Adsorption of sulfur dioxide in carbon nanotubes - gravimetric experiment and molecular dynamics simulation

Adsorption von Schwefeldioxid in Carbon Nanotubes - gravimetrische Experimente und molekulardynamische Simulation

Am Fachbereich Maschinenbau an der Technischen Universität Darmstadt zur Erlangung des Grades eines Doktor-Ingenieurs (Dr.-Ing.) genehmigte

DISSERTATION

vorgelegt von Dipl.-Ing. Frank G. Kühl aus Würzburg

Berichterstatter: Prof. Dr.-Ing. Manfred J. Hampe
Mitberichterstatter: Prof. Dr. Jörg J. Schneider

Tag der Einreichung: 05.04.2018
Tag der mündlichen Prüfung: 04.07.2018
Darmstadt 2018
D17

TECHNISCHE
UNIVERSITÄT
DARMSTADT

Dipl.-Ing. Frank G. Kühl

Dissertation
Thema: "Adsorption of sulfur dioxide in carbon nanotubes - gravimetric experiment and molecular dynamics simulation"
"Adsorption von Schwefeldioxid in Carbon Nanotubes - gravimetrische Experimente und molekulardynamische Simulation"

Am Fachbereich Maschinenbau an der Technischen Universität Darmstadt zur Erlangung des Grades eines Doktor-Ingenieurs (Dr.-Ing.) genehmigte

DISSERTATION

vorgelegt von Dipl.-Ing. Frank G. Kühl aus Würzburg

Berichterstatter: Prof. Dr.-Ing. Manfred J. Hampe
Mitberichterstatter: Prof. Dr. Jörg J. Schneider

Tag der Einreichung: 05.04.2018
Tag der mündlichen Prüfung: 04.07.2018
Darmstadt 2018
D17

urn:nbn:de:tuda-tuprints-81047
https://tuprints.ulb.tu-darmstadt.de/id/eprint/8104

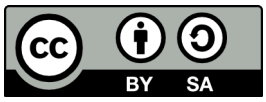

Abstract

In this work, isothermal adsorption of sulfur dioxide (SO_2) and nitrogen (N_2) at carbon nanotubes (CNTs) is studied in molecular dynamics simulation and gravimetric experiments in the temperature range from 0 °C to 125 °C and the pressure range from vacuum to 80 bar. The results are compared to each other and are in good agreement if the simulational data is adjusted by a scaling factor which is tied to the BET surface area of the respective CNTs.

In simulation, single-walled CNTs in a diameter range of 1.48 nm to 10.77 nm are regarded. Additionally, graphene was simulated in the two gas atmospheres. For a CNT(20/20) mixtures of SO_2 and N_2 were also studied and show a high attraction for SO_2.

Adsorption experiments with multi-walled CNTs, single-walled CNTs and vertically aligned CNTs in SO_2 show adsorbed amounts up to 22.7 $mmol g^{-1}$. For N_2 experiments the adsorbed amount is up to 1.49 $mmol g^{-1}$. From the adsorption isotherms heats of adsorption are derived. For SO_2 data the heats of adsorption are in the range between 18 and 30 $kJ mol^{-1}$. For N_2 data the heats of adsorption are in the range between 9 and 19 $kJ mol^{-1}$. Evaluations of adsorption isotherms from simulation deliver comparable heats of adsorption.

Acknowledgments

At this point I would like to take the opportunity to thank all people who have supported me in this work. First, I would like to thank Prof. Dr.-Ing. M.J. Hampe and the staff of the Institute of Thermal Process Engineering, who gave me the funding, opportunity, support and freedom to research the content of this work. For their encouragement and valuable discussions during lunch time and occasionally during the day I want to credit my fellow colleagues Sebastian, Stefan, Benjamin, Timurl, Becky and Maria. Heidi, Lidia, Birgit and Corinna helped me out with organizational and technical support.

A magnificent experience was the possibility to work with students at numerous occasions e.g. in recitations, lectures and during theses. Especially, the lectures 'Chemistry for Engineers' and 'Engineers in Society' were a great delight. Not only caused by numerous lecturers but also by the many tutors I was able to work with. At this occasion I want to thank especially the Writing Lab of TU Darmstadt for their support with tutors for the lecture 'Engineers in Society', namely the supervisor Lisa and her colleagues, with whom it was a pleasure to work with and supervise the up to 28 parallel seminar classes.

Here, I also want to recognize the students, Marius, Nico, Tingting, Franziska, Eugen, Hanna, Falko, who completed their Bachelor's or Master's degree under my supervision. Many thanks to all student assistants who gave a helping hand.

Special thanks go also to Prof. J.J. Schneider from the Eduard-Zintl-Institute of TU Darmstadt and his scientific staff, namely Deepu, Divya and Sandeep for providing sample material for adsorption measurement, BET measurements, SEM images and the excellent collaboration. For the TEM measurements I want to thank Jörg Engstler from TU Darmstadt for his work.

I also want to credit Edith for becoming my beloved wife and supporting me greatly during the writing process.

Not to forget my parents, brothers and sister who have always been there and encouraged during my studies. Finally, many thanks to all which are not named explicitly but supported me.

Contents

List of Figures

List of Tables

List of Symbols

Latin Letters

A	Amplitude of the linear driving force model	mg
a_i	Cohesion pressure of component i	bar
a_m	Cohesion pressure of the binary mixture	bar
A_{Te}	Adsorption constant in Temkin isotherm	bar^{-1}
b_i	Co-volume of component i	molm^{-3}
b_m	Co-volume of the binary mixture	molm^{-3}
b_{Te}	Adsorption constant in Temkin isotherm	$\mathrm{J\,gmol}^{-1}\,\mathrm{mmol}^{-1}$
F	Constant in Freundlich isotherm	$\mathrm{mmolg}^{-1}\mathrm{bar}^{-\mathrm{n_F}}$
G	Gibbs free energy	kJ
$\Delta_f G^\circ$	Standard Gibbs free energy of formation	kJmol^{-1}
$\Delta_f H^\circ$	Standard enthalpy of formation	kJmol^{-1}
$\Delta_{\mathrm{fus}} H_{T_f}$	Enthalpy of fusion at T_f	kJmol^{-1}
$\Delta_{\mathrm{sub}} H$	Enthalpy of sublimation	kJmol^{-1}
$\Delta_{\mathrm{vap}} H_{T_b}$	Enthalpy of vaporization at T_b	kJmol^{-1}
k	Kinetic constant of the linear driving force model	min^{-1}
K_{BET}	Constant in BET isotherm	–
k_{DA}	Constant in Dubinin Astakhov isotherm	$\mathrm{mol}^{\mathrm{n_{DA}}}/\mathrm{J}^{\mathrm{n_{DA}}}$
k_{DR}	Constant in Dubinin Raduskevich isotherm	$\mathrm{mol}^2\mathrm{J}^{-2}$
L	Constant in Langmuir isotherm	bar^{-1}
m	Molecule mass in DL Poly units	Da
M	Molecular weight	gmol^{-1}
m	Mass	g
m_{meas}	Measured mass	g
m_S	Mass of the sample	g
m_{SC}	Mass of the sample container	g
$m_{SC,meas}$	Measured vacuum mass of the sample container	g
m_{SC+S}	Mass of the sample container and sample	g
$m_{SC+S,\mathrm{meas}}$	Measured vacuum mass of the sample container and sample	g
$m_{S,\mathrm{meas}}$	Measured vacuum mass of the sample	g

n	Number of components in a system	–
$n_{\text{ads,ex}}$	Excess amount adsorbed per gram of sample	mmolg^{-1}
n_{DA}	Constant in Dubinin Astakhov isotherm	–
n_F	Power constant in Freundlich isotherm	–
n_i	Amount of moles of component i	mol
p_c	Critical pressure	bar
p	Pressure	Pa / bar
p_s	Saturation pressure	bar
p_{sat}	Saturation pressure at the respective temperature	bar
p_t	Triple point pressure	bar
p_{vp}	Vapor pressure	bar
Q_{BET}	Adsorbate loading in BET isotherm	mmolg^{-1}
Q_{DA}	Adsorbate loading in Dubinin Astakhov isotherm	mmolg^{-1}
Q_{DR}	Adsorbate loading in Dubinin Raduskevich isotherm	mmolg^{-1}
Q_F	Adsorbate loading in Freundlich isotherm	mmolg^{-1}
Q_L	Adsorbate loading in Langmuir isotherm	mmolg^{-1}
$q_{\text{max,BET}}$	Monomolecular loading in BET isotherm	mmolg^{-1}
$Q_{\text{max},L}$	Maximal adsorbate loading in Langmuir isotherm	mmolg^{-1}
$Q_{\text{max},T}$	Maximal adsorbate loading in Tóth isotherm	mmolg^{-1}
$q_{s,DA}$	Constant in Dubinin Astakhov isotherm	mmolg^{-1}
$q_{s,DR}$	Constant in Dubinin Raduskevich isotherm	mmolg^{-1}
Q_T	Adsorbate loading in Tóth isotherm	mmolg^{-1}
Q_{Te}	Adsorbate loading in Temkin isotherm	mmolg^{-1}
R	Ideal gas constant	$\text{J}\text{mol}^{-1}\,\text{K}^{-1}$
S	Entropy	JK^{-1}
$\Delta_f S°$	Standard entropy of formation	$\text{J}\text{mol}^{-1}\,\text{K}^{-1}$
S^{298K}	Entropy at 298 K	$\text{J}\text{mol}^{-1}\,\text{K}^{-1}$
S_{BET}	BET surface area	m^2g^{-1}
T	Temperature	K
T_b	Normal boiling point	K
T_c	Critical temperature	K
$T_{\text{decomp.}}$	Decomposition temperature	K
T_f	Normal fusion point	K
T	Constant in Tóth isotherm	$\text{mmol}\text{g}^{-1}\,\text{bar}^{-1}$
T_t	Triple point temperature	K
U	Inner energy	kJ

V	Volume	m^3
v	Molecule velocity in DL Poly units	Å/ps
$V_{m,i}$	Molar volume of component i	$molm^{-3}$
V_S	Volume of the sample	cm^3
V_{SC}	Volume of the sample container	cm^3
V_{SC+S}	Volume of the sample container and sample	cm^3
$V_{S,spec}$	Specific volume of the sample	cm^3g^{-1}

Greek Letters

β_i	Temperature dependent factor of the cohesion pressure in the Peng-Robinson equation for component i	–
η	Viscosity	μPa s
μ_i	Chemical potential of component i	$Jmol^{-1}$
ω	Acentric factor	–
ω_i	Acentric factor of component i	–
Φ	Number of phases in a system	–
ρ	Density	gcm^{-3}
ρ	Molar density	$molL^{-1}$
ρ_{meas}	Measured density of the fluid	gcm^{-3}
σ	Standard deviation of the fit error	g
ε_{DA}	Variable in Dubinin Astakhov isotherm	$Jmol^{-1}$
ε_{DR}	Variable in Dubinin Raduskevich isotherm	$Jmol^{-1}$

Indices

a	Adsorbent	–
a_0	Adsorbent in the absence of sorbate	–
s	Sorbate	–

Abbreviations

A	Adsorbent	
A_{ads}	Adsorbate	
Ar	Argon	
BET	Brunauer Emmett Teller	
CAS-#	Chemical abstract service number	–
CID	Compound identifier	–
CNH	Carbon nanohorn	

CNT	Carbon nanotube	
CO_2	Carbon dioxide	
CS_2	Carbon disulfide	
CVD	Chemical vapor deposition	
DA	Dubinin Astakhov	
DR	Dubinin Raduskevich	
DWCNT	Double-walled carbon nanotube	
EC-#	European Community number	–
EU	European Union	
GDS	Gas dosing system	
H_2	Hydrogen	
H_2O	Water	
HC	Hydrocarbons	
He	Helium	
HiPco	High pressure carbon monoxide method	
IAST	Ideal adsorbed solution theory	
ILV	Indicative limit value	mgm^{-3} or ppm
LJ	Lennard-Jones	
MD	Molecular dynamics	
MOF	Metal organic framework	
MSB	Magnetic suspension balance	
μVT	Grandcanonical simulation ensemble with constant chemical potential, volume and temperature	
MWCNT	Multi-walled carbon nanotube	
N_2	Nitrogen	
NPT	Simulation ensemble with constant number of sites, pressure and temperature	
NRTL	Non-random-two-liquid	
NTP	Normal temperature and pressure (293.15 K and 1 013.25 mbar)	
NVE	Microcanonical simulation ensemble with constant number of sites, volume and energy	
NVT	Canonical simulation ensemble with constant number of sites, volume and temperature	
OLV	Occupational limit value	mgm^{-3} or ppm
RAST	Real adsorbed solution theory	
S	Sorbate	

SO_2	Sulfur dioxide
SWCNT	Single-walled carbon nanotube
TSA	Temperature swing adsorption
VACNT	Vertically-aligned carbon nanotube
vdW	van-der-Waals
WS	Wong-Sandler

Natural Constants

e	Elementary charge	$1.602 \cdot 10^{-19}\,\mathrm{C}$
k_B	Boltzmann constant in DL Poly units	$0.831\,4\,\mathrm{JK}^{-1}$

1 Introduction

To study hazardous systems such as corrosive, toxic or acidic systems or systems in extreme experimental conditions such as high pressure, high or low temperature, etc. simulation can be superior to experiments. A precondition for this is that the simulation reflects the true system behavior well and allows to draw first conclusions whether experiments are necessary or need to be conducted at all. Especially, if these experiments need challenging precautions to account, e.g. for toxicity, corrosiveness, explosive atmospheres, etc.

As such a system, carbon nanotubes (CNTs) and pure sulfur dioxide SO_2 can be seen. Carbon nanotubes (CNTs) are a modification of carbon. As their name implies, they have a tubular structure in the nanoscale range. A simple way to describe CNTs is to imagine a single sheet of graphite, which is then called graphene. If you wrap this graphene around one axis, a tubular structure is established, a single-walled CNT (SWCNT). A good illustration of this is presented by Geim and Novoselov[1] shown in figure 1.1. In this illustration also graphite and a buckminsterfullerene are pictured.

Preliminary molecular dynamics simulations showed promising results for good adsorption behavior of SO_2 at (single-walled) carbon nanotubes ((SW)CNTs).[2] This behavior needed to be evaluated further in simulation and validated by appropriate experiments to show that simulation is a good representation of the studied conditions such as regarded pressures and temperatures and omit costly and hazardous experiments in pure SO_2 atmospheres for future studies. This preliminary study was the starting point of this work. Besides the validation of the simulation data, further simulations were carried out to allow a deeper insight in the adsorption behavior of different CNTs at various temperatures in SO_2, nitrogen (N_2) atmospheres and their mixtures.

Initially, it has to be clarified what carbon nanotubes (CNTs) are. They were first described by Kroto et al.[3] and Iijima et al.[4]. Their simple geometrical structure, which builds a cylindrical pore with fixed diameter and elongation along one axis, makes them interesting to study in theory and experiment. Depending on the preparation conditions the diameter, length and amount of walls can be tailored for CNTs[5] to produce single-walled carbon nanotubes (SWCNTs), multi-walled carbon nanotubes (MWCNTs) or vertical-aligned carbon nanotubes (VACNTs). Especially VACNTs are ideal to study in theory by e.g. molecular dynamics and to compare these results to results from experi-

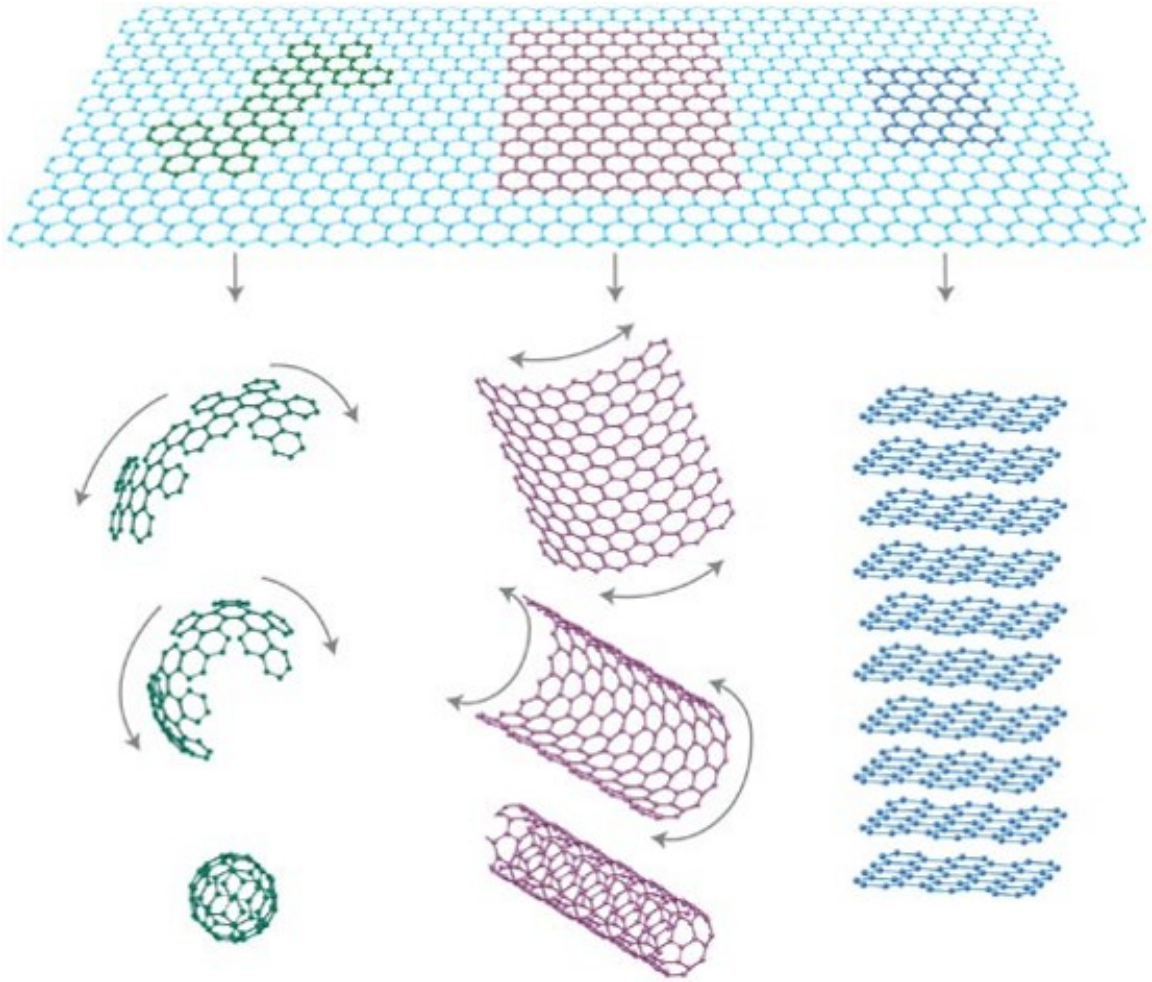

Figure 1.1.: Schematic of a sheet of graphene and how to form a fullerene, a (SW)CNT and graphite from it[1]

mental measurements. One reason for this is the well-ordered structure and the simple shape of the pores the CNTs form.

For CNTs already theoretical and/ or experimental studies with different molecules such as hydrogen (H_2), carbon dioxide (CO_2), nitrogen (N_2), argon (Ar), water (H_2O), carbon disulfide (CS_2) etc. exist.[6–13] Mostly in these studies single walled carbon nanotubes (SWCNTs) are studied. In this work also only SWCNTs were studied by simulation. In experiments different CNTs were studied such as MWCNTs, SWCNTs and VACNTs.

One model gas for CNT adsorption is sulfur dioxide which is described in literature only as a trace compound in a gas mixture (SO_2).[14,15] However, to get a better understanding of the adsorption behavior, pure gases should be studied first and then the results might be used to predict mixture adsorption behavior in different atmospheres.

SO_2 itself is a gas which has natural sources, e.g. volcanoes, but it is also a compound which is often released in trace compounds in different processes, e.g. burning of coal, wood or roasting of ores. Its acrid smell and acidic behavior even at low concentrations below 1 ppm make it a challenge to remove from, e.g. flue gases only with the help of adsorption. For this, the adsorption behavior of SO_2 needs to be studied in more detail to gain more knowledge about the capability of adsorption, e.g. by CNTs.

This work gives a deeper insight into the adsorption of SO_2 and N_2 at CNTs. For this different SWCNT were simulated in SO_2, N_2 and mixed atmospheres of the two gases. The results from the simulation were then compared to experimental studies of different CNT types which have been performed in a gravimetric apparatus. The gravimetric adsorption setup allowed to measure with pure SO_2, N_2 and CO_2 atmospheres. To account for buoyancy corrections also helium measurements could be performed.

In a last step simulation and experiment are compared to each other and show a good agreement for most of the studied cases. In experiment also further data such as reproducibility of the results, cycling and additional temperatures are studied to give a more detailed insight into the adsorption of SO_2 at CNTs.

2 Background information and literature review

In this chapter, an overview of adsorption is given including adsorption equilibria and selected adsorption models. Additionally, net, excess and absolute adsorption are distinguished which is important for presenting adsorption results. The principles of molecular dynamics are also shortly named as well as different setups for adsorption experiments. Production processes of carbon nanotubes and their geometrical structure are also presented. Finally, data on the used chemical media for the adsorptives, adsorbents and auxiliary substances are summarized.

2.1 Adsorption

According to the IUPAC definition adsorption is:
"*An increase in the concentration of a dissolved substance at the interface of a condensed and a liquid phase due to the operation of surface forces. Adsorption can also occur at the interface of a condensed and a gaseous phase.*"[16]
In simple terms, adsorption is a process in which atoms, molecules, ions or a combination of those adhere on a surface or an interface. The surface or interface can be solid or liquid. Furthermore, adsorption can be subdivided in the process of physisorption and chemisorption. The first one is adsorption due to weak van-der-Waals interactions and/or electrostatic forces arising from surface charge interactions of the adsorptive with the adsorbent forming the adsorbate phase (compare to figure 2.1). Usually physisorption has adsorption energies below $50\,\mathrm{kJmol^{-1}}$ ($\approx 0.5\,\mathrm{eV}$ per atom/ molecule/ ion)[17–20]. The latter one is adsorption due to the formation of chemical bonds to the surface. Chemisorption energies are typically above $50\,\mathrm{kJmol^{-1}}$. Generally, physisorption is easily reversible. To regenerate surfaces after chemisorption, high energies are required, and sometimes chemisorption is non-reversible, e.g. if a chemical reaction has occurred.

The adsorptive can either be a gas or gas mixture, a liquid or liquid mixture or a combination of those. Typically only gas (mixtures) or liquid (mixtures) are studied which adsorb on different adsorbents. In literature there is a variety of studies, here

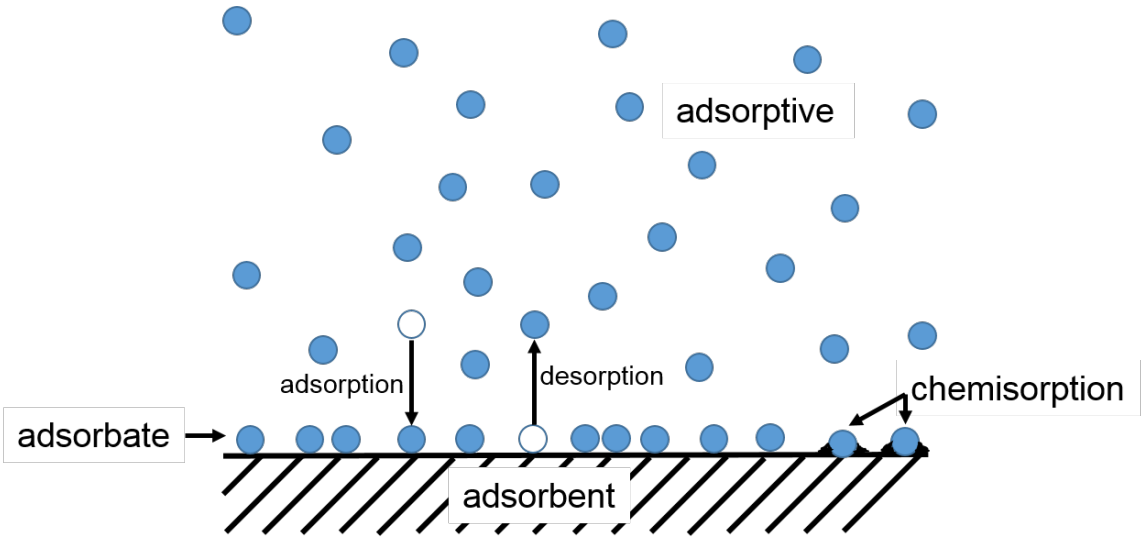

Figure 2.1.: Schematic of adsorption: an adsorptive adsorbs to an adsorbent to form an adsorbate layer, it can also desorb from the adsorbent. If strong adsorption is observed it is usually chemisorption with the surface

only a few are included exemplary, zeolites for purification and separation of gases, water adsorption on SWCNTs, adsorption at carbon molecular sieves, adsorption at activated carbon etc. [21–32].

In this work, adsorption is only limited to solid-gas adsorption. As solid adsorbent, many species can act. Some typical carbon-based adsorbents are activated carbons, carbon molecular sieves, carbon nanotubes, graphite, graphene etc. Non-carbon-based adsorbents are, e.g. silica, metal-organic frameworks (MOFs), zeolites, (non-carbon) molecular sieves etc.

2.1.1 Adsorption equilibria

To compare materials and make first estimations for their performance in adsorption, equilibria can give first hints. Typical equilibria, which are measured, are isotherms respectively isobars. These are measurements at constant temperature respectively pressure which yield in plots of the amount adsorbed over pressure respectively temperature. To evaluate the heat of adsorption also isosteres are of help. Isosteres are plots of the logarithmic pressure (typically $\ln(p)$) over the reciprocal temperature ($\frac{1}{T}$) at the same adsorbed amount.

In practice also the adsorption kinetics play a significant role to exploit a material for e.g. removal of a compound, storage of compounds, increase in the concentration of a compound. One way to study kinetics is to evaluate uptake curves by pressure, tem-

perature or composition step and study the time behavior of the uptake of a material. The kinetics as well as the achievable loading do influence breakthrough curves of, e.g. adsorption columns.

Thermodynamically a system is at an equilibrium state if the mechanical, thermal and chemical equilibrium for all phases Φ are achieved. This means pressure as well as temperature in all phases is constant and at the same value and that the chemical potential μ_i of component i in one phase is equal the chemical potentials of all components i in the other phases (compare equations 2.1, 2.2 and 2.3).

$$T^1 = T^2 = ... = T^\Phi \tag{2.1}$$

$$p^1 = p^2 = ... = p^\Phi \tag{2.2}$$

$$\mu_i^1 = \mu_i^2 = ... = \mu_i^\Phi \tag{2.3}$$

Thermodynamic fundamental equation and its amendment for usage in adsorption

To describe a system one can start from the thermodynamic fundamental equation 2.4:

$$dU(S,V,n_i) = TdS - pdV + \Sigma\mu_i dn_i \tag{2.4}$$

From equation 2.4 the Gibbs free energy (equation 2.5) can be derived with the help of Legendre transformations in the way that entropy S and volume V are substituted by temperature T and pressure p:

$$dG(T,p,n_i) = -SdT + Vdp + \Sigma\mu_i dn_i \tag{2.5}$$

Taking equation 2.5 and formulating it for an adsorbent a (in the prescence of a sorbate s) and the same adsorbent in the absence of a sorbate a_0 it gives[18,33]:

$$dG(T,p,n_a,n_s) = -SdT + Vdp + \mu_a dn_a + \mu_s dn_s \quad (2.6)$$

$$dG_{a_0}(T,p,n_{a_0},n_s=0) = -S_{a_0}dT + V_{a_0}dp + \mu_{a_0}dn_a \quad (2.7)$$

The differential Gibbs free energy for the sorbent G_s is obtained by the subtraction of equation 2.6 and 2.7[18,33]:

$$dG(T,p,n_a,n_s) = -S_s dT + V_s dp + (\mu_a - \mu_{a_0})dn_a + \mu_s dn_s \quad (2.8)$$

S_s and V_s are defined as:

$$S_s = S - S_{a_0} \quad (2.9)$$

$$V_s = V - V_{a_0} \quad (2.10)$$

Assuming that the sorbate volume V_s can be neglected in comparison to the vapor phase and assuming isothermal conditions equation 2.8 simplifies to[18,33]:

$$dG(T=\text{const},p,n_a,n_s) = (\mu_a - \mu_{a_0})dn_a + \mu_s dn_s \quad (2.11)$$

$$G(T=\text{const},p,n_a,n_s) = (\mu_a - \mu_{a_0})n_a + \mu_s n_s \quad (2.12)$$

Then the Gibbs free energy can easily be obtained by this equation by the knowledge of the chemical potentials in the equilibrium state of the adsorbed adsorbent μ_a, the pristine adsorbent μ_{a_0} and the adsorbate μ_s as well as the amount of moles of the adsorbent n_a and the adsorbate n_s.

2.1.2 Overview of adsorption models

There are many different models to describe adsorption isotherms and isobars. In this section, adsorption models are presented, which are employed in this work. These models are often empirical models and work only for certain instances in which they

have to be chosen respectively. Usually, they are fitted to experimental data, and the quality of the fit is a hint of the applicability of the respective model. Further adsorption models, which are not presented here, are, e.g. the models of Redlich Peterson [34], Radke Prausnitz [35], Kisliuk [36], the ideal adsorbed solution theory (IAST) [37], the real adsorbed solution theory (RAST) [38–40], etc.

Langmuir

The Langmuir adsorption isotherm is one of the first models to describe adsorption. It assumes a monomolecular covering of an adsorbent by a sorbate phase. Furthermore, it assumes that there is only a certain number of adsorption sites available and that these sites are equal to each other. Additionally is assumed that all adsorbed species do not interact with each other. To derive the equation for a Langmuirian isotherm a reaction equilibrium can be taken between the adsorbent A, sorbate S and adsorbed adsorbate A_{ads}:

$$\mathrm{A} + \mathrm{S} \rightleftharpoons \mathrm{A}_{\text{ads}} \tag{2.13}$$

Assuming that a steady state is reached this gives the following equation:

$$Q_L = Q_{\text{max},L} \frac{L \cdot p}{1 + L \cdot p} \text{ [41–43]} \tag{2.14}$$

With $Q_{\text{max},L}$ as the maximum loading of the adsorbent per gram adsorbent, L as the Langmuirian constant and p as the bulk pressure of the sorbate. Rearranging the equation into a linear form helps to judge whether a Langmuirian adsorption is achieved if the experimental data is also plotted in the same manner:

$$\frac{Q_L}{p} = Q_{\text{max},L} \cdot L - Q_L \cdot L \text{ [41–43]} \quad \text{or} \tag{2.15}$$

$$\frac{p}{Q_L} = \frac{1}{Q_{\text{max},L} \cdot L} + \frac{p}{Q_{\text{max},L}} \tag{2.16}$$

Freundlich

The Freundlich isotherm is an empirical isotherm model introduced by Ostwald, Boedecker and Freundlich in 1906.[44,45] Nowadays it is known as Freundlich adsorption isotherm model.[18] It has a simple polynomial approach:

$$Q_F = F \cdot p^{n_F} \text{ [42–45]} \tag{2.17}$$

With F as coefficient and n_F as exponent. A linearized form of the equation gives the following:

$$\log(Q_F) = \log(F) + n_F \log(p) \text{ [42,43,45]} \tag{2.18}$$

BET

The BET isotherm model was introduced by Brunauer, Emmett and Teller in 1938 and extends the Langmuirian theory from monomolecular to multimolecular adsorption.[46] It allows fitting S-shaped adsorption isotherms of type II according to the IUPAC definition.[47] The BET model may be written in the following form:

$$Q_{\mathrm{BET}} = \frac{K_{\mathrm{BET}} \cdot q_{\mathrm{max,BET}} \cdot p}{(p_{\mathrm{sat}} - p)\left(1 + (K_{\mathrm{BET}} - 1)\,\frac{p}{p_{\mathrm{sat}}}\right)} \text{ [43,46]} \tag{2.19}$$

For this model the saturation pressure of the adsorptive p_{sat} is needed. Characteristic constants for this model are K_{BET} and the monomolecular loading $Q_{\mathrm{max,BET}}$. From this monomolecular loading $Q_{\mathrm{max,BET}}$ the BET surface S_{BET} can be calculated, if e.g. the molecular cross-sectional area of the adsorbate is known. For N_2 at 77 K 0.162 nm^2 [48] is used widely, for CO_2 at 298 K it is 0.162 nm^2 [49] and for SO_2 at 273 K it is estimated to be 0.31 nm^2 [50]. A linear form of equation 2.19 is presented in the following and is usually used to determine the constants K_{BET} and $Q_{\mathrm{max,BET}}$:

$$\frac{p}{Q_{\mathrm{BET}} \cdot (p_{\mathrm{sat}} - p)} = \frac{(K_{\mathrm{BET}} - 1)}{K_{\mathrm{BET}} \cdot q_{\mathrm{max,BET}}} \cdot \frac{p}{p_{\mathrm{sat}}} + \frac{1}{K_{\mathrm{BET}} \cdot q_{\mathrm{max,BET}}} \text{ [18,43]} \tag{2.20}$$

The BET isotherm is usually only regarded and fitted in the range of $0.05 \leq \frac{p}{p_{\mathrm{sat}}} \leq 0.3$ to derive the constants.[47] This range can be extended or has to be reduced or shifted if the rules implemented and advocated by Rouquerol are not fulfilled.[51]

Dubinin Raduskevich - Dubinin Astakhov

The Dubinin-Raduskevich (DR) and the Dubinin-Astakhov (DA) adsorption isotherms are both empirical adsorption isotherm models. They have a similar equation structure. The equation for the DR isotherm (eq. 2.21 and 2.22) is a special case of the more general DA isotherm equation (eq. 2.23 and 2.24). However does the DA isotherm have an additional fitting parameter n_{DA} to linearize the adsorption isotherm over the whole range, if the adsorbed amount is plotted over the function $\varepsilon_{DA}^{n_{DA}}$ (equation 2.24).[52–54]

$$Q_{DR} = q_{s,DR} \cdot e^{-k_{DR} \cdot \varepsilon_{DR}^2} \text{ [54]} \tag{2.21}$$

$$\varepsilon_{DR} = RT \cdot \ln(1 + 1/p) \text{ [54]} \tag{2.22}$$

$$Q_{DA} = q_{s,DA} \cdot e^{-k_{DA} \cdot \varepsilon_{DA}^{n_{DA}}} \text{ [54]} \tag{2.23}$$

$$\varepsilon_{DA} = RT \cdot \ln(1 + 1/p) \text{ [54]} \tag{2.24}$$

The linear forms of the DR and the DA isotherm are given in equations 2.25 and 2.26.

$$\ln(Q_{DR}) = -k_{DR} \cdot \varepsilon_{DA}^2 + \ln\left(q_{s,DR}\right) \tag{2.25}$$

$$\ln(Q_{DA}) = -k_{DA} \cdot \varepsilon_{DA}^{n_{DA}} + ln\left(q_{s,DA}\right) \tag{2.26}$$

Tóth

Another empirical model is the Tóth isotherm introduced by J. Tóth (eq. 2.27).[55] The Tóth model was developed to deliver an improved fit in contrast to traditional Langmuirian fits.[56]

$$Q_T = Q_{\max,T} \frac{T \cdot p}{[1 + (T \cdot p)^{n_T}]^{\frac{1}{n_T}}} \text{ [42,43,55]} \tag{2.27}$$

Temkin

Another early model to describe adsorption isotherms is the model of Temkin (equation 2.28).[57] In this model, the adsorption energy of the sites is not equal and decreases linearly with increasing coverage of the adsorbent.[57–59]

$$Q_{Te} = \frac{RT}{b_{Te}} \ln(A_{Te} p)^{[42,43,57,60]} \tag{2.28}$$

Rearranging equation 2.28 into the linear form gives equation 2.29:

$$Q_{Te} = \frac{RT}{b_{Te}} \ln(p) + \frac{RT}{b_{Te}} \ln(A_{Te})^{[42,43,57,60]} \tag{2.29}$$

Virial-type thermal equation

To describe the adsorption isotherm also Virial-type thermal models can be used. They describe the pressure or the logarithmic pressure dependent on different variables, e.g. temperature T, amount adsorbed per gram adsorbent X. These models, in general, have a form of:

$$p = f(\frac{1}{T}, X, ...) \qquad \text{or} \tag{2.30}$$

$$\ln(p) = f(\frac{1}{T}, X, ...) \tag{2.31}$$

One exemplary equation of a Virial-type thermal model was first described by Czepirski and Jagiello[61] and may be simplified to the following form[56,62]:

$$\ln(p) = \frac{1}{T} \sum_{i=0}^{m} (a_i \cdot X^i) + \sum_{i=0}^{n} (b_i \cdot X^i) + \ln(X) \tag{2.32}$$

$$\tag{2.33}$$

m and n are parameters which can be chosen. a_i and b_i are derived through fitting methods to experimental data.

2.1.3 Determination of adsorption enthalpies

From the Gibbs free energy (equation 2.5) the heat of adsorption can be derived. In equilibrium the following equation holds for the bulk and the sorbate phase:

$$dG^{\text{bulk}} = dG^{s} \tag{2.34}$$

Taking isosteric conditions ($n = const.$), an equation similar to the Clausius-Clapeyron equation can be derived:

$$\left(\frac{\partial p}{\partial T}\right)_{n=\text{const}} = \frac{H^{\text{bulk}} - H^{s}}{RT^2} = \frac{\Delta_{\text{ads}}H}{RT^2} \tag{2.35}$$

This is equivalent to the more common plotting manner for isosteres, which is a plot of logarithmic pressure $\ln(p)$ over the inverse temperature T (compare figure 2.2):

$$\left(\frac{\partial \ln p}{\partial (1/T)}\right)_{n=\text{const}} = \frac{H^{\text{bulk}} - H^{s}}{R} = \frac{\Delta_{\text{ads}}H}{R} \tag{2.36}$$

To roughly estimate the heat of adsorption, if no measurements are present, the heat of condensation of the adsorptive can be taken and multiplied by a factor of 1.5 as a rule of thumb.[18,54] A more exact value can be derived from equation 2.36. It allows deriving the heat of adsorption in a graphical or an analytical manner. Graphically this is done by plotting the logarithmic equilibrium pressure over the inverse temperature of experimental adsorption isotherms of minimum two temperatures, which have the same adsorbed amount ($n_1 = n_2 = ... = n_n$ resp. $X_1 = X_2 = ... = X_n$). From this plot, the slope is estimated and yields the heat of adsorption by simple multiplication of the ideal gas constant R (compare figure 2.2). Analytically the equilibrium isotherms are fitted by a model, e.g. the Langmuir model, Freundlich model or a Virial-type model (these models are described in more detail in chapter 2.1.2). These models can then be rearranged into a form:

$$\ln(p) \quad = \quad f(\ln(p), \frac{1}{T}, ...) \tag{2.37}$$

One Virial-type thermal equation could be the following equation which yields for $m = 2$ and $n = 0$ to equation 2.39:

$$\ln(p) = \frac{1}{T}\sum_{i=0}^{m}(a_i \cdot X^i) + \sum_{i=0}^{n}(b_i \cdot X^i) + \ln(X) \tag{2.38}$$

$$\ln(p) = \frac{1}{T}\left(a_0 + a_1 \cdot X + a_2 \cdot X^2\right) + b_0 + \ln(X) \tag{2.39}$$

Deriving this equation for the isosteric heat of adsorption it gives:

$$\Delta_{ads}H = -R \cdot \left(a_0 + a_1 \cdot X + a_2 \cdot X^2\right) \tag{2.40}$$

With this, the isosteric heat of adsorption can be calculated over the whole range of the adsorbed amount (compare figure 2.2).

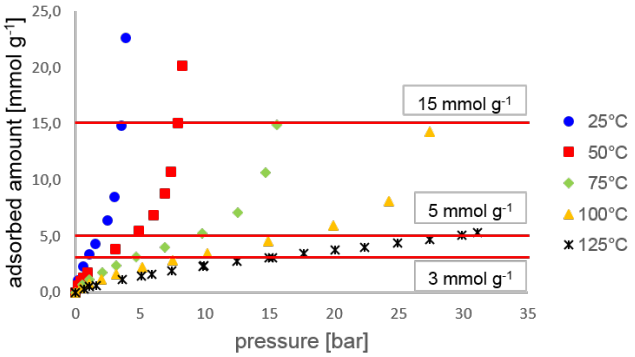

(a) Adsorption isotherms with isosteres

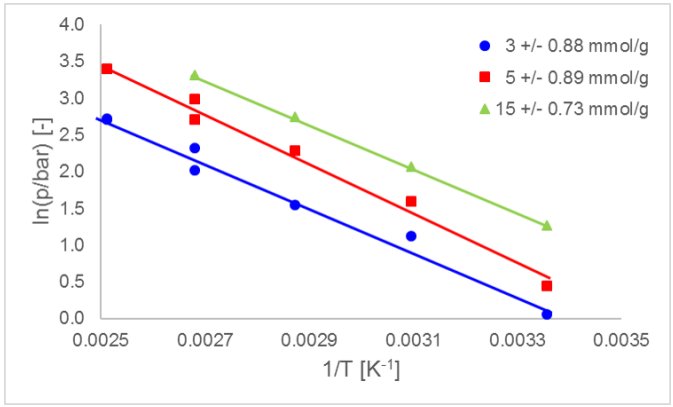

(b) $\ln(p)$-$\frac{1}{T}$ plot of isosteres to estimate the heat of adsorption from the slope

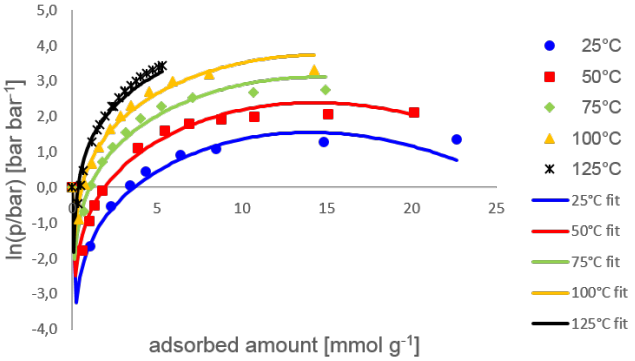

(c) Adsorption isotherms in a $\ln(p)$-adsorbed amount plot, experiments (symbols) isotherm fits by a Virial equation (lines)

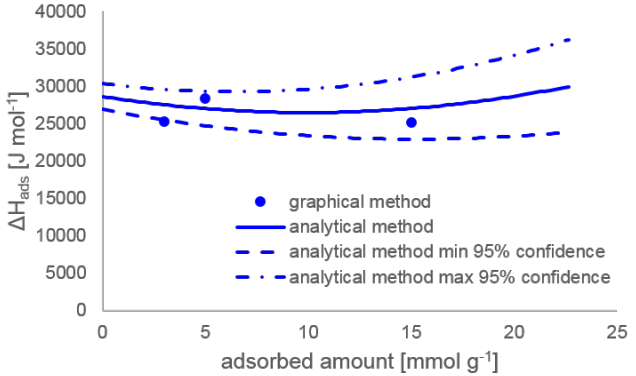

(d) Isosteric heat of adsorption estimated by the graphical method from b) (dots) and the analytical Virial fit from c) (line) with confidence interval

Figure 2.2.: Estimation of the heat of adsorption from experimental data from this work. a) Experimental values with isosteres, b) $\ln(p)$-$\frac{1}{T}$ plot of isosteres to estimate the heat of adsorption from the slope, c) adsorption isotherm in a $\ln(p)$-adsorbed amount plot with fitting lines and d) isosteric heat of adsorption from the graphical and and analytical method

2.1.4 Net, excess adsorption and absolute adsorption

Talking about adsorption one has to distinguish between net, excess and absolute adsorption. To illustrate this figure 2.3 shows the differences between the different adsorption definitions. Adsorption data can be presented in this three forms. Comparing adsorption data, one has to keep in mind that comparisons of, e.g. data from net and excess adsorption has to be treated with caution. The same accounts for data from absolute and excess adsorption.

To measure net adsorption, the sample volume is considered to be zero for the evaluation of the adsorbed amount. In fact, the sample volume itself is non-zero, but the adsorbed amount can be calculated by only knowing the sample mass and referring to it[63]. Excess adsorption considers the volume of the sample which has to be measured by a probe molecule. In practice, this probe molecule is often helium which is considered to be non-adsorbing or only very weakly adsorbing at room temperature and above. However it adsorbs to a very small amount[64–70] which is often negligible. With the sample volume estimated by the helium intrusion method, the excess adsorption can be calculated. Excess adsorption isotherms are the most commonly reported isotherms from experiments in literature. Absolute adsorption or total adsorption refers the adsorbed amount to the total volume of the adsorbent which includes all pores which are opened to the bulk phase. The total adsorbed amount is not easily accessible by measurements without making assumptions about, e.g. the density of the adsorbed phase in the pores. For e.g. MOFs or zeolites it is possible to calculate the total volume if the structural information is known and the volume is not changing during adsorption.[63,65] If it does change this is known as breathing.[71–73]

In this work, the shown isotherms from simulation are absolute adsorption isotherms. The reasons for this are: The structural information of the materials is known and it is assumed to be ideal. Additionally, there are no blocked areas which are not accessible by gas molecules. The experimental data, however, shows excess adsorption data. Here, pores which are not accessible by the probe molecule for the buoyancy correction are present. This is taken into account by the way the data is measured and evaluated. A comparison of the data from the simulation and the experiment is possible because the difference between excess adsorption and absolute adsorption of the studied systems under the studied conditions is covered by the adjustment factors which are used for the comparisons. These factors are introduced in the results (compare chapter 5.3).

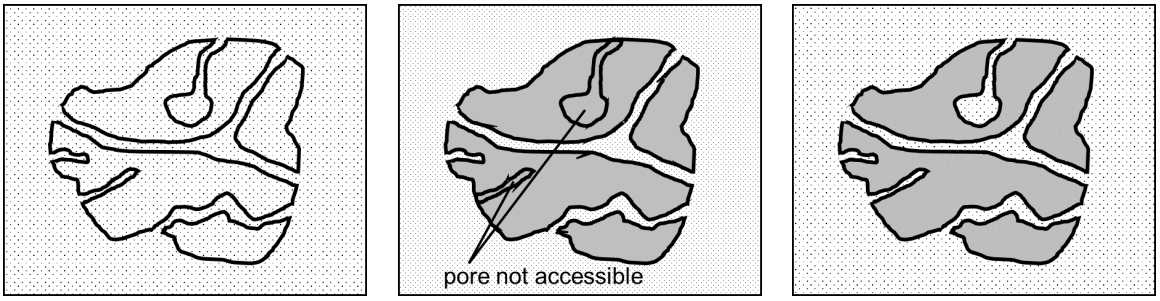

(a) Net adsorption **(b)** Excess adsorption **(c)** Absolute adsorption

Figure 2.3.: a) Net adsorption considers the solid volume to be zero for calculating the adsorbed amount, so only the mass has to be known, b) excess adsorption needs the measurement of the volume by a probe molecule e.g. helium which may not access all pores and c) absolute adsorption considers the true volume of the adsorbent

2.1.5 Adsorption kinetics

To study the kinetic behavior for the uptake of a gas from the experiments logged time evolution data from the measurements can be used. Therefore the logged mass change over time is evaluated. This time dependency can be fitted e.g. by a linear driving force model.[74] Equation 2.41 shows the fitting equation which was used for the evaluation. The code for the fitting is presented in appendix C.7. From the fit, the kinetic constant k and the amplitude A can be derived.

$$\Delta m = A \cdot \left(1 - e^{-k \cdot t}\right) \tag{2.41}$$

The amplitude is also dependent on the pressure step. Because of the way the data is measured the pressure steps vary, that is why the amplitude is not shown in this work and evaluated further. A typical evaluation of the kinetic constant is given in figure 2.4.

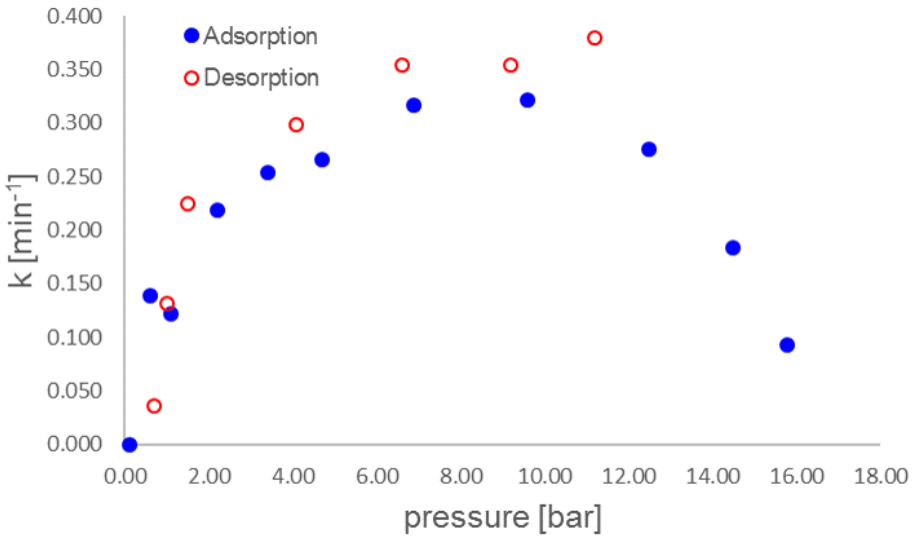

Figure 2.4.: Exemplary kinetic constants from experimental data of a VACNT at 75 °C in a SO_2 atmosphere from this work. The kinetic constant is shown for adsorption and desorption data over the pressure.

2.2 Molecular dynamics

The beginning of molecular dynamics (MD) is dating back to the middle of the last century. It was developed by Alder and Wainwright to initially study the phase transitions of hard spheres[75] and to study equilibrium and non-equilibrium problems of statistical mechanics[76]. Basically, it is a code to calculate the motion of particles, atoms, molecules or more general sites which interact with each other by different types of potential functions. For this, computers were of great help and still are of great help for bigger and bigger systems and more sophisticated models. The potential functions of the sites deliver the forces acting on the species in the system. With these forces Newtonian equations of motion are solved for one timestep Δt, predicting, e.g. the change in position and velocity of the species in the system after this timestep Δt. The results of the calculated changes are checked whether the boundary conditions of the simulation are met. The boundary conditions can be volume V, temperature T, pressure p, chemical potential μ, energy in the system E, number of particles in the system N. If yes, the system is updated, and the next timestep is calculated. If no, e.g. molecules are relaxed, the temperature is adjusted, the system size is adjusted etc.

Shortly summarized, molecular dynamics allow to study processes in molecular systems. These systems can consist of several hundred to thousand molecules. Nowadays these systems can also have sizes of several million particles. One of the early systems which were studied was liquid argon by Rahman.[77] One of the early realistic systems studied with molecular dynamics was water by Stillinger and Rahman.[78,79]

A great advantage of molecular dynamics is that system conditions can be studied which are not easy to measure in an experiment or where experiments have to be done under massive precautions because of extreme pressures, temperatures, corrosion conditions, etc. Also does molecular dynamics allow to study trajectories or forces acting on molecules which is sometimes not possible to do in an experiment. With special techniques, it is also possible to derive macroscopic values out of the simulation such as, e.g. thermal conductivity, diffusion coefficients, viscosity, adsorption properties etc.

Typically molecular dynamics simulations cover only small physical system sizes in the range of several or several hundred nm. Also, the simulated times in real times are low compared to times which are examined in experiments. Today the studied real times are in the range of a few ns, in some rare cases up to ms. A reason for this rather short times is the needed computational power for the systems and the small timesteps which have to be chosen. The timestep typically is in the range of ps. However, these limited times are sufficient to derive macroscopic properties from the system and to make it

possible to validate the simulation or compare it to macroscopic systems. Validation is needed especially for long simulation runs to show that numerical errors arising from integration do not accumulate and lead to faulty results. In the best case there are no numerical errors or they are averaged out during the simulation. Some basic consideration for molecular dynamics are summarized by Allen and Tildesley[80] and Frenkel and Smit[81].

Molecular dynamics simulations are carried out in so-called simulation ensembles. Some of these ensembles have special names such as the microcanonical ensemble (NVE ensemble), canonical ensemble (NVT ensemble), isobaric-isothermal ensemble (NPT ensemble) and the grand canonical ensemble (μVT).

To perform MD simulations a lot of different codes exist which were developed by different universities or institutions and are available for academic and/ or commercial use. Here only a few are named exemplary: Gromacs[82–88] , NAMD[89], Abalone[90], Vasp[91–93]. The code which was used in this work is DL Poly. It was programmed in the Daresbury Laboratory, England and is available for academical use. For this work different versions of DL Poly have been used, in the beginning, DL Poly 4.2[94] and later DL Poly 4.5[95].

2.3 Setups for adsorption experiments

Gas adsorption experiments are usually performed in either a volumetric or a gravimetric measuring system. Oscillometric and impedance spectroscopic setups are also used but not as frequent. Also, can a combination of different setups be used to study adsorption behavior. The outcome of the experiments is typically an adsorption isotherm. Isobares are measured not as frequent as isotherms, but they can also give valuable information for e.g. the study of temperature swing adsorption (TSA). In the setups, pure components or mixtures of components can be measured with different adsorbents or component mixtures with different adsorbents regarding their adsorption behavior. Here shortly the advantages and disadvantages of volumetric, gravimetric and mixed setups are presented. An overview of the history of adsorption measurements is given by, e.g. Kiefer and Robens[96] or Robens et. al.[97].

2.3.1 Volumetric adsorption

Volumetric setups were used for a long time, e.g. by Scheele in 1777[98,99], Chappuis in 1881[100], Langmuir in 1918[41], etc. In a volumetric apparatus, the volume is kept constant during the process. A scheme of a typical volumetric apparatus is given in

figure 2.5. In literature multiple setup assemblies can be found[29,96,101–106]. In most apparatus there is a vessel with an exactly known volume. To this vessel gas for sorption is applied and the pressure is measured. Then a valve is opened and the sorptive is introduced into a vessel with the sample. The volume of the sample has to be determined beforehand, e.g. by helium measurements. By knowing the volume of the storage vessel and the sample vessel with the sample the pressure drop without having any adsorption can be calculated by the use of equations of state. The measured pressure in an adsorption step is lower than the calculated pressure without adsorption happening. With this information the adsorbed amount can be calculated by the pressure difference.

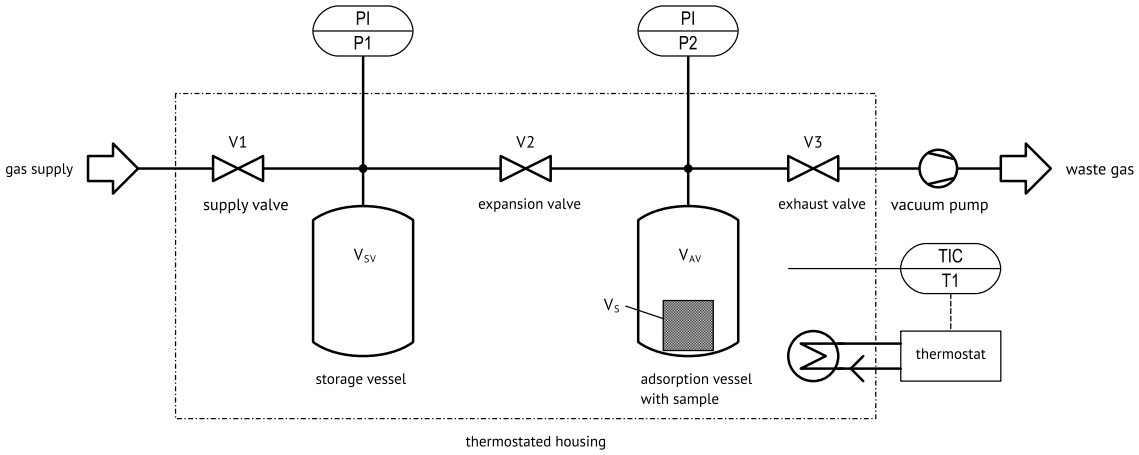

Figure 2.5.: Scheme of a typical volumetric apparatus to measure adsorption with a storage vessel with the volume V_{SV} and an adsorption vessel with the volume V_{AV} loaded with a sample with the sample volume V_S

The advantages of a volumetric setup are the simplicity of the setup and the necessity of only needing to measure pressure with the respective temperature.[104] Disadvantages of volumetric apparatuses are that a certain amount of adsorbent is needed to cause a change in pressure during the adsorption process which can be detected. Especially at very low pressures, this might be a problem. A mass change of the adsorptive during activation cannot be monitored and accounted in the experiments. At high pressures adsorption to the wall may play a major role which cannot be distinguished from adsorption to the adsorbent. Also, may it be difficult to judge if equilibrium is reached when changes in pressure are only very low or take a long time. Besides to this comes that errors from the adsorption steps accumulate during the measurement so that points measured towards the end have the highest uncertainty.[104]

2.3.2 Gravimetric adsorption

Balances have been used for several thousand years. A first application of balances which is tied to adsorption is the measurement of atmospheric humidity by a natural sponge reported already in the middle ages.[96,107,108] In 1861 the measurements under vacuum could be realized by the vacuum balance constructed by Deleuil[96,109]. It allowed investigating adsorption and desorption by varying the pressure in the measuring chamber. The early balances were usually simple beam balances (compare figure 2.6) which later got equipped with an electromagnetic measuring cell[110,111] (compare figure 2.6). These balances allow measuring adsorption isotherms if they are thermostated. A great disadvantage of these setups is that the counterweight or the measuring cell is exposed to the adsorptive and the respective temperature. This may cause problems such as corrosion, surface adsorption on the weighing parts or weighing drifts caused by temperature effects on the weighing cell. If the vacuum cell is made out of glass only low-pressure adsorption studies till a couple of bar are possible. Otherwise, the glass container will break.

The weighing cell can be placed outside of the measuring chamber to overcome the problems with the temperature, limited pressure and contact of the weighing cell with the adsorptive. The weight signal can be coupled either by a connecting rod or a magnetic coupling (compare figure 2.7). The disadvantage of the connecting rod is that it needs careful sealing which ideally does not affect the measurement and prevents the adsorptive from leaking to the environment, especially if hazardous adsorptives are used. These problems can easily be handled with a magnetic suspension balance, e.g. from Rubotherm (Bochum). Here the challenge is in a precise and low vibration floating of the suspension rod and the sample container with the sample inside the cell. Within this setup, this is realized by a level indicator which controls a current going through a coil of an electromagnet which lets a permanent magnet inside the measuring cell float. To the magnet, all measuring parts inside the cell are attached, e.g. permanent magnet with suspension rod and sample container with the sample (compare figure 2.7).

Overall disadvantages of gravimetric systems are that they have a certain complexity, e.g. the needed equipment such as weighing cell and its controlling, additional gas supply and (if applicable) suitable measuring chamber design. On the positive side, they have a high accuracy which is tied to the used microbalance. In comparison to volumetric setups, they need less sample material for measurements because the mass is monitored and not the change in pressure. Also, can the kinetics as well as the approach to equilibrium be studied. Wall sorption to the measuring cell does not play such a major

role because only the mass adsorbing to the sample and the floating parts are recorded. Additionally, if a suitable setup e.g. with a magnetic suspension balance is chosen high pressures (vacuum to 700 bar[112]) and temperatures (77 K to 673 K[113]) can be realized during measurement. In addtion, a gravimetric setup does allow to monitor a weight loss during activation and account for this for the experiment evaluation.[104]

2.3.3 Mixed setups

Sometimes also mixed experimental setups are used, e.g. a mixture of volumetric and gravimetric setups as described by Keller et al.[104]. They combine both techniques but limit the advantages of both techniques, e.g. a considerable amount of sample mass is needed for measurements, wall sorption may cause errors etc. Here these setups are not further addressed. One may have a look into the literature[104,114,115] for further information.

2.3.4 Volumetric vs. gravimetric

Overall volumetric setups are very simple in comparison to gravimetric setups which need a more sophisticated control especially if a magnetic suspension balance is used. On the other side volumetric setups have limitations towards low sample masses because only pressure changes can be monitored. These are depending on the size of the measuring cell and the adsorption capacity of the sample at the respective step, resulting in a detectable pressure change. With gravimetric setups, low sample masses are easier to handle because mass changes caused by adsorption are monitored which are usually more pronounced than pressure changes. Also, an already addressed disadvantage of volumetric setups is that uncertainty accumulates during the measurement which is caused by the setup design and how measurements are performed. For gravimetric setups, the uncertainty stays the same during the measuring process and is caused by the uncertainty of the used scale. So for this work, a gravimetric setup was chosen to do the experiments and to exploit the advantages of low sample masses, non-accumulating measurement uncertainties, being able to monitor the weight loss of the sample during activation and to allow kinetic studies of the adsorption process. Further details of the gravimetric setup used for the experimental part are given in chapter 4.1.

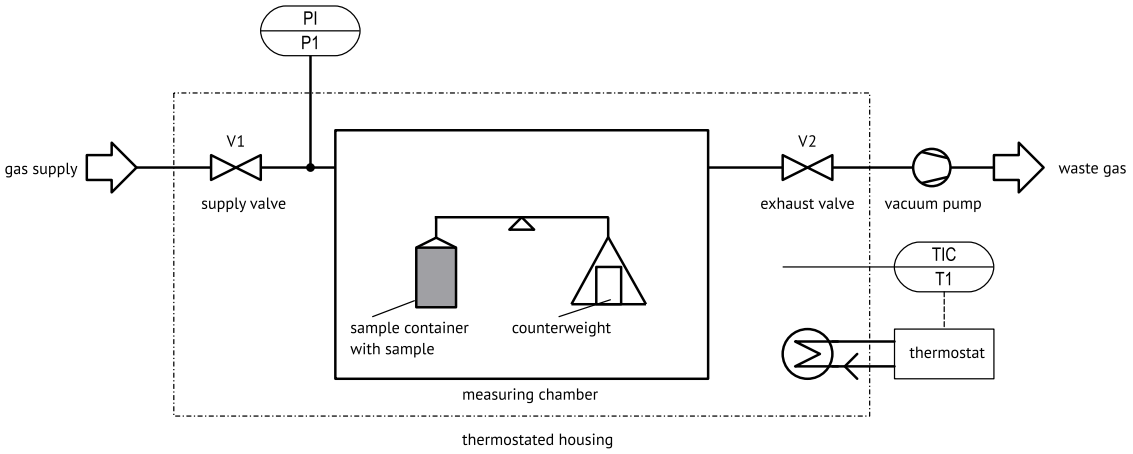

(a) beam balance

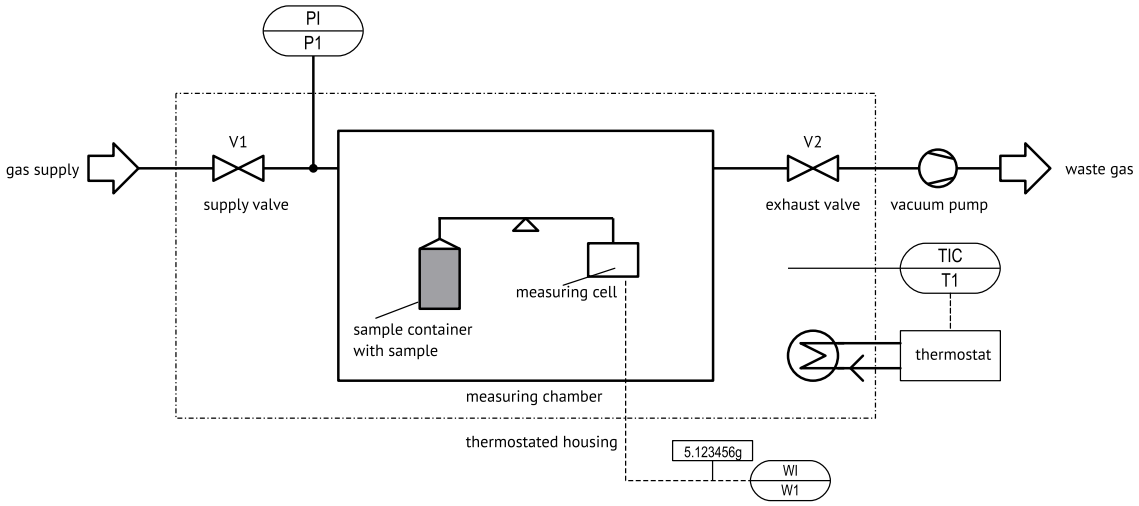

(b) beam balance with electromagnetic measuring cell

Figure 2.6.: Scheme of a) a beam balance and b) a beam balance with electromagnetic measuring cell

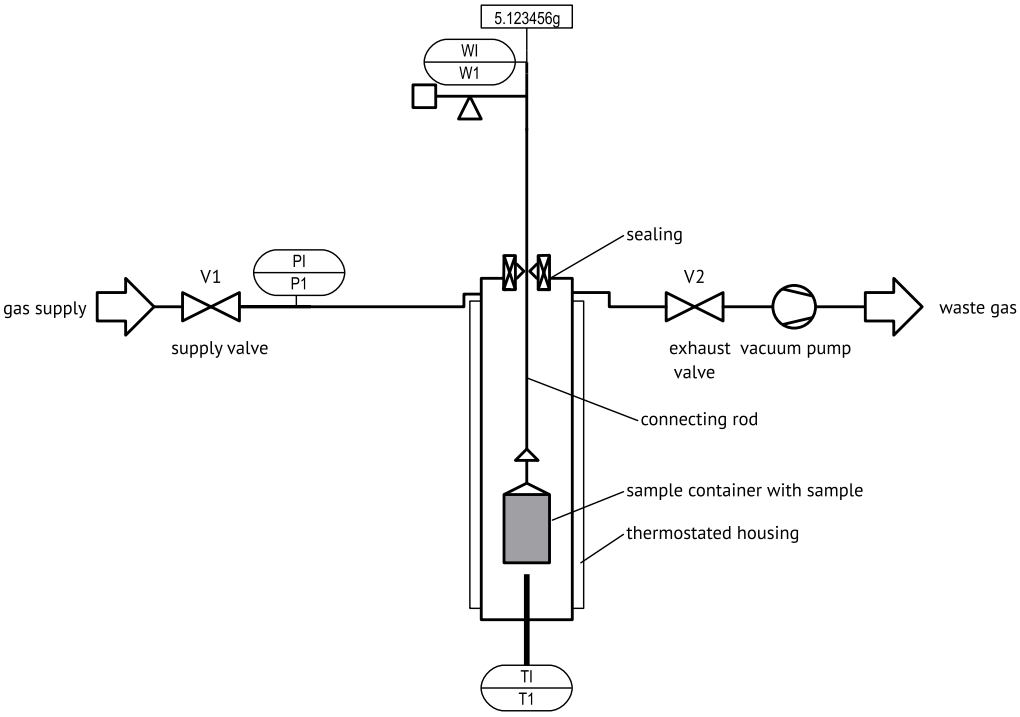

(a) mechanical sealed connection

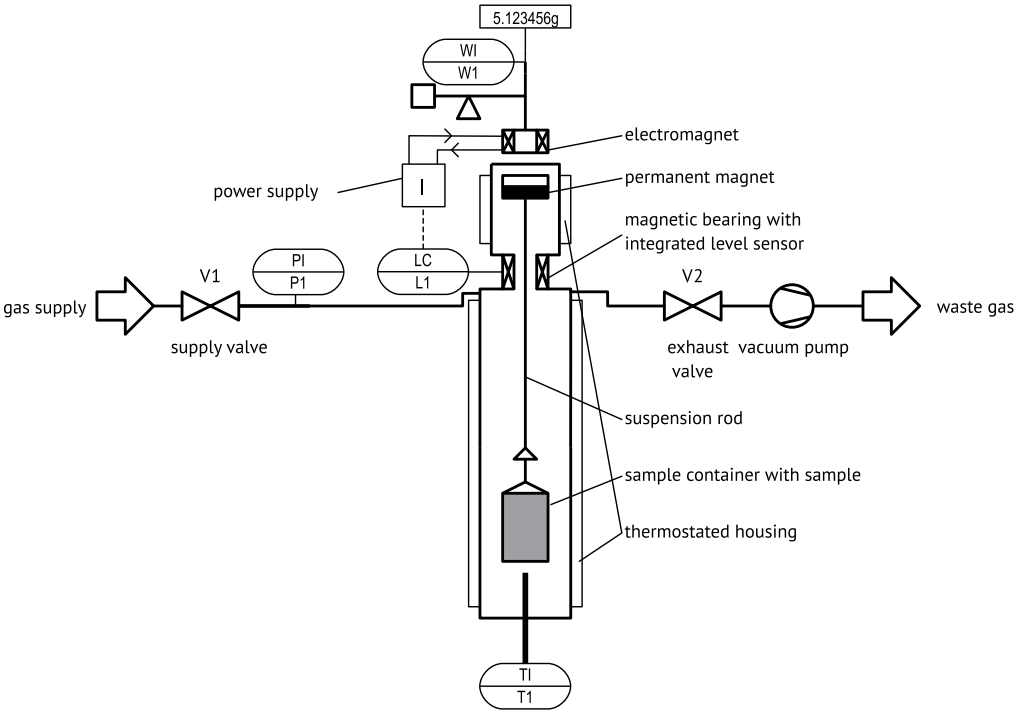

(b) closed measuring cell with magnetic coupling

Figure 2.7.: a) Scheme of a balance for adsorption experiments with a mechanical sealed connection to the measuring chamber and sample and b) scheme of a balance for adsorption experiments with a magnetic coupling to the measuring chamber and sample which allows high pressures and hazardous environments inside the closed measuring chamber

2.4 Determination of Adsorption isotherms

Adsorption isotherms can be determined by simulation and experiment. These isotherms can be used to benchmark adsorption materials for their usage in adsorption processes. Typical benchmarks are total uptake, selectivity for one component or component mixture, stability of the adsorbent regarding the conditions, e.g. temperature, pressure, humidity, acidity, etc.

The way adsorption isotherms are determined is described in more detail in chapter 3.3 for the performed simulations and in chapter 4.2 for the performed experiments.

2.5 CNTs

In the following sections, characteristics of CNTs are named such as production processes, geometrical structures, nomenclature for CNTs and electrical charging of CNTs.

2.5.1 Production of CNTs

CNTs can be synthesized via different production routes e.g. laser ablation[3,116–118], arc discharge method[4], chemical vapor deposition[119–121] (CVD), high-pressure carbon monoxide method[122] (HiPco), plasma enhanced CVD[5], aerosol assisted CVD[5]. Based on the production route and the conditions under which the CNTs are synthesized different CNTs can be produced such as single-walled CNTs (SWCNT), double-walled CNTs (DWCNT), multi-walled CNTs (MWCNT) or even other species such as carbon nanohorns (CNH). Also, can the shape of the CNTs be tailored such as diameter and length. Typical diameters range from a few Ångström to a few nanometer; typical lengths range from a few nanometer to millimeter or even in the centimeter range.

2.5.2 Geometrical structure

CNTs can appear in different structures as single-walled CNTs (SWCNT), double-walled CNT (DWCNT), multi-walled CNTs (MWCNT) and bundles of CNTs (compare to figure 2.8). Which type of CNTs are built is dependent on the production conditions. Then all types of CNTs can be arranged in different patterns (figure 2.9):

- without any pattern, as random packing
- in bundles, which can be packed randomly

- in defined structures, e.g. as vertically-aligned CNTs (VACNT)

Some theoretical considerations towards SWCNTs, MWCNTs and bundles of them were made by Peigney et al.[123]. They investigated the theoretical specific surface area of graphene, SWCNTs, MWCNTs and bundles of CNTs with the help of mathematical considerations.

A simple way to describe SWCNT is to name them after the number of elementary vectors n and m they consist of if the SWCNT is unwrapped into a graphene layer (figure 2.10). There exist three structures of CNTs, armchair, zigzag and chiral which are characterized by the number of elementary vectors of a graphene layer they hold. Armchair CNTs have the same amount of elementary vectors in both directions, they are (n/n) CNT or CNT(n/n). Zigzag CNT have only elementary vectors in one direction, they are (n/0) CNT or CNT(n/0). And chiral CNTs have elementary vectors in both directions, they are (n/m) CNT or CNT(n/m) ($n \neq m$). See figure 2.11 for an armchair, a zigzag and a chiral CNT. Additionally, can CNTs be capped on both ends, on only one end or completely uncapped. In this work, only uncapped CNTs were considered in the conducted simulations. Some theoretical consideration of half-capped CNTs were made by Asimov[124]. A nice description of a chiral CNT is given by Dekker[125] alongside with some electrical considerations concerning the conductance of CNTs.

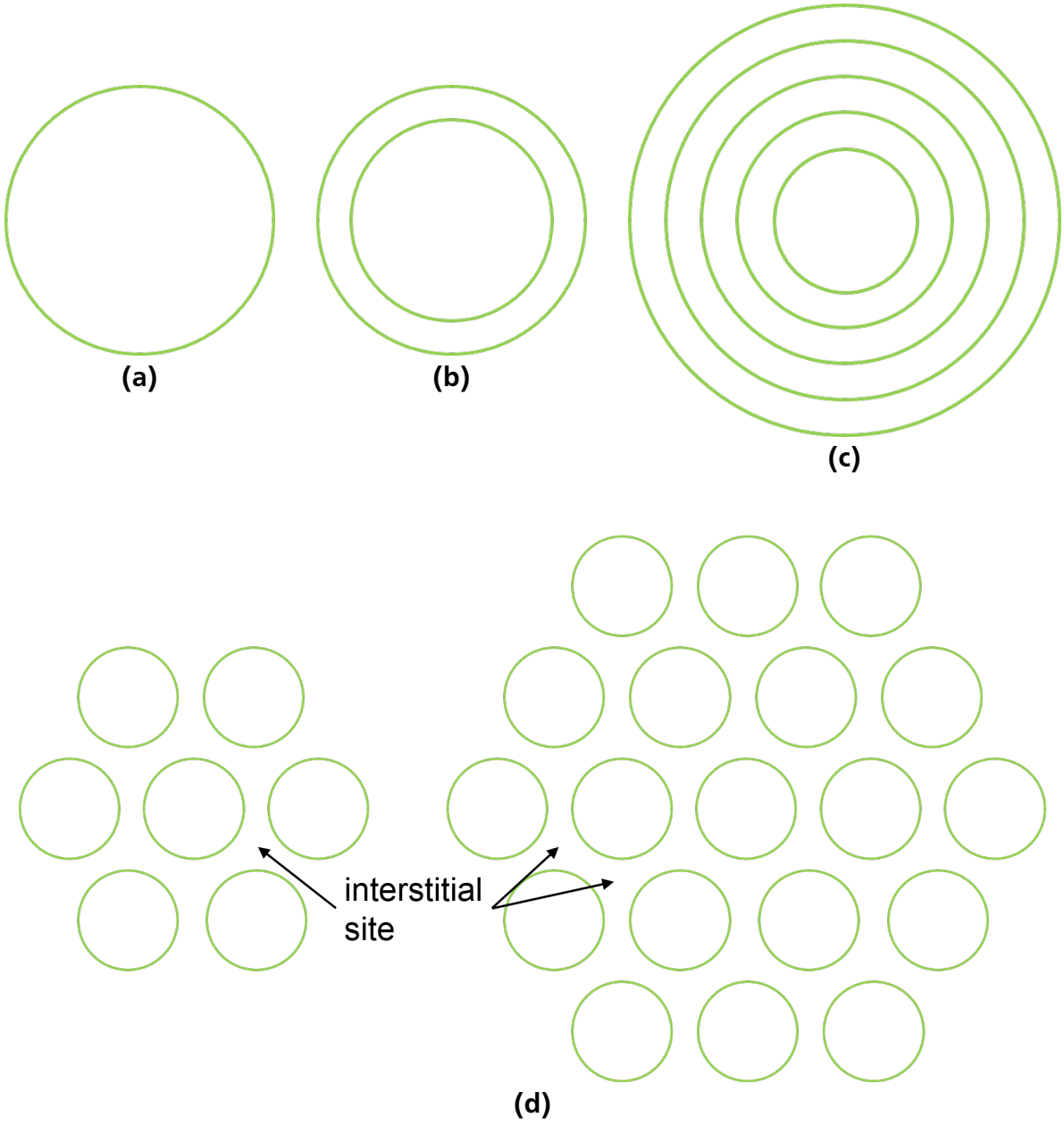

Figure 2.8.: Schematic of a) a single-walled CNT (SWCNT), b) double-walled CNT, c) multi-walled CNT (MWCNT) and d) bundles of CNTs (here two exemplary SWCNT bundles are shown and exemplary interstitial sites between the CNTs are indicated)

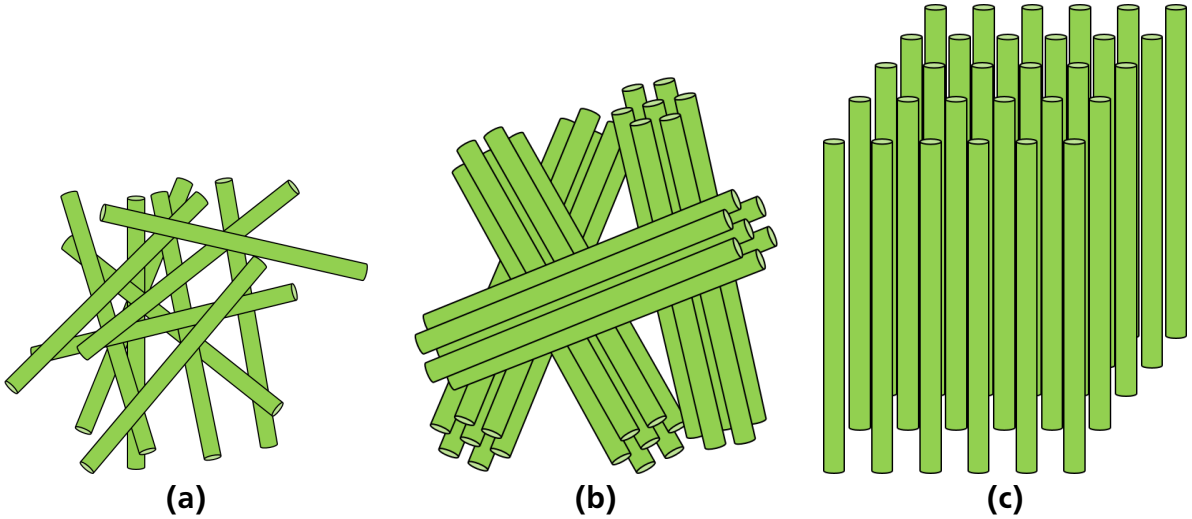

Figure 2.9.: Schematic of different CNT packings: a) random packing of single CNTs, b) random packing of CNT bundles and c) packing in defined and orderer structure as a vertically-aligned CNTs (VACNT)

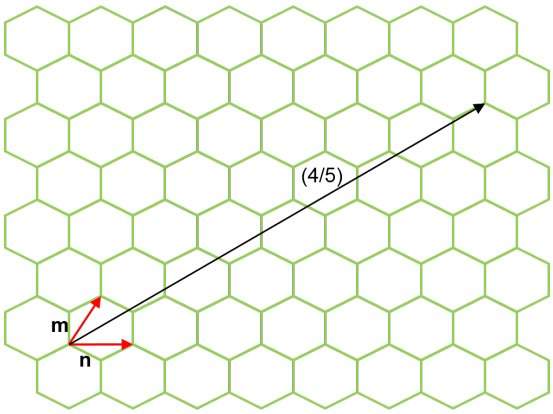

Figure 2.10.: Graphene with elementary vectors n and m which describe if an armchair, zigzag or chiral (SW)CNT is created, exemplary the vector for chiral SWCNT(4/5) is shown

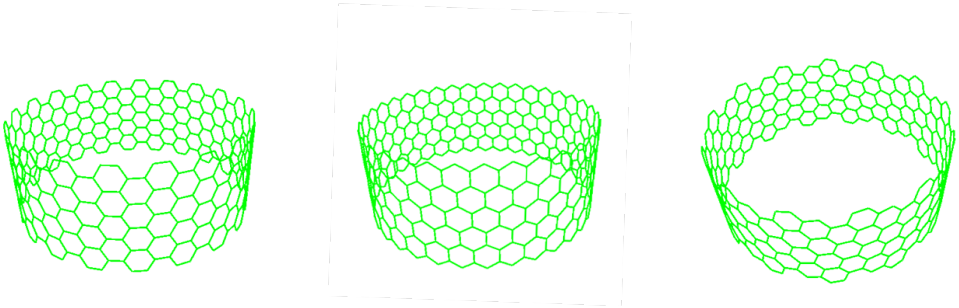

(a) SWCNT(20/20) **(b)** SWCNT(35/0) **(c)** SWCNT(26/13)

Figure 2.11.: a) Armchair, b) zigzag and c) chiral SWCNT (images generated from coordinates with gOpenMol[126])

2.5.3 Charging of CNTs

Applying charges to CNTs is possible. This is shown by various works which exploit CNTs as super-capacitors [127–135], electrodes [136,137] or fibers [138]. The specific capacity which the CNTs in the different applications can carry varies from 20 Fg^{-1} to 120 Fg^{-1} according to literature values. [127–138] Assuming that the voltage that can be applied to the CNTs is 1 V this translates to an elemental charge per carbon atom of a CNT of approximately 0.002 e to 0.015 e. In theory charges in this range should be applicable per carbon atom. So charging is also investigated in this work and its impact on the adsorption behavior of SO_2 is shown. However, preliminary studies conducted by Reinhardt [139] deliver specific charges up to approximately 50 nFg^{-1}. In her work she measured the charge of industrial grade CNTs under dry conditions in a plate capacitor without any electrolyte. This would only allow very low elementary charges per carbon atom. But this has to be investigated further.

2.6 Data on (used) chemical media

In this section, all major chemical substances used in this work are described with their physical and safety properties and the way they are used in this work. First, all adsorptive species are named, then investigated adsorbents are described. In the last section, auxiliary compounds such as gas washing agents or adsorption agents e.g. activated carbon Oxorbon K20 J are presented.

2.6.1 Adsorptive

As adsorptives helium (He), nitrogen (N_2), carbon dioxide (CO_2) and sulfur dioxide (SO_2) are used. Helium takes a special role as adsorptive as it is considered to be only very weakly adsorbing and therefore can be used to correct for buoyancy effects. Buoyancy arises from the gas atmosphere during measurement onto the probe material, the suspended sample container and the suspension. Especially at enhanced pressures, this needs to be considered and corrected. With N_2, CO_2 and SO_2, adsorption on different materials (described in section 2.6.2) is studied at different temperatures and pressure ranges from vacuum till pressures up to 80 bar.

Helium He

Helium is a noble gas and non-reactive. Under ambient conditions, air usually carries a helium content of only 5.2 ppm[140]. However, it should be avoided to inhale elevated helium concentrations as this can lead to suffocation. Under normal experimental conditions, only small quantities of helium are released, leading to non-noticeable concentration increases in the lab atmosphere.

All major physical properties of He are listed in table 2.1. For all experiments, helium distributed from Air Liquide was used. Further details about the gas purity and trace compounds are listed in table 2.2.

As already stated helium adsorption on any material is considered to be very weak, and therefore helium is often considered to be non-adsorbing especially at larger pore diameters[65,104,141]. In small pores helium may be adsorbing very weakly which is shown in the works of Gumma et al.[64] and Brandani et al.[65] and may cover some of the adsorption sites. In practice, this very weak adsorption does not alter the adsorbability for other gases significantly and does not play a major role regarding the achievable sample loadings in the experiments presented in this work. This leads to the assumption that helium measurements may be taken to do buoyancy correction and to estimate the sample volume. The procedure how this is done is described in detail in 4.2.2.

Nitrogen N_2

N_2 is a colorless and odorless gas. In nature, it is one of the major compounds in the air with a content of 78.08 %. Under ambient conditions it is considered as an inert gas which is non-hazardous and non-reactive. If the concentration inhaled by living beings is significantly enhanced compared to air, it may lead to suffocation. Under ambient conditions, N_2 is a supercritical fluid which does not influence the experiments done, and no precautions need to be taken for it because only small quantities are released during experiments.

All major physical properties of N_2 are listed in table 2.1. For all experiments nitrogen purchased from Air Liquide was used. Further details about the gas purity and trace compounds are listed in table 2.2.

Carbon dioxide CO_2

Carbon dioxide is also a colorless and odorless gas. In air CO_2 is present up to 0.04 %[142]. Carbon dioxide is relatively to air denser and can accumulate in cavities and close to the floor. Exposure to concentrations over 10 % over several minutes can

lead to suffocation[143,144]. Symptoms which can occur at different concentration levels from standard ambient conditions up to 8 % are summarized by Häggström[145]. The exposure limits for CO_2 given by the EU[146,147] and Germany[148] are set to 5 000 ppm and may only be exceeded by a factor of 2[148] for short periods. Its faint acid taste can be attributed to the formation of carbonic acid with water or saliva.

For all experiments, carbon dioxide, which is liquefied under pressure, purchased from Air Liquide was used. Further details about the gas purity and trace compounds are listed in table 2.2. The vapor pressure curve of CO_2 is shown in figure 2.12. All major physical properties of CO_2 are listed in table 2.1.

The liquefied CO_2 at approximately 58 bar is introduced from a dip-tube cylinder to a syringe pump to increase the pressure up to 100 bar to make adsorption experiments also at high pressures and supercritical conditions possible.

Sulfur dioxide SO_2

Sulfur dioxide is as all named gases a colorless gas. In contrast to the other gases, it has a characteristic, irritating, pungent smell and an acid taste[149,150] even at very low concentrations (0.1-0.47 ppm[149,150]). SO_2 can arise from natural sources such as volcanic activities. In industry, SO_2 is mostly produced by the roasting of pyrite or the combustion of elementary sulfur to produce in a further step the bulk chemical sulfuric acid[151]. Sulfur dioxide can be easily liquefied under ambient conditions. The vapor pressure curve of SO_2 is given in figure 2.12.

SO_2 should not be released to the environment, because of its harm to living beings and its corrosive behavior if in contact with water or the humidity from the air. Concentrations above several 100 ppm can already cause a severe toxic reaction in the human body such as pulmonary oedema[152]. Exposure limits are set in Germany to 1 ppm with no top limiting exceedance permitted for short time exposure.[148] The actions which are taken to prevent a release of SO_2 to the environment are described in more detail in chapter 4.1.

For all experiments, SO_2 liquefied under pressure purchased from Air Liquide was used. Further details about the gas purity and trace compounds are listed in table 2.2. To allow experiments at elevated pressure gaseous SO_2 is introduced into a syringe pump ISCO500D from Teledyne Isco which is cooled to temperatures well below 0 °C to condense the gas and compress it in a next step till pressures up to 40 bar are reached. All major physical properties of SO_2 are listed in table 2.1.

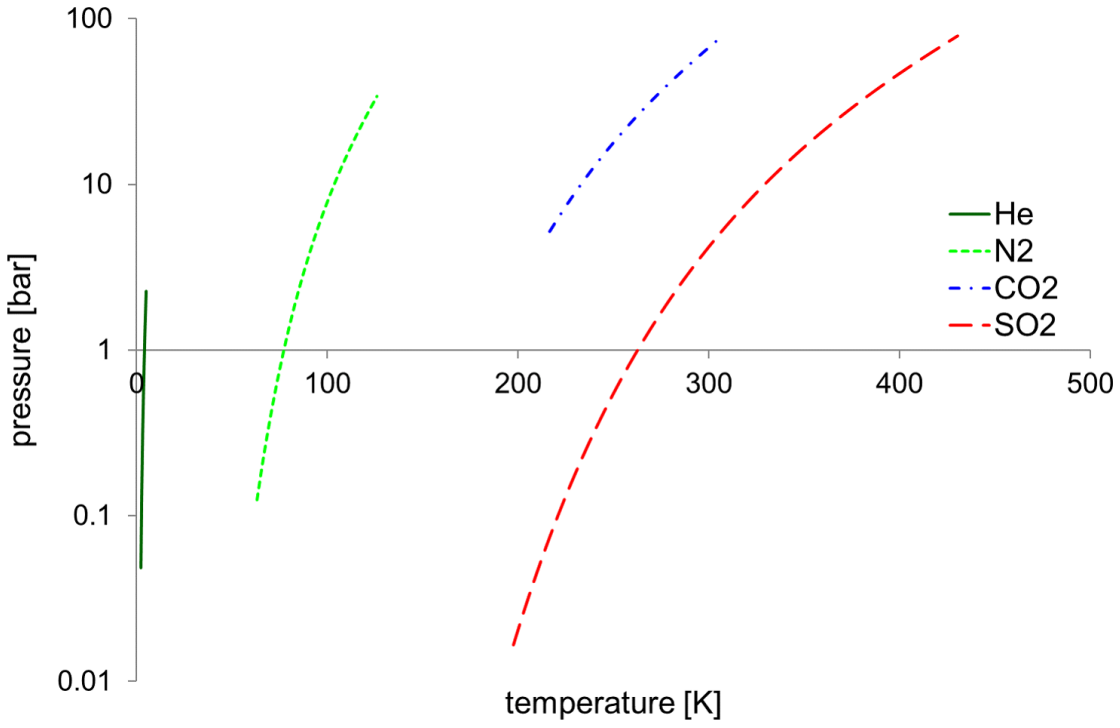

(a)

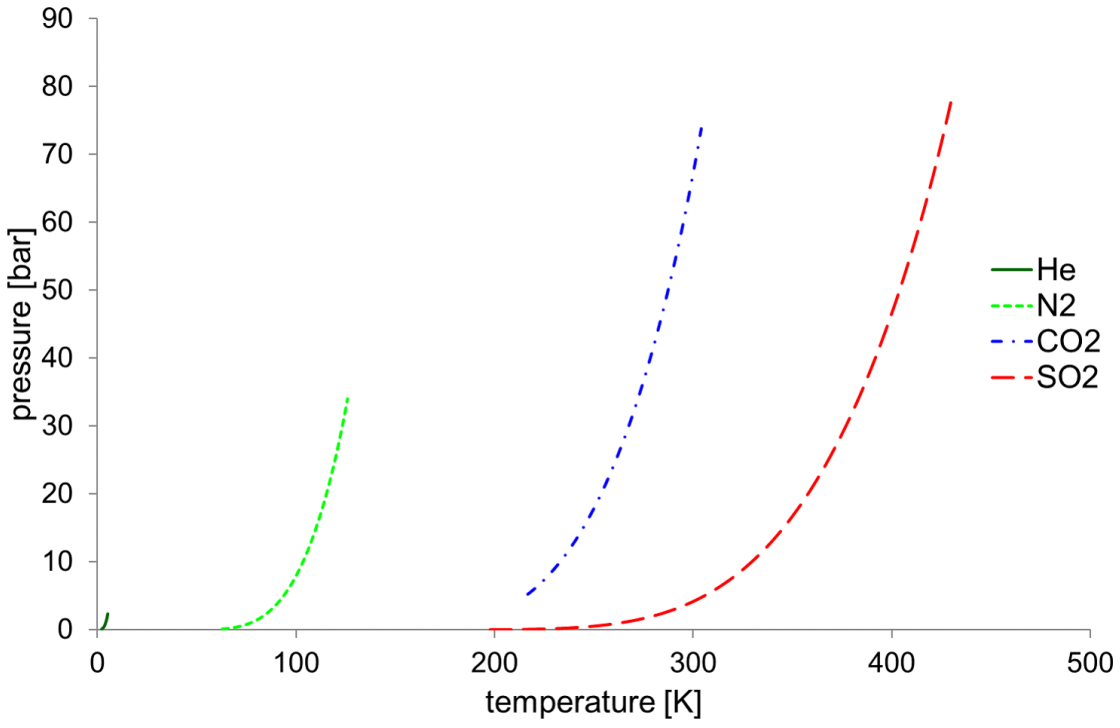

(b)

Figure 2.12.: Vapor pressure curve of helium He, nitrogen N_2, carbon dioxide CO_2 and sulfur dioxide SO_2 from the triple point to the critical point in (a) semilogarithmic and (b) normal scaling

Table 2.1.: Material properties of adsorptives

description	symbol	unit	CO_2	ref.	SO_2	ref.	N_2	ref.	He	ref.
Material descirption:										
Chemical Abstract Service number	CAS-#	[-]	124-38-9		7446-09-5		7727-37-9		7440-59-7	
European Community number	EC-#	[-]	204-696-9		231-195-2		231-738-9		231-168-5	
PubChem CID		[-]	280	[149]	1119	[149]	947	[149]	23987	[149]
Physical form at 20 °C and 1.013 bar		[-]	vapor	[153]	vapor	[153,154]	vapor	[153,155]	vapor	[153,156]
Appearance, description		[-]	colorless	[149,157]	colorless	[149,154]	colorless	[149,155]	colorless	[149,156]
Odor		[-]	odorless	[149,157]	characeristic, irritating, pungent smell	[149,154]	odorless	[149,155]	odorless	[149,156]
Threshold limit for sense of smell		[ppm]	-		0.1-0.47	[149]	-		-	
Taste		[-]	faint acid taste	[149]	acid taste	[149]	tasteless	[149]	tasteless	[149]
General properties:										
Molecular weight	M	[gmol^{-1}]	44.010	[149,153,158]	64.065	[149,153,158]	28.013	[149,153,158]	4.003	[149,153,158]
Normal boiling point	T_b	[K]	194.7	[158]	262.84-263.15	[149,153,158]	77.355	[153,158]	4.230	[153,158]
Normal fusion point	T_f	[K]	216.58	[158]	200.75	[153,158]	63.15	[149,153,158]	0.95-1.76	[149,158]
Triple point temperature	T_t	[K]	216.58	[153]	197.64	[153]	63.14	[153]	-	[149]
Triple point pressure	p_t	[bar]	5.185	[153]	0.0167	[153]	0.1252	[153]	-	[149]
Critical temperature	T_c	[K]	304.1282-304.19	[153,158]	430.64-430.75	[149,153]	126.192	[153]	5.1953	[153]
Critical pressure	p_c	[bar]	73.773-73.82	[153,158]	78.84	[149,153]	33.958	[153]	2.2746	[153]
Critical density	ρ_c	[molL^{-1}]	10.6249	[153]	8.195	[153]	11.1839	[153]	17.399	[153]
Water solubility at 20 °C and 1 bar		[mgL^{-1}]	2000	[157,158]	78097-107000	[149,158]	17.28	[158]	1.4-2.5	[149,156,158]
Relative density, liquid (Water = 1)		[-]	0.82	[157]	1.5	[154]				
Dipole moment		[Debye]	0.00	[158]	1.63	[153,158]	0.00	[158]	0.00	[153,158]
Acentric factor	ω	[-]	0.228	[158]	0.245-0.2557	[153,158]	0.0372-0.04	[153,158]	-0.382- -0.39	[153,158]
Decomposition temperature	$T_{\text{decomp.}}$	[K]	2273	[149]						
Viscosity at 20 °C and 1 bar	η	[μPa s]	14.674-15.05	[153,158]	12.897	[158]	17.544-17.573	[153,158]	19.611-19.857	[153,158]
Volatility:										
Vapor pressure at 20 °C	p_{vp}	[bar]	57.089	[153]	3.2915	[153]	-	[155,158]	-	[156,158]
Molar density at 20 °C and 1 bar	ρ	[molL^{-1}]	0.041266	[153]	0.041809	[153]	0.041058	[153]	0.041030	[153]
Relative density vapor (air = 1)		[-]	1.52	[157]	2.3	[154]			0.14	[149,156]

Table 2.1.: Material properties of adsorptives continued

description	symbol	unit	CO_2	ref.	SO_2	ref.	N_2	ref.	He	ref.
Exposure Limits:										
Indicative Limit Value (EU), 8h	ILV(EU)	[mgm^{-3}]	9000	[146,147]					-	
Indicative Limit Value (EU), 8h	ILV(EU)	[ppm]	5000	[146,147]					-	
Occupational limit value 8h, Germany	OLV	[mgm^{-3}]	9100	[148]	2.5	[148,159]	-		-	
Occupational limit value 8h, Germany	OLV	[ppm]	5000	[148]	1	[148,159]	-		-	
Top limiting exceedance factor OLV		[-]	2	[148]	1	[148,159]	-		-	
Thermodynamic properties:										
Enthalpy of fusion at T_f	$\Delta_{fus}H$	[$kJmol^{-1}$]								
Enthalpy of vaporization at T_b	$\Delta_{vap}H$	[$kJmol^{-1}$]	27.03	[158]	22.92-25.72	[149,153,158]	5.57-6.1	[149,153,158]	0.08	[158]
Enthalpy of sublimation	$\Delta_{sub}H$	[$kJmol^{-1}$]	25.2-27.2	[153]						
Standard enthalpy of formation	$\Delta_f H°$	[$kJmol^{-1}$]	-393.50	[153,158]	-296.80	[158]	0		0	
Standard entropy of formation	$\Delta_f S°$	[$Jmol^{-1}\,K^{-1}$]	3.020	[158]	11.070	[158]	0		0	
Standard Gibbs free energy of formation	$\Delta_f G°$	[$kJmol^{-1}$]	-394.40	[158]	-300.10	[158]	0		0	
Entropy at 298 K	S^{298K}	[$Jmol^{-1}\,K^{-1}$]	213.69-213.79	[153,158]	248.11	[158]	191.5	[158]	126.04	[158]

Table 2.2.: Purchased gases from Air liquide, their purities and trace compounds

compound	trademark	purity		impurities	
		percentage	abbreviated	compound	value
He	Alphagaz 1	99.999 %	5.0	H_2O	≤ 2 ppm
				O_2	≤ 2 ppm
				HC[a]	≤ 2 ppm
				N_2	≤ 5 ppm
N_2	Alphagaz 1	99.999 %	5.0	H_2O	≤ 3 ppm
				O_2	≤ 2 ppm
				HC[a]	≤ 0.2 ppm
CO_2		99.7 %	2.7	H_2O	≤ 200 ppm
CO_2		99.995 %	4.5	H_2O	≤ 5 ppm
				O_2	≤ 25 ppm
				HC[a]	≤ 1 ppm
				N_2	≤ 25 ppm
				CO	≤ 1 ppm
SO_2		99.98 wt−%	3.8	H_2O	≤ 10 ppmw
				H_2SO_4	≤ 50 ppmw

[a] HC = hydrocarbons

2.6.2 Adsorbents

In this work, different adsorbents are utilized to study their behavior in combination with different adsorptives. Some adsorbents are needed as auxiliary material such as the activated carbon Oxorbon K 20 J and zeolite 13X.

Adsorbents which are studied are activated carbons such as Desorex ED 43 and Norit R1 Extra. Also, different CNTs are tested such as commercial CNTs from Nanolab in the purities industrial grade and scientific grade and CNTs which are synthesized in the Schneider group of TU Darmstadt. A more detailed description is given in the following paragraphs.

2.6.2.1 Activated carbon

Activated carbons are one of the most common adsorbents which are widely used, e.g. in industrial, medical and household applications. In this work, the activated carbons Desorex ED43 and Norit R1 Extra are studied. Desorex ED43 was used as one of the first samples to test the experimental setup if adsorption isotherms could be obtained. The used Desorex ED43 sample was available at the institute and measured only with carbon dioxide.

Norit R1 Extra was measured in sulfur dioxide atmospheres close to room temperature and is one standard sample which is often measured in literature in nitrogen or carbon dioxide atmospheres as a reference.

2.6.2.2 Carbon nanotubes (CNTs)

As CNTs different samples have been used for measurement in nitrogen, carbon dioxide and sulfur dioxide atmospheres. Three sample types were bought in from NanoLab Inc. from Waltham Massachusetts namely industrial grade MWCNTs (product description: IG-CNT), scientific grade MWCNTs (product description: PD15L5-20) and scientific grade SWCNTs (product description: D1.5L1-5-S). Additionally, a sample VACNTs provided from the Schneider group of the Eduard-Zintl-Institute of the Chemistry Department of TU Darmstadt was tested in the experimental setup in sulfur dioxide atmospheres. For the scientific grade MWCNTs and SWCNTs from NanoLab, TEM and SEM images were provided by the Schneider group and are shown in figures 2.13 and 2.14. The TEM and SEM images of VACNTs were also provided by the Schneider group and are presented in figure 2.15[160,161]. The TEM images of the MWCNTs show that

multi-walled CNTs are present in the sample and the expected diameters are met. The SWCNT TEM images give a hint that also MWCNTs are present in the sample.

All measured CNTs are summarized in table 2.3.

Table 2.3.: Measured CNT types, diameters, lengths, product description, purity and supplier

CNT type	diameter [nm]	length [μm]	product description	purity [wt%]	supplier	ref.
MWCNT	10-30	5-20	IG-CNT	>85	NanoLab[a]	[162]
MWCNT	15±5	5-20	PD15L5-20	>95	NanoLab[b]	[162]
SWCNT	ca. 1.5	1-5	D1.5L1-5-S	>95	NanoLab[c]	[162]
VACNT	5-8[d]	1000-5000			TU Darmstadt[e]	[120,121]

[a] LOT 20120512, [b] LOT 20130820, [c] LOT 20121217, [d] intertube distance ≈ 15 nm,
[e] Schneider group, chemistry department, TU Darmstadt

2.6.2.3 Zeolite 13X

The zeolite 13X was supplied by Alfa Aesar. 3 mm-5 mm beads of the molecular sieve 13X were used to trap vacuum oil between the vacuum pump and the inlet of the gas dosing system and to prevent vapor of vacuum pump oil to enter the experimental setup and the sample chamber. It was also used to benchmark the experimental setup.

2.6.3 Other used or relevant chemicals

Furthermore, there are some chemicals which have been used to help perform the adsorption experiments. Especially experiments with sulfur dioxide needed a post-treatment of the SO_2 after leaving the manual gas dosing system. This is why it was washed by the gas washing agents hydrogen peroxide (H_2O_2), and sodium hydroxide (NaOH) in a two-stage gas washing unit followed by an absorbing column with impregnated activated carbon Oxorbon K 20 J from Donau Carbon. The gas scrubbing line is explained in more detail in chapter 4.1. H_2O_2 was purchased from Carl Roth as 35 wt−% bleach, NaOH as a solid in pellet form. Both were in a next step diluted to the desired concentrations of ≈ 6 wt−% for H_2O_2 and 0.5 molL^{-1} for NaOH. To the later bromothymol blue indicator was added.

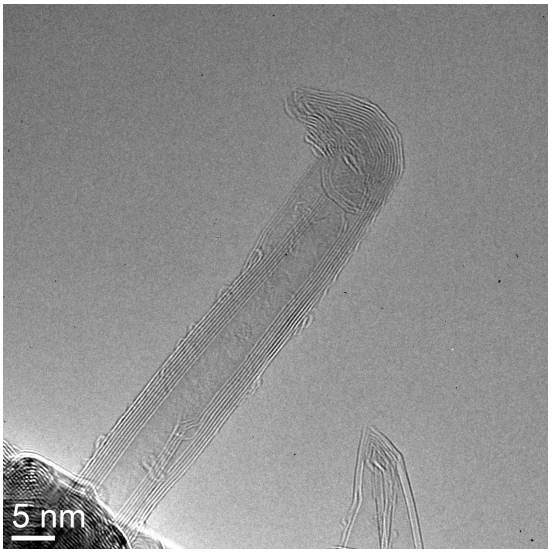

(a) Scientific grade MWCNT PD15L5-20

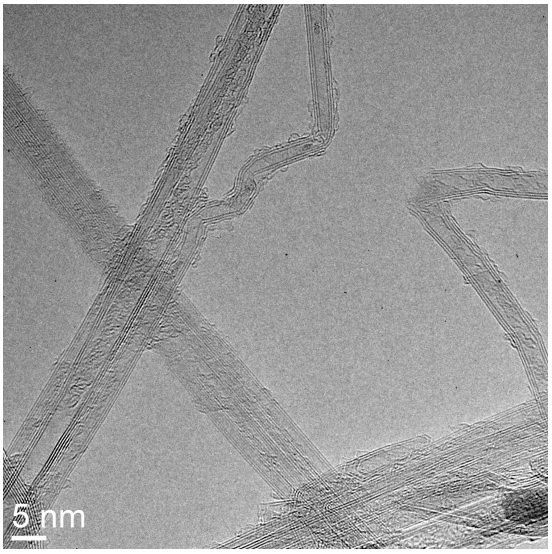

(b) Scientific grade SWCNT D1.5L1-5-S

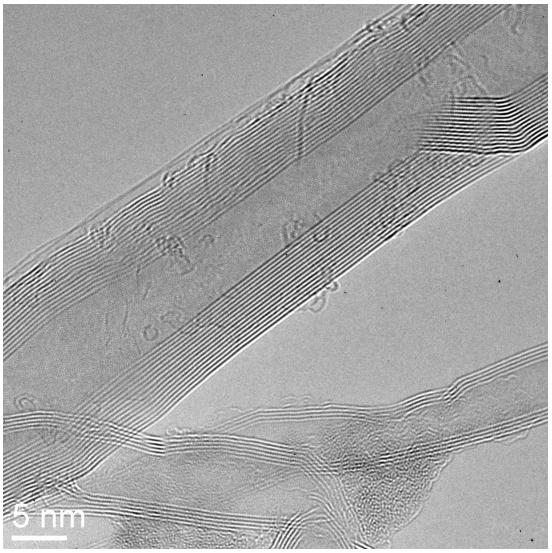

(c) Scientific grade MWCNT PD15L5-20

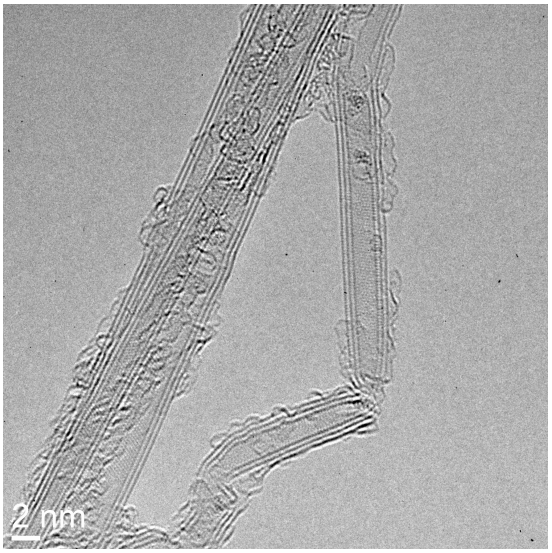

(d) Scientific grade SWCNT D1.5L1-5-S

Figure 2.13.: TEM images of CNTs from NanoLab a) MWCNT TEM image, b) SWCNT TEM image, c) MWCNT TEM image and d) SWCNT TEM image. The TEM images were provided by the Schneider group, Eduard-Zintl-Institute, Chemistry Department, TU Darmstadt.[161] (For the TEM images special acknowledgments to Dr. Jörg Engstler, Eduard-Zintl-Institute, Chemistry Department, TU Darmstadt)

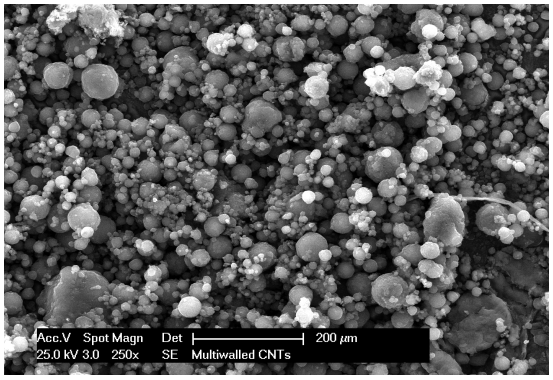

(a) Scientific grade MWCNT PD15L5-20 250x

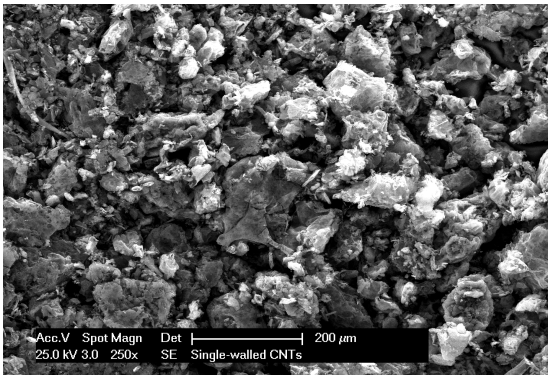

(b) Scientific grade SWCNT D1.5L1-5-S 250x

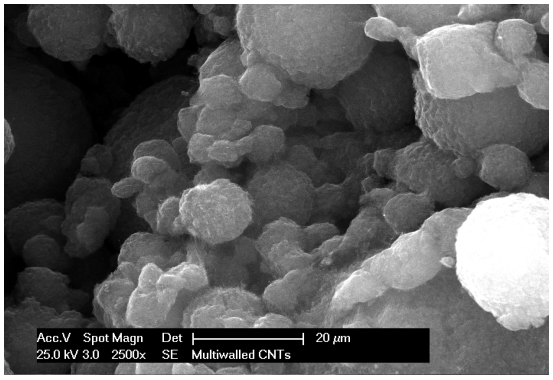

(c) Scientific grade MWCNT PD15L5-20 2500x

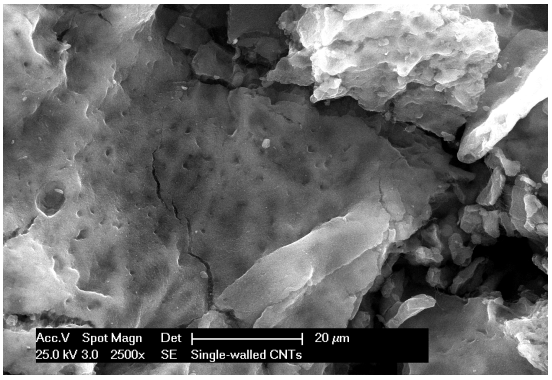

(d) Scientific grade SWCNT D1.5L1-5-S 2500x

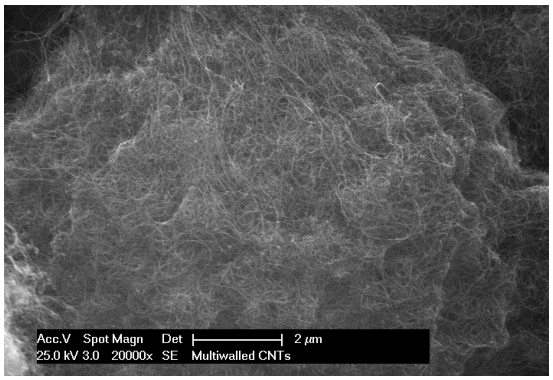

(e) Scientific grade MWCNT PD15L5-20 20000x

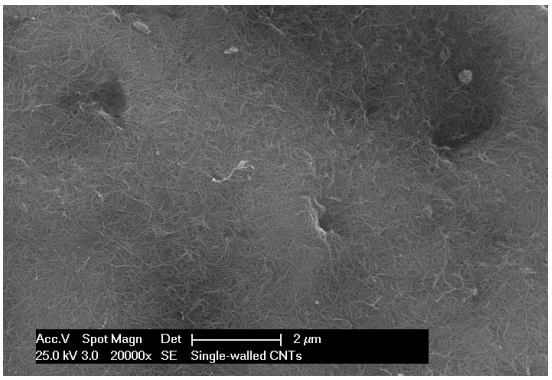

(f) Scientific grade SWCNT D1.5L1-5-S 20000x

Figure 2.14.: SEM images of CNTs from NanoLab a), c) and e) MWCNT SEM image, b), d) and f) SWCNT SEM image. The SEM images were provided by the Schneider group, chemistry department, TU Darmstadt.[161]

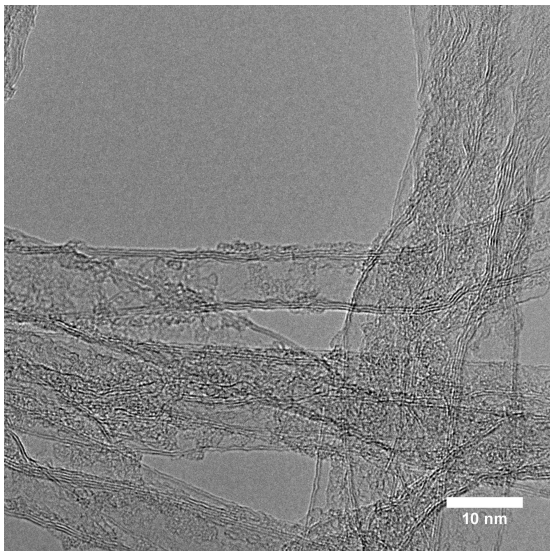

(a) TEM image of VACNT

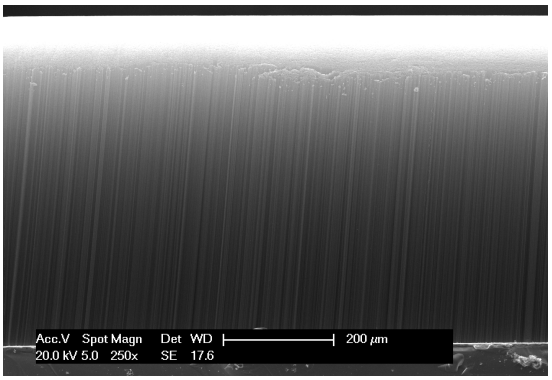

(b) SEM image of VACNT 250x

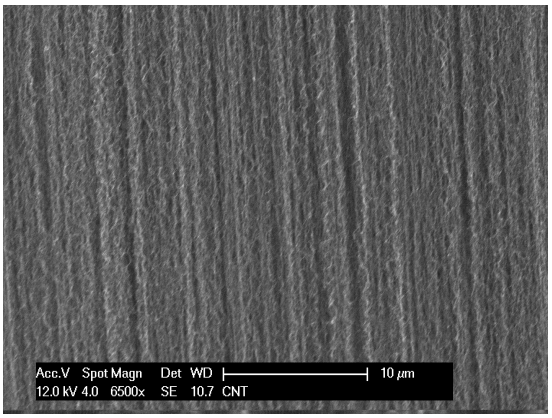

(c) SEM image of VACNT 6500x

Figure 2.15.: TEM and SEM images of VACNTs from Schneider group, chemistry department, TU Darmstadt a) VACNT TEM image (special acknowledgments to Dr. Jörg Engstler, chemistry department, TU Darmstadt), b) VACNT SEM image[160]

3 Simulation

In this work, simulations have been carried out with the simulation code DL Poly 4.2[163] or DL Poly 4.5[95]. The code of DL Poly 4.2 was modified to take two thermostats and flexible CNTs into account. The details for this are described in a previous work[2]. There it also was shown that flexible CNTs give the same results as rigid CNTs at a higher computational demand. Therefore in this work, only rigid CNTs are regarded. For graphene also only a rigid model was applied for the same reasons. Most of the simulations were carried out with the standard code of DL Poly 4.5. DL Poly allowed studying the adsorption behavior by inspecting the trajectories of the simulated molecules. As simulation ensemble in all cases, an ensemble with a constant number of molecules N, constant volume V and constant temperature T is chosen, also known as NVT ensemble. The used NVT ensemble incorporated a Nosé-Hoover type thermostat[164] to control the temperature. For all simulated cases a relaxation time of 0.1 ps is used for this type of thermostat. The time step for the simulations was 2 fs for cases with rigid CNTs or graphene.

3.1 Models for CNTs and graphene

As already mentioned, only rigid models were studied in this work. Some of the simulations were carried out with charged carbon materials. All further details concerning the simulation are described in the following sections

3.1.1 Rigid CNTs and graphene

The rigid CNT and rigid graphene model could easily be implemented into the DL Poly code, to take this into account frozen carbon atoms were used. These atoms do not change position during a simulation run and are fixed to their given spatial position. All forces acting on these atoms are truncated. Forces arising from these atoms are however simulated. Intramolecular interactions for the C atoms in the rigid model were neglected. The force field arising from the C atoms was modeled by a Lennard Jones (LJ) potential with the parameters $\sigma_{C-C} = 0.34\,\text{nm}$ and $\varepsilon_{C-C} = 0.36\,\text{kJmol}^{-1}$, obtained from AMBER force field[165].

3.1.2 Charging of CNTs and graphene

To charge the CNTs and graphene a partial charge was assigned to each carbon atom. This could be done easily in DL Poly by setting the respective value in the FIELD file for each atom or atom type. The partial charge is measured in elementary charges e. Typical charges applied to charge the carbon atoms were below 0.05 e.

3.2 Models for gases

For the simulated gases, rigid models have been applied, and all intramolecular interactions were neglected. This was done to keep the computational time lower. The used models did reproduce the bulk behavior of the gases reasonable as it was shown by Sokolic et al.[166,167], Arora and Sandler[168].

All geometrical and LJ parameters are summarized in the appendix A.1.

3.2.1 Sulfur dioxide

Sulfur dioxide was modeled as a three-sited rigid model. The S—O bond had a length of 143.4 pm and a fixed angle between the two S—O bonds of 119.5°[166]. A model of the SO_2 geometry can be seen in figure 3.1. Long range interactions of SO_2 were modeled by LJ potentials and coulombic potentials. The LJ potential parameters for S—S and O—O interactions are: $\sigma_{S-S} = 0.360\,50\,\text{nm}$, $\varepsilon_{S-S} = 1.229\,9\,\text{kJmol}^{-1}$, $\sigma_{O-O} = 0.299\,80\,\text{nm}$, $\varepsilon_{O-O} = 0.487\,0\,\text{kJmol}^{-1}$.

The dipole nature of SO_2 was considered by applying partial charges to the sulfur and oxygen atoms. The sulfur atom carried a partial charge of 0.46 e, and each oxygen atom carried a charge of −0.23 e.

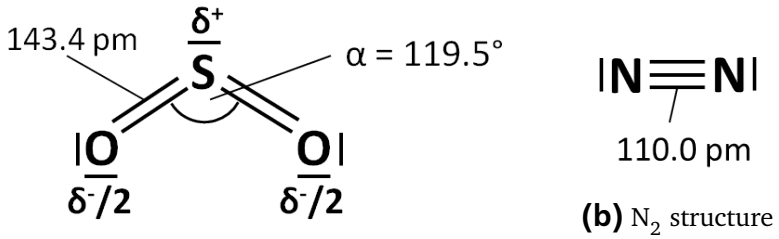

(a) SO_2 structure **(b)** N_2 structure

Figure 3.1.: Modeled geometry of a) a SO_2 molecule and b) a N_2 molecule

3.2.2 Nitrogen

Nitrogen was modeled with a two-sited rigid model. The N—N bond length was modeled to be 110 pm[168]. The geometry of the molecule is presented in figure 3.1. Its LJ potential parameters for the N—N interaction are $\sigma_{N-N} = 0.332\,00$ nm, $\varepsilon_{N-N} = 0.302\,6$ kJmol^{-1}.

3.2.3 Performance of molecular dynamics adsorption experiments

For the acquisition of data from molecular dynamics simulation a SWCNT or graphene and a fixed number of SO_2 and/ or N_2 molecules were placed into a simulation box with a fixed volume and the temperature was set to the desired value. Then the simulation was started till the equilibrium of the system was met. Meaning that adsorption had taken place and that the system did not change significantly. Then the adsorbed amount at the CNT or graphene and the bulk pressure was evaluated. With this, one data point of the adsorption isotherm is simulated. The other data points are achieved in the same manner by varying the number of gas molecules in the simulation box.

3.3 Evaluation of results

Results of the molecular dynamics simulations are trajectories and position of the molecules. Also, the velocity of each simulated site and all forces acting on it are saved and accessible for post-processing. In addition, accumulative data on the whole system is available such as the temperature of the whole system, total energy etc. Typically the trajectory data is saved every 2000 time steps which is equivalent to 4 ps (for the rigid case), in some cases the data is saved every 500 time steps which is equivalent to 1 ps (for the rigid case). From this data, most of the post-processing is done such as evaluation of the adsorbed amount, local density, (local) temperature, local pressure, selectivity of one compound, etc.

How the data is evaluated and processed is described in the following sections.

3.3.1 Post-processing of trajectory data

The trajectory data which is saved in the HISTORY file of DL Poly is post-processed in a first step by a fortran77 code which counts all molecules in a certain region of the simulation cell and calculates the density in this region. From the saved velocities of

each site, the molecular velocity v_i is estimated. With this information the temperature is calculated and averaged in each compartment by the following equation:

$$T = \frac{2}{3 \cdot k_B} \cdot \frac{1}{2} \cdot \Sigma_{i=1}^{N} m_i \cdot v_i^2 \tag{3.1}$$

k_B is the Boltzmann constant, m_i the mass of the respective molecule and N is the molecule count in the respective compartment of the respective species. The Fortran routine also distinguishes between the species of the compound and gives a molecule count and density value for SO_2 and N_2 separately for each compartment to evaluate this further.

3.3.2 Matlab post processing

In a next step, the results from the Fortran evaluation are processed further in a Matlab routine. A reason for this was to get graphs of the information and to allow to accumulate information of different compartments together. This is done for example for compartments where a bulk like gaseous phase is established. A reason for this was to show the information in a simplified way.

In the Matlab evaluation, the time evolution of the density in all compartments is shown. It is also used to judge whether the adsorption has reached a steady state. A simplified evaluation for the density profile is shown in figure 3.2 the corresponding simplified compartmentalization is shown in figure 3.3. A exemplary non-simplified compartmentalization can be found in appendix B.

If the density profiles show a steady state the adsorption process is considered to be completed. Based on this, the densities of each compartment for the last 100 000 time steps (which is 0.1 ns respectively 0.2 ns) are averaged to get a mean density. Similarly, this is also done to obtain a mean number count in each compartment to calculate the average loading of the material. Compartments with a gaseous density for the regarded compounds are considered to be bulk compartments. These compartments are used to estimate the bulk pressure in the simulation cell. This was done with the help of the estimated local density and the temperature in this/these compartment/s and a Peng-Robinson equation (equation 3.2). $V_{m,i}$ is the molar volume of the respective compound i and is the reciprocal molar density which is estimated in the previous step by the FORTRAN program.

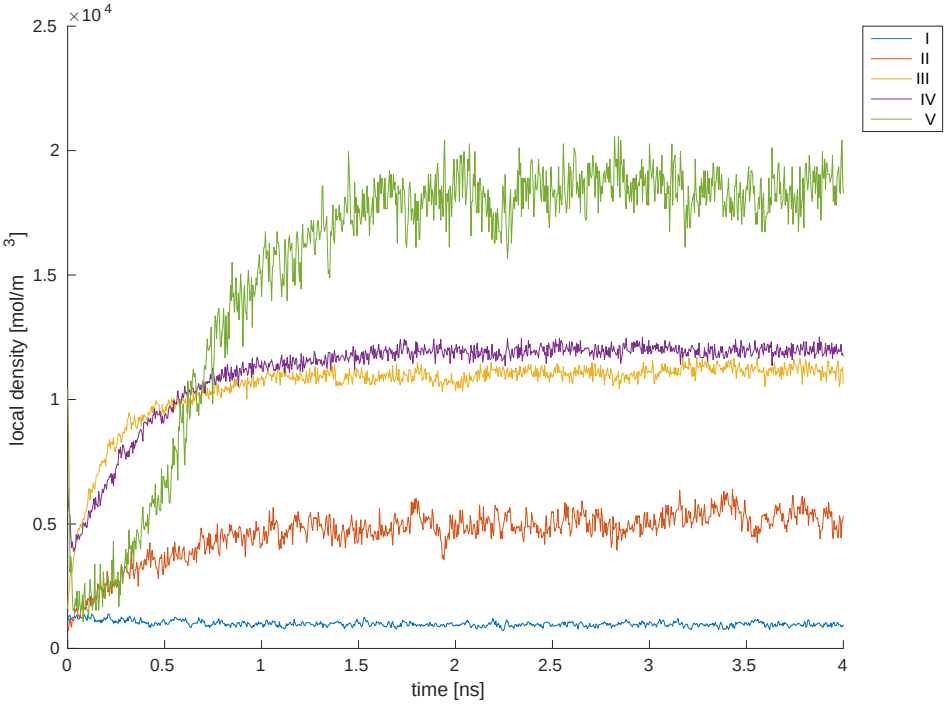

Figure 3.2.: SO_2 density in the simplified compartmentalization at a CNT(20/20) at $400\,\mathrm{K}$ and $26.3\,\mathrm{bar}$ bulk pressure in a pure SO_2 atmosphere

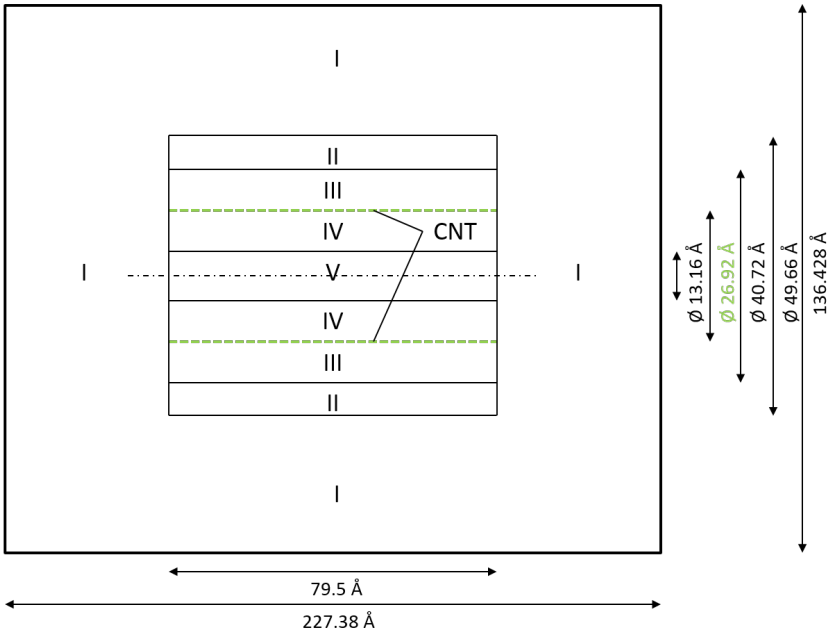

Figure 3.3.: Simplified compartmentalization of a CNT(20/20) at $400\,\mathrm{K}$

Table 3.1.: Parameters of the Peng Robinson equations for SO_2 and N_2 all taken from NIST[153]

		SO_2	N_2
T_c	[K]	430.64	126.20
p_c	[bar]	78.84	34.00
$p_s(T_r = 0.7)$	[bar]	4.3754	3.1184

For simulations with only one compound present e.g. SO_2 or N_2 the evaluation of the Peng Robinson equation is easy and given by equations 3.2, 3.3, 3.4, 3.5 and 3.6. Where a_i, b_i, β_i, ω_i and $T_{r,i}$ are the cohesion pressure, co-volume, temperature dependent factor, acentric factor and the reduced temperature of component i. Equations 3.3, 3.4, 3.5 and 3.6 are taken from Poling[169] or Pitzer[170]. The critical properties and the saturation properties at $T_r = 0.7$ are shortly summarized in table 3.1.

$$p_i = \frac{RT}{V_{m,i} - b_i} - \frac{a_i \beta_i}{V_{m,i}^2 + 2 b_i V_{m,i} - b_i^2} \quad i = SO_2, N_2 \tag{3.2}$$

$$a_i = \frac{0.457235 R^2 T_{c,i}^2}{p_{c,i}} \tag{3.3}$$

$$b_i = \frac{0.077796 R T_{c,i}}{p_{c,i}} \tag{3.4}$$

$$\beta_i = (1 + (0.37464 + 1.54226\omega_i - 0.26992\omega_i^2) \cdot \cdot(1 - T_{r,i}^{0.5}))^2 \tag{3.5}$$

$$\omega_i = -\log_{10}\left(\frac{p_{s,i}}{p_{c,i}}\right)_{T_{r,i}=0.7} - 1 \tag{3.6}$$

$$T_{r,i} = \frac{T}{T_{c,i}} \tag{3.7}$$

For mixtures the Peng-Robinson equation changes slightly (equation 3.8). The product of the cohesion pressure and the temperature dependent factor of the cohesion pressure are substituted by a_m, which is now the temperature dependent cohesion pressure of the mixture. The co-volume is substituted by b_m the co-volume of the mixture. These mixing parameters can be calculated by different mixing rules, e.g. the van-der-Waals (vdW) mixing rule or the Wong-Sandler (WS) mixing rule[171].

$$p_i = \frac{RT}{V_{m,i} - b_m} - \frac{a_m}{V_{m,i}^2 + 2b_m V_{m,i} - b_m^2} \quad i = \mathrm{SO_2}, \mathrm{N_2} \tag{3.8}$$

The calculation of the parameters a_m and b_m according to vdW is given by equations 3.9, 3.10 and 3.11. a_i and b_i are calculated according to equations 3.3 and 3.4. k_{ij} in equation 3.11 is an interaction parameter for the mixture of SO_2 and N_2 which shall be chosen to 0.008 according to Poling et. al[169] for the system SO_2/N_2. x_i and x_j are the molar ratios of SO_2 and N_2.

$$a_m = x_i^2 a_i \beta_i + 2x_i x_j \left(a_i \beta_i a_j \beta_j\right)^{0.5} \cdot \left(1 - k_{ij}\right) + x_j^2 a_j \beta_j \tag{3.9}$$
$$i, j = \mathrm{SO_2}, \mathrm{N_2}; i \neq j$$
$$b_m = x_i b_i + x_j b_j \tag{3.10}$$
$$k_{ij} = 0.008 \tag{3.11}$$

However, does the vdW mixing rule not reproduce the experimental phase diagram well which was shown by Marx[172]. For this reason, the Wong-Sandler mixing rule combined with the NRTL model for estimating the excess Gibbs free energy was chosen to represent the mixture SO_2/N_2 better. That this is reasonable for mixtures of SO_2 and N_2 was also shown in the work of Marx[172].

The same Peng-Robinson equation as in equation 3.8 is used for the Wong-Sandler mixing rule. The variables for the co-volume and the cohesion pressure change as described in the following equations 3.12 and 3.13[173]. Equations 3.14 to 3.19 give further details for the needed variables of equations 3.12 and 3.13[173]. The constant C (equation 3.14) is a characteristic constant for the Peng-Robinson equation and equals approximately 0.623 23[173], for other equations of state it is different e.g. for the Soave-Redlich-Kwong equation of state it is $C = \ln(2)$[173]. The excess Helmholtz energy can be approximated by the excess Gibbs free energy according to Kontogeorgis et al.[174] in combination with the Wong-Sandler mixing rule. As G^E model the NRTL model was chosen for approximation.

$$b_m = \frac{\sum_i \sum_j x_i x_j \left(b - \frac{a}{RT}\right)_{ij}}{1 - \frac{F^E}{CRT} - \sum_i x_i \frac{a_i}{RT b_i}} \quad i,j = \mathrm{SO_2}, \mathrm{N_2} \tag{3.12}$$

$$\frac{a_m}{b_m} = \sum_i x_i \frac{a_i}{b_i} + \frac{F^E}{C} \quad i = \mathrm{SO_2}, \mathrm{N_2} \tag{3.13}$$

$$C = 2^{-0.5} \ln\left(\sqrt{2} - 1\right) \tag{3.14}$$

$$\left(b - \frac{a}{RT}\right)_{ij} = \frac{\left(b_i - \frac{a_i}{RT}\right) + \left(b_j - \frac{a_j}{RT}\right)}{2}\left(1 - k_{ij}\right) \quad i,j = \mathrm{SO_2}, \mathrm{N_2} \tag{3.15}$$

$$F^E(P = \infty) \approx F^E(P \to 0) \approx G^E(P \to 0) \tag{3.16}$$

$$\frac{G^E}{RT} = x_i x_j \left[\frac{\tau_{ji} G_{ji}}{x_i + x_j G_{ji}} + \frac{\tau_{ij} G_{ij}}{x_j + x_i G_{ij}}\right] \quad i,j = \mathrm{SO_2}, \mathrm{N_2}; i \neq j \tag{3.17}$$

$$\frac{G^E}{RT} = 0 \quad i,j = \mathrm{SO_2}, \mathrm{N_2}; i = j \tag{3.18}$$

$$G_{ij} = \exp\left(-\alpha_{ij} \tau_{ij}\right) \quad i,j = \mathrm{SO_2}, \mathrm{N_2}; i \neq j \tag{3.19}$$

The values of the non-randomness constant for binary interactions α_{ij} (equation 3.20) are chosen according to the recommendation of Renon and Prausnitz for a liquid mixture of type IV[175]. What helped to choose a type IV mixture is the polarity of SO_2 and its positive deviation from the Trouton rule ($\Delta S_{v,\mathrm{SO_2}} = 94.9\,\mathrm{J mol^{-1}\,K^{-1}}$ [153] $> \Delta S_{v,Trouton} \approx 88\,\mathrm{J mol^{-1}\,K^{-1}}$). α_{ii} for a pure substance is 0 (equation 3.21). The temperature-dependent values for the NRTL coefficients $\tau_{\mathrm{N_2},\mathrm{SO_2}}$ and $\tau_{\mathrm{SO_2},\mathrm{N_2}}$ of the current system and the temperature-dependent coefficients k_{ij}, k_{ji} and k_{ii} are given in equations 3.22 to 3.25 and were determined in the work of Marx[172].

$$\alpha_{ij} = \alpha_{ji} = 0.48\,[175] \quad i,j = \mathrm{SO_2}, \mathrm{N_2}; i \neq j \tag{3.20}$$

$$\alpha_{ii} = 0 \quad i = \mathrm{SO_2}, \mathrm{N_2} \tag{3.21}$$

$$\tau_{\mathrm{N_2},\mathrm{SO_2}} = 6.055 - 0.015\,97\ \mathrm{K^{-1}}\,T \tag{3.22}$$

$$\tau_{\mathrm{SO_2},\mathrm{N_2}} = -3.388 + 0.013\,68\ \mathrm{K^{-1}}\,T \tag{3.23}$$

$$k_{ij} = k_{ji} = 0.29 + 0.001\,175\ \mathrm{K^{-1}}\,T \quad i,j = \mathrm{SO_2}, \mathrm{N_2}; i \neq j \tag{3.24}$$

$$k_{ii} = 0 \quad i = \mathrm{SO_2}, \mathrm{N_2} \tag{3.25}$$

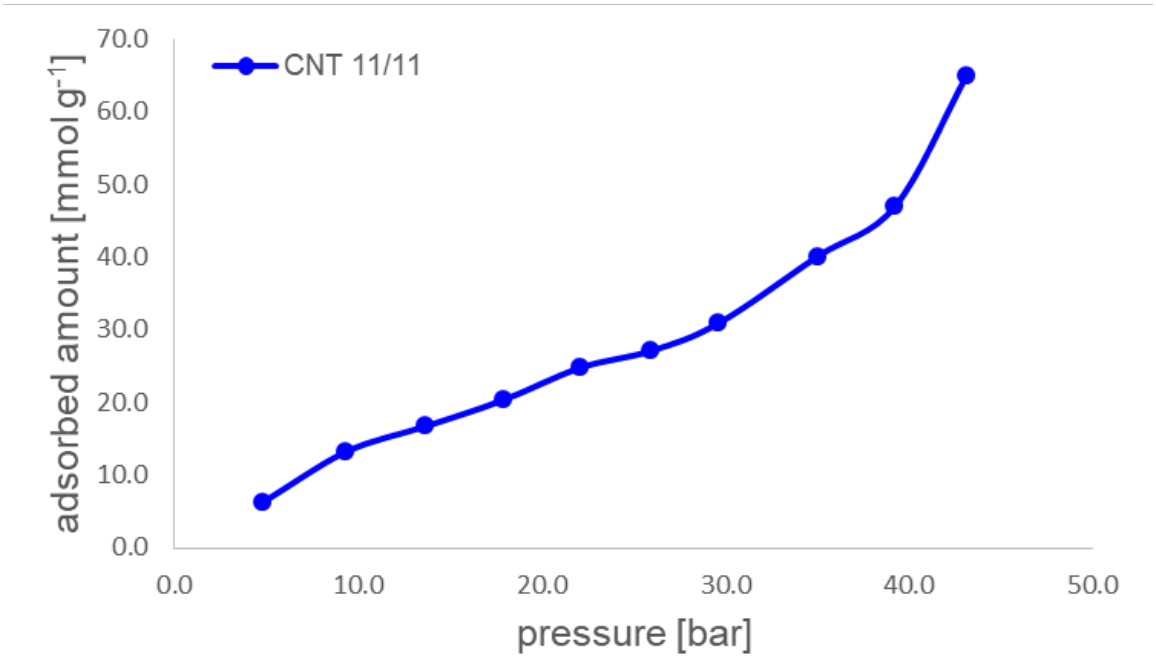

Figure 3.4.: Exemplary adsorption isotherm for a CNT

With the help of the Peng-Robinson equations for the pure substances (equation 3.2) and the mixture (equation 3.8) a pressure estimation in all compartments of the simulation cell can be done. However, do only the pressure estimations for the bulk compartments make sense. Compartments with adsorbed SO_2 or N_2 will only give a vague pressure estimation which might be the spreading pressure of the adsorbed phase.

Having now evaluated the adsorbed amount by the number count in the respective compartments, where a significantly increased density is established (in comparison to the bulk density), the temperature of the system, the bulk pressure and knowing the amount of carbon present in the CNT or graphene, the CNT or graphene loading can be evaluated and an adsorption isotherm can be drawn (figure 3.4).

4 Experiments

In this chapter the experimental setup to measure all experimental adsorption isotherms is described in detail as well as the procedure to obtain isotherms from the measured data.

4.1 Gravimetric adsorption setup

A gravimetric adsorption apparatus from Rubotherm of the IsoSORP® series is used[176–178]. For the first measurements, a standard setup consisting of magnetic suspension balance (MSB) and an automatic gas dosing system (GDS) was used. This setup had to be modified later to perform also experiments with pure SO_2 atmospheres. The modifications are described in detail in section 4.1.1. A scheme and P&I diagram of the initial setup can be seen in figure 4.1 and appendix A.3.

Before modifying, the setup allowed an operating range in pressure and temperature of 0 bar to 150 bar and 0 °C to 400 °C. In the temperature interval from 0 °C to 150 °C the measuring cell is thermostated by a double jacket which is attached to a Julabo thermostat F25. For higher temperatures, e.g. to activate the probe materials an inbuilt electrical heating coil is used.

All pipes inside the GDS and pipes to the measuring cell are automatically held at a temperature of 150 °C. This is done to prevent condensation of the measuring gases (namely CO_2 and SO_2) inside the GDS and to hinder condensed phases to harm the pressure sensors and dosing valves. All pipes from the gas cylinder cabinet to the GDS are not thermostated. To achieve a high enough back-pressure for carbon dioxide and sulfur dioxide these gases are pressurized with the help of an ISCO 500D syringe pump to pressures up to 160 bar. For CO_2 the pump is operated in an automatic mode with an automatic refill. CO_2 is also provided at a liquid state in the supply pipes due to the use of a cylinder with a riser pipe in the gas cabinet. Thus, the CO_2 pressure of provided CO_2 can be increased by the piston pump to the desired operating pressure. This was usually set to 100 bar.

SO_2 is supplied gaseous from the gas cylinder cabinet to reduce the hold up in the supply pipe. To pressurize the SO_2, the pump piston is cooled by a double jacket to temperatures below 0 °C to allow gaseous SO_2 at a pressure of approximately 3.5 bar to

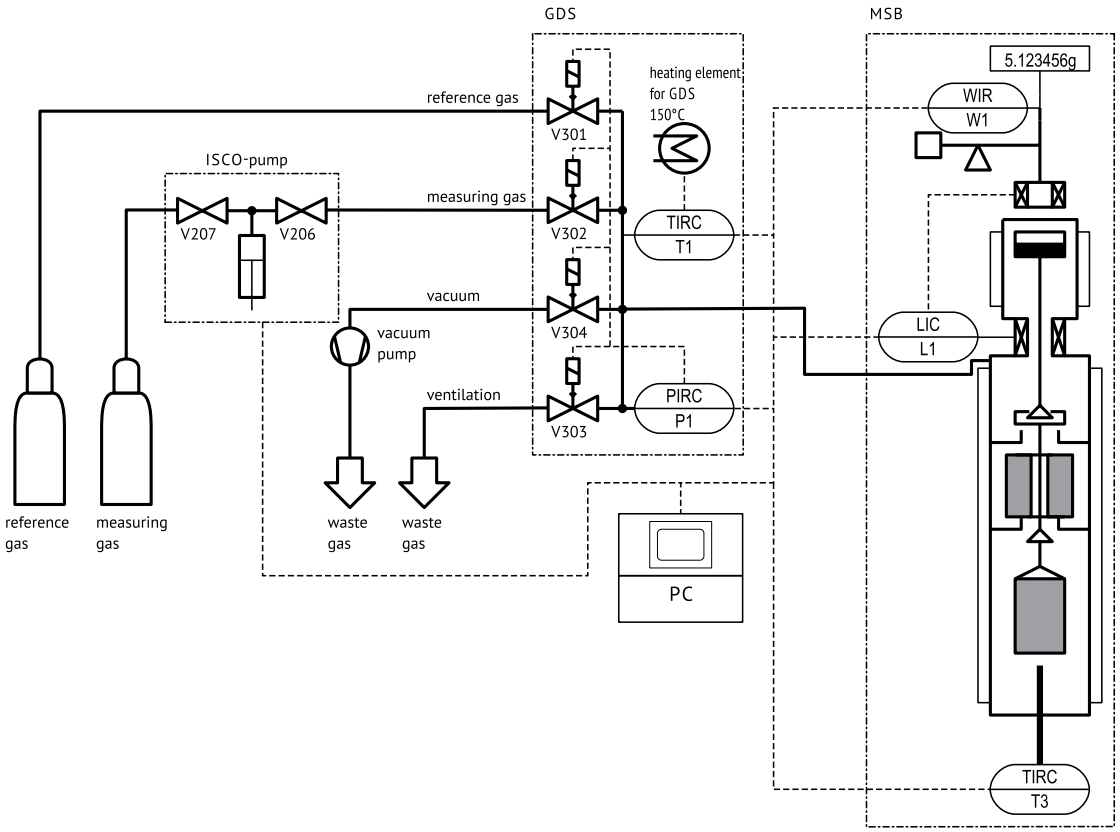

Figure 4.1.: Scheme of the experimental setup before modifications

condensate in the piston. After having (re)filled approximately 3 to 10 mL to the ISCO pump, sulfur dioxide which is condensed in the piston is also pressurized. Under SO_2 operating conditions the pump and the dosing of the experimental setup are operated manually and under observation of the operator.

Additionally to the gravimetric uptake, the gas density inside the measuring chamber can be measured by the MSB. This is done with a calibrated titanium sinker. The sinker allows with the help of the archimedical principle to calculate the density of the fluid in the measuring cell (see figure 4.2). Its vacuum mass and volume are known and the actual mass is measured. Assuming that volume change effects of the sinker only have a very minor impact, buoyancy on the sinker can be calculated by the mass difference. With this buoyancy, the density of the fluid can be determined. For more details see the manual "Procedure of Performing Gravimetric Adsorption Measurements"[179] from Rubotherm. The necessity for buoyancy corrections is discussed in more detail in section 4.2.2.

All data (e.g. current pressure, density, measured mass, temperature, time) are logged by a computer and stored for further evaluation.

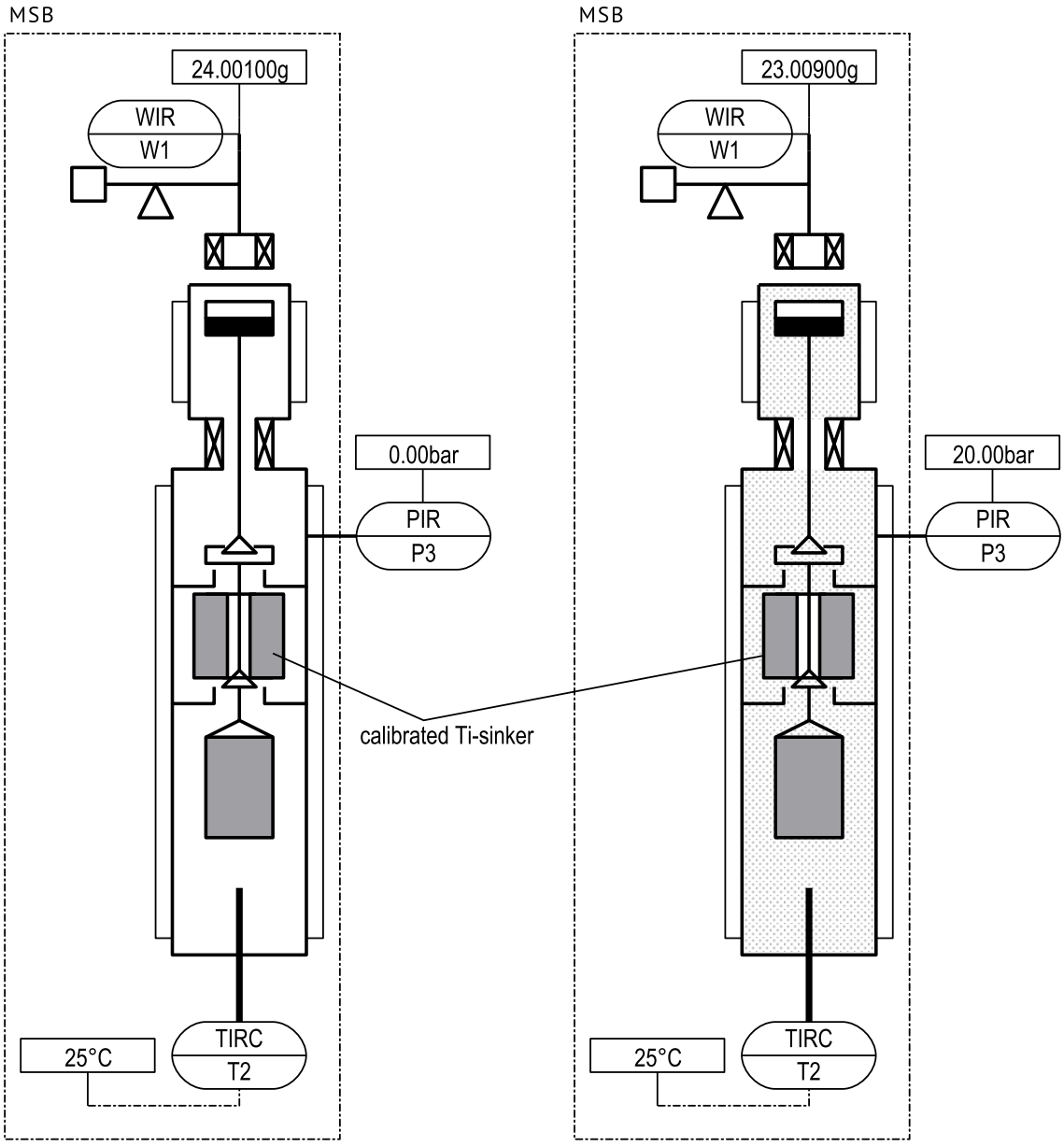

Figure 4.2.: Evaluation of the fluid density by a calibrated Ti-sinker with the help of the archimedical principle, left sinker in vacuum atmosphere with vacuum mass, right sinker in gas atmosphere with a reduced mass due to buoyancy effects

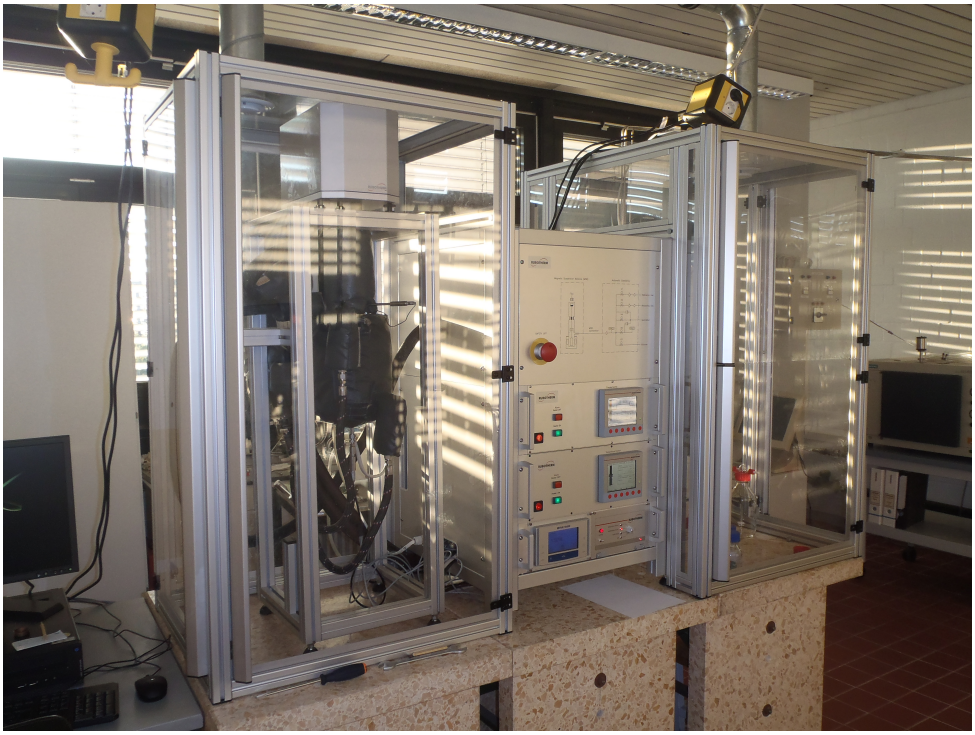

Figure 4.3.: Picture of the setup with its housing in the lab

To allow safe experimenting with sulfur dioxide the whole setup is housed in vented chambers, a picture of this is presented in figure 4.3.

For desorption and gas release out of the experimental setup, the ventilation is used for He, N_2 and CO_2 in an automatic mode. The released quantities of these gases are so small that ventilation directly to the environment is done. No exposure limits and indicative limits are reached. Also, if a pressure of 1 bar is attained the vacuum pump can be used directly with these gases without harming the vacuum pump.

When SO_2 is used the ventilation is done manually, and the vented gas is led to a gas scrubbing line (see fig. 4.4). This line consists of three gas-washing bottles and an adsorber column (length 1 m, $\varnothing_i$ 50 mm). The first gas-washing bottle is empty and mounted with the dip pipe towards the outlet. This is done to prevent that liquid of the following bottles is introduced to the GDS due to vacuum which is created by absorbed SO_2. The second gas-washing bottle is filled with $\approx$ 600 mL of a H_2O_2 with a concentration of $\approx$ 6 wt−%. In this bottle SO_2 reacts to sulphuric acid according to the following reaction:

$$SO_2 + H_2O_2 \longrightarrow H_2SO_4 \tag{4.1}$$

The third gas-washing bottle is filled with ≈ 600 mL of a 0.2 molL^{-1} NaOH solution and the indicator bromothymol blue. The purpose of this bottle is to absorb further SO_2 which was not absorbed in the previous bottle and to indicate if all H_2O_2 has reacted and the second bottle is saturated with SO_2. The reactions happening in the third bottle are partially reversible, and they are:

$$SO_2 + NaOH \rightleftharpoons NaHSO_3 \tag{4.2}$$

$$SO_2 + 2\,NaOH \rightleftharpoons Na_2SO_3 + H_2O \tag{4.3}$$

To remove last SO_2 contents, which were not trapped by the gas-washing bottles, an adsorber column with an impregnated activated carbon (Oxorbon K 20 J from Donau-Carbon[180]) is used. Finally, the exhaust of the adsorber column is connected to a water-jet pump which applies a constant flow of fresh air. It also spills the housing of the ISCO pump piston. These precautions are taken to omit a SO_2 concentration which is above the indicative exposure limit.

In theory 100 mL of a H_2O_2 solution with approximately 6 wt−% can absorb ≈ 0.2 mol (4.78 L at normal temperature and pressure (NTP)) SO_2 and 100 mL of a 0.2 molL^{-1} NaOH solution absorbs 0.101 6 mol (2.43 L at NTP) SO_2. Weidenfeller showed in his bachelor thesis that a sequential setup of 100 mL H_2O_2 with a concentration of 3 wt−% and 100 mL of a 0.1 molL^{-1} NaOH solution can absorb 0.122 7 mol (2.88 l at NTP) SO_2.[181] In comparison to Weidenfeller a higher concentration of H_2O_2 solution and NaOH solution is taken as well as a larger volume to allow to absorb higher quantities of SO_2. The maximum released amount of SO_2 during one experimental run, e.g. under 125 °C and 40 bar (the worst case), is maximum 8.3 L at NTP if a total volume of 200 mL for the measuring cell and the pipes is assumed. (This assumption overpredicts the actual volume significantly.) The released quantity of SO_2 is easily trapped by the described setup. A set of solution is usually exchanged after several runs at low temperatures and pressures or after one run at higher pressures to ensure that SO_2 is absorbed.

4.1.1 Modifications of the experimental setup

The experimental setup had unexpectedly to be modified to allow proper measurements with SO_2. A reason for this was the fact that the automatically operated needle valves of the GDS jammed after being in contact with pressurized, liquid sulfur dioxide. To

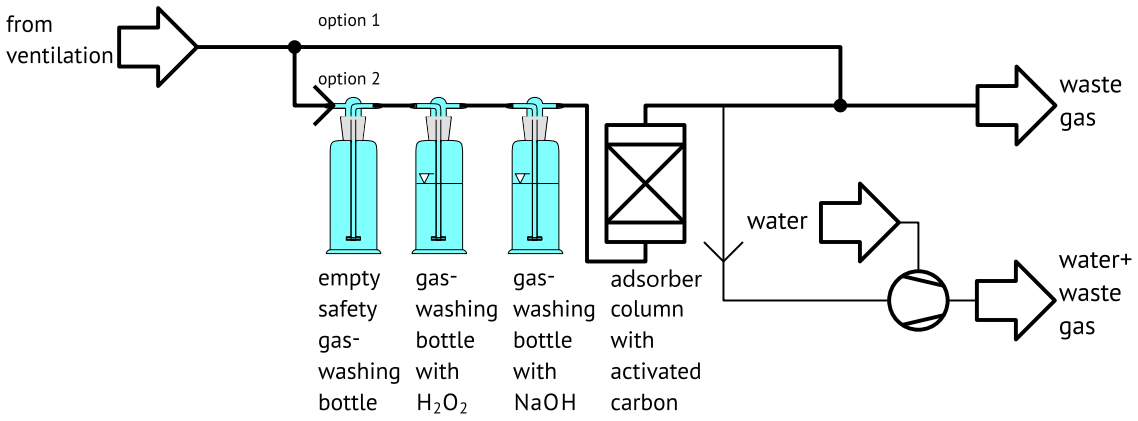

Figure 4.4.: Scheme of the gas scrubbing line, option 1: operation mode for non-hazardous gases, option 2: operation mode for SO_2 with the possibility to attach also a water jet pump to apply vacuum.

avoid this a manually operated bypass was delivered from Rubotherm. The amended scheme and flowchart can be seen in figure 4.5 and appendix A.4.

Additionally, the double-walled jack connections of the experimental setup were changed so that a disconnection of the double-walled jack was possible and the flow of the liquid thermostat could be short-circuited. One advantage of this was an easier mounting and unmounting of the double-walled jack and a reduction in the thermal inertia for the Julabo thermostat. Also did the as delivered flexible pipes easily leak at the soldering seam if being manipulated, which was necessary for mounting and unmounting the double-walled jack. The replacement parts were a set of new flexible and isolated pipes from Swagelok with quick disconnect coupler.

Charging of probe materials

A conceptual design how the experimental setup could be modified to apply charges in situ to the probe material was developed by Reinhardt in her bachelor thesis. [139] The principle of this design is that the measuring cell is slightly modified to allow to transfer charges into the cell by a connector which is welded into a redesigned measuring cell (compare figure 4.6). To apply the charge to the probe material the sample container is also modified to act as a capacitor which allows the probe material (e.g. CNTs) to be charged if the sample container is set to the zero position. The concept of the redesigned measuring cell was not implemented in this work, but might be studied in future works to show the impact of probe charging on the adsorption behavior in experiments. To prevent the charging of the all floating parts the sample container should be attached by an insulating hook, e.g. made out of glass.

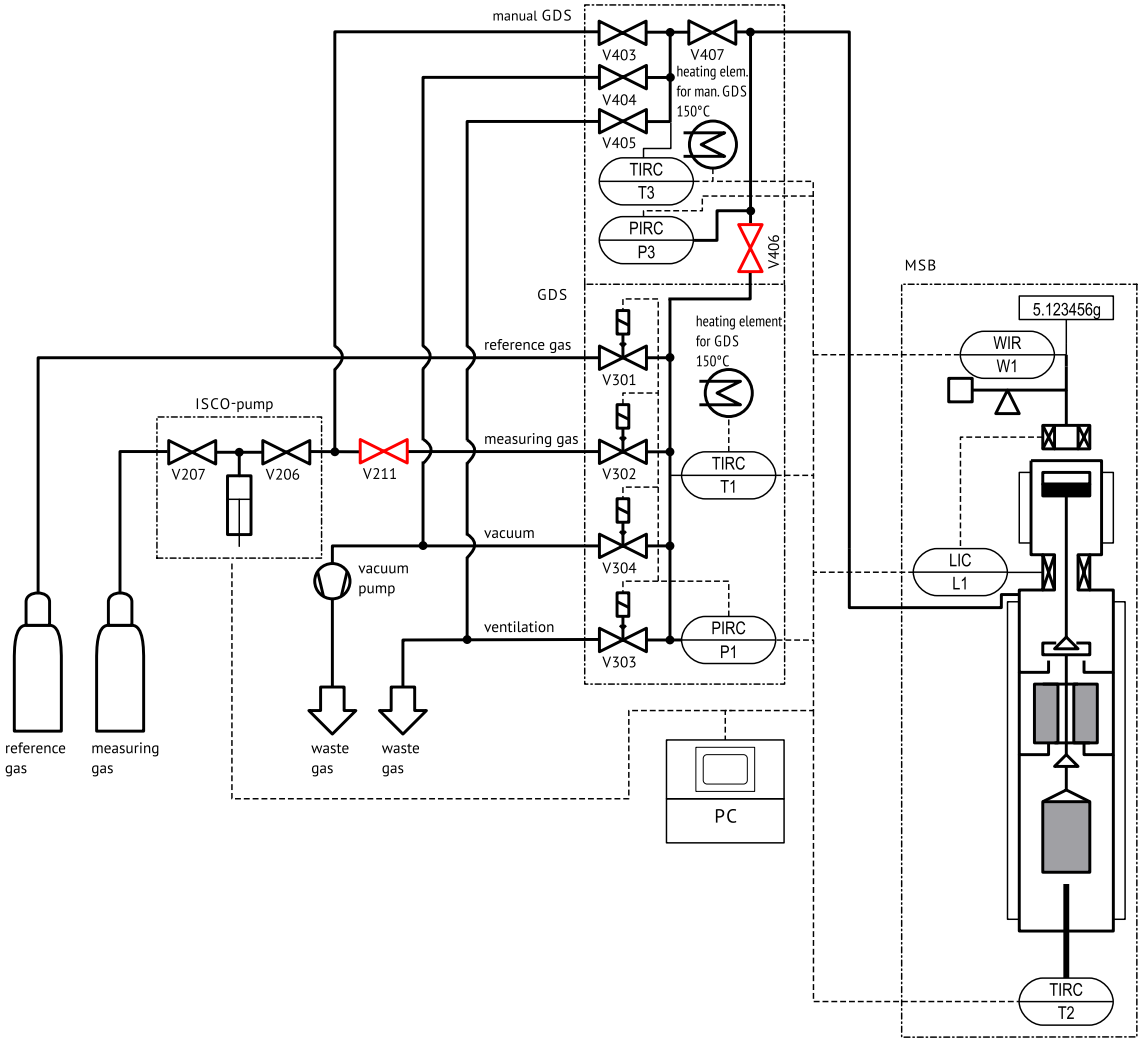

Figure 4.5.: Scheme of the experimental setup with bypass for high pressure SO_2 measurements

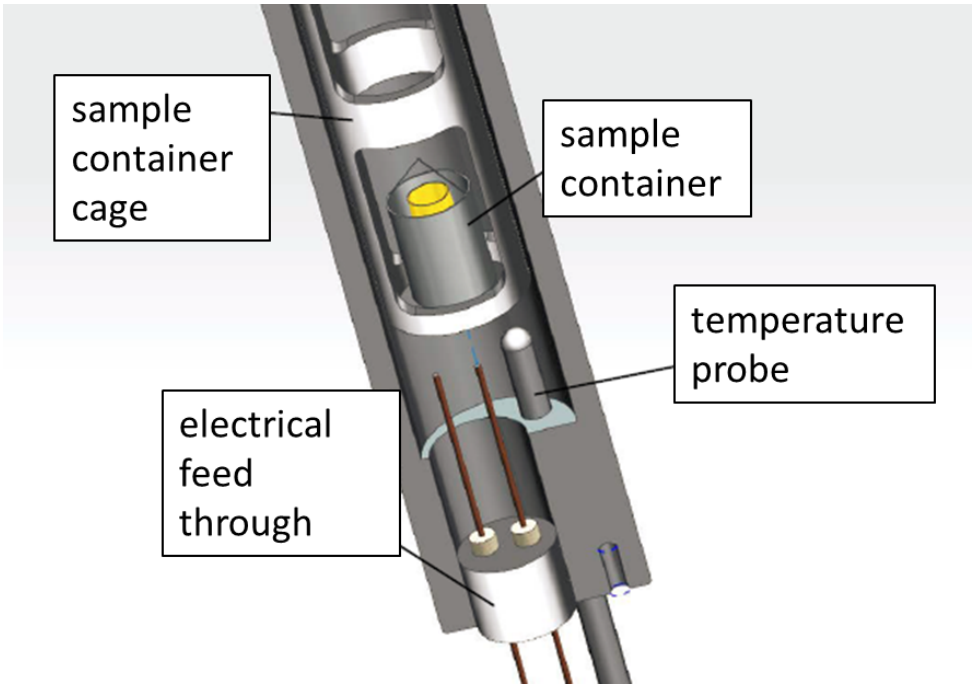

Figure 4.6.: Redesigned measuring cell to apply charges in situ to the probe material[139]

4.2 Determination of Adsorption isotherms

To measure and determine an adsorption isotherm with a gravimetric setup three measurements have to be performed. First, a calibration measurement of the blank setup, the so-called blank measurement, has to be done. Then a buoyancy measurement of the sample container with the sample is performed. These measurements are carried out with an inert gas, which is considered as non-adsorbing and has ideally no interactions with the sample material(s) and the experimental setup. Usually, helium is considered for this measurements and is used in this work. The third measurement is the measurement with the desired measuring gas or gas mixture atmosphere. Each measurement has to be performed at the same temperature. Usually, blank measurements only have to be conducted once and then do not need to be measured again, if the floating parts of the measuring cell are not changed or do not change due to reactions such as corrosion or oxidation.

In the following sections it is described what one can determine out of the blank measurement, buoyancy measurement and the measurement with the target gas/ gas mixture (in the following only named measurement).

Table 4.1.: List of blank measurement temperatures and year of measurement

temperature [°C]	year [-]
0	2014
20	2014
25	2013
25	2014
30	2014
40	2014
50	2014
60	2014
75	2013
80	2014
100	2014
125	2014
150	2014
175[†]	2013
200[†]	2013

[†] cell was heated by the electrical heating, coupling of the MSB was thermostatted to 100 °C by liquid thermostat

4.2.1 Blank measurement

As stated a blank measurement is only carried out once at each temperature if no changes to the floating parts inside the MSB are done. To perform a blank measurement, no probe material is inserted in the measuring cell. As gas He is applied and the experiment is started. Prior to the measurement with He the measuring chamber is heated to 300 °C under vacuum conditions ($p < 5 \cdot 10^{-2}$ bar) for 12 h. Then the cell is thermostatted to the temperature of the blank measurement (still under vacuum conditions), and then the blank measurement starts with a vacuum segment. The weight, temperature and pressure are logged in intervals of 20 s for a certain time period. For blank measurements, this period was usually 30 min per isotherm point. After this time the weight, temperature and pressure reached a steady state. Then pressure is in- or decreased incrementally to the next value. A typical table with pressure steps, times, recorded masses etc. is included in appendix A.2. All performed blank measurements with corresponding temperatures are listed in table 4.1.

Plotting the measured mass m of a blank measurement against the measured density ρ, one can determine the mass of the sample container and the volume of the sample

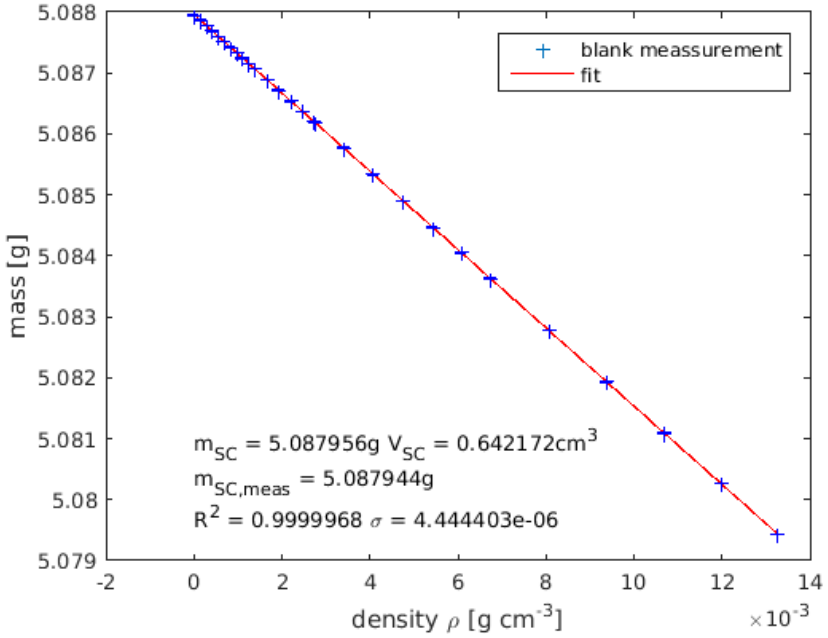

Figure 4.7.: Blank measurement ρ-m- chart with helium at 75 °C (+) and fit to the measured data (line), in the chart are also displayed the fit parameters for m_{SC}, V_{SC}, the measured vacuum mass of the sample container $m_{SC,meas}$ and the goodness of fit (R^2 and standard deviation σ)

container by a linear fit to the data points. The intercept of the line gives the mass of the sample container m_{SC}, and the negative slope gives the volume of the sample container V_{SC}. The fit equation can be summarized by the following equation:

$$m = m_{SC} + \rho \cdot V_{SC} \tag{4.4}$$

A typical plot of the mass against density, the goodness of fit and the estimated fitted parameters m_{SC} and V_{SC} is shown in figure 4.7. The measured vacuum mass $m_{SC,meas}$ (measured mass at $\rho = 0\,\mathrm{gcm^{-3}}$) and the fitted mass m_{SC} are in good agreement. A great advantage of measuring the density directly is that for the evaluation no assumption for the density has to be made, i.e. using an equation of state. This is of even greater advantage if gas mixtures are measured. Then the in situ density can be obtained directly and does not need to be derived from assumptions for the mixing behavior and presumable adsorption behavior of the different gases.

4.2.2 Buoyancy measurement

A buoyancy measurement is performed in a similar manner as a blank measurement. This time, sample material is introduced into the sample container. Prior to a buoyancy measurement also an activation of the sample material is performed. This is usually done for all measured CNTs at 300 °C and vacuum ($p < 5 \cdot 10^{-2}$ bar) for 12 h or sometimes shorter, if no change in the measured mass is observed anymore. As a gas for the buoyancy correction also He is used. Plotting the estimated data points for mass and density again in the same manner as described in 4.2.1 (see figure 4.8) and applying a linear fit to the data, the mass of the sample m_S and the volume of the sample V_S can be determined out of the fitted parameters (see equation 4.5, 4.6 and 4.7). With m_S and V_S the specific volume of the sample $V_{S,spec}$ can be calculated (see equation 4.8). Also, the measured vacuum mass of the sample $m_{S,meas}$ can be calculated out of the measured vacuum mass of sample container plus sample and the measured vacuum mass of the sample container (see equation 4.9).

$$m = m_{SC+S} + \rho \cdot V_{SC+S} \tag{4.5}$$

$$m_S = m_{SC+S} - m_{SC} \tag{4.6}$$

$$V_S = V_{SC+S} - V_{SC} \tag{4.7}$$

$$V_{S,\text{spec}} = \frac{V_S}{m_S} \tag{4.8}$$

$$m_{S,\text{meas}} = m_{SC+S,\text{meas}} - m_{SC,\text{meas}} \tag{4.9}$$

4.2.3 Measurement

Typically right after a buoyancy measurement, a measurement with the measuring gas is performed. The measuring gases are nitrogen N_2, carbon dioxide CO_2 and sulfur dioxide SO_2. The measurement also starts with a vacuum segment to establish the temperature and to measure again the vacuum mass of the sample. For all used samples it was shown that activation before a measurement has not to be performed if the sample was activated before the buoyancy measurement under the precondition that the gas for the buoyancy measurement is He. After the vacuum segment, the respective gas is introduced to the measuring chamber at a certain pressure. For measurements

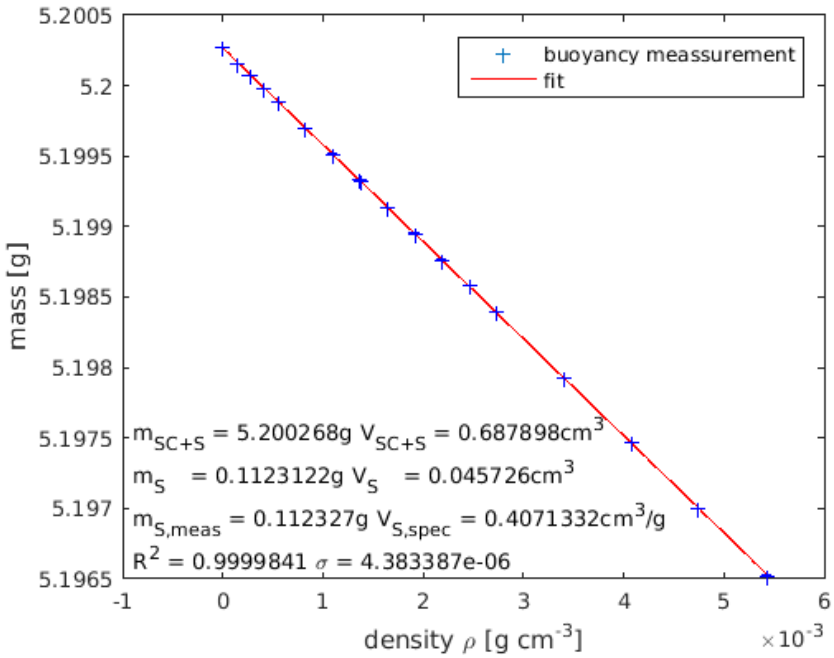

Figure 4.8.: Buoyancy measurement ρ-m- chart with helium at SWCNTs at 75 °C (+) and fit to the measured data (line), in the chart are also displayed the fit parameters for m_{SC+S}, V_{SC+S}, the calculated parameters of m_S, V_S, $V_{S,\mathrm{spec}}$, the calculated vacuum sample mass from the measured values $m_{S,\mathrm{meas}}$ and the goodness of fit (R^2 and standard deviation σ)

with N_2 and CO_2, this is done with the automatic gas dosing system. For measurements with SO_2 the manual gas dosing system is used.

A typical time to achieve equilibrium for measurements with N_2 and CO_2 is 30 min for the used samples. Then the next pressure step is or can be performed, and the data is logged. For SO_2, times to achieve equilibrium range from 20 min to 2 h. This is dependent on how close one is to the saturation pressure of SO_2. The closer the longer equilibrium times are needed. Equilibrium has to be reached to allow a proper evaluation of the data and to obtain the adsorption isotherm.

4.2.4 Evaluation of results

With the help of the sample container volume V_{SC}, sample container mass m_{SC}, sample volume V_S, sample mass m_S, measured mass m_{meas} and measured density ρ_{meas} the excess adsorbed amount $\Delta m_{\text{ads,ex}}$ for the respective pressure and temperature can be determined (compare equation 4.10). From this value the excess adsorbed amount $n_{\text{ads,ex}}$ per gram of sample can be calculated (see equation 4.11). The evaluation is done with the help of Matlab®. The code is presented in the appendix C.4. Also is the code functionality shortly summarized there.

$$\Delta m_{\text{ads,ex}} = m_{\text{meas}} - m_{SC} - m_S + \rho_{\text{meas}} \cdot (V_{SC} + V_S) \tag{4.10}$$

$$n_{\text{ads,ex}} = \frac{\Delta m_{\text{ads,ex}} \cdot 10^3\,\text{mmolmol}^{-1}}{M \cdot m_S} \quad \left[\text{mmolg}^{-1}\right] \tag{4.11}$$

Having evaluated each data point a plot of the excess adsorbed amount over the pressure gives the respective adsorption isotherm (see figure 4.9). In the figure, the excess adsorbed amount of SO_2 on SWCNTs from Nanolab is presented up to the saturation pressure. Also, is the adsorption and desorption branch shown. One can see that there is no hysteresis and that the isotherm shows a Type II behavior.

4.2.5 Measurements with charged materials

Measurements with charged materials were not conducted in this work. A study how the measurement cell needs to be modified was done in the work of Reinhardt.[139] With such a modified cell a static charge can be applied to the sample material by simply setting it to the zero position of the MSB and using the sample as a capacitor.

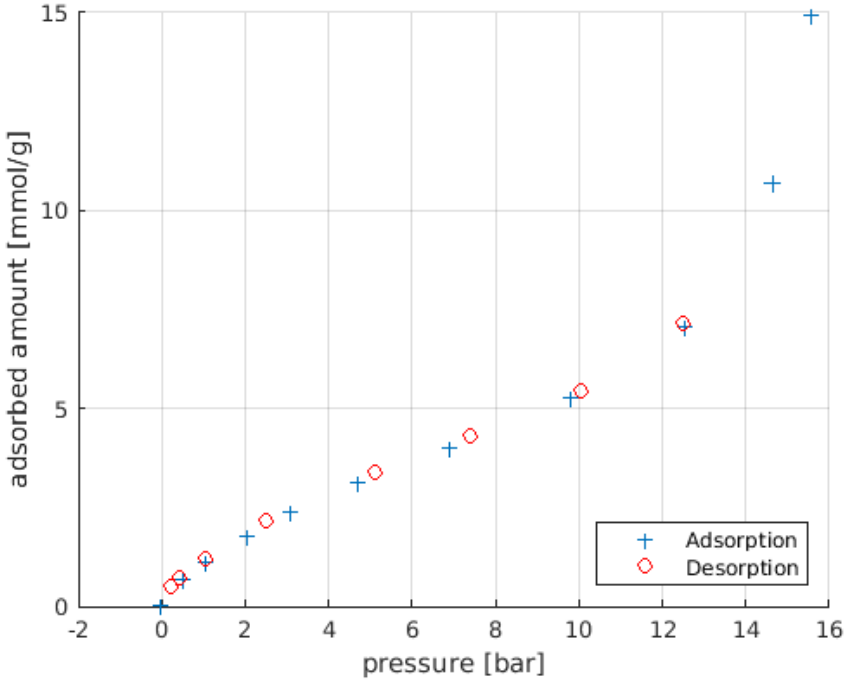

Figure 4.9.: Excess adsorbed amount over pressure at SWCNTs at 75 °C in a SO_2 atmosphere

4.2.6 Experimental errors

The quality of experimental data is dependent on the way the experiments are performed, and the errors occurring from the measurement equipment have an impact on the data. What is measured in all experiments is temperature, pressure and mass. These points are addressed in the following paragraphs.

Experimental error due to temperature deviations

The temperature is measured with a temperature transducer directly beneath the sample container. Additionally, the temperature of the double walled jack and the electrical heater is also measured. These three temperatures were consistent with each other throughout the experiments and did not show significant deviations. Therefore the temperature transducer in the measuring cell is considered to have delivered reliable data. A typical error for such a transducer is ±0.3 °C in the measured temperature range. Since there were only minor temperature deviations during the experiments, the temperature error is considered to be below ±0.5 °C for all measurements. Also is the thermal mass of the whole setup rather big and it takes approximately 4 h to set

a certain temperature, so that temperature fluctuations are considered to play only a very minor role if present at all. Temperature drifts are neglected for the experiments because no such drifts were seen in the data.

Experimental error due to pressure deviations

For the pressure transducer, two different pressure transducers are used in the automatic gas dosing system. One for the low pressure region below 40 bar and one for the region from 40 bar to 150 bar. In the low-pressure region, both pressure transducers were active and showed consistent values. In operation with the manual gas dosing system, only one additional pressure transducer with a measuring range from Vacuum to 40 bar was used. Which also showed consistent values to the two other pressure transducers. The error for the pressure in this work is ±2 % of the measured pressure. Usually, during one pressure step the pressure was changed in the very beginning and only adjusted if necessary by the automatic gas dosing system which was usually only applicable within the first 10 to 20 min. Then the pressure remained stable for the respective data point. Based on this the influence caused by pressure fluctuations on the experimental data are considered to be negligible.

Experimental error due to mass deviations

The mass could be measured in a resolution of 1 μg. During the experiment it typically fluctuated around a mean value ±30 μg. Since the mass or to be more precise the adsorbed amount (loading) is studied, the influence of the mass has to be examined in more depth. This was done by Ehmer[182]. A typical absolute mass error, which she evaluated from different measurements, was for the sample mass m_s and the mass of the sample container m_{SC} 500 μg. This has to be considered for the evaluation of the adsorbed amount. The adsorbed amount is calculated by formula 4.12:

$$X = \frac{m_{\text{meas}} - m_{SC} - m_S + \rho_{\text{meas}} \cdot (V_{SC} + V_S)}{m_S \cdot M_i} \quad i = \text{CO}_2, \text{N}_2, \text{SO}_2 \tag{4.12}$$

If the mass of the sample container (m_{SC}) or the sample m_S in equation 4.12 has a constant deviation, it causes only an offset in the adsorbed amount. The influence on the slope of the loading is negligible for the studied masses and pressures, which was shown in the work of Ehmer[182]. A constant deviation for the mass of the sample container and the sample can be assumed since they are measured before a sorption run, and they are assumed not to change during the experiment, e.g. no reaction is

taking place with the sample or the sample container, no deposition is happening, etc. To take into account these offset errors all measurements are corrected by the loading at vacuum conditions which has to be 0 mmolg^{-1}.

In equation 4.12 another source of errors can be the buoyancy correction. Here the sample container volume (V_{SC}) and the sample volume (V_S) have an impact and are more pronounced if the adsorbed amount is low, e.g. as for nitrogen measurements. Then errors in the buoyancy correction volumes can cause errors up to 5 to 10 % of the adsorbed amount at high pressures if only weak adsorption is happening. At low pressures (below 10 to 20 bar) the effect of the buoyancy correction is very minor.

Summing all these errors up the measured adsorbed amounts have a maximal uncertainty of 5 % of the shown value for SO_2 and CO_2 measurements and 10 % of the shown value for N_2 measurements.

4.2.7 Reproducibility

The measurements are well reproducible. This accounts especially for all measurements with different CNTs. To test this, a measurement with CO_2 at an industrial grade CNT was performed twice with the same sample. The procedure for each measurement was exactly the same. Meaning at first an activation at 300 °C, then a buoyancy measurement with He and the then the measurement with CO_2. Both times the same adsorbed amounts could be achieved (compare figure 4.10). The curves coincide within the experimental uncertainty very well.

The temperature difference for the curves arises from a defective temperature probe which was changed after the experiment, all other temperature probes which were logged and also inspected during the experiment showed comparable values. The defective temperature probe was, however, the master probe to control the thermostat. Since the offset during the measurement was constant, and the results agree well with each other no further measurements were conducted for this sample.

To benchmark whether the setup yields comparable experimental results, measurements with zeolite 13X 3 mm-5 mm beads were conducted and compared to literature values [183–188]. In the pressure region up to 10 bar, the experimental runs performed fit well to the literature data. Considering that relatively large 13X beads were chosen and that binder may have blocked some of the pores in comparison to the much smaller 13X pellets, e.g. utilized by Cavenati et al. [183] or even the powder as utilized by Rege et al. [184,185] (compare figure 4.11). In the high pressure region from 10 bar to 50 bar the adsorption is less pronounced as in the data of e.g. Cavenati et al. [183]. However, one

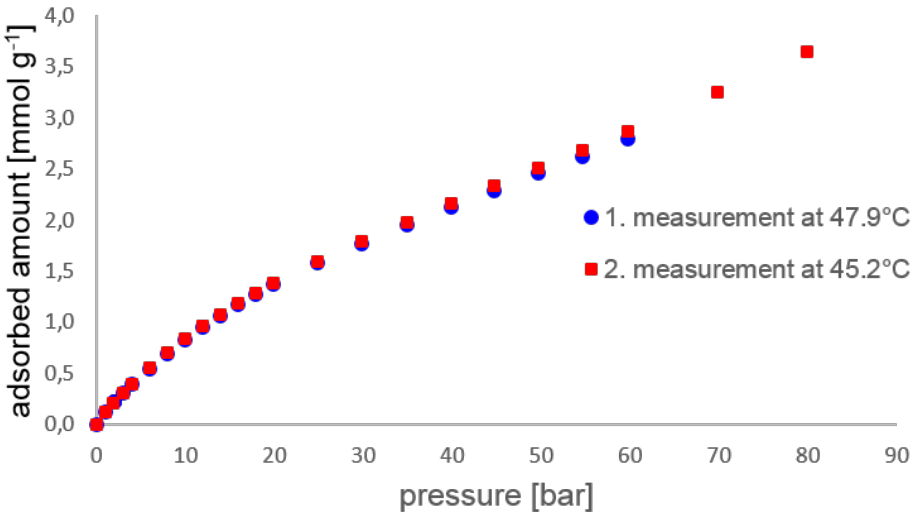

Figure 4.10.: Measurement of a industrial grade CNT in a CO_2 atmosphere at 50 °C twice to show reproducibility, the first measurement was done at 47.9 °C the second measurement was done at 45.2 °C, the deviations arise from a defective temperature probe which was changed after this experiment

needs to keep in mind that the bead size incorporated in the experiments was large and not powder-like which offers a higher surface area for adsorption. Also, one has to keep in mind that the data obtained from the experiment shows excess adsorption whereas the data from Rother and Fieback and Cavenati et al. presents data corrected to total adsorption, which leads to higher adsorbed amounts for their data (compare figure 4.12). Especially, in the region of higher pressures, the difference between excess and total amount adsorbed is increasing and has a higher impact on the measured values. Additionally, some pores and surfaces are blocked by binder material which reduces the adsorbed amount.

Summing the results with zeolite 13X up a considerable equivalence to the literature data is given which allows relying on the data measured in this work.

To study which amount of sample is needed to get the same result for each measurement Ehmer conducted several experiments with different sample masses and compared the results.[182] She showed for N_2 adsorption at industrial grade CNTs that with sample masses of approximately 20 mg the results of a measurement with 170 mg of sample could almost be reproduced. With a mass of 64 mg the measured curves coincide. With a lower mass of 6 mg the measurement of the 170 mg sample could not be reproduced.[182] Compare figure 4.13 to see the different masses and the measured results in comparison to the benchmark measured with 170 mg of sample.

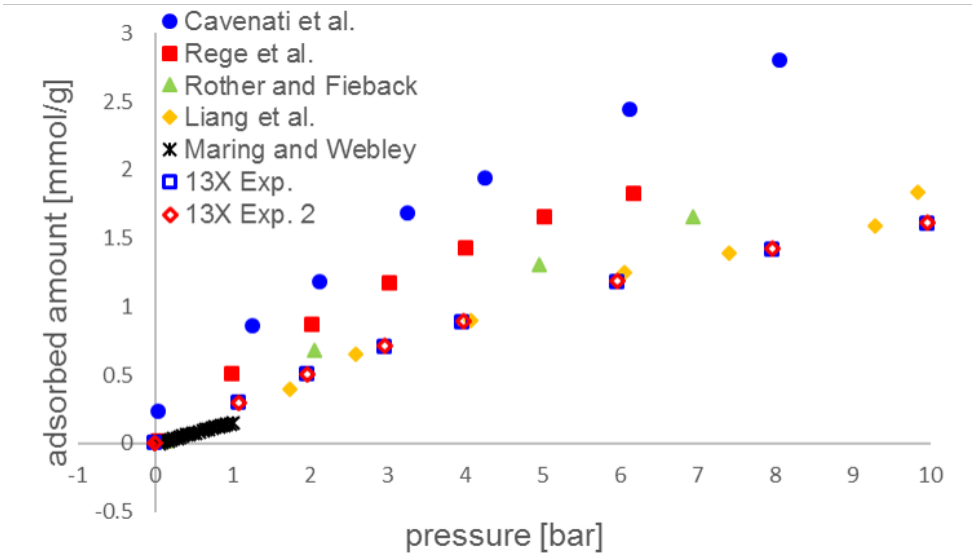

Figure 4.11.: Measurement of zeolite 13X in a N_2 atmosphere at 25 °C and comparison to data from Cavenati et al.[183], Rege et al.[185], Rother and Fieback[186], Liang et al.[187] and Maring and Webley[188] in the pressure region from vacuum to 10 bar

This leads to the assumption that for a measurement with a considerably low adsorbing gas such as N_2 a sample mass of minimally 50 mg should be used. The adsorbed amount of the low adsorbing gas gives then significant detectable masses which can be attributed to adsorption given reproducible results. With gases which adsorb better such as SO_2 also lower sample masses may be used as the adsorbed mass is higher resulting in a more pronounced mass change. Especially, as the curve of the 20 mg isotherm meets almost the isotherms with higher sample masses for the shown experiments with the weak adsorbing N_2.

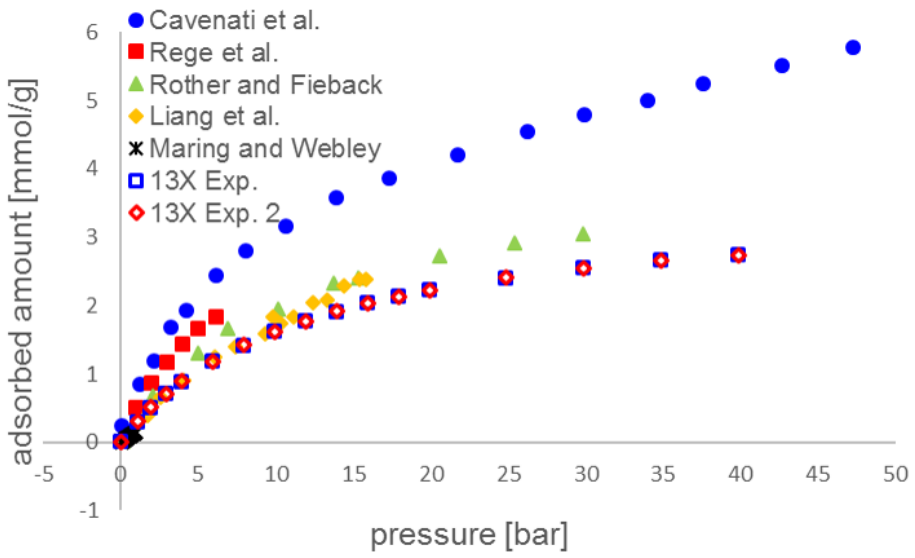

Figure 4.12.: Measurement of zeolite 13X in a N_2 atmosphere at $25\,^{\circ}\mathrm{C}$ and comparison to data from Cavenati et al.[183], Rege et al.[185], Rother and Fieback[186], Liang et al.[187] and Maring and Webley[188] in the pressure region from vacuum to $55\,\mathrm{bar}$

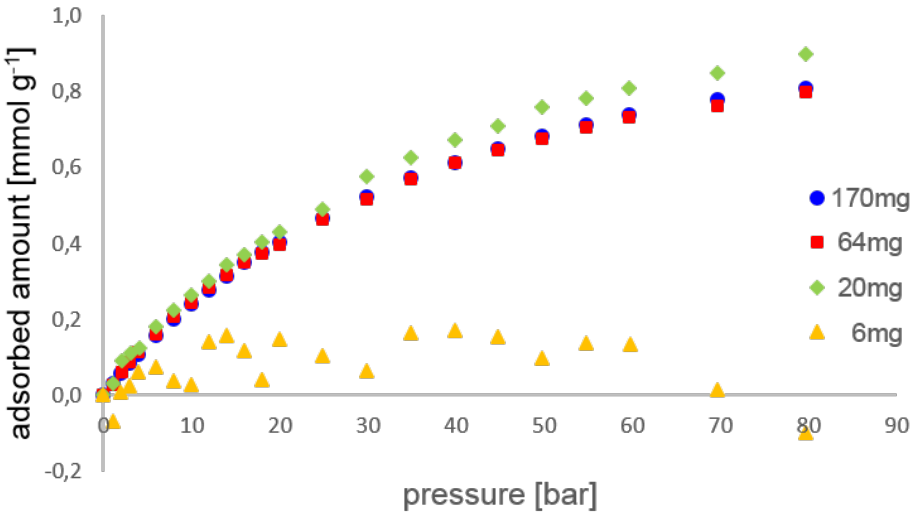

Figure 4.13.: Variation of the sample mass with industrial grade CNTs to check the minimum sample mass required for reproducibility with data from Ehmer[182]

5 Results and discussion

In this chapter, the results from simulation and experiment are presented and discussed. First, the simulational results are shown and assessed then the experimental results are shown and also assessed. In a last step, the simulation results and the experiments are compared to each other.

5.1 Results from MD

Isotherms shown in this section were obtained by MD simulation as described in chapter 3. First the simulations at (SW)CNTs are presented in SO_2 and N_2 atmospheres, then mixtures of SO_2 and N_2 are shown. In the simulation section SWCNTs are simply refered to as CNTs as only SWCNTs were simulated. Afterwards adsorption isotherms of SO_2 and N_2 on graphene are shown. All data of the simulation are summarized in appendix D.

5.1.1 CNTs

In simulation different CNTs with diameters in the range of 1.48 nm up to 10.77 nm (CNT(11/11) resp. CNT(80/80)) were studied in sulfur dioxide and nitrogen atmospheres. For some cases the temperature was changed in the range of 300 K to 400 K and for some cases charge was applied to the CNT. An overview of the studied CNTs, temperature, pressure range and charge gives table 5.1.

5.1.1.1 Adsorption studies with SO_2

Figure 5.1 shows the adsorbed amount of SO_2 on CNTs of different diameter at 400 K which have been simulated. What is noticeable is that diameter, and with the diameter, the size of the CNT does not seem to have a significant impact on the amount adsorbed. Only for the CNT(11/11), one can see that the amount adsorbed at lower and intermediate pressures is slightly lower than the amount adsorbed for the other CNTs. At higher pressures, the curve bends and has slightly higher adsorbed amounts. A reason for this could be capillary condensation inside the CNT alongside with confinement effects in

Table 5.1.: Studied CNTs, CNT diameters, CNT lengths, temperatures, bulk pressure range, gas composition and charge

CNT (n/m)	∅ [nm]	length [nm]	T [K]	range of p_{bulk} [bar]	x_{SO_2} [%]	charge [e][a]
CNT (11/11)	1.48	9.65	300	2.8- 3.7	100	0.000
CNT (11/11)	1.48	9.65	350	4.7-15.7	100	0.000
CNT (11/11)	1.48	9.65	400	4.8-43.1	100	0.000
CNT (11/11)	1.48	9.65	300	9.5-32.1	0	0.000
CNT (11/11)	1.48	9.65	350	9.6-32.7	0	0.000
CNT (11/11)	1.48	9.65	400	5.0-33.0	0	0.000
CNT(20/20)	2.69	7.95	300	3.0- 4.0	100	0.000
CNT(20/20)	2.69	7.95	350	5.2-14.0	100	0.000
CNT(20/20)	2.69	7.95	400	5.2-43.1	100	0.000
CNT(20/20)	2.69	7.95	400	9.5-29.7	100	0.010
CNT(20/20)	2.69	7.95	300	9.3-30.6	0	0.000
CNT(20/20)	2.69	7.95	350	9.9-31.1	0	0.000
CNT(20/20)	2.69	7.95	400	9.9-32.1	0	0.000
CNT(30/30)	4.04	12.33	400	7.2-43.6	100	0.000
CNT(40/40)	5.39	16.00	400	6.1-44.4	100	0.000
CNT(80/80)	10.77	10.87	400	13.8-44.4	100	0.000

[a] e denotes the elementary charge $1.602 \cdot 10^{-19}$ A s

the CNT which allow a denser packing of the SO_2 than in a condensed state. This is a behavior known from adsorbed phases in different systems. [189,190]

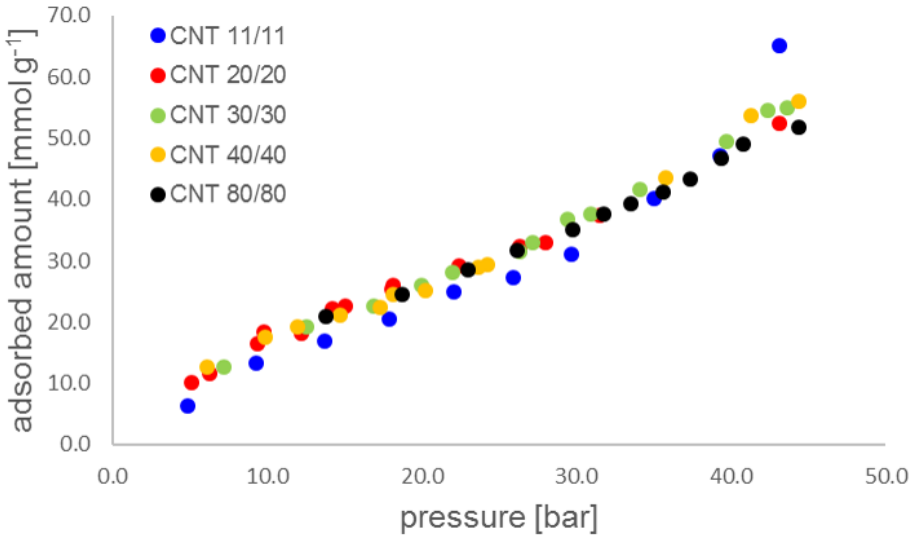

Figure 5.1.: Simulated total adsorbed amount of SO_2 of the CNTs CNT(11/11), CNT(20/20), CNT(30/30), CNT(40/40) and CNT(80/80) at 400 K

Varying the temperature of the simulations yields the well-known trend that at lower temperature more adsorption takes places (compare figure 5.2). Here, the narrower CNT(11/11) (diameter 1.48 nm) shows less adsorption than the larger CNT(20/20) (diameter 2.69 nm). At 350 K the beginning of the rise in adsorption for the CNT(11/11) towards saturation pressure (16.8 bar) can be seen, at 300 K no simulation close to the saturation pressure (4.2 bar) could be conducted, so this trend cannot be seen. But it is presumably present as well. Especially simulations at low pressures and temperature were computationally very demanding to reach equilibrium for the chosen approach of molecular dynamics. Therefore, only a few of them were carried out in this work.

Furthermore, the charging of a CNT(20/20) was simulated. For this purpose, an evenly distributed charge along the CNT was applied. This was done by assigning a partial charge of e.g. 0.01 e (e meaning elementary charge of $1.602 \cdot 10^{-19}$ A s) to each carbon atom of the CNT. In figure 5.3 the result of this simulation can be seen in combination with the same uncharged CNT(20/20) at 400 K. A charged CNT shows a higher amount of adsorbed SO_2 than the uncharged CNT due to the higher attraction of the CNT for the SO_2. The dipole nature of SO_2 may help to have this significant higher loading of the CNT.

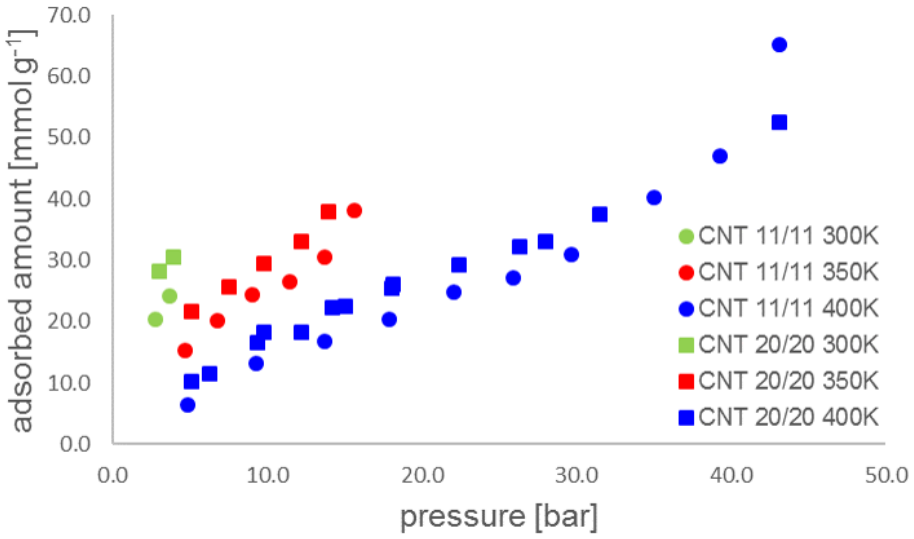

Figure 5.2.: Simulated total adsorbed amount of SO_2 of the CNTs CNT(11/11) and CNT(20/20) at $300\,\mathrm{K}$, $350\,\mathrm{K}$ and $400\,\mathrm{K}$

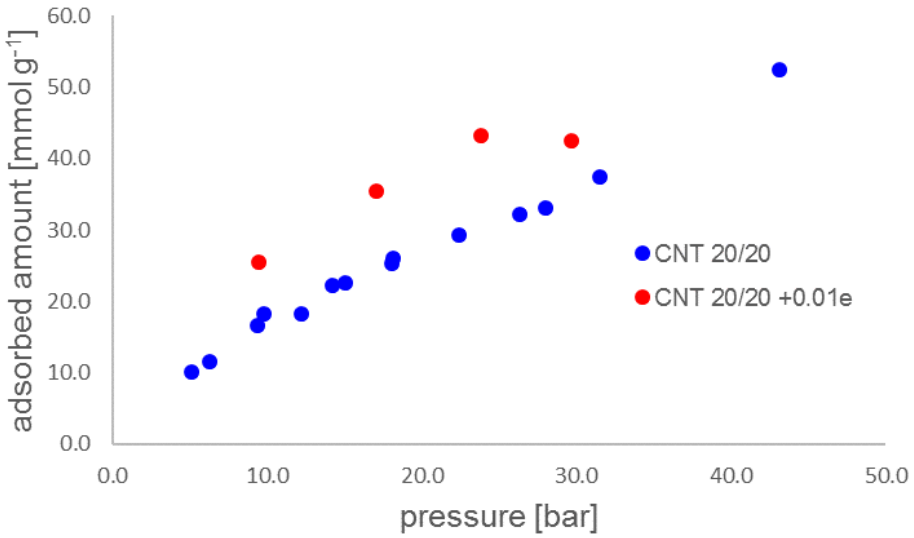

Figure 5.3.: Simulated total adsorbed amount of SO_2 of an uncharged and a charged CNT(20/20) at $400\,\mathrm{K}$, the charge applied was $0.01\,\mathrm{e}$ per carbon atom of the CNT

Model fits to the simulated data

As described in chapter 2.1.2 adsorption isotherms can usually be described with different models. For this, all data of one isotherm is taken and fitted with one or more models named in chapter 2.1.2. Some of the models allowed a fitting with the help of Matlab's fit command. For the simulated CNTs with smaller diameters a good fit to the data was possible with the Langmuir and Freundlich models. The BET, DR, DA and Toth isotherm model delivered a poor fit in most cases. A Temkin fit was not possible to obtain. An example of the fit results is given in figure 5.4. An overview which fit results could be obtained and how good they represent the data is given in table 5.2. For simulated data only fit results for the adsorption are presented as it is assumed that desorption data is the same for the carbon materials which have been simulated in this work. All further model fits can be found in appendix D as well as the data for the fitting parameters.

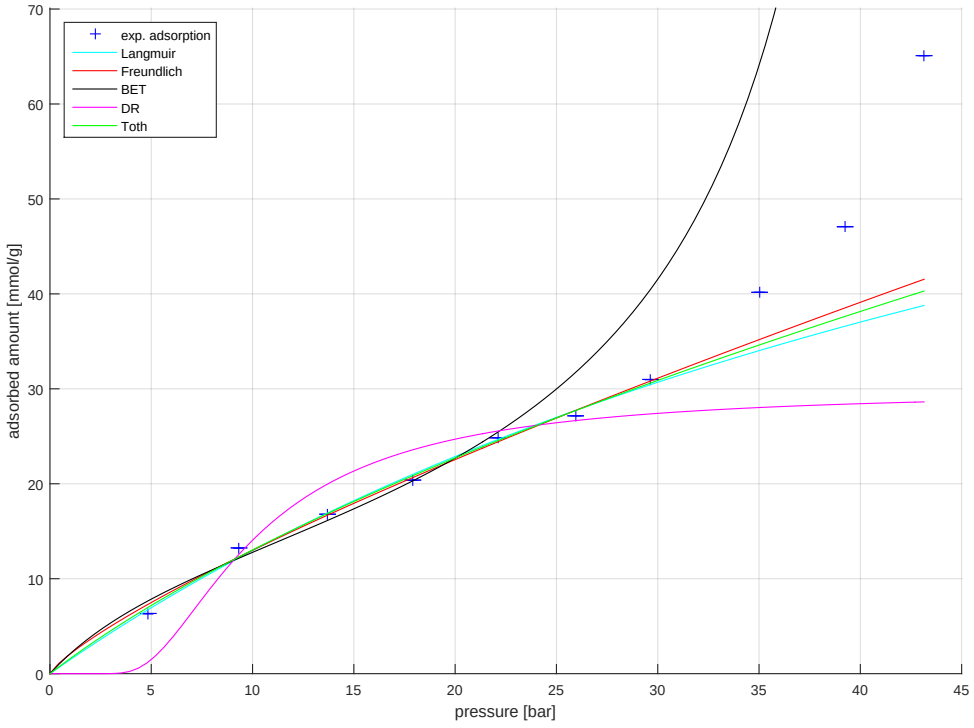

Figure 5.4.: Simulated data of a CNT(11/11) at 400 K in SO_2 atmosphere (+) and model fits to the simulated data (lines)

Analysis of adsorption in different compartments at the CNT

The advantage of molecular dynamics is that it is easy to state where the molecules are adsorbed and also how many are adsorbed if, e.g. one assigns compartments to the

Table 5.2.: Rating of the goodness of the model fits to the simulated data for different CNTs in SO_2 atmospheres and different temperatures (good fit (+), bad fit (-), no fit ( ))

CNT	T	Langmuir		Freundlich		BET		DR		DA		Temkin		Toth	
type	[°C]	Ads.	Des.	Ads.	Des.	Ads.	Des.	Ads.	Des.	Ads.	Des.	Ads.	Des.	Ads.	Des.
CNT(11/11)	25														
CNT(11/11)	75	+		+				-							
CNT(11/11)	125	+		+		-		-		-				+	
CNT(20/20)	25														
CNT(20/20)	75	+		+				-							
CNT(20/20)	125	+		+		-		-		+				+	
CNT(20/20) [a]	125	+		+				-		-				-	
CNT(30/30)	125	+		+		-		-		-					
CNT(40/40)	125	-		-		-		-		-					
CNT(80/80)	125	-		-				-		-					

[a] all carbon atoms carry a charge of 0.01 e

CNT as it was done in this work (compare figures B.1 and 3.3 in the appendix). With this approach different cases can be studied with one simulation:

- total adsorption at the CNT
- only adsorption at the outer surface of the CNT, e.g. if only capped CNTs are utilized
- adsorption at the inner surface of the CNT, e.g. the CNTs are embedded in a matrix which does not block the pores but does not allow accessibility to the outer surface of the CNT
- examination of the adsorbed amount in assigned regions, e.g. the first layer adsorbed at the CNT

The total adsorption at the CNTs was already presented in figure 5.1. The other mentioned cases are shown in the following figures 5.5 to 5.7. In figure 5.5 it is shown that more SO_2 adsorbs inside the CNT the larger the CNT diameter is. However, one can see that inside the CNT adsorption seems to come to a limiting value based on the CNT size and that some kind of saturation takes place which is pressure dependent on the CNT diameter. For the smaller CNT diameters, this is at a lower pressure than for the larger CNT diameters. For the CNTs CNT(40/40) and CNT(80/80), this cannot be seen anymore as clearly than for the smaller CNTs e.g. CNT(11/11). Also, the slope of the amount adsorbed inside the CNT does have an upper limit which is dependent on the pressure. The effect seen may be caused by the curvature radius of the CNTs. What can also be seen is that if the limiting values are eyed closely that for the small CNTs such as CNT(11/11) and CNT(20/20) the saturation limit seems to increase slightly with

pressure in the saturated region above 10 bar resp. 22 bar which might be caused by an increase in the packing of the SO_2 inside the CNTs and might be called confinement.

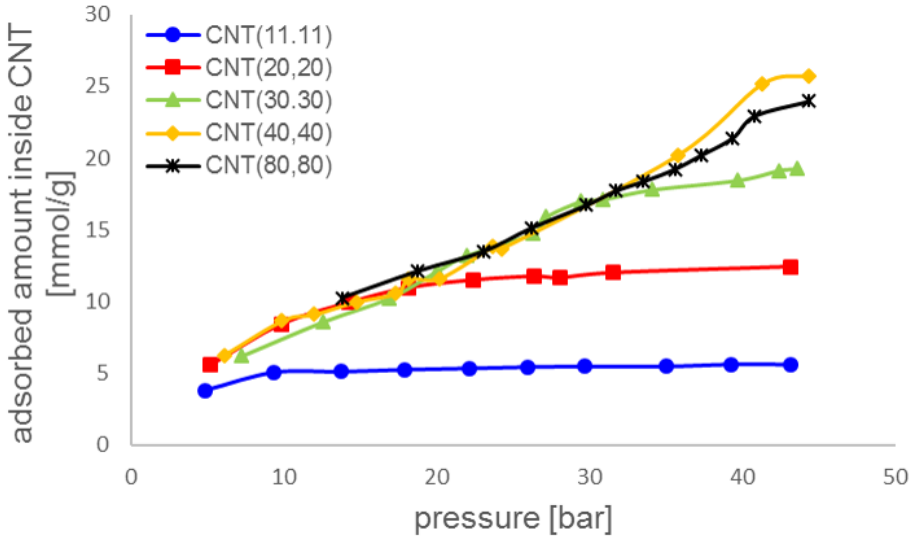

Figure 5.5.: Simulated adsorbed amount of SO_2 inside the CNT of the CNTs CNT(11/11), CNT(20/20), CNT(30/30), CNT(40/40) and CNT(80/80) at 400 K

If one takes a look at the adsorbed amount outside the CNT (figure 5.6), the situation is opposite. The larger the CNT, the lesser is adsorbed at the outer surface if higher pressures are regarded. For pressures below approximately 15 bar the adsorbed amount seems to be indifferent to the diameter of the CNT.

Inspecting the adsorbed amount in more detail gives further insight. Now having a look at the first layer adsorbed inside and outside the CNTs (figure 5.7 and figure 5.8), the same trends as for the adsorbed amounts inside and outside the CNTs seem to be shown. But it can also be seen that for the 1. layer inside the CNT a coverage limit seems to exist. The coverage limit is dependent on the diameter of the CNT and the pressure. The lower the diameter the lower the coverage limit and the lower the pressure the lower the limit which is reached. Especially for the CNT(11/11) and the CNT(20/20) it can also be seen again if the limit for adsorption is reached that with increasing pressure it seems to rise slightly which might also be a hint for denser packing or confinement effects caused by increasing pressure.

On the 1. layer outside the CNTs, a coverage limit is not as prominent established. Here, it can be seen that the smaller the diameter of the CNT, the bigger gets the adsorbed amount at the CNT. This can easily be assigned to the influence of the outer curvature of the CNTs. CNTs having a smaller diameter have a smaller curvature radius, resulting in leaving more space for SO_2 molecules outside the CNT for adsorption.

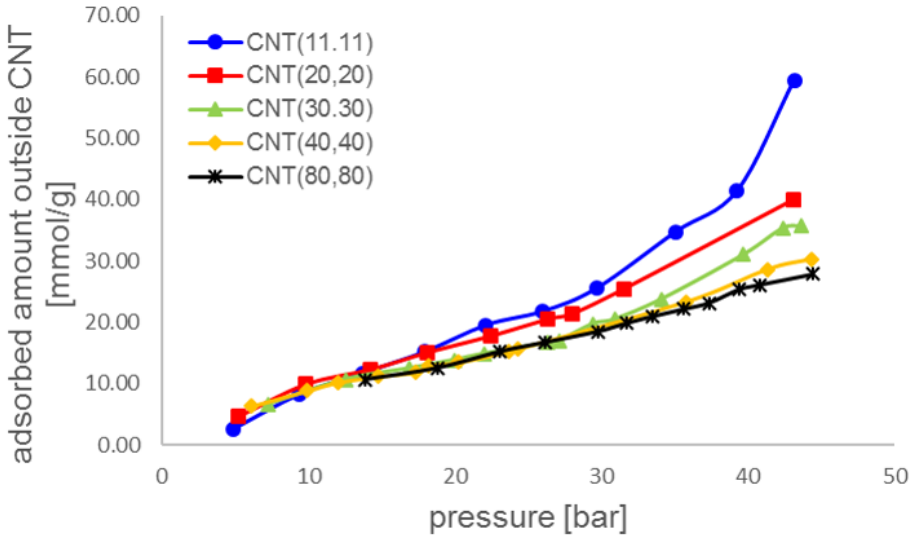

Figure 5.6.: Simulated adsorbed amount of SO_2 outside the CNT of the CNTs CNT(11/11), CNT(20/20), CNT(30/30), CNT(40/40) and CNT(80/80) at 400 K

If the ratio between the adsorbed amount inside the CNT and the total adsorbed amount is calculated and plotted against pressure, the smaller CNTs show at pressures below approximately 7.5 bar a higher adsorption inside the CNT than outside (compare figure 5.9). As already mentioned this may be caused by the curvature of the CNT which gives a higher attractive potential inside the CNT by the overlapping potentials of different carbon atoms. This trend, however, changes at pressures above approximately 7.5 bar. For the CNT(11/11) then adsorption outside the CNT is predominant, which could simply be because no more SO_2 molecules can enter the CNT and adsorption can only increase outside the CNT. For the CNT(20/20) adsorption outside the CNT is not as pronounced as for the CNT(11/11), but it can also be seen that at pressures above approximately 15 bar it plays a major role. Between roughly 7.5 bar and 15 bar the amount adsorbed inside and outside the CNT seems to be almost equivalent. Looking at greater CNT diameters (CNT(30/30), CNT(40/40) and CNT(80/80)) this behavior is seen over a wider or the whole range of studied pressures. An equal adsorbed amount in and outside the CNT means that the curvature seems to play only a minor or no role. E.g. for graphene the amount adsorbed on both sides of the graphene layer is equal in equilibrium and was also taken as a criterion that equilibrium was established (compare to chapter 5.1.2). To draw a first conclusion, large CNTs behave similar to graphene and seem to be indifferent to the curvature radius if the adsorbed amount inside and outside the CNT is compared. For graphene this behavior is expected and also holds in simulation (compare to the data shown in chapter 5.1.2).

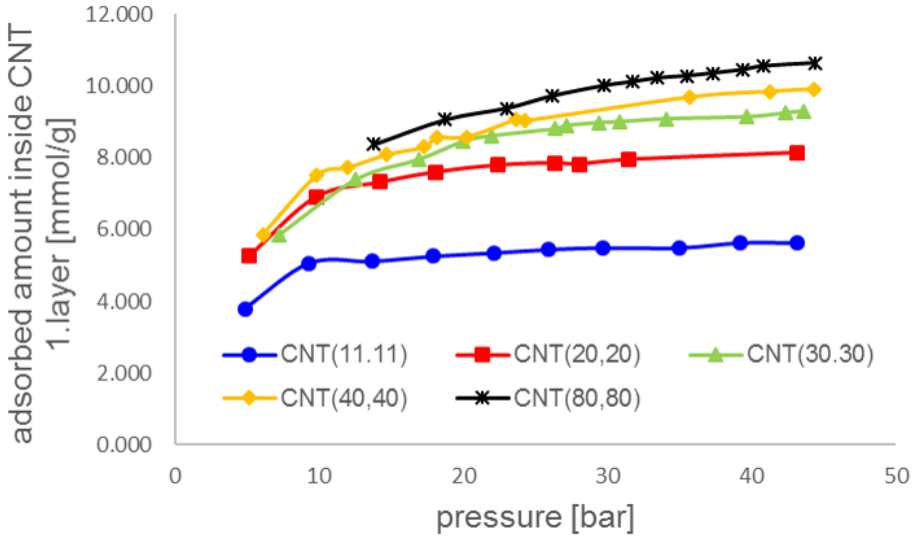

Figure 5.7.: Simulated adsorbed amount of SO_2 of the 1. layer inside the CNT of the CNTs CNT(11/11), CNT(20/20), CNT(30/30), CNT(40/40) and CNT(80/80) at 400 K

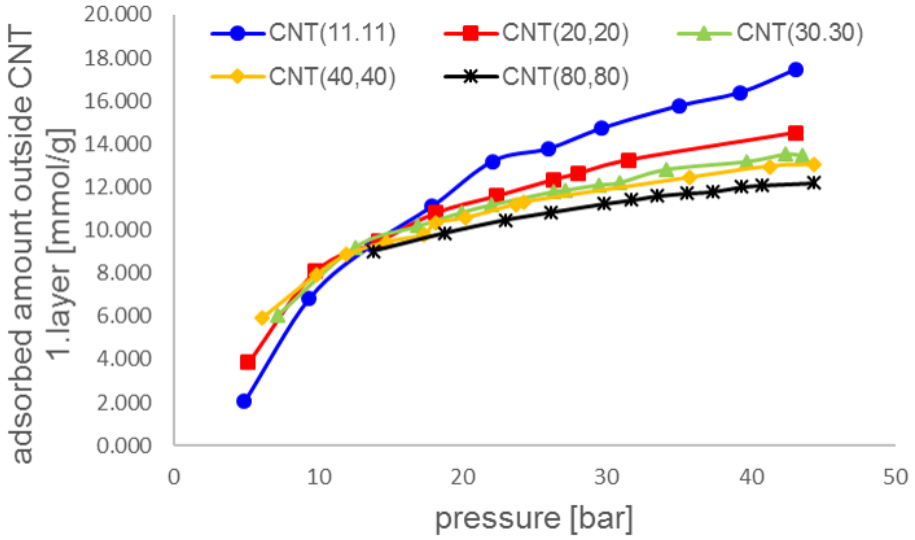

Figure 5.8.: Simulated adsorbed amount of SO_2 of the 1. layer outside the CNT of the CNTs CNT(11/11), CNT(20/20), CNT(30/30), CNT(40/40) and CNT(80/80) at 400 K

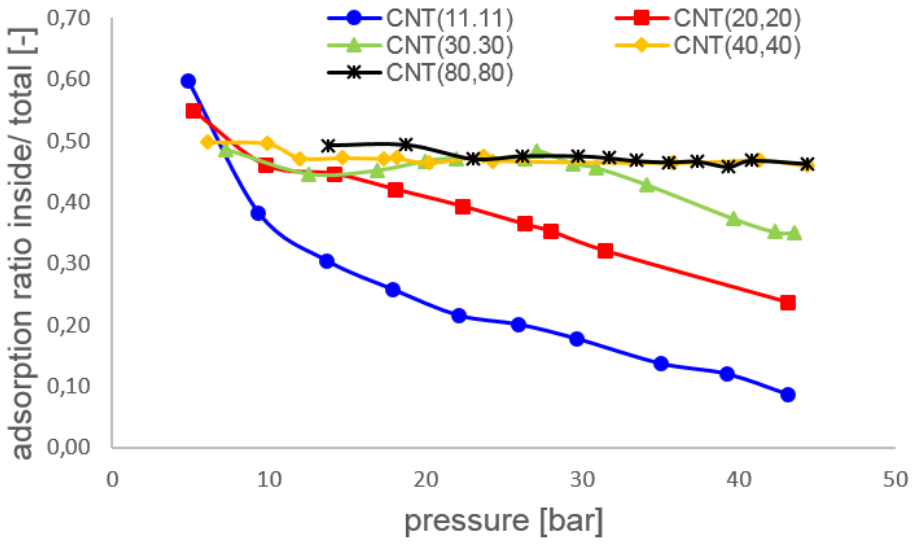

Figure 5.9.: Simulated ratio of the adsorbed amount of SO_2 inside the CNTs of the of the CNTs CNT(11/11), CNT(20/20), CNT(30/30), CNT(40/40) and CNT(80/80) at $400\,\mathrm{K}$ in comparison to the total amount adsorbed of SO_2 in these CNTs

5.1.1.2 Adsorption studies with N_2

Similar adsorption studies as for SO_2 have also be performed for N_2. In figure 5.10 the adsorbed amount of nitrogen at the CNT(11/11) and CNT(20/20) at the temperatures 300 K, 350 K and 400 K is shown. The simulations for the two CNTs have the expected temperature dependency, the higher the temperature, the less N_2 is adsorbed. For both CNTs, almost the same amount is adsorbed per temperature at the respective pressure, and no significant difference or dependency on the CNT diameter can be seen. One reason for this is that the adsorbed amount of N_2 is less than the adsorbed amount of SO_2 (compare figure 5.2) and that the nitrogen molecule is smaller and rod-shaped.

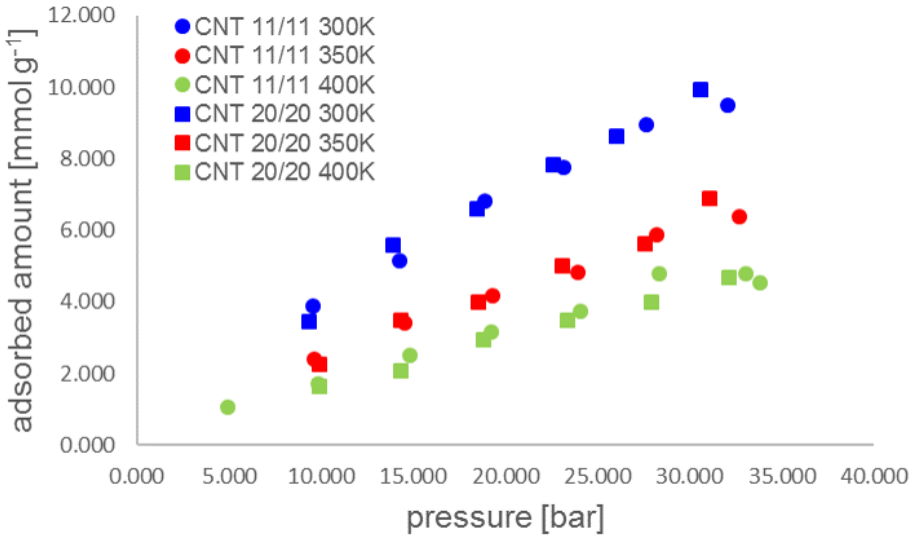

Figure 5.10.: Simulated total adsorbed amount of N_2 of the CNTs CNT(11/11) and CNT(20/20) at 300 K, 350 K and 400 K

The simulation showed that N_2 only seems to establish a monomolecular layer at the CNT surface. For this reason only the first layer inside and outside the CNT was studied in more detail (compare figure 5.11 and figure 5.12). The amount adsorbed inside and outside the CNT is almost the same for the two regarded CNT diameters. Deviations between the curves are within the uncertainty of the simulation for the studied cases for N_2. This represents also that less N_2 molecules are involved in the adsorption and that the fluctuation of a couple of molecules has a significant impact on the shown adsorbed amount.

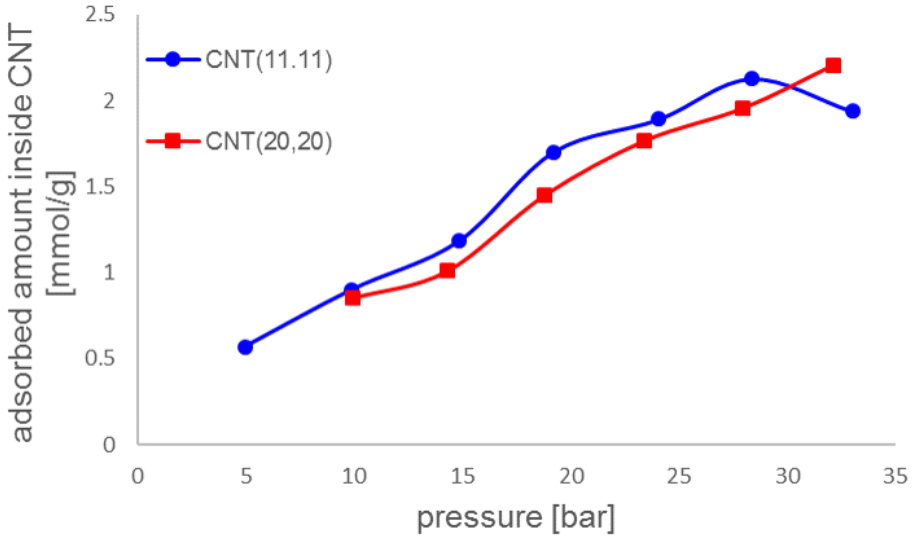

Figure 5.11.: Simulated adsorbed amount of N_2 of the 1. layer inside the CNT of the CNTs CNT(11/11) and CNT(20/20) at $400\,\mathrm{K}$

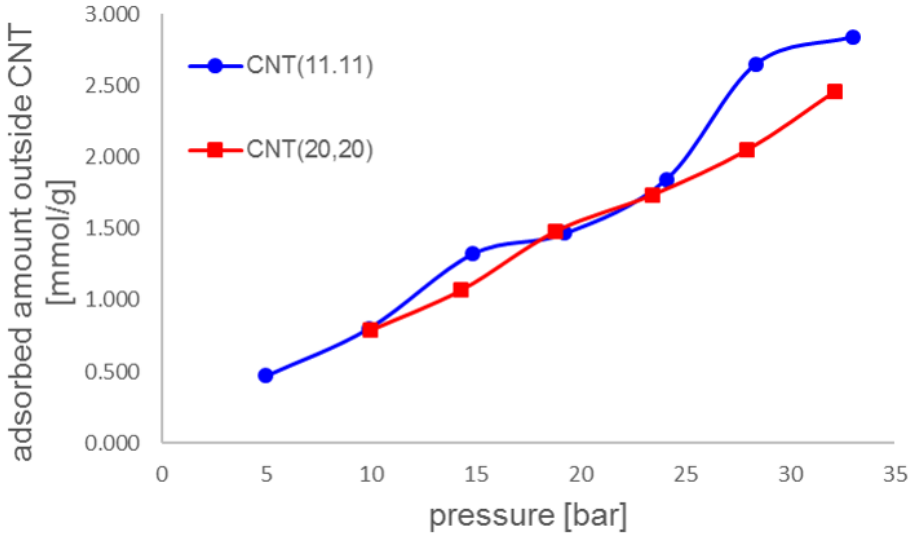

Figure 5.12.: Simulated adsorbed amount of N_2 of the 1. layer outside the CNT of the CNTs CNT(11/11) and CNT(20/20) at $400\,\mathrm{K}$

Due to the weak adsorption of N_2 onto the surface, no major difference between the adsorption inside and outside the CNTs can be seen. This is illustrated by figure 5.13 which shows the ratio of the adsorbed amount inside the CNT over the total adsorbed amount. This ratio is close to 0.5 with the mentioned fluctuation differences and does not show a preference for the inside or the outside or a limitation due to complete filling of the CNT.

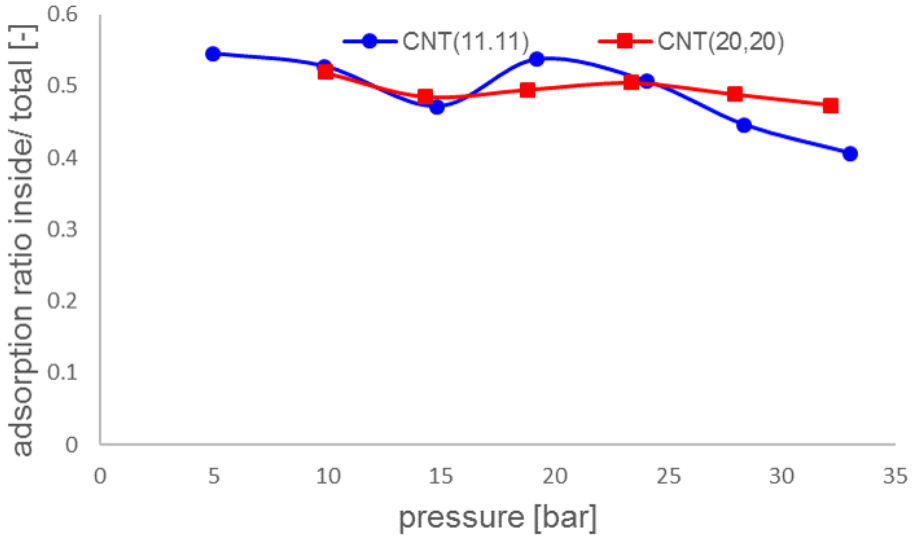

Figure 5.13.: Simulated ratio of the adsorbed amount of N_2 inside the CNTs of the CNTs CNT(11/11) and CNT(20/20) at $400\,\mathrm{K}$ in comparison to the total amount adsorbed of SO_2 in these CNTs

Model fits to the simulated data

Also fits for N_2 adsorption isotherms at CNTs are obtained by the simulated data. An exemplary result of the simulated data and its fits is presented in figure 5.14. An overview how well the fits represent the data and which fits could be performed is given in table 5.2. Further fits and data are presented in appendix D. Here also Langmuirian and Freundlich fits delivered an acceptable representation of the data. For the CNT(20/20) also the DA model is a good representation. For the CNT(11/11) at 125 °C Toth's model also delivers a reasonable fitting result. All other models give only a poor fit if a fit could be obtained at all.

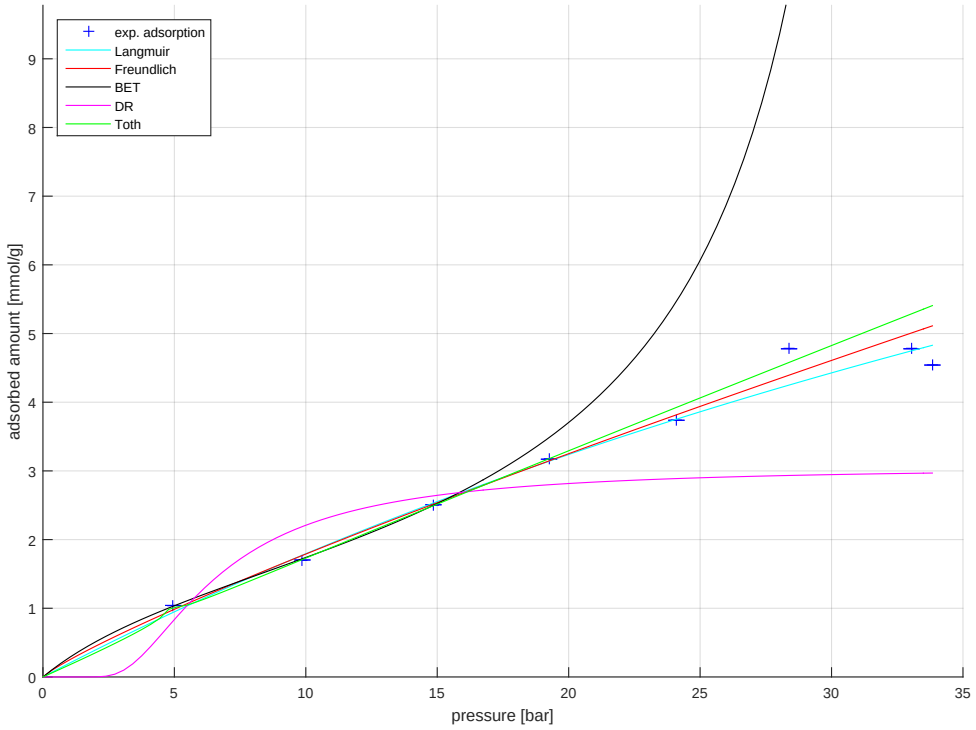

Figure 5.14.: Simulated data of a CNT(11/11) at 400 K in N_2 atmosphere (+) and model fits to the simulated data (lines)

5.1.1.3 Gas mixtures

In this section the adsorption of SO_2 and N_2 in different compositions is studied. To do so an initial gas composition $x_{i,0}$ was set in the simulation cell by the starting configuration (number of SO_2 and N_2 molecules). The total number of each molecule type was kept constant for each simulation run, and it was simulated till equilibrium was reached. Afterwards, the bulk composition y_i and the adsorbate composition x_i were

Table 5.3.: Rating of the goodness of the model fits to the simulated data for CNT(11/11) and CNT(20/20) in N_2 atmospheres and different temperatures (good fit (+), bad fit (-), no fit ( ))

CNT type	T [°C]	Langmuir Ads.	Langmuir Des.	Freundlich Ads.	Freundlich Des.	BET Ads.	BET Des.	DR Ads.	DR Des.	DA Ads.	DA Des.	Temkin Ads.	Temkin Des.	Toth Ads.	Toth Des.
CNT(11/11)	25	+		+				-		-					
CNT(11/11)	75	+		+				-							
CNT(11/11)	125	+		+		-		-		-				+	
CNT(20/20)	25	+		+				-		+					
CNT(20/20)	75	+		+				-		+					
CNT(20/20)	125	+		+				-		-					

estimated. In a next step the selectivity α_{ij} could be evaluated by equation 5.1 with the estimated compositions .[25,37,191]

$$\alpha_{ij} = \left(\frac{x_i}{x_j}\right) \cdot \left(\frac{y_j}{y_i}\right) \tag{5.1}$$

The adsorbed amounts of SO_2 and N_2 are presented in figure 5.15 and figure 5.16. The gas compositions indicated in the legend of this figures are the initial gas compositions of the mixture with respect to SO_2 before adsorption was taking place. For the compositions of 0 % and 100 % SO_2 the bulk gas composition has the same values and does not change during the simulation as no second gas is present in the simulation cell.

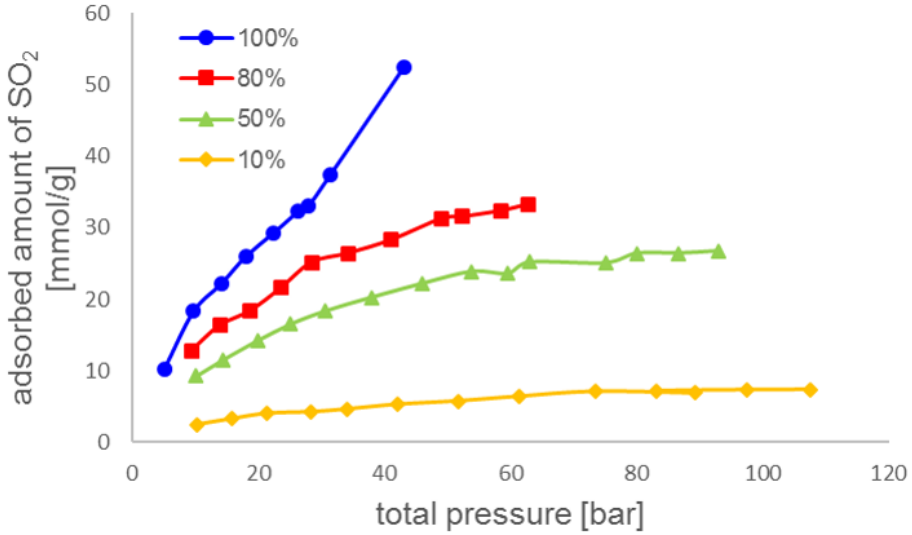

Figure 5.15.: Simulated adsorbed amount of SO_2 at CNT (20/20) at $400\,\mathrm{K}$ starting with different gas compositions of SO_2 and N_2

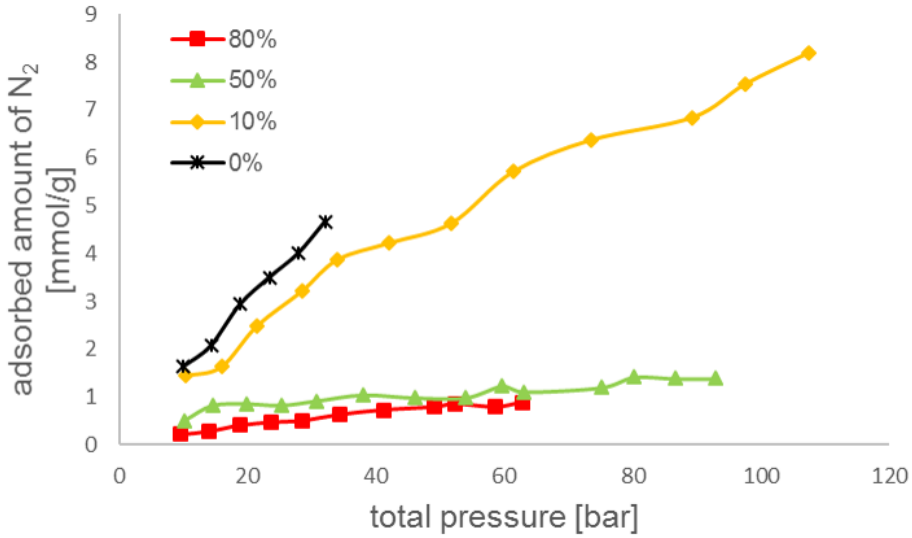

Figure 5.16.: Simulated adsorbed amount of N_2 at CNT (20/20) at $400\,\mathrm{K}$ starting with different gas compositions of SO_2 and N_2

The selectivity for SO_2 seems to be higher at medium gas compositions of SO_2 ($\approx$ 50 % SO_2) than gas compositions with low or high SO_2 content ($\approx$ 10 % or $\approx$ 80 % SO_2) (figure 5.17). Also does the selectivity seem to fluctuate around a mean value independent of the pressure in the studied pressure range, if the first data points of the 50 % mixture are ignored. Nevertheless the selectivity for SO_2 is for all studied compositions above 10 which shows a high adsorption attraction for SO_2.

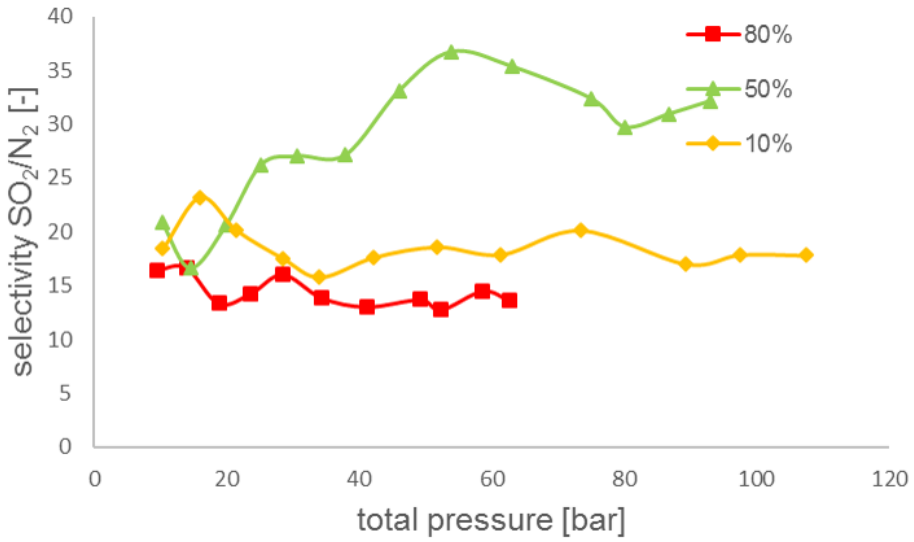

Figure 5.17.: Selectivity for SO_2 at CNT (20/20) at 400 K with different gas compositions of SO_2 and N_2over the total pressure from simulated data

5.1.2 Graphene

For graphene also some simulations have been conducted in SO_2 and N_2 atmospheres. An overview of the studied cases is given in table 5.4

Table 5.4.: Studied graphene cases, temperatures, pressure range, gas composition and charge

	width [nm]	length [nm]	T [K]	p_{bulk} range [bar]	x_{SO_2} [%]	charge [e][a]
Graphene	11.42	11.48	300	0.6 - 4.8	100	0.000
Graphene	11.42	11.48	350	2.6 - 7.3	100	0.000
Graphene	11.42	11.48	400	13.2 - 35.4	100	0.000
Graphene	11.42	11.48	300	0.6 - 4.8	100	0.002-0.010
Graphene	11.42	11.48	300	4.8 - 29.2	0	0.000
Graphene	11.42	11.48	350	4.0 - 28.5	0	0.000
Graphene	11.42	11.48	400	4.4 - 32.9	0	0.000

[a] e denotes the elementary charge $1.602 \cdot 10^{-19}$ A s

5.1.2.1 Adsorption studies with SO_2

Similar to the CNTs also graphene was studied in SO_2 atmospheres. For this, a layer of carbon atoms with the characteristic hexagonal pattern was placed in the simulation box, and different temperatures and amounts of molecules were applied. The resulting isotherms can be seen in figure 5.18. Here the same trend as for the CNTs at different temperatures can be observed.

Likewise to the CNTs, the 1. layer of the adsorbed phase was inspected. Here, a similar trend as for the 1. layer outside the CNT can be seen and that there is not yet a saturation or room limitation at the studied pressures for the temperatures 300 K, 350 K and 400 K established (see figure 5.19).

Furthermore, the simulations with graphene give a limiting value for the adsorption of SO_2 for the respective pressure as no curvature restrictions exist as for the CNTs. A comparison of the CNT cases and the graphene simulations is shown in figure 5.20. And the simulated adsorbed amount at graphene is above or at the same value as for the shown CNTs.

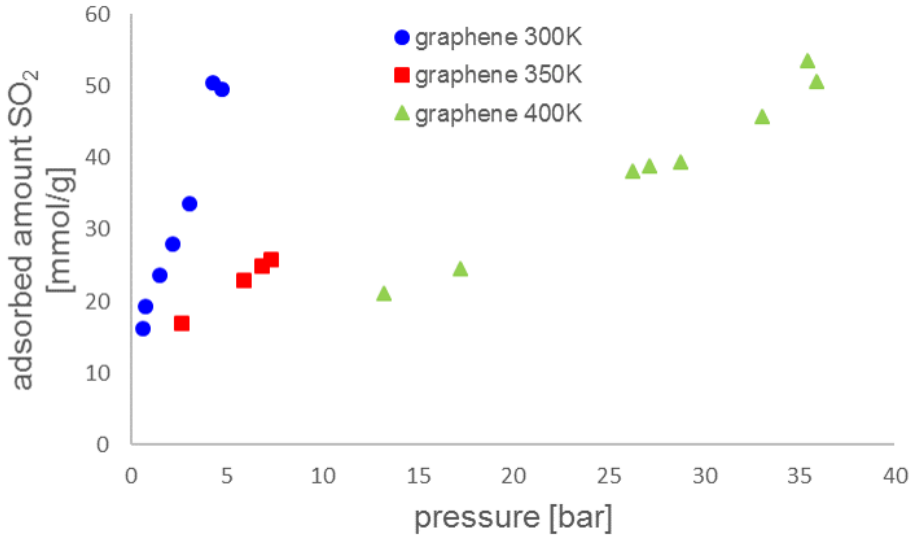

Figure 5.18.: Simulated total adsorbed amount of SO_2 on graphene at 300 K, 350 K and 400 K

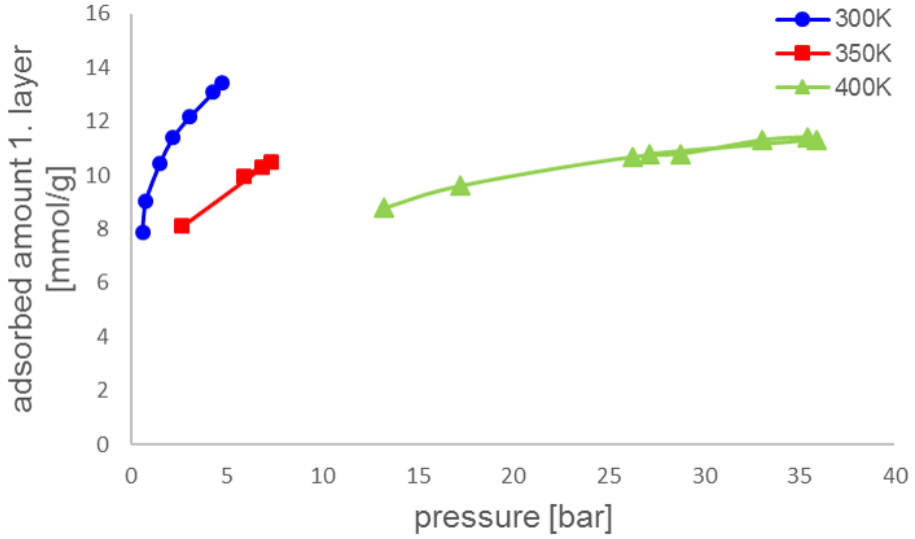

Figure 5.19.: Simulated adsorbed amount of the 1. SO_2 layer at graphene at 300 K, 350 K and 400 K

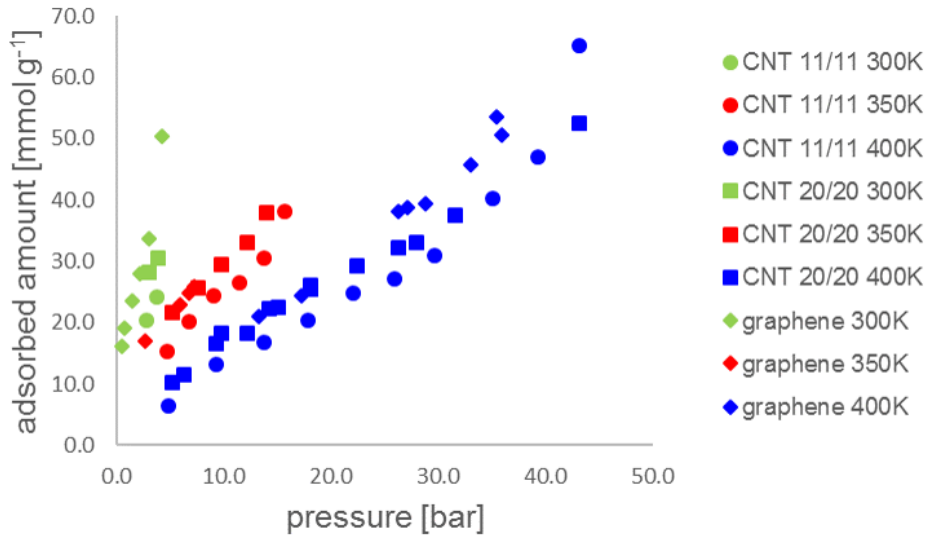

Figure 5.20.: Comparison of the simulated total adsorbed amount of SO_2 at graphene and CNTs at 300 K, 350 K and 400 K

At graphene also a variation of the applied charge was done. Therefore the same simulation setup was taken, and only the charge per carbon atom was varied. The temperature, number of molecules and geometrical system size were kept constant. However, it is obvious as more adsorption occurs the bulk pressure drops which means that at the same pressure even more SO_2 would be adsorbed. That is why figure 5.21 only gives an estimate how much the adsorption is increased by applying different charges to the carbon atoms. Would the same bulk pressures be simulated the adsorbed amount with higher charges would be even higher.

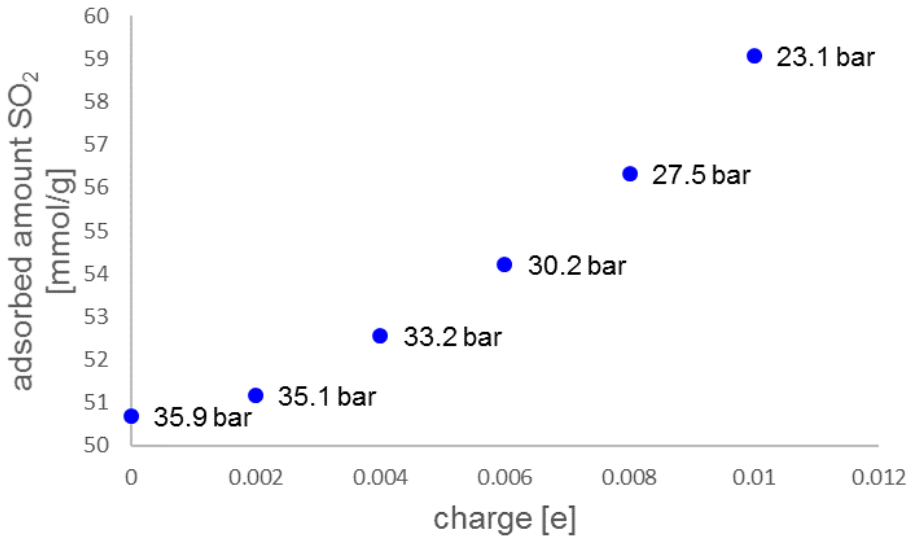

Figure 5.21.: Simulated adsorbed amount at graphene in SO_2 at $400\,\mathrm{K}$ with variation of the charge per carbon atom. For each data point the resulting simulated bulk pressure is presented in the chart next to the data point.

Model fits to the simulated data

Also, simulations of graphene in SO_2 atmospheres were fitted to the different adsorption models named previously. For the Langmuir and Freundlich model, the fits agree reasonable to the simulated data points. Toth's model does not represent the data very well but can be fitted. Again, the DR and DA model do show the least good fit of the data. The BET model and Temkin model could only be done for the studied case at 350 K. Exemplary figure 5.22 is presented for the fits on graphene. A table which fits can be done is presented in table 5.5 with a rating of the fit quality to the simulated data. Further data is presented in appendix D.

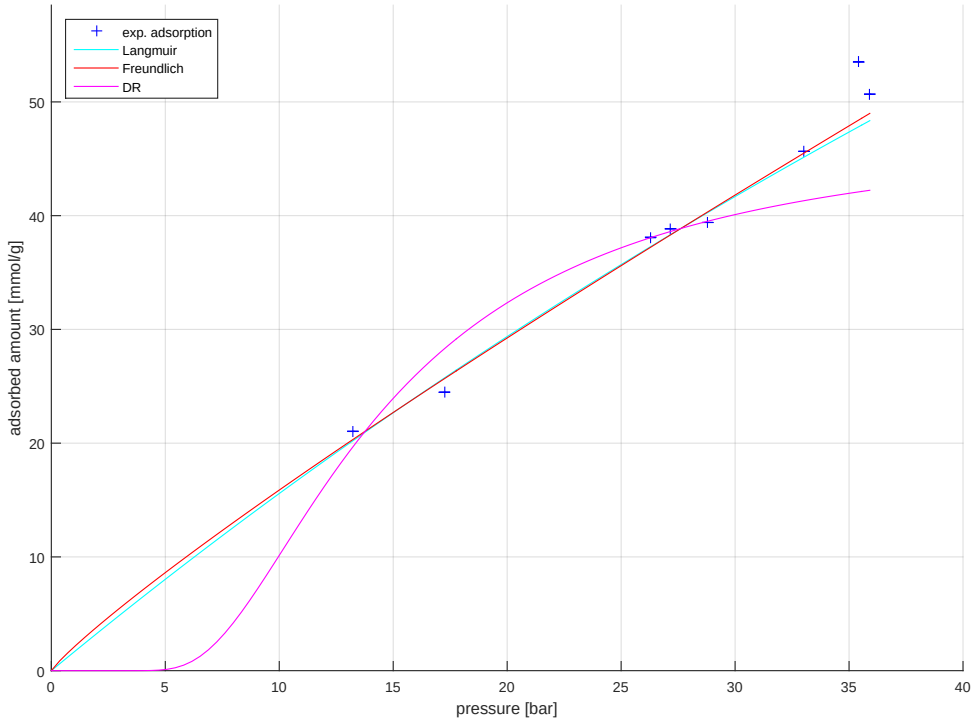

Figure 5.22.: Simulated data of graphene at 400 K in SO_2 atmosphere (+) and model fits to the simulated data (lines)

Table 5.5.: Rating of the goodness of the model fits to the simulated data for graphene in SO_2 atmospheres and different temperatures (good fit (+), bad fit (-), no fit ( ))

type	T	Langmuir		Freundlich		BET		DR		DA		Temkin		Toth	
	[°C]	Ads.	Des.	Ads.	Des.	Ads.	Des.	Ads.	Des.	Ads.	Des.	Ads.	Des.	Ads.	Des.
Graphene	25	+		+				-		-					
Graphene	75	+		+		+		-		-		+		-	
Graphene	125	+		+				-		-					

5.1.2.2 Adsorption studies with N_2

The adsorption of nitrogen on graphene was examined as well. As expected from simulations with CNTs the adsorption of N_2 on graphene was also weak. The temperatures 300 K, 350 K and 400 K were simulated and are shown in figure 5.23 in comparison with CNT data. The adsorption results of the simulations are in good agreement with each other.

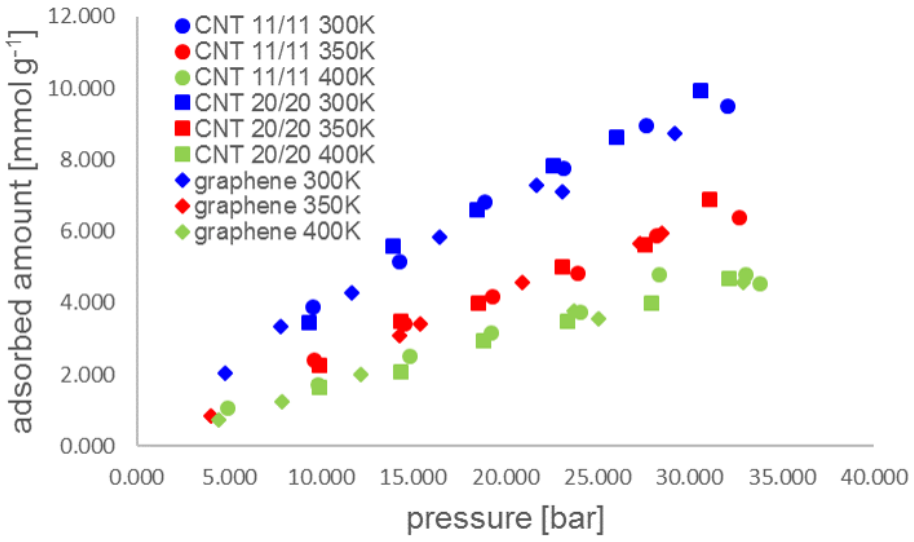

Figure 5.23.: Comparison of the simulated total adsorbed amount of N_2 at graphene and CNTs at 300 K, 350 K and 400 K

Model fits to the simulated data

Similarly, to the CNT data in nitrogen atmospheres also the graphene data in N_2 atmospheres was fitted to different adsorption models. The fits and the fit data is presented in the appendix D. For N_2 adsorbed on graphene the Langmuir, Freundlich and Toth model show a reasonable fitting behavior. The DA model shows for two of the three cases a reasonable agreement. The BET and DR model fits do not represent the simulated data well. The Temkin fit could not be performed with the simulated data for graphene at all.

5.1.3 Heat of adsorption

As mentioned in chapter 2.1.3 the heat of adsorption can be derived if isotherms at different temperatures are known. The data points obtained from simulation were taken and fitted with the described model from equation 2.39 and then the heat of adsorption is derived in the shown analytical manner. In figure 5.24 the heat of adsorption for SO_2 and N_2 is shown for a CNT(11/11), CNT(20/20) and graphene. It can be seen that SO_2 releases a higher heat of adsorption than N_2. For nitrogen, the curves for a CNT(11/11), CNT(20/20) and graphene are in good agreement. For sulfur dioxide, the curves for the CNT(11/11) and CNT(20/20) are close to each other. For the graphene, the heat of adsorption is estimated to be approximately 5 $kJmol^{-1}$ higher than for the CNTs. This might arise from the fact that graphene showed slightly higher adsorption at 400 K at higher pressures and that in the low-pressure region fewer data points were available than for the CNTs. This might have put greater weight on the fitting procedure to the higher adsorbed amount, yielding to a higher predicted heat of adsorption.

To make a comparison between the heat of adsorptions, the gained heat of adsorption was averaged over the adsorbed amount. In figure 5.25 the averaged values for the simulated CNT(11/11), CNT(20/20) and graphene is shown. The error bars represent the minimal and maximal heat of adsorption in the range of first molecules adsorbed till the full range adsorbed in an adsorbed amount-heat of adsorption plot.

What also has to be mentioned is that the value of the heat of adsorption is not influenced by the adjustment factors used for the simulated data to compare it to experiments. (The adjustment factors are introduced in more detail in chapter 5.3.) What is influenced by the adjustment factors is the maximal loading. The shape of all heat of adsorption curves remains the same.

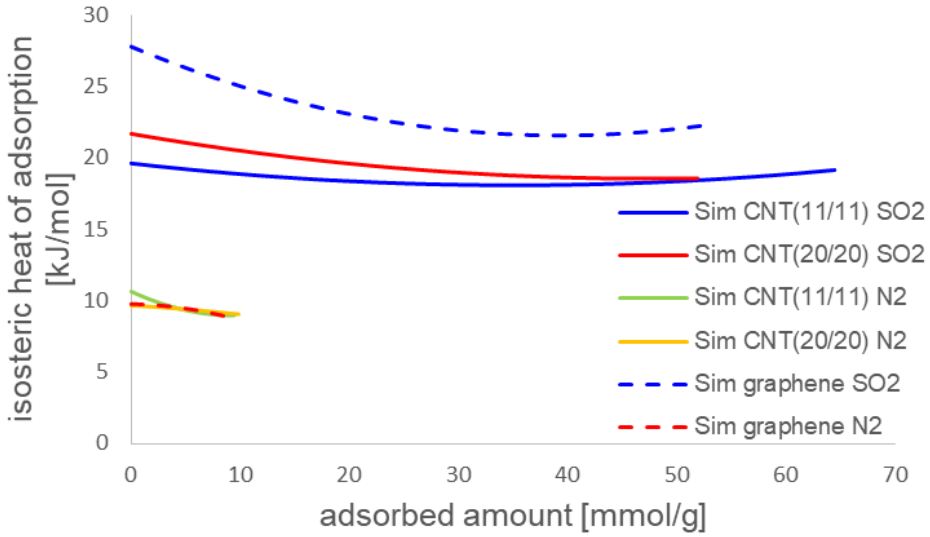

Figure 5.24.: Heat of adsorption over adsorbed amount from simulation for SO_2 and N_2 for a CNT(11/11), CNT(20/20) and graphene

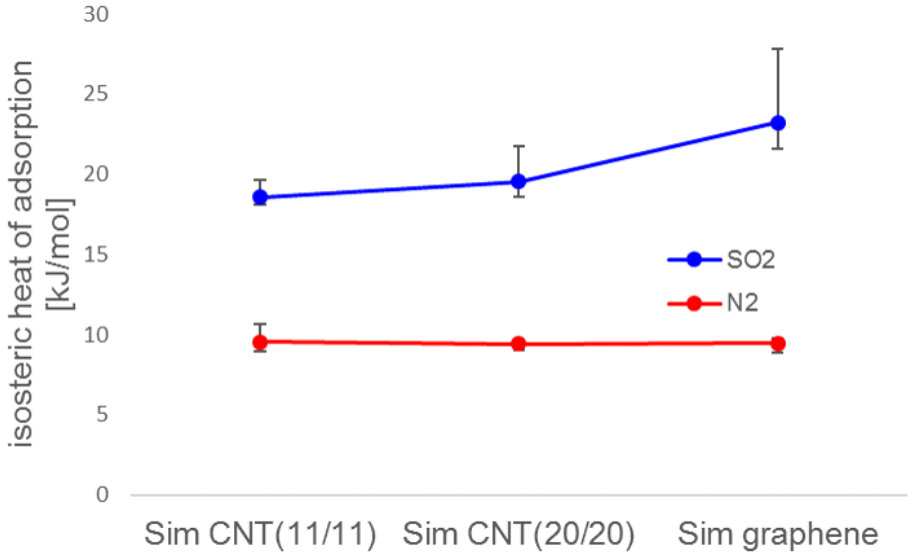

Figure 5.25.: Heat of adsorption from simulation for SO_2 and N_2 for a CNT(11/11), CNT(20/20) and graphene

5.2 Results from gravimetric experiments

In this section, the experimental data gained from the gravimetric setup is presented and discussed. The experimental setup itself is presented in more detail in chapter 4.1.

BET measurements in N_2 atmospheres at 77 K have been conducted on a commercial volumetric setup and are also presented in this section at the very beginning. They provide the BET surface area of the used materials.

5.2.1 BET measurements

The BET measurements have been performed by the Schneider group of the chemistry department from TU Darmstadt and Turek group of the Institute of Chemical and Electrochemical Process Engineering from TU Clausthal. The measurements were conducted on a commercial NOVA Station A from Quantachrom and an ASAP 2020 from Micromeritics. All BET measurements are done with nitrogen at 77 K. From these measurements, the BET surfaces of the nanotube samples could be obtained. The BET surface areas for the respective samples are presented in table 5.6. The BET data to this measurements can be found in the Appendix E.6. A combination of all N_2 isotherms at 77 K is given in figure 5.26. The BET surface area of the SWCNTs is smaller than expected. A reason for this could be that the sample contains also a portion of MWCNT as the TEM images in figure 2.13 show.

Table 5.6.: BET surface areas measured at 77 K with nitrogen

CNT type	BET $[m^2g^{-1}]$	
MWCNT ind. grade	239	
MWCNT	282	
SWCNT	552	
VACNT	492	[192]

5.2.2 Influence of the sample activation and the measurement order

To study the influence of the activation procedure on the probe materials of the CNTs, scientific grade MWCNTs were studied with nitrogen at different activation temperatures. Furthermore, an activated sample was compared to an unactivated sample. In an

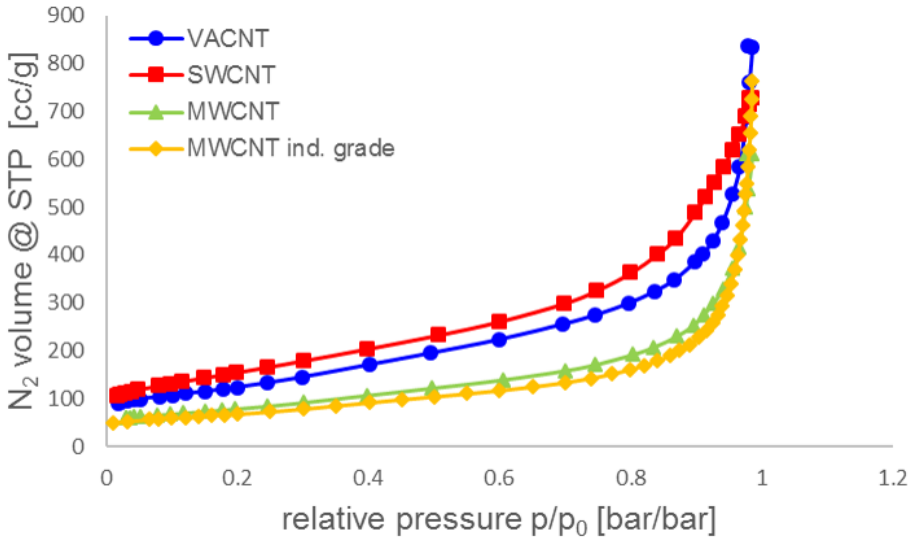

Figure 5.26.: N_2 BET isotherms of CNTs, MWCNTs, SWCNTs and VACNTs[192] at 77 K

additional run, the effect of the order of the buoyancy measurement was studied. The buoyancy measurement was first done directly after the activation, which is the normal procedure, and then a measurement is done with the sample. Secondly, the experiment was performed in the way that the activation was directly followed by the measurement with N_2. After that the buoyancy measurement was recorded.

Different activation temperatures

First, it was studied whether the activation temperature of the CNTs influences the measurement. Therefore, a scientific grade MWCNT was activated at 300 °C and then measured in a N_2 atmosphere at 125 °C. Then the same sample was activated at 150 °C and then also measured in a N_2 atmosphere at 125 °C. A comparison of the two adsorption isotherms showed that there was no significant difference depending on the activation temperature (see figure 5.27). So one can conclude that for unfunctionalized CNTs the activation temperature does not seem to play a major role.

Comparison of an activated CNT to an unactivated CNT

To have a closer look at the assumption from the previous paragraph activated and unactivated industrial grade CNTs were introduced to SO_2 at 25 °C. The measured data agree very well with each other, and it cannot be distinguished between the activated and the unactivated sample by having a look at the data points (see figure 5.28). What might have activated the unactivated sample was the helium measurement for

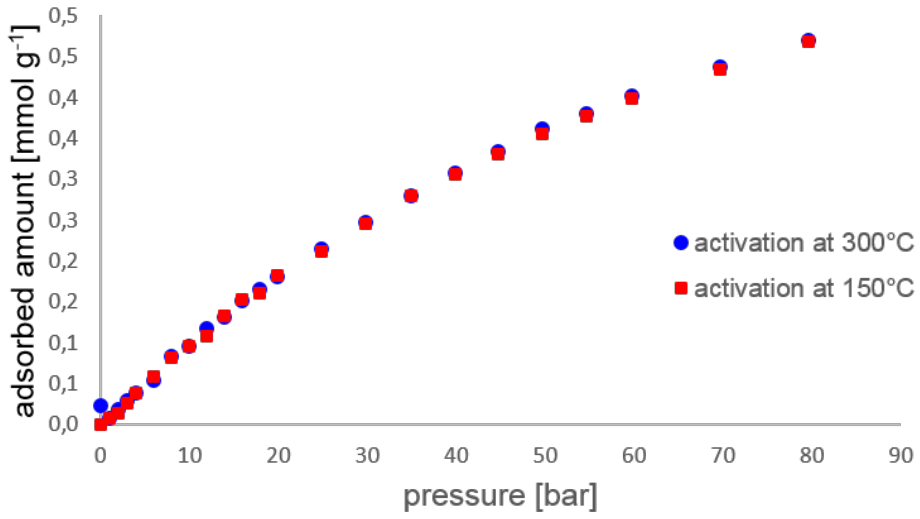

Figure 5.27.: Influence of the activation temperature on a MWCNT measured with N_2 at 125 °C (the data points for the activation at 300 °C and 150 °C coincide)

the buoyancy correction which was done as usual previous to the measurement with SO_2 and at the respective temperature of the measurement. Here this was 25 °C. This leads to an even further assumption that unfunctionalized CNTs do not need activation for measurement or are activated by a simple vacuum or helium flush at the measuring temperature. However, all following measurements were executed in the way that activation was followed by a buoyancy measurement and then by measurement with the measuring gas if it is not stated differently. This order is the usual order and is commonly accepted in the adsorption community.

Order of measurement He/N_2 or N_2/He

It was also studied if there is an influence on the evaluated data if the buoyancy measurement is done before the measurement with nitrogen or after the measurement with nitrogen. Therefore scientific grade MWCNTs were measured in the described orders. No difference between the measurements is seen. So it appears that it does not play a significant role if the buoyancy measurement is performed before or after the respective measurement (compare figure 5.29).

This is very unusual, but it could be seen throughout all measurements with CNTs that they barely show any hysteresis, which might be one of the reasons that it does not matter when the buoyancy measurement is performed if CNT materials are regarded. However, for all data (except for the described case) the buoyancy measurement was

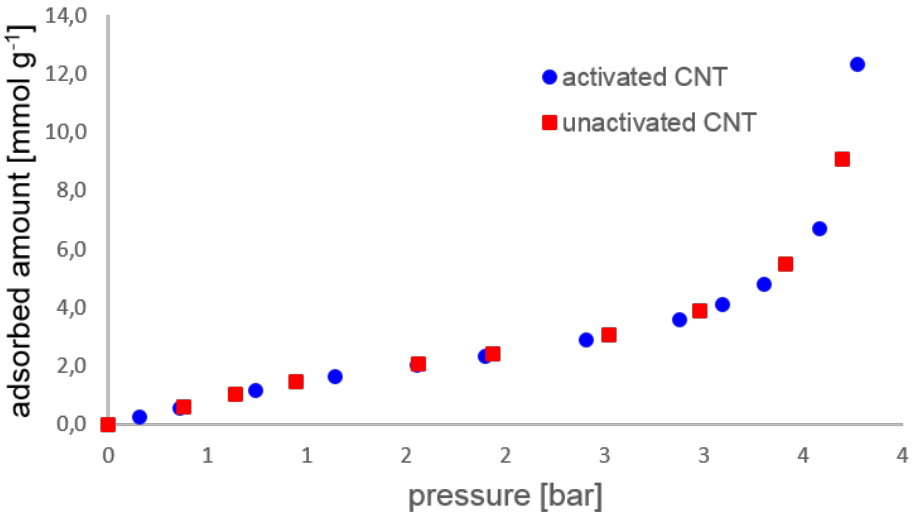

Figure 5.28.: Comparison of an activated CNT to an unactivated CNT measured in a SO_2 atmosphere at 25 °C (the measured data coincides)

done before the measurement with the respective gas which is also generally accepted in the adsorption community.

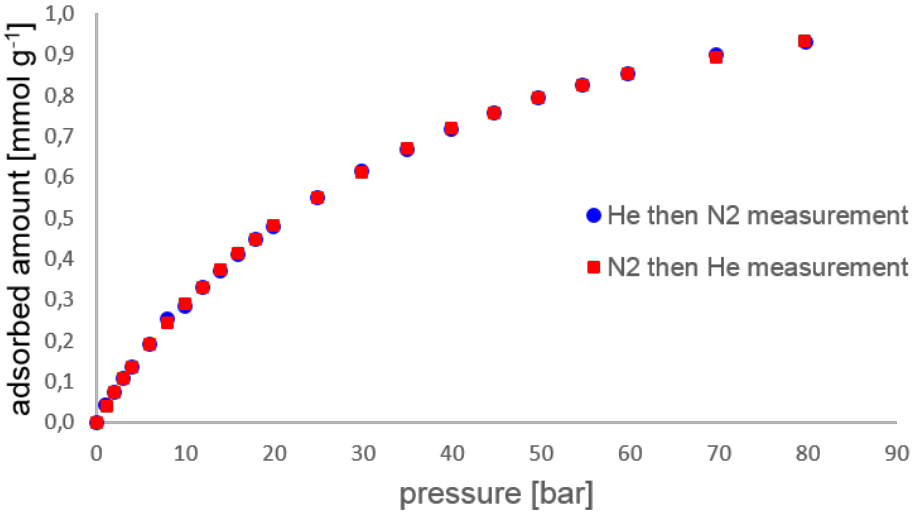

Figure 5.29.: Execution of the buoyancy measurement before and after the measurement with N_2 at scientific grade MWCNTs at 25 °C (the measured data coincides)

5.2.3 Cycling

For CNTs the cycling with CO_2 was also studied. It was analyzed whether the adsorbed amount is influenced by cycling. For this purpose a CNT sample was activated and measured in a helium atmosphere and then exposed to CO_2 at 40 °C in the pressure range from vacuum to 60 bar for the first cycle. Then the probe was desorbed to a pressure of 1 bar in various steps. From the pressure of 1 bar the second cycle was started. For all other cycles, the starting point for adsorption was also not vacuum but 1 bar. The amount adsorbed did not show a significant change in the uptake the more cycles were performed (see figure 5.30). Here in total nine cycles were performed which allow the conclusion that CNTs are excellent for ad- and desorption cycles regarding the reproducibility.

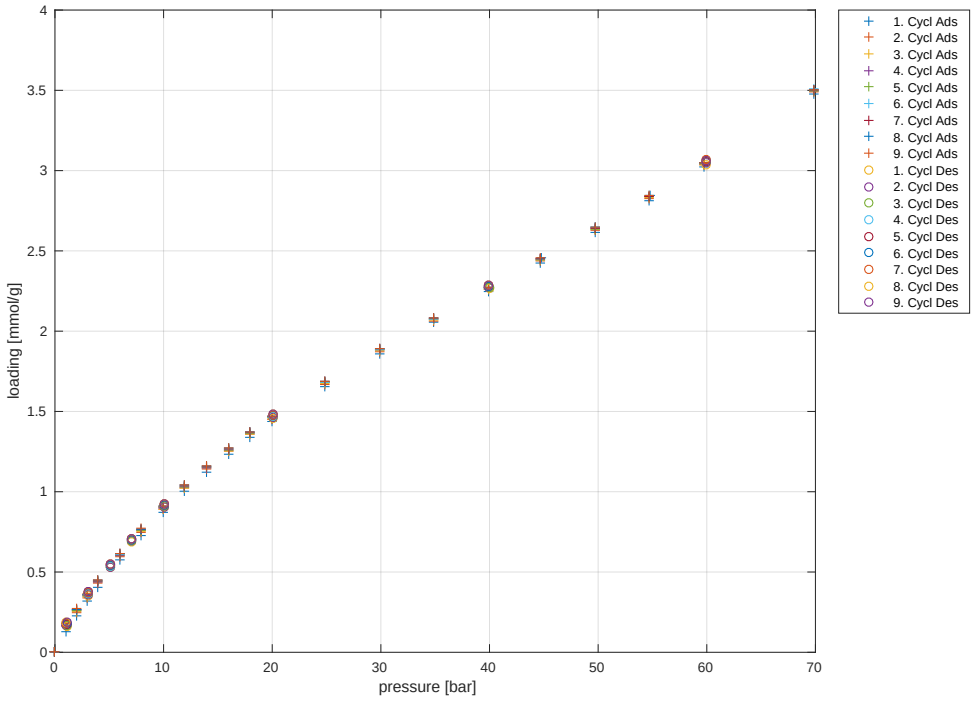

Figure 5.30.: Cycling with CO_2 at CNTs at 40 °C (the measured data coincides for most of the data points)

5.2.4 CNTs

In this section, the experiments conducted with the different CNT types namely industrial grade CNTs, MWCNTs, SWCNTs and VACNTs in various atmospheres (CO_2, SO_2 and N_2) are presented.

5.2.4.1 Adsorption studies with CO_2

First experiments with CNTs were done in CO_2 atmospheres. A reason for this was to get familiar with the measurement procedure with a relatively non-toxic gas. Additionally, should all functions of the setup be tested such as operability, leakage rate, response time for inputs etc. The results of these measurements are presented in figure 5.31. The measurement at 25 °C shows only data beyond approximately 1.5 bar because of an error with the pressure transducer beforehand which allowed no data logging. The isotherms at 0 °C and 25 °C were measured to the saturation pressure. The other isotherms were measured to 60 bar respectively 50 bar. The trends of the isotherms are as expected. The desorption data coincides very good with the adsorption data and is presented in the appendix E.

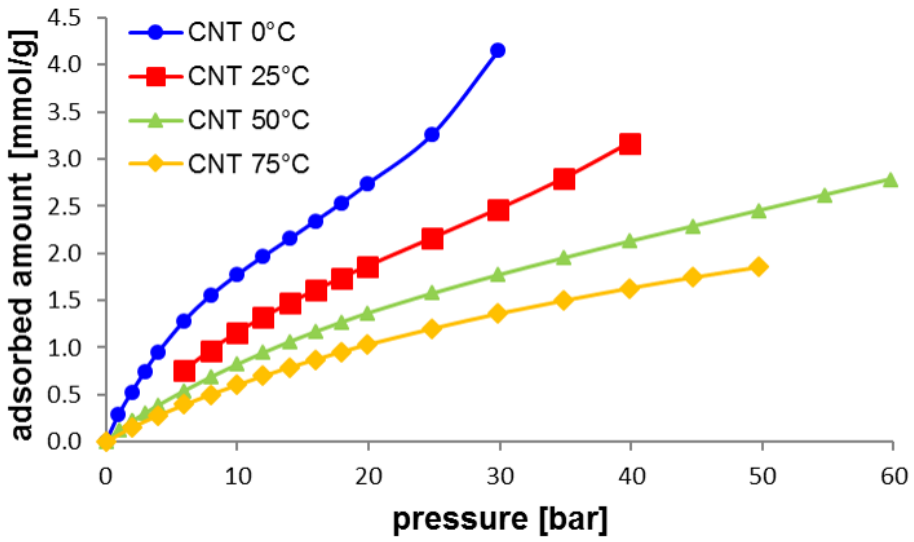

Figure 5.31.: Adsorption isotherms of CNTs in CO_2 atmosphere at the temperatures 0 °C, 25 °C, 50 °C and 75 °C

Model fits to the experimental data with CO_2

The model fits to the experimental data for adsorption and desorption is presented for all cases in appendix E. An overview of the fits which could be performed and how well the experimental data is represented is given in table 5.7. In figure 5.32 exemplary the obtained fits from experimental data on industrial grade CNTs in CO_2 atmospheres is presented. It can be seen that the Langmuir, Freundlich and DA models fit well to the experimental data for ad- and desorption. The BET model gives a good representation

of the data until medium pressures. DR and Temkin's model do not give a good fit result over the whole range and represent only parts of the data or do not show a good fitting behavior at all.

Table 5.7.: Rating of the goodness of the model fits to the experimental data for industrial grade CNTs in CO_2 atmospheres and different temperatures (good fit (+), bad fit (-), no fit ( ))

CNT	T	Langmuir		Freundlich		BET		DR		DA		Temkin		Toth	
type	[°C]	Ads.	Des.	Ads.	Des.	Ads.	Des.	Ads.	Des.	Ads.	Des.	Ads.	Des.	Ads.	Des.
CNT	0	+	+	+	+	+	+	-	-	+	+		-		
CNT	25	+	-	+	-	+		-	-	+					
CNT	50	+	+	+	+	+	+	-	-	+	+		-		
CNT[a]	50	+	+	+	+	+	+	-	-	+	+		-		
CNT	75	+	+	+	+	+	+	-	-		+		-		

[a] 2. cycle

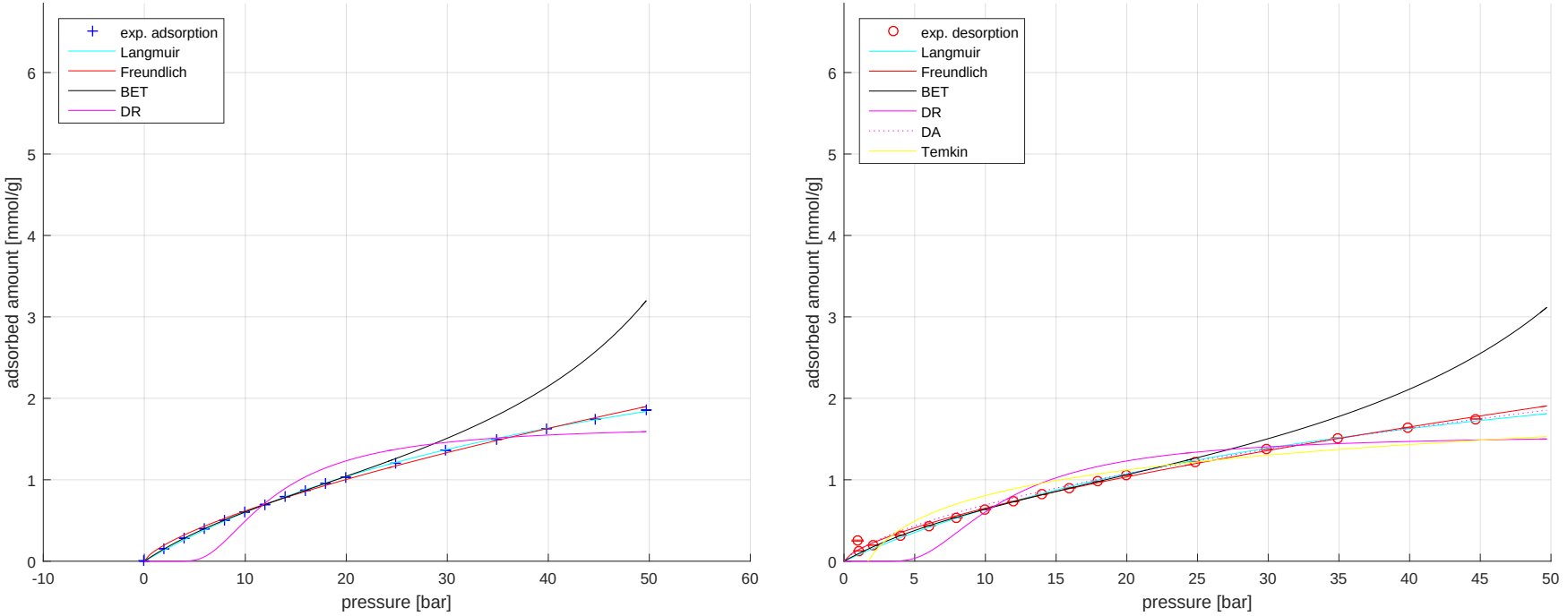

(a) adsorption **(b)** desorption

Figure 5.32.: Experimental data of industrial grade CNTs at 75 °C in CO_2 atmosphere (+ (adsorption data)/ ∘ (desorption data)) and model fits to the simulated data (lines) for the adsorption (a) and desorption data (b)

5.2.4.2 Adsorption studies with SO_2

In experiments with SO_2 atmospheres various CNT types were studied at temperatures between 25 °C and 125 °C at pressures up to the respective saturation pressure or pressures close to 40 bar. The 40 bar limit was a system limitation of the measurements with the manually operated gas dosing system.

CNT

Adsorption at industrial grade CNTs from Nanolab Inc. shows that at low temperatures the highest adsorption can be achieved (compare figure 5.33). Close to the saturation pressure a steep increase of the adsorption can be seen which might arise from capillary condensation. For the temperature of 125 °C this increase cannot be seen because the saturation pressure of approximately 46 bar was not in reach for the used experimental setup. In figure 5.33 only the adsorption branch of each measurement is presented. The desorption data for SO_2 is almost identical with the adsorption data which was discussed already earlier in 5.2.3 and allows the conclusion that only physisorption is taking place. All experimental points are listed in appendix E. There, a graph is shown which includes the adsorption and desorption branch of each measurement.

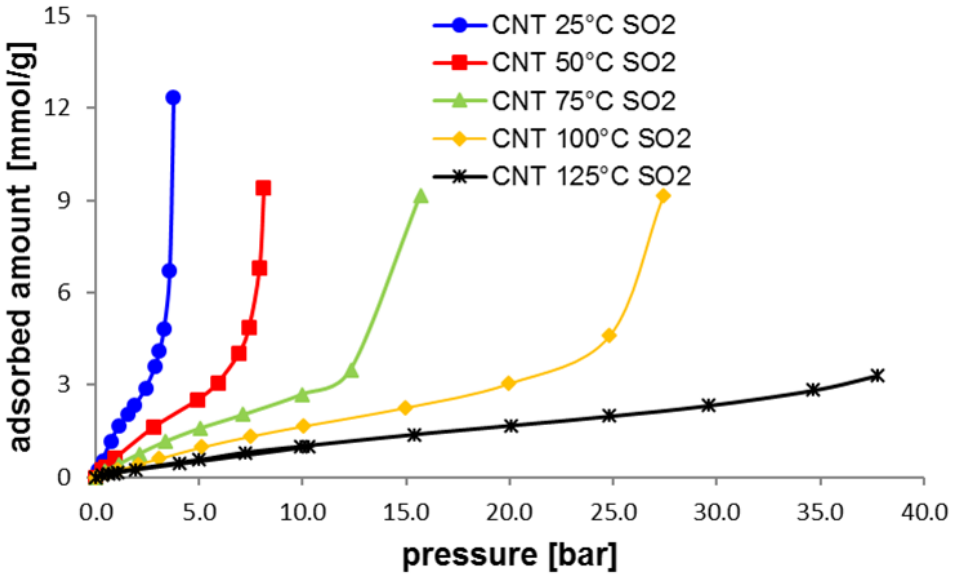

Figure 5.33.: Adsorption isotherms of industrial grade CNTs in SO_2 atmosphere at the temperatures 25 °C, 50 °C, 75 °C, 100 °C, 125 °C

MWCNT

The adsorption behavior at the MWCNTs from Nanolab Inc. (compare figure 5.34) is similar to the adsorption behavior described in the previous section. Here, however, the MWCNTs have a higher adsorption capacity than the CNTs. One reason for this is the higher purity of the MWCNTs in comparison to the CNTs which results in higher BET surface area (see table 5.6).

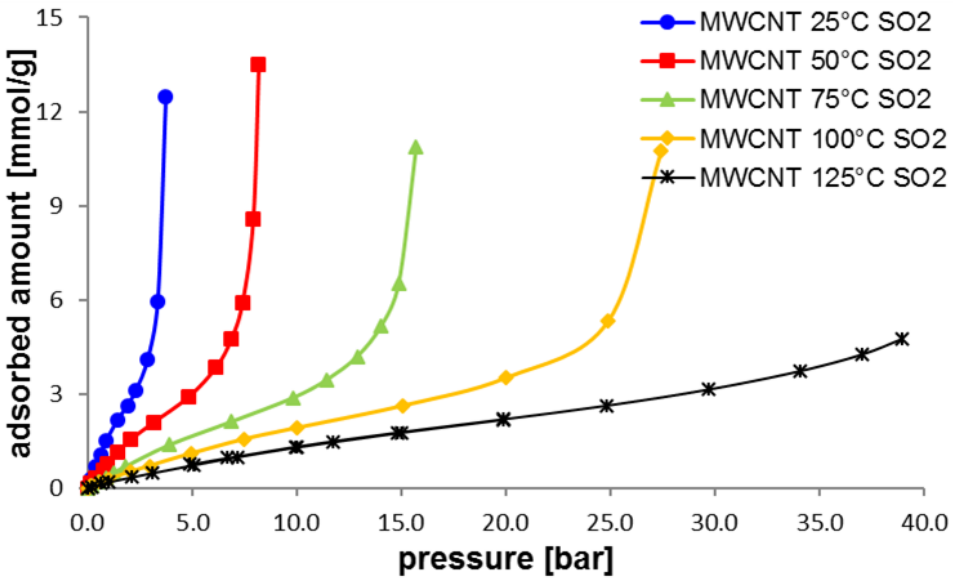

Figure 5.34.: Adsorption isotherms of MWCNTs in SO_2 atmosphere at the temperatures 25 °C, 50 °C, 75 °C, 100 °C, 125 °C

SWCNT

The SWCNTs from Nanolab show again a higher adsorption behavior than the MWCNTs and CNTs (compare figure 5.35). These CNTs have the highest BET surface area of the studied CNTs (see table 5.6). All other trends are similar to the already described trends.

VACNT

The VACNTs were provided by the Schneider group of the chemistry department of TU Darmstadt and showed a slightly lower BET surface area than the SWCNTs. This can also be seen in the adsorption isotherm in figure 5.36. They display a lower capacity for SO_2 than the SWCNTs. However, the capacity is higher than for the studied MWCNTs. For the VACNTs only the temperatures 25 °C, 50 °C and 75 °C were studied. The almost equivalent loading of the last data point of each isotherm is by coincidence that the

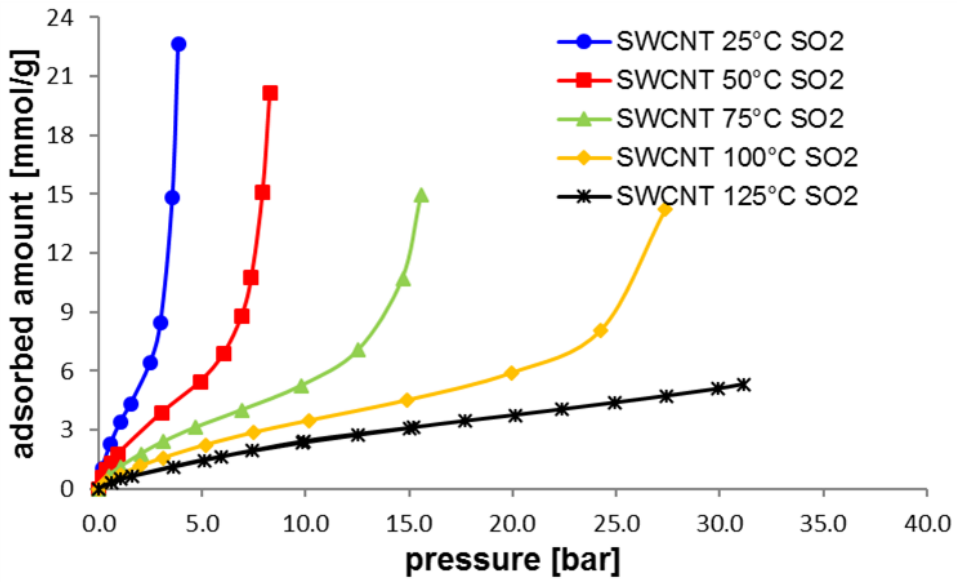

Figure 5.35.: Adsorption isotherms of SWCNTs in SO_2 atmosphere at the temperatures 25 °C, 50 °C, 75 °C, 100 °C, 125 °C

last data point (at saturation pressure) always takes the longest to reach equilibrium and that in the case for the VACNT for the last data point of each adsorption series equilibrium was not fully established. However, the general trends are met, and the data can be compared to the other studied CNT types. The expected trends are met and these CNTs also showed no significant hysteresis for the uptake during and after desorption.

Model fits to the experimental data with SO_2

For all experiments with the various CNT types in SO_2 atmospheres model fits with the described models were done. Exemplary, the fits to SWCNTs adsorption and desorption data at 75 °C are shown in figure 5.37. All fits and data tied to experimental data in SO_2 atmospheres are presented in appendix E. Table 5.8 gives an overview which fits could be performed and how well they represent the data. It can be mentioned that for all CNT types in SO_2 atmosphere Langmuir, Freundlich and DA fits could be performed which represent the data for low to medium relative pressures well. Deviations from these models show the data points towards the end of an isotherm in the region where the significant rise in adsorption can be seen. Temkin's and Toth's model could only be fitted to some cases, in most cases no fit could be performed with these models for the measured data or a poor fitting result is obtained. The fits with the DR model could be performed, however, do they only show a poor correlation to the experimental data. The BET model which should be applicable to fit a multilayer behavior of the

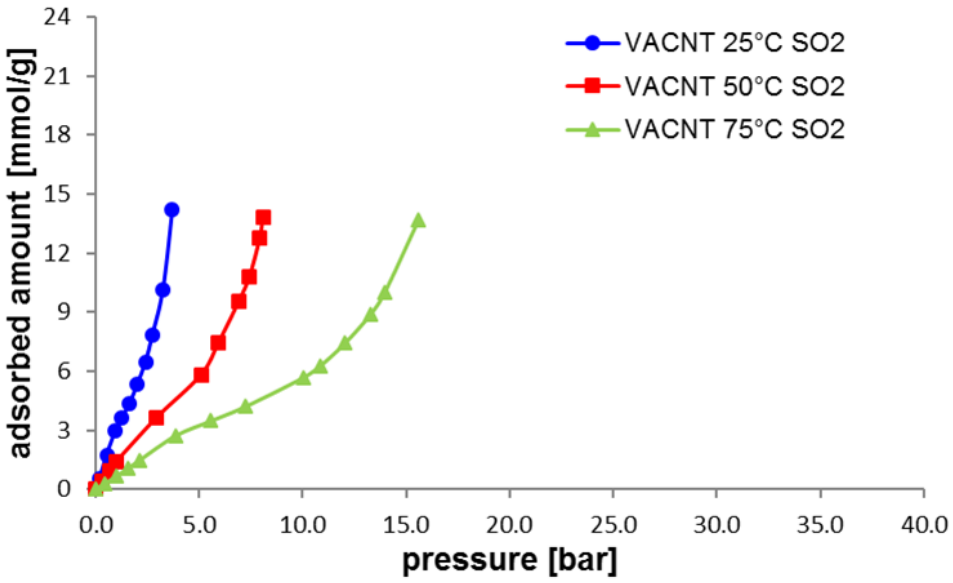

Figure 5.36.: Adsorption isotherms of VACNTs in SO_2 atmosphere at the temperatures 25 °C, 50 °C, 75 °C

adsorption isotherm, especially in the region towards the saturation pressure, did only show an acceptable correspondence to the measured data for low to medium pressures. Towards the saturation pressure, the BET model overpredicts the experimental data. This might be a hint that if longer equilibrium times are allowed at higher pressures a higher adsorbed amount might be achieved.

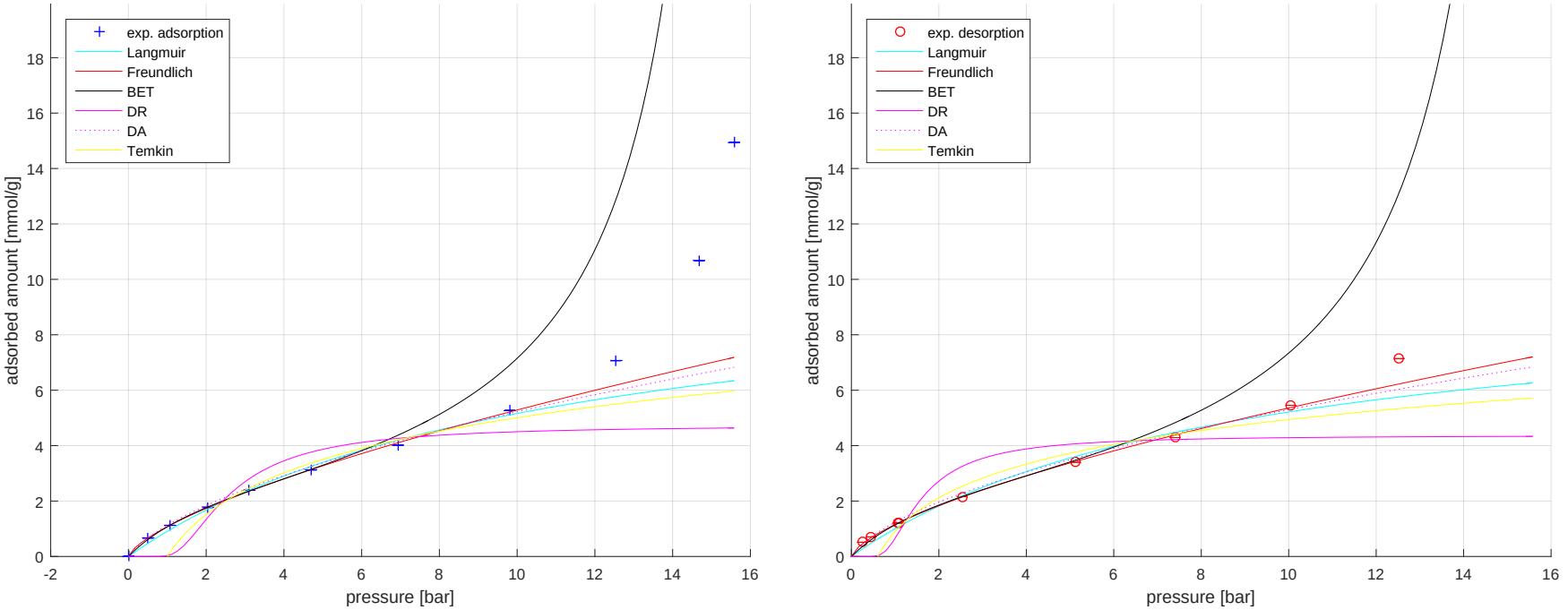

(a) adsorption **(b)** desorption

Figure 5.37.: Experimental data of SWCNTs at 75 °C in SO_2 atmosphere (+ (adsorption data)/ ∘ (desorption data)) and model fits to the simulated data (lines) for the adsorption (a) and desorption data (b)

Table 5.8.: Rating of the goodness of the model fits to the experimental data for different CNT types in SO_2 atmospheres and different temperatures (good fit (+), bad fit (-), no fit ( ))

CNT	T	Langmuir		Freundlich		BET		DR		DA		Temkin		Toth	
type	[°C]	Ads.	Des.	Ads.	Des.	Ads.	Des.	Ads.	Des.	Ads.	Des.	Ads.	Des.	Ads.	Des.
VACNT	15	+	+	+	+	+	+	-	-		+		-		
VACNT	25	+	+	+	+	+	+	-	-		+	-	-		
VACNT	35	+	+	+	+	+	+	-	-	+	+	-	-	+	+
VACNT	50	+	+	+	+	+	+	-	-	+	+		-		
VACNT	75	+	+	+	+	+	+	-	-		+		-		
SWCNT	25	+	+	+	+	+	+	-	-		+			+	+
SWCNT	50	+	+	+	+	+	+	-	-	+	+		-		+
SWCNT	75	+	+	+	+	+	+	-	-	+	+	-	-		
SWCNT[a]	75	+	+	+	+	+	+	-	-	+	+	-	-		
SWCNT	100	+	+	+	+	+	+	-	-	+	+		-		
SWCNT	125	+	+	+	+	+	+	-	-	+	+		-		
MWCNT	25	+	+	+	+	+	+	-	-	+	+		-		
MWCNT	50	+	+	+	+	-	-	-	-	+	-	-	+		
MWCNT	75	+	+	+	+			-	-	+	-		-		
MWCNT	100	+	+	+	+	+	+	-	-	+	+	-	+		
MWCNT	125	+	+	+	+	+	+	-	-		+				
CNT	25	+	+	+	+	+	+	-	-	+	+				
CNT[a]	25	+		+		+		-		+					
CNT[b]	25	+		+		+		-		+					
CNT	50	+	+	+	+		+	-	-	+	+		+		
CNT	75	+	+	+	+	-		-	-			-			
CNT	100	+	+	+	+	+	+	-	-	+	+	-	-		
CNT	125	+	+	+	+	+	+	-	-	+	+				

[a] 2. cycle
[b] no activation of the sample performed

5.2.4.3 Adsorption studies with N_2

For the experiments in N_2 atmospheres also different CNT types were utilized. All measured data points can be found in appendix E. The experiments with N_2 were performed before the experimental setup was equipped with the manual gas dosing system. This allowed in theory measurements up to 150 bar. For the N_2 measurements only pressures up to 80 bar were conducted.

CNT

The isotherms in figure 5.38 show weak adsorption of nitrogen at the industrial grade CNTs which is almost an order of magnitude lower than for SO_2 adsorption. The curves at 100 °C and 125 °C are close to each other which they should not be. Reasons for this are unclear and have to be further investigated. Overall show the isotherms a Langmuirian type adsorption behavior. The adsorption capacity is not reached, because there exists no saturation pressure for N_2 at the studied conditions and pressures beyond 80 bar were not considered to study.

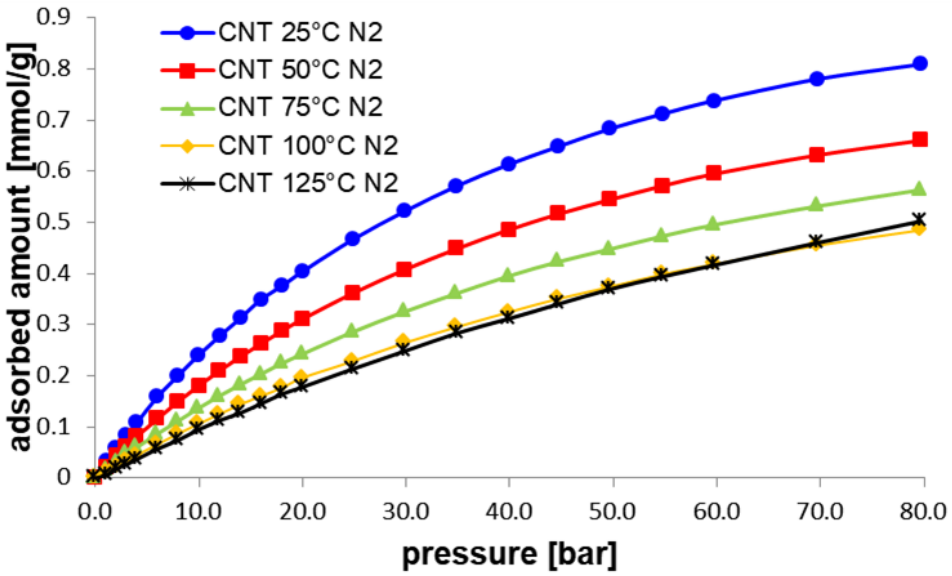

Figure 5.38.: Adsorption isotherms of CNTs in N_2 atmosphere at the temperatures 25 °C, 50 °C, 75 °C, 100 °C, 125 °C

MWCNT

MWCNTs have a slightly higher adsorption capacity for N_2 than CNTs do. Nevertheless, the adsorption is very weak. In figure 5.39 the adsorption isotherms show the expected behavior especially the curves at 100 °C and 125 °C have the expected trend and do not coincide as they do for CNTs.

SWCNT

For the SWCNTs only three temperatures are studied namely 25 °C, 75 °C and 125 °C (figure 5.40). The trends are as expected.

VACNT

The VACNTs were not studied in Nitrogen atmospheres. One reason for this was that the experimental setup was limited to 40 bar when VACNTs were available for studying, and that the adsorbed amount was expected to be in the region between the MWCNTs and SWCNTs. Meaning that the adsorption capacity for N_2 is very low in comparison to SO_2 and that these measurements do not deliver any further information.

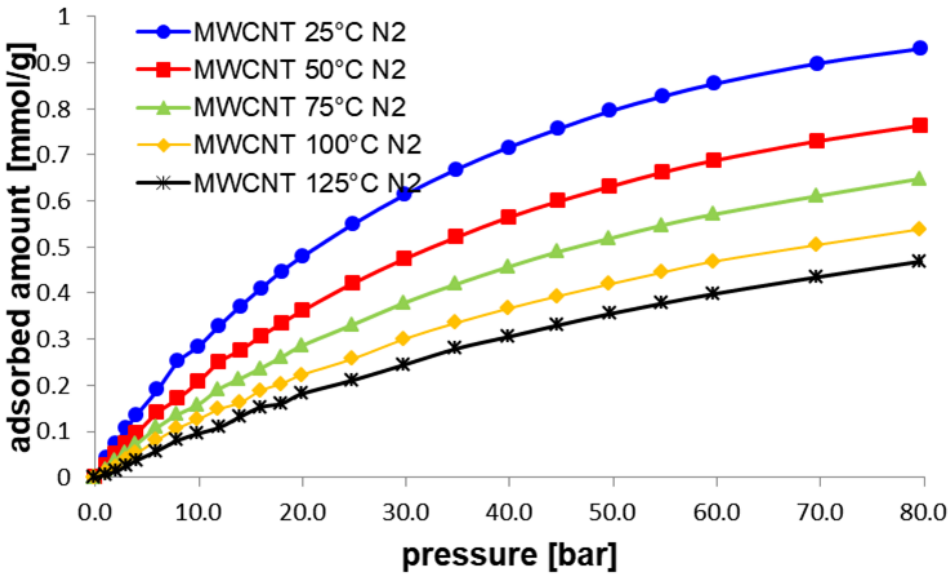

Figure 5.39.: Adsorption isotherms of MWCNTs in N_2 atmosphere at the temperatures 25 °C, 50 °C, 75 °C, 100 °C, 125 °C

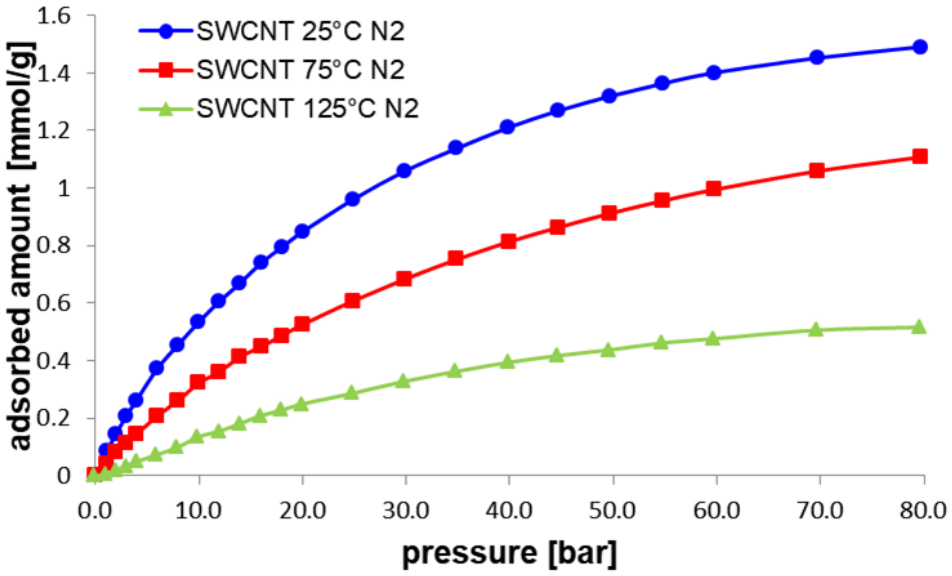

Figure 5.40.: Adsorption isotherms of SWCNTs in N_2 atmosphere at the temperatures 25 °C, 75 °C, 125 °C

Model fits to the experimental data with N_2

For the adsorption isotherm of all CNT types measured in a N_2 atmosphere, the Langmuir fits give the best representation of the experimental data (compare exemplary figure 5.41). DA and Temkin fits show also a good agreement to the data for most cases. Toth's model fits could not be obtained for the data in the N_2 atmospheres. Deviations from the experimental points can be seen particularly for the fits with the BET model which show a pole point. This might be attributed to the assumption that the saturation pressure of N_2 is equal to the critical pressure for N_2, because of the fact that a saturation pressure for N_2 does not exist in the regarded temperature region. Further information which fits could be done and how they are rated is given in table 5.9. All other fits and data to the fits are presented in appendix E.

Table 5.9.: Rating of the goodness of the model fits to the experimental data for different CNT types in N_2 atmospheres and different temperatures (good fit (+), bad fit (-), no fit ( ))

CNT	T	Langmuir		Freundlich		BET		DR		DA		Temkin		Toth	
type	[°C]	Ads.	Des.	Ads.	Des.	Ads.	Des.	Ads.	Des.	Ads.	Des.	Ads.	Des.	Ads.	Des.
SWCNT	25	+	+	+	+	-	-	-	-		+	+	+		
SWCNT	75	+	+	+	+	-	-	-	-	+	+	+	+		
SWCNT	125	+	+		+	-	-	-	-	+	+	+	+		
MWCNT	25	+	+	+	+	-	-	-	-		+	+	-		
MWCNT[a]	25	+	+	+	+	-	-	-	-		+	+	-		
MWCNT	50	+	+	+	+	-	-	-	-	+	+	+	-		
MWCNT	75	+	+	+	+	-	-	-	-		+	+	+		
MWCNT	100	+	+	+	+	-	-	-	-	+	+	+	-		
MWCNT[b]	125	+	+	-	+	-	-	-	-	+	+	+	-		
MWCNT[c]	125	+	+	-	+	-	-	-	-	+	+	+	-		
CNT	0	+	+	-	-	-	-	-	-		+	+	+		
CNT	25	+	+	-	+	-	-	-	-		+	+	+		
CNT	40	+	+	-	+	-	-	-	-	+	+	+	+		
CNT	50	+	+	-	+	-	-	-	-	+	+	+	+		
CNT	75	+	+	-	+	-	-	-	-	+	+	+	+		
CNT	100	+	+	+	+	-	-	-	-	+	+	+	+		
CNT	125	+	+	+	+	-	-	-	-	+	+	+	+		

[a] 2. cycle
[b] activation temperature 300 °C
[c] activation temperature 150 °C

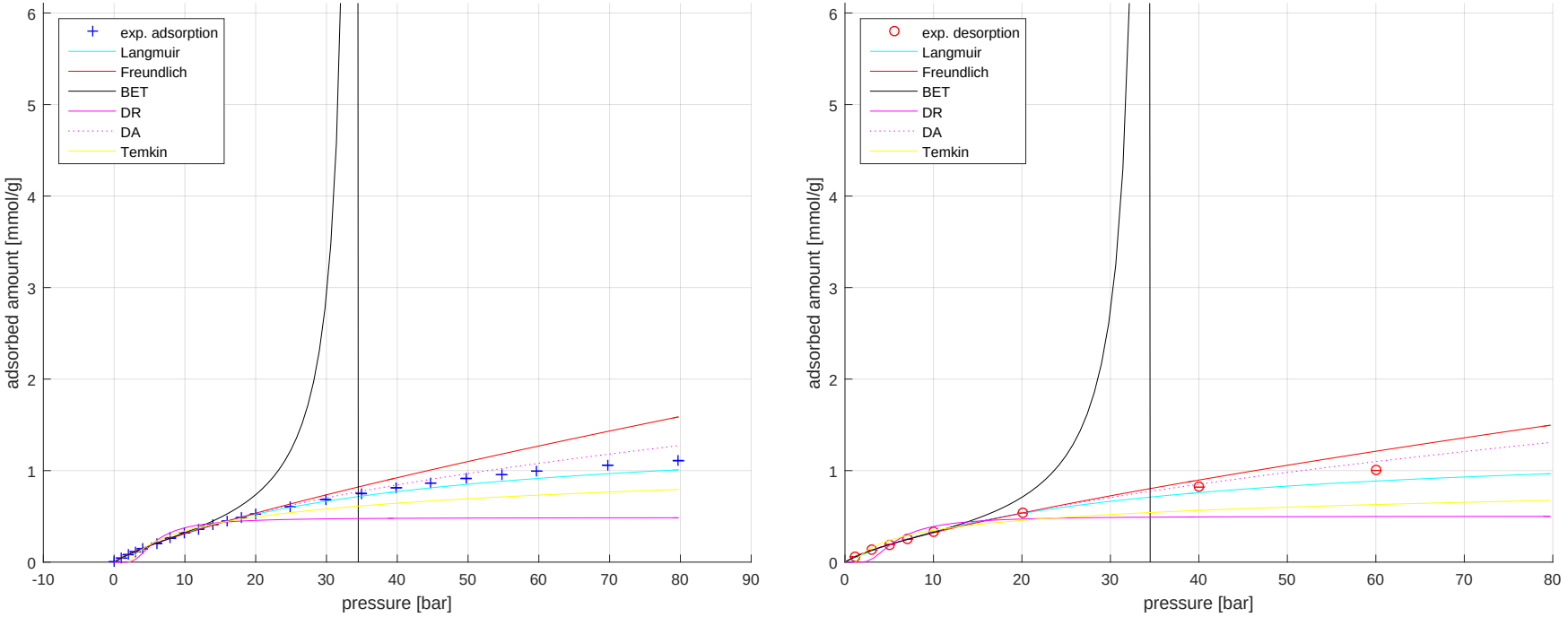

(a) adsorption **(b)** desorption

Figure 5.41.: Experimental data of SWCNTs at 75 °C in N_2 atmosphere (+ (adsorption data)/ ∘ (desorption data)) and model fits to the simulated data (lines) for the adsorption (a) and desorption data (b)

5.2.5 Heat of adsorption

From the experimental data, the heat of adsorption for the studied materials can be derived. This is also done with the analytical model described in chapter 2.1.3. For all studied CNTs (VACNT, SWCNT, MWCNT and CNT) in SO_2, the heats of adsorption are in the same range and agree good to each other. In figure 5.42 the heat of adsorption for the different CNT types is shown over the amount adsorbed. In the graph, only the adsorption branch was used to gain the heat of adsorption. The desorption data is in a similar range and agrees to the shown plot. A comparison is given in figure 5.43 were the averaged heats of adsorption for VACNT, SWCNT, MWCNT and CNT in SO_2 are shown with the maximal and minimal value from the fits in figure 5.42 as error bars.

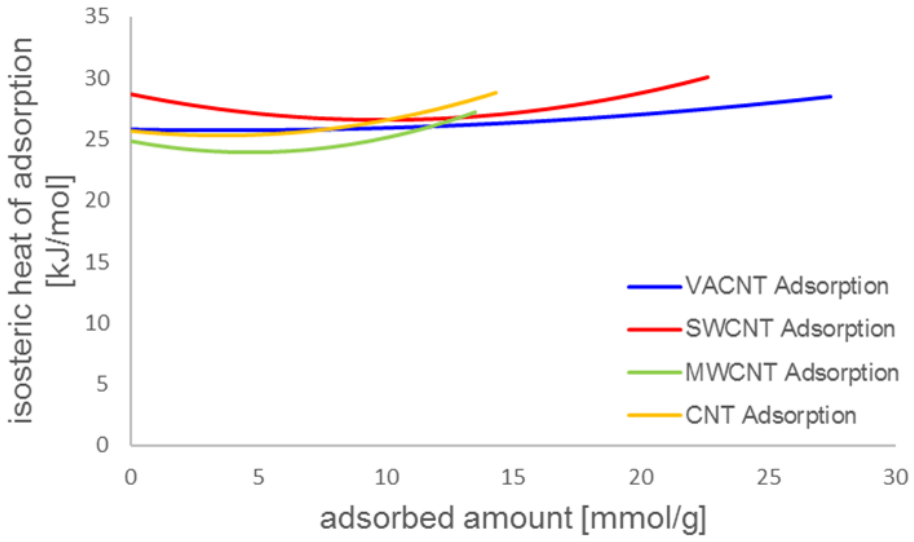

Figure 5.42.: Heat of adsorption derived from the adsorption branch over adsorbed amount from experiment for SO_2 at VACNT, SWCNT, MWCNT and CNT

For nitrogen, the same evaluations have been done. In figure 5.44 the heat of adsorption from the averaged heats of adsorption are shown for the adsorption and desorption branch of the experimental data from SWCNT, MWCNT and CNT. The data agree quite well with each other. What can be seen is that the narrower the CNTs and the higher the purity of the CNTs the higher is the heat of adsorption. However, all data is still in a comparable range.

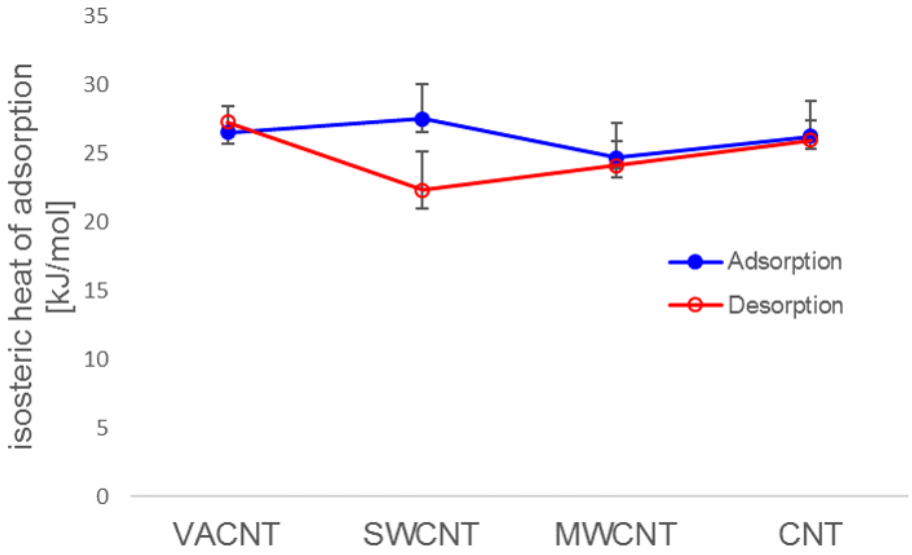

Figure 5.43.: Heat of adsorption from experiment for SO_2 at VACNT, SWCNT, MWCNT and CNT

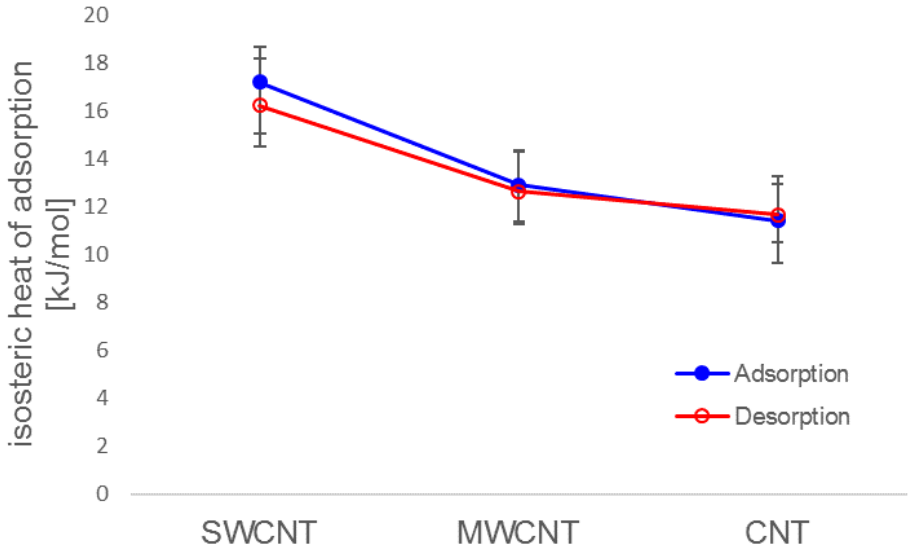

Figure 5.44.: Heat of adsorption from experiment for N_2 at SWCNT, MWCNT and CNT

5.2.6 Kinetics

From the logged data of each adsorption point over time, it was possible to derive the kinetics. This was done by fitting the measured weight difference over the time for a pressure step with a linear driving force model as described in 2.1.5. To have a closer look at the kinetic constants, these are plotted over the respective pressure. In figures 5.45 to 5.47 the kinetic constants over pressure are presented for different temperatures and CNT types in SO_2 and N_2 atmospheres.

For N_2, only data from the desorption branch was regarded. The reason for this was that in the adsorption branch the fitting procedure was not applicable to the logged time steps. For an evaluation of the adsorption branch, a shorter time step has to be evaluated. Additionally, the buoyancy does play a major role in this step which covers the uptake over time and makes an estimation difficult. What can be seen from the data for N_2 is that the kinetic constant is higher at pressures below 20 bar (see figures 5.45 to 5.47, charts on the right side). Above 20 bar the kinetic constant seems to be almost the same for all pressure steps and close to 1 min^{-1}. What is also remarkable is that for N_2 the kinetic constant is almost the same for all shown CNT types at one pressure step. One reason for this could be that the measurement was done in the automatic mode of the experimental setup and that the measurements were run with the same procedure. Also, it can be seen that the equilibrium for each step was reached relatively quickly after a couple of minutes after the respective pressure step.

For SO_2, data from the adsorption and desorption branch was evaluated (see figures 5.45 to 5.47, charts on the left side). Here the kinetic constant is significantly lower than for N_2 measurements. Mostly the values deviate between 0.2 min^{-1} and 0.5 min^{-1}. What is also obvious is that the data points do not coincide as clearly as for N_2. However, the constants show a trend. For all CNT types, they have a more or less comparable value which is dependent on the pressure. From vacuum to low pressures the kinetic constants is increasing. At medium pressures, the kinetic constants seem to establish a plateau and are decreasing at higher pressures. The decrease at higher pressures coincides approximately with the region when capillary condensation seems to take place, and the isotherms show a steep increase. Also at the low-pressure region, a similarly steep increase can be seen. So one conclusion might be that the value of the kinetic constant is dependent on the slope of the isotherm. But this has to be investigated further and is beyond the scope of this work.

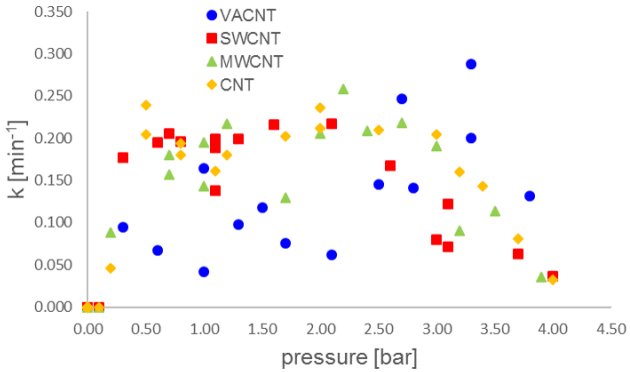

(a) SO_2 25 °C

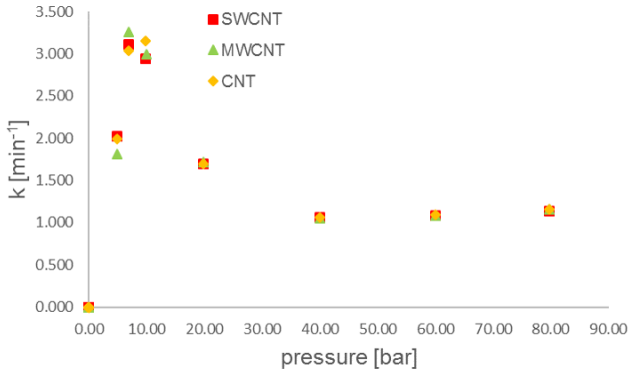

(b) N_2 25 °C

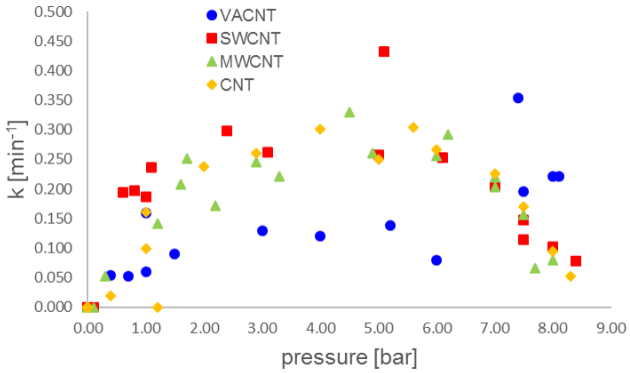

(c) SO_2 50 °C

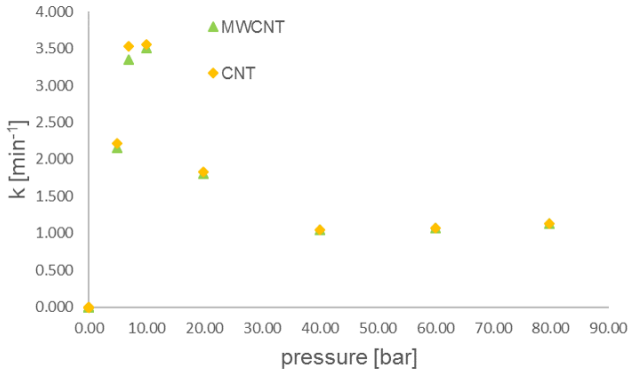

(d) N_2 50 °C

Figure 5.45.: Kinetics derived from experimental data at VACNT, SWCNT, MWCNT and CNT at the temperatures 25 °C and 50 °C for SO_2 and N_2

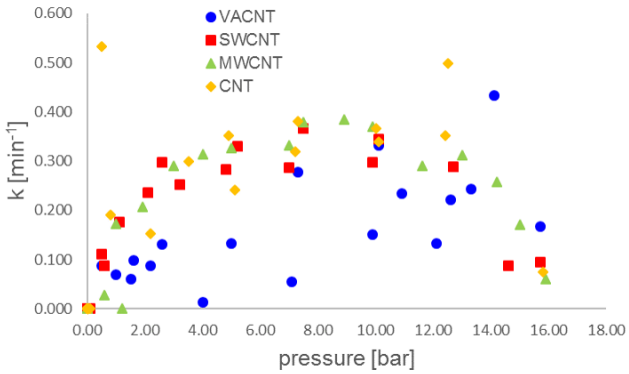

(a) SO_2 75 °C

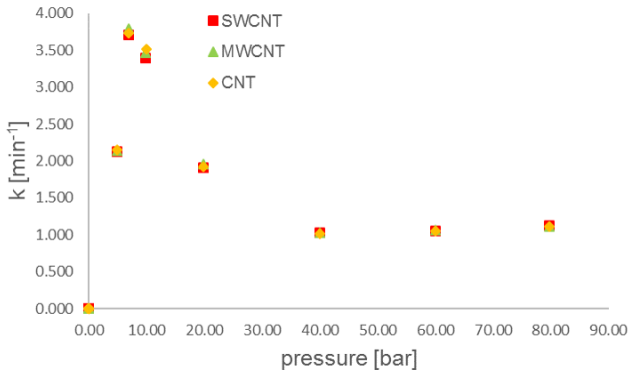

(b) N_2 75 °C

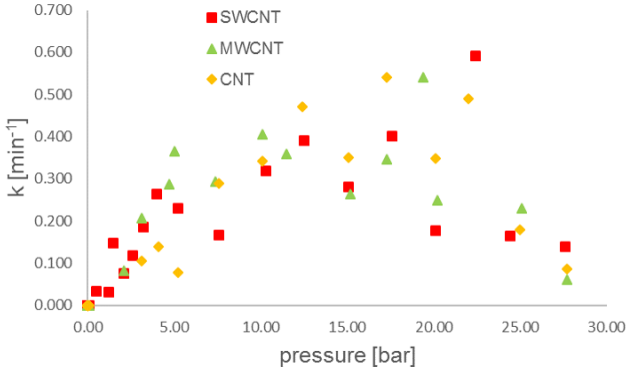

(c) SO_2 100 °C

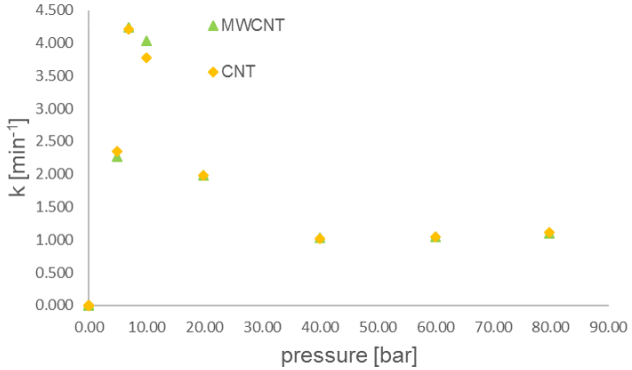

(d) N_2 100 °C

Figure 5.46.: Kinetics derived from experimental data at VACNT, SWCNT, MWCNT and CNT at the temperatures 75 °C and 100 °C for SO_2 and N_2

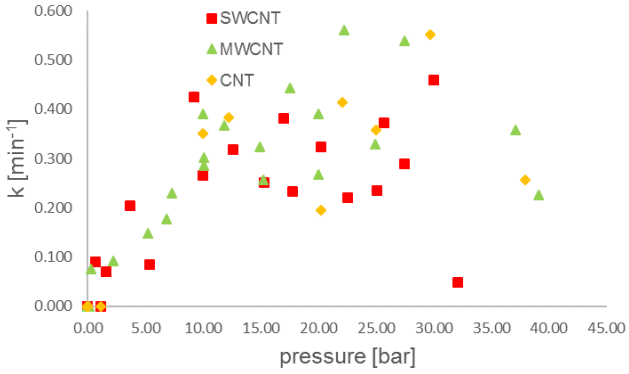

(a) SO_2 125 °C

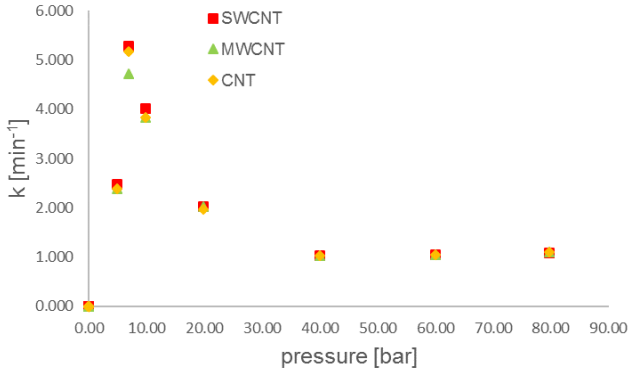

(b) N_2 125 °C

Figure 5.47.: Kinetics derived from experimental data at VACNT, SWCNT, MWCNT and CNT at the temperature 125 °C for SO_2 and N_2

5.3 Comparison of MD simulations with experiments

To validate the simulations a comparison between the simulated data and the experiments needs to be done. In this section data from simulation and experiment are combined and discussed. As already mentioned are the simulations based on ideal CNTs with complete accessibility. No blocking and no defects are considered. Having a first look on the data gained from simulation and the experimental data one can see right away, that the data from the simulated CNTs and the experimental CNT do not match up if these facts are not considered. As a correction for the simulated data, the BET surface area in comparison to the theoretical surface area[123] is taken. Additionally, the impurities of the CNTs are considered by the stated purity of the manufacturer, e.g. for industrial grade CNTs from Nanolab 85 wt−% pure carbon. With this in mind, the simulated data of the industrial grade CNTs has to be corrected by a factor of 0.077 which can be calculated by equation 5.2. For the studied MWCNTs, SWCNTs and VACNTs the correction factors are determined analogically and have a value of 0.102, 0.199 and 0.187.

$$\text{correction factor} = \frac{\text{measured BET surface area}}{\text{theoretical BET surface area}} \cdot \text{carbon content} = \tag{5.2}$$

$$= \frac{239\,\mathrm{m^2 g^{-1}}}{2\,630\,\mathrm{m^2 g^{-1}}} \cdot 0.85 = 0.077 \tag{5.3}$$

CNTs

Applying these correction factors and plotting the experimental data for industrial grade CNTs and adjusted simulation data one gets figure 5.48 for SO_2 and figure 5.49 for N_2.

The adjusted simulation data and the experimental data points are in good agreement with each other. At lower temperatures, the simulation is underpredicting the experimental values, which might be due to the arrangement of the industrial grade CNTs. They form bundles, and therefore interstitial sites are formed which are not simulated. These interstitial sites create additional pores which are especially filled up with SO_2 if its pressure gets closer to the saturation pressure. This explains as well why the experimental curves show a steep increase towards the saturation pressure.

For N_2 the simulation is slightly overpredicting the adsorbed amount. Considering, that only weak adsorption with N_2 is happening minor changes in the LJ-potential of

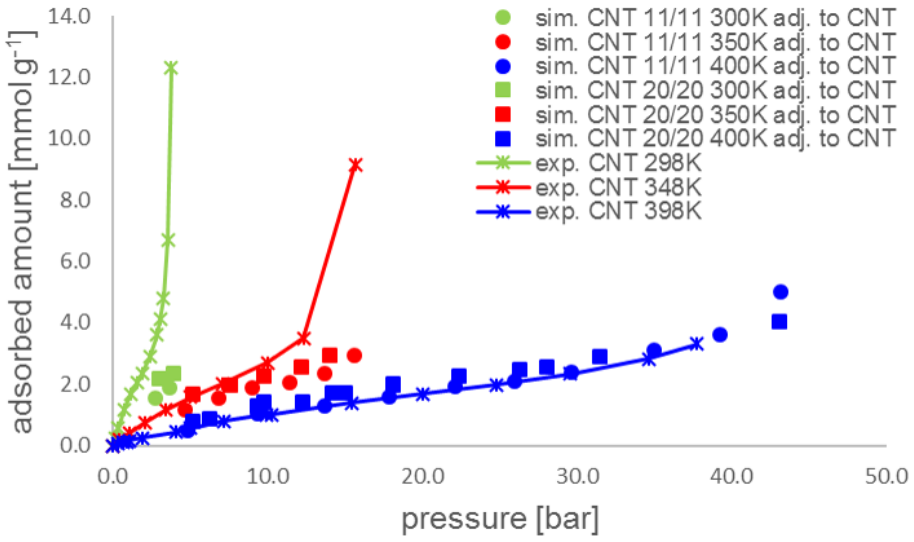

Figure 5.48.: Comparison of the adjusted simulated total adsorbed amount of SO_2 at CNTs to experimental measurements at CNTs at 300 K, 350 K and 400 K

N_2 might fix this. However, since the experimental data is only slightly overpredicted a parameter tuning was not done. For nitrogen at these temperatures no saturation pressure exists. This does not lead to such a steep increase in the experimental data as it can be seen for SO_2.

MWCNTs

Similar to the industrial grade CNTs also MWCNTs are compared to the simulated and experimental data. Here only the data for SO_2 is presented in figure 5.50 which again is in good agreement.

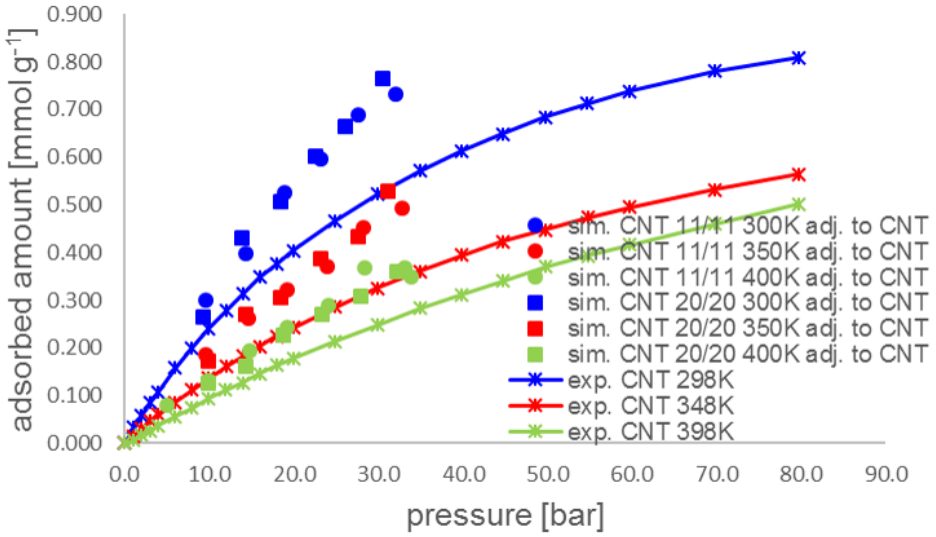

Figure 5.49.: Comparison of the adjusted simulated total adsorbed amount of N_2 at CNTs to experimental measurements at CNTs at $300\,\mathrm{K}$, $350\,\mathrm{K}$ and $400\,\mathrm{K}$

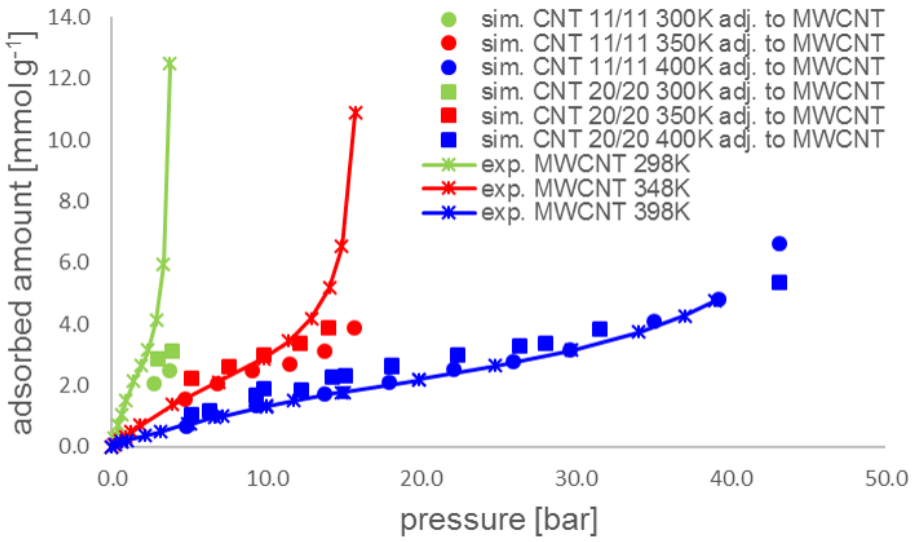

Figure 5.50.: Comparison of the adjusted simulated total adsorbed amount of SO_2 at MWCNTs to experimental measurements at MWCNTs at $300\,\mathrm{K}$, $350\,\mathrm{K}$ and $400\,\mathrm{K}$

SWCNTs

The same accounts for SWCNTs in figure 5.51, were the adjusted simulated data is in very good agreement with the experiment. Especially, if one is focusing on the simulated data of the CNT(11/11) which has roughly the same CNT diameter as the CNTs used in the experiment ($\approx 1.5\,\mathrm{nm}$). Here, the simulated curves at the temperatures 350 K and 400 K also show a slight increase in adsorption at higher pressures. The CNT(20/20) does not show this behavior at the simulated pressures. This increase might arise due to the smaller geometry of the CNT(11/11) but does fit even better to the experimental data.

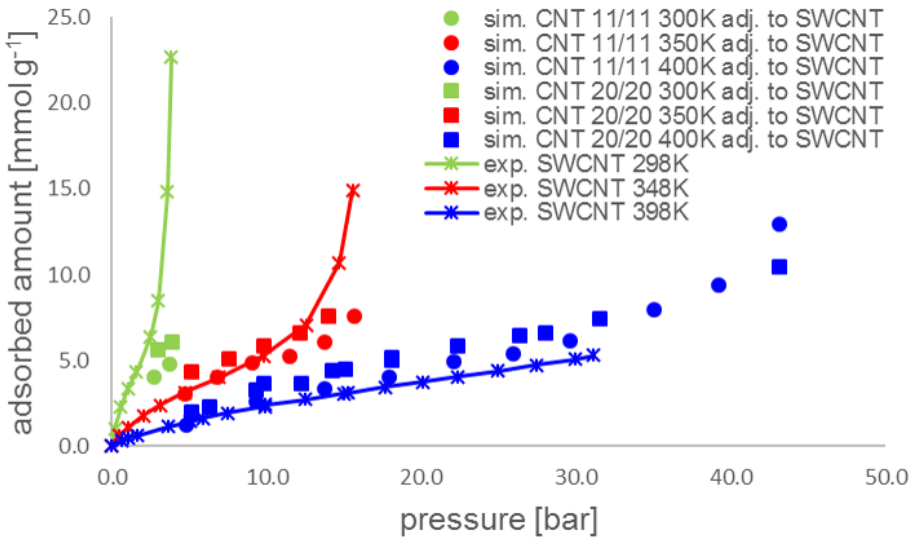

Figure 5.51.: Comparison of the adjusted simulated total adsorbed amount of SO_2 at SWCNTs to experimental measurements at SWCNTs at 300 K, 350 K and 400 K

VACNTs

For the VACNTs only the temperatures of 298 K and 348 K have been measured in the experiment. As for the other CNT cases, the adjusted simulated values agree well to the two temperatures. So the assumption that the simulated data at 400 K will agree to the experimental data may be applicable. The measured VACNTs also formed bundles because they were sheared of their substrate to provide enough VACNT mass to fit into the sample container for a gravimetric measurement. One can see that the increase in adsorbed amount towards the saturation pressure is not as pronounced as for the other CNT types. This might arise from the fact the bundles of CNTs still keep their alignment in one direction for the bundles and only have more ordered interstitial sites than unordered CNTs samples have.

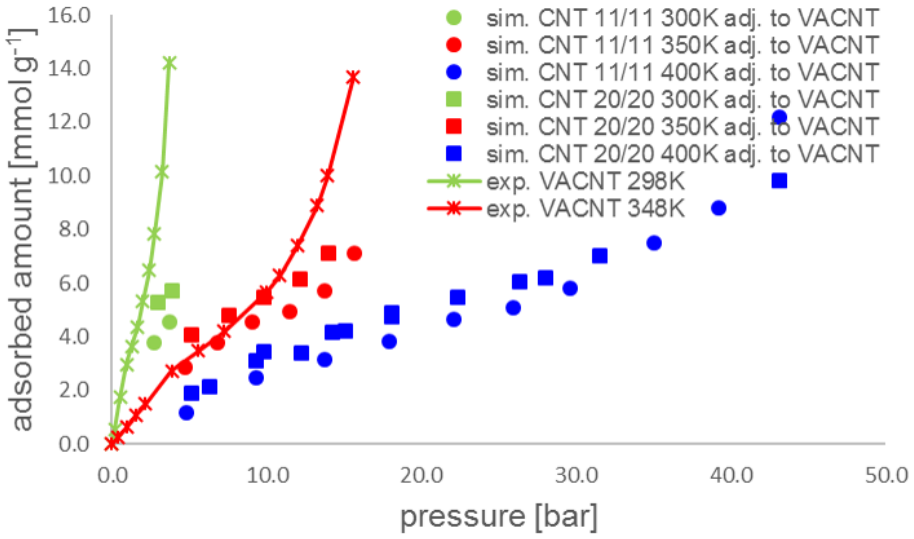

Figure 5.52.: Comparison of the adjusted simulated total adsorbed amount of SO_2 at VACNTs to experimental measurements at VACNTs at 300 K and 350 K, simulative data at 400 K is only shown for completeness

5.3.1 Heat of adsorption

A comparison of the heats of adsorption from experiment and simulation shows that the simulation is slightly underpredicting the heat of adsorption for both SO_2 and N_2 at the CNTs (compare figure 5.53 and figure 5.54). Considering that the simulation does not take into account impurities and defects which may cause higher adsorption the results are in a reasonable agreement with each other. In practice, this means that higher heats of adsorption may be expected than evaluated from simulation but the region of the heats of adsorption is met in reasonable boundaries.

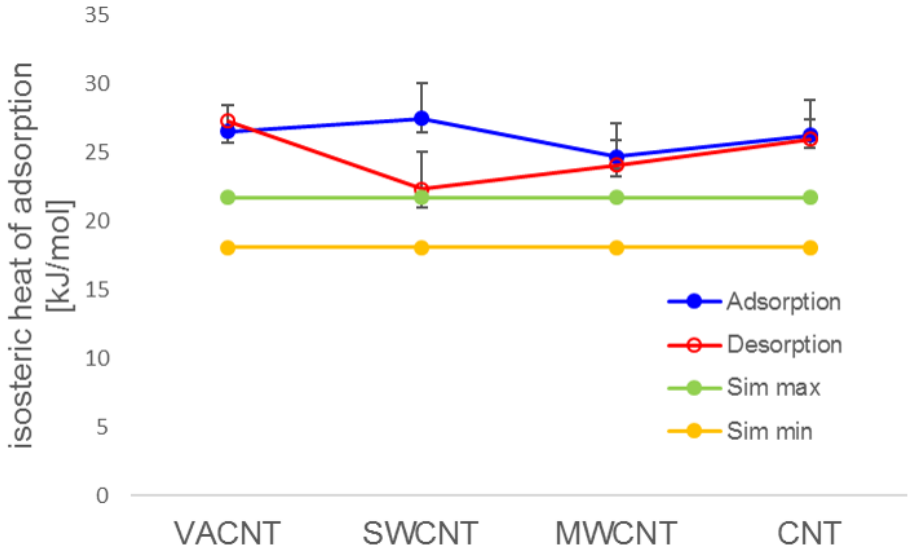

Figure 5.53.: Comparison of the heat of adsorption from experiment and simulation for SO_2 at VACNT, SWCNT, MWCNT and CNT

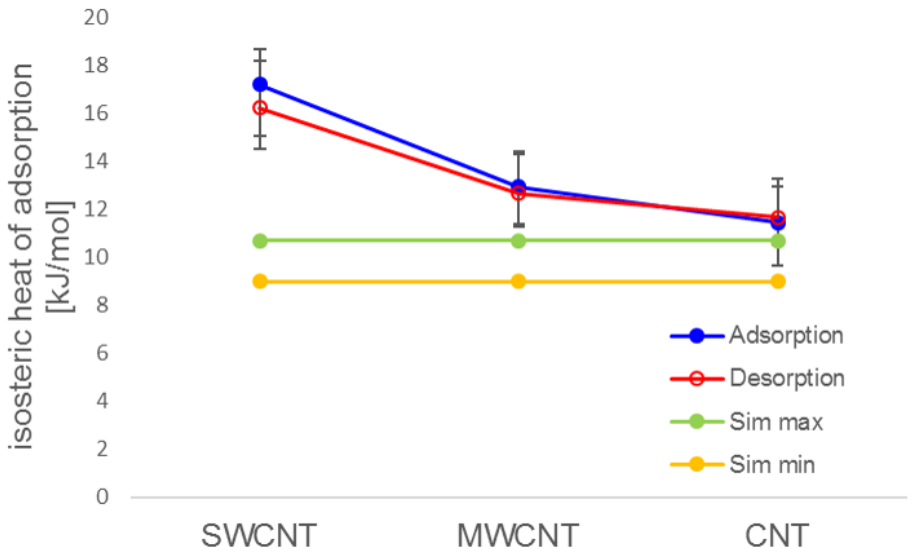

Figure 5.54.: Comparison of the heat of adsorption from experiment and simulation for N_2 at VACNT, SWCNT, MWCNT and CNT

6 Summary and open questions

6.1 Summary

In this work adsorption data from molecular dynamics simulations of SWCNTs in SO_2 and N_2 atmospheres is compared to experiments of different CNT types in the same atmospheres. The regarded temperatures range from 273 K to 400 K. Pressure data ranges from vacuum to the saturation pressure of the respective gas at the regarded temperature or at the utmost to 80 bar. From the simulated and experimental data heats of adsorption were derived and compared to each other. To all data, different adsorption models (e.g. Langmuir, Freundlich, BET, Dubinin-Raduskevich, etc.) were fitted and are presented as well as rated with regard to their applicability.

It is shown that molecular dynamics simulations are capable of predicting adsorption isotherms of different CNT types. A precondition for this is that the BET surface area of the respective CNT is considered and used as a scaling factor for the simulated data with ideal SWCNTs. From simulation and experiments also the kinetic constants for a linear driving force model are derived and compared to each other. In simulation mixture atmospheres of SO_2 and N_2 were studied and their selectivity was computed. High selectivity for SO_2 can be expected out of the simulated data.

Moreover, simulation allowed to study the influence of charges applied to the adsorbents. Therefore an even charge distribution was assumed which yielded to a significant higher adsorption capability. A study for modifying the experimental setup to employ charges in situ was also conducted.

The simulation also showed that the size of the CNT only plays a minor role for the overall adsorption. Splitting the adsorbed amount up into the amount adsorbed inside and outside a CNT a diameter dependency can be seen. This might be interesting if capped CNTs are studied.

In the experiments, good reproducibility of the gained isotherms was shown. Also, the studied CNTs for the studied gases gave a good cycling behavior. Overall, the studied CNTs showed almost no hysteresis, and adsorption to them was completely reversible.

6.2 Open questions

Points which could be covered in future works are the experimental measurement of mixture atmospheres. The experimental setup could be modified to be capable to measure charged materials. With the capability of measuring charged materials, the charge which can be applied to CNTs under dry conditions should be investigated further. The impact of the charge on the adsorption behavior should also be studied in more detail, if charging can increase the adsorbed amount as significant as expected from simulation. Also, the kinetic behavior of the adsorption process of the different gases could be studied in more depth to draw further conclusions. Additionally, further simulation should be conducted with a Monte Carlo code to allow to access adsorption at low pressures and to refine the adsorption isotherms gained from simulation. Confinement effects could also be addressed in future work by experiment and simulation.

Bibliography

[1] A. K. Geim and K. S. Novoselov. The rise of graphene. *Nat Mater*, 6(3):183–191, 2007. doi:10.1038/nmat1849.

[2] Frank Kühl. *Molecular dynamic simulation of sulfur-dioxide in carbon nanotubes*. Diplomarbeit, TU Darmstadt, Darmstadt, 10.05.2011.

[3] H. W. Kroto, J. R. Heath, S. C. O'Brien, R. F. Curl, and R. E. Smalley. C_{60}: Buckminsterfullerene. *Nature*, 318(6042):162–163, 1985. doi:10.1038/318162a0.

[4] Sumio Iijima. Helical microtubules of graphitic carbon. *Nature*, 354(6348):56–58, 1991. doi:10.1038/354056a0.

[5] D. M. Guldi and Nazario Martin. *Carbon nanotubes and related structures: Synthesis, characterization, functionalization, and applications*. Wiley-VCH, Weinheim, 2010.

[6] Alessio Alexiadis and Stavros Kassinos. Molecular dynamic simulations of carbon nanotubes in CO_2 atmosphere. *Chemical Physics Letters*, 460(4-6):512–516, 2008. doi:10.1016/j.cplett.2008.06.050.

[7] Kourosh Malek and Muhammad Sahimi. Molecular dynamics simulations of adsorption and diffusion of gases in silicon-carbide nanotubes. *The Journal of Chemical Physics*, 132(1):014310, 2010. doi:10.1063/1.3284542.

[8] Anastasios I. Skoulidas, David S. Sholl, and J. Karl Johnson. Adsorption and diffusion of carbon dioxide and nitrogen through single-walled carbon nanotube membranes. *The Journal of Chemical Physics*, 124(5):054708, 2006. doi:10.1063/1.2151173.

[9] Anastasios Skoulidas, David Ackerman, J. Johnson, and David Sholl. Rapid transport of gases in carbon nanotubes. *Physical Review Letters*, 89(18):185901, 2002. doi:10.1103/PhysRevLett.89.185901.

[10] M. Bienfait, P. Zeppenfeld, N. Dupont-Pavlovsky, M. Muris, M. Johnson, T. Wilson, M. DePies, and O. Vilches. Thermodynamics and structure of hydrogen, methane, argon, oxygen, and carbon dioxide adsorbed on single-wall carbon nanotube

bundles. *Physical Review B*, 70(3):035410, 2004. doi:10.1103/PhysRevB.70.035410.

[11] Alessio Alexiadis and Stavros Kassinos. Molecular simulation of water in carbon nanotubes. *Chemical Reviews*, 108(12):5014–5034, 2008. doi:10.1021/cr078140f.

[12] Mousumi Mani Biswas and Tahir Cagin. Simulation studies on hydrogen sorption and its thermodynamics in covalently linked carbon nanotube scaffold. *The journal of physical chemistry. B*, 114(43):13752–13763, 2010. doi:10.1021/jp1027806.

[13] Kholmirzo Kholmurodov. Molecular dynamics simulations of the interaction of carbon nanotube and a carbon disulfide solvent. *Natural Science*, 02(08):902–910, 2010. doi:10.4236/ns.2010.28111.

[14] Xuan Peng and Dapeng Cao. Computational screening of porous carbons, zeolites, and metal organic frameworks for desulfurization and decarburization of biogas, natural gas, and flue gas. *AIChE Journal*, 59(8):2928–2942, 2013. doi:10.1002/aic.14046.

[15] Wenjuan Wang, Xuan Peng, and Dapeng Cao. Capture of trace sulfur gases from binary mixtures by single-walled carbon nanotube arrays: a molecular simulation study. *Environmental science & technology*, 45(11):4832–4838, 2011. doi:10.1021/es1043672.

[16] Miloslav Nič, Jiří Jirát, Bedřich Košata, Aubrey Jenkins, and Alan McNaught, editors. *IUPAC Compendium of Chemical Terminology*. IUPAC, Research Triagle Park, NC, 2009. doi:10.1351/goldbook.

[17] Marie-Catharine Desjonquères and Daniel Spanjaard. *Concepts in surface physics*. SPRINGER, Berlin, 2. ed., corr. print edition, 1998.

[18] Werner Kast. *Adsorption aus der Gasphase: Ingenieurwissenschaftliche Grundlagen und technische Verfahren*. VCH, Weinheim, 1988.

[19] D. Amari, J. M. Lopez Cuesta, N. P. Nguyen, R. Jerrentrup, and J. L. Ginoux. Chemisorption and physisorption of CO_2 on cation exchanged zeolites A, X and MOR. *Journal of Thermal Analysis*, 38(4):1005–1015, 1992. doi:10.1007/BF01979434.

[20] Drew Myers. *Surfaces, Interfaces, and Colloids*. John Wiley & Sons, Inc, New York, USA, 2nd edition, 1999. doi:10.1002/0471234990.

[21] M. Ackley. Application of natural zeolites in the purification and separation of gases. *Microporous and Mesoporous Materials*, 61(1-3):25–42, 2003. doi:10.1016/S1387-1811(03)00353-6.

[22] Sandeep Agnihotri, Pyoungchung Kim, Yijing Zheng, José P. B. Mota, and Liangcheng Yang. Regioselective competitive adsorption of water and organic vapor mixtures on pristine single-walled carbon nanotube bundles. *Langmuir : the ACS journal of surfaces and colloids*, 24(11):5746–5754, 2008. doi:10.1021/la7036197.

[23] Y.-S Bae and C.-H Lee. Sorption kinetics of eight gases on a carbon molecular sieve at elevated pressure. *Carbon*, 43(1):95–107, 2005. doi:10.1016/j.carbon.2004.08.026.

[24] Ricardo Eugenio Bazan. *Adsorptionsuntersuchungen von methanhaltigen Gasgemischen an Aktivkohle Norit R1*. Dissertation, Universität Leipzig, Leipzig, 22.03.2010.

[25] Silvio Beutekamp. *Adsorptionsgleichgewichte der reinen Gase Methan, Kohlendioxid, Stickstoff und deren binärer Gemische an verschiedenartigen porösen Stoffen*. Dissertation, Universität Leipzig, Leipzig, 10.07.2001.

[26] Burcu Selen Caglayan and A. Erhan Aksoylu. CO_2 adsorption on chemically modified activated carbon. *Journal of Hazardous Materials*, 252-253:19–28, 2013. doi:10.1016/j.jhazmat.2013.02.028.

[27] Melina C. Castrillon, Karine O. Moura, Caiuã A. Alves, Moises Bastos-Neto, Diana C. S. Azevedo, Jörg Hofmann, Jens Möllmer, Wolf-Dietrich Einicke, and Roger Gläser. CO_2 and H_2S removal from CH_4-rich streams by adsorption on activated carbons modified with K_2CO_3 , NaOH, or Fe_2O_3. *Energy & Fuels*, 30(11):9596–9604, 2016. doi:10.1021/acs.energyfuels.6b01667.

[28] S. García, J. J. Pis, F. Rubiera, and C. Pevida. Predicting mixed-gas adsorption equilibria on activated carbon for precombustion CO_2 capture. *Langmuir*, 29(20):6042–6052, 2013. doi:10.1021/la4004998.

[29] Jens Möllmer, Marcus Lange, Andreas Möller, Christin Patzschke, Karolin Stein, Daniel Lässig, Jörg Lincke, Roger Gläser, Harald Krautscheid, and Reiner Staudt.

Pure and mixed gas adsorption of CH_4 and N_2 on the metal–organic framework Basolite® A100 and a novel copper-based 1,2,4-triazolyl isophthalate MOF. *Journal of Materials Chemistry*, 22(20):10274, 2012. doi:10.1039/c2jm15734a.

[30] Ranjani V. Siriwardane, Ming-Shing Shen, and Edward P. Fisher. Adsorption of CO_2, N_2, and O_2 on natural zeolites. *Energy & Fuels*, 17(3):571–576, 2003. doi:10.1021/ef020135l.

[31] Diana P. Vargas, L. Giraldo, and J. C. Moreno-Piraján. Study of CO_2 adsorption in functionalized carbon. *Adsorption*, 19(2-4):323–329, 2013. doi:10.1007/s10450-012-9454-7.

[32] *Ullmann's Encyclopedia of Industrial Chemistry*. Wiley-VCH Verlag GmbH & Co. KGaA, Weinheim and Germany, 2000.

[33] Douglas Morris Ruthven. *Principles of adsorption and adsorption processes*. A Wiley-Interscience publication. Wiley, New York, 1984.

[34] O. Redlich and D. L. Peterson. A useful adsorption isotherm. *Journal of Physical Chemistry*, 63(6):1024, 1959. doi:10.1021/j150576a611.

[35] C. J. Radke and J. M. Prausnitz. Adsorption of organic solutes from dilute aqueous solution of activated carbon. *Industrial & Engineering Chemistry Fundamentals*, 11(4):445–451, 1972. doi:10.1021/i160044a003.

[36] P. Kisliuk. The sticking probabilities of gases chemisorbed on the surfaces of solids. *Journal of Physics and Chemistry of Solids*, 3(1-2):95–101, 1957. doi:10.1016/0022-3697(57)90054-9.

[37] A. L. Myers and J. M. Prausnitz. Thermodynamics of mixed-gas adsorption. *AIChE Journal*, 11(1):121–127, 1965. doi:10.1002/aic.690110125.

[38] Orhan Talu and Imre Zwiebel. Multicomponent adsorption equilibria of nonideal mixtures. *AIChE Journal*, 32(8):1263–1276, 1986. doi:10.1002/aic.690320805.

[39] M. Sakuth, J. Meyer, and J. Gmehling. Measurement and prediction of binary adsorption equilibria of vapors on dealuminated Y-zeolites (DAY). *Chemical Engineering and Processing: Process Intensification*, 37(4):267–277, 1998. doi:10.1016/S0255-2701(98)00038-5.

[40] A. Erto, A. Lancia, and D. Musmarra. A modelling analysis of PCE/TCE mixture adsorption based on Ideal Adsorbed Solution Theory. *Separation and Purification Technology*, 80(1):140–147, 2011. doi:10.1016/j.seppur.2011.04.021.

[41] Irving Langmuir. The adsorption of gases on plane surfaces of glass, mica and platinum. *Journal of the American Chemical Society*, 40(9):1361–1403, 1918. doi:10.1021/ja02242a004.

[42] G. Limousin, J.-P. Gaudet, L. Charlet, S. Szenknect, V. Barthès, and M. Krimissa. Sorption isotherms: A review on physical bases, modeling and measurement. *Applied Geochemistry*, 22(2):249–275, 2007. doi:10.1016/j.apgeochem.2006.09.010.

[43] Christoph Hinz. Description of sorption data with isotherm equations. *Geoderma*, 99(3-4):225–243, 2001. doi:10.1016/S0016-7061(00)00071-9.

[44] H. Freundlich. *Über die Adsorption in Lösungen*. W. Engelmann, 1906. URL: https://books.google.de/books?id=9a7kcQAACAAJ.

[45] H. Freundlich. Über die Adsorption in Lösungen. *Zeitschrift für Physikalische Chemie*, (57):385–470, 1907.

[46] Stephen Brunauer, P. H. Emmett, and Edward Teller. Adsorption of gases in multimolecular layers. *Journal of the American Chemical Society*, 60(2):309–319, 1938. doi:10.1021/ja01269a023.

[47] Matthias Thommes, Katsumi Kaneko, Alexander V. Neimark, James P. Olivier, Francisco Rodriguez-Reinoso, Jean Rouquerol, and Kenneth S.W. Sing. Physisorption of gases, with special reference to the evaluation of surface area and pore size distribution (IUPAC technical report). *Pure and Applied Chemistry*, 87(9-10), 2015. doi:10.1515/pac-2014-1117.

[48] Ismail M. K. Ismail. Cross-sectional areas of adsorbed nitrogen, argon, krypton, and oxygen on carbons and fumed silicas at liquid nitrogen temperature. *Langmuir*, 8(2):360–365, 1992. doi:10.1021/la00038a006.

[49] Ranjani V. Siriwardane, Ming-Shing Shen, Edward P. Fisher, and James A. Poston. Adsorption of CO_2 on molecular sieves and activated carbon. *Energy & Fuels*, 15(2):279–284, 2001. doi:10.1021/ef000241s.

[50] Peter J. Branton, Peter G. Hall, Mona Treguer, and Kenneth S. W. Sing. Adsorption of carbon dioxide, sulfur dioxide and water vapour by MCM-41, a model

mesoporous adsorbent. *Journal of the Chemical Society, Faraday Transactions*, 91(13):2041, 1995. doi:10.1039/FT9959102041.

[51] J. Rouquerol, P. Llewellyn, and F. Rouquerol. Is the BET equation applicable to microporous adsorbents? In *Characterization of Porous Solids VII - Proceedings of the 7th International Symposium on the Characterization of Porous Solids (COPS-VII), Aix-en-Provence, France, 26-28 May 2005*, volume 160 of *Studies in Surface Science and Catalysis*, pages 49–56. Elsevier, 2007. doi:10.1016/S0167-2991(07)80008-5.

[52] M. M. Dubinin and V. A. Astakhov. Description of adsorption equilibria of vapors on zeolites over wide ranges of temperature and pressure. In Edith M. Flanigen and Leonard B. Sand, editors, *Molecular Sieve Zeolites-II*, volume 102 of *Advances in Chemistry*, pages 69–85. AMERICAN CHEMICAL SOCIETY, WASHINGTON, D. C., 1971. doi:10.1021/ba-1971-0102.ch044.

[53] M. M. Dubinin and L. V. Radushkevich. Evaluation of microporous materials with a new isotherm. In *Dokl. Akad. Nauk SSSR 1947*, volume 55, pages 331–334.

[54] S. G. Chen and R. T. Yang. Theoretical basis for the potential theory adsorption isotherms. The Dubinin-Radushkevich and Dubinin-Astakhov equations. *Langmuir*, 10(11):4244–4249, 1994. doi:10.1021/la00023a054.

[55] J. Tóth. State equations of the solid gas interface layer. *Acta Chimica Academiae Scientiarum Hungaricae*, (69):311–317, 1971.

[56] unknown. The micro report, 2017. URL: http://micro-report.com/isotherm-models/toth/ [cited 20.02.2017].

[57] M. I. Temkin and V. Pyzhev. Recent modifications to Langmuir isotherms. *Acta Physicochima USSR*, (12):217–222, 1940.

[58] Chaim Aharoni and Moshe Ungarish. Kinetics of activated chemisorption. part 2.—theoretical models. *Journal of the Chemical Society, Faraday Transactions 1: Physical Chemistry in Condensed Phases*, 73:456–464, 1977. doi:10.1039/F19777300456.

[59] M. I. Temkin and V. Pyzhev. Kinetics of the synthesis of ammonia on promoted iron catalysts. *Acta Physicochima USSR*, 13:851–861, 1939.

[60] K.Y Foo and B.H Hameed. Insights into the modeling of adsorption isotherm systems. *Chemical Engineering Journal*, 156(1):2–10, 2010. doi:10.1016/j.cej.2009.09.013.

[61] Leszek Czepirski and Jacek JagieŁŁo. Virial-type thermal equation of gas—solid adsorption. *Chemical Engineering Science*, 44(4):797–801, 1989. doi:10.1016/0009-2509(89)85253-4.

[62] Shaheen A. Al-Muhtaseb and James A. Ritter. New virial-type model for predicting single- and multicomponent isosteric heats of adsorption. *Industrial & Engineering Chemistry Research*, 37(2):684–696, 1998. doi:10.1021/ie970577y.

[63] Orhan Talu. Net adsorption of gas/vapor mixtures in microporous solids. *The Journal of Physical Chemistry C*, 117(25):13059–13071, 2013. doi:10.1021/jp4021382.

[64] Sasidhar Gumma and Orhan Talu. Gibbs dividing surface and helium adsorption. *Adsorption*, 9(1):17–28, 2003. doi:10.1023/A:1023859112985.

[65] Stefano Brandani, Enzo Mangano, and Lev Sarkisov. Net, excess and absolute adsorption and adsorption of helium. *Adsorption*, 22(2):261–276, 2016. doi:10.1007/s10450-016-9766-0.

[66] John M. Fernbacher and Leonard A. Wenzel. Adsorption equilibria at high pressures in the helium-nitrogen-activated carbon system. *Industrial & Engineering Chemistry Fundamentals*, 11(4):457–465, 1972. doi:10.1021/i160044a005.

[67] F. A. P. Maggs, P. H. Schwabe, and J. H. Williams. Adsorption of helium on carbons: Influence on measurement of density. *Nature*, 186(4729):956–958, 1960. doi:10.1038/186956b0.

[68] P. Malbrunot, D. Vidal, J. Vermesse, R. Chahine, and T. K. Bose. Adsorbent helium density measurement and its effect on adsorption isotherms at high pressure. *Langmuir*, 13(3):539–544, 1997. doi:10.1021/la950969e.

[69] Isao Suzuki, Kazuhiko Kakimoto, and Shoichi Oki. Volumetric determination of adsorption of helium over some zeolites with a temperature–compensated, differential tensimeter having symmetrical design. *Review of Scientific Instruments*, 58(7):1226–1230, 1987. doi:10.1063/1.1139659.

[70] S. Sircar. Measurement of Gibbsian surface excess. *AIChE Journal*, 47(5):1169–1176, 2001. doi:10.1002/aic.690470522.

[71] Helge Reinsch, Renjith S. Pillai, Renee Siegel, Jurgen Senker, Alexandra Lieb, Guillaume Maurin, and Norbert Stock. Structure and properties of Al-MIL-53-ADP, a breathing MOF based on the aliphatic linker molecule adipic acid. *Dalton transactions (Cambridge, England : 2003)*, 45(10):4179–4186, 2016. doi:10.1039/c5dt03510d.

[72] Mays Alhamami, Huu Doan, and Chil-Hung Cheng. A review on breathing behaviors of metal-organic-frameworks (MOFs) for gas adsorption. *Materials*, 7(4):3198–3250, 2014. doi:10.3390/ma7043198.

[73] Bin Mu, Feng Li, Yougui Huang, and Krista S. Walton. Breathing effects of CO_2 adsorption on a flexible 3D lanthanide metal–organic framework. *Journal of Materials Chemistry*, 22(20):10172, 2012. doi:10.1039/C2JM15721G.

[74] S. Sircar and J. R. Hufton. Why does the linear driving force model for adsorption kinetics work. *Adsorption*, 6(2):137–147, 2000. doi:10.1023/A:1008965317983.

[75] B. J. Alder and T. E. Wainwright. Phase transition for a hard sphere system. *The Journal of Chemical Physics*, 27(5):1208–1209, 1957. doi:10.1063/1.1743957.

[76] B. J. Alder and T. E. Wainwright. Studies in molecular dynamics. I. General method. *The Journal of Chemical Physics*, 31(2):459–466, 1959. doi:10.1063/1.1730376.

[77] A. Rahman. Correlations in the motion of atoms in liquid argon. *Physical Review*, 136(2A):A405–A411, 1964. doi:10.1103/PhysRev.136.A405.

[78] Frank H. Stillinger and Aneesur Rahman. Improved simulation of liquid water by molecular dynamics. *The Journal of Chemical Physics*, 60(4):1545–1557, 1974. doi:10.1063/1.1681229.

[79] Aneesur Rahman and Frank H. Stillinger. Propagation of sound in water. A molecular-dynamics study. *Physical Review A*, 10(1):368–378, 1974. doi:10.1103/PhysRevA.10.368.

[80] M. P. Allen and D. J. Tildesley. *Computer simulation of liquids*. Clarendon Press and Oxford University Press, Oxford [England], New York, 1989.

[81] Daan Frenkel and Berend Smit. *Understanding molecular simulation: From algorithms to applications*, volume 1 of *Computational science series*. Academic Press, San Diego, Californien, 2. edition, 2009.

[82] H.J.C. Berendsen, D. van der Spoel, and R. van Drunen. GROMACS: A message-passing parallel molecular dynamics implementation. *Computer Physics Communications*, 91(1-3):43–56, 1995. doi:10.1016/0010-4655(95)00042-E.

[83] Erik Lindahl, Berk Hess, and van der Spoel, David. GROMACS 3.0: A package for molecular simulation and trajectory analysis. *Journal of Molecular Modeling*, 7(8):306–317, 2001. doi:10.1007/s008940100045.

[84] van der Spoel, David, Erik Lindahl, Berk Hess, Gerrit Groenhof, Alan E. Mark, and Herman J. C. Berendsen. GROMACS: fast, flexible, and free. *Journal of Computational Chemistry*, 26(16):1701–1718, 2005. doi:10.1002/jcc.20291.

[85] Berk Hess, Carsten Kutzner, van der Spoel, David, and Erik Lindahl. GROMACS 4: Algorithms for highly efficient, load-balanced, and scalable molecular simulation. *Journal of Chemical Theory and Computation*, 4(3):435–447, 2008. doi:10.1021/ct700301q.

[86] Sander Pronk, Szilard Pall, Roland Schulz, Per Larsson, Par Bjelkmar, Rossen Apostolov, Michael R. Shirts, Jeremy C. Smith, Peter M. Kasson, van der Spoel, David, Berk Hess, and Erik Lindahl. GROMACS 4.5: a high-throughput and highly parallel open source molecular simulation toolkit. *Bioinformatics (Oxford, England)*, 29(7):845–854, 2013. doi:10.1093/bioinformatics/btt055.

[87] Stefano Markidis and Erwin Laure, editors. *Solving Software Challenges for Exascale*. Lecture Notes in Computer Science. Springer International Publishing, Cham, 2015. doi:10.1007/978-3-319-15976-8.

[88] Mark James Abraham, Teemu Murtola, Roland Schulz, Szilárd Páll, Jeremy C. Smith, Berk Hess, and Erik Lindahl. GROMACS: High performance molecular simulations through multi-level parallelism from laptops to supercomputers. *SoftwareX*, 1-2:19–25, 2015. doi:10.1016/j.softx.2015.06.001.

[89] James C. Phillips, Rosemary Braun, Wei Wang, James Gumbart, Emad Tajkhorshid, Elizabeth Villa, Christophe Chipot, Robert D. Skeel, Laxmikant Kale, and Klaus Schulten. Scalable molecular dynamics with NAMD. *Journal of Computational Chemistry*, 26(16):1781–1802, 2005. doi:10.1002/jcc.20289.

[90] Abalone, 2015. URL: http://www.biomolecular-modeling.com/Abalone/ [cited 24.02.2017].

[91] G. Kresse and J. Hafner. Ab initio molecular dynamics for liquid metals. *Physical Review B*, 47(1):558–561, 1993. doi:10.1103/PhysRevB.47.558.

[92] G. Kresse and J. Furthmüller. Efficiency of ab-initio total energy calculations for metals and semiconductors using a plane-wave basis set. *Computational Materials Science*, 6(1):15–50, 1996. doi:10.1016/0927-0256(96)00008-0.

[93] G. Kresse and J. Furthmüller. Efficient iterative schemes for ab initio total-energy calculations using a plane-wave basis set. *Physical Review B*, 54(16):11169–11186, 1996. doi:10.1103/PhysRevB.54.11169.

[94] W. Smith, T.R Forester, and I.T Todorov. *THE DL POLY 2 USER MANUAL, Version 2.19*. STFC Daresbury Laboratory Daresbury, Warrington WA4 4AD Cheshire, UK, April 2008.

[95] Ilian T. Todorov, William Smith, Kostya Trachenko, and Martin T. Dove. DL_POLY_3: new dimensions in molecular dynamics simulations via massive parallelism. *Journal of Materials Chemistry*, 16(20):1911, 2006. doi:10.1039/b517931a.

[96] Susanne Kiefer and E. Robens. Some intriguing items in the history of volumetric and gravimetric adsorption measurements. *Journal of Thermal Analysis and Calorimetry*, 94(3):613–618, 2008. doi:10.1007/s10973-008-9351-1.

[97] Erich Robens and Shanath Jayaweera. Early history of adsorption measurements. *Adsorption Science & Technology*, 32(6):425–442, 2014. doi:10.1260/0263-6174.32.6.425.

[98] Carl Wilhelm Scheele. Chemische Abhandlung von der Luft und dem Feuer, 1777. URL: http://runeberg.org/scheelch/ [cited 09.03.2017].

[99] Carl Wilhelm Scheele. *Chemische Abhandlung von der Luft und dem Feuer*. Salzwasser-Verlag Gmbh, Paderborn, 2013.

[100] P. Chappuis. Ueber die Absorption der Kohlensäure durch Holzkohle und deren Abhängigkeit von Druck und Temperatur. *Annalen der Physik*, 248(2):161–180, 1881. doi:10.1002/andp.18812480202.

[101] Francesco Albergamo. *Etude par diffusion de neutrons des propriétés dynamiques de l'hélium liquide confiné dans des milieux poreux*. Dissertation, Université Paris XI, Paris, 30.11.2001.

[102] William D. Harkins and George Jura. Surfaces of Solids. XIII. A vapor adsorption method for the determination of the area of a solid without the assumption of a molecular area, and the areas occupied by nitrogen and other molecules on the

surface of a solid. *Journal of the American Chemical Society*, 66(8):1366–1373, 1944. doi:10.1021/ja01236a048.

[103] Youngsan Ju, Yongha Park, Dooyoung Park, Jae-Jeong Kim, and Chang-Ha Lee. Adsorption kinetics of CO_2, CO, N_2 and CH_4 on zeolite LiX pellet and activated carbon granule. *Adsorption*, 21(5):419–432, 2015. doi:10.1007/s10450-015-9683-7.

[104] Jürgen U. Keller and Reiner Staudt. *Gas adsorption equilibria: Experimental methods and adsorptive isotherms*. SPRINGER, New York, 2005.

[105] Hyeon-Hui Lee, Hae-Jung Kim, Yao Shi, David Keffer, and Chang-Ha Lee. Competitive adsorption of CO_2/CH_4 mixture on dry and wet coal from subcritical to supercritical conditions. *Chemical Engineering Journal*, 230:93–101, 2013. doi:10.1016/j.cej.2013.06.036.

[106] S.W Rutherford and J.E Coons. Adsorption dynamics of carbon dioxide in molecular sieving carbon. *Carbon*, 41(3):405–411, 2003. doi:10.1016/S0008-6223(02)00318-4.

[107] E. Gerland and F. Trautmüller. *Geschichte der physikalischen Experimentierkunst*. Wilhelm Engelmann, Leipzig, 1899.

[108] N. Cusanus. Idiota de staticis experimentis, 1450. URL: http://www.cusanus-portal.de/content/fw.php?werk=30&fw=179 [cited 12.03.2017].

[109] Dieter Hoffmann, editor. *Genauigkeit und Präzision in der Geschichte der Wissenschaften und des Alltags: Vorträge*, volume 4 of *PTB-Texte*. Wirtschaftsverl. NW, Bremerhaven, 1996.

[110] F. Emich and Emil Abderhalden. *Handbuch der biologischen Arbeitsmethoden: Einrichtung und Gebrauch der zu chemischen Zwecken verwendbaren Mikrowaagen*. Urban & Schwarzenberg, Berlin, Wien, 1921.

[111] M. G. Urbain and M. A. Haller. Sur une balance-laboratoire à compensation électromagnétique à l'etude des systèmes qui dégagent des gaz avec une vitesse sensible. *Comptes Rendus Hebdomadaires des Séances de l'Académie des Sciences*, (154):347–349, 1912. URL: http://gallica.bnf.fr/ark:/12148/bpt6k31070/f369.image [cited 13.03.2017].

[112] Rubotherm. Waage und Dosiersystem: Druckbereich, 2017. URL: http://www.rubotherm.de/sorptionsmessung-automatisch.html [cited 05.02.2016].

[113] Rubotherm. Temperaturregelung, 2017. URL: http://www.rubotherm.de/sorptionsmessung-temperaturregelung.html [cited 05.02.2016].

[114] F. Dreisbach, R. Staudt, and J. U. Keller. High pressure adsorption data of methane, nitrogen, carbon dioxide and their binary and ternary mixtures on activated carbon. *Adsorption*, 5(3):215–227, 1999. doi:10.1023/A:1008914703884.

[115] J. U. Keller, R. Staudt, and M. Tomalla. Volume-gravimetric measurements of binary gas adsorption equilibria. *Berichte der Bunsengesellschaft für physikalische Chemie*, 96(1):28–32, 1992. doi:10.1002/bbpc.19920960105.

[116] T. Guo, P. Nikolaev, A. Thess, D. T. Colbert, and R. E. Smalley. Catalytic growth of single-walled manotubes by laser vaporization. *Chemical Physics Letters*, 243(1-2):49–54, 1995. doi:10.1016/0009-2614(95)00825-O.

[117] J. A. Isaacs, A. Tanwani, M. L. Healy, and L. J. Dahlben. Economic assessment of single-walled carbon nanotube processes. *Journal of Nanoparticle Research*, 12(2):551–562, 2010. doi:10.1007/s11051-009-9673-3.

[118] Justyna Chrzanowska, Jacek Hoffman, Artur Małolepszy, Marta Mazurkiewicz, Tomasz A. Kowalewski, Zygmunt Szymanski, and Leszek Stobinski. Synthesis of carbon nanotubes by the laser ablation method: Effect of laser wavelength. *physica status solidi (b)*, 252(8):1860–1867, 2015. doi:10.1002/pssb.201451614.

[119] M. José-Yacamán, M. Miki-Yoshida, L. Rendón, and J. G. Santiesteban. Catalytic growth of carbon microtubules with fullerene structure. *Applied Physics Letters*, 62(6):657–659, 1993. doi:10.1063/1.108857.

[120] Deepu J. Babu, Marcus Lange, Gennady Cherkashinin, Alexander Issanin, Reiner Staudt, and Jörg J. Schneider. Gas adsorption studies of CO_2 and N_2 in spatially aligned double-walled carbon nanotube arrays. *Carbon*, 61:616–623, 2013. doi:10.1016/j.carbon.2013.05.045.

[121] Joshi, R. Engstler, J., L. Houben, M. Bar Sadan, A. Weidenkaff, P. Mandaliev, A. Issanin, and J. J. Schneider. Catalyst composition, morphology and reaction pathway in the growth of super-long carbon nanotubes. *ChemCatChem*, 2(9):1069–1073, 2010. doi:10.1002/cctc.201000037.

[122] Pavel Nikolaev, Michael J. Bronikowski, R.Kelley Bradley, Frank Rohmund, Daniel T. Colbert, K.A Smith, and Richard E. Smalley. Gas-phase catalytic growth

of single-walled carbon nanotubes from carbon monoxide. *Chemical Physics Letters*, 313(1-2):91–97, 1999. doi:10.1016/S0009-2614(99)01029-5.

[123] A. Peigney, Ch. Laurent, E. Flahaut, R. R. Bacsa, and A. Rousset. Specific surface area of carbon nanotubes and bundles of carbon nanotubes. *Carbon*, 39(4):507–514, 2001. doi:10.1016/S0008-6223(00)00155-X.

[124] Daniel Asimov. Geometry of capped nanocylinders. AT&T Labs - Research, 1998.

[125] Cees Dekker. Carbon nanotubes as molecular quantum wires. *Physics Today*, 52(5):22, 1999. doi:10.1063/1.882658.

[126] Leif Laaksonen. gOpenMol, 2005.

[127] Chunming Niu, Enid K. Sichel, Robert Hoch, David Moy, and Howard Tennent. High power electrochemical capacitors based on carbon nanotube electrodes. *Applied Physics Letters*, 70(11):1480, 1997. doi:10.1063/1.118568.

[128] Po-Chiang Chen, Guozhen Shen, Saowalak Sukcharoenchoke, and Chongwu Zhou. Flexible and transparent supercapacitor based on In_2O_3 nanowire/carbon nanotube heterogeneous films. *Applied Physics Letters*, 94(4):043113, 2009. doi:10.1063/1.3069277.

[129] Chunsheng Du and Ning Pan. High power density supercapacitor electrodes of carbon nanotube films by electrophoretic deposition. *Nanotechnology*, 17(21):5314–5318, 2006. doi:10.1088/0957-4484/17/21/005.

[130] Tao Chen and Liming Dai. Flexible supercapacitors based on carbon nanomaterials. *Journal of Materials Chemistry A*, 2(28):10756, 2014. doi:10.1039/C4TA00567H.

[131] Duy Tho Pham, Tae Hoon Lee, Dinh Hoa Luong, Fei Yao, Arunabha Ghosh, Viet Thong Le, Tae Hyung Kim, Bing Li, Jian Chang, and Young Hee Lee. Carbon nanotube-bridged graphene 3D building blocks for ultrafast compact supercapacitors. *ACS Nano*, 9(2):2018–2027, 2015. doi:10.1021/nn507079x.

[132] Ricardo Quintero, Dong Young Kim, Kei Hasegawa, Yuki Yamada, Atsuo Yamada, and Suguru Noda. Important factors for effective use of carbon nanotube matrices in electrochemical capacitor hybrid electrodes without binding additives. *RSC Adv*, 5(21):16101–16111, 2015. doi:10.1039/c4ra16560h.

[133] Hui Xia, Yu Wang, Jianyi Lin, and Li Lu. Hydrothermal synthesis of MnO_2/CNT nanocomposite with a CNT core/porous MnO_2 sheath hierarchy architecture for supercapacitors. *Nanoscale Research Letters*, 7(1):33, 2012. doi:10.1186/1556-276X-7-33.

[134] Qinghong Wang, Lifang Jiao, Hongmei Du, Yijing Wang, and Huatang Yuan. Fe_3O_4 nanoparticles grown on graphene as advanced electrode materials for supercapacitors. *Journal of Power Sources*, 245:101–106, 2014. doi:10.1016/j.jpowsour.2013.06.035.

[135] Elzbieta Frackowiak and François Béguin. Carbon materials for the electrochemical storage of energy in capacitors. *Carbon*, 39(6):937–950, 2001. doi:10.1016/S0008-6223(00)00183-4.

[136] Jesse Smithyman, Andrew Moench, Richard Liang, Jim P. Zheng, Ben Wang, and Chuck Zhang. Binder-free composite electrodes using carbon nanotube networks as a host matrix for activated carbon microparticles. *Applied Physics A*, 107(3):723–731, 2012. doi:10.1007/s00339-012-6790-0.

[137] Chien-Te Hsieh, Hsisheng Teng, Wei-Yu Chen, and Yu-Shun Cheng. Synthesis, characterization, and electrochemical capacitance of amino-functionalized carbon nanotube/carbon paper electrodes. *Carbon*, 48(15):4219–4229, 2010. doi:10.1016/j.carbon.2010.07.021.

[138] Yan Feng, Ningning Feng, and Guixiang Du. Wearable carbon nanotube fibers for energy storage. *International Journal of Electrochemical Science*, 7(12):12432–12439, 2012. URL: http://www.electrochemsci.org/papers/vol7/71212432.pdf.

[139] Hanna Reinhardt. *Konstruktion einer Messzelle für elektrisch aufladbare Adsorbentien*. Bachelor thesis, TU Darmstadt, Darmstadt, 04.01.2016.

[140] B. M. Oliver, James G. Bradley, and Harry Farrar. Helium concentration in the Earth's lower atmosphere. *Geochimica et Cosmochimica Acta*, 48(9):1759–1767, 1984. doi:10.1016/0016-7037(84)90030-9.

[141] Irena Senkovska and Stefan Kaskel. High pressure methane adsorption in the metal-organic frameworks $Cu_3(btc)_2$, $Zn_2(bdc)_2$dabco, and $Cr_3F(H_2O)_2O(bdc)_3$. *Microporous and Mesoporous Materials*, 112(1-3):108–115, 2008. doi:10.1016/j.micromeso.2007.09.016.

[142] Umweltbundesamt. Kohlendioxid-Konzentration in der Atmosphäre (Monatsmittel), 11.02.2016. URL: http://www.umweltbundesamt.de/daten/klimawandel/atmosphaerische-kohlendioxid-konzentration [cited 28.05.216].

[143] Nigel J. Langford. Carbon dioxide poisoning. *Toxicological Reviews*, 24(4):229–235, 2005. doi:10.2165/00139709-200524040-00003.

[144] Stephen Mallinger. OSHA Hazard information BulletinsPotential carbon dioxide (CO_2) asphyxiation hazard when filling stationary low pressure CO_2 supply systems, 1996. URL: https://www.osha.gov/dts/hib/hib_data/hib19960605.html [cited 15.11.2016].

[145] Mikael Häggström. Main symptoms of carbon dioxide toxicity, 28.02.2009. URL: https://commons.wikimedia.org/wiki/File:Main_symptoms_of_carbon_dioxide_toxicity.png [cited 28.05.2016].

[146] European Commission. Commission directive on establishing indicative limit values by implementing Council Directive 80/1107/EEC on the protection of workers from the risks related to exposure to chemical, physical and biological agents at work: 91/322/EEC, 29.May.1991. URL: http://eur-lex.europa.eu/legal-content/EN/TXT/PDF/?uri=CELEX:01991L0322-20060301&from=EN [cited 09.01.2016].

[147] European Commission. Commission directive 2006/15/EC of 7 february 2006 establishing a second list of indicative occupational exposure limit values in implementation of Council Directive 98/24/EC and amending Directives 91/322/EEC and 2000/39/EC. *Official Journal of the European Union*, 49(L38):36–38, 2006. URL: http://eur-lex.europa.eu/legal-content/EN/TXT/?uri=OJ:L:2006:038:TOC [cited 09.01.2016].

[148] Bundesanstalt für Arbeitsschutz und Arbeitsmedizin. Technische Regel für Gefahrstoffe - Arbeitsplatzgrenzwerte: TRGS 900, 01.2006.

[149] Pubchem. URL: http://pubchem.ncbi.nlm.nih.gov/ [cited 30.12.2017].

[150] Committee on Acute Exposure Guideline Levels. *Acute exposure guideline levels for selected airborne chemicals: Volume 8*. The compass series. National Academy Press, Washington, D.C, 2010. URL: http://search.ebscohost.com/login.aspx?direct=true&scope=site&db=nlebk&db=nlabk&AN=319145.

[151] Vollrath Hopp, editor. *Grundlagen der chemischen Technologie*. WILEY-VCH Verlag GmbH, Weinheim, Germany, 2001. doi:10.1002/9783527625055.

[152] OSHA. Occupational health guideline for sulfur dioxide.

[153] Nist chemistry webbook. URL: http://webbook.nist.gov/ [cited 30.12.2017].

[154] Air Liquide. Sicherheitsdatenblatt Schwefeldioxid: gemäß RL 1907/2006/EG (REACH): 113-ALD, 30.09.2010.

[155] Air Liquide. Sicherheitsdatenblatt Stickstoff: gemäß RL 1907/2006/EG (REACH): 089A, 04.03.2015.

[156] Air Liquide. Sicherheitsdatenblatt Helium: gemäß RL 1907/2006/EG (REACH): 061A_01-ALD, 12.08.2010.

[157] Air Liquide. Sicherheitsdatenblatt Kohlendioxid: gemäß RL 1907/2006/EG (REACH): 018A, 02.07.2015.

[158] Carl L. Yaws and William Braker. *Matheson gas data book*. Matheson Tri-Gas and McGraw-Hill, Parsippany, NJ and New York, 7th ed edition, 2001.

[159] Bundesanstalt für Arbeitsschutz und Arbeitsmedizin. Begründung zu Schwefeldioxid in Technische Regel für Gefahrstoffe - Arbeitsplatzgrenzwerte: TRGS 900 SO_2, 10.2011.

[160] Divya Puthusseri and Jörg Engstler. SEM and TEM images of VACNTs and N_2 BET data on VACNT at 77K: Email, jpg, tiff, txt files and personal communication, 27.06.2017.

[161] Deepu Babu and Jörg Engstler. SEM and TEM images of industrial grade MWCNTs, scientific grade MWCNTs and scientific grade SWCNTs from NanoLab Inc.: Email, tiff files and personal communication, 30.01.2018.

[162] NanoLab Inc. Nanolab products: Carbon nanotubes and nanomaterials. URL: http://www.nano-lab.com/ [cited 27.03.2017].

[163] W. Smith and T. R. Forester. DL_POLY_2.0: A general-purpose parallel molecular dynamics simulation package. *Journal of Molecular Graphics*, 14(3):136–141, 1996. doi:10.1016/S0263-7855(96)00043-4.

[164] William Hoover. Canonical dynamics: Equilibrium phase-space distributions. *Physical Review A*, 31(3):1695–1697, 1985. doi:10.1103/PhysRevA.31.1695.

[165] David A. Pearlman, David A. Case, James W. Caldwell, Wilson S. Ross, Thomas E. Cheatham, Steve DeBolt, David Ferguson, George Seibel, and Peter Kollman. AMBER, a package of computer programs for applying molecular mechanics, normal

mode analysis, molecular dynamics and free energy calculations to simulate the structural and energetic properties of molecules. *Computer Physics Communications*, 91(1-3):1–41, 1995. doi:10.1016/0010-4655(95)00041-D.

[166] F. Sokolic, Y. Guissani, and B. Guillot. Computer simulation of liquid sulfur dioxide: comparison of model potentials. *The Journal of Physical Chemistry*, 89(14):3023–3026, 1985. doi:10.1021/j100260a014.

[167] F. Sokolić, Y. Guissani, and B. Guillot. Molecular dynamics simulations of thermodynamic and structural properties of liquid SO_2. *Molecular Physics*, 56(2):239–253, 1985. doi:10.1080/00268978500102291.

[168] Gaurav Arora and Stanley I. Sandler. Mass transport of O_2 and N_2 in nanoporous carbon (C_{168} schwarzite) using a quantum mechanical force field and molecular dynamics simulations. *Langmuir*, 22(10):4620–4628, 2006. doi:10.1021/la053062h.

[169] Bruce E. Poling, J. M. Prausnitz, and John P. O'Connell. *The properties of gases and liquids*. McGraw-Hill, New York, 5 edition, 2001.

[170] Kenneth S. Pitzer, David Z. Lippmann, R. F. Curl, Charles M. Huggins, and Donald E. Petersen. The volumetric and thermodynamic properties of fluids. II. Compressibility factor, vapor pressure and entropy of vaporization. *Journal of the American Chemical Society*, 77(13):3433–3440, 1955. doi:10.1021/ja01618a002.

[171] Wong, David Shan Hill and Stanley I. Sandler. A theoretically correct mixing rule for cubic equations of state. *AIChE Journal*, 38(5):671–680, 1992. doi:10.1002/aic.690380505.

[172] Falko Marx. *Modellierung des Dampf-flüssig-Gleichgewichtes des Systems Schwefeldioxid-Stickstoff mit Zustandsgleichungen*. Bachelor thesis, TU Darmstadt, Darmstadt, 26.09.2016.

[173] Hasan Orbey and Stanley I. Sandler. A comparison of various cubic equation of state mixing rules for the simultaneous description of excess enthalpies and vapor-liquid equilibria. *Fluid Phase Equilibria*, 121(1-2):67–83, 1996. doi:10.1016/0378-3812(96)03030-0.

[174] Georgios M. Kontogeorgis and Philippos Coutsikos. Thirty years with EoS/G^e models—What have we learned? *Industrial & Engineering Chemistry Research*, 51(11):4119–4142, 2012. doi:10.1021/ie2015119.

[175] Henri Renon and J. M. Prausnitz. Local compositions in thermodynamic excess functions for liquid mixtures. *AIChE Journal*, 14(1):135–144, 1968. doi:10.1002/aic.690140124.

[176] F. Dreisbach, R. Staudt, M. Tomalla, and J. U. Keller. Measurement of adsorption equilibria of pure and mixed corrosive gases: The magnetic suspension balance. In M. Douglas LeVan, editor, *Fundamentals of Adsorption*, volume 356 of *The Kluwer International Series in Engineering and Computer Science*, pages 259–268. Springer US, Boston, MA, 1996. doi:10.1007/978-1-4613-1375-5{\textunderscore}31.

[177] F. Dreisbach and H. W. Lösch. Magnetic suspension balance for simultaneous measurement of a sample and the density of the measuring fluid. *Journal of Thermal Analysis and Calorimetry*, 62(2):515–521, 2000. doi:10.1023/A:1010179306714.

[178] F. Dreisbach, H. W. Lösch, and P. Harting. Highest pressure adsorption equilibria data: Measurement with magnetic suspension balance and analysis with a new adsorbent/adsorbate-volume. *Adsorption*, 8(2):95–109, 2002. doi:10.1023/A:1020431616093.

[179] Rubotherm. Manual: Procedure of performing gravimetric adsorption measurements.

[180] DonauCarbon. Oxorbon K 20 J, 2016. URL: http://www.donau-carbon.com/Products---Solutions/Aktivkohle/Produktubersicht.aspx [cited 26.07.2016].

[181] Marius Weidenfeller. *Entwurf eines Verfahrens zur absatzweisen Adsorption von Schwefeldioxid*. Bachelor thesis, TU Darmstadt, Darmstadt, 03.12.2012.

[182] Franziska Ehmer. *Messung und Auswertung von Adsorptionsisothermen unter der Berücksichtigung des Einflusses des Auftriebs bei gravimetrischen Adsorptionsversuchen*. Bachelor thesis, TU Darmstadt, Darmstadt, 03.05.2016.

[183] Simone Cavenati, Carlos A. Grande, and Alírio E. Rodrigues. Adsorption equilibrium of methane, carbon dioxide, and nitrogen on zeolite 13X at high pressures. *Journal of Chemical & Engineering Data*, 49(4):1095–1101, 2004. doi:10.1021/Je0498917.

[184] Salil U. Rege, Ralph T. Yang, and Mark A. Buzanowski. Sorbents for air prepurification in air separation. *Chemical Engineering Science*, 55(21):4827–4838, 2000. doi:10.1016/S0009-2509(00)00122-6.

[185] Salil U. Rege, Ralph T. Yang, Kangyi Qian, and Mark A. Buzanowski. Air-prepurification by pressure swing adsorption using single/layered beds. *Chemical Engineering Science*, 56(8):2745–2759, 2001. doi:10.1016/S0009-2509(00)00531-5.

[186] J. Rother and T. Fieback. Multicomponent adsorption measurements on activated carbon, zeolite molecular sieve and metal–organic framework. *Adsorption*, 19(5):1065–1074, 2013. doi:10.1007/s10450-013-9527-2.

[187] Zhijian Liang, Marc Marshall, and Alan L. Chaffee. Comparison of Cu-BTC and zeolite 13X for adsorbent based CO_2 separation. *Energy Procedia*, 1(1):1265–1271, 2009. doi:10.1016/j.egypro.2009.01.166.

[188] Brian Joseph Maring and Paul A. Webley. A new simplified pressure/vacuum swing adsorption model for rapid adsorbent screening for CO_2 capture applications. *International Journal of Greenhouse Gas Control*, 15:16–31, 2013. doi:10.1016/j.ijggc.2013.01.009.

[189] Sumant Patankar, Siddharth Gautam, Gernot Rother, Andrey Podlesnyak, Georg Ehlers, Tingting Liu, David R. Cole, and David L. Tomasko. Role of confinement on adsorption and dynamics of ethane and an ethane–CO_2 mixture in mesoporous CPG silica. *The Journal of Physical Chemistry C*, 120(9):4843–4853, 2016. doi:10.1021/acs.jpcc.5b09984.

[190] Amber Janda, Bess Vlaisavljevich, Li-Chiang Lin, Berend Smit, and Alexis T. Bell. Effects of zeolite structural confinement on adsorption thermodynamics and reaction kinetics for monomolecular cracking and dehydrogenation of n-butane. *Journal of the American Chemical Society*, 138(14):4739–4756, 2016. doi:10.1021/jacs.5b11355.

[191] Ravichandar Babarao, Zhongqiao Hu, Jianwen Jiang, Shaji Chempath, and Stanley I. Sandler. Storage and separation of CO_2 and CH_4 in silicalite, C_{168} schwarzite, and IRMOF-1: a comparative study from Monte Carlo simulation. *Langmuir: the ACS journal of surfaces and colloids*, 23(2):659–666, 2007. doi:10.1021/la062289p.

[192] Deepu J. Babu, Divya Puthusseri, Frank G. Kühl, Sherif Okeil, Michael Bruns, Manfred Hampe, and Jörg J. Schneider. $SO2_2$ gas adsorption on carbon nanomaterials: a comparative study. *Beilstein journal of nanotechnology*, 9:1782–1792, 2018. doi:10.3762/bjnano.9.169.

[193] H. A. Lorentz. Ueber die Anwendung des Satzes vom Virial in der kinetischen Theorie der Gase. *Annalen der Physik*, 248(1):127–136, 1881. doi:10.1002/andp.18812480110.

[194] Daniel M. Berthelot and M.H Becquerel. Sur le mélange des gaz. *Physique*, pages 1703–1706, 1898.

[195] MaryBeth H. Ketko, Ganesh Kamath, and Jeffrey J. Potoff. Development of an optimized intermolecular potential for sulfur dioxide. *The Journal of Physical Chemistry B*, 115(17):4949–4954, 2011. doi:10.1021/jp2010524.

A Appendix

A.1 LJ parameter and geometrical data for simulated molecules

In this section the LJ parameter and geometrical parameters of each molecule in the simulation are summarized. Table A.1 shows the LJ parameters. Mixed LJ parameters are estimated according to the rules of Lorentz[193] and Berthelot[194].

Table A.1.: Lennard-Jones parameter for the simulations

	ε_{ij} [kJ mol^{-1}]	σ_{ij} [Å]	q [e]
S-S[166]	1.2299	3.6050	+0.460
O-O[166]	0.4870	2.9980	-0.230
S-S[195]	0.6136	3.3900	+0.590
O-O[195]	0.6568	3.0500	-0.295
C-C[6]	0.3600	3.4000	-
N-N[168]	0.3026	3.3200	-

In table A.2 the geometrical information of all molecules are given.

Table A.2.: Geometrical information of the species for the simulations

bond length [pm]		angle [°]	
S-O[166]	143.4	∠OSO	119.5
C-C[6]	141		
N-N[168]	110		

A.2 Typical blank measurement

In table A.3 the equilibrium data of a typical blank measurement is presented. T, $\sigma(T)$, p, $\sigma(p)$, m_{meas}, Δm_{meas}, $\sigma(m_{meas})$, ρ_{meas} denote the temperature, standard deviation of the temperature within the last minutes of each segment, pressure, standard deviation of the pressure within the last minutes of each segment, measured mass, measured mass difference, standard deviation of the measured mass within the last minutes of each segment, measured density.

Table A.3.: Equilibrium data of a blank measurement at 25 °C

segment	duration [min]	T [°C]	$\sigma(T)$ [°C]	p [bar]	$\sigma(p)$ [bar]	m_{meas} [g]	Δm_{meas} [g]	$\sigma(m_{meas})$ [g]	ρ_{meas} [gcm^{-3}]
1	240	25.00	0.000000	-0.040	0.0000	5.088446	0.000010	0.000001	0.000000
2	20	25.00	0.000000	1.039	0.0032	5.088330	-0.000117	0.000002	0.000171
3	20	25.00	0.000000	2.030	0.0000	5.088225	-0.000222	0.000003	0.000333
4	20	25.00	0.000000	3.031	0.0032	5.088120	-0.000328	0.000001	0.000494
5	20	25.00	0.000000	4.030	0.0000	5.088022	-0.000426	0.000001	0.000656
6	20	25.00	0.000000	6.030	0.0000	5.087814	-0.000633	0.000000	0.000975
7	20	25.00	0.000000	8.030	0.0000	5.087609	-0.000838	0.000001	0.001298
8	20	25.00	0.000000	10.020	0.0000	5.087405	-0.001042	0.000002	0.001617
9	20	25.00	0.000000	12.020	0.0000	5.087197	-0.001250	0.000001	0.001937
10	20	25.00	0.000000	14.020	0.0000	5.086992	-0.001456	0.000002	0.002257
11	20	25.00	0.000000	16.020	0.0000	5.086788	-0.001660	0.000002	0.002575
12	20	25.00	0.000000	18.020	0.0000	5.086581	-0.001867	0.000001	0.002894
13	20	25.00	0.000000	20.020	0.0000	5.086380	-0.002068	0.000001	0.003211
14	20	25.00	0.000000	24.890	0.0000	5.085885	-0.002562	0.000001	0.003979
15	20	25.00	0.000000	29.850	0.0000	5.085377	-0.003070	0.000011	0.004756
16	20	25.00	0.000000	34.880	0.0000	5.084888	-0.003560	0.000001	0.005541
17	20	25.00	0.000000	39.870	0.0000	5.084376	-0.004071	0.000002	0.006340
18	20	25.00	0.000000	44.700	0.0000	5.083897	-0.004551	0.000003	0.007086
19	20	25.00	0.000000	49.676	0.0052	5.083411	-0.005037	0.000001	0.007849
20	20	25.00	0.000000	54.680	0.0000	5.082919	-0.005529	0.000002	0.008617
21	20	25.00	0.000000	59.670	0.0000	5.082429	-0.006019	0.000001	0.009377
22	20	25.00	0.000000	69.669	0.0032	5.081455	-0.006992	0.000001	0.010896
23	20	25.00	0.000000	79.667	0.0048	5.080495	-0.007953	0.000001	0.012400
24	20	25.00	0.000000	60.027	0.0048	5.082405	-0.006042	0.000002	0.009429
25	20	25.10	0.000000	40.030	0.0000	5.084386	-0.004062	0.000002	0.006342
26	20	25.20	0.000000	20.030	0.0000	5.086417	-0.002030	0.000001	0.003178
27	20	25.30	0.000000	10.000	0.0000	5.087444	-0.001003	0.000001	0.001582
28	20	25.10	0.000000	7.030	0.0000	5.087748	-0.000699	0.000001	0.001106
29	20	25.00	0.000000	5.030	0.0000	5.087953	-0.000495	0.000001	0.000786
30	20	25.00	0.000000	3.031	0.0032	5.088160	-0.000287	0.000001	0.000465
31	20	25.00	0.000000	1.041	0.0032	5.088360	-0.000088	0.000002	0.000141

A.3 P&I diagram of the experimental setup after installation

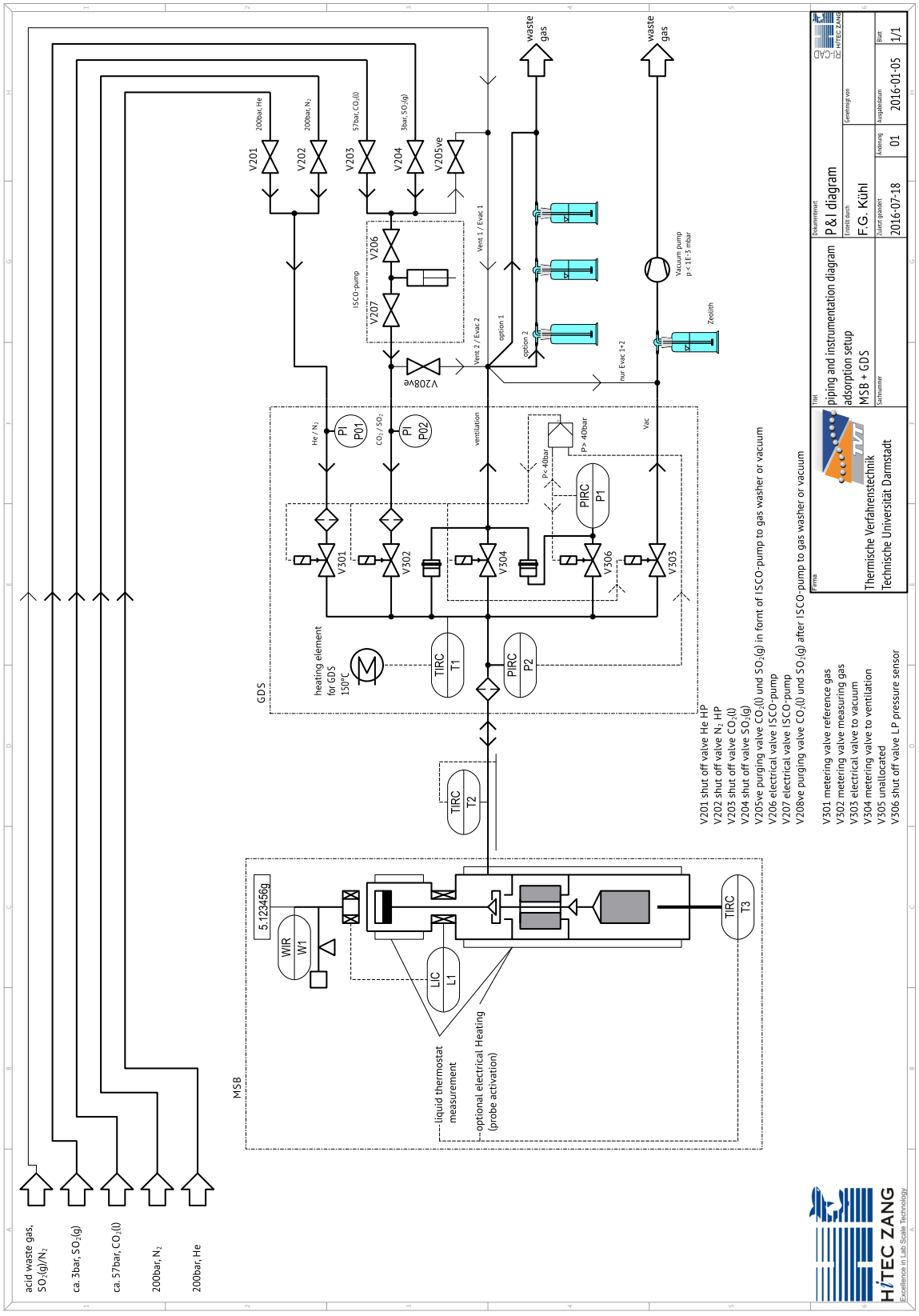

A.4 P&I diagram of the experimental setup after modification

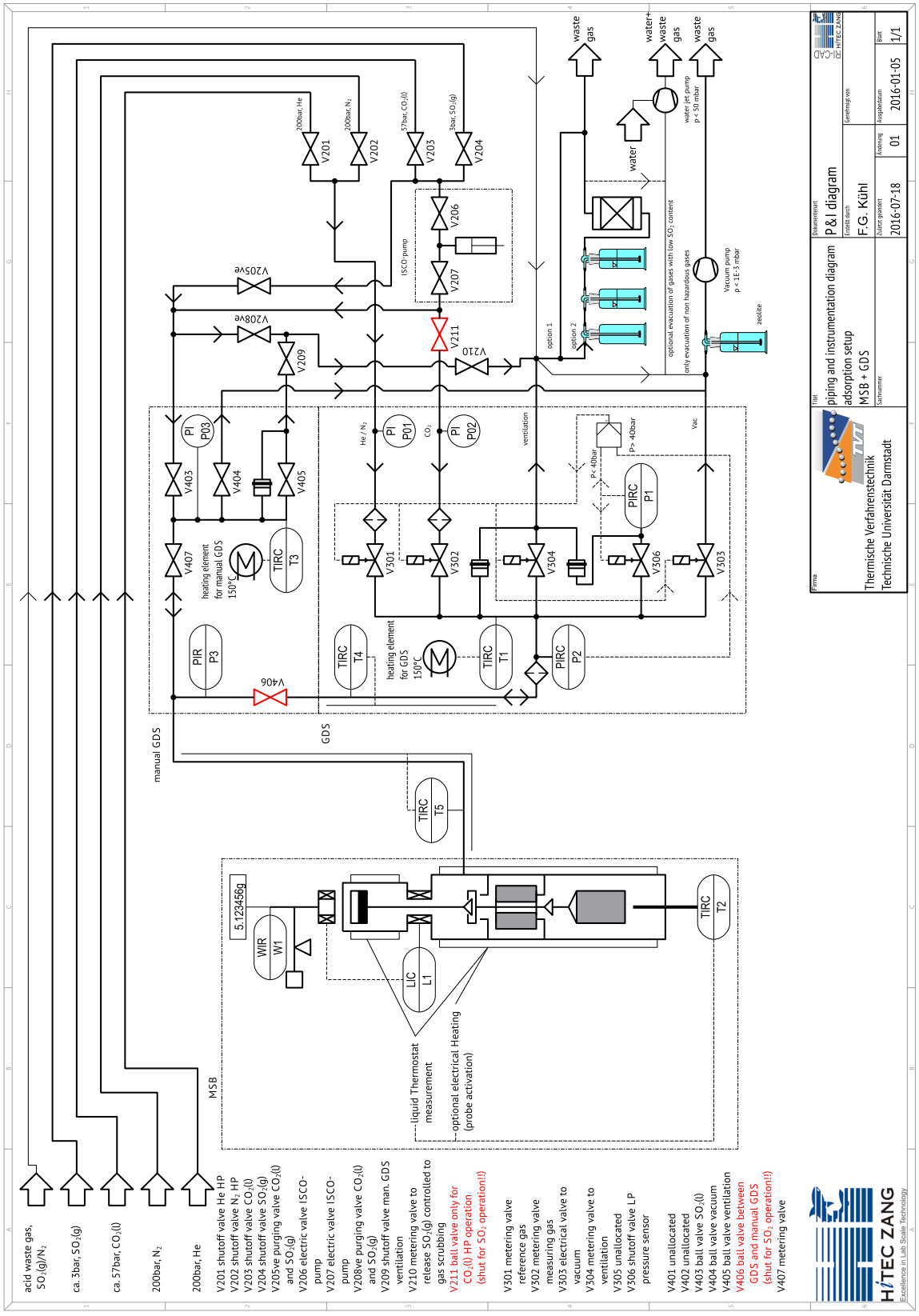

B Input and Output files

B.1 Boundary

The boundary file is a input file which gives the information of the structure of the compartments in a simulation cell. A typical boundary file looks as following:

```
       136.4280000000          0.0000000000          0.0000000000
         0.0000000000        136.4280000000          0.0000000000
         0.0000000000          0.0000000000        227.3800000000
    4
erste Grenze gross genug waehlen (+/-1), falls Molekuelschwerpunkt
   ausserhalb der Systembox liegt dieser noch erfasst wird
-114.69     -85.00
 -85.00     -70.00
 -70.00     -55.00
 -55.00     -40.40

    9
erste Grenze gross genung waehlen
 320.00      55.00
  55.00      40.00
  40.00      33.78
  33.78      29.31
  29.31      24.83
  24.83      20.36
  20.36      13.47
  13.47       6.58
   6.58       0.00

    4
erste Grenze ist Ende der tube
  39.11      55.00
  55.00      70.00
  70.00      85.00
  85.00     113.69
```

The first three lines give the box size of the simulation cell. Whereas the y-direction value is a dummy value which is not needed in the further evaluation.

In the next line the number of compartments in front of the CNT/graphene (in z-direction) is given. the next line(s) is a comment line, Then the compartment boundaries for the slab like compartments in front of the CNT/graphene are given, first the lower boundary and the the upper boundary.

In the next section again the number of compartments is given. The next line is again a comment line. Then the boundaries of the compartment are given. Here first the upper and then the lower boundary have to be typed in. The created compartments do now have a hollow-cylindrical shape, which allows a better compartmentation in and around the CNT. For graphene evaluations usually this sections does not have any compartment.

In the next section again the number of compartments is given first. The next line is again a comment line. Then the lower and upper boundary of the slab like compartment is given.

A graphical representation how these compartments look like is presented in figure B.1.

To simplify the compartmentalization all comparments which are at some distance of the CNT/ graphene surface can be treated as a big bulk compartment. A simplified compartmentalization is presented in figure B.2.

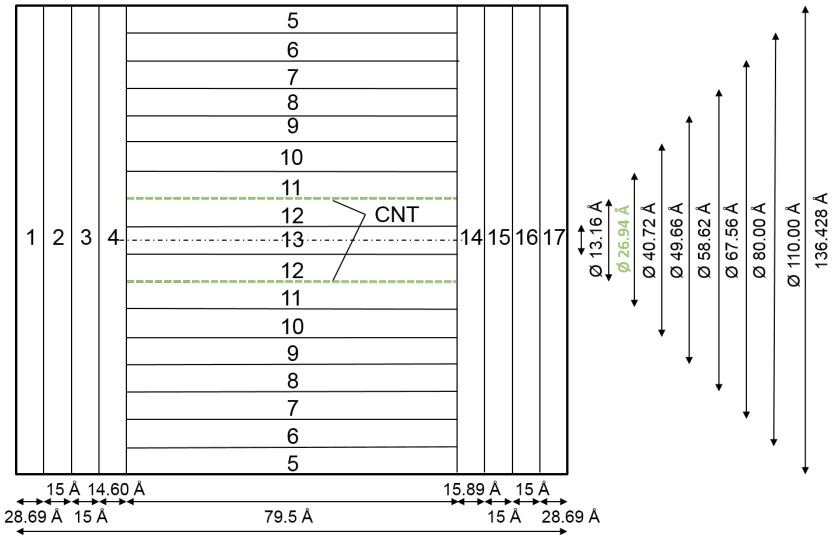

Figure B.1.: Compartmentalization of a CNT(20/20) at $400\,\mathrm{K}$

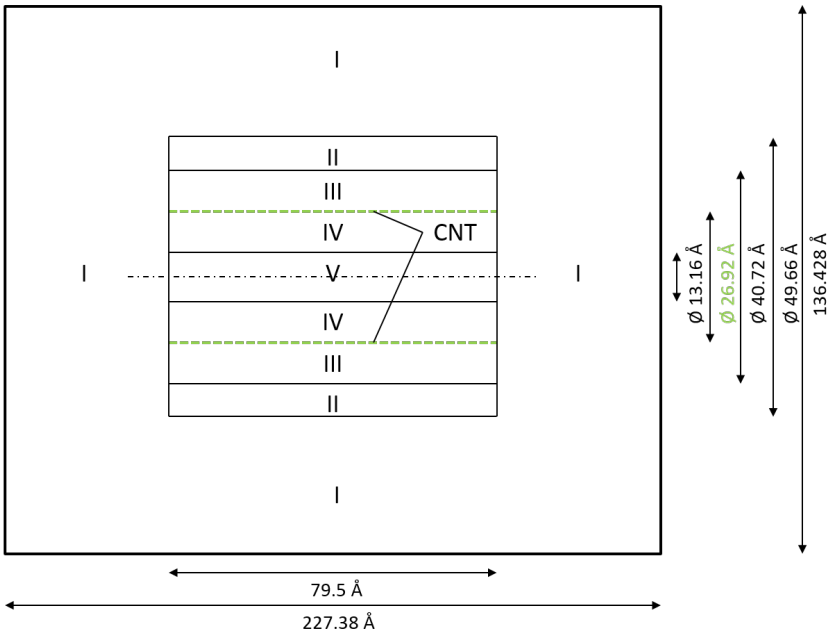

Figure B.2.: Compartmentalization of a CNT(20/20) at $400\,\mathrm{K}$ simplified

C Code

C.1 Fortran code densTempN

In this section the Fortran77 code to evaluate the HISTORY file is presented which counts the molecules in certain compartments for each printed trajectory to allow the determination of the molecule count in the respective compartment, local density and local temperature. The molecule count and the local density is evaluated in each compartment for SO_2 and N_2 separately and printed into the output file denslocN. As a further input file boundary is needed. This file provides the information of the compartment arrangement.

```
      PROGRAM ExtractOutput
C     ::::::::::::::::::::::::::::::::::::::::::::::::::::::::::::::::
C     ::Purpose: Evaluate HISTORY file
C     ::Input: HISTORY, boundary
C     ::Output: denslocN, TempC
C     ::By Frank Kuehl
C     ::Date: 02.11.2010
C     ::::::::::::::::::::::::::::::::::::::::::::::::::::::::::::::::

        CALL ID
        CALL ExOutOff
        CALL SgnOff
      END

C     ================================================================
      SUBROUTINE ID
C     ::::::::::::::::::::::::::::::::::::::::::::::::::::::::::::::::
C     ::Purpose: To Print Identifying Information
C     ::::::::::::::::::::::::::::::::::::::::::::::::::::::::::::::::

        WRITE(6,*)
        WRITE(6,*) 'calculate local density out of History file data'
        WRITE(6,*) 'By Frank Kuehl'
        WRITE(6,*) 'Date: 06.01.2015 (last modified)'
        WRITE(6,*)
```

```
        RETURN
      END
C     ==========================================================================
      SUBROUTINE ExOutOff
C     ::::::::::::::::::::::::::::::::::::::::::::::::::::::::::::::::::::::::
C     ::Purpose: To extract postion data from History file
C     ::Input: HISTORY, boundary
C     ::Output: denslocN, TempC
C     ::::::::::::::::::::::::::::::::::::::::::::::::::::::::::::::::::::::::

C     eof = end of file condition
      INTEGER eof
      INTEGER tsn
      LOGICAL f
      DOUBLE PRECISION coor(3),coor2(3),coor3(3),tstep
      DOUBLE PRECISION vel(3),vel2(3),vel3(3)
      DOUBLE PRECISION force(3),force2(3),force3(3)
      CHARACTER title*80,ubstr*3,lbstr*3,mstr*3
      CHARACTER str1*8,str2*8,str3*8
      INTEGER iatm1,itam2,itam3,keytrj,imcon,namts,nstep
      DOUBLE PRECISION wghtchar1(2),wghtchar2(2),wghtchar3(2)
      DOUBLE PRECISION mass,xs,ys,zs,x,vx,vy,vz,v,xbox(3)
      DOUBLE PRECISION Ekin, T
      CHARACTER titlestep*8
      DOUBLE PRECISION xstp,ystp,zstp
      INTEGER ncount(30),ncountchk,ncountchkold,slabs,hollows,slabs2
      INTEGER ncountchkSO2,ncountchkN2
      INTEGER ncountC,ncountN(30),boundarycount
      DOUBLE PRECISION dens(30),zlb(30),zub(30),Tmean(30),Tmeanout(30)
      DOUBLE PRECISION densN(30),TmeanN(30),TmeanoutN(30)
      DOUBLE PRECISION denssys,denssysN
      DOUBLE PRECISION rlb(30),rub(30),Ekinsum,xchk

      DATA eof/0/

      iatm1 = 0
      iatm2 = 0
      iatm3 = 0
      ncountchk = 0
      ncountchkold = 0
      ncountchkSO2 = 0
      ncountchkN2 = 0
      ncount(:) = 0
      boundarycount = 0
```

```
      OPEN(12, FILE = 'boundary')

c     read box size, deprecated is extracted from HISTORY
c     xbox(2) should be chosen big enough that all molecules in
c     the compartment furthest away from the CNT are taken into
c     account
      READ(12,'(3F20.10)',IOSTAT = eof) xbox(1),xbox(3),xbox(3)
      READ(12,'(3F20.10)',IOSTAT = eof) xbox(3),xbox(2),xbox(3)
      READ(12,'(3F20.10)',IOSTAT = eof) xbox(3),xbox(3),xbox(3)
      WRITE(*,*) xbox(1),xbox(2),xbox(3)

c     read boundaries for density evalutaion
c     read number of slabs before hollows
      READ(12,'(i5)',IOSTAT = eof) slabs
      WRITE(*,*)slabs

      READ(12,*,IOSTAT =eof)
      DO i=1,slabs
         READ(12,'(2F10.5)',IOSTAT = eof) zlb(i),zub(i)
      END DO

      READ(12,*,IOSTAT =eof)

c     read number of hollows
      READ(12,'(i5)',IOSTAT = eof) hollows
      WRITE(*,*)hollows

      READ(12,*,IOSTAT =eof)
      DO i=0,(hollows-1)
         READ(12,'(2F10.5)',IOSTAT = eof) rub(20-i),rlb(20-i)
      END DO

      READ(12,*,IOSTAT =eof)

c     read number of slabs after hollows
      READ(12,'(i5)',IOSTAT = eof) slabs2
      WRITE(*,*)slabs2

      READ(12,*,IOSTAT =eof)
      DO i=1,slabs2
         READ(12,'(2F10.5)',IOSTAT = eof) zlb(20+i),zub(20+i)
      END DO
```

```
c      first boundary is decreased by 1 Ang to catch molecules
c      ranging over the periodic boundaries
       zlb(1) = zlb(1) - 1
c      last boundary is increased by 1 Ang to catch molecules
c      ranging over the periodic boundaries
       zub(20 + slabs2) = zub(20 + slabs2) + 1
c      first radius for hollows is choosen big enough
       rub(20) = xbox(2)

       Ekinsum = 0

       OPEN(10, FILE = 'HISTORY')
       OPEN(11, FILE = 'denslocN')
       OPEN(13, FILE = 'TempC')

       READ(10,'(A,/,3I10)', IOSTAT = eof) title,keytrj,imcon,natms
       keytrj = 0

       DO WHILE (eof .EQ. 0)

      0 READ(10,'(A8,2I10,2I2,2F20.6)', IOSTAT = eof) titlestep,nstep,
      1    natms,keytrj,imcon,tstep
       READ(10,*) xstp
       READ(10,*) ystp,ystp
       READ(10,*) zstp,zstp,zstp
       keytrj = 0

       IF (boundarycount .EQ. 0) THEN
         boundarycount = 1
         WRITE(*,*) xstp,ystp,zstp
         xbox(1) = xstp
         xbox(2) = ystp
         xbox(3) = zstp
       ENDIF

       ubstr = '    '
       ncountC = 0

          DO WHILE ((ubstr .NE. 'tim') .AND. (eof .EQ. 0))

          mstr = '    '
          lbstr = '    '

      0    READ(10,'(A,/,/,/,/,A,/,/,/,/,A)',IOSTAT = eof) ubstr,
```

```
     1       mstr,lbstr
             BACKSPACE(10)
             BACKSPACE(10)
             BACKSPACE(10)
             BACKSPACE(10)
             BACKSPACE(10)
             BACKSPACE(10)
             BACKSPACE(10)
             BACKSPACE(10)

C     read coordinates of C
             IF ((ubstr .EQ. 'C   ')) THEN
                BACKSPACE(10)
     0          READ(10,'(A8,I10,2F12.6)',IOSTAT = eof) str1,iatm1,
     1             wghtchar1
     0          READ(10,*,IOSTAT = eof)
     1             coor,vel,force

                   mass = wghtchar1(1)
C     calculation of the molecule-velocity
     0             vx = vel(1)
     0             vy = vel(2)
     0             vz = vel(3)

                      ncountC = ncountC + 1
                      v = vx*vx + vy*vy + vz*vz
                      Ekin = 0.5 * mass * v
                      T = 2 * Ekin / (3*0.831451115)
                      TmeanC = (TmeanC + T)
                      TmeanoutC = TmeanC / ncountC
             ENDIF

C     read coordinates of SO2
     0       IF ((ubstr .EQ. 'S   ') .AND. (lbstr .EQ. 'O   ') .AND.
     1          (mstr .EQ. 'O   ')) THEN
                BACKSPACE(10)
     0          READ(10,'(A8,I10,2F12.6)',IOSTAT = eof) str1,iatm1,
     1             wghtchar1
     0          READ(10,*,IOSTAT = eof)
     1             coor,vel,force
     0          READ(10,'(A8,I10,2F12.6)',IOSTAT = eof) str2,iatm2,
     1             wghtchar2
     0          READ(10,*,IOSTAT = eof)
     1             coor2,vel2,force2
```

```
     0          READ(10,'(A8,I10,2F12.6)',IOSTAT = eof) str3,iatm3,
     1             wghtchar3
     0          READ(10,*,IOSTAT = eof)
     1             coor3,vel3,force3

C     calculation of the center of mass
                mass = wghtchar1(1) + wghtchar2(1) + wghtchar3(1)
     0          xs = 1/(mass) *
     1             (wghtchar1(1) * coor(1) + wghtchar2(1) * coor2(1) +
     2             wghtchar3(1) * coor3(1))
     0          ys = 1/(mass) *
     1             (wghtchar1(1) * coor(2) + wghtchar2(1) * coor2(2) +
     2             wghtchar3(1) * coor3(2))
     0          zs = 1/(mass) *
     1             (wghtchar1(1) * coor(3) + wghtchar2(1) * coor2(3) +
     2             wghtchar3(1) * coor3(3))

C     calculation of the molecule-velocity
     0             vx = (wghtchar1(1) * vel(1) + wghtchar2(1) * vel2(1)
     1                + wghtchar3(1) * vel3(1)) / mass
     0             vy = (wghtchar1(1) * vel(2) + wghtchar2(1) * vel2(2)
     1                + wghtchar3(1) * vel3(2)) / mass
     0             vz = (wghtchar1(1) * vel(3) + wghtchar2(1) * vel2(3)
     1                + wghtchar3(1) * vel3(3)) / mass

C     correction of the center of mass if SO2 ranges over the periodic
C     boundaries
               DO i = 1,3
                 IF (i .EQ. 1) x = xs
                 IF (i .EQ. 2) x = ys
                 IF (i .EQ. 3) x = zs

     0           IF (((coor2(i) - x) .GT. 3) .OR. ((coor2(i) - x)
     1              .LT. -3)) THEN
     0             IF     ((coor(i) .GT. 0) .AND. (coor2(i) .GT. 0))
     1              THEN
                    coor3(i) = coor3(i) + xbox(i)
     0             ELSEIF ((coor(i) .GT. 0) .AND. (coor3(i) .GT. 0))
     1              THEN
                    coor2(i) = coor2(i) + xbox(i)
     0             ELSEIF ((coor2(i) .GT. 0) .AND. (coor3(i) .GT. 0))
     1              THEN
                    coor(i) = coor(i) + xbox(i)
     0             ELSEIF ((coor(i) .LT. 0) .AND. (coor2(i) .LT. 0))
```

```
     1               THEN
                     coor3(i) = coor3(i) - xbox(i)
     0              ELSEIF ((coor(i) .LT. 0) .AND. (coor3(i) .LT. 0))
     1               THEN
                     coor2(i) = coor2(i) - xbox(i)
     0              ELSEIF ((coor2(i) .LT. 0) .AND. (coor3(i) .LT. 0))
     1               THEN
                     coor(i) = coor(i) - xbox(i)
                    ENDIF
     0              x = 1/(mass) *
     1               (wghtchar1(1) * coor(i) + wghtchar2(1) *
     2                coor2(i) + wghtchar3(1) * coor3(i))

                    IF (i .EQ. 1) xs = x
                    IF (i .EQ. 2) ys = x
                    IF (i .EQ. 3) zs = x
                  ENDIF
                END DO

C     Do loop for slabs till the beginning of the CNT
                DO i = 1,slabs
                   IF ((zs .GE. zlb(i)) .AND. (zs .LT. zub(i))) THEN
                      ncount(i) = ncount(i) + 1
     0                dens(i) = ncount(i) /6.02214179d23 /
     1                   (xbox(1) * xbox(2) * 1d-30 * (zub(i)-zlb(i)))
                      v = vx*vx + vy*vy + vz*vz
                      Ekin = 0.5 * mass * v
                      T = 2 * Ekin / (3*0.831451115)
                      Tmean(i) = (Tmean(i) + T)
                      Tmeanout(i) = Tmean(i) / ncount(i)
                   ENDIF
                END DO

C      Do loop for (hollow) cylinder in and around the CNT
                DO j = 20,20-hollows+1,-1
     0             IF ((zs .GE. zub(i-1)) .AND. (zs .LT. zlb(21)) .AND.
     1                (xs*xs + ys*ys .GE.
     2                rlb(j)*rlb(j)) .AND. (xs*xs + ys*ys .LT.
     3                rub(j)*rub(j))) THEN

                      ncount(j) = ncount(j) + 1

                      IF (j .EQ. 20) THEN
     0                   dens(j) = ncount(j) /6.02214179d23 /
```

```
     1                    ((zlb(21)-zub(slabs))*1d-30 * (xbox(1)
     2                    * xbox(2) - 3.1415 * rlb(j)*rlb(j)))
                       ELSE
     0                    dens(j) = ncount(j) /6.02214179d23 /
     1                    ((zlb(21)-zub(slabs))*1d-30 * 3.1415 *
     2                    (rub(j)*rub(j) - rlb(j)*rlb(j)))
                       ENDIF
                       v = vx*vx + vy*vy + vz*vz
                       Ekin = 0.5 * mass * v
                       T = 2 * Ekin / (3*0.831451115)
                       Tmean(j) = (Tmean(j) + T)
                       Tmeanout(j) = Tmean(j) / ncount(j)
                    ENDIF
                 END DO

C     Do loop for slabs after the end of the CNT
                 DO k = 21,20+slabs2
                    IF ((zs .GE. zlb(k)) .AND. (zs .LT. zub(k))) THEN
                       ncount(k) = ncount(k) + 1
     0                 dens(k) = ncount(k) /6.02214179d23 /
     1                    (xbox(1) * xbox(2) * 1d-30 * (zub(k)-zlb(k)))
                       v = vx*vx + vy*vy + vz*vz
                       Ekin = 0.5 * mass * v
                       T = 2 * Ekin / (3*0.831451115)
                       Tmean(k) = (Tmean(k) + T)
                       Tmeanout(k) = Tmean(k) / ncount(k)
                    ENDIF
                 END DO
              END IF

C ************************************************************
C     read coordinates of N2
     0       IF ((ubstr .EQ. 'N   ') .AND.
     1           (mstr .EQ. 'N   ')) THEN
                 BACKSPACE(10)
     0           READ(10,'(A8,I10,2F12.6)',IOSTAT = eof) str1,iatm1,
     1              wghtchar1
     0           READ(10,*,IOSTAT = eof)
     1              coor,vel,force
     0           READ(10,'(A8,I10,2F12.6)',IOSTAT = eof) str2,iatm2,
     1              wghtchar2
     0           READ(10,*,IOSTAT = eof)
     1              coor2,vel2,force2
```

```
C     calculation of the center of mass
                mass = wghtchar1(1) + wghtchar2(1)
     0          xs = 1/(mass) *
     1             (wghtchar1(1) * coor(1) + wghtchar2(1) * coor2(1))
     0          ys = 1/(mass) *
     1             (wghtchar1(1) * coor(2) + wghtchar2(1) * coor2(2))
     0          zs = 1/(mass) *
     1             (wghtchar1(1) * coor(3) + wghtchar2(1) * coor2(3))

C     calculation of the molecule-velocity
     0             vx = (wghtchar1(1) * vel(1) + wghtchar2(1) * vel2(1)
     1                ) / mass
     0             vy = (wghtchar1(1) * vel(2) + wghtchar2(1) * vel2(2)
     1                ) / mass
     0             vz = (wghtchar1(1) * vel(3) + wghtchar2(1) * vel2(3)
     1                ) / mass

C     correction of the center of mass if N2 ranges over the periodic
C     boundaries
                DO i = 1,3
                  IF (i .EQ. 1) x = xs
                  IF (i .EQ. 2) x = ys
                  IF (i .EQ. 3) x = zs

     0            IF (((coor2(i) - x) .GT. 3) .OR. ((coor2(i) - x)
     1               .LT. -3)) THEN
     0              IF      ((x .GT. 0) .AND. (coor2(i) .GT. 0))
     1               THEN
                     coor(i) = coor(i) + xbox(i)
     0              ELSEIF ((x .GT. 0) .AND. (coor2(i) .LT. 0))
     1               THEN
                     coor2(i) = coor2(i) + xbox(i)
     0              ELSEIF ((x .LE. 0) .AND. (coor2(i) .GT. 0))
     1               THEN
                     coor2(i) = coor2(i) - xbox(i)
     0              ELSEIF ((x .LE. 0) .AND. (coor2(i) .LT. 0))
     1               THEN
                     coor(i) = coor(i) - xbox(i)
                    ENDIF
     0              x = 1/(mass) *
     1               (wghtchar1(1) * coor(i) + wghtchar2(1) *
     2                coor2(i))

                    IF (i .EQ. 1) xs = x
```

```
                IF (i .EQ. 2) ys = x
                IF (i .EQ. 3) zs = x
              ENDIF
            END DO

C     Do loop for slabs till the beginning of the CNT
            DO i = 1,slabs
              IF ((zs .GE. zlb(i)) .AND. (zs .LT. zub(i))) THEN
                ncountN(i) = ncountN(i) + 1
     0          densN(i) = ncountN(i) /6.02214179d23 /
     1            (xbox(1) * xbox(2) * 1d-30 * (zub(i)-zlb(i)))
                v = vx*vx + vy*vy + vz*vz
                Ekin = 0.5 * mass * v
                T = 2 * Ekin / (3*0.831451115)
                TmeanN(i) = (TmeanN(i) + T)
                TmeanoutN(i) = TmeanN(i) / ncountN(i)
              ENDIF
            END DO

C      Do loop for (hollow) cylinder in and around the CNT
            DO j = 20,20-hollows+1,-1
     0        IF ((zs .GE. zub(i-1)) .AND. (zs .LT. zlb(21)) .AND.
     1          (xs*xs + ys*ys .GE.
     2          rlb(j)*rlb(j)) .AND. (xs*xs + ys*ys .LT.
     3          rub(j)*rub(j))) THEN

                ncountN(j) = ncountN(j) + 1

                IF (j .EQ. 20) THEN
     0            densN(j) = ncountN(j) /6.02214179d23 /
     1              ((zlb(21)-zub(slabs))*1d-30 * (xbox(1)
     2              * xbox(2) - 3.1415 * rlb(j)*rlb(j)))
                ELSE
     0            densN(j) = ncountN(j) /6.02214179d23 /
     1              ((zlb(21)-zub(slabs))*1d-30 * 3.1415 *
     2              (rub(j)*rub(j) - rlb(j)*rlb(j)))
                ENDIF
                v = vx*vx + vy*vy + vz*vz
                Ekin = 0.5 * mass * v
                T = 2 * Ekin / (3*0.831451115)
                TmeanN(j) = (TmeanN(j) + T)
                TmeanoutN(j) = TmeanN(j) / ncountN(j)
              ENDIF
            END DO
```

```
C     Do loop for slabs after the end of the CNT
            DO k = 21,20+slabs2
               IF ((zs .GE. zlb(k)) .AND. (zs .LT. zub(k))) THEN
                  ncountN(k) = ncountN(k) + 1
     0            densN(k) = ncountN(k) /6.02214179d23 /
     1               (xbox(1) * xbox(2) * 1d-30 * (zub(k)-zlb(k)))
                  v = vx*vx + vy*vy + vz*vz
                  Ekin = 0.5 * mass * v
                  T = 2 * Ekin / (3*0.831451115)
                  TmeanN(k) = (TmeanN(k) + T)
                  TmeanoutN(k) = TmeanN(k) / ncountN(k)
               ENDIF
            END DO
         END IF
      END DO

      DO i = 1,slabs
     0    WRITE(11,'(2I10,2E12.4,I10,2E12.4,I10)') nstep,i,dens(i),
     1       Tmeanout(i),ncount(i),densN(i),TmeanoutN(i),ncountN(i)
         Tmeansys = Tmeansys + Tmean(i) + TmeanN(i)
         denssys = denssys + dens(i)
         denssysN = denssysN + densN(i)
         ncountchkSO2 = ncountchkSO2 + ncount(i)
         ncountchkN2 = ncountchkN2 + ncountN(i)
         ncountchk = ncountchk + ncount(i) + ncountN(i)
      END DO

      DO i = 20,20-hollows+1,-1
     0    WRITE(11,'(2I10,2E12.4,I10,2E12.4,I10)') nstep,i,dens(i),
     1       Tmeanout(i),ncount(i),densN(i),TmeanoutN(i),ncountN(i)
         Tmeansys = Tmeansys + Tmean(i) + TmeanN(i)
         denssys = denssys + dens(i)
         denssysN = denssysN + densN(i)
         ncountchkSO2 = ncountchkSO2 + ncount(i)
         ncountchkN2 = ncountchkN2 + ncountN(i)
         ncountchk = ncountchk + ncount(i) + ncountN(i)
      END DO

      DO i = 21,20+slabs2
     0    WRITE(11,'(2I10,2E12.4,I10,2E12.4,I10)') nstep,i,dens(i),
     1       Tmeanout(i),ncount(i),densN(i),TmeanoutN(i),ncountN(i)
         Tmeansys = Tmeansys + Tmean(i) + TmeanN(i)
         denssys = denssys + dens(i)
```

```
            denssysN = denssysN + densN(i)
            ncountchkSO2 = ncountchkSO2 + ncount(i)
            ncountchkN2 = ncountchkN2 + ncountN(i)
            ncountchk = ncountchk + ncount(i) + ncountN(i)
          END DO

C     output of the temperature of the tube
      0       WRITE(13,'(I10,E12.4,I10)') nstep,TmeanoutC,
      1          ncountC
            TmeanC = 0

          Tmeansys = Tmeansys / (ncountchk - ncountchkold)
          denssys = denssys / ((slabs + hollows + slabs2))
          denssysN = denssysN / ((slabs + hollows + slabs2))
      0   WRITE(11,'(2I10,2E12.4,I10,2E12.4,I10)') nstep,i,denssys,
      1       Tmeansys,ncountchkSO2,denssysN,Tmeansys,ncountchkN2

          Tmeansys = 0
          denssys = 0
          denssysN = 0
          ncountchkold = ncountchk
          ncount(:) = 0
          ncountN(:) = 0
          Tmean(:) = 0
          TmeanN(:) = 0
          dens(:) = 0
          densN(:) = 0

          BACKSPACE(10)
        END DO
        RETURN
        END

C     ================================================================
        SUBROUTINE SgnOff
C     ::::::::::::::::::::::::::::::::::::::::::::::::::::::::::::::::
C     ::Purpose: To print an end message indicating normal end of
C     ::program, and to close the output file
C     ::::::::::::::::::::::::::::::::::::::::::::::::::::::::::::::::

        WRITE(*,*)
        WRITE(*,*) '<<<End of Program>>>'
        CLOSE(10)
        CLOSE(11)
```

```
      CLOSE(12)
      CLOSE(13)

      RETURN
      END
```

C.2 Matlab code graphische_Auswertung_denslocN

Routine to evaluate the file denslocN in Matlab. The result are plots of local temperature over time, local density of each compartment over time for SO_2 and N_2. For the compartments directly at the CNT/graphene surface the local densities of SO_2 and N_2 and the respective compartments is given in two additional plots. Last the molecule count for SO_2 and N_2 is presented for the refined compartments.

```
clear all;
clc;
load('denslocN')

denslocN2 = denslocN;

% Startwert fuer Slab-Zaehlung
Anz_slabs = 1;

% while Schleife um Anzahl der Slabs zu ermitteln (einschliesslich eines
% zusaetzlichen Slabs wegen  der Aufsummierung aller Slabs, Schleife zaehlt
    aber
% einen Slab zu viel, deshalb danach Abzug des zuviel gezaehlten (Startwert
% 0 fuer Anz_slabs nicht moeglich
while denslocN2(Anz_slabs,1) == denslocN2(1,1)
   Anz_slabs = Anz_slabs + 1;
end
Anz_slabs = Anz_slabs - 1;


for j = 1:1:Anz_slabs
    for i = 1:1:size(denslocN2,1)/Anz_slabs
        step(i,1) = denslocN2 ((i - 1)*Anz_slabs + j,1); % timestep
%        slabnr (i,1) = denslocN2 ((i - 1)*Anz_slabs + j,2); %
   Teilgebietsnummer
        locdens(i,j) = denslocN2 ((i - 1)*Anz_slabs + j,3); % lokale Dichte
            SO_2
        locTemp(i,j) = denslocN2 ((i - 1)*Anz_slabs + j,4); % lokale
           Temperatur
```

```
        MolAnz(i,j) = denslocN2 ((i - 1)*Anz_slabs + j,5); % Molekuelanzahl
            SO_2 in Teilgebiet
        locdensN(i,j) = denslocN2 ((i - 1)*Anz_slabs + j,6); % lokale
            Dichte N_2
        locTemp_N(i,j) = denslocN2 ((i - 1)*Anz_slabs + j,7); % lokale
            Temperatur
        MolAnzN(i,j) = denslocN2 ((i - 1)*Anz_slabs + j,8); %
            Molekuelanzahl N_2 in Teilgebiet
    end
end

for i = 1:1:Anz_slabs - 1
    leg(i,1) = i;
end
leg = char(num2str(leg));
t = char('mean value');
leg = strvcat(leg,t);

% Teil =[5 7 8 9 10];
Teil =[5 10 11 12 13];
timestep = 0.002;
numbering = ['  I';' II';'III';' IV';'  V'];
%numbering = ['  I';' II';'III'];

for i = 1:1:size(Teil,2)
    legTeilt(i,1) = Teil(1,i);
    legTeileinfach(i,:) = numbering(i,:);
    if (i > 1)
        legTeileinfachAnz(i-1,:) = numbering(i,:);
    end
end
legTeil = char(num2str(legTeilt));
legTeileinfach = char(num2str(legTeileinfach));
legTeileinfachAnz = char(num2str(legTeileinfachAnz));
legTeilTitle =(num2str(legTeilt));
TitleTeil = strcat(num2str(numbering),' compartment',legTeilTitle);

step = step*timestep/1000;

% figure(1)
figure('Color','white','Toolbar','none','Position',get(0,'ScreenSize'))
hold on
set(gca,'LineStyleOrder',{':','-','--','-.'});
```

```
plot(step(:,1),locTemp); %FGK hier um _N ergaenzen fuer reine N2
    Simulationen
% title ('Temperatur');
xlabel('step');
ylabel('Temperatur in [K]');
legend(leg,'Location','BestOutside');
set(gca,'XGrid','on');
set(gca,'YGrid','on');
hold off
orient landscape
saveas(gcf,'lokale_Werte_Temp','pdf');

% figure(2)
figure('Color','white','Toolbar','none','Position',get(0,'ScreenSize'))
hold on
set(gca,'LineStyleOrder',{':','-','--','-.'});
plot(step(:,1),locdens);
title ('lokale Dichte SO_2');
xlabel('step');
ylabel('lokale Dichte in [mol/m^3]');
legend(leg,'Location','BestOutside');
set(gca,'XGrid','on');
%set(gca,'XMinorGrid','on');
set(gca,'YGrid','on');
%set(gca,'YMinorGrid','on');
hold off
orient landscape
saveas(gcf,'lokale_Werte_dens','pdf');

% figure(3)
figure('Color','white','Toolbar','none','Position',get(0,'ScreenSize'))
hold on
set(gca,'LineStyleOrder',{':','-','--','-.'});
plot(step(:,1),locdensN);
title ('lokale Dichte N_2');
xlabel('step');
ylabel('lokale Dichte in [mol/m^3]');
legend(leg,'Location','BestOutside');
set(gca,'XGrid','on');
%set(gca,'XMinorGrid','on');
set(gca,'YGrid','on');
%set(gca,'YMinorGrid','on');
hold off
orient landscape
```

```
saveas(gcf,'lokale_Werte_densN2','pdf');

% figure(4)
figure('Color','white','Toolbar','none','Position',get(0,'ScreenSize'))
hold on
set(gca,'XGrid','on','YGrid','on','fontsize',13);
% set(gca,'XGrid','on','YGrid','on','YMinorGrid','on','fontsize',13);
plot(step(:,1),locdens(:,Teil))
title ('lokale Dichte SO_2');
xlabel('time [ns]');
ylabel('lokale Dichte [mol/m^3]');
legend(legTeileinfach,'Location','BestOutside');
hold off
orient landscape
saveas(gcf,'lokale_Werte_dens_relevant','pdf');

% figure(5)
figure('Color','white','Toolbar','none','Position',get(0,'ScreenSize'))
hold on
set(gca,'XGrid','on','YGrid','on','fontsize',13);
% set(gca,'XGrid','on','YGrid','on','YMinorGrid','on','fontsize',13);
plot(step(:,1),locdensN(:,Teil))
title ('lokale Dichte N_2');
xlabel('time [ns]');
ylabel('lokale Dichte [mol/m^3]');
legend(legTeileinfach,'Location','BestOutside');
hold off
orient landscape
saveas(gcf,'lokale_Werte_densN2_relevant','pdf');

% figure(6)
figure('Color','white','Toolbar','none','Position',get(0,'ScreenSize'))
hold on
% set(gca,'XGrid','on','YGrid','on','YMinorGrid','on','fontsize',13);
subplot(2,1,1); plot(step(:,1),MolAnz(:,[Teil(2) Teil(3) Teil(4) Teil(5)]))
set(gca,'XGrid','on','YGrid','on','fontsize',13);
title ('Molekuelanzahl SO_2');
xlabel('time [ns]');
ylabel('number of SO_2 molecules [-]');
legend(legTeileinfachAnz,'Location','BestOutside');
subplot(2,1,2); plot(step(:,1),MolAnzN(:,[Teil(2) Teil(3) Teil(4) Teil(5)])
    )
set(gca,'XGrid','on','YGrid','on','fontsize',13);
title ('Molekuelanzahl N_2');
```

```
xlabel('time [ns]');
ylabel('number of N_2 molecules [-]');
legend(legTeileinfachAnz,'Location','BestOutside');
hold off
orient landscape
saveas(gcf,'lokale_Molekuelanzahl_relevant','pdf');
```

C.3 Matlab code ZustandswerteN2_corr_p

Routine to evaluate the file denslocN in Matlab. Here additionally the pressure in each compartment is calculated by a Peng-Robinson equation of state using either the van-der-Waals mixing rule or the Wong-Sandler mixing rule. In the shown code the Wong-Sandler mixing rule is active and the van-der-Waals mixing rule is commented out. All respective equations are shown in chapter 3.3.

```
clear all;
clc;

% SO_2
R = 8.314472; % [J/(mol*K)]
T_c = 430.64; % [K] lt. NIST
p_c = 78.840*10^5; % [Pa] lt. NIST
a = 0.457235*R^2*T_c^2/p_c;
b = 0.077796*R*T_c/p_c;
omega = 0.256; % acentric factor

% N_2
T_c_N = 126.192; % [K] lt. NIST
p_c_N = 33.958*10^5; % [Pa] lt. NIST
a_N = 0.457235*R^2*T_c_N^2/p_c_N;
b_N = 0.077796*R*T_c_N/p_c_N;
omega_N = 0.0372; % azentric factor acc. to  Pitzer, Corresponding States
    for perfect liquids, J Chem Phys, 7, 583-590, 1939

%%%%%%%%%%%%%%%%%%%%%%%%%%%%%%%%%%%%%%%%%%%%%%%%%%%%%%%%%%%%%%%%%%%%%%%%%%%%%%%%
load('denslocN')
densloc = denslocN;

% Startwert fuer Slab-Zaehlung
Anz_slabs = 1;

% while Schleife um Anzahl der Slabs zu ermitteln (einschliesslich
```

```
% zusaetzlichen Slab wegen Aufsummierung aller Slabs, Schleife zaehlt aber
% einen Slab zu viel, deshalb danach Abzug des zuviel gezaehlten (Startwert
% 0 fuer Anz_slabs nicht moeglich
while densloc(Anz_slabs,1) == densloc(1,1)
   Anz_slabs = Anz_slabs + 1;
end
Anz_slabs = Anz_slabs - 1;


for j = 1:1:Anz_slabs-1
    for i = 1:1:size(densloc,1)/Anz_slabs
        step(i,1) = densloc ((i - 1)*Anz_slabs + j,1); % timestep
%        slabnr (i,1) = densloc ((i - 1)*Anz_slabs + j,2); %
    Teilgebietsnummer
        locdens(i,j) = densloc ((i - 1)*Anz_slabs + j,3); % lokale Dichte
        locTemp(i,j) = densloc ((i - 1)*Anz_slabs + j,4); % lokale
            Temperatur
        MolAnz(i,j) = densloc ((i - 1)*Anz_slabs + j,5); % Molekuelanzahl
            in Teilgebiet
        locdens_N(i,j) = densloc ((i - 1)*Anz_slabs + j,6); % lokale Dichte
             N2
        locTemp_N(i,j) = densloc ((i - 1)*Anz_slabs + j,7); % lokale
            Temperatur N2
        MolAnzN(i,j) = densloc ((i - 1)*Anz_slabs + j,8); % Molekuelanzahl
            in Teilgebiet

        % FGK for pure N2 evaluations uncomment the following line:
        % locTemp(i,j) = locTemp_N(i,j);

        % mole ratio x in the repsective compartment j at timestep i for
        % SO_2
        x(i,j) = (MolAnz(i,j))./(MolAnz(i,j)+MolAnzN(i,j));

        % SO_2
        T_r = locTemp(i,j) / T_c;
        alpha = (1 + (0.37464 + 1.54226*omega - 0.26992*omega^2)*(1-T_r
            ^0.5))^2;
        p(i,j) = R*locTemp(i,j)/(1/locdens(i,j) - b) - a*alpha /((1/locdens
            (i,j))^2 + 2*b*(1/locdens(i,j))- b^2);

        % N_2
        T_r_N = locTemp_N(i,j) / T_c_N;
        alpha_N = (1 + (0.37464 + 1.54226*omega_N - 0.26992*omega_N^2)*(1-
            T_r_N^0.5))^2;
```

```
        p_N(i,j) = R*locTemp_N(i,j)/(1/locdens_N(i,j) - b_N) - a_N*alpha_N
            /((1/locdens_N(i,j))^2 + 2*b_N*(1/locdens_N(i,j))- b_N^2);

%         % vdW mixing rule
%         % calculation of parameters a, a_N, b and b_N for the mixture a
    and
%         % a_N = a_m and b and b_N = b_m
%         % according to Shibata and Sandler, Ind Eng Chem Rev (1989), 28,
    1893-1898
%
%         % SO2
%         T_r = locTemp(i,j) / T_c;
%         alpha = (1 + (0.37464 + 1.54226*omega - 0.26992*omega^2)*(1-T_r
    ^0.5))^2;
%         % N2
%         T_r_N = locTemp_N(i,j) / T_c_N;
%         alpha_N = (1 + (0.37464 + 1.54226*omega_N - 0.26992*omega_N^2)
    *(1-T_r_N^0.5))^2;
%
%         a_m = x(i,j)*x(i,j)*a*alpha + 2*x(i,j)*(1-x(i,j))*(a*alpha*a_N*
    alpha_N)^(0.5)*(1-0.08) + (1-x(i,j))*(1-x(i,j))*a_N*alpha_N; % k_ij =
    0.08 according to Prausnitz for SO2/N2
%         b_m = x(i,j)*b + (1-x(i,j))*b_N;
%
%         % SO_2_new
%         p_new(i,j) = R*locTemp(i,j)/(1/locdens(i,j) - b_m) - a_m /((1/
    locdens(i,j))^2 + 2*b_m*(1/locdens(i,j))- b_m^2);
%
%         % N_2_new
%         p_N_new(i,j) = R*locTemp_N(i,j)/(1/locdens_N(i,j) - b_m) - a_m
    /((1/locdens_N(i,j))^2 + 2*b_m*(1/locdens_N(i,j))- b_m^2);


        % Wong Sandler mixing rule with NRTL as G^E model
        % calculation of parameters a, a_N, b and b_N, for the mixture a_m
            and
        % b_m with the help of tau_N2SO2, tau_SO2N2, k_ij, alpha_ij, C,
        % G_N2SO2, G_SO2N2, GE, b_ij
        % according to Shibata and Sandler, Ind Eng Chem Rev (1989), 28,
            1893-1898
        % SO2
        T_r = locTemp(i,j) / T_c;
        alpha = (1 + (0.37464 + 1.54226*omega - 0.26992*omega^2)*(1-T_r
            ^0.5))^2;
```

```
        % N2
        T_r_N = locTemp_N(i,j) / T_c_N;
        alpha_N = (1 + (0.37464 + 1.54226*omega_N - 0.26992*omega_N^2)*(1-
            T_r_N^0.5))^2;

        C = 2^(-0.5)*log(2^(0.5) - 1); % constant for the PR equation and
            the used mixing rule
        k_ij = 0.29 + 0.001175 *locTemp(i,j); % interaction parameter
        tau_N2SO2 = 6.055 - 0.01597 * locTemp(i,j); % NRTL binary parameter
        tau_SO2N2 = -3.388 + 0.01368 * locTemp(i,j); % NRTL binary
            parameter
        alpha_ij = 0.48; % NRTL binary interaction parameter

        G_N2SO2 = exp(alpha_ij * tau_N2SO2); % excess Gibbs free energy for
             the binary interaction N2/SO2 for the NRTL model
        G_SO2N2 = exp(alpha_ij * tau_SO2N2); % excess Gibbs free energy for
             the binary interaction SO2/N2 for the NRTL model
        GE = x(i,j)*(1-x(i,j)) * (((tau_SO2N2*G_SO2N2)/((1-x(i,j)) + x(i,j)
            *G_SO2N2)) + ((tau_N2SO2*G_N2SO2)/(x(i,j) + (1-x(i,j))*G_N2SO2))
            ); % G^E/RT excess Gibbs free energy per RT

        b_ij = (1-x(i,j))^2 * (b_N - (a_N/(R*locTemp(i,j)))) + 2*(1-x(i,j))
            *x(i,j)*((((b_N - (a_N/(R*locTemp(i,j)))) + (b - (a/(R*locTemp(i
            ,j))))))/2) * (1 - k_ij) ) + (x(i,j))^2 * (b - (a/(R*locTemp(i,j)
            ))); % parameter to calculate b_m

        b_m = b_ij/(1 - GE/C - (((x(i,j)*a)/(R*locTemp(i,j)*b)) + (((1-x(i,
            j))*a_N)/(R*locTemp(i,j)*b_N))));
        a_m_help = x(i,j)*a/b + (1-x(i,j))*a_N/b_N + GE*R*locTemp(i,j)/C; %
             a_m/b_m
        a_m = a_m_help * b_m;

        % SO_2_new
        p_new(i,j) = R*locTemp(i,j)/(1/locdens(i,j) - b_m) - a_m /((1/
            locdens(i,j))^2 + 2*b_m*(1/locdens(i,j))- b_m^2);

        % N_2_new
        p_N_new(i,j) = R*locTemp_N(i,j)/(1/locdens_N(i,j) - b_m) - a_m
            /((1/locdens_N(i,j))^2 + 2*b_m*(1/locdens_N(i,j))- b_m^2);

    end
end

for i = 1:1:Anz_slabs - 1
```

```
    leg(i,1) = i;
end
leg = char(num2str(leg));

% Teil =[5 7 8 9 10];
Teil =[5 10 11 12 13];
bulk =[1 2 3 4 5];
timestep = 0.002;
numbering = ['  I';' II';'III';' IV';'  V'];
%numbering = ['  I';' II';'III'];

for i = 1:1:size(Teil,2)
    legTeilt(i,1) = Teil(1,i);
    legTeileinfach(i,:) = numbering(i,:);
    if (i>1)
        legTeileinfachAnz(i-1,:) = numbering(i,:);
    end
end
legTeil = char(num2str(legTeilt));
legTeileinfach = char(num2str(legTeileinfach));
legTeileinfachAnz = char(num2str(legTeileinfachAnz));
legTeilTitle =(num2str(legTeilt));
TitleTeil = strcat(num2str(numbering),' compartment',legTeilTitle);

step = step*timestep/1000;

% figure(1)
figure('Color','white','Toolbar','none','Position',get(0,'ScreenSize'))
hold on
%set(gca,'LineStyleOrder',{':','-','--','-.'});
set(gca,'LineStyleOrder',{':','-','—','-.'},'XGrid','on','YGrid','on','
    YMinorGrid','on','fontsize',13);
plot(step(:,1),p_new/10^5);
% title ('Temperatur');
xlabel('time [ns]');
ylabel('partial pressure SO_2 [bar]');
legend(leg,'Location','BestOutside');
hold off

% figure(2)
figure('Color','white','Toolbar','none','Position',get(0,'ScreenSize'))
hold on
%set(gca,'LineStyleOrder',{':','-','--','-.'});
```

```
set(gca,'LineStyleOrder',{':','-','--','-.'},'XGrid','on','YGrid','on','
    YMinorGrid','on','fontsize',13);
plot(step(:,1),p_N_new/10^5);
% title ('Temperatur');
xlabel('time [ns]');
ylabel('partial pressure N_2 [bar]');
legend(leg,'Location','BestOutside');
hold off

% figure(3)
figure('Color','white','Toolbar','none','Position',get(0,'ScreenSize'))
hold on
%set(gca,'LineStyleOrder',{':','-','--','-.'});
set(gca,'LineStyleOrder',{':','-','--','-.'},'XGrid','on','XMinorGrid','on'
    ,'YGrid','on','YMinorGrid','on','fontsize',13);
plot(step(:,1),locdens);
title ('local density SO_2');
xlabel('time [ns]');
ylabel('local density [mol/m^3]');
legend(leg,'Location','BestOutside');
hold off

% figure(4)
figure('Color','white','Toolbar','none','Position',get(0,'ScreenSize'))
hold on
%set(gca,'LineStyleOrder',{':','-','--','-.'});
set(gca,'LineStyleOrder',{':','-','--','-.'},'XGrid','on','XMinorGrid','on'
    ,'YGrid','on','YMinorGrid','on','fontsize',13);
plot(step(:,1),locdens_N);
title ('local density N_2');
xlabel('time [ns]');
ylabel('local density [mol/m^3]');
legend(leg,'Location','BestOutside');
hold off

% figure(5)
figure('Color','white','Toolbar','none','Position',get(0,'ScreenSize'))
hold on
%set(gca,'LineStyleOrder',{':','-','--','-.'});
set(gca,'LineStyleOrder',{':','-','--','-.'},'XGrid','on','YGrid','on','
    YMinorGrid','on','fontsize',13);
subplot(4,1,1); plot(step(:,1),p_new(:,Teil)/10^5)
% title ('Temperatur');
xlabel('time [ns]');
```

```
ylabel('partial pressure SO_2 [bar]');
legend(legTeil,'Location','BestOutside');
set(gca,'LineStyleOrder',{':','-','--','-.'});
subplot(4,1,2); plot(step(:,1),p_N_new(:,Teil)/10^5);
xlabel('time [ns]');
ylabel('partial pressure N_2 [bar]');
legend(legTeil,'Location','BestOutside');
set(gca,'LineStyleOrder',{':','-','--','-.'});
subplot(4,1,3); plot(step(:,1),(p_new(:,bulk) + p_N_new(:,bulk))/10^5);
xlabel('time [ns]');
ylabel('bulk pressure [bar]');
legend('1','2','3','4','5','Location','BestOutside');
set(gca,'LineStyleOrder',{':','-','--','-.'});
subplot(4,1,4); plot(step(:,1),locTemp(:,Teil)); % FGK hier _N bei locTemp
    hinzufuegen fuer N2 Simulationen
xlabel('time [ns]');
ylabel('Temperature [K]');
legend(legTeil,'Location','BestOutside');
hold off
orient landscape
saveas(gcf,'Zust_N_lokale_Werte_pressure','pdf');

% figure(6)
figure('Color','white','Toolbar','none','Position',get(0,'ScreenSize'))
hold on
set(gca,'XGrid','on','YGrid','on','YMinorGrid','on','fontsize',13);
plot(step(:,1),locdens(:,Teil))
%title (TitleTeil);
xlabel('time [ns]');
ylabel('local density SO_2 [mol/m^3]');
legend(legTeileinfach,'Location','BestOutside');
set(gca,'LineStyleOrder',{':','-','--','-.'});
hold off
orient landscape
saveas(gcf,'Zust_N_lokale_Werte_density_relevant','pdf');

% figure(7)
figure('Color','white','Toolbar','none','Position',get(0,'ScreenSize'))
hold on
set(gca,'XGrid','on','YGrid','on','YMinorGrid','on','fontsize',13);
plot(step(:,1),locdens_N(:,Teil))
%title (TitleTeil);
xlabel('time [ns]');
ylabel('local density N_2 [mol/m^3]');
```

```
legend(legTeileinfach,'Location','BestOutside');
set(gca,'LineStyleOrder',{':','-','--','-.'});
hold off
orient landscape
saveas(gcf,'Zust_N_lokale_Werte_density_relevant_N2','pdf');

xrange = 5900000 / 2000 + 1;

for i = xrange:size(p,1)
    % SO_2
    step_adj(i-xrange+1,1) = step (i,1);
    adjusted_plot_p(i-xrange+1,:) = p_new(i,:);
    adjusted_plot_T(i-xrange+1,:) = locTemp(i,:);
    adjusted_plot_dens(i-xrange+1,:) = locdens(i,:);
    adjusted_plot_count(i-xrange+1,:) = MolAnz(i,:);

    adjusted_plot_x(i-xrange+1,:) = x(i,:);

    %N_2
    adjusted_plot_p_N(i-xrange+1,:) = p_N_new(i,:);
    adjusted_plot_T_N(i-xrange+1,:) = locTemp_N(i,:);
    adjusted_plot_dens_N(i-xrange+1,:) = locdens_N(i,:);
    adjusted_plot_count_N(i-xrange+1,:) = MolAnzN(i,:);
end

% SO_2
mean_pressure = mean(adjusted_plot_p)/10^5
mean_pressure_adj = mean(adjusted_plot_p(:,Teil))/10^5
mean_temperature = mean(adjusted_plot_T)
mean_temperature_adj = mean(adjusted_plot_T(:,Teil))
mean_density = mean(adjusted_plot_dens)
mean_density_adj = mean(adjusted_plot_dens(:,Teil))
mean_SO2_count = round(mean(adjusted_plot_count))

mean_x = mean(adjusted_plot_x)
mean_x_adj = mean(adjusted_plot_x(:,Teil))

save('Zust_N_mean_pressure.txt','mean_pressure','-ASCII','-DOUBLE','-TABS')
save('Zust_N_mean_temperature.txt','mean_temperature','-ASCII','-DOUBLE','-
    TABS')
save('Zust_N_mean_density.txt','mean_density','-ASCII','-DOUBLE','-TABS')
save('Zust_N_SO2_count.txt','mean_SO2_count','-ASCII','-DOUBLE','-TABS')
save('Zust_N_x.txt','mean_x','-ASCII','-DOUBLE','-TABS')
```

```
% N_2
mean_pressure_N = mean(adjusted_plot_p_N)/10^5
mean_pressure_adj_N = mean(adjusted_plot_p_N(:,Teil))/10^5
mean_temperature_N = mean(adjusted_plot_T_N)
mean_temperature_adj_N = mean(adjusted_plot_T_N(:,Teil))
mean_density_N = mean(adjusted_plot_dens_N)
mean_density_adj_N = mean(adjusted_plot_dens_N(:,Teil))
mean_N2_count = round(mean(adjusted_plot_count_N))

save('Zust_N_mean_pressure_N.txt','mean_pressure_N','-ASCII','-DOUBLE','-
    TABS')
save('Zust_N_mean_density_N.txt','mean_density_N','-ASCII','-DOUBLE','-TABS
    ')
save('Zust_N_N2_count.txt','mean_N2_count','-ASCII','-DOUBLE','-TABS')
save('Zust_N_mean_temperature_N.txt','mean_temperature_N','-ASCII','-DOUBLE
    ','-TABS')

% FGK mean_temperature um _N ergaenzen fuer N2 Simulationen;
save('Zust_N_all.txt','mean_density','mean_SO2_count','mean_pressure','
    mean_density_N','mean_N2_count','mean_pressure_N','mean_temperature','
    mean_x','-ASCII','-DOUBLE','-TABS')

% figure(8)
figure('Color','white','Toolbar','none','Position',get(0,'ScreenSize'))
hold on
subplot(5,1,1); plot(step_adj(:,1),adjusted_plot_dens(:,Teil));
title(TitleTeil);
xlabel('time [ns]');
ylabel('\rho_{SO_2} [mol/m^3]');
legend(legTeileinfach,'Location','BestOutside');
set(gca,'XGrid','on','YGrid','on','YMinorGrid','on','fontsize',13);
subplot(5,1,2); plot(step_adj(:,1),adjusted_plot_dens_N(:,Teil));
xlabel('time [ns]');
ylabel('\rho_{N_2} [mol/m^3]');
legend(legTeileinfach,'Location','BestOutside');
set(gca,'XGrid','on','YGrid','on','YMinorGrid','on','fontsize',13);
subplot(5,1,3); plot(step_adj(:,1),adjusted_plot_p(:,Teil)/10^5)
xlabel('time [ns]');
ylabel('p_{SO_2} [bar]');
% legend(legTeil,'Location','BestOutside');
legend(legTeileinfach,'Location','BestOutside')
set(gca,'XGrid','on','YGrid','on','YMinorGrid','on','fontsize',13);
subplot(5,1,4); plot(step_adj(:,1),adjusted_plot_p_N(:,Teil)/10^5)
xlabel('time [ns]');
```

```
ylabel('p_{N_2} [bar]');
% legend(legTeil,'Location','BestOutside');
legend(legTeileinfach,'Location','BestOutside')
set(gca,'XGrid','on','YGrid','on','YMinorGrid','on','fontsize',13);
subplot(5,1,5); plot(step_adj(:,1),adjusted_plot_T(:,Teil));
xlabel('time [ns]');
ylabel('T [K]');
legend(legTeileinfach,'Location','BestOutside');
set(gca,'XGrid','on','YGrid','on','YMinorGrid','on','fontsize',13);
hold off
orient landscape
saveas(gcf,'Zust_N_lokale_Werte_pressure_adjusted','pdf');

% figure(9)
figure('Color','white','Toolbar','none','Position',get(0,'ScreenSize'))
hold on
subplot(2,1,1); plot(step_adj(:,1),adjusted_plot_count(:,[Teil(2) Teil(3)
    Teil(4) Teil(5)]));
% title(TitleTeil);
xlabel('time [ns]');
ylabel('local number of SO_2 molecules [-]');
legend(legTeileinfachAnz,'Location','BestOutside');
set(gca,'XGrid','on','YGrid','on','YMinorGrid','on','fontsize',13);
subplot(2,1,2); plot(step_adj(:,1),adjusted_plot_count_N(:,[Teil(2) Teil(3)
     Teil(4) Teil(5)]));
xlabel('time [ns]');
ylabel('local number of N_2 molecules [-]');
legend(legTeileinfachAnz,'Location','BestOutside');
set(gca,'XGrid','on','YGrid','on','YMinorGrid','on','fontsize',13);
hold off
orient landscape
saveas(gcf,'Zust_N_lokale_Molekuelanzahl_adjusted','pdf');

% figure(10)
figure('Color','white','Toolbar','none','Position',get(0,'ScreenSize'))
hold on
%set(gca,'LineStyleOrder',{':','-','--','-.'});
set(gca,'LineStyleOrder',{':','-','--','-.'},'XGrid','on','XMinorGrid','on'
    ,'YGrid','on','YMinorGrid','on','fontsize',13);
plot(step(:,1),x);
title ('molar ratio x(SO_2)');
xlabel('time [ns]');
ylabel('molar ratio x(SO_2) [-]');
legend(leg,'Location','BestOutside');
```

```
hold off
orient landscape
saveas(gcf,'Zust_N_lokaler_Molenbruch','pdf');

% figure(11)
figure('Color','white','Toolbar','none','Position',get(0,'ScreenSize'))
hold on
%set(gca,'LineStyleOrder',{':','-','--','-.'});
set(gca,'LineStyleOrder',{':','-','--','-.'},'XGrid','on','YGrid','on','
    YMinorGrid','on','fontsize',13);
subplot(4,2,1); plot(step(:,1),p(:,Teil)/10^5)
% title ('Temperatur');
xlabel('time [ns]');
ylabel('p(SO_2) [bar]');
legend(legTeil,'Location','BestOutside');
set(gca,'LineStyleOrder',{':','-','--','-.'});
subplot(4,2,3); plot(step(:,1),p_N(:,Teil)/10^5);
xlabel('time [ns]');
ylabel('p(N_2) [bar]');
legend(legTeil,'Location','BestOutside');
set(gca,'LineStyleOrder',{':','-','--','-.'});
subplot(4,2,5); plot(step(:,1),(p_new(:,bulk))/10^5);
xlabel('time [ns]');
ylabel('bulk p_{new}(SO_2) [bar]');
legend('1','2','3','4','5','Location','BestOutside');
set(gca,'LineStyleOrder',{':','-','--','-.'});
subplot(4,2,7); plot(step(:,1),locTemp(:,Teil)); % FGK hier _N bei locTemp
    hinzufuegen fuer N2 Simulationen
xlabel('time [ns]');
ylabel('Temperature [K]');
legend(legTeil,'Location','BestOutside');
set(gca,'LineStyleOrder',{':','-','--','-.'},'XGrid','on','YGrid','on','
    YMinorGrid','on','fontsize',13);
subplot(4,2,2); plot(step(:,1),p_new(:,Teil)/10^5)
% title ('Temperatur');
xlabel('time [ns]');
ylabel('p_{new}(SO_2) [bar]');
legend(legTeil,'Location','BestOutside');
set(gca,'LineStyleOrder',{':','-','--','-.'});
subplot(4,2,4); plot(step(:,1),p_N_new(:,Teil)/10^5);
xlabel('time [ns]');
ylabel('p_{new}(N_2) [bar]');
legend(legTeil,'Location','BestOutside');
set(gca,'LineStyleOrder',{':','-','--','-.'});
```

```
subplot(4,2,6); plot(step(:,1),(p_N_new(:,bulk))/10^5);
xlabel('time [ns]');
ylabel('bulk p_{new}(N_2) [bar]');
legend('1','2','3','4','5','Location','BestOutside');
set(gca,'LineStyleOrder',{':','-','--','-.'});
subplot(4,2,8); plot(step(:,1),locTemp(:,Teil)); % FGK hier _N bei locTemp
    hinzufuegen fuer N2 Simulationen
xlabel('time [ns]');
ylabel('Temperature [K]');
legend(legTeil,'Location','BestOutside');
set(gca,'LineStyleOrder',{':','-','--','-.'},'XGrid','on','YGrid','on','
    YMinorGrid','on','fontsize',13);
hold off
orient landscape
saveas(gcf,'Zust_N_Uebersicht','pdf');

% figure(12)
figure('Color','white','Toolbar','none','Position',get(0,'ScreenSize'))
hold on
%set(gca,'LineStyleOrder',{':','-','--','-.'});
set(gca,'LineStyleOrder',{':','-','--','-.'},'XGrid','on','YGrid','on','
    YMinorGrid','on','fontsize',13);
subplot(4,1,1); plot(step(:,1),(p(:,Teil)-p_new(:,Teil))/10^5)
% title ('Temperatur');
xlabel('time [ns]');
ylabel('p(SO_2) - p_{new}(SO_2) [bar]');
legend(legTeil,'Location','BestOutside');
set(gca,'LineStyleOrder',{':','-','--','-.'});
subplot(4,1,2); plot(step(:,1),(p_N(:,Teil)-p_N_new(:,Teil))/10^5);
xlabel('time [ns]');
ylabel('p(N_2) - p_{new}(N_2) [bar]');
legend(legTeil,'Location','BestOutside');
set(gca,'LineStyleOrder',{':','-','--','-.'});
subplot(4,1,3); plot(step(:,1),((p(:,bulk) + p_N(:,bulk))-(p_new(:,bulk) +
    p_N_new(:,bulk)))/10^5);
xlabel('time [ns]');
ylabel('total bulk p - total bulk p_{new} [bar]');
legend('1','2','3','4','5','Location','BestOutside');
set(gca,'LineStyleOrder',{':','-','--','-.'});
subplot(4,1,4); plot(step(:,1),locTemp(:,Teil)); % FGK hier _N bei locTemp
    hinzufuegen fuer N2 Simulationen
xlabel('time [ns]');
ylabel('Temperature [K]');
legend(legTeil,'Location','BestOutside');
```

```
hold off

% figure(13)
figure('Color','white','Toolbar','none','Position',get(0,'ScreenSize'))
hold on
subplot(2,1,1);plot(step(:,1),(p(:,bulk))/10^5);
xlabel('time [ns]');
ylabel('bulk p(SO2) [bar]');
legend('1','2','3','4','5','Location','BestOutside');
set(gca,'LineStyleOrder',{':','-','--','-.'});
subplot(2,1,2); plot(step(:,1),(p_new(:,bulk))/10^5);
xlabel('time [ns]');
ylabel('bulk p_{new}(SO2) [bar]');
legend('1','2','3','4','5','Location','BestOutside');
hold off
```

C.4 Matlab code blank_equ_m_corr

In this matlab code the blank, buoyancy and measurement data from the experimental setup is used to post-process and correct for buoyancy effects caused by the blank setup and the pristine sample on the measured data. Therefore, the respective blank data file, buoyancy data file and measurement data file is read in and stored into different variables. Here in the given code, exemplary a VACNT sample in SO_2 atmosphere at 25 °C is shown. From the blank data, as described in chapter 4.2, the sample container mass and volume is derived. The same is done for the sample mass and volume based on the buoyancy data. With this information the adsorption isotherm can be plotted. The data is saved from this file to be available for further post-processing e.g. fitting operations.

```
clear all;
format long;

% insert file names of buoyancy measurement and measurement

%%%%%%%%%%%%%%%%%%%%%%%%%%%%%%%%%%%%%%%%%%%%%%%%%%%%%%%%%%%%%%%%%%%%%%%%%%%%%%%%
%%%% VACNT SO2
%%%%%%%%%%%%%%%%%%%%%%%%%%%%%%%%%%%%%%%%%%%%%%%%%%%%%%%%%%%%%%%%%%%%%%%%%%%%%%%%

% VACNT and SO2 15C 'results/VACNT_SO2_15C.mat'
% buoyancy_data = 'VACNT_He_15C_20170320.equ'; %FGK
% measurement_data = 'VACNT_SO2_15C_20170321.equ'; %FGK
```

```
% VACNT and SO2 25C 'results/VACNT_SO2_25C.mat'
 buoyancy_data = 'VACNT_He_25C_20170313.equ'; %FGK
 measurement_data = 'VACNT_SO2_25C_20170314.equ'; %FGK

% VACNT and SO2 35C 'results/VACNT_SO2_35C.mat'
% buoyancy_data = 'VACNT_He_35C_20170327.equ'; %FGK
% measurement_data = 'VACNT_SO2_35C_20170328.equ'; %FGK

% VACNT and SO2 50C 'results/VACNT_SO2_50C.mat'
% buoyancy_data = 'VACNT_He_50C_20170410.equ'; %FGK
% measurement_data = 'VACNT_SO2_50C_20170411.equ'; %FGK

% VACNT and SO2 75C 'results/VACNT_SO2_75C.mat'
% buoyancy_data = 'VACNT_He_75C_20170403.equ'; %FGK
% measurement_data = 'VACNT_SO2_75C_20170404_combined.equ'; %FGK

%%%%%%%%%%%%%%%%%%%%%%%%%%%%%%%%%%%%%%%%%%%%%%%%%%%%%%%%%%%%%%%%%%%%%%%%%%%%%%%
%%%%%%%%%%%%%%%%%%%%%%%%%%%%%%%%%%%%%%%%%%%%%%%%%%%%%%%%%%%%%%%%%%%%%%%%%%%%%%%
%%%%%%%%%%%%%%%%%%%%%%%%%%%%%%%%%%%%%%%%%%%%%%%%%%%%%%%%%%%%%%%%%%%%%%%%%%%%%%%

% choose right temperature for blank measurement by setting 'blank_input'
% to the right value (possible: 0, 20, 25.2013, 25.2014, 30, 40, 50, 60,
    75, 80, 100, 125, 150, 175, 200)
blank_input = 25.2013;

% choose right messuring gas 0 = CO2; 1 = SO2; 2 = N2
meassuring_gas = 1;

if (meassuring_gas == 0) % CO2
    Molar_mass_gas = 44.0095; %[g mol{-1}] (data from NIST)
elseif (meassuring_gas == 1) % SO2
    Molar_mass_gas = 64.064; %[g mol{-1}] (data from NIST)
elseif (meassuring_gas == 2) % N2
    Molar_mass_gas = 28.0234; %[g mol{-1}] (data from NIST)
end

% blank input
if (blank_input == 0)
    blank_data = 'blank/He_blank_0C_2014.equ';
elseif (blank_input == 20)
    blank_data = 'blank/He_blank_20C_2014.equ';
elseif (blank_input == 25.2013)
    blank_data = 'blank/He_blank_25C_2013.equ';
```

```
elseif (blank_input == 25.2014)
    blank_data = 'blank/He_blank_25C_2014.equ';
elseif (blank_input == 30)
    blank_data = 'blank/He_blank_30C_2014.equ';
elseif (blank_input == 40)
    blank_data = 'blank/He_blank_40C_2014.equ';
elseif (blank_input == 50)
    blank_data = 'blank/He_blank_50C_2014.equ';
elseif (blank_input == 60)
    blank_data = 'blank/He_blank_60C_2014.equ';
elseif (blank_input == 75)
    blank_data = 'blank/He_blank_75C_2013.equ';
elseif (blank_input == 80)
    blank_data = 'blank/He_blank_80C_2014.equ';
elseif (blank_input == 100)
    blank_data = 'blank/He_blank_100C_2013.equ';
elseif (blank_input == 125)
    blank_data = 'blank/He_blank_125C_2014.equ';
elseif (blank_input == 150)
    blank_data = 'blank/He_blank_150C_2014.equ';
elseif (blank_input == 175)
    blank_data = 'blank/He_blank_175C_el_2013.equ';
elseif (blank_input == 200)
    blank_data = 'blank/He_blank_200C_el_2013.equ';
end

%%%%%%%%%%%%%%%%%%%%%%%%%%%%%%%%%%%%%%%%%%%%%%%%%%%%%%%%%%%%%%%%%%%%%%%%%%%%%%%%
% blank data
fid = fopen(blank_data,'r');

Title_blank = textscan(fid,'%s %s %s %s %s %*[^\n]',1);
date_blank = textscan(fid,'%s %s %s %*[^\n]',1);
experimenter_blank = textscan(fid,'%s %s %s %*[^\n]',1);
comment_blank = textscan(fid,'%s %s %s %*[^\n]',1);
empty1 = textscan(fid,'%s %*[^\n]',1);
Title1_blank = textscan(fid,'%s %s %*[^\n]',1);
empty2 = textscan(fid,'%s %*[^\n]',1);
Title2_blank = textscan(fid,'%s %s %s %s %s %s %s %s %s %*[^\n]',1,'
    delimiter', ';');
Values_blank = textscan(fid,'%f %f %f %f %f %f %f %f %f %s %*[^\n]','
    delimiter', ';');
fclose(fid);

segment_blank = Values_blank{1,1}; % segement Nr.
```

```
temperature_blank = Values_blank{1,2}; % Temperatur [°C]
sigma_temperature_blank = Values_blank{1,3}; % Sigma der Temperatur im
    Segement/ der letzten betrachteten Periode [°C]
pressure_blank = Values_blank{1,4}; % Druck [bar]
sigma_pressure_blank = Values_blank{1,5}; % Sigma des Drucks im Segement/
    der letzten betrachteten Periode [bar]
mass_blank = Values_blank{1,6}; % corr. weight am Ende des Segments [g]
massdiff_blank = Values_blank{1,7}; % corr. weight difference am Ende des
    Segments [g]
sigma_mass_blank = Values_blank{1,8}; % Sigma des Drucks im Segement/ der
    letzten betrachteten Periode [g]
density_blank = Values_blank{1,9}; % gas density [g/cm^3]

% corrections
density_blank = density_blank - density_blank(1); % offset correction for
    density

[blank_fit,blank_gof] = fit(density_blank,mass_blank,'poly1','Exclude',[1])
    ;
coeff_blank_fit = coeffvalues(blank_fit);

m_SC = coeff_blank_fit(1,2) % [g]
V_SC = -coeff_blank_fit(1,1) % [cm^3]

m_SC_meas = mass_blank(1) % [g]

%%%%%%%%%%%%%%%%%%%%%%%%%%%%%%%%%%%%%%%%%%%%%%%%%%%%%%%%%%%%%%%%%%%%%%%%%%%%
% buoyancy data
fid = fopen(buoyancy_data,'r');

Title_buoy = textscan(fid,'%s %s %s %s %s %*[^\n]',1);
date_buoy = textscan(fid,'%s %s %s %*[^\n]',1);
experimenter_buoy = textscan(fid,'%s %s %s %*[^\n]',1);
comment_buoy = textscan(fid,'%s %s %s %*[^\n]',1);
empty1 = textscan(fid,'%s %*[^\n]',1);
Title1_buoy = textscan(fid,'%s %s %*[^\n]',1);
empty2 = textscan(fid,'%s %*[^\n]',1);
Title2_buoy = textscan(fid,'%s %s %s %s %s %s %s %s %s %*[^\n]',1,'
    delimiter', ';');
Values_buoy = textscan(fid,'%f %f %f %f %f %f %f %f %f %s %*[^\n]','
    delimiter', ';');
fclose(fid);

segment_buoy = Values_buoy{1,1}; % segement Nr.
```

```
temperature_buoy = Values_buoy{1,2}; % Temperatur [°C]
sigma_temperature_buoy = Values_buoy{1,3}; % Sigma der Temperatur im
    Segement/ der letzten betrachteten Periode [°C]
pressure_buoy = Values_buoy{1,4}; % Druck [bar]
sigma_pressure_buoy = Values_buoy{1,5}; % Sigma des Drucks im Segement/ der
     letzten betrachteten Periode [bar]
mass_buoy = Values_buoy{1,6}; % corr. weight am Ende des Segments [g]
massdiff_buoy = Values_buoy{1,7}; % corr. weight difference am Ende des
    Segments [g]
sigma_mass_buoy = Values_buoy{1,8}; % Sigma des Drucks im Segement/ der
    letzten betrachteten Periode [g]
density_buoy = Values_buoy{1,9}; % gas density [g/cm^3]

% corrections
density_buoy = density_buoy - density_buoy(1); % offset correction for
    density

[buoyancy_fit,buoyancy_gof] = fit(density_buoy,mass_buoy,'poly1','Exclude'
    ,[1]);
coeff_buoyancy_fit = coeffvalues(buoyancy_fit);

m_SC_S = coeff_buoyancy_fit(1,2) % [g]
V_SC_S = -coeff_buoyancy_fit(1,1) % [cm^3]

m_S = m_SC_S - m_SC % [g]
V_S = V_SC_S - V_SC % [cm^3]
V_S_spec = V_S/m_S % [cm^3/g]
m_S_meas = mass_buoy(1) - mass_blank(1) % [g]

%%%%%%%%%%%%%%%%%%%%%%%%%%%%%%%%%%%%%%%%%%%%%%%%%%%%%%%%%%%%%%%%%%%%%%%%%%%%%%%
% measurement data
fid = fopen(measurement_data,'r');

Title_meas = textscan(fid,'%s %s %s %s %s %*[^\n]',1);
date_meas = textscan(fid,'%s %s %s %*[^\n]',1);
experimenter_meas = textscan(fid,'%s %s %s %*[^\n]',1);
comment_meas = textscan(fid,'%s %s %s %*[^\n]',1);
empty1 = textscan(fid,'%s %*[^\n]',1);
Title1_meas = textscan(fid,'%s %s %*[^\n]',1);
empty2 = textscan(fid,'%s %*[^\n]',1);
Title2_meas = textscan(fid,'%s %s %s %s %s %s %s %s %s %*[^\n]',1,'
    delimiter', ';');
Values_meas = textscan(fid,'%f %f %f %f %f %f %f %f %f %s %*[^\n]','
    delimiter', ';');
```

```
fclose(fid);

segment_meas = Values_meas{1,1}; % segement Nr.
temperature_meas = Values_meas{1,2}; % Temperatur [°C]
sigma_temperature_meas = Values_meas{1,3}; % Sigma der Temperatur im
    Segement/ der letzten betrachteten Periode [°C]
pressure_meas = Values_meas{1,4}; % Druck [bar]
sigma_pressure_meas = Values_meas{1,5}; % Sigma des Drucks im Segement/ der
     letzten betrachteten Periode [bar]
mass_meas = Values_meas{1,6}; % corr. weight am Ende des Segments [g]
massdiff_meas = Values_meas{1,7}; % corr. weight difference am Ende des
    Segments [g]
sigma_mass_meas = Values_meas{1,8}; % Sigma des Drucks im Segement/ der
    letzten betrachteten Periode [g]
density_meas = Values_meas{1,9}; % gas density [g/cm^3]

% corrections
density_meas = density_meas - density_meas(1); % offset correction for
    density
pressure_meas = pressure_meas -(0.06); % FGK offset correction for pressure

[measurement_fit,gof] = fit(density_meas,mass_meas,'poly1','Exclude',[1]);
coeff_measurement_fit = coeffvalues(measurement_fit);

%m_SC_S = coeff_buoyancy_fit(1,2) % [g]
V_SC_S_A = -coeff_measurement_fit(1,1) % [cm^3];

%m_S = m_SC_S - m_SC % [g]
%V_S = V_SC_S - V_SC % [cm^3]

% delta_m = mass_meas - m_SC - m_S + density_meas*(V_SC + V_S); % delta_m
    calculated with the fitted values
delta_m = mass_meas - m_SC_meas - m_S_meas + density_meas*(V_SC + V_S); %
    delta_m calculated with the measured values
delta_m = delta_m - delta_m(1); % FGK offset correction with vacuum mass

% calculation of the net adsorbed amount according to O. Talu, J. Phys.
% Chem C, 2013, 117, 13059-13071
delta_m_net = mass_meas - m_SC_meas - m_S_meas + density_meas*(V_SC); %
    delta_m calculated with the measured values
delta_m_net = delta_m_net - delta_m(1); % FGK offset correction with vacuum
     mass

[max_mass,max_index] = max(pressure_meas);
```

```
for i = 1:max_index
    pressure_ads(i) = pressure_meas(i);
    delta_m_ads(i) = delta_m(i);
    sigma_mass_meas_ads(i) = sigma_mass_meas(i);

    delta_m_net_ads(i) = delta_m_net(i);
end
for i = max_index+1:size(delta_m,1)
    pressure_des(i-max_index) = pressure_meas(i);
    delta_m_des(i-max_index)  = delta_m(i);
    sigma_mass_meas_des(i-max_index) = sigma_mass_meas(i);

    delta_m_net_des(i-max_index) = delta_m_net(i);
end

%%%%%%%%%%%%%%%%%%%%%%%%%%%%%%%%%%%%%%%%%%%%%%%%%%%%%%%%%%%%%%%%%%%%%%%%%%%%%%%

figure(1)
plot(blank_fit,'r-',density_blank,mass_blank,'+')
hold on
errorbar(density_blank,mass_blank,sigma_mass_blank,'+b')
xlabel('density \rho [g cm^{-3}]')
ylabel('mass [g]')
legend('blank measurement','fit')
text(min(density_blank),min(mass_blank),{['m_{SC} = ',num2str(m_SC,7),'g','
    V_{SC} = ',num2str(V_SC,7),'cm^{3}'];['m_{SC,meas} = ',num2str(
   m_SC_meas,7),'g'];['R^2 = ',num2str(blank_gof.rsquare,7),' \sigma = ',
   num2str(blank_gof.rmse,7)]},'VerticalAlignment','bottom','
   HorizontalAlignment','left')
hold off

figure(2)
plot(buoyancy_fit,'r-',density_buoy,mass_buoy,'+')
hold on
errorbar(density_buoy,mass_buoy,sigma_mass_buoy,'+b')
xlabel('density \rho [g cm^{-3}]')
ylabel('mass [g]')
legend('buoyancy measurement','fit')
text(min(density_buoy),min(mass_buoy),{['m_{SC+S} = ',num2str(m_SC_S,7),'g'
   ,' V_{SC+S} = ',num2str(V_SC_S,7),'cm^{3}'];['m_{S    } = ',num2str(m_S
   ,7),'g',' V_{S    } = ',num2str(V_S,7),'cm^{3}'];['m_{S,meas} = ',num2str
   (m_S_meas,7),'g',' V_{S,spec} = ',num2str(V_S_spec,7),'cm^{3}/g'];['R^2
```

```
    = ',num2str(buoyancy_gof.rsquare,7),' \sigma = ',num2str(buoyancy_gof.
    rmse,7)]},'VerticalAlignment','bottom','HorizontalAlignment','left')
% FGK for saving to pdf edit x and y position of text field
%text(min(density_buoy)-0.0009,min(mass_buoy),{['m_{SC+S} = ',num2str(
    m_SC_S,7),'g',' V_{SC+S} = ',num2str(V_SC_S,7),'cm^{3}'];['m_{S    } = ',
    num2str(m_S,7),'g',' V_{S    } = ',num2str(V_S,7),'cm^{3}'];['m_{S,meas}
    = ',num2str(m_S_meas,7),'g',' V_{S,spec} = ',num2str(V_S_spec,7),'cm
    ^{3}/g'];['R^2 = ',num2str(buoyancy_gof.rsquare,7),' \sigma = ',num2str(
    buoyancy_gof.rmse,7)]},'VerticalAlignment','bottom','HorizontalAlignment
    ','left')
hold off

figure(3)
%plot(pressure_meas,delta_m*1e3/Molar_mass_gas/m_S,'+')
hold on
errorbar(pressure_meas,delta_m*1e3/Molar_mass_gas/m_S,sigma_mass_meas*1e3/
    Molar_mass_gas/m_S,'+b')
xlabel('pressure [bar]')
ylabel('adsorbed amount [mmol/g]')
grid on
hold off

figure(4)
hold on
%plot(pressure_ads,delta_m_ads*1e3/Molar_mass_gas/m_S,'+')
%plot(pressure_des,delta_m_des*1e3/Molar_mass_gas/m_S,'or')
errorbar(pressure_ads,delta_m_ads*1e3/Molar_mass_gas/m_S,
    sigma_mass_meas_ads*1e3/Molar_mass_gas/m_S,'+b')
errorbar(pressure_des,delta_m_des*1e3/Molar_mass_gas/m_S,
    sigma_mass_meas_des*1e3/Molar_mass_gas/m_S,'or')

%errorbar(pressure_ads,delta_m_net_ads*1e3/Molar_mass_gas/m_S,
    sigma_mass_meas_ads*1e3/Molar_mass_gas/m_S,'+c')
%errorbar(pressure_des,delta_m_net_des*1e3/Molar_mass_gas/m_S,
    sigma_mass_meas_des*1e3/Molar_mass_gas/m_S,'og')
xlabel('pressure [bar]');
ylabel('adsorbed amount [mmol/g]');
legend('Adsorption','Desorption','Location','SouthEast');
%legend('Adsorption','Desorption','net Adsorption','net Desorption','
    Location','SouthEast');
grid on
hold off

% Variables to save:
```

```
delta_m_plot = delta_m*1e3/Molar_mass_gas/m_S; % [mmol/g]
sigma_mass_meas_plot =sigma_mass_meas*1e3/Molar_mass_gas/m_S; %[mmol/g]
delta_m_plot_ads = delta_m_ads*1e3/Molar_mass_gas/m_S; % [mmol/g]
delta_m_plot_des = delta_m_des*1e3/Molar_mass_gas/m_S; % [mmol/g]
sigma_mass_meas_plot_ads =sigma_mass_meas_ads*1e3/Molar_mass_gas/m_S; %[
    mmol/g]
sigma_mass_meas_plot_des =sigma_mass_meas_des*1e3/Molar_mass_gas/m_S; %[
    mmol/g]

exceldata_ads = [pressure_ads;delta_m_ads*1e3/Molar_mass_gas/m_S]'
exceldata_des = [pressure_des;delta_m_des*1e3/Molar_mass_gas/m_S]'

save('exceldata_ads.txt','exceldata_ads','-ASCII','-DOUBLE','-TABS');
save('exceldata_des.txt','exceldata_des','-ASCII','-DOUBLE','-TABS');

save('results/VACNT_SO2_25C.mat','blank_input','density_blank','mass_blank'
    ,'sigma_mass_blank','m_SC','V_SC','m_SC_meas', ...
     'density_buoy','mass_buoy','sigma_mass_buoy','m_SC_S', 'V_SC_S','V_S','
        m_S_meas','V_S_spec', ...
     'pressure_meas','delta_m_plot','sigma_mass_meas_plot','temperature_meas
        ','sigma_temperature_meas', ...
     'pressure_ads','pressure_des','delta_m_plot_ads','delta_m_plot_des','
        sigma_mass_meas_plot_ads','sigma_mass_meas_plot_des', ...
     'delta_m','delta_m_ads','delta_m_des');

orient landscape
saveas(gcf,'results/VACNT_SO2_25C','pdf');

figure(8)
hold on
%plot(pressure_meas,temperature_meas,'+b')
errorbar(pressure_meas,temperature_meas,sigma_temperature_meas,'+b')
xlabel('pressure [bar]')
ylabel('temperature [°C]')
grid on
hold off
```

C.5 Matlab code fit_ads_models

In this matlab code the data saved from the code presented in C.4 is loaded by the routine described in C.8 and the adsorption isotherms are tried to be fitted with different models. The models which can be fitted with this code are the Langmuir, Freundlich,

BET, Dubinin-Raduskevich, Dubinin-Astakhov, Temkin and Toth adsorption isotherm models. The fit can be triggered by setting the respective fit variable to 1 e.g. Langmuir_ads. Also, it can be chosen which pressure range shall be excluded for fitting. For the BET method therefore the upper and lower bound of the fraction of p_sat can be chosen. After the fitting procedure the fits can be inspected by the different plots produced. The last two plots display the enabled fit models and experimental data for the adsorption and desorption branch and are saved.

```
clear all;
close all;
format long;

Masse = zeros(1,8);
Delta_m = zeros(1,3);
X = zeros(1,3);
p = zeros(1,3);
T = zeros(1,2);
sigma = zeros(1,4);
A =zeros(1,2);
B =zeros(1,2);

%%
%%%%%%%%%%%%%%%%%%%%%%%%%%%%%%%%%%%%%%%%%%%%%%%%%%%%%%%%%%%%%%%%%%%%%%%%%%%%%%%%
%%%% VACNT SO2 high pressure
%%%%%%%%%%%%%%%%%%%%%%%%%%%%%%%%%%%%%%%%%%%%%%%%%%%%%%%%%%%%%%%%%%%%%%%%%%%%%%%%

% load('results/VACNT_SO2_15C.mat');   ii = 1;
% blank_input = 15; % [°C]
% [Masse,Delta_m,X,p,T,sigma,A,B] = readdata(Masse,Delta_m,X,p,T,sigma,A,B
    ,...
%       ii,m_SC,m_SC_meas,m_SC_S,...
%       m_S_meas,V_SC,V_SC_S,V_S,V_S_spec,delta_m,delta_m_ads,delta_m_des,...
%       delta_m_plot,delta_m_plot_ads,delta_m_plot_des,pressure_meas,...
%       pressure_ads,pressure_des,temperature_meas,sigma_mass_meas_plot,...
%       sigma_mass_meas_plot_ads,sigma_mass_meas_plot_des,
    sigma_temperature_meas);

load('results/VACNT_SO2_25C.mat'); ii = 1;
blank_input = 25; % [°C]
[Masse,Delta_m,X,p,T,sigma,A,B] = readdata(Masse,Delta_m,X,p,T,sigma,A,B
    ,...
     ii,m_SC,m_SC_meas,m_SC_S,...
     m_S_meas,V_SC,V_SC_S,V_S,V_S_spec,delta_m,delta_m_ads,delta_m_des,...
```

```
    delta_m_plot,delta_m_plot_ads,delta_m_plot_des,pressure_meas,...
    pressure_ads,pressure_des,temperature_meas,sigma_mass_meas_plot,...
    sigma_mass_meas_plot_ads,sigma_mass_meas_plot_des,
        sigma_temperature_meas);

% load('results/VACNT_SO2_35C.mat');   ii = 1;
% blank_input = 35; % [°C]
% [Masse,Delta_m,X,p,T,sigma,A,B] = readdata(Masse,Delta_m,X,p,T,sigma,A,B
    ,...
%     ii,m_SC,m_SC_meas,m_SC_S,...
%     m_S_meas,V_SC,V_SC_S,V_S,V_S_spec,delta_m,delta_m_ads,delta_m_des,...
%     delta_m_plot,delta_m_plot_ads,delta_m_plot_des,pressure_meas,...
%     pressure_ads,pressure_des,temperature_meas,sigma_mass_meas_plot,...
%     sigma_mass_meas_plot_ads,sigma_mass_meas_plot_des,
    sigma_temperature_meas);

figure(1)
hold on
%plot(pressure_ads,delta_m_ads*1e3/Molar_mass_gas/m_S,'+')
%plot(pressure_des,delta_m_des*1e3/Molar_mass_gas/m_S,'or')
errorbar(pressure_ads,delta_m_plot_ads,sigma_mass_meas_plot_ads,'+b')
errorbar(pressure_des,delta_m_plot_des,sigma_mass_meas_plot_des,'or')
xlabel('pressure [bar]');
ylabel('adsorbed amount [mmol/g]');
legend('Adsorption','Desorption','Location','SouthEast');
grid on
hold off

%%%%%%%%%%%%%%%%%%%%%%%%%%%%%%%%%%%%%%%%%%%%%%%%%%%%%%%%%%%%%%%%%%%%%%%%%%%%%%%
%%%%%%%  Fit  %%%%%%%%%%%%%%%%%%%%%%%%%%%%%%%%%%%%%%%%%%%%%%%%%%%%%%%%%%%%%%%%
%%%%%%%%%%%%%%%%%%%%%%%%%%%%%%%%%%%%%%%%%%%%%%%%%%%%%%%%%%%%%%%%%%%%%%%%%%%%%%%

% FGK choose right messuring gas 0 = CO2; 1 = SO2; 2 = N2
meassuring_gas = 1;

exceldata_ads = [pressure_ads;delta_m_plot_ads]';
exceldata_des = [pressure_des;delta_m_plot_des]';

% FGK choose fit to be performed 1 = will be done 0 = will not be done
Langmuir_ads = 1;
Langmuir_des = 1;
Freundlich_ads = 1;
Freundlich_des = 1;
BET_ads = 1;
```

```
BET_des = 1;
DR_ads = 1;
DR_des = 1;
DA_ads = 1;
DA_des = 1;
Temkin_ads = 0;
Temkin_des = 0;
Toth_ads = 0;
Toth_des = 0;

if (meassuring_gas == 0) % CO2
    Molar_mass_gas = 44.0095; %[g mol{-1}] (data from NIST)
elseif (meassuring_gas == 1) % SO2
    Molar_mass_gas = 64.064; %[g mol{-1}] (data from NIST)
elseif (meassuring_gas == 2) % N2
    Molar_mass_gas = 28.0234; %[g mol{-1}] (data from NIST)
end

%set saturation pressure
if (meassuring_gas == 0) % CO2
    if (blank_input == 0)
        p_sat = 34.851; % CO2, T = 0°C
    elseif (blank_input == 25)
        p_sat = 64.342; % CO2, T = 25°C
    else
        p_sat = 73.773; % CO2, p_c, T_c = 30.9782°C
    end
elseif (meassuring_gas == 1) % SO2
    if (blank_input == 25)
        p_sat = 3.9238; % SO2, T = 25°C
    elseif (blank_input == 15)
        p_sat = 2.7711; % SO2, T = 15°C
    elseif (blank_input == 35)
        p_sat = 5.415; % SO2, T = 35°C
    elseif (blank_input == 40)
        p_sat = 6.3061; % SO2, T = 40°C
    elseif (blank_input == 50)
        p_sat = 8.4178; % SO2, T = 50°C
    elseif (blank_input == 75)
        p_sat = 16.006; % SO2, T = 75°C
    elseif (blank_input == 100)
        p_sat = 27.784; % SO2, T = 100°C
    elseif (blank_input == 125)
        p_sat = 45.022; % SO2, T = 125°C
```

```
    end
elseif (meassuring_gas == 2) % N2
    p_sat = 33.958; % N2, P_c, T_c = -146,958°C
end

R = 8.314; % ideal gas constant

% FGK to set limit for values to be excluded [bar]
excludevar_help = 0.7*p_sat;
excludecoeff_BET_lower = 0.05; % set lower boundary for BET fit typically
    0.05
excludecoeff_BET_upper = 0.5; % set lower boundary for BET fit typically
    0.30

%%%%%%%%%%%%%%%%%%%%%%%%%%%%%%%%%%%%%%%%%%%%%%%%%%%%%%%%%%%%%%%%%%%%%%%%%%%%
% Langmuir model: Langmuir = K_L*q_max*p/(1 + K_L*p);
% variables:
% K_L: Langmuir Sorption coefficient;
% q_max: maximal sorbable concentration / pressure
% p: pressure / concentration of the sorbate

x = exceldata_ads(:,1);
excludevar_ads = [x < 0.0 | x > excludevar_help];

p_ads = x;
ads_amount_ads = exceldata_ads(:,2);
exclude_Langmuir_ads = excludevar_ads;

Langmuir = 'K_L*q_max*x/(1 + K_L*x)';
startPoints_Langmuir = [0.01 100];

if (Langmuir_ads)
    Langmuir_fit_ads = fit(x,ads_amount_ads,Langmuir,'Start',
        startPoints_Langmuir,'Exclude',exclude_Langmuir_ads)

    Langmuir_coeffs_ads = coeffvalues(Langmuir_fit_ads);
    Langmuir_confint_ads = confint(Langmuir_fit_ads);
else
    Langmuir_coeffs_ads = [0 0];
    Langmuir_confint_ads = [0 0;0 0];
end

x = exceldata_des(:,1);
excludevar_des = [x < 0.0 | x > excludevar_help];
```

```
p_des = x;
ads_amount_des = exceldata_des(:,2);
exclude_Langmuir_des = excludevar_des;

if (Langmuir_des)
    Langmuir_fit_des = fit(x,ads_amount_des,Langmuir,'Start',
        startPoints_Langmuir,'Exclude',exclude_Langmuir_des)

    Langmuir_coeffs_des = coeffvalues(Langmuir_fit_des);
    Langmuir_confint_des = confint(Langmuir_fit_des);
else
    Langmuir_coeffs_des = [0 0];
    Langmuir_confint_des = [0 0;0 0];
end

%%%%%%%%%%%%%%%%%%%%%%%%%%%%%%%%%%%%%%%%%%%%%%%%%%%%%%%%%%%%%%%%%%%%%%%%%%%%%%%
% Freundllich model: Freundlich = K*p^n;
% variables:
% K: Freundlich Sorption coefficient;
% n: Freundlich exponent;
% p: pressure / concentration of the sorbate;

x = exceldata_ads(:,1);
p_ads = x;
exclude_Freundlich_ads = excludevar_ads;

Freundlich = 'K*x^n';
startPoints_Freundlich = [10 0.5];

if (Freundlich_ads)
    Freundlich_fit_ads = fit(x,ads_amount_ads,Freundlich,'Start',
        startPoints_Freundlich,'Exclude',exclude_Freundlich_ads)

    Freundlich_coeffs_ads = coeffvalues(Freundlich_fit_ads);
    Freundlich_confint_ads = confint(Freundlich_fit_ads);
else
    Freundlich_coeffs_ads = [0 0];
    Freundlich_confint_ads = [0 0;0 0];
end

x = exceldata_des(:,1);
p_des = x;
exclude_Freundlich_des = excludevar_des;
```

```
if (Freundlich_des)
    Freundlich_fit_des = fit(x,ads_amount_des,Freundlich,'Start',
        startPoints_Freundlich,'Exclude',exclude_Freundlich_des)

    Freundlich_coeffs_des = coeffvalues(Freundlich_fit_des);
    Freundlich_confint_des = confint(Freundlich_fit_des);
else
    Freundlich_coeffs_des = [0 0];
    Freundlich_confint_des = [0 0;0 0];
end

%%%%%%%%%%%%%%%%%%%%%%%%%%%%%%%%%%%%%%%%%%%%%%%%%%%%%%%%%%%%%%%%%%%%%%%%%%%%%%%
% BET model: BET = K_BET*q_max_BET*C_eq / [(C_sat - C_eq)*(1 + ((K_BET - 1)
    *C_eq) / C_sat)];
% variables:
% K_BET: BET Sorption coefficient;
% q_max_BET: maximal sorbate concentration in one layer;
% C_eq : pressure of the bulk;
% C_sat: saturation pressure

x = exceldata_ads(:,1);
p_ads = x;
if (meassuring_gas == 0) % CO2
    if (blank_input == 0)
        p_sat_BET = 34.851; % CO2, T = 0°C
        BET = 'K_BET*q_max_BET*x / ((34.851 - x)*(1 + ((K_BET - 1)*x) /
            34.851))';
    elseif (blank_input == 25)
        p_sat_BET = 64.342; % CO2, T = 25°C
        BET = 'K_BET*q_max_BET*x / ((64.342 - x)*(1 + ((K_BET - 1)*x) /
            64.342))';
    else
        p_sat_BET = 73.773; % CO2, p_c, T_c = 30.9782°C
        BET = 'K_BET*q_max_BET*x / ((73.773 - x)*(1 + ((K_BET - 1)*x) /
            73.773))';
    end
elseif (meassuring_gas == 1) % SO2
    if (blank_input == 25)
        p_sat_BET = 3.9238; % SO2, T = 25°C
        BET = 'K_BET*q_max_BET*x / ((3.9238 - x)*(1 + ((K_BET - 1)*x) /
            3.9238))';
    elseif (blank_input == 15)
        p_sat_BET = 2.7711; % SO2, T = 15°C
```

```
        BET = 'K_BET*q_max_BET*x / ((2.7711 - x)*(1 + ((K_BET - 1)*x) /
            2.7711))';
    elseif (blank_input == 35)
        p_sat_BET = 5.415; % SO2, T = 35°C
        BET = 'K_BET*q_max_BET*x / ((5.415 - x)*(1 + ((K_BET - 1)*x) /
            5.415))';
    elseif (blank_input == 40)
        p_sat_BET = 6.3061; % SO2, T = 40°C
        BET = 'K_BET*q_max_BET*x / ((6.3061 - x)*(1 + ((K_BET - 1)*x) /
            6.3061))';
    elseif (blank_input == 50)
        p_sat_BET = 8.4178; % SO2, T = 50°C
        BET = 'K_BET*q_max_BET*x / ((8.4178 - x)*(1 + ((K_BET - 1)*x) /
            8.4178))';
    elseif (blank_input == 75)
        p_sat_BET = 16.006; % SO2, T = 75°C
        BET = 'K_BET*q_max_BET*x / ((16.006 - x)*(1 + ((K_BET - 1)*x) /
            16.006))';
    elseif (blank_input == 100)
        p_sat_BET = 27.784; % SO2, T = 100°C
        BET = 'K_BET*q_max_BET*x / ((27.784 - x)*(1 + ((K_BET - 1)*x) /
            27.784))';
    elseif (blank_input == 125)
        p_sat_BET = 45.022; % SO2, T = 125°C
        BET = 'K_BET*q_max_BET*x / ((45.022 - x)*(1 + ((K_BET - 1)*x) /
            45.022))';
    end
elseif (meassuring_gas == 2) % N2
    p_sat_BET = 33.958; % N2, P_c, T_c = -146,958°C
    BET = 'K_BET*q_max_BET*x / ((33.958 - x)*(1 + ((K_BET - 1)*x) / 33.958)
        )';
end

excludevar_ads_2 = [x < excludecoeff_BET_lower*p_sat_BET | x >
    excludecoeff_BET_upper*p_sat_BET];
startPoints_BET = [20 0.8];

exclude_BET_ads = excludevar_ads_2;

if (BET_ads)
    BET_fit_ads = fit(x,ads_amount_ads,BET,'Start',startPoints_BET,'Exclude
        ',exclude_BET_ads)

    BET_coeffs_ads = coeffvalues(BET_fit_ads);
```

```
    BET_confint_ads = confint(BET_fit_ads);
else
    BET_coeffs_ads = [0 0];
    BET_confint_ads = [0 0;0 0];
end

x = exceldata_des(:,1);
p_des = x;
excludevar_des_2 = [x < excludecoeff_BET_lower*p_sat_BET | x >
   excludecoeff_BET_upper*p_sat_BET];
exclude_BET_des = excludevar_des_2;

if (BET_des)
    BET_fit_des = fit(x,ads_amount_des,BET,'Start',startPoints_BET,'Exclude
        ',exclude_BET_des)

    BET_coeffs_des = coeffvalues(BET_fit_des);
    BET_confint_des = confint(BET_fit_des);
else
    BET_coeffs_des = [0 0];
    BET_confint_des = [0 0;0 0];
end

%%%%%%%%%%%%%%%%%%%%%%%%%%%%%%%%%%%%%%%%%%%%%%%%%%%%%%%%%%%%%%%%%%%%%%%%%%%%%%%
% Dubinin-Radushkevich model: DR = q_s*exp(-k_DR*epsilon^2); epsilon =
% R*T*ln(1+ 1/p)
% variables:
% q_s: DR theoretical saturation loading;
% k_DR : DR isotherm constant
% epsilon: DR isotherm constant, dependant on Temperature and pressure
% R: ideal gas constant
% T: temperature

x = exceldata_ads(:,1);
p_ads = x;
exclude_DR_ads = excludevar_ads;
R = 8.314;
epsilon_ads = R*(blank_input + 273.15)*log(1 + 1./(p_ads*1e5));
epsilon_des = R*(blank_input + 273.15)*log(1 + 1./(p_des*1e5));

% DR = q_s*exp(-k_DR*((R*T*log(1+ 1/p))^2));
if (blank_input == 0)
    DR = 'q_s*exp(-k_DR*((8.314*(0+273.15)*log(1+ 1./(x*1e5))).^2))'; % T
        =0°C
```

```
elseif (blank_input == 15)
    DR = 'q_s*exp(-k_DR*((8.314*(15+273.15)*log(1+ 1./(x*1e5))).^2))'; % T
        =15°C
elseif (blank_input == 25)
    DR = 'q_s*exp(-k_DR*((8.314*(25+273.15)*log(1+ 1./(x*1e5))).^2))'; % T
        =25°C
elseif (blank_input == 35)
    DR = 'q_s*exp(-k_DR*((8.314*(35+273.15)*log(1+ 1./(x*1e5))).^2))'; % T
        =35°C
elseif (blank_input == 40)
    DR = 'q_s*exp(-k_DR*((8.314*(40+273.15)*log(1+ 1./(x*1e5))).^2))'; % T
        =40°C
elseif (blank_input == 50)
    DR = 'q_s*exp(-k_DR*((8.314*(50+273.15)*log(1+ 1./(x*1e5))).^2))'; % T
        =50°C
elseif (blank_input == 75)
    DR = 'q_s*exp(-k_DR*((8.314*(75+273.15)*log(1+ 1./(x*1e5))).^2))'; % T
        =75°C
elseif (blank_input == 100)
    DR = 'q_s*exp(-k_DR*((8.314*(100+273.15)*log(1+ 1./(x*1e5))).^2))'; % T
         =100°C
elseif (blank_input == 125)
    DR = 'q_s*exp(-k_DR*((8.314*(125+273.15)*log(1+ 1./(x*1e5))).^2))'; % T
         =125°C
elseif (blank_input == 150)
    DR = 'q_s*exp(-k_DR*((8.314*(150+273.15)*log(1+ 1./(x*1e5))).^2))'; % T
         =150°C
end

startPoints_DR = [6000 5];

if (DR_ads)
    DR_fit_ads = fit(x,ads_amount_ads,DR,'Start',startPoints_DR,'Exclude',
        exclude_DR_ads)

    DR_coeffs_ads = coeffvalues(DR_fit_ads);
    DR_confint_ads = confint(DR_fit_ads);
else
    DR_coeffs_ads = [0 0];
    DR_confint_ads = [0 0;0 0];
end

x = exceldata_des(:,1);
p_des = x;
```

```
exclude_DR_des = excludevar_des;

if  (DR_des)
    DR_fit_des = fit(x,ads_amount_des,DR,'Start',startPoints_DR,'Exclude',
        exclude_DR_des)

    DR_coeffs_des = coeffvalues(DR_fit_des);
    DR_confint_des = confint(DR_fit_des);
else
    DR_coeffs_des = [0 0];
    DR_confint_des = [0 0;0 0];
end

%%%%%%%%%%%%%%%%%%%%%%%%%%%%%%%%%%%%%%%%%%%%%%%%%%%%%%%%%%%%%%%%%%%%%%%%%%%%%%%
% Dubinin-Astakhov model: DA = q_s_DA*exp(-k_DA*epsilon_DA^n_DA);
    epsilon_DA =
% R*T*ln(1+ 1/p)
% variables:
% q_s_DA: DA theoretical saturation loading;
% k_DA : DA isotherm constant
% epsilon_DA: DA isotherm constant, dependant on Temperature and pressure
% R: ideal gas constant
% T: temperature

x = exceldata_ads(:,1);
p_ads = x;
exclude_DA_ads = excludevar_ads;
R = 8.314;
epsilon_ads_DA = R*(blank_input + 273.15)*log(1 + 1./(p_ads*1e5));
epsilon_des_DA = R*(blank_input + 273.15)*log(1 + 1./(p_des*1e5));

% DA = q_s_DA*exp(-k_DA*((R*T*log(1+ 1/p))^n_DA));
if (blank_input == 0)
    DA = 'q_s_DA*exp(-k_DA*((8.314*(0+273.15)*log(1+ 1./(x*1e5))).^n_DA))';
         % T =0°C
elseif (blank_input == 15)
    DA = 'q_s_DA*exp(-k_DA*((8.314*(15+273.15)*log(1+ 1./(x*1e5))).^n_DA))'
        ; % T =15°C
elseif (blank_input == 25)
    DA = 'q_s_DA*exp(-k_DA*((8.314*(25+273.15)*log(1+ 1./(x*1e5))).^n_DA))'
        ; % T =25°C
elseif (blank_input == 35)
    DA = 'q_s_DA*exp(-k_DA*((8.314*(35+273.15)*log(1+ 1./(x*1e5))).^n_DA))'
        ; % T =35°C
```

```
elseif (blank_input == 40)
    DA = 'q_s_DA*exp(-k_DA*((8.314*(40+273.15)*log(1+ 1./(x*1e5))).^n_DA))'
        ; % T =40°C
elseif (blank_input == 50)
    DA = 'q_s_DA*exp(-k_DA*((8.314*(50+273.15)*log(1+ 1./(x*1e5))).^n_DA))'
        ; % T =50°C
elseif (blank_input == 75)
    DA = 'q_s_DA*exp(-k_DA*((8.314*(75+273.15)*log(1+ 1./(x*1e5))).^n_DA))'
        ; % T =75°C
elseif (blank_input == 100)
    DA = 'q_s_DA*exp(-k_DA*((8.314*(100+273.15)*log(1+ 1./(x*1e5))).^n_DA))
        '; % T =100°C
elseif (blank_input == 125)
    DA = 'q_s_DA*exp(-k_DA*((8.314*(125+273.15)*log(1+ 1./(x*1e5))).^n_DA))
        '; % T =125°C
elseif (blank_input == 150)
    DA = 'q_s_DA*exp(-k_DA*((8.314*(150+273.15)*log(1+ 1./(x*1e5))).^n_DA))
        '; % T =150°C
end

startPoints_DA = [100 2 5];

if (DA_ads)
    DA_fit_ads = fit(x,ads_amount_ads,DA,'Start',startPoints_DA,'Exclude',
        exclude_DA_ads)

    DA_coeffs_ads = coeffvalues(DA_fit_ads);
    DA_confint_ads = confint(DA_fit_ads);
else
    DA_coeffs_ads = [0 0 0];
    DA_confint_ads = [0 0;0 0;0 0];
end

x = exceldata_des(:,1);
p_des = x;
exclude_DA_des = excludevar_des;

if  (DA_des)
    DA_fit_des = fit(x,ads_amount_des,DA,'Start',startPoints_DA,'Exclude',
        exclude_DA_des)

    DA_coeffs_des = coeffvalues(DA_fit_des);
    DA_confint_des = confint(DA_fit_des);
else
```

```
    DA_coeffs_des = [0 0 0];
    DA_confint_des = [0 0;0 0;0 0];
end

%%%%%%%%%%%%%%%%%%%%%%%%%%%%%%%%%%%%%%%%%%%%%%%%%%%%%%%%%%%%%%%%%%%%%%%%%%%%%%%
%% Temkin model: Temkin = R*T/b_T*ln(A_T*p)
%% variables:
%% A_T: Temkin constant
%% b_T: Temkin constant
%% R: ideal gas constant
%% T: temperature
%
x = exceldata_ads(:,1);
p_ads = x;
exclude_Temkin_ads = [x < 2.0 | x > excludevar_help];

Temkin = 'RTb_T*log(A_T*x)'; % varibale RTb_T = R*T/b_T
startPoints_Temkin = [1 0.4];

if (Temkin_ads)
    Temkin_fit_ads = fit(x,ads_amount_ads,Temkin,'Start',startPoints_Temkin
        ,'Exclude',exclude_Temkin_ads)

    Temkin_coeffs_ads = coeffvalues(Temkin_fit_ads);
    Temkin_confint_ads = confint(Temkin_fit_ads);
else
    Temkin_coeffs_ads = [0 0];
    Temkin_confint_ads = [0 0;0 0];
end

x = exceldata_des(:,1);
p_des = x;
exclude_Temkin_des = [x < 1.0 | x > excludevar_help];

if (Temkin_des)
    Temkin_fit_des = fit(x,ads_amount_des,Temkin,'Start',startPoints_Temkin
        ,'Exclude',exclude_Temkin_des)

    Temkin_coeffs_des = coeffvalues(Temkin_fit_des);
    Temkin_confint_des = confint(Temkin_fit_des);
else
    Temkin_coeffs_des = [0 0];
    Temkin_confint_des = [0 0;0 0];
end
```

```
%%%%%%%%%%%%%%%%%%%%%%%%%%%%%%%%%%%%%%%%%%%%%%%%%%%%%%%%%%%%%%%%%%%%%%%%%%%%%%%%
% Toth model: Toth = (K_T*p)/(a_T + p)^(1/t);
% variables:
% K_T: Toth Sorption coefficient;
% a_T: Toth Sorption coefficient;
% t: Toth exponent;
% p: pressure / concentration of the sorbate;

x = exceldata_ads(:,1);
p_ads = x;
exclude_Toth_ads = excludevar_ads;

Toth = '(K_T*x)/(a_T + x)^(1/t)';
startPoints_Toth = [10 0.5 0.5];

if (Toth_ads)
    Toth_fit_ads = fit(x,ads_amount_ads,Toth,'Start',startPoints_Toth,'
       Exclude',exclude_Toth_ads)

    Toth_coeffs_ads = coeffvalues(Toth_fit_ads);
    Toth_confint_ads = confint(Toth_fit_ads);
else
    Toth_coeffs_ads = [0 0 0];
    Toth_confint_ads = [0 0 0;0 0 0];
end

x = exceldata_des(:,1);
p_des = x;
exclude_Toth_des = excludevar_des;

if (Toth_des)
    Toth_fit_des = fit(x,ads_amount_des,Toth,'Start',startPoints_Toth,'
       Exclude',exclude_Toth_des)

    Toth_coeffs_des = coeffvalues(Toth_fit_des);
    Toth_confint_des = confint(Toth_fit_des);
else
    Toth_coeffs_des = [0 0 0];
    Toth_confint_des = [0 0 0; 0 0 0];
end

%%
% save fitvariables
```

```
kkk_Langmuir = [Langmuir_coeffs_ads' Langmuir_confint_ads
    Langmuir_coeffs_des' Langmuir_confint_des]; % [K_L;q_max]
kkk_Freundlich = [Freundlich_coeffs_ads' Freundlich_confint_ads
    Freundlich_coeffs_des' Freundlich_confint_des]; % [K;n]
kkk_BET = [BET_coeffs_ads' BET_confint_ads BET_coeffs_des' BET_confint_des
    ]; % [K_BET;q_max_BET]
kkk_DR = [DR_coeffs_ads' DR_confint_ads DR_coeffs_des' DR_confint_des]; % [
    k_DR;q_s]
kkk_Temkin = [Temkin_coeffs_ads' Temkin_confint_ads Temkin_coeffs_des'
    Temkin_confint_des]; % [A_T;RTb_T]
kkk_Toth = [Toth_coeffs_ads' Toth_confint_ads' Toth_coeffs_des'
    Toth_confint_des']; % [K_T;a_T;t]

save('fitparameter.txt','kkk_Langmuir','kkk_Freundlich','kkk_BET','kkk_DR',
    'kkk_Temkin','kkk_Toth','-ASCII','-DOUBLE','-TABS');

%%

figure (5)
hold on
% y,x,numbering from left to right, top to bottom
if (Langmuir_ads) subplot(3,3,1); plot(Langmuir_fit_ads,p_ads,
    ads_amount_ads,exclude_Langmuir_ads); title('Langmuir'); grid on; end
if (Langmuir_des) subplot(3,3,2); plot(Langmuir_fit_des,p_des,
    ads_amount_des,exclude_Langmuir_des); grid on; legend off; end
subplot(3,3,3); plot(ads_amount_ads,ads_amount_ads./p_ads,ads_amount_des,
    ads_amount_des./p_des); xlabel('m_{ads}'); ylabel('m_{ads}/p'); grid on;

if (Freundlich_ads) subplot(3,3,4); plot(Freundlich_fit_ads,p_ads,
    ads_amount_ads,exclude_Freundlich_ads); title('Freundlich'), grid on;
    legend off; end
if (Freundlich_des) subplot(3,3,5); plot(Freundlich_fit_des,p_des,
    ads_amount_des,exclude_Freundlich_des); grid on; legend off; end
subplot(3,3,6); plot(log(p_ads),log(ads_amount_ads),log(p_des),log(
    ads_amount_des)); xlabel('ln(p)'); ylabel('ln(m_{ads})'); grid on;

if (BET_ads) subplot(3,3,7); plot(BET_fit_ads,p_ads,ads_amount_ads,
    exclude_BET_ads); title('BET'), grid on; legend off; end
if (BET_des) subplot(3,3,8); plot(BET_fit_des,p_des,ads_amount_des,
    exclude_BET_des); grid on; legend off; end
subplot(3,3,9); plot(p_ads./p_sat_BET,p_ads./(ads_amount_ads.*(p_sat_BET-
    p_ads)),p_des./p_sat_BET,p_des./(ads_amount_des.*(p_sat_BET-p_des)));
    xlabel('(p/p_{s})'); ylabel('p/(m_{ads}*(p_{s} - p))'); grid on;
```

```
hold off


figure (6)
hold on
% y,x,numbering from left to right, top to bottom
if (DR_ads) subplot(3,3,1); plot(DR_fit_ads,p_ads,ads_amount_ads,
    exclude_DR_ads); title('Dubinin Raduskevich'); grid on; end
if (DR_des) subplot(3,3,2); plot(DR_fit_des,p_des,ads_amount_des,
    exclude_DR_des); grid on;legend off; end
subplot(3,3,3); plot(epsilon_ads.^2,log(ads_amount_ads),epsilon_des.^2,log(
    ads_amount_des)); xlabel('\epsilon ^2'); ylabel('log(m_{ads})'); grid on
    ; legend off;

if (Temkin_ads) subplot(3,3,4); plot(Temkin_fit_ads,p_ads,ads_amount_ads,
    exclude_Temkin_ads); title('Temkin'); grid on; legend off; end
if (Temkin_des) subplot(3,3,5); plot(Temkin_fit_des,p_des,ads_amount_des,
    exclude_Temkin_des); grid on; end
subplot(3,3,6); plot(log(p_ads),ads_amount_ads,log(p_des),ads_amount_des);
    xlabel('p'); ylabel('m_{ads}'); grid on;

if (Toth_ads) subplot(3,3,7); plot(Toth_fit_ads,p_ads,ads_amount_ads);
    title('Toth'), grid on; legend off; end
if (Toth_des) subplot(3,3,8); plot(Toth_fit_des,p_des,ads_amount_des); grid
     on; end
subplot(3,3,9); plot(log(p_ads),log(ads_amount_ads),log(p_des),log(
    ads_amount_des)); xlabel('ln(p)'); ylabel('ln(X)'); grid on;

% find all indices where the pressure is greater than 0 bar
x = exceldata_ads(:,1);
index_ads = find(x > 0.0); %p_ads has to be greater than 0.0 bar
p_ads = exceldata_ads(index_ads,1);
ads_amount_ads = exceldata_ads(index_ads,2);

% for DR plot:
R = 8.134;
epsilon_ads = R*(blank_input + 273.15)*log(1 + 1./p_ads);
epsilon_des = R*(blank_input + 273.15)*log(1 + 1./p_des);

%store old values
p_ads_old = p_ads;
p_des_old = p_des;
ads_amount_ads_old = ads_amount_ads;
ads_amount_des_old = ads_amount_des;
```

```
epsilon_ads_old = R*(blank_input + 273.15)*log(1 + 1./(p_ads*1e5));
epsilon_des_old = R*(blank_input + 273.15)*log(1 + 1./(p_des*1e5));

%pull the full data range
p_ads = exceldata_ads(:,1);
p_des = exceldata_des(:,1);
ads_amount_ads = exceldata_ads(:,2);
ads_amount_des = exceldata_des(:,2);
epsilon_ads = R*(blank_input + 273.15)*log(1 + 1./(p_ads*1e5));
epsilon_des = R*(blank_input + 273.15)*log(1 + 1./(p_des*1e5));
p_BET_sec_ads = p_ads(p_ads > 0.05*p_sat_BET & p_ads < 0.3*p_sat_BET);
p_BET_sec_des = p_des(p_des > 0.05*p_sat_BET & p_des < 0.3*p_sat_BET);
ads_amount_ads_BET_sec = ads_amount_ads(p_ads > 0.05*p_sat_BET & p_ads <
    0.3*p_sat_BET);
ads_amount_des_BET_sec = ads_amount_des(p_des > 0.05*p_sat_BET & p_des <
    0.3*p_sat_BET);

if (DA_ads)
    n_DA_ads = DR_coeffs_ads(2);
else
    n_DA_ads = 0;
end
if (DA_des)
    n_DA_des = DR_coeffs_des(2);
else
    n_DA_des = 0;
end

%,epsilon_ads.^n_DA_ads,log(ads_amount_ads),'-c+',epsilon_des.^n_DA_des,log
    (ads_amount_des),'-m+'

figure (7)
subplot(2,3,1); plot(1./p_ads,1./ads_amount_ads,'-b+',1./p_des,1./
    ads_amount_des,'-r+'); title('Langmuir'); xlabel('1/p'); ylabel('1/m_{
    ads}'); grid on;
subplot(2,3,2); plot(log(p_ads),log(ads_amount_ads),'-b+',log(p_des),log(
    ads_amount_des),'-r+'); title('Freundlich / Toth'); xlabel('ln(p)');
    ylabel('ln(m_{ads})'); grid on;
subplot(2,3,3); plot(p_ads./p_sat_BET,p_ads./(ads_amount_ads.*(p_sat_BET-
    p_ads)),'-b+',p_des./p_sat_BET,p_des./(ads_amount_des.*(p_sat_BET-p_des)
    ),'-r+'); title('BET'); xlabel('(p/p_{s})'); ylabel('p/(m_{ads}*(p_{s} -
     p))'); grid on;
subplot(2,3,4); plot(epsilon_ads.^2,log(ads_amount_ads),'-b+',epsilon_des
    .^2,log(ads_amount_des),'-r+',epsilon_ads.^n_DA_ads,log(ads_amount_ads),
```

```
    '-c+',epsilon_des.^n_DA_des,log(ads_amount_des),'-m+'); title('Dubinin
    Raduskevich / Dubinin Astakhov'); xlabel('\epsilon ^2'); ylabel('log(m_{
    ads})'); grid on;
subplot(2,3,5); plot(log(p_ads),ads_amount_ads,'-b+',log(p_des),
    ads_amount_des,'-r+'); title('Temkin'); xlabel('ln(p)'); ylabel('m_{ads}
    '); grid on;
subplot(2,3,6); plot(p_BET_sec_ads./p_sat_BET,p_BET_sec_ads./(
    ads_amount_ads_BET_sec.*(p_sat_BET-p_BET_sec_ads)),'-b+',p_BET_sec_des./
    p_sat_BET,p_BET_sec_des./(ads_amount_des_BET_sec.*(p_sat_BET-
    p_BET_sec_des)),'-r+'); title('BET 0.05p_{sat}<p<0.3p_{sat}'); xlabel('(
    p/p_{s})'); ylabel('p/(m_{ads}*(p_{s} - p))'); grid on;

%%
%%%%%%%%%%%%%%%%%%%%%%%%%%%%%%%%%%%%%%%%%%%%%%%%%%%%%%%%%%%%%%%%%%%%%%%%%%%%
% for presenting
%%%%%%%%%%%%%%%%%%%%%%%%%%%%%%%%%%%%%%%%%%%%%%%%%%%%%%%%%%%%%%%%%%%%%%%%%%%%

xx = linspace(0,max(p_ads),1000)';
Langmuir_plot_ads = Langmuir_coeffs_ads(1).*Langmuir_coeffs_ads(2).*xx./(1
    + Langmuir_coeffs_ads(1).*xx);
Freundlich_plot_ads = Freundlich_coeffs_ads(1).*xx.^Freundlich_coeffs_ads
    (2);
BET_plot_ads = BET_coeffs_ads(1).*BET_coeffs_ads(2).*xx ./ ((p_sat_BET - xx
    ).*(1 + ((BET_coeffs_ads(1) - 1).*xx) ./ p_sat_BET));
DR_plot_ads = DR_coeffs_ads(2).*exp(-DR_coeffs_ads(1).*((R .*(blank_input
    +273.15).*log(1+ 1./(xx*1e5))).^2));
Temkin_plot_ads = Temkin_coeffs_ads(2).*log(Temkin_coeffs_ads(1).*xx); %
    varibale RTb_T = R*T/b_T
Toth_plot_ads = (Toth_coeffs_ads(1)*xx)./(Toth_coeffs_ads(2) + xx).^(1/
    Toth_coeffs_ads(3));
DA_plot_ads = DA_coeffs_ads(3).*exp(-DA_coeffs_ads(1).*((R .*(blank_input
    +273.15).*log(1+ 1./(xx*1e5))).^DA_coeffs_ads(2)));

figure(2)
hold on
%plot(pressure_ads,delta_m_ads*1e3/Molar_mass_gas/m_S,'+')
%plot(pressure_des,delta_m_des*1e3/Molar_mass_gas/m_S,'or')
errorbar(pressure_ads,delta_m_plot_ads,sigma_mass_meas_plot_ads,'+b','
    DisplayName','exp. adsorption')
%errorbar(pressure_des,delta_m_plot_des,sigma_mass_meas_plot_des,'or','
    DisplayName','exp. desorption')
if (Langmuir_ads)    plot(xx,Langmuir_plot_ads,'c','DisplayName','Langmuir')
    ;     end
```

```
if (Freundlich_ads) plot(xx,Freundlich_plot_ads,'r','DisplayName','
    Freundlich');end
if (BET_ads)          plot(xx,BET_plot_ads,'k','DisplayName','BET');
                  end
if (DR_ads)           plot(xx,DR_plot_ads,'m','DisplayName','DR');
                    end
if (DA_ads)           plot(xx,DA_plot_ads,'m:','DisplayName','DA');
                   end
if (Temkin_ads)       plot(xx,Temkin_plot_ads,'y','DisplayName','Temkin');
           end
if (Toth_ads)         plot(xx,Toth_plot_ads,'g','DisplayName','Toth');
               end
xlabel('pressure [bar]');
ylabel('adsorbed amount [mmol/g]');
legend('-DynamicLegend','Location','NorthWest');
ylim([0 max(delta_m_plot_ads)+5]);
grid on
hold off

% FGK for saving plot
orient landscape
saveas(gcf,'results/VACNT_SO2_25C_fit_ads','pdf');

Langmuir_plot_des = Langmuir_coeffs_des(1).*Langmuir_coeffs_des(2).*xx./(1
    + Langmuir_coeffs_des(1).*xx);
Freundlich_plot_des = Freundlich_coeffs_des(1).*xx.^Freundlich_coeffs_des
    (2);
BET_plot_des = BET_coeffs_des(1).*BET_coeffs_des(2).*xx ./ ((p_sat_BET - xx
    ).*(1 + ((BET_coeffs_des(1) - 1).*xx) ./ p_sat_BET));
DR_plot_des = DR_coeffs_des(2).*exp(-DR_coeffs_des(1).*((R .*(blank_input
    +273.15).*log(1+ 1./(xx*1e5))).^2));
Temkin_plot_des = Temkin_coeffs_des(2).*log(Temkin_coeffs_des(1).*xx); %
    varibale RTb_T = R*T/b_T
Toth_plot_des = (Toth_coeffs_des(1)*xx)./(Toth_coeffs_des(2) + xx).^(1/
    Toth_coeffs_des(3));
DA_plot_des = DA_coeffs_des(3).*exp(-DA_coeffs_des(1).*((R .*(blank_input
    +273.15).*log(1+ 1./(xx*1e5))).^DA_coeffs_des(2)));

figure(3)
hold on
%plot(pressure_ads,delta_m_ads*1e3/Molar_mass_gas/m_S,'+')
%plot(pressure_des,delta_m_des*1e3/Molar_mass_gas/m_S,'or')
%errorbar(pressure_ads,delta_m_plot_ads,sigma_mass_meas_plot_ads,'+b','
    DisplayName','exp. adsorption')
```

```
errorbar(pressure_des,delta_m_plot_des,sigma_mass_meas_plot_des,'or','
    DisplayName','exp. desorption')
if (Langmuir_des)    plot(xx,Langmuir_plot_des,'c','DisplayName','Langmuir')
    ;     end
if (Freundlich_des) plot(xx,Freundlich_plot_des,'r','DisplayName','
    Freundlich');end
if (BET_des)          plot(xx,BET_plot_des,'k','DisplayName','BET');
                  end
if (DR_des)           plot(xx,DR_plot_des,'m','DisplayName','DR');
                   end
if (DA_des)           plot(xx,DA_plot_des,'m:','DisplayName','DA');
                  end
if (Temkin_des)       plot(xx,Temkin_plot_des,'y','DisplayName','Temkin');
           end
if (Toth_des)         plot(xx,Toth_plot_des,'g','DisplayName','Toth');
                end
xlabel('pressure [bar]');
ylabel('adsorbed amount [mmol/g]');
legend('-DynamicLegend','Location','NorthWest');
ylim([0 max(delta_m_plot_ads)+5]);
grid on
hold off

% FGK for saving plot
orient landscape
saveas(gcf,'results/VACNT_SO2_35C_fit_des','pdf');
```

C.6 Matlab code fit_ads_models_Virial

In this matlab code the data saved from the code presented in C.4 is loaded by the routine described in C.8 and the described Virial model is tried to fit to all given isotherms to evaluate the heat of adsorption for the given adsorbent/adsorptive combination. The Virial model to which the data is fitted to is:

$$ln(p) = \frac{1}{T}\sum_{i=0}^{m}(a_i * X^i) + \sum_{i=0}^{n}(b_i * X^i) + ln(X) \tag{C.1}$$

For the fit m is set to 2 and n is set to 0. T is the temperature in Kelvin and X stands for the adsorbed amount in $\mathrm{mmol\,g^{-1}}$. The code displays the fits to the adsorption branches for all temperatures and the desorption branches to all temperatures and gives

a plot of the isosteric heats of adsorption for the adsorption and desorption over the adsorbed amount with a 95 % confidence intervall. The heat of adsorption is calculated as following by the fitted coefficients a_0 to a_2:

$$\Delta H_{ads} = -R \cdot \left(a_0 + a_1 \cdot X + a_2 \cdot X^2\right) \tag{C.2}$$

```
clear all;
close all;
format long;

R = 8.314; %[J mol^{1} K^{-1}] ideal gas constant
Masse = zeros(1,8);
Delta_m = zeros(1,3);
X = zeros(1,3);
p = zeros(1,3);
T = zeros(1,2);
sigma = zeros(1,4);
A =zeros(1,2);
B =zeros(1,2);

%%%%%%%%%%%%%%%%%%%%%%%%%%%%%%%%%%%%%%%%%%%%%%%%%%%%%%%%%%%%%%%%%%%%%%%%%%%%%%%
%%%% VACNT SO2 high pressure
%%%%%%%%%%%%%%%%%%%%%%%%%%%%%%%%%%%%%%%%%%%%%%%%%%%%%%%%%%%%%%%%%%%%%%%%%%%%%%%

load('results/VACNT_SO2_15C.mat'); ii = 1;
[Masse,Delta_m,X,p,T,sigma,A,B] = readdata(Masse,Delta_m,X,p,T,sigma,A,B
    ,...
    ii,m_SC,m_SC_meas,m_SC_S,...
    m_S_meas,V_SC,V_SC_S,V_S,V_S_spec,delta_m,delta_m_ads,delta_m_des,...
    delta_m_plot,delta_m_plot_ads,delta_m_plot_des,pressure_meas,...
    pressure_ads,pressure_des,temperature_meas,sigma_mass_meas_plot,...
    sigma_mass_meas_plot_ads,sigma_mass_meas_plot_des,
        sigma_temperature_meas);

load('results/VACNT_SO2_25C.mat'); ii = 2;
[Masse,Delta_m,X,p,T,sigma,A,B] = readdata(Masse,Delta_m,X,p,T,sigma,A,B
    ,...
    ii,m_SC,m_SC_meas,m_SC_S,...
    m_S_meas,V_SC,V_SC_S,V_S,V_S_spec,delta_m,delta_m_ads,delta_m_des,...
    delta_m_plot,delta_m_plot_ads,delta_m_plot_des,pressure_meas,...
    pressure_ads,pressure_des,temperature_meas,sigma_mass_meas_plot,...
```

```
    sigma_mass_meas_plot_ads,sigma_mass_meas_plot_des,
        sigma_temperature_meas);

load('results/VACNT_SO2_35C.mat'); ii = 3;
[Masse,Delta_m,X,p,T,sigma,A,B] = readdata(Masse,Delta_m,X,p,T,sigma,A,B
    ,...
    ii,m_SC,m_SC_meas,m_SC_S,...
    m_S_meas,V_SC,V_SC_S,V_S,V_S_spec,delta_m,delta_m_ads,delta_m_des,...
    delta_m_plot,delta_m_plot_ads,delta_m_plot_des,pressure_meas,...
    pressure_ads,pressure_des,temperature_meas,sigma_mass_meas_plot,...
    sigma_mass_meas_plot_ads,sigma_mass_meas_plot_des,
        sigma_temperature_meas);

load('results/VACNT_SO2_50C.mat'); ii = 4;
[Masse,Delta_m,X,p,T,sigma,A,B] = readdata(Masse,Delta_m,X,p,T,sigma,A,B
    ,...
    ii,m_SC,m_SC_meas,m_SC_S,...
    m_S_meas,V_SC,V_SC_S,V_S,V_S_spec,delta_m,delta_m_ads,delta_m_des,...
    delta_m_plot,delta_m_plot_ads,delta_m_plot_des,pressure_meas,...
    pressure_ads,pressure_des,temperature_meas,sigma_mass_meas_plot,...
    sigma_mass_meas_plot_ads,sigma_mass_meas_plot_des,
        sigma_temperature_meas);

load('results/VACNT_SO2_75C.mat'); ii = 5;
[Masse,Delta_m,X,p,T,sigma,A,B] = readdata(Masse,Delta_m,X,p,T,sigma,A,B
    ,...
    ii,m_SC,m_SC_meas,m_SC_S,...
    m_S_meas,V_SC,V_SC_S,V_S,V_S_spec,delta_m,delta_m_ads,delta_m_des,...
    delta_m_plot,delta_m_plot_ads,delta_m_plot_des,pressure_meas,...
    pressure_ads,pressure_des,temperature_meas,sigma_mass_meas_plot,...
    sigma_mass_meas_plot_ads,sigma_mass_meas_plot_des,
        sigma_temperature_meas);

figure(1) % adsorption and desorption isotherms
% figure('Name','figure(1) adsorption and desorption isotherms','
    NumberTitle','off')
for ii=1:2:(size(A,2)-1) % column
    plot(A(:,ii),A(:,ii+1),'+','DisplayName',['Ads. ',num2str(T(1,(ii+1))),
        ' °C'])
    hold on
    plot(B(:,ii),B(:,ii+1),'o','DisplayName',['Des. ',num2str(T(1,(ii+1))),
        ' °C'])
end
xlabel('pressure p [bar]')
```

```
ylabel('adsorbed amount X [mmol\cdotg^{-1}]')
legend('-DynamicLegend','Location','Best')
grid on
hold off

figure(2) % adsorption and desorption isotherms
for ii=1:2:(size(A,2)-1) % column
    plot(A(:,ii+1),log(A(:,ii)),'+','DisplayName',['Ads. ',num2str(T(1,(ii
        +1))),' °C'])
    hold on
    plot(B(:,ii+1),log(B(:,ii)),'o','DisplayName',['Des. ',num2str(T(1,(ii
        +1))),' °C'])
end
ylabel('ln(p/1bar) [bar bar^{-1}]')
xlabel('adsorbed amount X [mmol\cdotg^{-1}]')
legend('-DynamicLegend','Location','Best')
grid on
hold off

%%%%%%%%%%%%%%%%%%%%%%%%%%%%%%%%%%%%%%%%%%%%%%%%%%%%%%%%%%%%%%%%%%%%%%%%%%%%
%%%%%%% Fit %%%%%%%%%%%%%%%%%%%%%%%%%%%%%%%%%%%%%%%%%%%%%%%%%%%%%%%%%%%%%%%
%%%%%%%%%%%%%%%%%%%%%%%%%%%%%%%%%%%%%%%%%%%%%%%%%%%%%%%%%%%%%%%%%%%%%%%%%%%%

%%%%%%%%%%%%%%%%%%%%%%%%%%%%%%%%%%%%%%%%%%%%%%%%%%%%%%%%%%%%%%%%%%%%%%%%%%%%
% Virial model: ln(p) = 1/T sum_i=0^l1 (a_i*n^i) + sum_i=0^l2 (b_i*n^i) +
% ln(n)
% T = temperature
% a_i = coefficient
% b_i = coefficient
% n = adsorbed amount
% l1 = parameter
% l2 = parameter

% adsorption
counterhelp=0;
excludevar_help = 20;

for ii=1:2:size(A,2)-1
  counter=0;
    for jj=1:size(A,1)
        counter = counter+1;
        if A(jj,ii)~=0
            counterhelp=counterhelp+1;
```

```
            x(counterhelp,1) = A(counter,ii+1);
            y(counterhelp,1) = T(counter,ii+1) + 273.15;
            excludevar_ads(counterhelp,1) = [A(counter,ii) < 0.1];%| x >
                excludevar_help];

            lnp_ads(counterhelp,1) = log(A(counter,ii));
            p_ads(counterhelp,1) = A(counter,ii);
        end
    end
end

Virial_2_0 = '1/y *(a_0 + a_1*x + a_2*x^2) + b_0 + log(x)';
Virial_2_0_fit_ads = fit([x,y],lnp_ads,Virial_2_0) %,'Start',
    startPoints_Virial_2_0,'Exclude',exclude_Virial_2_0)

Virial_2_0_coeffs_ads = coeffvalues(Virial_2_0_fit_ads);
Virial_2_0_confint_ads = confint(Virial_2_0_fit_ads);

%desorption
counterhelp=0;
excludevar_help = 20;

for ii=1:2:size(B,2)-1
  counter=0;
    for jj=1:size(B,1)
        counter = counter+1;
        if B(jj,ii)~=0
            counterhelp=counterhelp+1;

            x_des(counterhelp,1) = B(counter,ii+1);
            y_des(counterhelp,1) = T(counter,ii+1) + 273.15;
            excludevar_ads(counterhelp,1) = [B(counter,ii) < 0.1];%| x >
                excludevar_help];

            lnp_des(counterhelp,1) = log(B(counter,ii));
            p_des(counterhelp,1) = B(counter,ii);
        end
    end
end

Virial_2_0_des = '1/y *(a_0 + a_1*x + a_2*x^2) + b_0 + log(x)';
Virial_2_0_fit_des = fit([x_des,y_des],lnp_des,Virial_2_0_des) %,'Start',
    startPoints_Virial_2_0_des,'Exclude',exclude_Virial_2_0_des)
```

```
Virial_2_0_coeffs_des = coeffvalues(Virial_2_0_fit_des);
Virial_2_0_confint_des = confint(Virial_2_0_fit_des);

figure(3)
plot(Virial_2_0_fit_ads,[x,y],lnp_ads)
hold on
title('adsorption branch');
xlabel('adsorbed amount [mmol g^{-1}]');
ylabel('temperature [K]');
zlabel('ln(p/1bar)');
legend('-DynamicLegend','Location','Best');
hold off

figure(4)
plot(Virial_2_0_fit_des,[x_des,y_des],lnp_des)
hold on
title('desorption branch');
xlabel('adsorbed amount [mmol g^{-1}]');
ylabel('temperature [K]');
zlabel('ln(p/1bar)');
legend('-DynamicLegend','Location','Best');
hold off

figure(5) % adsorption isotherms adsorption branch
for ii=1:2:(size(A,2)-1) % column
    n_plot = linspace(0.1,max(A(:,ii+1)),100)';
    lnp_plot = 1/(T(1,(ii+1))+273.15)*(Virial_2_0_coeffs_ads(1) +
       Virial_2_0_coeffs_ads(2)*n_plot + Virial_2_0_coeffs_ads(3)*n_plot
       .^2) + Virial_2_0_coeffs_ads(4) + log(n_plot);

    hold on
    plot(A(:,ii+1),log(A(:,ii)),'+','DisplayName',[num2str(T(1,(ii+1))),' °C
       '])
    plot(n_plot,lnp_plot,'DisplayName',[num2str(T(1,(ii+1))),' °C fit'])
end
title('adsorption branch');
ylabel('ln(p/1bar) [bar bar^{-1}]')
xlabel('adsorbed amount X [mmol\cdotg^{-1}]')
legend('-DynamicLegend','Location','Best')
grid on
hold off

figure(6) % adsorption isotherms desorption branch
for ii=1:2:(size(B,2)-1) % column
```

```
    n_plot_des = linspace(0.1,max(B(:,ii+1)),100)';
    lnp_plot_des = 1/(T(1,(ii+1))+273.15)*(Virial_2_0_coeffs_des(1) +
        Virial_2_0_coeffs_des(2)*n_plot_des + Virial_2_0_coeffs_des(3)*
        n_plot_des.^2) + Virial_2_0_coeffs_des(4) + log(n_plot_des);

    hold on
    plot(B(:,ii+1),log(B(:,ii)),'o','DisplayName',[num2str(T(1,(ii+1))),' °C
        '])
    plot(n_plot_des,lnp_plot_des,'DisplayName',[num2str(T(1,(ii+1))),' °C
        fit'])
end
title('desorption branch');
ylabel('ln(p/1bar) [bar bar^{-1}]')
xlabel('adsorbed amount X [mmol\cdotg^{-1}]')
legend('-DynamicLegend','Location','Best')
grid on
hold off

n_q_st = linspace(0,max(x),100)';
q_st_Virial_2_0 = -R*(Virial_2_0_coeffs_ads(1) + Virial_2_0_coeffs_ads(2)*
    n_q_st + Virial_2_0_coeffs_ads(3)*n_q_st.^2);

q_st_Virial_2_0_min = -R*(Virial_2_0_confint_ads(1,1) +
    Virial_2_0_confint_ads(1,2)*n_q_st + Virial_2_0_confint_ads(1,3)*n_q_st
    .^2);
q_st_Virial_2_0_max = -R*(Virial_2_0_confint_ads(2,1) +
    Virial_2_0_confint_ads(2,2)*n_q_st + Virial_2_0_confint_ads(2,3)*n_q_st
    .^2);

n_q_st_des = linspace(0,max(x_des),100)';
q_st_Virial_2_0_des = -R*(Virial_2_0_coeffs_des(1) + Virial_2_0_coeffs_des
    (2)*n_q_st_des + Virial_2_0_coeffs_des(3)*n_q_st_des.^2);

q_st_Virial_2_0_des_min = -R*(Virial_2_0_confint_des(1,1) +
    Virial_2_0_confint_des(1,2)*n_q_st_des + Virial_2_0_confint_des(1,3)*
    n_q_st_des.^2);
q_st_Virial_2_0_des_max = -R*(Virial_2_0_confint_des(2,1) +
    Virial_2_0_confint_des(2,2)*n_q_st_des + Virial_2_0_confint_des(2,3)*
    n_q_st_des.^2);

figure(7)
plot(n_q_st,q_st_Virial_2_0/1000,'b')
hold on
plot(n_q_st,q_st_Virial_2_0_min/1000,'b--')
```

```
plot(n_q_st_des,q_st_Virial_2_0_des/1000,'r')
plot(n_q_st_des,q_st_Virial_2_0_des_min/1000,'r--')

plot(n_q_st,q_st_Virial_2_0_max/1000,'b--')
plot(n_q_st_des,q_st_Virial_2_0_des_max/1000,'r--')
xlabel('adsorbed amount [mmol g^{-1}]');
ylabel('isosteric heat of adsorption [kJ mol^{-1}]');
legend('heat of adsorption adsorption branch','95% confidence intervall','
    heat of adsorption desorption branch','95% confidence intervall','
    location','best')
hold off

% Values for saving
maxloading_ads = max(x); % max. loading adsorption branch
maxloading_des = max(x_des); % max. loading desorption branch

avg_q_st_ads = mean(q_st_Virial_2_0)/1000; % mean heat of adsorption
    adsorption branch
avg_q_st_des = mean(q_st_Virial_2_0_des/1000); % mean heat of adsorption
    desorption branch
min_q_st_ads = min(q_st_Virial_2_0)/1000; % min. heat of adsorption
    adsorption branch
max_q_st_ads = max(q_st_Virial_2_0)/1000; % max. heat of adsorption
    adsorption branch
min_q_st_des = min(q_st_Virial_2_0_des/1000); % min. heat of adsorption
    desorption branch
max_q_st_des = max(q_st_Virial_2_0_des/1000); % max. heat of adsorption
    desorption branch

q_st_save = [avg_q_st_ads min_q_st_ads max_q_st_ads;avg_q_st_des
    min_q_st_des max_q_st_des];

orient landscape
saveas(gcf,'results/VACNT_SO2_heat_of_ads','pdf');
save('exceldata_heat_of_ads.txt','Virial_2_0_coeffs_ads','
    Virial_2_0_confint_ads','Virial_2_0_coeffs_des','Virial_2_0_confint_des'
    ,'maxloading_ads','maxloading_des','q_st_save','-ASCII','-DOUBLE','-TABS
    ');

figure(8) % adsorption isotherms
for ii=1:2:(size(A,2)-1) % column
    n_plot = linspace(0.1,max(A(:,ii+1)),100)';
```

```
    lnp_plot = 1/(T(1,(ii+1))+273.15)*(Virial_2_0_coeffs_ads(1) +
        Virial_2_0_coeffs_ads(2)*n_plot + Virial_2_0_coeffs_ads(3)*n_plot
        .^2) + Virial_2_0_coeffs_ads(4) + log(n_plot);

    hold on
    plot(A(:,ii),A(:,ii+1),'+','DisplayName',[num2str(T(1,(ii+1))),' °C'])
    plot(exp(lnp_plot),n_plot,'DisplayName',[num2str(T(1,(ii+1))),' °C fit'
        ])
end
xlabel('p [bar]')
ylabel('adsorbed amount X [mmol\cdotg^{-1}]')
legend('-DynamicLegend','Location','Best')
grid on
hold off

figure(9) % adsorption isotherms
for ii=1:2:(size(B,2)-1) % column
    n_plot_des = linspace(0.1,max(B(:,ii+1)),100)';
    lnp_plot_des = 1/(T(1,(ii+1))+273.15)*(Virial_2_0_coeffs_des(1) +
        Virial_2_0_coeffs_des(2)*n_plot_des + Virial_2_0_coeffs_des(3)*
        n_plot_des.^2) + Virial_2_0_coeffs_des(4) + log(n_plot_des);

    hold on
    plot(B(:,ii),B(:,ii+1),'o','DisplayName',[num2str(T(1,(ii+1))),' °C'])
    plot(exp(lnp_plot_des),n_plot_des,'DisplayName',[num2str(T(1,(ii+1))),'
        °C fit'])
end
xlabel('p [bar]')
ylabel('adsorbed amount X [mmol\cdotg^{-1}]')
legend('-DynamicLegend','Location','Best')
grid on
hold off
```

C.7 Matlab code k_ads_des

In this matlab code experimental data from the logged time evolution files is imported and chopped into the experimental segments. For each segment the uptake over time is plotted and fitted with a linear driving force model[74]. The fitted value for the amplitude A and time constant k (compare equation C.3) are then plotted and saved for further evaluation.

$$\Delta m = A \cdot \left(1 - e^{-k \cdot t}\right) \tag{C.3}$$

```
clear all; close all;
clc;
%%%%%%%%%%%%%%%%%%%%%%%%%%%%%%%%%%%%%%%%%%%%%%%%%%%%%%%%%%%%%%%%%%%%%%%%%%%%%%%%
%%%% VACNT SO2
%%%%%%%%%%%%%%%%%%%%%%%%%%%%%%%%%%%%%%%%%%%%%%%%%%%%%%%%%%%%%%%%%%%%%%%%%%%%%%%%

% VACNT and SO2 15C
% filename = 'VACNT_SO2_15C.csv'; %FGK

% VACNT and SO2 25C
filename = 'VACNT_25C_SO2.csv'; %FGK

% VACNT and SO2 35C
% filename = 'VACNT_SO_35C.csv'; %FGK

% VACNT and SO2 50C
% filename = 'VACNT_SO2_50C.csv'; %FGK

% VACNT and SO2 75C adsorption branch
% filename = 'VACNT_SO2_75C.csv'; %FGK

% VACNT and SO2 75C desorption branch
% filename = 'VACNT_SO_75C_2.csv'; %FGK

%%%%%%%%%%%%%%%%%%%%%%%%%%%%%%%%%%%%%%%%%%%%%%%%%%%%%%%%%%%%%%%%%%%%%%%%%%%%%%%%
% Import routine
%%%%%%%%%%%%%%%%%%%%%%%%%%%%%%%%%%%%%%%%%%%%%%%%%%%%%%%%%%%%%%%%%%%%%%%%%%%%%%%%
% Initialize variables.
delimiter = ';';
startRow = 2;

% Read columns of data as strings:
% For more information, see the TEXTSCAN documentation.
formatSpec = '%s%s%s%s%s%s%s%s%s%s%s%s%s%s%s%s%s%[^\n\r]';

% Open the text file.
fileID = fopen(filename,'r');
```

```
% Read columns of data according to format string.
% This call is based on the structure of the file used to generate this
% code. If an error occurs for a different file, try regenerating the code
% from the Import Tool.
dataArray = textscan(fileID, formatSpec, 'Delimiter', delimiter, '
    HeaderLines' ,startRow-1, 'ReturnOnError', false);

% Close the text file.
fclose(fileID);

% Convert the contents of columns containing numeric strings to numbers.
% Replace non-numeric strings with NaN.
raw = repmat({''},length(dataArray{1}),length(dataArray)-1);
for col=1:length(dataArray)-1
    raw(1:length(dataArray{col}),col) = dataArray{col};
end
numericData = NaN(size(dataArray{1},1),size(dataArray,2));

for col=[1,2,3,4,5,6,7,8,9,10,11,12,13]
    % Converts strings in the input cell array to numbers. Replaced non-
        numeric
    % strings with NaN.
    rawData = dataArray{col};
    for row=1:size(rawData, 1);
        % Create a regular expression to detect and remove non-numeric
            prefixes and
        % suffixes.
        regexstr = '(?<prefix>.*?)(?<numbers>([-]*(\d+[\,]*)+[\.]{0,1}\d*[
            eEdD]{0,1}[-+]*\d*[i]{0,1})|([-]*(\d+[\,]*)*[\.]{1,1}\d+[eEdD
            ]{0,1}[-+]*\d*[i]{0,1}))(?<suffix>.*)';
        try
            result = regexp(rawData{row}, regexstr, 'names');
            numbers = result.numbers;

            % Detected commas in non-thousand locations.
            invalidThousandsSeparator = false;
            if any(numbers==',');
                thousandsRegExp = '^\d+?(\,\d{3})*\.{0,1}\d*$';
                if isempty(regexp(thousandsRegExp, ',', 'once'));
                    numbers = NaN;
                    invalidThousandsSeparator = true;
                end
            end
            % Convert numeric strings to numbers.
```

```
            if ~invalidThousandsSeparator;
                numbers = textscan(strrep(numbers, ',', ''), '%f');
                numericData(row, col) = numbers{1};
                raw{row, col} = numbers{1};
            end
        catch me
        end
    end
end

% Convert the contents of columns with dates to MATLAB datetimes using date
% format string.
try
    dates{14} = datetime(dataArray{14}, 'Format', 'HH:mm:ss', 'InputFormat'
        , 'HH:mm:ss');
catch
    try
        % Handle dates surrounded by quotes
        dataArray{14} = cellfun(@(x) x(2:end-1), dataArray{14}, '
            UniformOutput', false);
        dates{14} = datetime(dataArray{14}, 'Format', 'HH:mm:ss', '
            InputFormat', 'HH:mm:ss');
    catch
        dates{14} = repmat(datetime([NaN NaN NaN]), size(dataArray{14}));
    end
end

anyBlankDates = cellfun(@isempty, dataArray{14});
anyInvalidDates = isnan(dates{14}.Hour) - anyBlankDates;
dates = dates(:,14);

% Split data into numeric and cell columns.
% rawNumericColumns = raw(:, [1,2,3,4,5,6,7,8]); orig
rawNumericColumns = raw(:, [1,2,3,4,5,6,7,8,9,10,11,12,13]);
% rawCellColumns = raw(:, [9,10,11,12,13,15,16]); orig
rawCellColumns = raw(:, [15,16]);

% Replace non-numeric cells with NaN
R = cellfun(@(x) ~isnumeric(x) && ~islogical(x),rawNumericColumns); % Find
    non-numeric cells
rawNumericColumns(R) = {NaN}; % Replace non-numeric cells

% Allocate imported array to column variable names
No = cell2mat(rawNumericColumns(:, 1));
```

```
Time = cell2mat(rawNumericColumns(:, 2)); % [min]
T = cell2mat(rawNumericColumns(:, 3)); % [Celsius]
calT = cell2mat(rawNumericColumns(:, 4)); % [Celsius]
p = cell2mat(rawNumericColumns(:, 5)); % [bar]
m = cell2mat(rawNumericColumns(:, 6)); % [g]
m_corr = cell2mat(rawNumericColumns(:, 7)); % [g]
delta_m_corr = cell2mat(rawNumericColumns(:, 8)); % [g]
m_MP2 = cell2mat(rawNumericColumns(:, 9)); % [g]
delta_m_MP2_corr = cell2mat(rawNumericColumns(:, 10)); % [g]
density = cell2mat(rawNumericColumns(:, 11)); % [g cm^-3]
t_ZP = cell2mat(rawNumericColumns(:, 12)); % [min]
m_ZP = cell2mat(rawNumericColumns(:, 13)); % [g]

SystemDate = dates{:, 1};
SystemTime = rawCellColumns(:, 1);
VarName16 = rawCellColumns(:, 2);

% For code requiring serial dates (datenum) instead of datetime, uncomment
% the following line(s) below to return the imported dates as datenum(s).
% SystemDate=datenum(SystemDate);

%% Clear temporary variables
clearvars filename delimiter startRow formatSpec fileID dataArray ans raw
    col numericData rawData row regexstr result numbers
    invalidThousandsSeparator thousandsRegExp me dates blankDates
    anyBlankDates invalidDates anyInvalidDates rawNumericColumns
    rawCellColumns R;

%%%%%%%%%%%%%%%%%%%%%%%%%%%%%%%%%%%%%%%%%%%%%%%%%%%%%%%%%%%%%%%%%%%%%%%%%%%%%%%
% Evaluation
%%%%%%%%%%%%%%%%%%%%%%%%%%%%%%%%%%%%%%%%%%%%%%%%%%%%%%%%%%%%%%%%%%%%%%%%%%%%%%%

ind = find((No == 0));
Segmentsplit = [ind];
No_segments = size(Segmentsplit,1)-1;

ind = find(t_ZP > 0);
ZPsplit = [ind];

time_mat = NaN(size(delta_m_corr,1),No_segments);
delta_m_corr_mat = NaN(size(delta_m_corr,1),No_segments);

for i = 1:No_segments
    leg(i,1) = i;
```

```
    p_split(i,1) = p(Segmentsplit(i));
    for j = Segmentsplit(i):(Segmentsplit(i+1)-2)
        time_mat(j-(i-1),i) = Time(j) - Time(Segmentsplit(i)+1);
        delta_m_corr_mat(j-(i-1),i) = delta_m_corr(j) - delta_m_corr(
            Segmentsplit(i)+1);
    end
end

leg = char(num2str(leg));

[p_max,max_index] = max(p_split);

for i = 1:max_index
    p_ads(i) = p_split(i);
end
for i = max_index+1:size(p_split,1)
    p_des(i-max_index) = p_split(i);
end

figure(100)
hold on
set(gca,'LineStyleOrder',{'-','--','-.',':'});
plot(time_mat,(delta_m_corr_mat*1000))
legend(leg)
xlabel('time [min]')
ylabel('mass [mg]')
hold off

for i = 2:No_segments

    coeff_Func_fit_A(i) = NaN;
    coeff_Func_fit_k(i) = NaN;

    if(i~=40 && i~=41 && i~=42 && i~=43 && i~=44) % FGK to exclude Segments
         with a poor fit or no possible fit
        x = time_mat([(Segmentsplit(i)-(i-2)):(Segmentsplit(i+1)-(i+1))],i)
            ; % time vector of each segment
        y = delta_m_corr_mat([Segmentsplit(i)-(i-2):(Segmentsplit(i+1)-(i
            +1))],i)*1000; % recorded delta_m_corr of each segment
        %exclude_x = [x == 'NaN'];

        % fit function
        Func = 'A*(1-exp(-k*x))';
        startPoints_Func = [3 0.5];
```

```
        %Func_fit = fit(x,y,Func,'Start',startPoints_Func,'Exclude',
            exclude_x)
        [Func_fit,gof,fitinfo] = fit(x,y,Func,'Start',startPoints_Func)
        coeff_Func_fit = coeffvalues(Func_fit);

        coeff_Func_fit_A(i) = coeff_Func_fit(1,1);
        coeff_Func_fit_k(i) = coeff_Func_fit(1,2);

        figure(i)
        plot(Func_fit,x,y);
        hold on
        xlabel('time [min]')
        ylabel('mass [mg]')
        hold off
        orient landscape
        saveas(gcf,['results/fit_Segment_',num2str(i)],'pdf');
    end

    SegmentVec = 1:i;
end

coeff_Func_fit_A
coeff_Func_fit_k

figure(101)
[hAx,h1,h2] = plotyy(SegmentVec,coeff_Func_fit_A,SegmentVec,
    coeff_Func_fit_k);
hold on
xlabel('Segment');
ylabel(hAx(1),'A [mg]');
ylabel(hAx(2),'k [min^{-1}]');
set(h1,'Marker','+','MarkerSize',8,'LineStyle','none');
set(h2,'Marker','+','MarkerSize',8,'LineStyle','none');
hold off
orient landscape
saveas(gcf,'results/fit_A_k_over_Segment','pdf');

figure(102)
subplot(2,1,1); plot(p_ads,coeff_Func_fit_A(1:max_index),'+');
hold on
plot(p_des,coeff_Func_fit_A(max_index+1:size(p_split,1)),'o');
xlabel('pressure [bar]');
ylabel('A [mg]');
```

```
subplot(2,1,2); plot(p_ads,coeff_Func_fit_k(1:max_index),'+');
hold on
plot(p_des,coeff_Func_fit_k(max_index+1:size(p_split,1)),'o');
xlabel('pressure [bar]');
ylabel('k [min^{-1}]');
%set(h1,'Color','b','Marker','+','MarkerSize',8,'LineStyle','none');
%set(h2,'Marker','+','MarkerSize',8,'LineStyle','none');
%set(h3,'Color','b','Marker','o','MarkerSize',8,'LineStyle','none');
%set(h4,'Marker','o','MarkerSize',8,'LineStyle','none');
hold off
orient landscape
saveas(gcf,'results/fit_A_k_over_pressure','pdf');

p_split = p_split';
%save variables
save('results/p_A_k.txt','p_split','coeff_Func_fit_A','coeff_Func_fit_k','-
    ASCII','-DOUBLE','-TABS')
```

C.8 Matlab code readdata

Function which is utilized by the Matlab programs fit_ads_models (see C.5) and fit_ads_models_Virial (see C.6) to read in saved data which was produced by the program blank_equ_m_corr (see C.4). The function puts the data it into the variables Masse, Delta_m, X, p, T, sigma, A and B for further processing.

```
function [Masse,Delta_m,X,p,T,sigma,A,B] = readdata(Masse,Delta_m,X,p,T,
    sigma,A,B,ii,m_SC,m_SC_meas,m_SC_S,m_S_meas,V_SC,V_SC_S,V_S,V_S_spec,
    delta_m,delta_m_ads,delta_m_des,delta_m_plot,delta_m_plot_ads,
    delta_m_plot_des,pressure_meas,pressure_ads,pressure_des,
    temperature_meas,sigma_mass_meas_plot,sigma_mass_meas_plot_ads,
    sigma_mass_meas_plot_des,sigma_temperature_meas)

Masse(ii,1) = m_SC; % [g] mass sample container from fit
Masse(ii,2) = m_SC_meas; % [g] measured mass sample container
Masse(ii,3) = m_SC_S; % [g] mass sample container + sample from fit
Masse(ii,4) = m_S_meas; % [g] measured mass sample
Masse(ii,5) = V_SC; % [cm^3] volume sample container
Masse(ii,6) = V_SC_S; % [cm^3] volume sample container + sample
Masse(ii,7) = V_S; % [cm^3] volume sample
Masse(ii,8) = V_S_spec; % [cm^3/g] volume sample per gramm

Delta_m(1:size(delta_m,1),3*(ii-1)+1) = delta_m; % [g] absolute adsorbed
    amount
```

```
Delta_m(1:size(delta_m_ads,2),3*(ii-1)+2) = delta_m_ads'; % [g] absolute
    adsorbed amount adsorption branch
Delta_m(1:size(delta_m_des,2),3*(ii-1)+3) = delta_m_des'; % [g] absolute
    adsorbed amount desorption branch

X(1:size(delta_m_plot,1),3*(ii-1)+1) = delta_m_plot; % [mmol/g] amount
    adsorbed per gramm sample
X(1:size(delta_m_plot_ads,2),3*(ii-1)+2) = delta_m_plot_ads'; % [mmol/g]
    amount adsorbed per gramm sample adsorption branch
X(1:size(delta_m_plot_des,2),3*(ii-1)+3) = delta_m_plot_des'; % [mmol/g]
    amount adsorbed per gramm sample desorption branch

p(1:size(pressure_meas,1),3*(ii-1)+1) = pressure_meas; % [bar] meassuered
    pressure
p(1:size(pressure_ads,2),3*(ii-1)+2) = pressure_ads'; % [bar] meassuered
    pressure adsorption branch
p(1:size(pressure_des,2),3*(ii-1)+3) = pressure_des'; % [bar] meassuered
    pressure desorption branch

T(1:size(temperature_meas,1),2*ii) = temperature_meas; % [°C] measured
    temperature

sigma(1:size(sigma_mass_meas_plot,1),4*(ii-1)+1) = sigma_mass_meas_plot; %
    [mmol/g] standard deviation adsorbed amount per gramm sample
sigma(1:size(sigma_mass_meas_plot_ads,2),4*(ii-1)+2) =
    sigma_mass_meas_plot_ads'; % [mmol/g] standard deviation adsorbed amount
     per gramm sample adsorption branch
sigma(1:size(sigma_mass_meas_plot_des,2),4*(ii-1)+3) =
    sigma_mass_meas_plot_des'; % [mmol/g] standard deviation adsorbed amount
     per gramm sample desorption branch
sigma(1:size(sigma_temperature_meas,1),4*(ii-1)+4) = sigma_temperature_meas
    ; % [°C] standard deviation temperature

A(1:size(p,1),2*ii-1) = p(:,3*(ii-1)+2);% generate A-Matrix with adsorption
     branch data
A(1:size(p,1),2*ii) = X(:,3*(ii-1)+2);

B(1:size(p,1),2*ii-1) = p(:,3*(ii-1)+3);% generate B-Matrix with desorption
     branch data
B(1:size(p,1),2*ii) = X(:,3*(ii-1)+3);
end
```

D Data from simulation

Here, the data gained from simulation is presented. The following tables show relevant parameters of the simulation setup such as used CNT type or graphene, simulated gas(es), temperature T, number of C atoms of the CNT or graphene layer, incorporated box size x, y and z, number of gas molecules, number of time steps simulated, the bulk concentration y_{bulk} which is estimated from the non-absorbed phase, the bulk pressure p which is also estimated from the non-absorbed phase and the absorbed amount of the respective gas $X(i)$ $i = \mathrm{SO}_2, \mathrm{N}_2$.

If fits to the simulated data could be performed the fits are shown. The fit parameters are shown at the end of each section as tables.

D.1 SWCNT and SO_2

D.1.1 CNT(11/11) and SO_2 at 300 K

Table D.1.: CNT(11/11) and SO_2 at 300 K

sample:		CNT(11/11)						
gas(es):		SO_2						
temperature in [K]:		300.00						
# of C-atoms :		1760						
boxsize		# of molecules		# of time	y_{bulk}	p	X(SO_2)	X(N_2)
x,y	z	SO_2	N_2	steps				
[nm]	[nm]	[−]	[−]	[10^6]	[−]	[bar]	[mmolg^{-1}]	
35.3535	47.1380	4500	0	10.0	4.302	2.786	21.619	0.000
31.9065	42.5420	4500	0	10.0	5.121	3.622	25.735	0.000

D.1.2 CNT(11/11) and SO_2 at 350 K

Table D.2.: CNT(11/11) and SO_2 at 350 K

sample:	CNT(11/11)
gas(es):	SO_2
temperature in [K]:	350.00
# of C-atoms :	1760

boxsize x,y [nm]	boxsize z [nm]	# of molecules SO_2 [−]	# of molecules N_2 [−]	# of time steps [10^6]	y_{bulk} [−]	p [bar]	X(SO_2) [mmolg^{-1}]	X(N_2) [mmolg^{-1}]
31.4355	41.9140	4500	0	5.0	3.041	4.708	15.280	0.000
27.2145	36.2860	4500	0	3.0	4.001	6.826	20.105	0.000
24.4830	32.6440	4500	0	3.0	4.848	9.033	24.363	0.000
22.4835	29.9780	4500	0	2.5	5.262	11.483	26.444	0.000
20.9040	27.8720	4500	0	2.0	6.072	13.713	30.513	0.000
19.0000	26.0000	4500	0	2.5	7.569	15.651	38.034	0.000

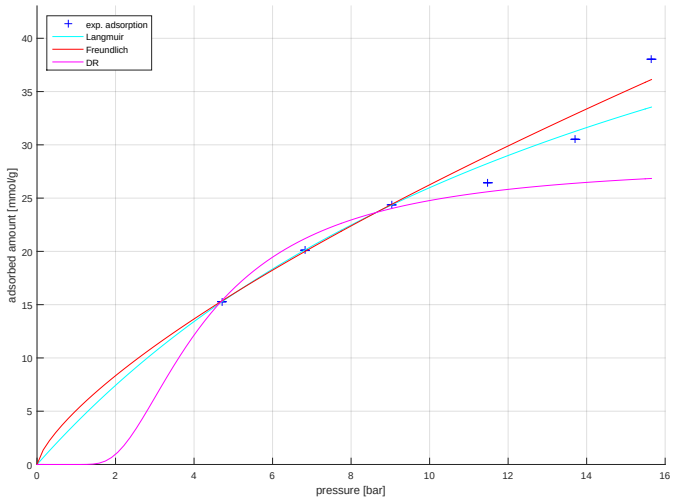

Figure D.1.: CNT(11/11) and SO_2 at 350 K data (marks) and fits (lines) adsorption branch

D.1.3 CNT(11/11) and SO_2 at 400 K

Table D.3.: CNT(11/11) and SO_2 at 400 K

sample:	CNT(11/11)
gas(es):	SO_2
temperature in [K]:	400.00
# of C-atoms :	1760

boxsize		# of molecules		# of time	y_{bulk}	p	X(SO_2)	X(N_2)
x,y [nm]	z [nm]	SO_2 [−]	N_2 [−]	steps [10^6]	[−]	[bar]	[mmolg^{-1}]	
33.0780	44.1040	4500	0	2.0	1.261	4.849	6.339	0.000
25.9770	34.6360	4500	0	2.0	2.636	9.333	13.246	0.000
22.4325	29.9100	4500	0	1.5	3.342	13.706	16.794	0.000
20.1225	26.8300	4500	0	1.5	4.057	17.914	20.389	0.000
18.4155	24.5540	4500	0	1.0	4.942	22.099	24.836	0.000
17.0535	22.7380	4460	0	1.0	5.404	25.949	27.154	0.000
15.8970	21.1960	4440	0	1.0	6.166	29.650	30.986	0.000
14.8635	19.8180	4420	0	1.0	7.992	35.029	40.163	0.000
13.8780	18.5040	4420	0	1.0	9.367	39.249	47.070	0.000
12.3150	16.4200	4420	0	1.0	12.954	43.145	65.093	0.000

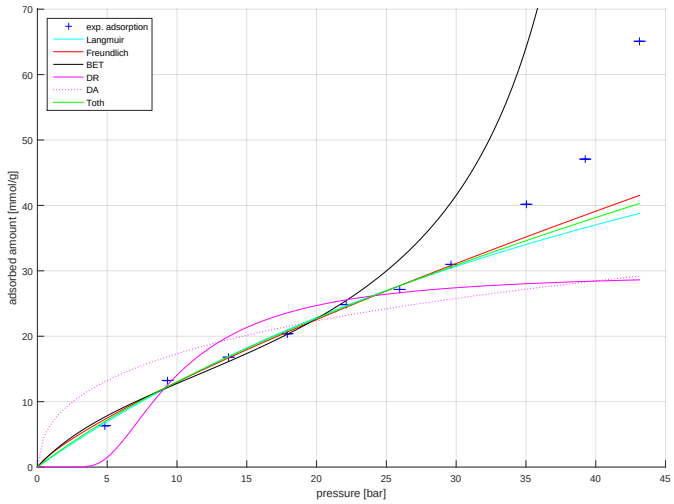

Figure D.2.: CNT(11/11) and SO_2 at 400 K data (marks) and fits (lines) adsorption branch

D.1.4 CNT(20/20) and SO_2 at 300 K

Table D.4.: CNT(20/20) and SO_2 at 300 K

sample:			CNT(20/20)					
gas(es):			SO_2					
temperature in [K]:			300.00					
# of C-atoms :			2640					
boxsize		# of molecules		# of time	y_{bulk}	p	X(SO_2)	X(N_2)
x,y	z	SO_2	N_2	steps				
[nm]	[nm]	[−]	[−]	[10^6]	[−]	[bar]	[mmolg^{-1}]	
35.3535	47.1380	5328	0	9.0	5.604	2.993	28.163	0.000
31.9065	42.5420	5328	0	6.0	6.075	3.936	30.528	0.000

D.1.5 CNT(20/20) and SO_2 at 350 K

Table D.5.: CNT(20/20) and SO_2 at 350 K

sample:	CNT(20/20)
gas(es):	SO_2
temperature in [K]:	350.00
# of C-atoms :	2640

boxsize x,y [nm]	boxsize z [nm]	# of molecules SO_2 [−]	# of molecules N_2 [−]	# of time steps [10^6]	y_{bulk} [−]	p [bar]	X(SO_2) [mmolg^{-1}]	X(N_2) [mmolg^{-1}]
31.4355	41.9140	5328	0	7.0	4.305	5.159	21.635	0.000
27.2145	36.2860	5328	0	7.0	5.096	7.575	25.608	0.000
24.4830	32.6440	5268	0	4.0	5.843	9.797	29.361	0.000
22.4835	29.9780	5248	0	3.0	6.565	12.200	32.988	0.000
20.9040	27.8720	5248	0	3.0	7.563	13.997	38.003	0.000

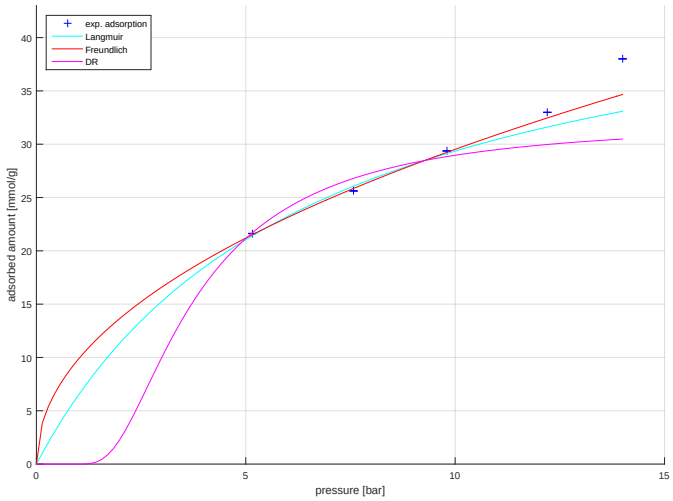

Figure D.3.: CNT(20/20) and SO_2 at 350 K data (marks) and fits (lines) adsorption branch

D.1.6 CNT(20/20) and SO_2 at 400 K

Table D.6.: CNT(20/20) and SO_2 at 400 K

sample:	CNT(20/20)
gas(es):	SO_2
temperature in [K]:	400.00
# of C-atoms :	2640

boxsize x,y [nm]	boxsize z [nm]	# of molecules SO_2 [−]	# of molecules N_2 [−]	# of time steps [10^6]	y_{bulk} [−]	p [bar]	X(SO_2) [mmolg^{-1}]	X(N_2) [mmolg^{-1}]
26.4670	44.1110	3364	0	10.0	1.000	5.157	10.155	0.000
20.7850	34.6400	3364	0	5.0	1.000	9.803	18.292	0.000
17.9520	29.9200	3364	0	5.0	1.000	14.235	22.202	0.000
16.0920	26.8200	3364	0	3.0	1.000	18.124	26.018	0.000
14.7360	24.5600	3364	0	2.0	1.000	22.387	29.204	0.000
13.6428	22.7380	3364	0	2.0	1.000	26.342	32.231	0.000
10.5980	22.2558	2454	0	1.0	1.000	28.031	33.051	0.000
9.9090	22.7907	2680	0	1.0	1.000	31.525	37.435	0.000
12.3150	16.4200	4360	0	1.0	1.000	43.123	52.415	0.000

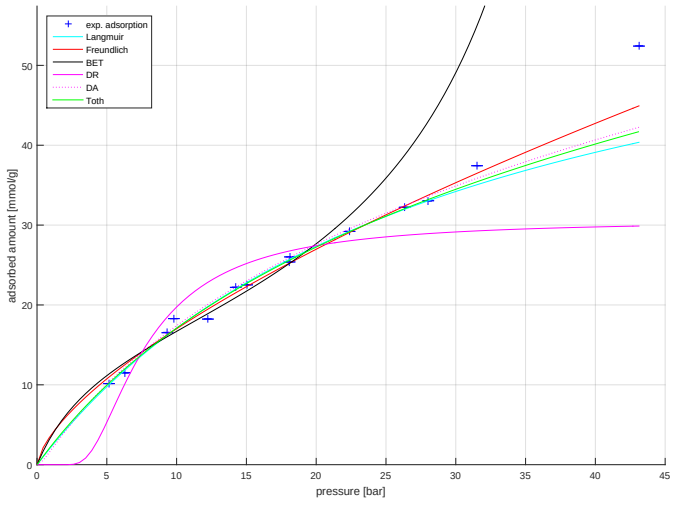

Figure D.4.: CNT(20/20) and SO_2 at 400 K data (marks) and fits (lines) adsorption branch

D.1.7 Charged CNT(20/20) and SO_2 at 400 K

Table D.7.: Charged CNT(20/20) with 0.01 e per C atom and SO_2 at 400 K

sample:	CNT(20/20)
gas(es):	SO_2/N_2
temperature in [K]:	400.00
# of C-atoms :	2640

boxsize		# of molecules		# of time	y_{bulk}	p	X(SO_2)	X(N_2)
x,y [nm]	z [nm]	SO_2 [−]	N_2 [−]	steps [10^6]	[−]	[bar]	[mmolg^{-1}]	
20.7850	34.6400	3364	0	2.0	0.000	9.483	25.545	0.000
16.0920	26.8200	3364	0	2.0	0.000	17.045	35.480	0.000
13.6428	22.7380	3364	0	1.0	0.000	23.814	43.238	0.000
9.9090	22.7907	2680	0	1.0	0.000	29.674	42.513	0.000

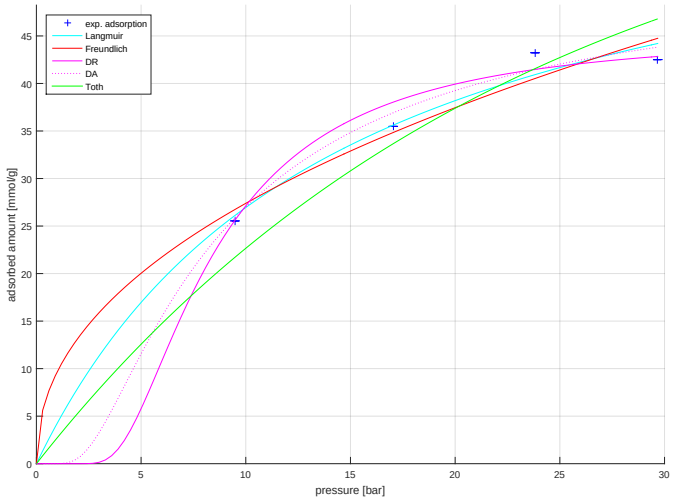

Figure D.5.: charged CNT(20/20) with 0.01 e per C atom and SO_2 at 400 K data (marks) and fits (lines) adsorption branch

D.1.8 CNT(30/30) and SO_2 at 400 K

Table D.8.: CNT(30/30) and SO_2 at 400 K

sample:		CNT(30/30)						
gas(es):		SO_2						
temperature in [K]:		400.00						
# of C-atoms :		6120						
boxsize		# of molecules		# of time	y_{bulk}	p	X(SO_2)	X(N_2)
x,y	z	SO_2	N_2	steps				
[nm]	[nm]	[−]	[−]	[10^6]	[−]	[bar]	[mmolg^{-1}]	
26.5355	35.3780	4420	0	3.0	0.000	7.228	12.761	0.000
21.0585	28.0780	4420	0	2.0	0.000	12.537	19.250	0.000
18.3975	24.5500	4420	0	2.0	0.000	16.895	22.692	0.000
16.7145	22.2860	4420	0	2.0	0.000	19.969	25.916	0.000
15.5160	20.6880	4300	0	2.0	0.000	21.969	28.039	0.000
13.8705	18.4940	4260	0	2.0	0.000	26.322	31.372	0.000
13.2660	17.6880	4260	0	2.0	0.000	27.137	32.882	0.000
12.7560	17.0080	4240	0	2.0	0.000	29.435	36.705	0.000
12.3150	16.4200	4220	0	1.5	0.000	30.898	37.589	0.000
12.3150	20.5250	5275	0	1.0	0.000	34.118	41.562	0.000
16.4200	16.4200	7680	0	1.0	0.000	39.674	49.438	0.000
16.4200	20.5250	9600	0	1.0	0.000	42.361	54.445	0.000
16.4200	22.1670	10368	0	2.5	0.000	43.590	54.907	0.000

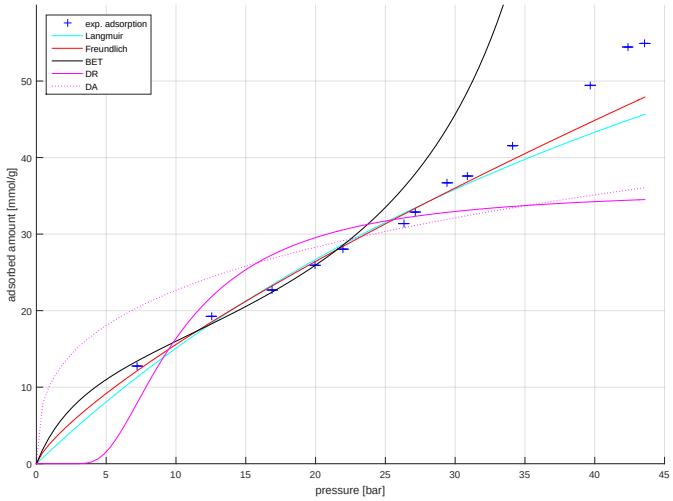

Figure D.6.: CNT(30/30) and SO_2 at $400\,\mathrm{K}$ data (marks) and fits (lines) adsorption branch

D.1.9 CNT(40/40) and SO_2 at 400 K

Table D.9.: CNT(40/40) and SO_2 at 400 K

sample:		CNT(40/40)						
gas(es):		SO_2						
temperature in [K]:		400.00						
# of C-atoms :		10560						
boxsize		# of molecules		# of time steps	y_{bulk}	p	X(SO_2)	X(N_2)
x,y [nm]	z [nm]	SO_2 [−]	N_2 [−]	[10^6]	[−]	[bar]	[mmolg^{-1}]	
26.5355	35.3780	4420	0	3.0	0.000	6.105	12.599	0.000
21.0585	28.0780	4420	0	3.0	0.000	9.877	17.456	0.000
18.3975	24.5500	4260	0	1.5	0.000	11.986	19.262	0.000
16.7145	22.2860	4340	0	1.5	0.000	14.719	21.099	0.000
15.5160	20.6880	4340	0	1.5	0.000	17.322	22.384	0.000
13.8705	18.4940	4180	0	1.5	0.000	18.152	24.497	0.000
13.2660	17.6880	4180	0	1.5	0.000	20.220	25.033	0.000
12.7560	21.2600	5125	0	1.5	0.000	23.692	29.022	0.000
12.3150	20.5250	5075	0	1.5	0.000	24.281	29.314	0.000
16.4200	20.5250	9550	0	2.0	0.000	35.751	43.451	0.000
20.5250	20.5250	15075	0	2.5	0.000	41.303	53.724	0.000
20.5250	24.6300	18090	0	3.0	0.000	44.373	55.987	0.000

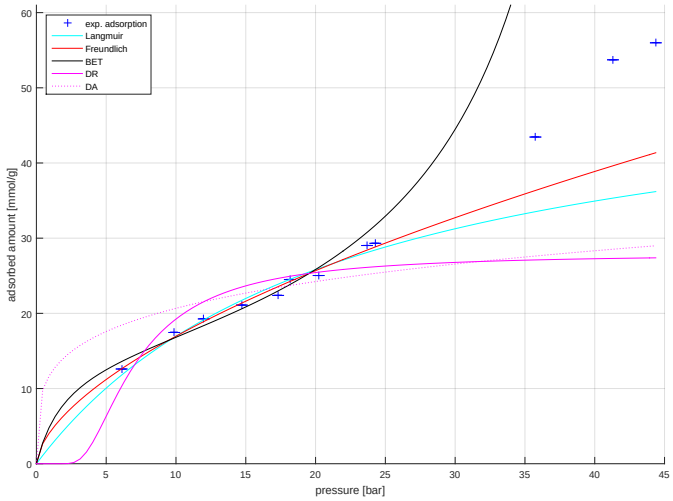

Figure D.7.: CNT(40/40) and SO_2 at $400\,\mathrm{K}$ data (marks) and fits (lines) adsorption branch

D.1.10 CNT(80/80) and SO_2 at 400 K

Table D.10.: CNT(80/80) and SO_2 at 400 K

sample:		CNT(80/80)						
gas(es):		SO_2						
temperature in [K]:		400.00						
# of C-atoms :		14400						
boxsize		# of molecules		# of time	y_{bulk}	p	X(SO_2)	X(N_2)
x,y	z	SO_2	N_2	steps				
[nm]	[nm]	[−]	[−]	[10^6]	[−]	[bar]	[mmolg^{-1}]	
35.0975	35.0975	15325	0	3.0	0.000	13.811	20.815	0.000
30.6625	30.6625	15175	0	3.0	0.000	18.762	24.561	0.000
27.8575	27.8575	15125	0	1.5	0.000	23.021	28.597	0.000
25.8600	25.8600	14925	0	1.5	0.000	26.162	31.766	0.000
24.3350	24.3350	15175	0	1.5	0.000	29.790	35.148	0.000
23.1175	23.1175	14975	0	1.5	0.000	31.717	37.496	0.000
22.1100	22.1100	14675	0	1.5	0.000	33.476	39.224	0.000
21.2600	21.2600	14800	0	1.5	0.000	35.574	41.288	0.000
20.5250	20.5250	14925	0	1.5	0.000	37.347	43.324	0.000
20.5250	24.6300	17910	0	2.5	0.000	39.375	46.700	0.000
20.5250	28.7350	20895	0	3.0	0.000	40.816	49.001	0.000
22.9880	28.7350	26250	0	3.0	0.000	44.385	51.748	0.000

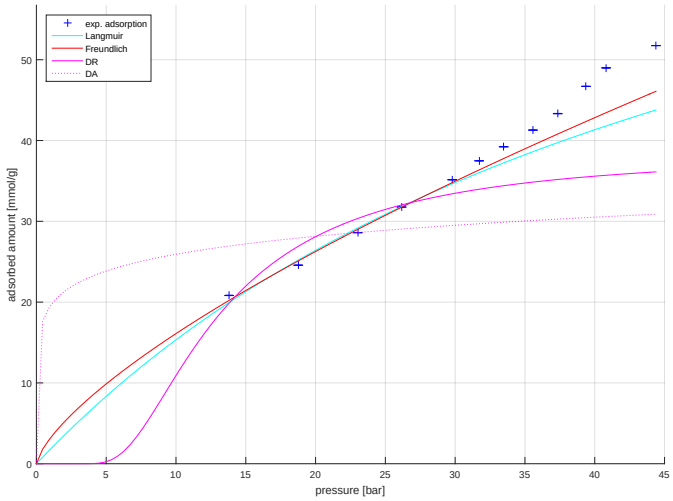

Figure D.8.: CNT(80/80) and SO_2 at $400\,\mathrm{K}$ data (marks) and fits (lines) adsorption branch

Table D.11.: Model fit parameter for CNT data and SO_2 - Langmuir model

Adsorption T [K]	k_L	k_L min	k_L max	q_max	q_max min	q_max max
CNT(11/11)						
300						
350	0.0601	0.0452	0.0751	69.2011	57.2401	81.1621
400	0.0154	0.0071	0.0237	97.2555	58.1604	136.3505
CNT(20/20)						
300						
350	0.1531	-0.2428	0.5491	48.5239	-9.4686	106.5164
400	0.0331	0.0255	0.0408	68.6173	58.7487	78.4860
400[a]	0.0698	-0.0243	0.1640	65.5341	29.0090	102.0593
CNT(30/30)						
400	0.0151	0.0053	0.0250	114.8621	60.3790	169.3453
CNT(40/40)						
400	0.0457	0.0259	0.0655	54.0326	41.0829	66.9822
CNT(80/80)						
400	0.0193	0.0039	0.0346	95.0106	42.8313	147.1899

[a] charged with 0.01 e

Table D.12.: Model fit parameter for CNT data and SO_2 - Freundlich model

Adsorption T [K]	K	K min	K max	n	n min	n max
CNT(11/11)						
300						
350	5.0836	3.0274	7.1397	0.7130	0.5108	0.9152
400	2.0846	1.5148	2.6543	0.7948	0.7068	0.8828
CNT(20/20)						
300						
300	9.8259	2.8986	16.7531	0.4777	0.1357	0.8198
400	3.6910	3.0763	4.3057	0.6640	0.6072	0.7207
400[a]	9.6871	-2.6623	22.0366	0.4514	0.0376	0.8652
CNT(30/30)						
400	2.6864	1.9737	3.3990	0.7632	0.6802	0.8462
CNT(40/40)						
400	4.2763	3.3854	5.1673	0.5983	0.5265	0.6702
CNT(80/80)						
400	3.1711	1.9840	4.3583	0.7057	0.5876	0.8238

[a] charged with 0.01 e

Table D.13.: Model fit parameter for CNT data and SO_2 - BET model

Adsorption T [K]	K_BET	K_BET min	K_BET max	q_max_BET	q_max_BET max	q_max_BET min
CNT(11/11)						
300						
350						
400	7.1078	0.4107	13.8049	14.8343	11.7611	17.9075
CNT(20/20)						
300						
350						
400	10.9974	4.6710	17.3238	17.1215	15.3634	18.8796
400[a]						
CNT(30/30)						
400	12.9523	1.8239	24.0807	15.8143	14.0862	17.5425
CNT(40/40)						
400	21.8086	-0.1858	43.8030	15.1811	13.6753	16.6869
CNT(80/80)						
400						

[a] charged with 0.01 e

Table D.14.: Model fit parameter for CNT data and SO_2 - DR model

Adsorption T [K]	k_DR	k_DR min	k_DR max	q_s	q_s min	q_s max
CNT(11/11)						
300						
350	16936.7825	-20273.2353	54146.8003	28.3743	6.6419	50.1067
400	71638.8263	12332.2218	130945.4308	29.8005	22.6869	36.9142
CNT(20/20)						
300						
350	13051.6176	-26378.3856	52481.6208	32.1573	8.9656	55.3491
400	41765.7822	24513.2473	59018.3172	30.5943	26.9599	34.2286
400[a]	49146.1247	11567.3707	86724.8786	45.4228	37.4429	53.4028
CNT(30/30)						
400	75078.1356	26037.0820	124119.1891	35.9684	30.2336	41.7031
CNT(40/40)						
400	35439.1274	16423.7055	54454.5493	27.9056	24.4952	31.3161
CNT(80/80)						
400	120206.0556	42661.7711	197750.3401	38.5054	30.8003	46.2105

[a] charged with 0.01 e

Table D.15.: Model fit parameter for CNT data and SO_2 - Temkin model

Adsorption T [K]	A_T	A_T min	A_T max	RTb_T	RTb_T min	RTb_T max
CNT(11/11)						
300						
350						
400						
CNT(20/20)						
300						
350						
400						
400[a]						
CNT(30/30)						
400						
CNT(40/40)						
400						
CNT(80/80)						
400						

[a] charged with 0.01 e

Table D.16.: Model fit parameter for CNT data and SO_2 - Tóth model

Adsorption T [K]	K_T	K_T min	K_T max	a_T	a_T min	a_T max	t	t min	tmax
CNT(11/11)									
300									
350									
400	3.6936	-13.8018	21.1890	10.4041	-76.1665	96.9748	2.8952	-6.2547	12.0452
CNT(20/20)									
300									
350									
400	14.8567	-46.0149	75.7282	14.8368	-27.7080	57.3815	1.4860	-0.5440	3.5160
400[a]	26283	-95825271	95877838	90.6189	-34833	35014	0.4927	-154.5377	155.5232
CNT(30/30)									
400									
CNT(40/40)									
400									
CNT(80/80)									
400									

[a] charged with 0.01 e

D.2 SWCNT and N_2

D.2.1 CNT(11/11) and N_2 at 300 K

Table D.17.: CNT(11/11) and N_2 at 300 K

sample:	CNT(11/11)
gas(es):	N_2
temperature in [K]:	300.00
# of C-atoms :	1760

boxsize x,y [nm]	boxsize z [nm]	# of molecules SO_2 [−]	# of molecules N_2 [−]	# of time steps [10^6]	y_{bulk} [−]	p [bar]	X(SO_2) [mmolg^{-1}]	X(N_2) [mmolg^{-1}]
24.0765	32.1020	0	4500	2.0	0.000	9.543	0.000	3.879
21.0270	28.0360	0	4500	2.0	0.000	14.265	0.000	5.156
19.1010	25.4680	0	4500	2.0	0.000	18.902	0.000	6.812
17.7300	23.6400	0	4500	2.0	0.000	23.157	0.000	7.758
16.6830	22.2440	0	4480	2.0	0.000	27.645	0.000	8.941
15.8460	21.1280	0	4480	2.0	0.000	32.102	0.000	9.509

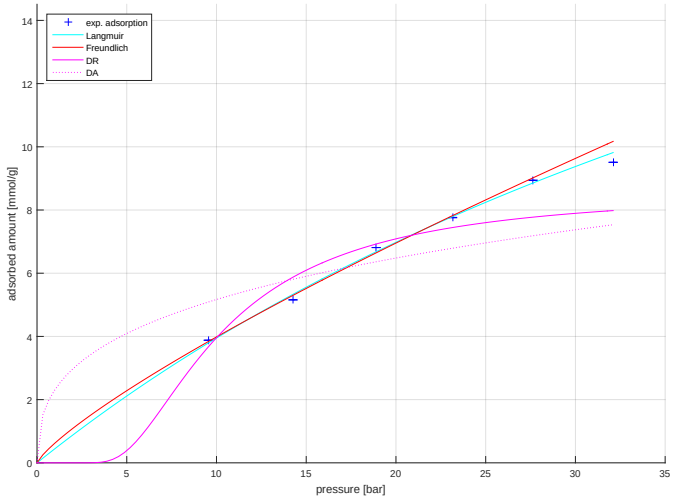

Figure D.9.: CNT(11/11) and N_2 at 300 K data (marks) and fits (lines) adsorption branch

D.2.2 CNT(11/11) and N_2 at 350 K

Table D.18.: CNT(11/11) and N_2 at 350 K

sample:	CNT(11/11)
gas(es):	N_2
temperature in [K]:	350.00
# of C-atoms :	1760

boxsize x,y [nm]	boxsize z [nm]	# of molecules SO_2 [−]	# of molecules N_2 [−]	# of time steps [10^6]	y_{bulk} [−]	p [bar]	X(SO_2) [mmolg^{-1}]	X(N_2) [mmolg^{-1}]
25.3695	33.8260	0	4500	2.0	0.000	9.661	0.000	2.413
22.1685	29.5580	0	4500	2.0	0.000	14.568	0.000	3.406
20.1480	26.8640	0	4500	2.0	0.000	19.276	0.000	4.163
18.7095	24.9460	0	4500	2.0	0.000	23.934	0.000	4.825
17.6115	23.4820	0	4500	3.0	0.000	28.192	0.000	5.866
16.7355	22.3140	0	4480	2.0	0.000	32.742	0.000	6.386

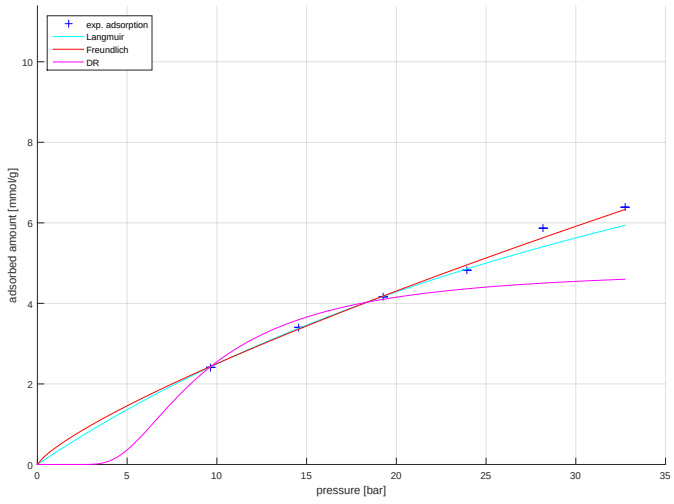

Figure D.10.: CNT(11/11) and N_2 at 350 K data (marks) and fits (lines) adsorption branch

D.2.3 CNT(11/11) and N_2 at 400 K

Table D.19.: CNT(11/11) and N_2 at 400 K

sample:		CNT(11/11)						
gas(es):		N_2						
temperature in [K]:		400.00						
# of C-atoms :		1760						
boxsize		# of molecules		# of time	y_{bulk}	p	X(SO_2)	X(N_2)
x,y	z	SO_2	N_2	steps				
[nm]	[nm]	[−]	[−]	[10^6]	[−]	[bar]	[mmolg^{-1}]	
33.4200	44.5600	0	4500	3.0	0.000	4.956	0.000	1.041
26.5380	35.3840	0	4500	2.0	0.000	9.870	0.000	1.703
23.1945	30.9260	0	4500	3.5	0.000	14.855	0.000	2.507
21.0840	28.1120	0	4500	3.0	0.000	19.252	0.000	3.170
19.5840	26.1120	0	4500	3.0	0.000	24.099	0.000	3.737
18.4395	24.5860	0	4500	3.0	0.000	28.384	0.000	4.778
17.5245	23.3660	0	4500	2.0	0.000	33.837	0.000	4.541
17.5245	23.3660	0	4500	4.0	0.000	33.044	0.000	4.778

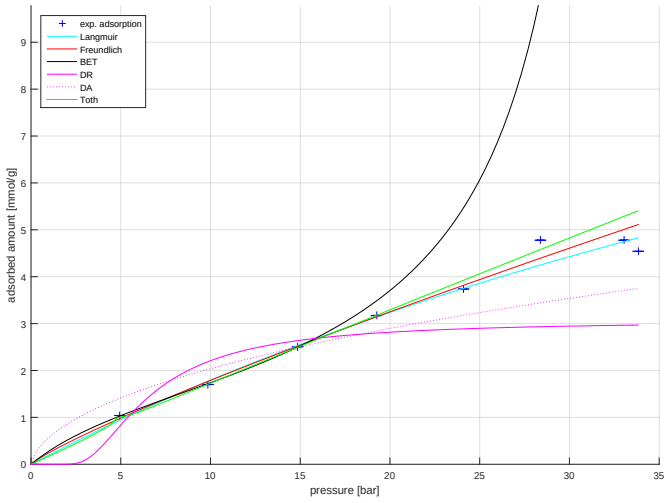

Figure D.11.: CNT(11/11) and N_2 at 400 K data (marks) and fits (lines) adsorption branch

D.2.4 CNT(20/20) and N_2 at 300 K

Table D.20.: CNT(20/20) and N_2 at 300 K

sample:			CNT(20/20)					
gas(es):			N_2					
temperature in [K]:			300.00					
# of C-atoms :			2640					
boxsize		# of molecules		# of time	y_{bulk}	p	X(SO_2)	X(N_2)
x,y [nm]	z [nm]	SO_2 [−]	N_2 [−]	steps [10^6]	[−]	[bar]	[mmolg^{-1}]	
24.0765	32.1020	0	4420	2.0	0.000	9.326	0.000	3.438
21.0270	28.0360	0	4420	3.0	0.000	13.926	0.000	5.582
19.1010	25.4680	0	4420	2.0	0.000	18.455	0.000	6.591
17.7300	23.6400	0	4380	2.0	0.000	22.595	0.000	7.821
16.6830	22.2440	0	4340	2.0	0.000	26.030	0.000	8.641
15.8460	21.1280	0	4400	2.0	0.000	30.573	0.000	9.934

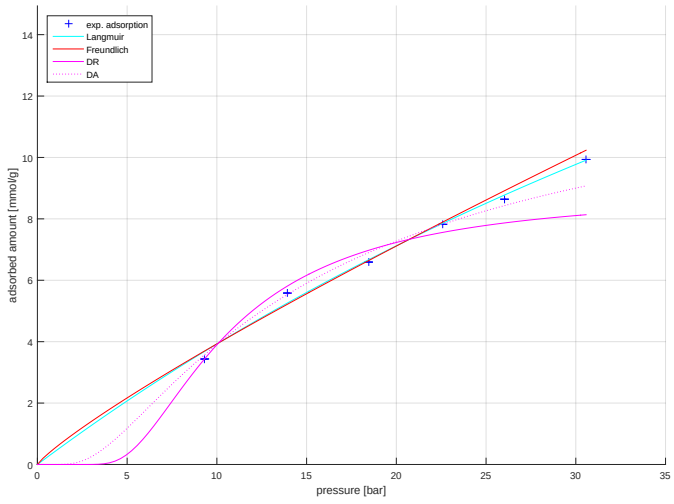

Figure D.12.: CNT(20/20) and N_2 at 300 K data (marks) and fits (lines) adsorption branch

D.2.5 CNT(20/20) and N_2 at 350 K

Table D.21.: CNT(20/20) and N_2 at 350 K

sample:		CNT(20/20)						
gas(es):		N_2						
temperature in [K]:		350.00						
# of C-atoms :		2640						
boxsize		# of molecules		# of time	y_{bulk}	p	X(SO_2)	X(N_2)
x,y [nm]	z [nm]	SO_2 [−]	N_2 [−]	steps [10^6]	[−]	[bar]	[mmolg^{-1}]	
25.3695	33.8260	0	4480	2.0	0.000	9.900	0.000	2.239
22.1685	29.5580	0	4420	3.0	0.000	14.351	0.000	3.501
20.1480	26.8640	0	4420	2.0	0.000	18.513	0.000	3.974
18.7095	24.9460	0	4420	2.0	0.000	23.112	0.000	5.014
17.6115	23.4820	0	4380	2.0	0.000	27.608	0.000	5.614
16.7355	22.3140	0	4340	2.0	0.000	31.116	0.000	6.875

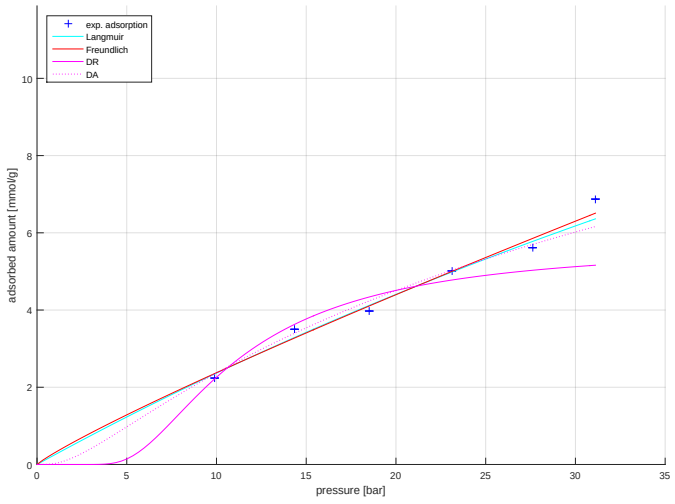

Figure D.13.: CNT(20/20) and N_2 at 350 K data (marks) and fits (lines) adsorption branch

D.2.6 CNT(20/20) and N_2 at 400 K

Table D.22.: CNT(20/20) and N_2 at 400 K

sample:	CNT(20/20)
gas(es):	N_2
temperature in [K]:	400.00
# of C-atoms :	2640

boxsize x,y [nm]	boxsize z [nm]	# of molecules SO_2 [−]	# of molecules N_2 [−]	# of time steps [10^6]	y_{bulk} [−]	p [bar]	X(SO_2) [mmolg^{-1}]	X(N_2) [mmolg^{-1}]
26.5380	35.3840	0	4500	3.0	0.000	9.930	0.000	1.640
23.1945	30.9260	0	4420	3.4	0.000	14.306	0.000	2.081
21.0840	28.1112	0	4420	3.0	0.000	18.814	0.000	2.933
19.5840	26.1120	0	4420	3.0	0.000	23.402	0.000	3.501
18.4395	24.5860	0	4420	3.0	0.000	27.947	0.000	4.005
17.5260	23.3680	0	4380	2.0	0.000	32.152	0.000	4.668

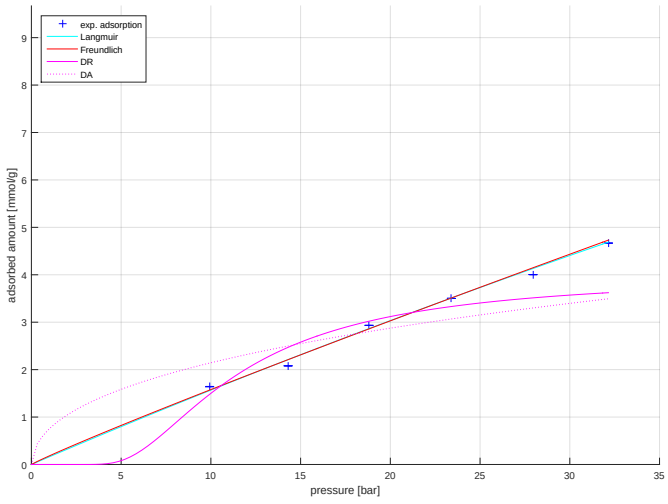

Figure D.14.: CNT(20/20) and N_2 at 400 K data (marks) and fits (lines) adsorption branch

Table D.23.: Model fit parameter for CNT data and N_2 - Langmuir model

Adsorption T [K]	k_L	k_L min	k_L max	q_max	q_max min	q_max max
CNT(11/11)						
300	0.0152	-0.0060	0.0364	29.9833	-2.7461	62.7126
350	0.0199	-0.0091	0.0490	15.0440	-1.6486	31.7366
400	0.0121	-0.0168	0.0409	16.6400	-16.8142	50.0942
CNT(20/20)						
300	0.0114	-0.0230	0.0459	38.2297	-56.8415	133.3010
350	0.0081	-0.0250	0.0412	31.6910	-81.2957	144.6778
400	0.0035	-0.0213	0.0283	46.0624	-257.7418	349.8667

Table D.24.: Model fit parameter for CNT data and N_2 - Freundlich model

Adsorption T [K]	K	K min	K max	n	n min	n max
CNT(11/11)						
300	0.6260	0.2422	1.0097	0.8037	0.5934	1.0140
350	0.4137	-0.1281	0.9556	0.7820	0.3077	1.2563
400	0.2463	0.1186	0.3741	0.8612	0.6713	1.0510
CNT(20/20)						
300	0.5458	-0.1210	1.2126	0.8571	0.4356	1.2786
350	0.3079	-0.0796	0.6955	0.8875	0.4564	1.3187
400	0.1815	-0.0104	0.3735	0.9395	0.5797	1.2994

Table D.25.: Model fit parameter for CNT data and N_2 - BET model

Adsorption T [K]	K_BET	K_BET min	K_BET max	q_max_BET	q_max_BET max	q_max_BET min
CNT(11/11)						
300						
350						
400	6.3536	0.3886	12.3186	1.6902	1.2912	2.0891
CNT(20/20)						
300						
350						
400						

Table D.26.: Model fit parameter for CNT data and N_2 - DR model

Adsorption T [K]	k_DR	k_DR min	k_DR max	q_s	q_s min	q_s max
CNT(11/11)						
300	132061.0820	2500.9612	261621.2027	8.6063	5.5863	11.6263
350	81141.4897	-83541.6920	245824.6714	4.8876	1.1997	8.5755
400	30892.8591	-30551.3278	92337.0461	3.0539	1.1694	4.9384
CNT(20/20)						
300	140034.8152	62674.3629	217395.2676	8.8838	6.9998	10.7677
350	114844.7445	22622.4422	207067.0468	5.6755	3.8511	7.5000
400	93080.3879	-15772.9662	201933.7420	3.9807	2.0596	5.9017

Table D.27.: Model fit parameter for CNT data and N_2 - Temkin model

Adsorption T [K]	A_T	A_T min	A_T max	RTb_T	RTb_T min	RTb_T max
CNT(11/11)						
300						
350						
400						
CNT(20/20)						
300						
350						
400						

Table D.28.: Model fit parameter for CNT data and N_2 - Tóth model

Adsorption T [K]	K_T	K_T min	K_T max	a_T	a_T min	a_T max	t	t min	tmax
CNT(11/11)									
300									
350									
400	0.1866	0.1217	0.2515	-4.8796	-6.1148	-3.6445	21.7144	-45.1975	88.6264
CNT(20/20)									
300									
350									
400									

D.3 SWCNT and mixtures of SO_2 and N_2

D.3.1 CNT(20/20) and 10% SO_2/N_2 mixture at 400 K

Table D.29.: CNT(20/20) and a mixture of 10% SO_2 in N_2 at 400 K

sample:		CNT(20/20)						
gas(es):		SO_2/N_2						
temperature in [K]:		400.00						
# of C-atoms :		2640						
boxsize		# of molecules		# of time	y_{bulk}	p	X(SO_2)	X(N_2)
x,y	z	SO_2	N_2	steps				
[nm]	[nm]	[−]	[−]	[10^6]	[−]	[bar]	[mmolg^{-1}]	
25.9770	34.6360	448	4032	8.0	0.085	10.317	2.491	1.451
22.4325	29.9100	446	3974	6.0	0.080	15.939	3.311	1.640
20.1225	26.8300	441	3979	5.0	0.074	21.475	4.037	2.491
18.4155	24.5540	429	3980	5.0	0.070	28.479	4.258	3.217
17.0535	22.7380	436	3904	5.0	0.070	34.046	4.636	3.879
15.8970	21.1960	439	3958	5.0	0.066	42.119	5.298	4.226
14.8635	19.8180	439	3958	3.0	0.063	51.788	5.771	4.636
13.8780	18.5040	442	3978	3.0	0.059	61.380	6.402	5.708
12.9180	17.2240	434	3961	3.0	0.052	73.500	7.096	6.371
12.4560	16.6080	439	3960	3.0	0.056	89.331	6.875	6.844
12.0540	16.0720	437	3903	3.0	0.054	83.139	7.159	7.317
11.6980	15.5980	431	3902	3.0	0.052	97.517	7.317	7.537
11.3820	15.1760	416	3877	3.0	0.048	107.542	7.348	8.200

D.3.2 CNT(20/20) and 50% SO_2/N_2 mixture at 400 K

Table D.30.: CNT(20/20) and a mixture of 50% SO_2 in N_2 at 400 K

sample:		CNT(20/20)						
gas(es):		SO_2/N_2						
temperature in [K]:		400.00						
# of C-atoms :		2640						
boxsize		# of molecules		# of time	y_{bulk}	p	X(SO_2)	X(N_2)
x,y	z	SO_2	N_2	steps				
[nm]	[nm]	[−]	[−]	[10^6]	[−]	[bar]	[mmolg^{-1}]	
25.9770	34.6360	2236	2236	4.0	0.467	10.225	9.240	0.505
22.4325	29.9100	2212	2208	2.5	0.458	14.530	11.543	0.820
20.1225	26.8300	2214	2206	2.0	0.447	19.924	14.192	0.852
18.4155	24.5540	2199	2207	2.0	0.435	25.207	16.526	0.820
17.0535	22.7380	2172	2168	3.0	0.426	30.735	18.355	0.915
15.8970	21.1960	2188	2192	2.0	0.417	37.968	20.247	1.041
14.8635	19.8180	2186	2195	2.0	0.407	46.091	22.202	0.978
13.8780	18.5040	2209	2211	1.5	0.399	53.931	23.874	0.978
13.5660	18.0880	2213	2207	1.5	0.403	59.653	23.590	1.230
12.9180	17.2240	2191	2197	1.0	0.392	63.090	25.167	1.104
12.4560	16.6080	2190	2194	1.0	0.393	75.075	25.072	1.198
12.0540	16.0720	2170	2170	1.0	0.385	80.162	26.428	1.419
11.6985	15.5980	2142	2163	1.0	0.381	86.723	26.428	1.388
11.3820	15.1760	2111	2147	1.0	0.375	92.956	26.744	1.388

D.3.3 CNT(20/20) and 80% SO_2/N_2 mixture at 400 K

Table D.31.: CNT(20/20) and a mixture of 80% SO_2 in N_2 at 400 K

sample:		CNT(20/20)						
gas(es):		SO_2/N_2						
temperature in [K]:		400.00						
# of C-atoms :		2640						
boxsize		# of molecules		# of time	y_{bulk}	p	X(SO_2)	X(N_2)
x,y	z	SO_2	N_2	steps				
[nm]	[nm]	[−]	[−]	[10^6]	[−]	[bar]	[mmolg^{-1}]	
25.9770	34.6360	3568	896	2.5	0.779	9.490	12.836	0.221
22.4325	29.9100	3539	881	2.5	0.775	13.936	16.336	0.284
20.1225	26.8300	3537	883	1.5	0.771	18.836	18.418	0.410
18.4155	24.5540	3501	885	1.5	0.762	23.703	21.603	0.473
17.0535	22.7380	3471	869	2.0	0.756	28.509	25.135	0.505
15.8970	21.1960	3485	883	1.5	0.751	34.373	26.428	0.631
14.8635	19.8180	3489	877	1.5	0.749	41.162	28.289	0.725
13.8780	18.5040	3534	886	2.5	0.743	49.208	31.285	0.788
13.5660	18.0880	3536	884	2.5	0.743	52.329	31.506	0.852
12.9180	17.2240	3500	884	2.0	0.739	58.626	32.358	0.788
12.4560	16.6080	3483	882	2.0	0.735	62.765	33.241	0.883

D.3.4 CNT(20/20) and different SO_2/N_2 mixtures at 400 K

Table D.32.: CNT(20/20) and different SO_2/N_2 mixtures at 400 K

sample:		CNT(20/20)						
gas(es):		SO_2/N_2						
temperature in [K]:		400.00						
# of C-atoms :		2640						
boxsize		# of molecules		# of time	y_{bulk}	p	X(SO_2)	X(N_2)
x,y [nm]	z [nm]	SO_2 [−]	N_2 [−]	steps [10^6]	[−]	[bar]	[mmolg^{-1}]	
14.8635	19.8180	439	3958	3.0	0.063	50.103	5.771	6.308
14.8635	19.8180	875	3518	3.5	0.137	48.002	10.660	4.951
14.8635	19.8180	1308	3077	2.0	0.218	48.916	14.949	3.974
14.8635	19.8180	1749	2636	1.5	0.309	48.178	18.733	2.807
14.8635	19.8180	2628	1752	1.5	0.514	44.306	25.104	1.514
14.8635	19.8180	3056	1316	1.5	0.631	42.961	26.113	1.135
14.8635	19.8180	3928	437	1.5	0.873	39.131	30.371	0.378
14.8635	19.8180	3928	437	10.0	0.864	40.089	36.363	0.189

D.4 Graphene and SO_2

D.4.1 Graphene and SO_2 at 300 K

Table D.33.: Graphene and SO_2 at 300 K

sample:	graphene
gas(es):	SO_2
temperature in [K]:	300.00
# of C-atoms :	5076

boxsize x,y [nm]	boxsize z [nm]	# of molecules SO_2 [−]	# of molecules N_2 [−]	# of time steps [10^6]	y_{bulk} [−]	p [bar]	X(SO_2) [mmolg^{-1}]	X(N_2) [mmolg^{-1}]
11.4210	14.1800	3200	0	3.0	1.000	4.305	50.421	0.000
11.4210	14.1800	2200	0	2.0	1.000	3.043	33.625	0.000
11.4210	14.1800	1800	0	2.0	1.000	2.199	27.966	0.000
11.4210	14.1800	1500	0	2.0	1.000	1.493	23.570	0.000
11.4210	14.1800	1200	0	2.0	1.000	0.764	19.191	0.000
11.4210	14.1800	1000	0	2.0	1.000	0.575	16.107	0.000

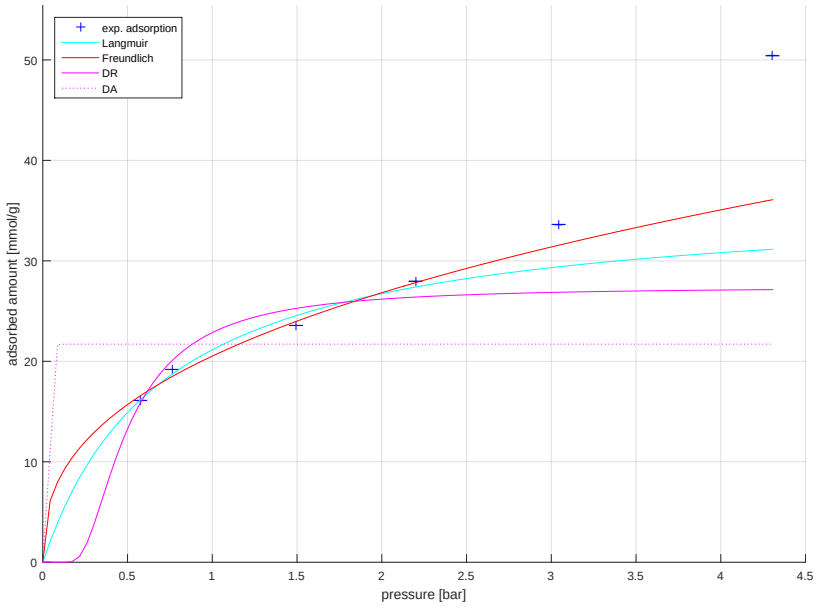

Figure D.15.: Graphene and SO_2 at 300 K fits

D.4.2 Graphene and SO_2 at 350 K

Table D.34.: Graphene and SO_2 at 350 K

sample:		graphene						
gas(es):		SO_2						
temperature in [K]:		350.00						
# of C-atoms :		5076						
boxsize		# of molecules		# of time	y_{bulk}	p	X(SO_2)	X(N_2)
x,y [nm]	z [nm]	SO_2 [−]	N_2 [−]	steps [10^6]	[−]	[bar]	[mmolg^{-1}]	
11.4210	25.1484	1200	0	2.0	1.000	2.647	16.895	0.000
11.4210	35.9084	2200	0	2.0	1.000	6.840	24.850	0.000
11.4210	25.0848	1800	0	2.0	1.000	5.897	22.964	0.000
11.4210	30.6592	2200	0	2.0	1.000	7.308	25.867	0.000

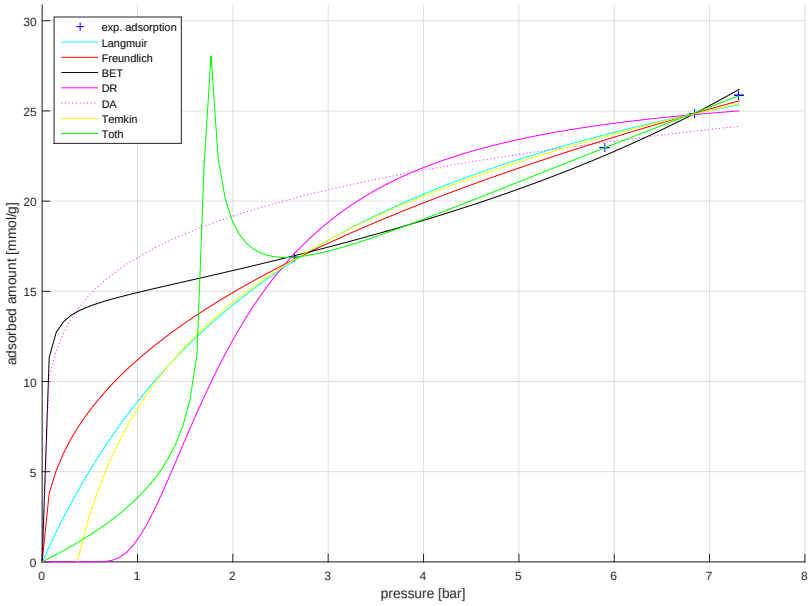

Figure D.16.: Graphene and SO_2 at 350 K fits

D.4.3 Graphene and SO_2 at 400 K

Table D.35.: Graphene and SO_2 at 400 K

sample:	graphene
gas(es):	SO_2
temperature in [K]:	400.00
# of C-atoms :	5076

boxsize x,y [nm]	boxsize z [nm]	# of molecules SO_2 [−]	# of molecules N_2 [−]	# of time steps [10^6]	y_{bulk} [−]	p [bar]	X(SO_2) [mmolg^{-1}]	X(N_2) [mmolg^{-1}]
11.4210	22.7380	2000	0	1.0	1.000	13.230	21.044	0.000
11.4210	21.1960	2420	0	1.0	1.000	17.243	24.473	0.000
11.4210	18.2380	3380	0	1.5	1.000	26.294	38.103	0.000
11.4210	36.4760	6760	0	6.0	1.000	35.910	50.684	0.000
11.4210	17.2240	3380	0	2.0	1.000	27.169	38.858	0.000
11.4210	16.6080	3920	0	6.0	1.000	28.804	39.399	0.000
11.4210	16.0720	3920	0	1.0	1.000	33.031	45.648	0.000
11.4210	15.1760	4500	0	2.0	1.000	35.421	53.505	0.000

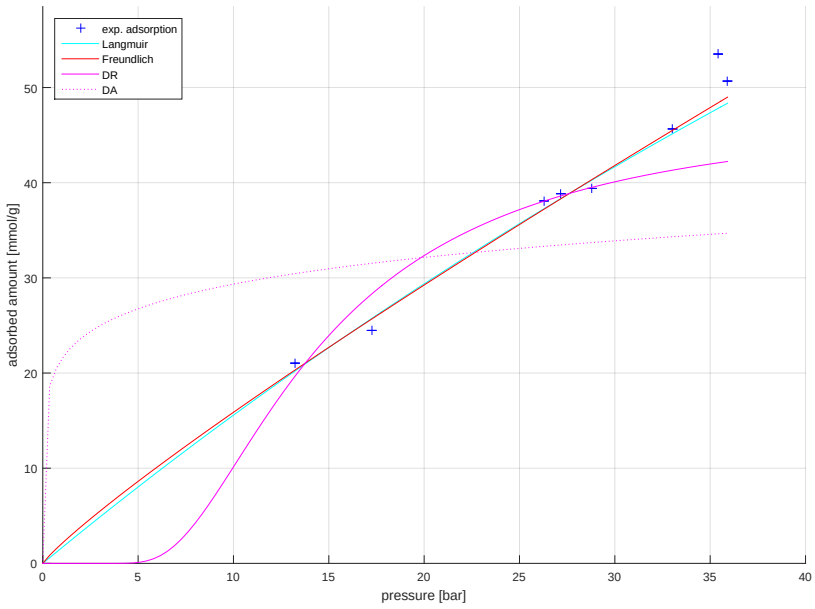

Figure D.17.: Graphene and SO_2 at 400 K fits

D.4.4 Charge variation graphene and SO_2 at 400 K

Table D.36.: Graphene with different charges and SO_2 at 400 K

sample:			graphene					
gas(es):			SO_2					
temperature in [K]:			400.00					
# of C-atoms :			5076					
boxsize		# of molecules		# of time	y_{bulk}	p	X(SO_2)	X(N_2)
x,y	z	SO_2	N_2	steps				
[nm]	[nm]	[−]	[−]	[10^6]	[−]	[bar]	[mmolg^{-1}]	
11.4210	36.4760	6760	0	3.0[a]	1.000	35.137	51.159	0.000
11.4210	36.4760	6760	0	3.0[b]	1.000	33.163	52.570	0.000
11.4210	36.4760	6760	0	4.0[c]	1.000	30.248	54.227	0.000
11.4210	36.4760	6760	0	1.5[d]	1.000	27.502	56.343	0.000
11.4210	36.4760	6760	0	2.0[e]	1.000	23.137	59.082	0.000

[a] charged with 0.002 e
[b] charged with 0.004 e
[c] charged with 0.006 e
[d] charged with 0.008 e
[e] charged with 0.010 e

Table D.37.: Model fit parameter for graphene data and SO_2 - Langmuir, Freundlich, BET and DR model

Adsorption - Langmuir model						
T [K]	k_L	k_L min	k_L max	q_max	q_max min	q_max max
300	1.3901	0.3785	2.4017	36.3563	26.5056	46.2070
350	0.3291	0.0729	0.5852	35.8768	26.0801	45.6734
400	0.0064	-0.0068	0.0197	257.4977	-198.9898	713.9852
Adsorption - Freundlich model						
T [K]	K	K min	K max	n	n min	n max
300	20.5169	18.9828	22.0510	0.3868	0.2599	0.5137
350	11.2006	9.0022	13.3991	0.4147	0.3061	0.5233
400	2.0864	0.6907	3.4822	0.8814	0.6731	1.0896
Adsorption - BET model						
T [K]	K_BET	K_BET min	K_BET max	q_max_BET	q_max_BET max	q_max_BET min
300						
350	821.3571	-18816.4431	20459.1573	14.2546	13.3130	15.1962
400						
Adsorption - DR model						
T [K]	k_DR	k_DR min	k_DR max	q_s	q_s min	q_s max
300	308.0779	22.5279	593.6278	27.4022	20.9810	33.8235
350	3823.7103	891.8529	6755.5678	26.4771	22.8005	30.1538
400	147515.8318	75745.8082	219285.8554	47.6135	39.1655	56.0616

Table D.38.: Model fit parameter for graphene data and SO_2 - Temkin and Tóth model

Adsorption - Temkin model						
T [K]	A_T	A_T min	A_T max	RTb_T	RTb_T min	RTb_T max
300						
350	2.7164	0.2011	5.2317	8.4994	5.5791	11.4196
400						

Adsorption - Tóth model									
T [K]	K_T	K_T min	K_T max	a_T	a_T min	a_T max	t	t min	tmax
300									
350	6.2426	3.4735	9.0117	-1.7120	-3.0254	-0.3987	3.0293	0.9992	5.0593
400									

D.5 Graphene and N_2

D.5.1 Graphene and N_2 at 300 K

Table D.39.: Graphene and N_2 at 300 K

sample:	graphene
gas(es):	N_2
temperature in [K]:	300.00
# of C-atoms :	5076

boxsize x,y [nm]	boxsize z [nm]	# of molecules SO_2 [−]	# of molecules N_2 [−]	# of time steps [10^6]	y_{bulk} [−]	p [bar]	X(SO_2) [mmolg^{-1}]	X(N_2) [mmolg^{-1}]
11.4210	40.4560	0	720	1.5	0.000	4.796	0.000	2.018
11.4210	32.1020	0	980	1.0	0.000	7.785	0.000	3.330
11.4210	28.0360	0	1280	1.0	0.000	11.682	0.000	4.297
11.4210	25.4680	0	1620	1.0	0.000	16.415	0.000	5.839
11.4210	23.6400	0	2000	1.0	0.000	21.687	0.000	7.299
11.4210	22.2440	0	2000	1.0	0.000	23.108	0.000	7.102
11.4210	21.1280	0	2420	1.0	0.000	29.209	0.000	8.743

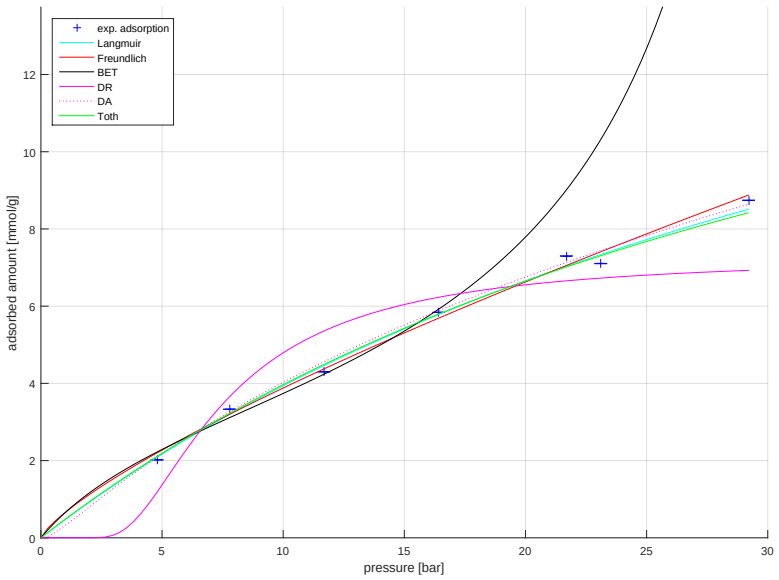

Figure D.18.: Graphene and N_2 at 300 K data (marks) and fits (lines) adsorption branch

D.5.2 Graphene and N_2 at 350 K

Table D.40.: Graphene and N_2 at 350 K

sample:	graphene
gas(es):	N_2
temperature in [K]:	350.00
# of C-atoms :	5076

boxsize x,y [nm]	boxsize z [nm]	# of molecules SO_2 [−]	# of molecules N_2 [−]	# of time steps [10^6]	y_{bulk} [−]	p [bar]	X(SO_2) [mmolg^{-1}]	X(N_2) [mmolg^{-1}]
11.4210	42.6100	0	500	1.0	0.000	3.990	0.000	0.837
11.4210	29.5580	0	1280	1.0	0.000	14.227	0.000	3.084
11.4210	26.8640	0	1280	1.0	0.000	15.373	0.000	3.395
11.4210	24.9460	0	1620	1.0	0.000	20.958	0.000	4.560
11.4210	23.4820	0	2000	1.0	0.000	27.312	0.000	5.659
11.4210	22.3140	0	2000	1.0	0.000	28.468	0.000	5.938

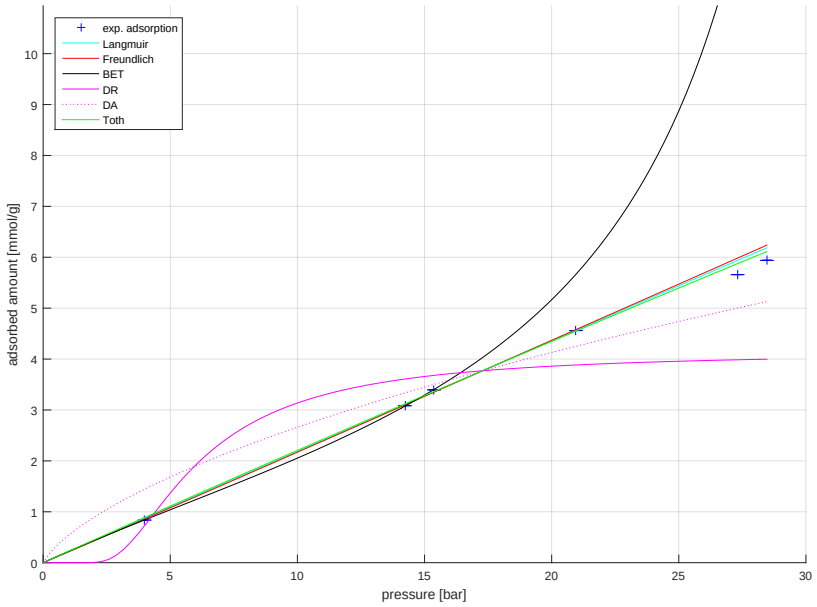

Figure D.19.: Graphene and N_2 at 350 K data (marks) and fits (lines) adsorption branch

D.5.3 Graphene and N_2 at 400 K

Table D.41.: Graphene and N_2 at 400 K

sample:	graphene
gas(es):	N_2
temperature in [K]:	400.00
# of C-atoms :	5076

boxsize x,y [nm]	boxsize z [nm]	# of molecules SO_2 [−]	# of molecules N_2 [−]	# of time steps [10^6]	y_{bulk} [−]	p [bar]	X(SO_2) [mmolg^{-1}]	X(N_2) [mmolg^{-1}]
11.4210	44.5600	0	500	1.0	0.000	4.449	0.000	0.738
11.4210	35.3840	0	720	1.0	0.000	7.880	0.000	1.230
11.4210	30.9260	0	980	1.0	0.000	12.163	0.000	2.001
11.4210	26.1120	0	1620	1.0	0.000	23.737	0.000	3.756
11.4210	24.5860	0	1620	1.0	0.000	25.066	0.000	3.543
11.4210	23.3660	0	2000	1.0	0.000	32.948	0.000	4.576

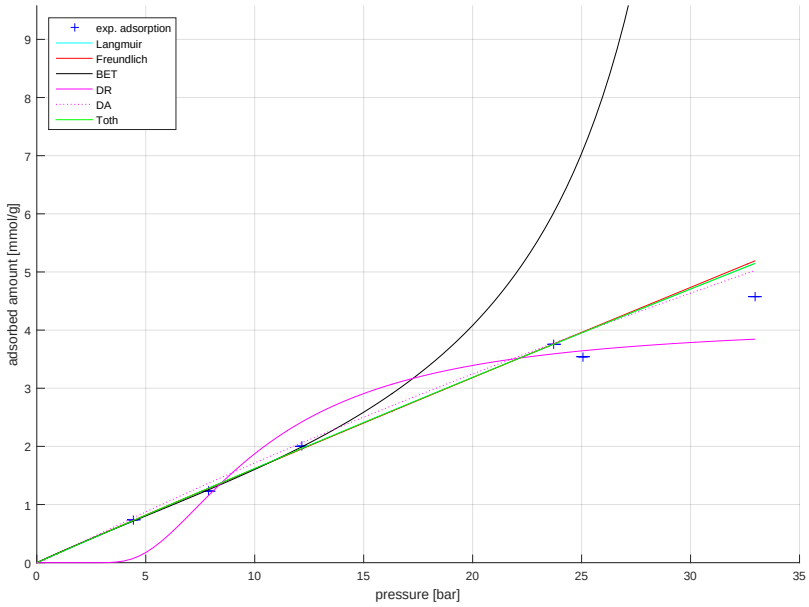

Figure D.20.: Graphene and N_2 at 400 K data (marks) and fits (lines) adsorption branch

Table D.42.: Model fit parameter for graphene data and N_2 - Langmuir, Freundlich, BET and DR model

Adsorption - Langmuir model						
T [K]	k_L	k_L min	k_L max	q_max	q_max min	q_max max
300	0.0224	0.0069	0.0378	21.5388	10.9249	32.1526
350	0.0003	-0.0075	0.0081	653.5247	-14445.8415	15752.8909
400	0.0016	-0.0057	0.0089	101.3020	-339.4625	542.0665
Adsorption - Freundlich model						
T [K]	K	K min	K max	n	n min	n max
300	0.6557	0.3991	0.9123	0.7721	0.6370	0.9073
350	0.2124	0.1518	0.2730	1.0094	0.9095	1.1092
400	0.1693	0.1172	0.2214	0.9793	0.8747	1.0840
Adsorption - BET model						
T [K]	K_BET	K_BET min	K_BET max	q_max_BET	q_max_BET max	q_max_BET min
300	7.2482	-1.5033	15.9998	3.5098	2.5656	4.4541
350	2.9528	1.5446	4.3610	2.6252	2.2174	3.0329
400	2.8187	-1.7932	7.4306	2.0927	0.4993	3.6862
Adsorption - DR model						
T [K]	k_DR	k_DR min	k_DR max	q_s	q_s min	q_s max
300	70977.0659	16139.7125	125814.4193	7.2739	5.5811	8.9667
350	34484.7955	-47266.0099	116235.6008	4.1362	1.9774	6.2951
400	75476.8535	-55310.9635	206264.6705	4.1345	0.8103	7.4586

Table D.43.: Model fit parameter for graphene data and N_2 - Temkin and Tóth model

Adsorption - Temkin model									
T [K]	A_T	A_T min	A_T max	RTb_T	RTb_T min	RTb_T max			
300									
350									
400									
Adsorption - Tóth model									
T [K]	K_T	K_T min	K_T max	a_T	a_T min	a_T max	t	t min	tmax
300	55.6119	-6014.9928	6126.2166	52.6961	-1135.1709	1240.5631	0.8372	-13.8172	15.4916
350	0.9623	-2732.3847	2734.3093	176.6665	-309773	310126	3.5496	-5713.4328	5720.5320
400	0.6428	-1702.6198	1703.9053	149.6508	-264366	264666	3.6806	-5870.4783	5877.8395

D.6 Heat of adsorption

Here the parameters for the fits of the Virial-type thermal equation are given for the different CNT types and graphene which were simulated. In the tables also the fitting values for the 95 % confidence interval are given.

Table D.44.: Fit parameters for Virial-type thermal equation for different simulated CNT types and graphene and SO_2

Adsorption type	fit				min. 95% confidence intervall				max. 95% confidence intervall			
	a_0	a_1	a_2	b_0	a_0	a_1	a_2	b_0	a_0	a_1	a_2	b_0
CNT(11/11)	-2363.627	10.497	-0.149	5.360	-2551.071	5.808	-0.215	4.920	-2176.183	15.186	-0.083	5.801
CNT(20/20)	-2613.406	15.951	-0.168	5.443	-2818.154	9.481	-0.274	5.054	-2408.657	22.422	-0.062	5.833
graphene	-3347.835	38.140	-0.486	6.293	-3598.606	24.696	-0.678	5.752	-3097.063	51.585	-0.293	6.834

Table D.45.: Fit parameters for Virial-type thermal equation for different simulated CNT types and graphene and N_2

Adsorption type	fit				min. 95% confidence intervall				max. 95% confidence intervall			
	a_0	a_1	a_2	b_0	a_0	a_1	a_2	b_0	a_0	a_1	a_2	b_0
CNT(11/11)	-1283.577	42.846	-2.258	4.753	-1436.851	21.493	-4.081	4.407	-1130.302	64.198	-0.435	5.099
CNT(20/20)	-1165.029	5.153	0.234	4.757	-1296.579	-13.865	-1.326	4.465	-1033.478	24.170	1.795	5.050
graphene	-1177.279	1.462	1.217	4.795	-1289.212	-15.732	-0.582	4.512	-1065.345	18.657	3.015	5.079

E Experimental data

Here, the experimental data of all measurements is presented. All measured points are tabulated for each temperature measured. Besides the sample and gas, the exact temperature is given and its deviation throughout a measurement. The measured sample mass $m_{S,meas}$ and estimated sample volume V_S (from the buoyancy measurements with He) is presented. Additionally to the pressure p and adsorbed amount X, the in situ measured fluid density ρ_{meas} and measured mass change of the sample is tabulated.

A graph of the shown data points is also included which displays the adsorption points as + and the desorption points as o. If applicable, also two graphs are included which show the isotherms gained by model fits for the adsorption branch and the desorption branch. Only the model fits which could be obtained by a fitting procedure with matlab are presented. The following model fits might be shown:

- Langmuir
- Freundlich
- BET
- Dubinin Raduskevich (DR)
- Dubinin Astakhov (DA)
- Tóth
- Temkin

Also, the parameters gained from all fits which could be obtained are summarized in a table. For the respective temperature the parameter is given and with min and max which are the 95 % percent confidence interval values for the parameter.

E.1 CNT

E.1.1 CNT and SO_2 at 25 °C

Table E.1.: CNT and SO_2 at 25 °C

sample:	CNT		
gas:	SO_2		
temperature in [°C]:	25.1	+0.0	-0.0
$m_{S,meas}$ in [mg]:	122.05		
V_S in [cm^3]:	0.055377		

p [bar]	X [$mmolg^{-1}$]	ρ_{meas} [gcm^{-3}]	Δm_{meas} [g]
0.00	0.0000	0.000000	0.000000
0.16	0.2503	0.000385	0.001957
0.36	0.5544	0.000934	0.004335
0.74	1.1632	0.001922	0.009095
1.14	1.6519	0.002981	0.012917
1.56	2.0320	0.004102	0.015888
1.90	2.3320	0.005046	0.018235
2.41	2.8771	0.006492	0.022497
2.88	3.6026	0.007813	0.028169
3.09	4.1021	0.008418	0.032075
3.30	4.8153	0.009034	0.037651
3.58	6.7140	0.009836	0.052498
3.77	12.3339	0.010416	0.096441
2.94	3.8518	0.007989	0.030118
1.90	2.4073	0.005054	0.018823
1.00	1.5680	0.002602	0.012260
0.68	1.1453	0.001764	0.008955
0.44	0.7595	0.001140	0.005939
0.18	0.3718	0.000465	0.002907

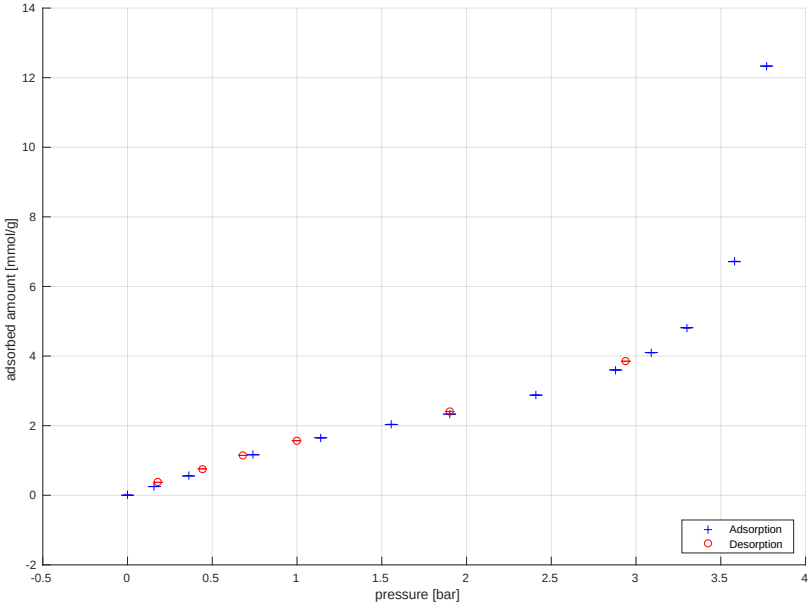

Figure E.1.: CNT and SO_2 at 25 °C

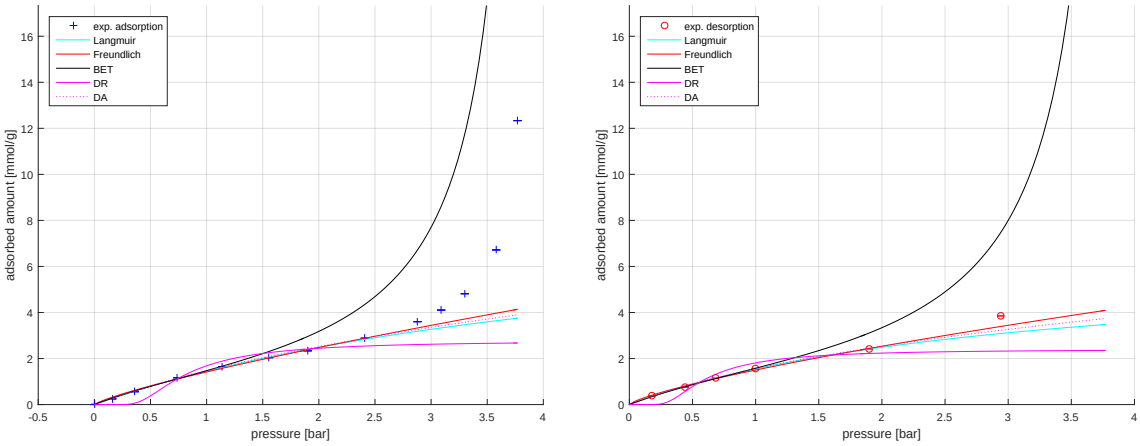

(a) adsorption **(b)** desorption

Figure E.2.: CNT and SO_2 at 25 °C data (marks) and fits (lines) adsorption branch (a) and desorption branch (b)

E.1.2 Unactivated CNT and SO_2 at 25 °C

Table E.2.: Unactivated CNT and SO_2 at 25 °C

sample:	CNT unactivated		
gas:	SO_2		
temperature in [°C]:	25.1	+0.0	-0.0
$m_{S,meas}$ in [mg]:	103.67		
V_S in [cm^3]:	0.040545		

p [bar]	X [$mmolg^{-1}$]	ρ_{meas} [gcm^{-3}]	Δm_{meas} [g]
0.00	0.0000	0.000000	0.000000
0.38	0.6101	0.000985	0.004052
0.64	1.0374	0.001675	0.006890
0.95	1.4690	0.002485	0.009757
1.56	2.0702	0.004151	0.013750
1.94	2.4073	0.005186	0.015989
2.52	3.0654	0.006834	0.020360
2.98	3.8876	0.008143	0.025821
3.41	5.4664	0.009393	0.036308
3.70	9.0949	0.010231	0.060408
3.03	4.1493	0.008278	0.027560
1.93	2.4740	0.005177	0.016432
1.00	1.6080	0.002653	0.010681

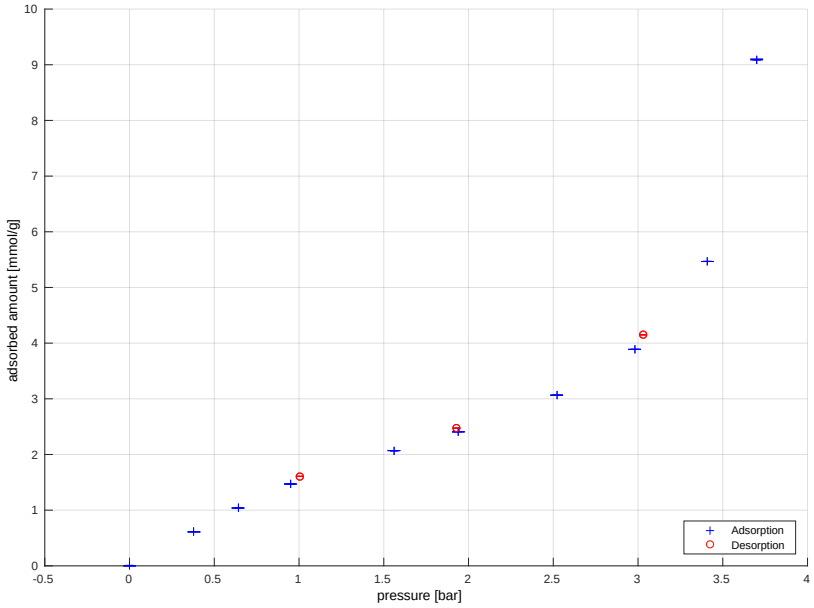

Figure E.3.: Unactivated CNT and SO_2 at 25 °C

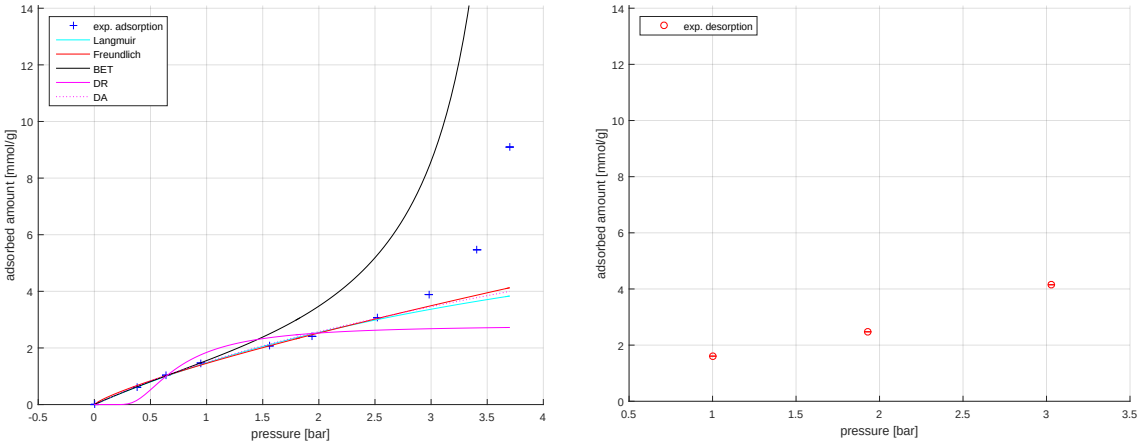

(a) adsorption **(b)** desorption

Figure E.4.: Unactivated CNT and SO_2 at 25 °C data (marks) and fits (lines) adsorption branch (a) and desorption branch (b)

E.1.3 CNT and SO_2 at 50 °C

Table E.3.: CNT and SO_2 at 50 °C

sample:	CNT		
gas:	SO_2		
temperature in [°C]:	50.0	+0.1	-0.2
$m_{S,meas}$ in [mg]:	129.13		
V_S in [cm^3]:	0.055621		

p [bar]	X [mmolg^{-1}]	ρ_{meas} [gcm^{-3}]	Δm_{meas} [g]
0.00	0.0000	0.000000	0.000000
0.31	0.2195	0.000751	0.001816
0.52	0.3424	0.001260	0.002832
0.94	0.6034	0.002274	0.004992
2.83	1.6273	0.006984	0.013462
4.93	2.5140	0.012545	0.020798
5.90	3.0726	0.015232	0.025419
6.90	4.0067	0.018099	0.033145
7.40	4.8550	0.019555	0.040164
7.91	6.8124	0.021085	0.056356
8.13	9.4166	0.021713	0.077899
6.52	3.6525	0.016986	0.030216
5.47	2.8452	0.013998	0.023538
3.95	2.1381	0.009918	0.017687
1.94	1.2729	0.004730	0.010530
0.96	0.6698	0.002303	0.005541
0.65	0.4750	0.001547	0.003930
0.26	0.2429	0.000623	0.002010

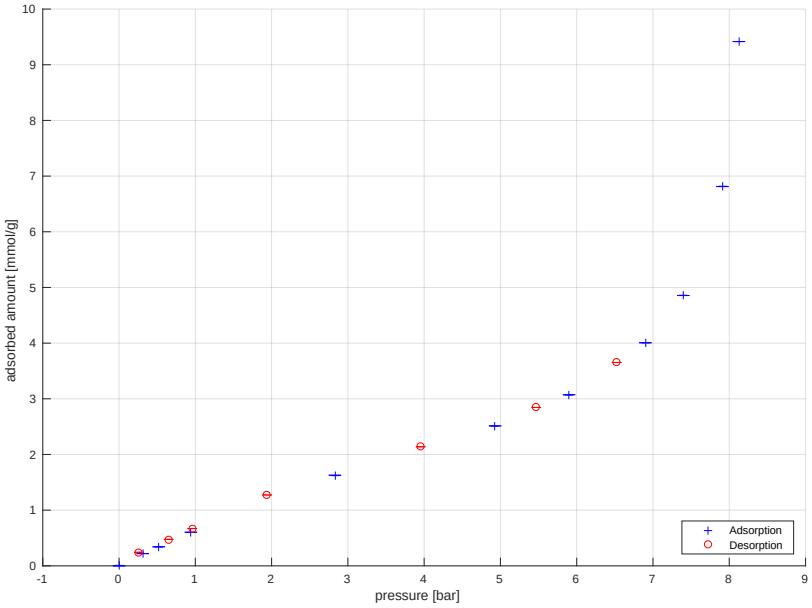

Figure E.5.: CNT and SO_2 at 50 °C

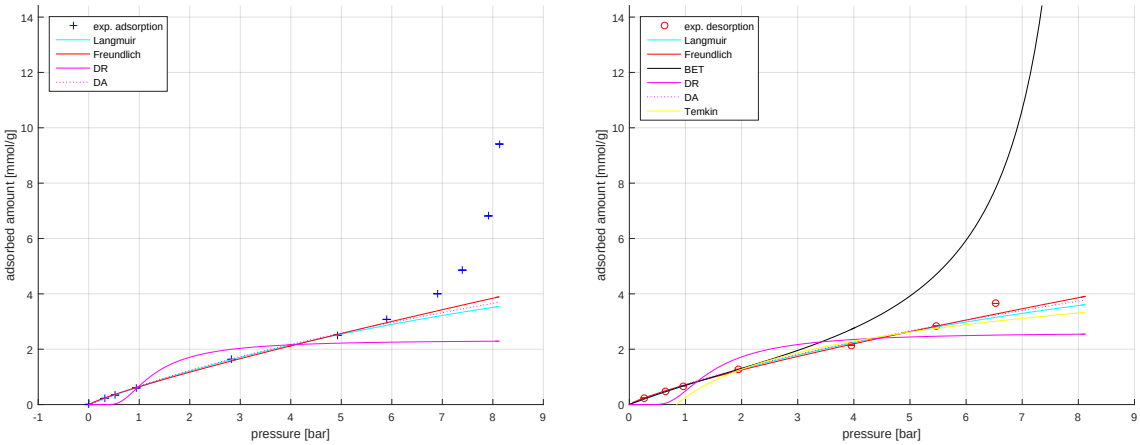

(a) adsorption **(b)** desorption

Figure E.6.: CNT and SO_2 at 50 °C data (marks) and fits (lines) adsorption branch (a) and desorption branch (b)

E.1.4 CNT and SO_2 at 75 °C

Table E.4.: CNT and SO_2 at 75 °C

sample:	CNT		
gas:	SO_2		
temperature in [°C]:	74.9	+0.5	-0.1
$m_{S,meas}$ in [mg]:	148.32		
V_S in [cm^3]:	0.063229		

p [bar]	X [$mmolg^{-1}$]	ρ_{meas} [gcm^{-3}]	Δm_{meas} [g]
0.00	0.0000	0.000000	0.000000
0.46	0.1919	0.001033	0.001824
1.13	0.4185	0.002531	0.003976
2.13	0.7570	0.004807	0.007193
3.40	1.1556	0.007775	0.010979
5.05	1.5788	0.011745	0.015001
7.14	2.0263	0.016980	0.019253
9.99	2.6937	0.024561	0.025593
12.33	3.4960	0.031221	0.033216
15.69	9.1588	0.041772	0.087020
12.48	3.6009	0.031680	0.034213
9.92	2.6972	0.024358	0.025627
7.25	2.0821	0.017265	0.019783
4.87	1.5777	0.011312	0.014990
0.76	0.3481	0.001688	0.003308
0.77	0.3465	0.001716	0.003292
0.77	0.3463	0.001712	0.003291
0.77	0.3462	0.001720	0.003289
0.77	0.3462	0.001716	0.003289
0.43	0.2346	0.000949	0.002229

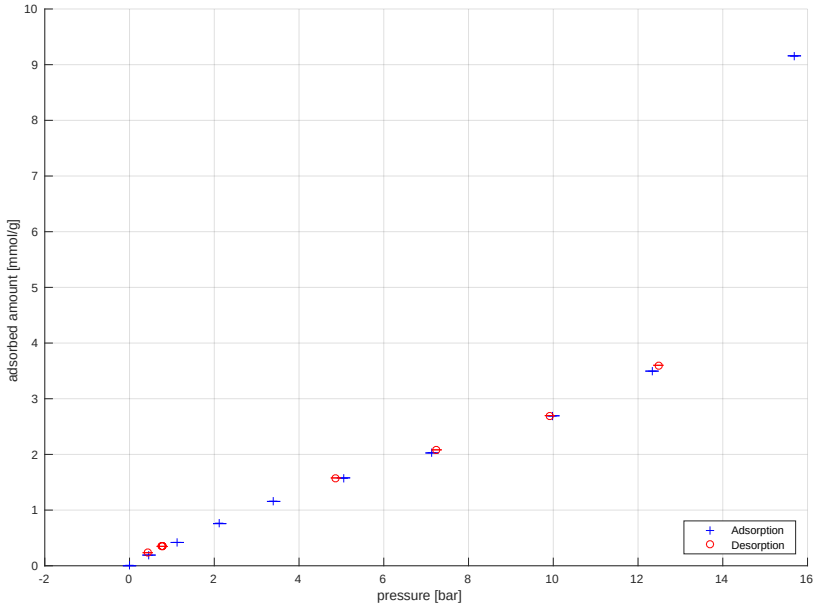

Figure E.7.: CNT and SO_2 at 75 °C

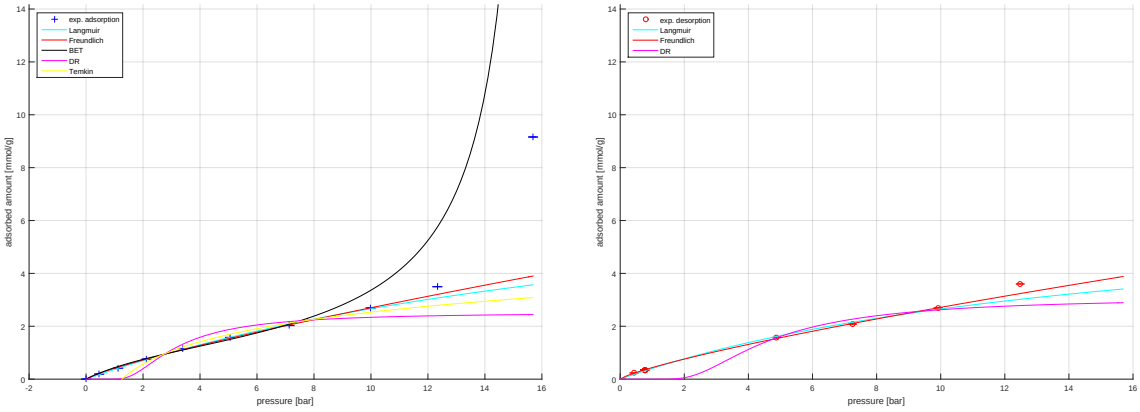

(a) adsorption **(b)** desorption

Figure E.8.: CNT and SO_2 at 75 °C data (marks) and fits (lines) adsorption branch (a) and desorption branch (b)

E.1.5 CNT and SO_2 at 100 °C

Table E.5.: CNT and SO_2 at 100 °C

sample:	CNT		
gas:	SO_2		
temperature in [°C]:	99.9	+0.8	-0.3
$m_{S,meas}$ in [mg]:	95.68		
V_S in [cm^3]:	0.043238		

p [bar]	X [mmolg^{-1}]	ρ_{meas} [gcm^{-3}]	Δm_{meas} [g]
0.00	0.0000	0.000000	0.000000
0.55	0.1298	0.001158	0.000796
1.07	0.2311	0.002255	0.001417
2.05	0.4190	0.004337	0.002569
3.06	0.6070	0.006479	0.003721
5.13	0.9795	0.010995	0.006004
7.50	1.3347	0.016391	0.008181
10.01	1.6583	0.022338	0.010165
14.95	2.2611	0.034970	0.013860
19.95	3.0401	0.049276	0.018635
24.83	4.5932	0.065448	0.028155
27.44	9.1512	0.075416	0.056094
22.01	3.5447	0.055780	0.021728
17.20	2.6316	0.041218	0.016131
12.36	2.0006	0.028184	0.012263
7.47	1.3931	0.016286	0.008539
4.03	0.8585	0.008536	0.005262
2.57	0.5979	0.005375	0.003665
1.55	0.4080	0.003207	0.002501
1.03	0.3145	0.002134	0.001928
0.56	0.2230	0.001158	0.001367

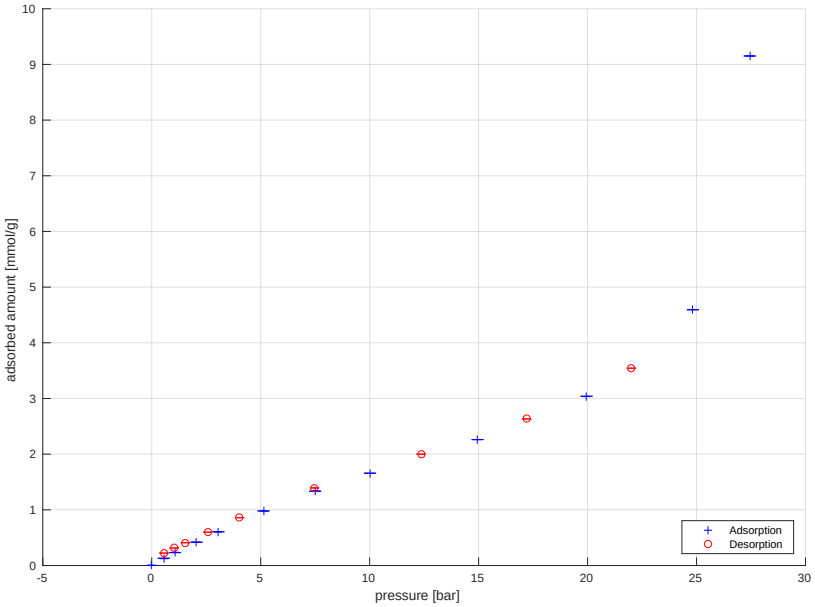

Figure E.9.: CNT and SO_2 at 100 °C

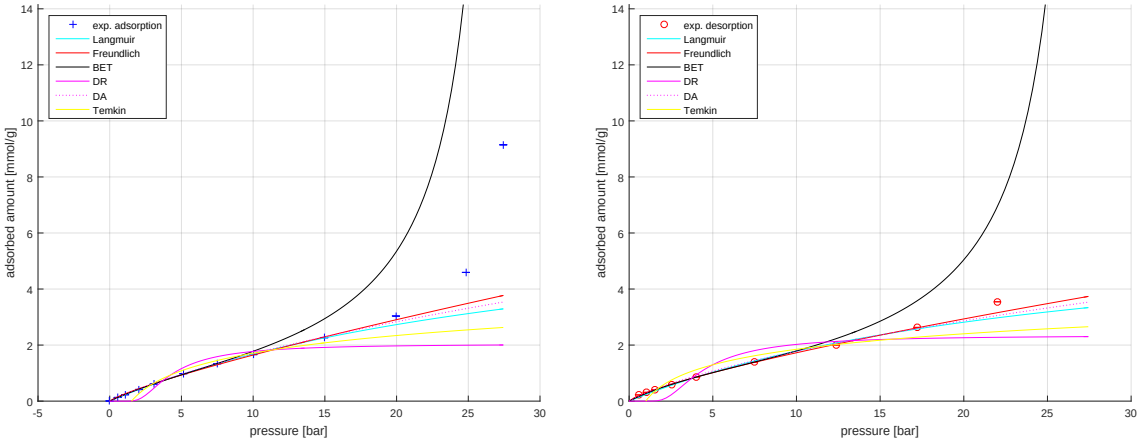

(a) adsorption **(b)** desorption

Figure E.10.: CNT and SO_2 at 100 °C data (marks) and fits (lines) adsorption branch (a) and desorption branch (b)

E.1.6 CNT and SO_2 at 125 °C

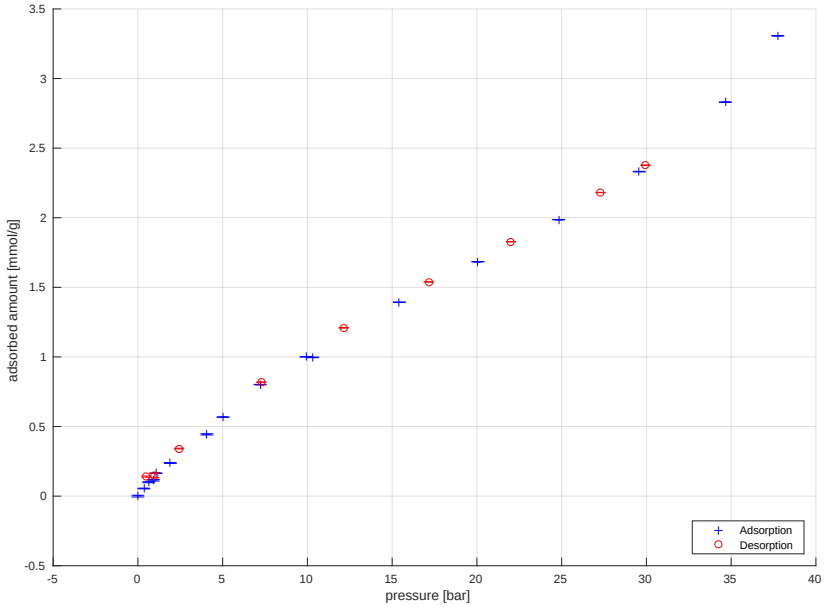

Figure E.11.: CNT and SO_2 at 125 °C

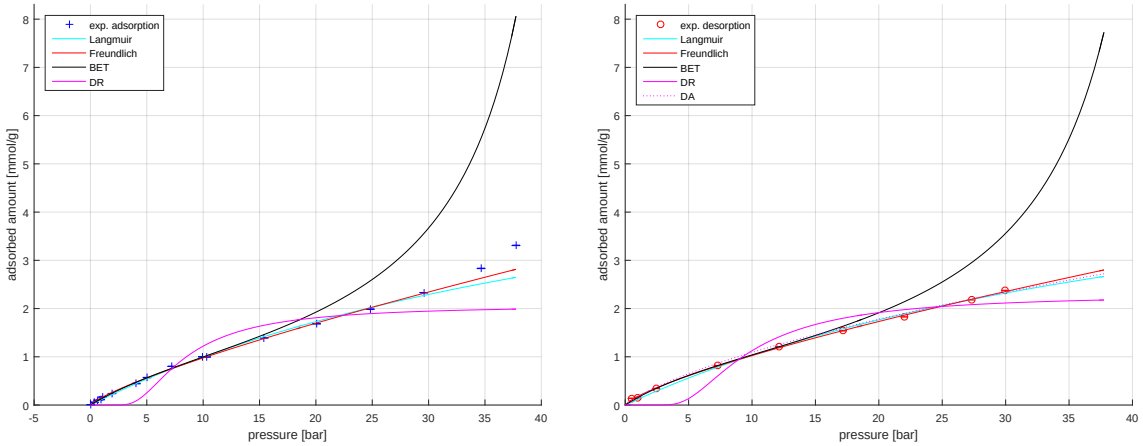

(a) adsorption **(b)** desorption

Figure E.12.: CNT and SO_2 at 125 °C data (marks) and fits (lines) adsorption branch (a) and desorption branch (b)

Table E.6.: CNT and SO_2 at 125 °C

sample:	CNT		
gas:	SO_2		
temperature in [°C]:	124.7	+0.2	-0.1
$m_{S,meas}$ in [mg]:	121.80		
V_S in [cm^3]:	0.017812		

p [bar]	X [$mmolg^{-1}$]	ρ_{meas} [gcm^{-3}]	Δm_{meas} [g]
0.00	0.0000	0.000000	0.000000
0.35	0.0543	0.000668	0.000424
0.64	0.0999	0.001165	0.000780
0.91	0.1135	0.001380	0.000886
1.91	0.2380	0.003618	0.001858
4.07	0.4438	0.007686	0.003466
7.21	0.8013	0.014771	0.006258
10.31	0.9966	0.021254	0.007783
1.06	0.1647	0.002084	0.001286
5.02	0.5677	0.010010	0.004433
9.92	1.0007	0.020409	0.007815
15.42	1.3933	0.032933	0.010881
20.06	1.6840	0.044462	0.013151
24.82	1.9863	0.057253	0.015512
29.57	2.3312	0.071445	0.018205
34.65	2.8303	0.088650	0.022102
37.75	3.3071	0.100664	0.025826
29.95	2.3771	0.072525	0.018563
27.30	2.1809	0.064411	0.017031
22.01	1.8278	0.049501	0.014274
17.16	1.5389	0.037139	0.012018
12.14	1.2091	0.025334	0.009443
7.28	0.8187	0.014702	0.006393
2.42	0.3418	0.004772	0.002669
0.99	0.1481	0.001378	0.001156
0.50	0.1405	0.000937	0.001098

Table E.7.: Model fit parameter for CNT data and SO_2 - Langmuir model

Adsorption						
T [°C]	k_L	k_L min	k_L max	q_max	q_max min	q_max max
25	0.1959	0.1247	0.2670	8.8349	6.4499	11.2199
25[a]	0.2145	0.1258	0.3033	8.0466	5.4895	10.6038
50	0.0716	0.0649	0.0783	9.6446	8.9414	10.3479
75	0.0433	0.0317	0.0550	8.8147	7.0095	10.6199
100	0.0295	0.0264	0.0326	7.3600	6.7695	7.9505
125	0.0178	0.0138	0.0219	6.5782	5.4819	7.6746
Desorption						
T [°C]	k_L	k_L min	k_L max	q_max	q_max min	q_max max
25	0.3267	0.2367	0.4168	6.2987	5.0822	7.5152
25[a]						
50	0.0837	0.0361	0.1312	8.9237	5.1711	12.6763
75	0.0633	0.0389	0.0878	6.8410	5.0441	8.6380
100	0.0367	0.0188	0.0545	6.6537	4.4167	8.8907
125	0.0197	0.0110	0.0284	6.2575	4.3434	8.1716

[a] unactivated CNT

Table E.8.: Model fit parameter for CNT data and SO_2 - Freundlich model

Adsorption T [°C]	K	K min	K max	n	n min	n max
25	1.4169	1.3469	1.4869	0.8076	0.7355	0.8797
25[a]	1.3890	1.3205	1.4574	0.8283	0.7350	0.9216
50	0.6462	0.5911	0.7013	0.8574	0.7974	0.9174
75	0.4121	0.3817	0.4426	0.8165	0.7794	0.8535
100	0.2477	0.2250	0.2703	0.8222	0.7834	0.8609
125	0.1562	0.1450	0.1675	0.7962	0.7723	0.8202
Desorption						
T [°C]	K	K min	K max	n	n min	n max
25	1.5011	1.4049	1.5974	0.7560	0.6472	0.8647
25[a]						
50	0.7102	0.6546	0.7658	0.8141	0.7612	0.8669
75	0.4378	0.4183	0.4573	0.7927	0.7709	0.8145
100	0.2966	0.2786	0.3146	0.7650	0.7409	0.7890
125	0.1798	0.1605	0.1991	0.7562	0.7219	0.7904

[a] unactivated CNT

Table E.9.: Model fit parameter for CNT data and SO_2 - BET model

Adsorption						
T [°C]	K_BET	K_BET min	K_BET max	q_max_BET	q_max_BET max	q_max_BET min
25	3.7091	-9.3725	16.7907	1.9632	-1.3169	5.2432
25[a]	2.3958	2.1574	2.6342	2.4521	2.3032	2.6009
50						
75	3.4464	1.8829	5.0099	1.8910	1.3887	2.3933
100	3.9991	2.4250	5.5733	1.6447	1.3211	1.9683
125	4.6890	1.5181	7.8598	1.3553	0.9062	1.8045
Desorption						
T [°C]	K_BET	K_BET min	K_BET max	q_max_BET	q_max_BET max	q_max_BET min
25	4.0504	-3.1668	11.2677	2.0263	0.2347	3.8179
25[a]						
50	3.5575	2.3109	4.8040	1.8982	1.5243	2.2720
75	0.0000	0.0000	0.0000	0.0000	0.0000	0.0000
100	5.5946	4.6847	6.5045	1.5118	1.4018	1.6217
125	5.9039	5.6781	6.1298	1.2884	1.2688	1.3080

[a] unactivated CNT

Table E.10.: Model fit parameter for CNT data and SO_2 - DR model

Adsorption T [°C]	k_DR	k_DR min	k_DR max	q_s	q_s min	q_s max
25	35.0686	21.9832	48.1540	3.7950	2.9439	4.6462
25[a]	32.1084	23.8691	40.3476	3.3933	2.7951	3.9914
50	59.1022	24.3279	93.8765	3.2454	2.1799	4.3110
75	124.3704	75.7525	172.9883	3.5545	2.6512	4.4578
100	166.6567	107.6586	225.6548	2.9354	2.2550	3.6159
125	295.3402	224.2426	366.4377	2.9177	2.4621	3.3733
Desorption						
T [°C]	k_DR	k_DR min	k_DR max	q_s	q_s min	q_s max
25	27.3121	10.8442	43.7800	3.3044	1.9453	4.6634
25[a]	0.0000	0.0000	0.0000	0.0000	0.0000	0.0000
50	64.9965	28.7455	101.2475	3.6047	2.4292	4.7801
75	57.4790	36.0863	78.8717	2.7428	2.2611	3.2245
100	158.4400	76.6446	240.2355	3.1572	2.2187	4.0957
125	337.4704	195.5704	479.3704	3.2193	2.4315	4.0072

[a] unactivated CNT

Table E.11.: Model fit parameter for CNT data and SO_2 - Temkin model

Adsorption T [°C]	A_T	A_T min	A_T max	RTb_T	RTb_T min	RTb_T max
25						
25[a]						
50						
75	0.7945	0.4282	1.1609	1.2228	0.8337	1.6119
100	0.6593	0.3903	0.9283	0.9078	0.6601	1.1554
125						
Desorption T [°C]	**A_T**	**A_T min**	**A_T max**	**RTb_T**	**RTb_T min**	**RTb_T max**
25						
25[a]						
50	1.1918	-2.3140	4.6976	1.4675	-1.4385	4.3735
75						
100	1.0148	0.4247	1.6049	0.7981	0.5350	1.0612
125						

[a] unactivated CNT

Table E.12.: Model fit parameter for CNT data and SO_2 - Tóth model

Adsorption									
T [°C]	K_T	K_T min	K_T max	a_T	a_T min	a_T max	t	t min	tmax
25									
25[a]									
50									
75									
100									
125									
Desorption									
T [°C]	K_T	K_T min	K_T max	a_T	a_T min	a_T max	t	t min	tmax
25									
25[a]									
50									
75									
100									
125									

[a] unactivated CNT

E.1.8 CNT and N_2 at 0 °C

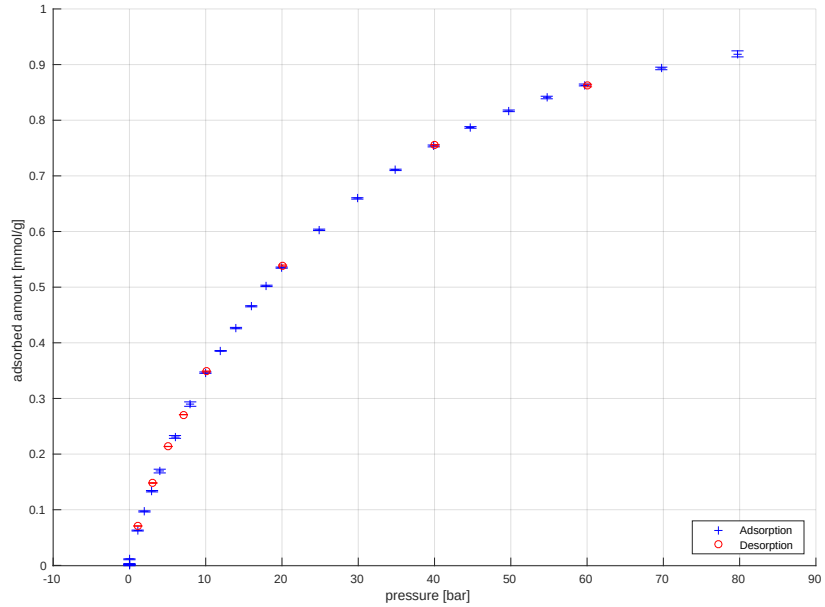

Figure E.13.: CNT and N_2 at 0 °C

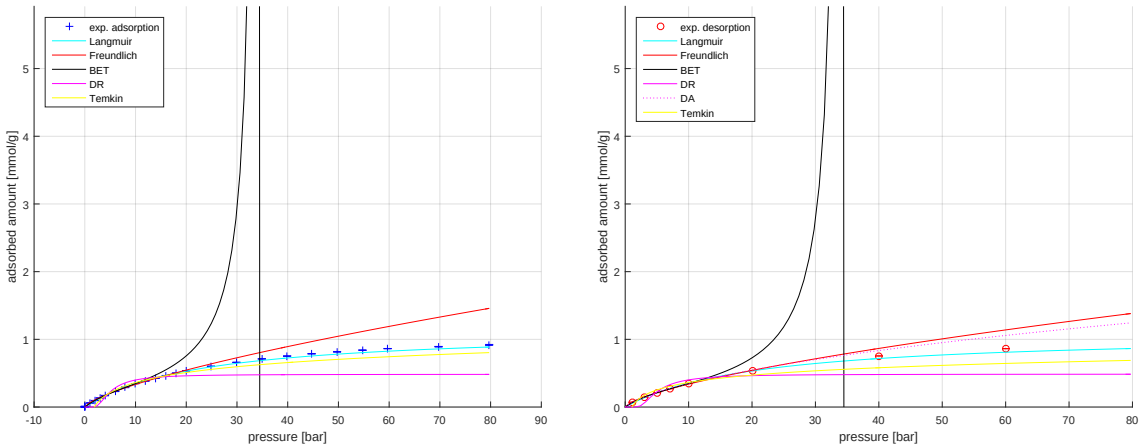

(a) adsorption **(b)** desorption

Figure E.14.: CNT and N_2 at 0 °C data (marks) and fits (lines) adsorption branch (a) and desorption branch (b)

Table E.13.: CNT and N_2 at 0 °C

sample:	CNT		
gas:	N_2		
temperature in [°C]:	1.0	+0.6	-0.1
$m_{S,meas}$ in [mg]:	170.71		
V_S in [cm^3]:	0.073773		

p [bar]	X [$mmolg^{-1}$]	ρ_{meas} [gcm^{-3}]	Δm_{meas} [g]
0.00	0.0000	0.000000	0.000000
0.00	0.0013	-0.000007	0.000006
0.00	0.0026	-0.000016	0.000013
0.00	0.0109	-0.000019	0.000052
1.08	0.0626	0.001301	0.000300
1.97	0.0970	0.002399	0.000464
2.96	0.1333	0.003622	0.000638
3.97	0.1695	0.004871	0.000812
5.97	0.2308	0.007332	0.001105
7.97	0.2898	0.009810	0.001388
9.96	0.3464	0.012295	0.001659
11.96	0.3855	0.014747	0.001846
13.97	0.4265	0.017237	0.002042
15.97	0.4656	0.019726	0.002230
17.97	0.5023	0.022215	0.002405
19.96	0.5351	0.024699	0.002562
24.87	0.6031	0.030832	0.002888
29.88	0.6595	0.037103	0.003158
34.89	0.7108	0.043393	0.003404
39.89	0.7538	0.049851	0.003610
44.71	0.7871	0.055921	0.003769
49.73	0.8169	0.062228	0.003912
54.71	0.8408	0.068494	0.004027
59.71	0.8634	0.074797	0.004135
69.73	0.8931	0.087385	0.004277
79.72	0.9193	0.099895	0.004402
60.07	0.8623	0.075186	0.004130
40.06	0.7548	0.050002	0.003615
20.08	0.5388	0.024808	0.002580
10.08	0.3485	0.012396	0.001669
7.08	0.2709	0.008692	0.001297
5.08	0.2136	0.006229	0.001023
3.08	0.1481	0.003766	0.000709
1.11	0.0708	0.001335	0.000339

E.1.9 CNT and N_2 at 25 °C

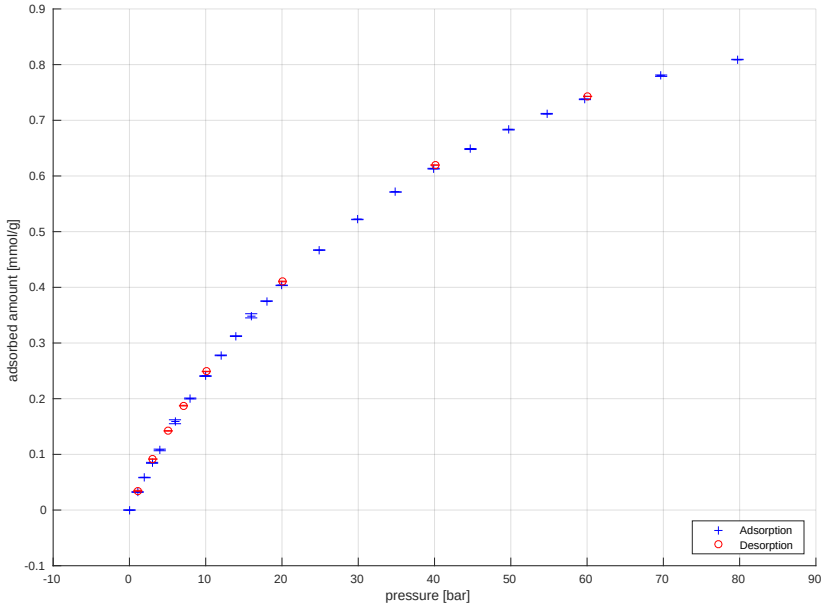

Figure E.15.: CNT and N_2 at 25 °C

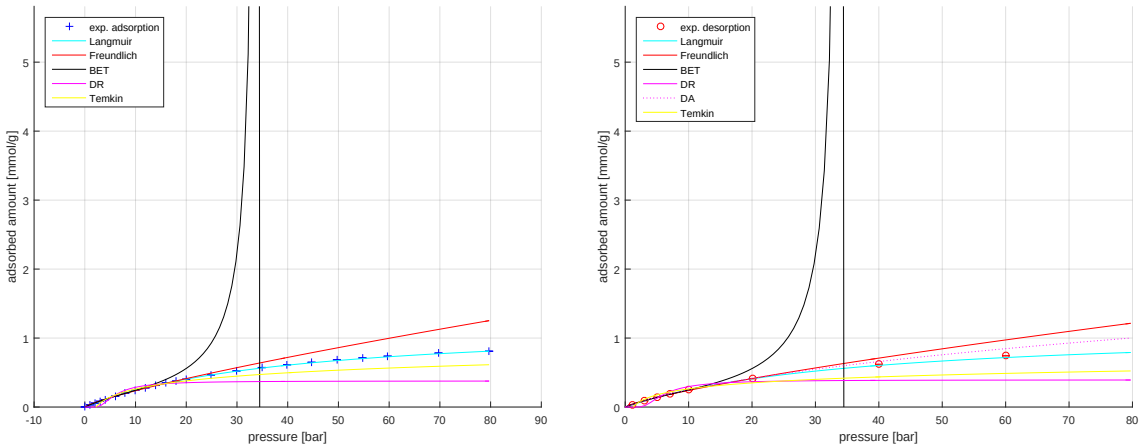

(a) adsorption **(b)** desorption

Figure E.16.: CNT and N_2 at 25 °C data (marks) and fits (lines) adsorption branch (a) and desorption branch (b)

Table E.14.: CNT and N_2 at 25 °C

sample:	CNT		
gas:	N_2		
temperature in [°C]:	25.3	+0.3	-0.0
$m_{S,meas}$ in [mg]:	171.37		
V_S in [cm^3]:	0.077599		

p [bar]	X [$mmol g^{-1}$]	ρ_{meas} [$g cm^{-3}$]	Δm_{meas} [g]
0.00	0.0000	0.000000	0.000000
1.07	0.0324	0.001178	0.000156
1.97	0.0584	0.002181	0.000280
2.97	0.0848	0.003293	0.000407
3.97	0.1079	0.004416	0.000518
5.97	0.1586	0.006665	0.000762
7.97	0.2004	0.008909	0.000962
9.97	0.2406	0.011161	0.001156
11.98	0.2778	0.013423	0.001334
13.97	0.3124	0.015673	0.001500
15.97	0.3489	0.017936	0.001676
17.98	0.3753	0.020197	0.001802
19.97	0.4035	0.022448	0.001938
24.88	0.4669	0.028005	0.002242
29.88	0.5219	0.033663	0.002507
34.89	0.5712	0.039347	0.002743
39.88	0.6131	0.045161	0.002945
44.71	0.6484	0.050626	0.003114
49.71	0.6832	0.056265	0.003281
54.71	0.7117	0.061906	0.003418
59.72	0.7377	0.067544	0.003543
69.71	0.7801	0.078770	0.003746
79.71	0.8091	0.089899	0.003886
60.07	0.7430	0.067935	0.003568
40.06	0.6196	0.045378	0.002976
20.07	0.4105	0.022624	0.001972
10.08	0.2488	0.011331	0.001195
7.08	0.1875	0.007945	0.000901
5.08	0.1421	0.005688	0.000683
3.08	0.0915	0.003435	0.000440
1.10	0.0346	0.001208	0.000166

E.1.10 CNT and N_2 at 25 °C, sample mass 64 mg

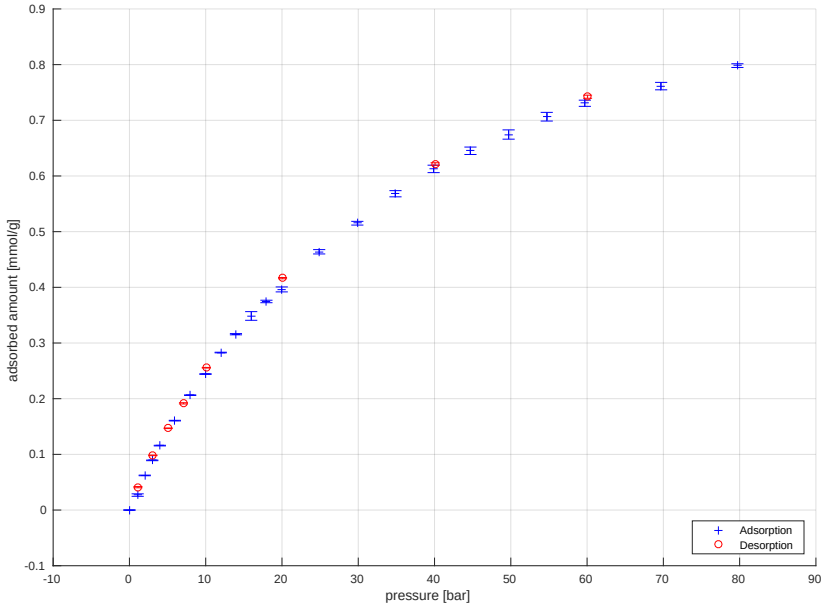

Figure E.17.: CNT and N_2 at 25 °C, sample mass 64 mg [182]

Table E.15.: CNT and N_2 at 25 °C, sample mass 64 mg[182]

sample:	CNT		
gas:	N_2		
temperature in [°C]:	25.1	+0.2	-0.1
$m_{S,meas}$ in [mg]:	64.15		
V_S in [cm^3]:	0.028356		

p [bar]	X [mmolg^{-1}]	ρ_{meas} [gcm^{-3}]	Δm_{meas} [g]
0.00	0.0000	0.000000	0.000000
1.08	0.0269	0.001209	0.000048
2.01	0.0622	0.002251	0.000112
2.99	0.0892	0.003341	0.000160
3.99	0.1158	0.004458	0.000208
5.96	0.1606	0.006664	0.000289
7.96	0.2063	0.008920	0.000371
9.97	0.2442	0.011191	0.000439
11.97	0.2829	0.013452	0.000509
13.96	0.3158	0.015714	0.000568
15.97	0.3486	0.017989	0.000627
17.96	0.3746	0.020243	0.000674
19.97	0.3963	0.022524	0.000713
24.88	0.4639	0.028109	0.000834
29.88	0.5152	0.033786	0.000926
34.88	0.5681	0.039469	0.001022
39.88	0.6127	0.045313	0.001102
44.71	0.6453	0.050801	0.001160
49.71	0.6745	0.056462	0.001213
54.71	0.7064	0.062132	0.001270
59.71	0.7306	0.067775	0.001314
69.71	0.7614	0.079026	0.001369
79.71	0.7982	0.090226	0.001435
60.07	0.7423	0.068172	0.001335
40.07	0.6215	0.045556	0.001118
20.08	0.4165	0.022726	0.000749
10.08	0.2556	0.011396	0.000460
7.08	0.1917	0.007999	0.000345
5.08	0.1469	0.005735	0.000264
3.08	0.0982	0.003474	0.000177
1.12	0.0411	0.001262	0.000074

E.1.11 CNT and N_2 at 25 °C, sample mass 20 mg

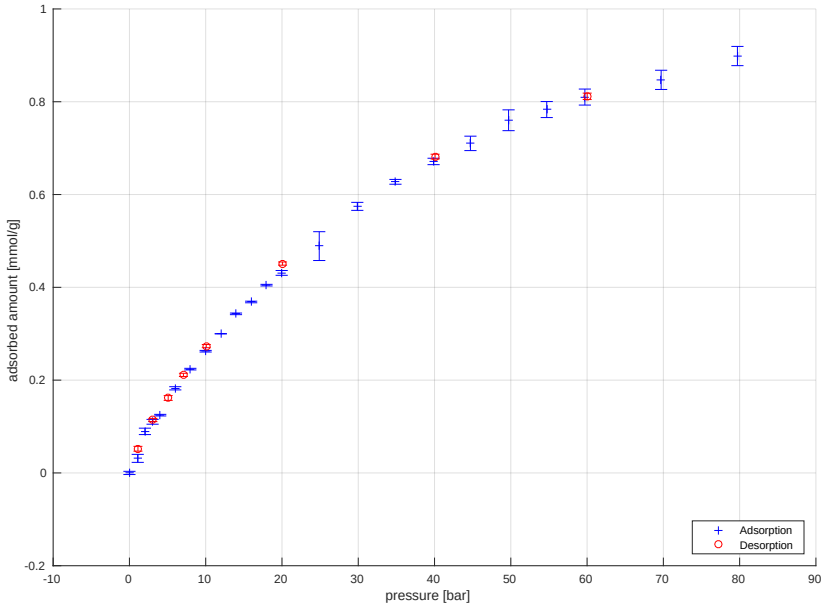

Figure E.18.: CNT and N_2 at 25 °C, sample mass 20 mg [182]

Table E.16.: CNT and N_2 at 25 °C, sample mass 20 mg[182]

sample:	CNT		
gas:	N_2		
temperature in [°C]:	25.1	+0.2	-0.0
$m_{S,meas}$ in [mg]:	20.67		
V_S in [cm^3]:	0.009423		

p [bar]	X [$mmol g^{-1}$]	ρ_{meas} [$g cm^{-3}$]	Δm_{meas} [g]
0.00	0.0000	0.000000	0.000000
1.09	0.0314	0.001207	0.000018
2.03	0.0896	0.002249	0.000052
3.04	0.1102	0.003319	0.000064
4.04	0.1245	0.004388	0.000072
6.01	0.1824	0.006552	0.000106
7.99	0.2237	0.008732	0.000130
9.99	0.2623	0.010951	0.000152
11.98	0.2999	0.013163	0.000174
13.97	0.3429	0.015392	0.000199
15.96	0.3684	0.017624	0.000213
17.97	0.4047	0.019887	0.000234
19.96	0.4311	0.022132	0.000250
24.88	0.4889	0.027718	0.000283
29.88	0.5745	0.033381	0.000333
34.88	0.6274	0.039064	0.000364
39.88	0.6713	0.044891	0.000389
44.71	0.7103	0.050362	0.000412
49.71	0.7601	0.056030	0.000440
54.71	0.7832	0.061688	0.000454
59.71	0.8101	0.067331	0.000469
69.71	0.8472	0.078576	0.000491
79.71	0.8985	0.089760	0.000521
60.01	0.8117	0.067750	0.000470
40.07	0.6817	0.045324	0.000395
20.08	0.4512	0.022612	0.000261
10.08	0.2733	0.011340	0.000158
7.08	0.2113	0.007961	0.000122
5.08	0.1615	0.005709	0.000094
3.08	0.1141	0.003456	0.000066
1.12	0.0521	0.001250	0.000030

E.1.12 CNT and N_2 at 25 °C, sample mass 6 mg

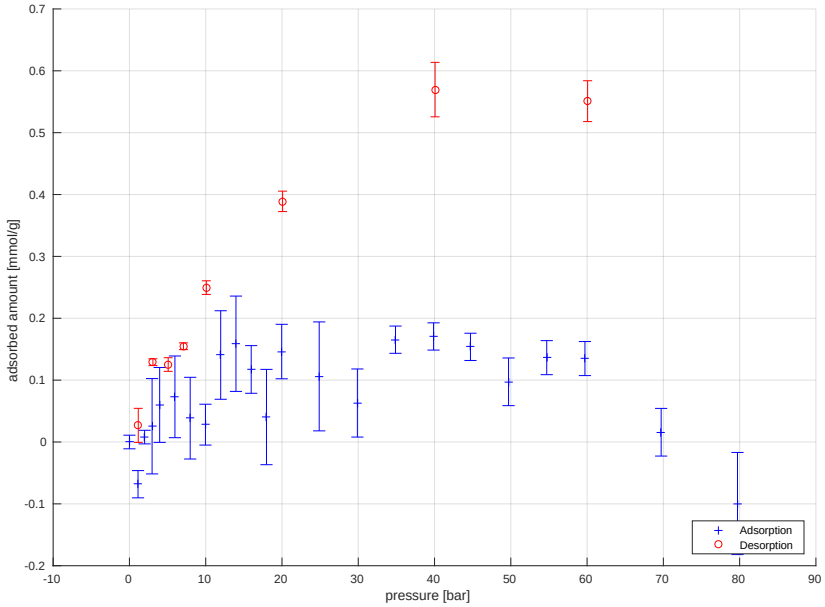

Figure E.19.: CNT and N_2 at 25 °C, sample mass 6 mg[182]

Table E.17.: CNT and N_2 at 25 °C, sample mass 6 mg[182]

sample:	CNT		
gas:	N_2		
temperature in [°C]:	25.1	+0.4	-0.1
$m_{S,meas}$ in [mg]:	6.48		
V_S in [cm^3]:	0.001345		

p [bar]	X [$mmolg^{-1}$]	ρ_{meas} [gcm^{-3}]	Δm_{meas} [g]
0.00	0.0000	0.000000	0.000000
1.13	-0.0682	0.001257	-0.000012
1.99	0.0079	0.002247	0.000001
2.97	0.0255	0.003365	0.000005
3.96	0.0599	0.004494	0.000011
5.96	0.0730	0.006758	0.000013
7.97	0.0385	0.009021	0.000007
9.96	0.0280	0.011283	0.000005
11.97	0.1406	0.013558	0.000026
13.97	0.1588	0.015825	0.000029
15.97	0.1173	0.018086	0.000021
17.97	0.0403	0.020351	0.000007
19.96	0.1462	0.022621	0.000027
24.88	0.1061	0.028206	0.000019
29.88	0.0630	0.033899	0.000011
34.88	0.1654	0.039588	0.000030
39.87	0.1706	0.045419	0.000031
44.71	0.1538	0.050908	0.000028
49.70	0.0973	0.056563	0.000018
54.71	0.1363	0.062231	0.000025
59.72	0.1349	0.067886	0.000025
69.71	0.0158	0.079129	0.000003
79.72	-0.0994	0.090328	-0.000018
60.07	0.5509	0.068302	0.000100
40.07	0.5696	0.045611	0.000104
20.08	0.3890	0.022716	0.000071
10.08	0.2496	0.011372	0.000045
7.08	0.1548	0.007975	0.000028
5.08	0.1252	0.005711	0.000023
3.08	0.1290	0.003444	0.000023
1.16	0.0269	0.001259	0.000005

E.1.13 CNT and N_2 at 40 °C

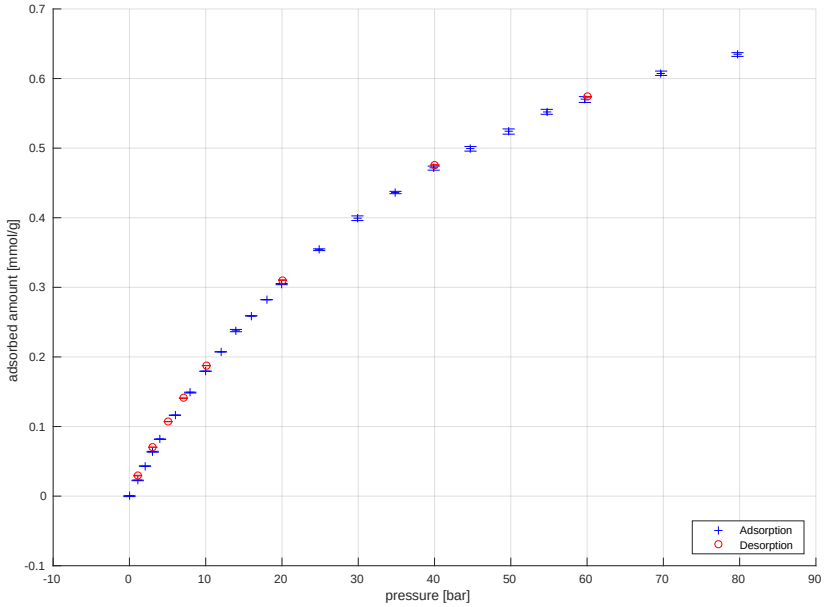

Figure E.20.: CNT and N_2 at 40 °C

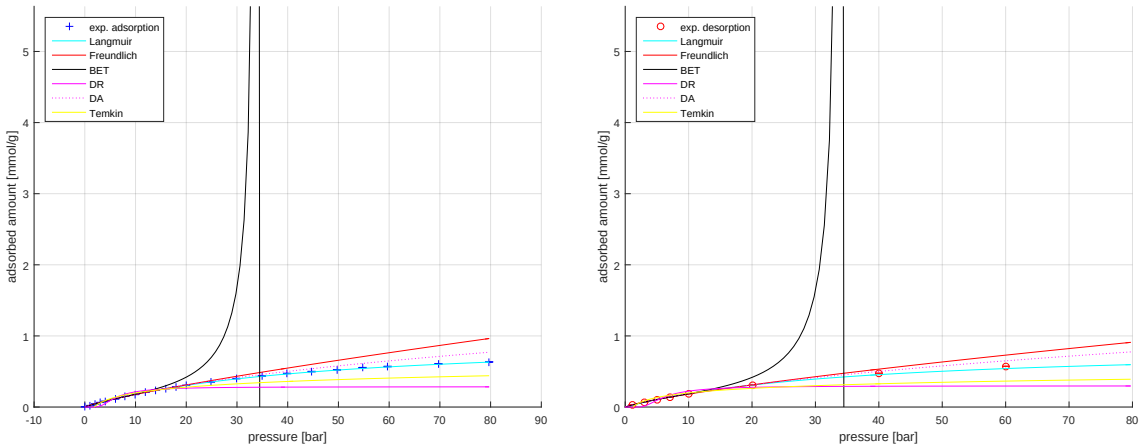

(a) adsorption **(b)** desorption

Figure E.21.: CNT and N_2 at 40 °C data (marks) and fits (lines) adsorption branch (a) and desorption branch (b)

Table E.18.: CNT and N_2 at 40 °C

sample:	CNT		
gas:	N_2		
temperature in [°C]:	48.7	+0.2	-0.1
$m_{S,meas}$ in [mg]:	170.66		
V_S in [cm^3]:	0.073629		

p [bar]	X [$mmolg^{-1}$]	ρ_{meas} [gcm^{-3}]	Δm_{meas} [g]
0.00	0.0000	0.000000	0.000000
1.08	0.0226	0.001115	0.000108
2.04	0.0432	0.002116	0.000207
3.05	0.0638	0.003174	0.000305
4.01	0.0818	0.004166	0.000391
5.97	0.1163	0.006218	0.000556
7.97	0.1488	0.008310	0.000712
9.98	0.1795	0.010405	0.000859
11.97	0.2074	0.012483	0.000992
13.96	0.2379	0.014584	0.001138
15.96	0.2591	0.016663	0.001239
17.98	0.2823	0.018767	0.001351
19.96	0.3047	0.020839	0.001458
24.88	0.3541	0.025980	0.001694
29.89	0.3994	0.031215	0.001911
34.88	0.4363	0.036421	0.002087
39.89	0.4714	0.041775	0.002255
44.72	0.4992	0.046787	0.002388
49.72	0.5240	0.051969	0.002507
54.71	0.5523	0.057144	0.002642
59.71	0.5699	0.062295	0.002727
69.71	0.6077	0.072569	0.002907
79.71	0.6347	0.082758	0.003036
60.05	0.5738	0.062624	0.002745
40.06	0.4760	0.041964	0.002277
20.07	0.3105	0.020982	0.001485
10.08	0.1875	0.010533	0.000897
7.08	0.1408	0.007395	0.000674
5.08	0.1070	0.005300	0.000512
3.08	0.0703	0.003208	0.000336
1.08	0.0295	0.001118	0.000141

E.1.14 CNT and N_2 at 50 °C

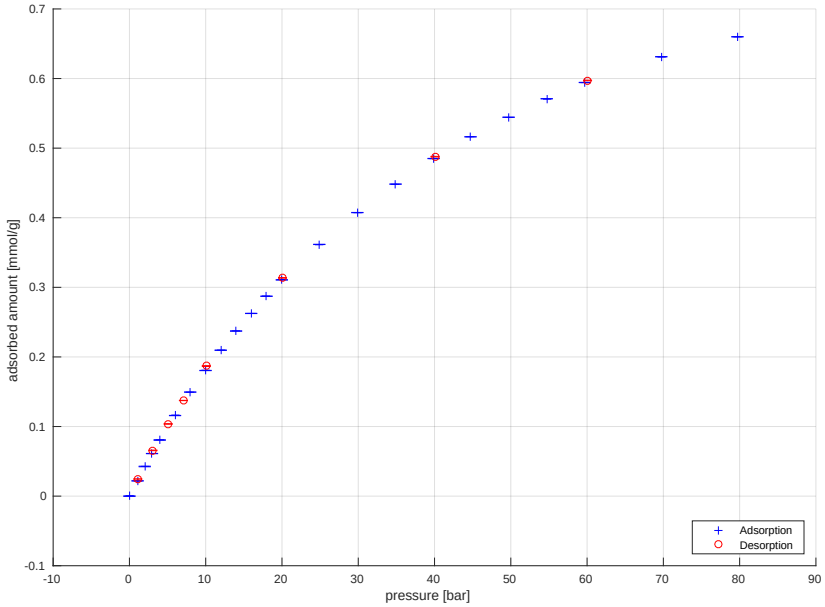

Figure E.22.: CNT and N_2 at 50 °C

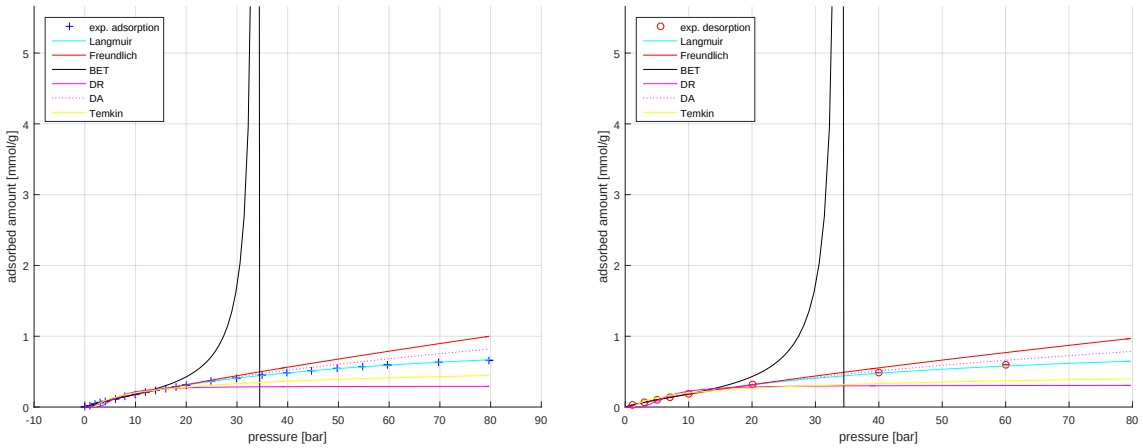

(a) adsorption **(b)** desorption

Figure E.23.: CNT and N_2 at 50 °C data (marks) and fits (lines) adsorption branch (a) and desorption branch (b)

Table E.19.: CNT and N_2 at 50 °C

sample:	CNT		
gas:	N_2		
temperature in [°C]:	50.6	+0.5	-0.2
$m_{S,meas}$ in [mg]:	170.66		
V_S in [cm^3]:	0.076123		

p [bar]	X [$mmolg^{-1}$]	ρ_{meas} [gcm^{-3}]	Δm_{meas} [g]
0.00	0.0000	0.000000	0.000000
1.07	0.0219	0.001108	0.000105
2.01	0.0426	0.002078	0.000204
2.96	0.0612	0.003069	0.000293
3.97	0.0806	0.004116	0.000386
5.98	0.1158	0.006203	0.000554
7.97	0.1495	0.008276	0.000715
9.98	0.1805	0.010366	0.000863
11.97	0.2097	0.012434	0.001003
13.98	0.2372	0.014512	0.001135
15.96	0.2625	0.016564	0.001256
17.97	0.2872	0.018644	0.001374
19.98	0.3107	0.020734	0.001486
24.89	0.3617	0.025833	0.001730
29.88	0.4074	0.031007	0.001949
34.89	0.4483	0.036185	0.002145
39.88	0.4851	0.041490	0.002321
44.72	0.5163	0.046474	0.002470
49.71	0.5444	0.051606	0.002604
54.71	0.5710	0.056733	0.002731
59.71	0.5943	0.061850	0.002843
69.73	0.6313	0.072044	0.003020
79.71	0.6600	0.082134	0.003157
60.06	0.5973	0.062187	0.002857
40.06	0.4878	0.041661	0.002333
20.07	0.3136	0.020852	0.001500
10.08	0.1869	0.010481	0.000894
7.08	0.1374	0.007366	0.000657
5.08	0.1037	0.005286	0.000496
3.08	0.0657	0.003205	0.000314
1.10	0.0241	0.001142	0.000115

E.1.15 CNT and N_2 at 75 °C

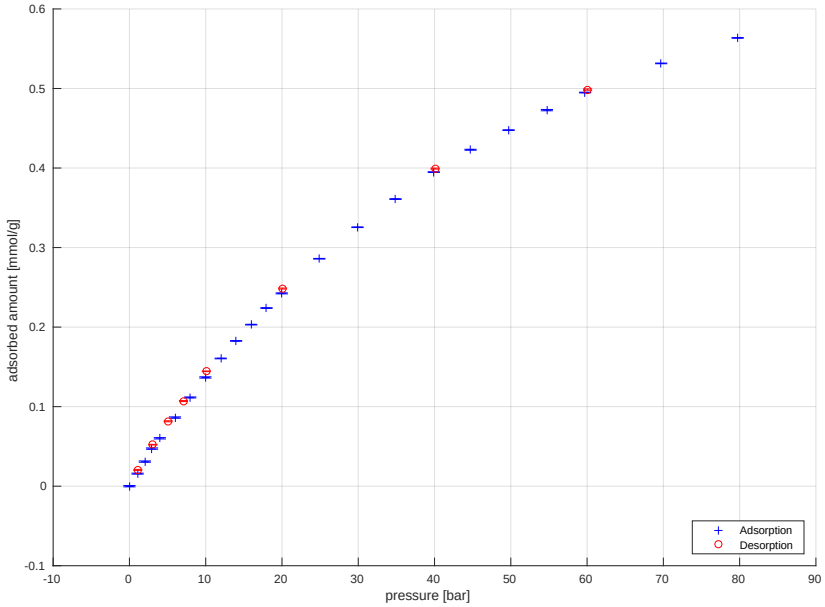

Figure E.24.: CNT and N_2 at 75 °C

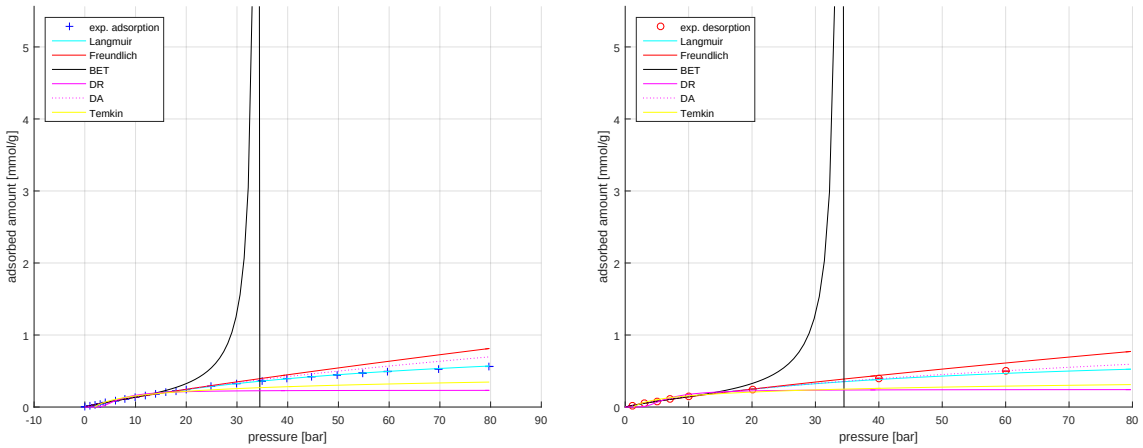

(a) adsorption **(b)** desorption

Figure E.25.: CNT and N_2 at 40 °C data (marks) and fits (lines) adsorption branch (a) and desorption branch (b)

Table E.20.: CNT and N_2 at 75 °C

sample:	CNT		
gas:	N_2		
temperature in [°C]:	75.4	+0.7	-0.3
$m_{S,meas}$ in [mg]:	171.25		
V_S in [cm^3]:	0.077346		

p [bar]	X [$mmolg^{-1}$]	ρ_{meas} [gcm^{-3}]	Δm_{meas} [g]
0.00	0.0000	0.000000	0.000000
1.07	0.0158	0.001024	0.000076
2.02	0.0309	0.001931	0.000148
2.96	0.0473	0.002849	0.000227
3.99	0.0602	0.003819	0.000289
5.97	0.0863	0.005725	0.000414
7.97	0.1116	0.007653	0.000535
9.96	0.1367	0.009569	0.000656
11.97	0.1606	0.011500	0.000770
13.98	0.1826	0.013422	0.000876
15.96	0.2031	0.015318	0.000975
17.97	0.2239	0.017243	0.001075
19.97	0.2424	0.019152	0.001163
24.89	0.2859	0.023862	0.001372
29.90	0.3256	0.028639	0.001562
34.88	0.3610	0.033392	0.001732
39.90	0.3949	0.038284	0.001895
44.72	0.4230	0.042845	0.002030
49.71	0.4476	0.047557	0.002148
54.73	0.4728	0.052282	0.002269
59.74	0.4949	0.056966	0.002375
69.71	0.5315	0.066262	0.002551
79.74	0.5636	0.075536	0.002705
60.07	0.4987	0.057237	0.002393
40.06	0.3993	0.038387	0.001916
20.07	0.2485	0.019222	0.001193
10.08	0.1444	0.009637	0.000693
7.08	0.1070	0.006755	0.000513
5.08	0.0816	0.004833	0.000391
3.08	0.0522	0.002915	0.000250
1.10	0.0205	0.001011	0.000098

E.1.16 CNT and N_2 at 100 °C

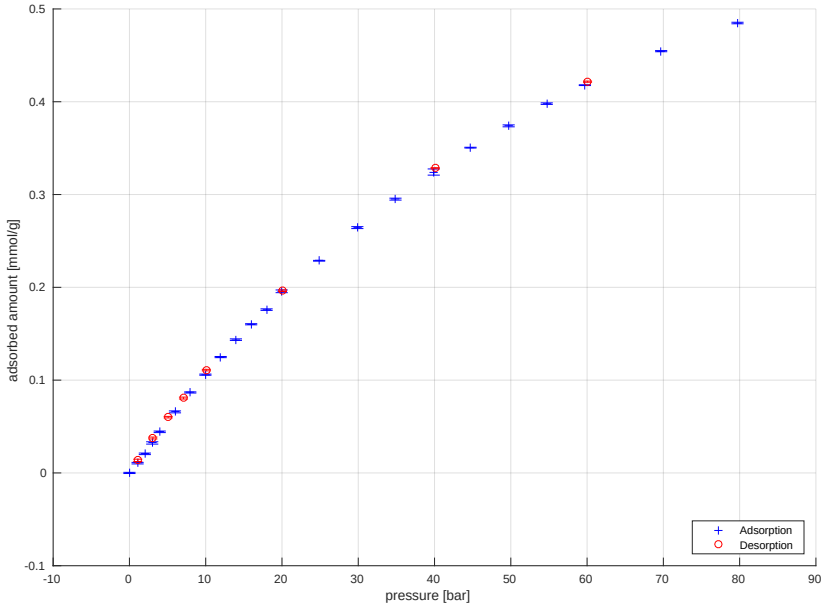

Figure E.26.: CNT and N_2 at 100 °C

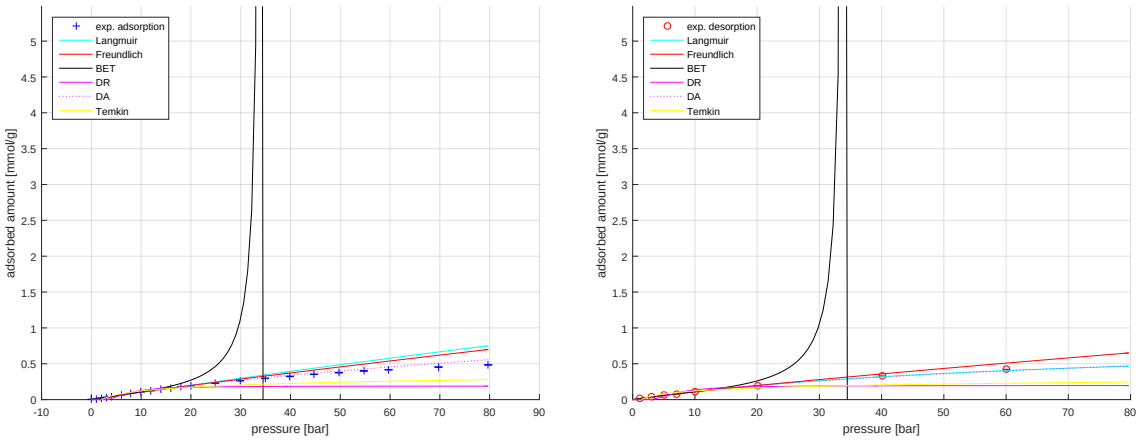

(a) adsorption **(b)** desorption

Figure E.27.: CNT and N_2 at 100 °C data (marks) and fits (lines) adsorption branch (a) and desorption branch (b)

Table E.21.: CNT and N_2 at 100 °C

sample:	CNT		
gas:	N_2		
temperature in [°C]:	100.0	+0.4	-0.2
$m_{S,meas}$ in [mg]:	172.13		
V_S in [cm^3]:	0.078893		

p [bar]	X [$mmolg^{-1}$]	ρ_{meas} [gcm^{-3}]	Δm_{meas} [g]
0.00	0.0000	0.000000	0.000000
1.07	0.0105	0.000948	0.000051
2.02	0.0206	0.001793	0.000099
2.99	0.0323	0.002663	0.000155
3.97	0.0443	0.003543	0.000213
5.97	0.0658	0.005342	0.000316
7.98	0.0867	0.007140	0.000416
9.96	0.1059	0.008925	0.000508
11.96	0.1248	0.010714	0.000599
13.96	0.1436	0.012495	0.000689
15.96	0.1602	0.014289	0.000769
17.98	0.1760	0.016093	0.000845
19.96	0.1957	0.017858	0.000939
24.87	0.2286	0.022235	0.001097
29.88	0.2644	0.026689	0.001269
34.88	0.2950	0.031108	0.001416
39.90	0.3243	0.035660	0.001556
44.71	0.3505	0.039893	0.001682
49.72	0.3740	0.044271	0.001795
54.71	0.3980	0.048634	0.001910
59.71	0.4179	0.052984	0.002006
69.71	0.4545	0.061627	0.002181
79.72	0.4848	0.070200	0.002327
60.06	0.4216	0.053263	0.002024
40.07	0.3283	0.035776	0.001576
20.07	0.1963	0.017944	0.000942
10.08	0.1108	0.009009	0.000532
7.08	0.0807	0.006319	0.000387
5.08	0.0601	0.004526	0.000288
3.08	0.0376	0.002726	0.000181
1.09	0.0136	0.000946	0.000065

E.1.17 CNT and N_2 at 125 °C

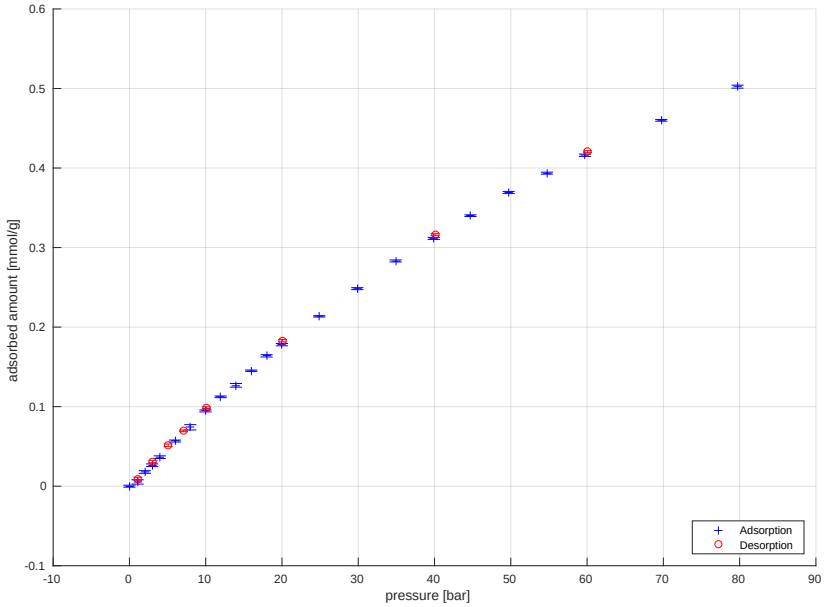

Figure E.28.: CNT and N_2 at 125 °C

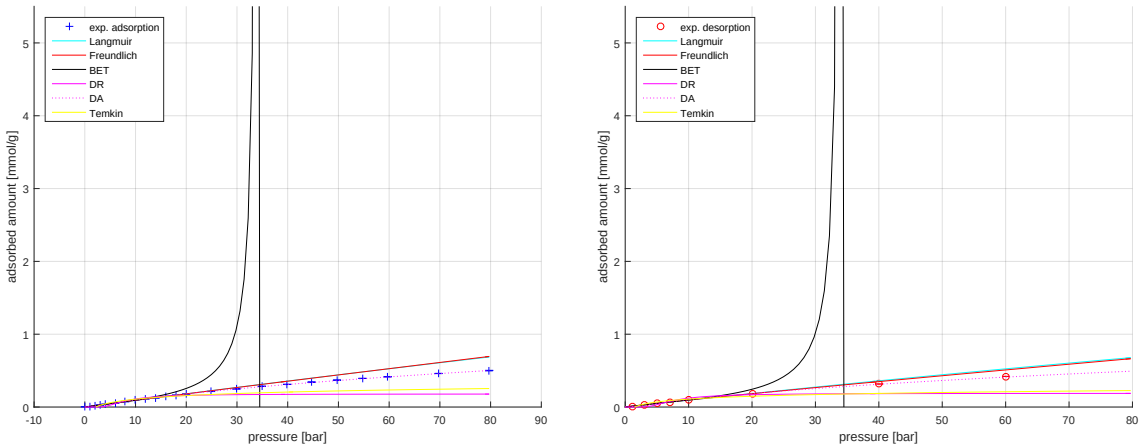

(a) adsorption **(b)** desorption

Figure E.29.: CNT and N_2 at 40 °C data (marks) and fits (lines) adsorption branch (a) and desorption branch (b)

Table E.22.: CNT and N_2 at 125 °C

sample:	CNT		
gas:	N_2		
temperature in [°C]:	125.1	+0.2	-0.2
$m_{S,meas}$ in [mg]:	171.84		
V_S in [cm^3]:	0.086896		

p [bar]	X [$mmol g^{-1}$]	ρ_{meas} [$g cm^{-3}$]	Δm_{meas} [g]
0.00	0.0000	0.000000	0.000000
1.07	0.0054	0.000884	0.000026
2.02	0.0178	0.001676	0.000085
2.97	0.0264	0.002471	0.000126
3.98	0.0365	0.003315	0.000175
5.98	0.0568	0.004992	0.000272
7.98	0.0740	0.006678	0.000355
9.96	0.0946	0.008338	0.000453
11.96	0.1123	0.010005	0.000538
13.96	0.1268	0.011674	0.000607
15.97	0.1452	0.013351	0.000695
17.98	0.1639	0.015034	0.000785
19.99	0.1780	0.016706	0.000852
24.89	0.2135	0.020788	0.001023
29.88	0.2484	0.024934	0.001189
34.90	0.2832	0.029084	0.001356
39.90	0.3115	0.033316	0.001492
44.71	0.3401	0.037266	0.001629
49.72	0.3693	0.041353	0.001769
54.73	0.3935	0.045425	0.001885
59.73	0.4161	0.049468	0.001993
69.72	0.4599	0.057509	0.002203
79.72	0.5023	0.065487	0.002406
60.06	0.4206	0.049727	0.002014
40.07	0.3162	0.033435	0.001514
20.07	0.1829	0.016781	0.000876
10.08	0.0987	0.008428	0.000473
7.08	0.0696	0.005914	0.000333
5.08	0.0514	0.004236	0.000246
3.08	0.0310	0.002554	0.000149
1.09	0.0093	0.000873	0.000045

Table E.23.: Model fit parameter for CNT data and N_2 - Langmuir model

Adsorption						
T [°C]	k_L	k_L min	k_L max	q_max	q_max min	q_max max
0	0.0433	0.0050	0.0050	1.1435	0.0835	0.0835
25	0.0248	0.0014	0.0014	1.2199	0.0525	0.0525
40	0.0224	0.0014	0.0014	0.9842	0.0455	0.0455
50	0.0200	0.0006	0.0006	1.0862	0.0239	0.0239
75	0.0153	0.0013	0.0013	1.0348	0.0690	0.0690
100	0.0011	0.0052	0.0052	9.0625	41.1875	41.1875
125	0.0009	0.0035	0.0035	10.1563	38.6522	38.6522
Desorption						
T [°C]	k_L	k_L min	k_L max	q_max	q_max min	q_max max
0	0.0480	0.0147	0.0147	1.0901	0.2111	0.2111
25	0.0276	0.0018	0.0018	1.1506	0.0548	0.0548
40	0.0278	0.0054	0.0054	0.8653	0.1216	0.1216
50	0.0225	0.0012	0.0012	1.0089	0.0416	0.0416
75	0.0208	0.0036	0.0036	0.8432	0.1130	0.1130
100	0.0145	0.0009	0.0009	0.8708	0.0445	0.0445
125	0.0016	0.0076	0.0076	6.0938	28.7336	28.7336

Table E.24.: Model fit parameter for CNT data and N_2 - Freundlich model

Adsorption T [°C]	K	K min	K max	n	n min	n max
0	0.0650	0.0047	0.0047	0.7104	0.0273	0.0273
25	0.0371	0.0031	0.0031	0.8036	0.0310	0.0310
40	0.0268	0.0023	0.0023	0.8183	0.0322	0.0322
50	0.0260	0.0019	0.0019	0.8330	0.0276	0.0276
75	0.0185	0.0012	0.0012	0.8639	0.0234	0.0234
100	0.0127	0.0010	0.0010	0.9159	0.0302	0.0302
125	0.0098	0.0010	0.0010	0.9734	0.0386	0.0386
Desorption						
T [°C]	K	K min	K max	n	n min	n max
0	0.0712	0.0066	0.0066	0.6771	0.0357	0.0357
25	0.0400	0.0060	0.0060	0.7796	0.0572	0.0572
40	0.0306	0.0030	0.0030	0.7747	0.0378	0.0378
50	0.0278	0.0043	0.0043	0.8112	0.0581	0.0581
75	0.0214	0.0018	0.0018	0.8183	0.0319	0.0319
100	0.0147	0.0015	0.0015	0.8652	0.0372	0.0372
125	0.0112	0.0014	0.0014	0.9315	0.0445	0.0445

Table E.25.: Model fit parameter for CNT data and N_2 - BET model

Adsorption						
T [°C]	K_BET	K_BET min	K_BET max	q_max_BET	q_max_BET max	q_max_BET min
0	5.6579	0.2155	0.2155	0.3490	0.0056	0.0056
25	4.3021	0.6581	0.6581	0.2673	0.0193	0.0193
40	4.1366	0.5279	0.5279	0.2018	0.0123	0.0123
50	3.9663	0.4677	0.4677	0.2062	0.0118	0.0118
75	3.8005	0.4594	0.4594	0.1583	0.0095	0.0095
100	2.9066	0.8275	0.8275	0.1386	0.0217	0.0217
125	2.3241	0.5235	0.5235	0.1366	0.0183	0.0183
Desorption						
T [°C]	K_BET	K_BET min	K_BET max	q_max_BET	q_max_BET max	q_max_BET min
0	7.0377	0.7423	0.7423	0.3283	0.0124	0.0124
25	4.8096	1.3117	1.3117	0.2625	0.0309	0.0309
40	4.9517	0.7374	0.7374	0.1955	0.0124	0.0124
50	4.1957	0.7694	0.7694	0.2062	0.0174	0.0174
75	4.5388	0.8153	0.8153	0.1549	0.0123	0.0123
100	3.7927	0.7208	0.7208	0.1270	0.0116	0.0116
125	3.0703	0.6867	0.6867	0.1231	0.0145	0.0145

Table E.26.: Model fit parameter for CNT data and N_2 - DR model

Adsorption T [°C]	k_DR	k_DR min	k_DR max	q_s	q_s min	q_s max
0	244.5597	54.9786	54.9786	0.6511	0.0767	0.0767
25	276.7660	67.4395	67.4395	0.5274	0.0765	0.0765
40	270.7376	64.1292	64.1292	0.4014	0.0578	0.0578
50	270.6504	65.9591	65.9591	0.4127	0.0621	0.0621
75	268.1422	67.0719	67.0719	0.3301	0.0533	0.0533
100	274.9753	63.9410	63.9410	0.2753	0.0440	0.0440
125	286.7252	64.3956	64.3956	0.2663	0.0442	0.0442
Desorption						
T [°C]	k_DR	k_DR min	k_DR max	q_s	q_s min	q_s max
0	254.0585	140.1409	140.1409	0.6749	0.2393	0.2393
25	285.9625	126.5385	126.5385	0.5555	0.1772	0.1772
40	272.4612	128.8746	128.8746	0.4195	0.1430	0.1430
50	280.5181	119.5477	119.5477	0.4354	0.1382	0.1382
75	264.7587	121.8831	121.8831	0.3459	0.1196	0.1196
100	268.0454	115.1510	115.1510	0.2837	0.0956	0.0956
125	279.3164	112.1888	112.1888	0.2782	0.0926	0.0926

Table E.27.: Model fit parameter for CNT data and N_2 - Temkin model

Adsorption						
T [°C]	A_T	A_T min	A_T max	RTb_T	RTb_T max	RTb_T min
0	0.5472	0.1092	0.1092	0.2129	0.0243	0.0243
25	0.4680	0.1041	0.1041	0.1695	0.0235	0.0235
40	0.5459	0.1435	0.1435	0.1167	0.0184	0.0184
50	0.5437	0.1496	0.1496	0.1182	0.0196	0.0196
75	0.5241	0.1522	0.1522	0.0929	0.0165	0.0165
100	0.4880	0.1387	0.1387	0.0760	0.0138	0.0138
125	0.4643	0.1410	0.1410	0.0704	0.0140	0.0140
Desorption						
T [°C]	A_T	A_T min	A_T max	RTb_T	RTb_T max	RTb_T min
0	0.9977	0.8135	0.8135	0.1574	0.1574	0.0670
25	0.8173	0.6705	0.6705	0.1253	0.1253	0.0589
40	0.8503	0.7507	0.7507	0.0927	0.0927	0.0461
50	0.7828	0.6621	0.6621	0.0962	0.0962	0.0477
75	0.7903	0.7057	0.7057	0.0752	0.0752	0.0391
100	0.7427	0.6771	0.6771	0.0600	0.0600	0.0329
125	0.6865	0.6408	0.6408	0.0565	0.0565	0.0330

Table E.28.: Model fit parameter for CNT data and N_2 - Tóth model

Adsorption T [°C]	K_T	K_T min	K_T max	a_T	a_T min	a_T max	t	t min	tmax
0									
25									
40									
50									
75									
100									
125									
Desorption **T [°C]**	**K_T**	**K_T min**	**K_T max**	**a_T**	**a_T min**	**a_T max**	**t**	**t min**	**tmax**
0									
25									
40									
50									
75									
100									
125									

Table E.29.: CNT and CO_2 at 0 °C

sample:	CNT		
gas:	CO_2		
temperature in [°C]:	0.2	+5.9	-0.2
$m_{S,meas}$ in [mg]:	138.70		
V_S in [cm^3]:	0.062815		

p [bar]	X [mmolg^{-1}]	ρ_{meas} [gcm^{-3}]	Δm_{meas} [g]
0.00	0.0000	0.000000	0.000000
0.96	0.2886	0.001842	0.001762
1.96	0.5293	0.003811	0.003232
2.96	0.7487	0.005800	0.004571
3.96	0.9495	0.007821	0.005797
5.96	1.2864	0.011933	0.007853
7.96	1.5532	0.016161	0.009482
9.97	1.7726	0.020498	0.010822
11.97	1.9693	0.024948	0.012023
13.97	2.1554	0.029520	0.013159
15.96	2.3462	0.034271	0.014324
17.96	2.5381	0.039188	0.015496
19.96	2.7431	0.044322	0.016747
24.87	3.2668	0.057929	0.019944
29.88	4.1491	0.073749	0.025331
20.08	2.7015	0.044326	0.016493
10.07	1.6885	0.020426	0.010308
5.07	1.0400	0.009919	0.006349
3.07	0.7033	0.005929	0.004294
1.08	0.3058	0.002045	0.001867

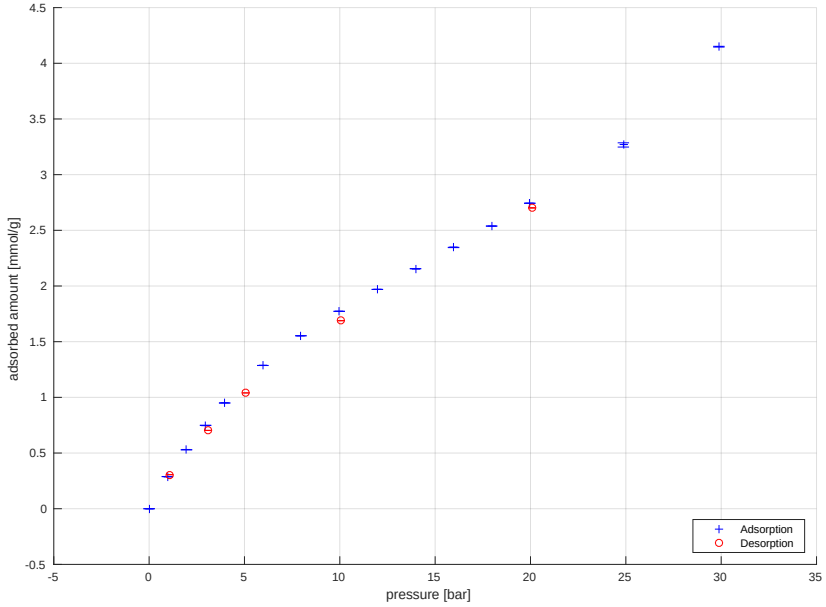

Figure E.30.: CNT and CO_2 at 0 °C

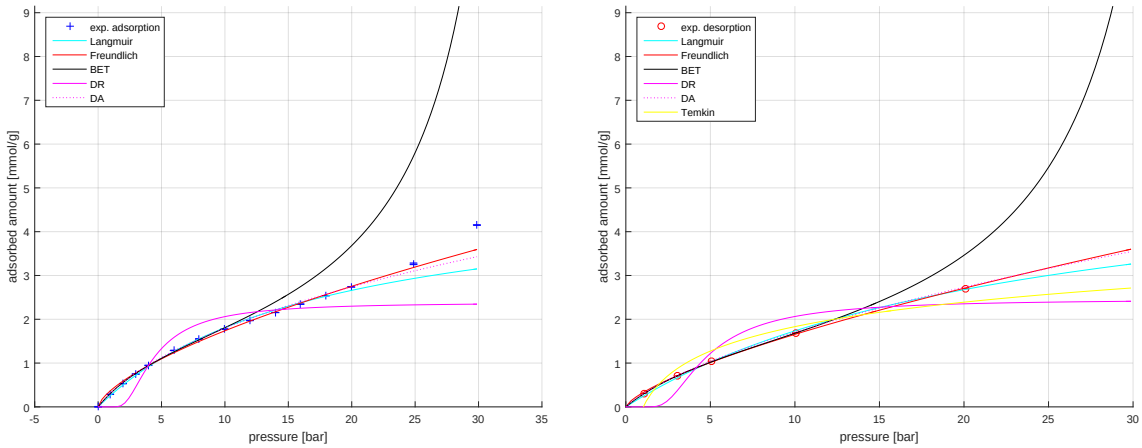

(a) adsorption **(b)** desorption

Figure E.31.: CNT and CO_2 at 0 °C data (marks) and fits (lines) adsorption branch (a) and desorption branch (b)

E.1.20 CNT and CO_2 at 25 °C

Table E.30.: CNT and CO_2 at 25 °C

sample:	CNT		
gas:	CO_2		
temperature in [°C]:	21.9	+0.4	-0.8
$m_{S,meas}$ in [mg]:	139.33		
V_S in [cm^3]:	0.062096		

p [bar]	X [$mmolg^{-1}$]	ρ_{meas} [gcm^{-3}]	Δm_{meas} [g]
1.45	0.0000	0.000000	0.000000
5.98	0.8077	0.010550	0.004953
7.97	1.0181	0.014356	0.006244
9.96	1.2017	0.018261	0.007370
11.96	1.3662	0.022279	0.008379
13.96	1.5159	0.026397	0.009297
15.96	1.6548	0.030613	0.010149
17.96	1.7862	0.034948	0.010955
19.96	1.9106	0.039402	0.011718
24.88	2.2077	0.050957	0.013540
29.88	2.5123	0.063686	0.015409
34.88	2.8386	0.077664	0.017410
39.88	3.2141	0.093732	0.019713
32.23	-0.5568	0.042579	-0.003415
13.36	1.4323	0.018668	0.008785
10.08	-0.8754	0.000000	-0.005369

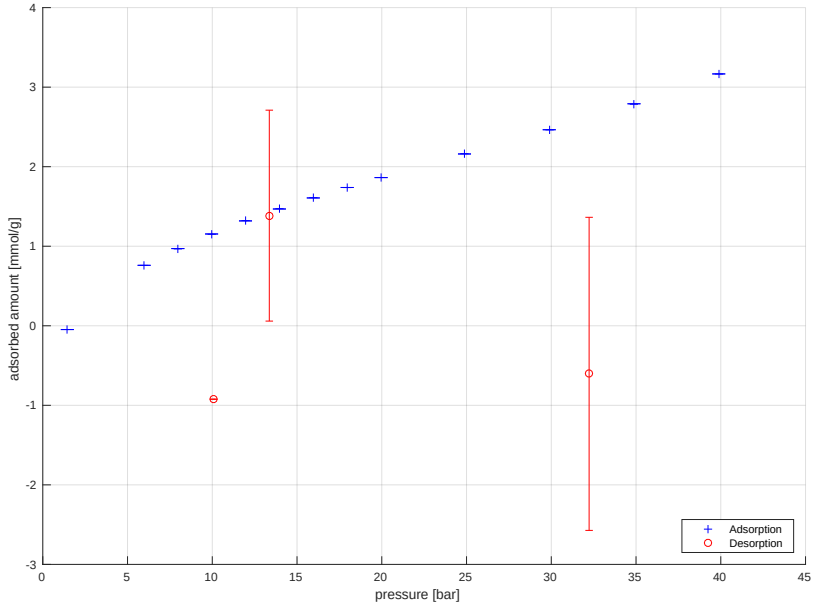

Figure E.32.: CNT and CO_2 at 25 °C

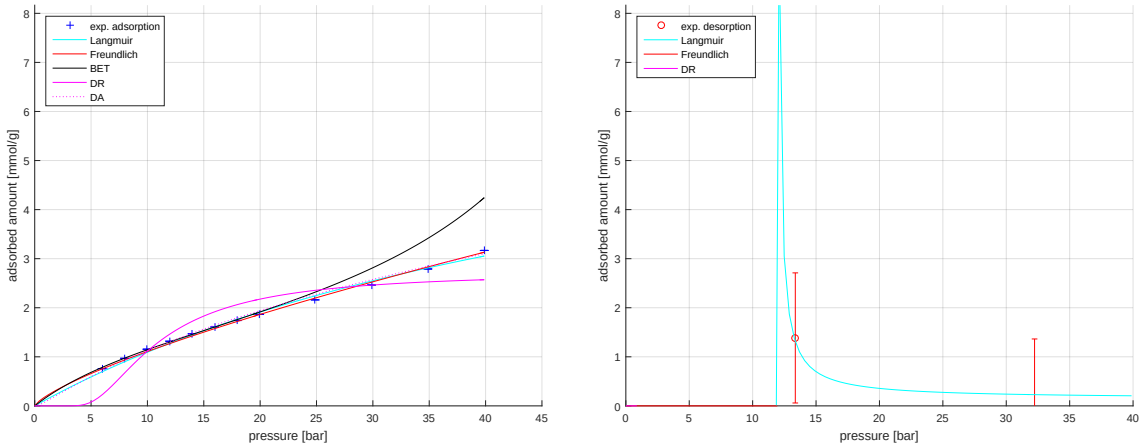

(a) adsorption **(b)** desorption

Figure E.33.: CNT and CO_2 at 25 °C data (marks) and fits (lines) adsorption branch (a) and desorption branch (b)

E.1.21 CNT and CO_2 at 50 °C

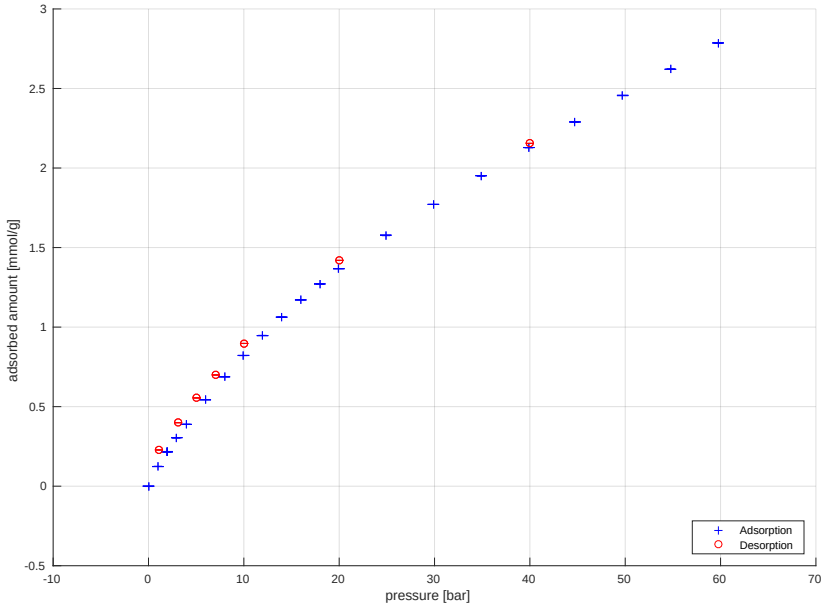

Figure E.34.: CNT and CO_2 at 50 °C

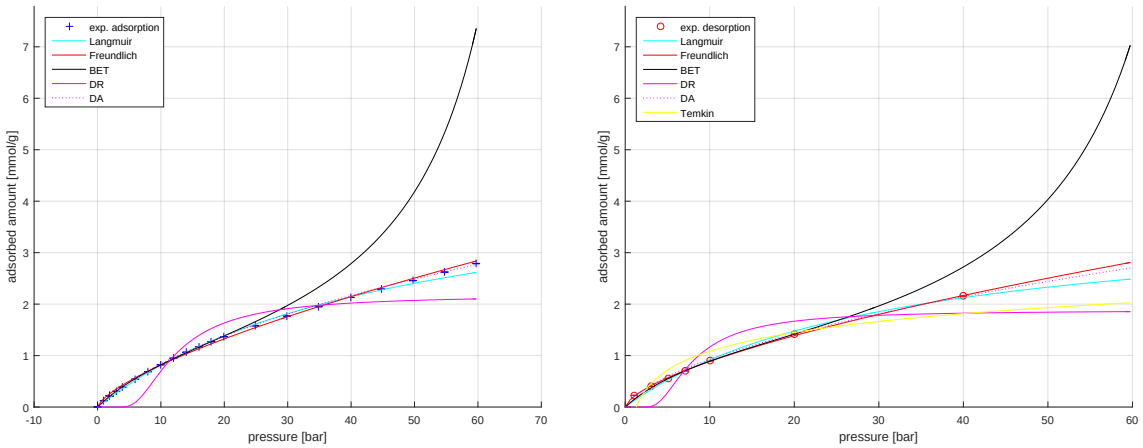

(a) adsorption **(b)** desorption

Figure E.35.: CNT and CO_2 at 0 °C data (marks) and fits (lines) adsorption branch (a) and desorption branch (b)

Table E.31.: CNT and CO_2 at 50 °C

sample:	CNT		
gas:	CO_2		
temperature in [°C]:	47.9	+0.1	-0.2
$m_{S,meas}$ in [mg]:	128.49		
V_S in [cm^3]:	0.057909		

p [bar]	X [$mmolg^{-1}$]	ρ_{meas} [gcm^{-3}]	Δm_{meas} [g]
0.00	0.0000	0.000000	0.000000
0.99	0.1233	0.001626	0.000697
1.96	0.2164	0.003243	0.001224
1.96	0.2173	0.003245	0.001229
1.96	0.2178	0.003240	0.001231
2.96	0.3050	0.004907	0.001725
3.96	0.3881	0.006578	0.002195
5.96	0.5432	0.009999	0.003072
7.96	0.6875	0.013473	0.003888
9.96	0.8216	0.017010	0.004646
11.96	0.9465	0.020605	0.005352
13.96	1.0624	0.024282	0.006008
15.96	1.1708	0.028026	0.006621
17.96	1.2713	0.031826	0.007190
19.96	1.3671	0.035706	0.007731
24.88	1.5775	0.045577	0.008921
29.88	1.7712	0.056139	0.010016
34.89	1.9518	0.067279	0.011038
39.90	2.1286	0.079502	0.012038
44.73	2.2895	0.091727	0.012948
49.73	2.4560	0.105333	0.013889
54.74	2.6204	0.120053	0.014819
59.74	2.7863	0.136163	0.015757
39.97	2.1546	0.079712	0.012185
20.05	1.4191	0.035862	0.008025
10.07	0.8971	0.017230	0.005073
7.07	0.6989	0.011950	0.003953
5.08	0.5546	0.008493	0.003136
3.08	0.3991	0.005086	0.002257
1.08	0.2275	0.001732	0.001287

E.1.22 CNT and CO_2 at 50 °C, second measurement

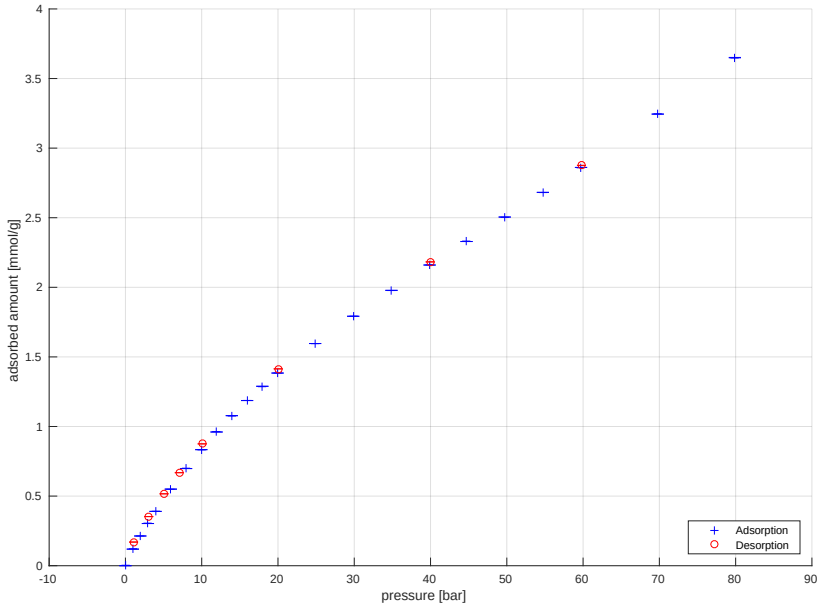

Figure E.36.: CNT and CO_2 at 50 °C second measurement

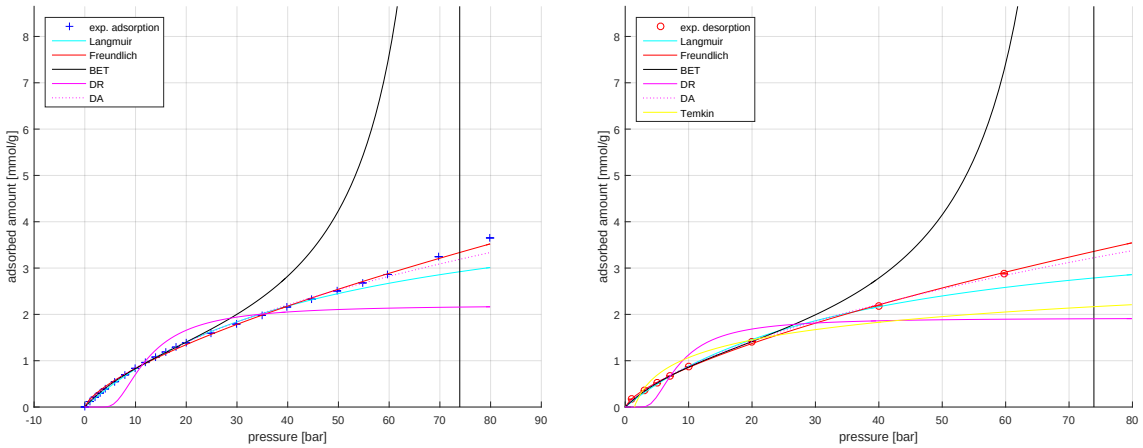

(a) adsorption **(b)** desorption

Figure E.37.: CNT and CO_2 at 50 °C second measurement data (marks) and fits (lines) adsorption branch (a) and desorption branch (b)

Table E.32.: CNT and CO_2 at 50 °C, second measurement

sample:	CNT		
gas:	CO_2		
temperature in [°C]:	45.2	+0.1	-0.1
$m_{S,meas}$ in [mg]:	128.73		
V_S in [cm^3]:	0.057769		

p [bar]	X [$mmol g^{-1}$]	ρ_{meas} [$g cm^{-3}$]	Δm_{meas} [g]
0.01	0.0000	0.000000	0.000000
0.98	0.1189	0.001624	0.000674
1.96	0.2133	0.003258	0.001209
2.96	0.3028	0.004944	0.001716
3.96	0.3900	0.006631	0.002210
5.96	0.5500	0.010069	0.003116
7.96	0.6978	0.013582	0.003953
9.96	0.8336	0.017144	0.004723
11.96	0.9605	0.020784	0.005442
13.96	1.0778	0.024485	0.006107
15.96	1.1865	0.028280	0.006722
17.96	1.2888	0.032150	0.007302
19.96	1.3840	0.036073	0.007841
24.88	1.5961	0.046094	0.009043
29.87	1.7920	0.056841	0.010153
34.89	1.9781	0.068270	0.011207
39.89	2.1602	0.080738	0.012239
44.73	2.3290	0.093316	0.013195
49.74	2.5049	0.107381	0.014192
54.74	2.6821	0.122721	0.015196
59.74	2.8612	0.139595	0.016211
69.80	3.2445	0.180250	0.018382
79.91	3.6501	0.236213	0.020680
59.80	2.8759	0.140312	0.016293
39.96	2.1827	0.081089	0.012366
20.04	1.4141	0.036298	0.008012
10.07	0.8752	0.017422	0.004958
7.07	0.6681	0.012066	0.003785
5.07	0.5163	0.008570	0.002925
3.07	0.3527	0.005145	0.001999
1.08	0.1697	0.001772	0.000961

E.1.23 CNT and CO_2 at 75 °C

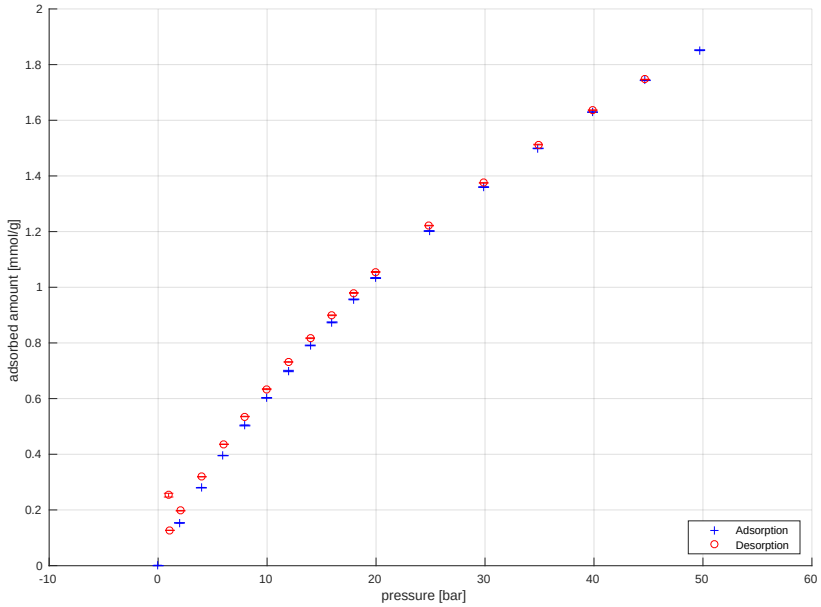

Figure E.38.: CNT and CO_2 at 75 °C

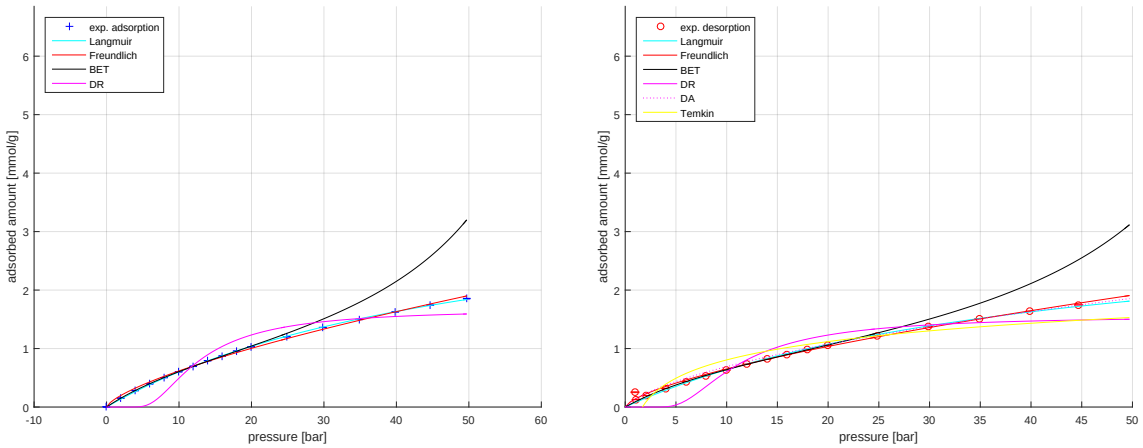

(a) adsorption **(b)** desorption

Figure E.39.: CNT and CO_2 at 75 °C data (marks) and fits (lines) adsorption branch (a) and desorption branch (b)

Table E.33.: CNT and CO_2 at 75 °C

sample:	CNT		
gas:	CO_2		
temperature in [°C]:	73.8	+0.0	-0.1
$m_{S,meas}$ in [mg]:	142.83		
V_S in [cm^3]:	0.062729		

p [bar]	X [$mmolg^{-1}$]	ρ_{meas} [gcm^{-3}]	Δm_{meas} [g]
0.00	0.0000	0.000000	0.000000
1.96	0.1535	0.002972	0.000965
3.97	0.2796	0.006057	0.001758
5.96	0.3950	0.009159	0.002483
7.96	0.5033	0.012309	0.003164
9.96	0.6026	0.015489	0.003788
11.96	0.6991	0.018724	0.004395
13.96	0.7909	0.022003	0.004972
15.96	0.8740	0.025300	0.005494
17.96	0.9565	0.028680	0.006013
19.96	1.0330	0.032072	0.006494
24.88	1.2020	0.040647	0.007556
29.88	1.3599	0.049694	0.008548
34.87	1.4990	0.059052	0.009423
39.87	1.6292	0.068955	0.010241
44.70	1.7437	0.078751	0.010961
49.70	1.8519	0.089318	0.011641
44.70	1.7467	0.078748	0.010980
39.88	1.6364	0.068975	0.010287
34.88	1.5128	0.059274	0.009509
29.88	1.3750	0.049688	0.008643
24.87	1.2216	0.040651	0.007679
19.96	1.0550	0.032082	0.006632
17.96	0.9797	0.028667	0.006158
15.96	0.8994	0.025336	0.005653
13.96	0.8170	0.022028	0.005136
11.96	0.7316	0.018747	0.004599
9.96	0.6339	0.015510	0.003985
7.96	0.5357	0.012314	0.003367
6.05	0.4359	0.009299	0.002740
4.01	0.3192	0.006119	0.002006
2.06	0.1970	0.003131	0.001238
1.08	0.1267	0.001625	0.000796

E.1.24 CNT and CO_2 at 40 °C cycling experiment with 30 min equilibration time

Table E.34.: CNT and CO_2 at 40 °C 9 cycles with 30 min equilibration time per data point

sample:	CNT		
gas:	CO_2		
temperature in [°C]:	41.9	+0.5	-0.1
$m_{S,meas}$ in [mg]:	139.38		
V_S in [cm^3]:	0.062038		

p [bar]	X [$mmolg^{-1}$]	ρ_{meas} [gcm^{-3}]	Δm_{meas} [g]
1. cycle			
0.00	0.0000	0.000000	0.000000
0.98	0.1261	0.001637	0.000773
1.95	0.2248	0.003288	0.001378
2.95	0.3186	0.004993	0.001953
3.95	0.4075	0.006712	0.002498
5.95	0.5757	0.010206	0.003529
7.95	0.7299	0.013754	0.004474
9.95	0.8732	0.017388	0.005352
11.95	1.0038	0.021072	0.006153
13.95	1.1241	0.024832	0.006890
15.95	1.2363	0.028671	0.007578
17.95	1.3403	0.032574	0.008215
19.95	1.4382	0.036551	0.008815
24.87	1.6572	0.046748	0.010158
29.87	1.8606	0.057719	0.011405
34.87	2.0527	0.069377	0.012582
39.88	2.2461	0.082237	0.013768
44.72	2.4276	0.095277	0.014880
49.71	2.6176	0.109932	0.016044
54.72	2.8153	0.126099	0.017256
59.73	3.0233	0.144160	0.018531
69.83	3.4792	0.188704	0.021325
59.94	3.0381	0.145089	0.018622

Table E.34.: CNT and CO_2 with 30 min equilibration time per data point continued

p [bar]	X [mmolg^{-1}]	ρ_{meas} [gcm^{-3}]	Δm_{meas} [g]
39.97	2.2649	0.082601	0.013883
20.04	1.4597	0.036737	0.008947
10.06	0.9023	0.017571	0.005531
7.07	0.6864	0.012161	0.004207
5.06	0.5281	0.008636	0.003237
3.06	0.3547	0.005171	0.002174
1.07	0.1629	0.001767	0.000999
2. cycle			
1.06	0.1838	0.001781	0.001126
1.95	0.2717	0.003283	0.001665
2.95	0.3637	0.004996	0.002229
3.95	0.4523	0.006716	0.002772
5.95	0.6176	0.010200	0.003785
7.95	0.7706	0.013751	0.004723
9.95	0.9123	0.017376	0.005592
11.95	1.0419	0.021067	0.006386
13.95	1.1616	0.024832	0.007120
15.95	1.2714	0.028656	0.007793
17.95	1.3746	0.032563	0.008426
19.95	1.4712	0.036568	0.009017
24.86	1.6873	0.046752	0.010342
29.87	1.8906	0.057738	0.011588
34.86	2.0789	0.069402	0.012743
39.86	2.2709	0.082282	0.013919
44.70	2.4516	0.095337	0.015027
49.69	2.6402	0.110017	0.016183
54.70	2.8376	0.126182	0.017393
59.69	3.0361	0.144182	0.018609
69.69	3.4490	0.188275	0.021141
60.06	3.1056	0.145794	0.019036
40.06	2.3002	0.082695	0.014099

Table E.34.: CNT and CO_2 with 30 min equilibration time per data point continued

p [bar]	X [mmolg^{-1}]	ρ_{meas} [gcm^{-3}]	Δm_{meas} [g]
20.06	1.4800	0.036733	0.009071
10.06	0.9235	0.017590	0.005660
7.06	0.7118	0.012196	0.004363
5.06	0.5548	0.008670	0.003401
3.07	0.3812	0.005204	0.002336
1.10	0.1944	0.001848	0.001192
3. cycle			
1.06	0.1894	0.001799	0.001161
1.95	0.2832	0.003318	0.001736
2.96	0.3709	0.005022	0.002273
3.95	0.4535	0.006728	0.002780
5.95	0.6183	0.010228	0.003790
7.95	0.7763	0.013795	0.004758
9.95	0.9166	0.017412	0.005618
11.95	1.0436	0.021092	0.006397
13.95	1.1621	0.024862	0.007123
15.95	1.2746	0.028701	0.007813
17.95	1.3779	0.032614	0.008446
19.95	1.4746	0.036607	0.009039
24.86	1.6895	0.046795	0.010356
29.86	1.8923	0.057787	0.011599
34.86	2.0828	0.069465	0.012766
39.86	2.2733	0.082354	0.013934
44.69	2.4546	0.095416	0.015046
49.69	2.6430	0.110106	0.016200
54.69	2.8383	0.126279	0.017397
59.69	3.0418	0.144337	0.018644
69.69	3.4548	0.188446	0.021176
60.06	3.1084	0.145886	0.019053
40.06	2.3004	0.082715	0.014100
20.06	1.4828	0.036743	0.009088

Table E.34.: CNT and CO_2 with 30 min equilibration time per data point continued

p [bar]	X [mmolg^{-1}]	ρ_{meas} [gcm^{-3}]	Δm_{meas} [g]
10.06	0.9251	0.017586	0.005670
7.06	0.7130	0.012189	0.004370
5.06	0.5547	0.008658	0.003400
3.07	0.3830	0.005194	0.002347
1.10	0.1937	0.001828	0.001187
4. cycle			
1.06	0.1910	0.001786	0.001171
1.95	0.2848	0.003302	0.001746
2.96	0.3722	0.005002	0.002281
3.95	0.4546	0.006706	0.002786
5.95	0.6200	0.010211	0.003800
7.95	0.7766	0.013772	0.004760
9.95	0.9172	0.017395	0.005622
11.95	1.0442	0.021076	0.006401
13.95	1.1632	0.024843	0.007130
15.95	1.2748	0.028681	0.007814
17.95	1.3775	0.032599	0.008443
19.95	1.4738	0.036590	0.009034
24.87	1.6878	0.046786	0.010345
29.86	1.8918	0.057774	0.011595
34.86	2.0815	0.069460	0.012759
39.86	2.2748	0.082367	0.013943
44.69	2.4533	0.095434	0.015037
49.69	2.6423	0.110144	0.016196
54.69	2.8390	0.126357	0.017402
59.69	3.0397	0.144432	0.018631
69.69	3.4537	0.188763	0.021169
60.06	3.1108	0.146076	0.019067
40.06	2.3004	0.082819	0.014100
20.06	1.4803	0.036790	0.009074
10.06	0.9247	0.017628	0.005668

Table E.34.: CNT and CO_2 with 30 min equilibration time per data point continued

p [bar]	X [mmolg^{-1}]	ρ_{meas} [gcm^{-3}]	Δm_{meas} [g]
7.07	0.7132	0.012226	0.004371
5.07	0.5563	0.008690	0.003410
3.07	0.3833	0.005215	0.002349
1.10	0.1948	0.001847	0.001194
5. cycle			
1.06	0.1909	0.001802	0.001170
1.96	0.2858	0.003326	0.001752
2.96	0.3750	0.005025	0.002298
3.95	0.4560	0.006731	0.002795
5.95	0.6219	0.010233	0.003812
7.95	0.7784	0.013800	0.004771
9.95	0.9197	0.017418	0.005637
11.95	1.0461	0.021095	0.006412
13.95	1.1663	0.024867	0.007149
15.95	1.2774	0.028704	0.007830
17.95	1.3805	0.032618	0.008461
19.95	1.4762	0.036608	0.009048
24.87	1.6899	0.046813	0.010358
29.87	1.8944	0.057806	0.011612
34.87	2.0853	0.069504	0.012782
39.87	2.2755	0.082379	0.013948
44.70	2.4556	0.095463	0.015052
49.70	2.6461	0.110165	0.016219
54.70	2.8420	0.126322	0.017420
59.70	3.0414	0.144341	0.018642
69.70	3.4493	0.188451	0.021142
60.06	3.1088	0.145918	0.019055
40.06	2.3017	0.082742	0.014108
20.06	1.4832	0.036751	0.009091
10.06	0.9250	0.017596	0.005669
7.07	0.7140	0.012206	0.004376

Table E.34.: CNT and CO_2 with 30 min equilibration time per data point continued

p [bar]	X [mmolg^{-1}]	ρ_{meas} [gcm^{-3}]	Δm_{meas} [g]
5.07	0.5564	0.008678	0.003410
3.07	0.3834	0.005212	0.002350
1.09	0.1952	0.001848	0.001197
6. cycle			
1.06	0.1917	0.001810	0.001175
1.96	0.2854	0.003338	0.001749
2.96	0.3736	0.005036	0.002290
3.95	0.4548	0.006746	0.002788
5.95	0.6207	0.010247	0.003804
7.95	0.7769	0.013820	0.004762
9.95	0.9192	0.017451	0.005634
11.95	1.0460	0.021140	0.006412
13.95	1.1654	0.024912	0.007143
15.95	1.2765	0.028740	0.007824
17.95	1.3803	0.032659	0.008460
19.95	1.4770	0.036649	0.009053
24.87	1.6918	0.046848	0.010370
29.87	1.8945	0.057846	0.011612
34.86	2.0854	0.069539	0.012782
39.87	2.2788	0.082463	0.013968
44.69	2.4560	0.095534	0.015054
49.70	2.6464	0.110267	0.016221
54.70	2.8445	0.126484	0.017435
59.70	3.0472	0.144572	0.018678
69.69	3.4626	0.188947	0.021223
60.06	3.1164	0.146158	0.019102
40.06	2.3059	0.082827	0.014134
20.06	1.4862	0.036780	0.009110
10.06	0.9273	0.017608	0.005684
7.06	0.7148	0.012208	0.004382
5.07	0.5575	0.008676	0.003417

Table E.34.: CNT and CO_2 with 30 min equilibration time per data point continued

p [bar]	X [mmolg^{-1}]	ρ_{meas} [gcm^{-3}]	Δm_{meas} [g]
3.07	0.3848	0.005207	0.002359
1.09	0.1951	0.001841	0.001196
7. cycle			
1.06	0.1913	0.001798	0.001172
1.96	0.2859	0.003327	0.001752
2.96	0.3745	0.005021	0.002296
3.95	0.4551	0.006729	0.002790
5.95	0.6215	0.010226	0.003810
7.95	0.7776	0.013800	0.004766
9.95	0.9185	0.017416	0.005630
11.95	1.0465	0.021103	0.006415
13.95	1.1651	0.024865	0.007141
15.95	1.2760	0.028709	0.007821
17.95	1.3790	0.032628	0.008452
19.95	1.4756	0.036624	0.009045
24.86	1.6902	0.046821	0.010360
29.86	1.8924	0.057818	0.011599
34.86	2.0839	0.069518	0.012773
39.86	2.2749	0.082419	0.013944
44.69	2.4575	0.095509	0.015063
49.69	2.6472	0.110234	0.016226
54.69	2.8431	0.126425	0.017427
59.69	3.0473	0.144507	0.018678
69.69	3.4567	0.188849	0.021187
60.06	3.1123	0.146143	0.019076
40.06	2.3045	0.082849	0.014125
20.06	1.4842	0.036798	0.009097
10.06	0.9269	0.017630	0.005681
7.06	0.7144	0.012227	0.004379
5.07	0.5578	0.008696	0.003419
3.06	0.3843	0.005223	0.002356

Table E.34.: CNT and CO_2 with 30 min equilibration time per data point continued

p [bar]	X [mmolg^{-1}]	ρ_{meas} [gcm^{-3}]	Δm_{meas} [g]
1.10	0.1952	0.001856	0.001196
8. cycle			
1.06	0.1916	0.001812	0.001174
1.96	0.2858	0.003335	0.001752
2.96	0.3747	0.005030	0.002297
3.95	0.4563	0.006739	0.002797
5.95	0.6218	0.010238	0.003811
7.95	0.7781	0.013805	0.004769
9.95	0.9195	0.017425	0.005636
11.95	1.0469	0.021109	0.006417
13.95	1.1664	0.024882	0.007149
15.95	1.2774	0.028714	0.007830
17.95	1.3804	0.032626	0.008461
19.95	1.4766	0.036617	0.009051
24.86	1.6921	0.046825	0.010372
29.86	1.8942	0.057814	0.011611
34.86	2.0864	0.069518	0.012788
39.86	2.2768	0.082409	0.013956
44.69	2.4590	0.095495	0.015072
49.70	2.6469	0.110204	0.016224
54.70	2.8414	0.126393	0.017416
59.69	3.0438	0.144455	0.018656
69.69	3.4561	0.188673	0.021184
60.06	3.1120	0.146047	0.019075
40.06	2.3016	0.082805	0.014107
20.06	1.4835	0.036779	0.009093
10.06	0.9259	0.017614	0.005675
7.07	0.7139	0.012220	0.004376
5.07	0.5569	0.008691	0.003413
3.06	0.3831	0.005219	0.002348
1.09	0.1955	0.001856	0.001198

Table E.34.: CNT and CO_2 with 30 min equilibration time per data point continued

p [bar]	X [mmolg^{-1}]	ρ_{meas} [gcm^{-3}]	Δm_{meas} [g]
9. cycle			
1.06	0.1922	0.001813	0.001178
1.96	0.2849	0.003338	0.001746
2.96	0.3745	0.005039	0.002295
3.95	0.4558	0.006749	0.002794
5.95	0.6202	0.010244	0.003801
7.95	0.7773	0.013819	0.004764
9.95	0.9191	0.017447	0.005634
11.95	1.0474	0.021135	0.006420
13.95	1.1659	0.024906	0.007146
15.95	1.2768	0.028745	0.007826
17.95	1.3803	0.032652	0.008460
19.95	1.4772	0.036648	0.009055
24.86	1.6924	0.046856	0.010374
29.86	1.8951	0.057856	0.011616
34.86	2.0869	0.069565	0.012791
39.86	2.2796	0.082489	0.013973
44.69	2.4599	0.095580	0.015078
49.70	2.6504	0.110314	0.016245
54.70	2.8462	0.126540	0.017446
59.69	3.0496	0.144651	0.018692
69.69	3.4607	0.188985	0.021212
60.06	3.1163	0.146201	0.019101
40.06	2.3038	0.082854	0.014121
20.06	1.4852	0.036794	0.009103
10.06	0.9281	0.017618	0.005689
7.06	0.7155	0.012218	0.004386
5.07	0.5579	0.008688	0.003419
3.06	0.3851	0.005215	0.002360
1.09	0.1968	0.001850	0.001206

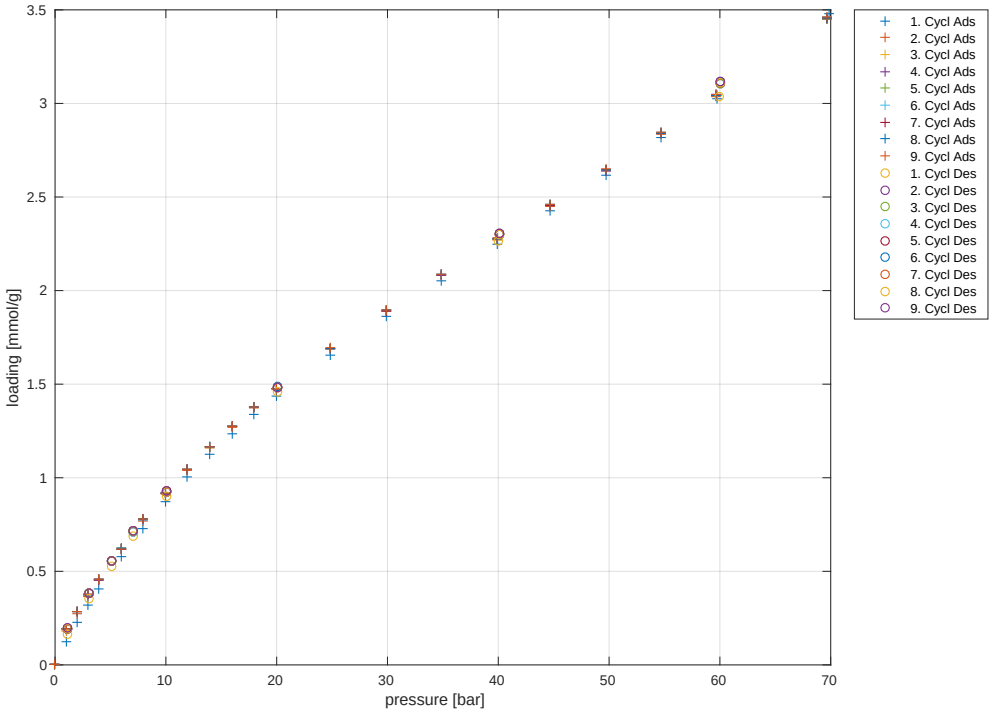

Figure E.40.: CNT and CO_2 at $40\,^{\circ}\mathrm{C}$ 9 cycles with $30\,\mathrm{min}$ equilibration time per data point

E.1.25 CNT and CO_2 at 40 °C cycling experiment with 2 h equilibration time

Table E.35.: CNT and CO_2 at 40 °C 9 cycles with 2 h equilibration time per data point

sample:	CNT		
gas:	CO_2		
temperature in [°C]:	41.9	+0.5	-0.1
$m_{S,meas}$ in [mg]:	139.38		
V_S in [cm^3]:	0.062038		

p [bar]	X [$mmolg^{-1}$]	ρ_{meas} [gcm^{-3}]	Δm_{meas} [g]
1. cycle			
0.00	0.0000	0.000000	0.000000
0.98	0.1261	0.001637	0.000773
1.95	0.2248	0.003288	0.001378
2.95	0.3186	0.004993	0.001953
3.95	0.4075	0.006712	0.002498
5.95	0.5757	0.010206	0.003529
7.95	0.7299	0.013754	0.004474
9.95	0.8732	0.017388	0.005352
11.95	1.0038	0.021072	0.006153
13.95	1.1241	0.024832	0.006890
15.95	1.2363	0.028671	0.007578
17.95	1.3403	0.032574	0.008215
19.95	1.4382	0.036551	0.008815
24.87	1.6572	0.046748	0.010158
29.87	1.8606	0.057719	0.011405
34.87	2.0527	0.069377	0.012582
39.88	2.2461	0.082237	0.013768
44.72	2.4276	0.095277	0.014880
49.71	2.6176	0.109932	0.016044
54.72	2.8153	0.126099	0.017256
59.73	3.0233	0.144160	0.018531
69.83	3.4792	0.188704	0.021325
59.94	3.0381	0.145089	0.018622

Table E.35.: CNT and CO_2 with 2 h equilibration time per data point continued

p [bar]	X [mmolg^{-1}]	ρ_{meas} [gcm^{-3}]	Δm_{meas} [g]
39.97	2.2649	0.082601	0.013883
20.04	1.4597	0.036737	0.008947
10.06	0.9023	0.017571	0.005531
7.07	0.6864	0.012161	0.004207
5.06	0.5281	0.008636	0.003237
3.06	0.3547	0.005171	0.002174
1.07	0.1629	0.001767	0.000999
2. cycle			
1.07	0.1614	0.001774	0.000989
1.95	0.2487	0.003290	0.001524
2.95	0.3408	0.005000	0.002089
3.95	0.4292	0.006725	0.002631
5.95	0.5955	0.010204	0.003650
7.95	0.7491	0.013757	0.004592
9.95	0.8902	0.017374	0.005456
11.95	1.0207	0.021054	0.006256
13.95	1.1406	0.024821	0.006991
15.95	1.2518	0.028654	0.007673
17.95	1.3554	0.032560	0.008308
19.95	1.4521	0.036541	0.008900
24.86	1.6680	0.046737	0.010224
29.87	1.8709	0.057737	0.011467
34.87	2.0631	0.069433	0.012646
39.88	2.2573	0.082351	0.013836
44.72	2.4395	0.095396	0.014952
49.73	2.6304	0.110072	0.016123
54.73	2.8256	0.126210	0.017319
59.75	3.0333	0.144266	0.018592
69.84	3.4924	0.188877	0.021406
59.93	3.0463	0.145128	0.018672
39.95	2.2700	0.082554	0.013914

Table E.35.: CNT and CO_2 with 2 h equilibration time per data point continued

p [bar]	X [mmolg^{-1}]	ρ_{meas} [gcm^{-3}]	Δm_{meas} [g]
20.04	1.4655	0.036743	0.008982
10.06	0.9075	0.017590	0.005562
7.06	0.6921	0.012195	0.004242
5.06	0.5319	0.008678	0.003260
3.06	0.3583	0.005222	0.002196
1.07	0.1661	0.001795	0.001018
3. cycle			
1.07	0.1653	0.001782	0.001013
1.95	0.2546	0.003286	0.001561
2.95	0.3471	0.004990	0.002128
3.95	0.4355	0.006709	0.002670
5.95	0.6011	0.010190	0.003684
7.95	0.7541	0.013746	0.004622
9.95	0.8941	0.017383	0.005481
11.95	1.0246	0.021094	0.006280
13.95	1.1450	0.024865	0.007018
15.95	1.2561	0.028687	0.007699
17.95	1.3589	0.032589	0.008329
19.95	1.4559	0.036574	0.008924
24.87	1.6742	0.046765	0.010262
29.88	1.8763	0.057733	0.011501
34.88	2.0674	0.069412	0.012672
39.88	2.2605	0.082319	0.013855
44.72	2.4416	0.095388	0.014966
49.71	2.6321	0.110070	0.016134
54.72	2.8292	0.126297	0.017342
59.73	3.0388	0.144410	0.018626
69.83	3.4949	0.189250	0.021422
59.93	3.0548	0.145465	0.018724
39.96	2.2745	0.082704	0.013941
20.04	1.4699	0.036789	0.009010

Table E.35.: CNT and CO_2 with 2 h equilibration time per data point continued

p [bar]	X [mmolg^{-1}]	ρ_{meas} [gcm^{-3}]	Δm_{meas} [g]
10.06	0.9121	0.017609	0.005591
7.07	0.6967	0.012198	0.004271
5.07	0.5356	0.008679	0.003283
3.07	0.3628	0.005212	0.002224
1.07	0.1700	0.001805	0.001042
4. cycle			
1.07	0.1688	0.001803	0.001035
1.95	0.2575	0.003311	0.001578
2.95	0.3495	0.005016	0.002142
3.95	0.4378	0.006744	0.002683
5.95	0.6040	0.010241	0.003702
7.95	0.7576	0.013797	0.004644
9.95	0.8996	0.017422	0.005514
11.95	1.0310	0.021116	0.006320
13.95	1.1507	0.024868	0.007053
15.95	1.2615	0.028706	0.007732
17.95	1.3644	0.032610	0.008363
19.95	1.4611	0.036601	0.008956
24.87	1.6789	0.046809	0.010291
29.87	1.8816	0.057805	0.011533
34.87	2.0735	0.069492	0.012709
39.88	2.2663	0.082405	0.013891
44.72	2.4480	0.095480	0.015005
49.72	2.6388	0.110172	0.016174
54.73	2.8373	0.126363	0.017391
59.74	3.0440	0.144419	0.018658
69.83	3.4988	0.189064	0.021446
59.94	3.0555	0.145293	0.018728
39.95	2.2764	0.082577	0.013953
20.03	1.4723	0.036761	0.009024
10.06	0.9154	0.017601	0.005611

Table E.35.: CNT and CO_2 with 2 h equilibration time per data point continued

p [bar]	X [mmolg^{-1}]	ρ_{meas} [gcm^{-3}]	Δm_{meas} [g]
7.07	0.6988	0.012195	0.004283
5.06	0.5392	0.008669	0.003305
3.07	0.3657	0.005201	0.002241
1.07	0.1741	0.001789	0.001067
5. cycle			
1.07	0.1738	0.001788	0.001065
1.96	0.2616	0.003293	0.001604
2.95	0.3538	0.004994	0.002169
3.95	0.4420	0.006711	0.002709
5.95	0.6080	0.010203	0.003727
7.95	0.7611	0.013762	0.004665
9.95	0.9024	0.017388	0.005531
11.95	1.0326	0.021088	0.006329
13.95	1.1522	0.024844	0.007062
15.95	1.2624	0.028677	0.007738
17.95	1.3659	0.032581	0.008372
19.95	1.4633	0.036565	0.008969
24.87	1.6804	0.046757	0.010300
29.87	1.8828	0.057727	0.011540
34.88	2.0746	0.069408	0.012716
39.88	2.2676	0.082279	0.013899
44.71	2.4471	0.095316	0.014999
49.72	2.6376	0.110018	0.016167
54.73	2.8363	0.126214	0.017385
59.74	3.0426	0.144284	0.018649
69.83	3.4981	0.188970	0.021442
59.93	3.0567	0.145254	0.018736
39.95	2.2791	0.082615	0.013970
20.03	1.4751	0.036759	0.009042
10.06	0.9180	0.017594	0.005627
7.06	0.7018	0.012187	0.004302

Table E.35.: CNT and CO_2 with 2 h equilibration time per data point continued

p [bar]	X [mmolg^{-1}]	ρ_{meas} [gcm^{-3}]	Δm_{meas} [g]
5.06	0.5420	0.008658	0.003322
3.07	0.3698	0.005192	0.002267
1.07	0.1773	0.001790	0.001087
6. cycle			
1.07	0.1743	0.001792	0.001068
1.95	0.2634	0.003300	0.001614
2.95	0.3563	0.005007	0.002184
3.95	0.4445	0.006733	0.002724
5.95	0.6107	0.010230	0.003744
7.95	0.7640	0.013770	0.004683
9.95	0.9054	0.017387	0.005549
11.95	1.0361	0.021086	0.006351
13.95	1.1551	0.024834	0.007080
15.95	1.2666	0.028672	0.007763
17.95	1.3690	0.032586	0.008391
19.95	1.4657	0.036586	0.008984
24.87	1.6839	0.046809	0.010322
29.87	1.8859	0.057807	0.011560
34.87	2.0783	0.069516	0.012739
39.88	2.2723	0.082456	0.013928
44.72	2.4532	0.095543	0.015037
49.72	2.6451	0.110245	0.016213
54.73	2.8431	0.126436	0.017426
59.75	3.0506	0.144500	0.018698
69.84	3.5066	0.189193	0.021494
59.93	3.0601	0.145312	0.018757
39.95	2.2809	0.082652	0.013981
20.03	1.4772	0.036793	0.009055
10.06	0.9195	0.017632	0.005636
7.06	0.7038	0.012230	0.004314
5.07	0.5441	0.008710	0.003335

Table E.35.: CNT and CO_2 with 2 h equilibration time per data point continued

p [bar]	X [mmolg^{-1}]	ρ_{meas} [gcm^{-3}]	Δm_{meas} [g]
3.06	0.3708	0.005227	0.002273
1.07	0.1794	0.001811	0.001100
7. cycle			
1.07	0.1778	0.001807	0.001090
1.95	0.2669	0.003309	0.001636
2.96	0.3592	0.005020	0.002202
3.95	0.4470	0.006738	0.002740
5.95	0.6122	0.010231	0.003752
7.95	0.7662	0.013782	0.004696
9.95	0.9074	0.017419	0.005562
11.95	1.0379	0.021120	0.006362
13.95	1.1574	0.024891	0.007094
15.95	1.2679	0.028725	0.007772
17.95	1.3715	0.032628	0.008406
19.95	1.4690	0.036602	0.009004
24.87	1.6865	0.046804	0.010337
29.88	1.8884	0.057787	0.011575
34.87	2.0805	0.069461	0.012752
39.88	2.2703	0.082366	0.013915
44.71	2.4534	0.095441	0.015038
49.71	2.6434	0.110158	0.016202
54.72	2.8420	0.126397	0.017420
59.73	3.0501	0.144529	0.018696
69.83	3.5063	0.189381	0.021492
59.95	3.0677	0.145570	0.018803
39.96	2.2862	0.082722	0.014013
20.03	1.4800	0.036797	0.009071
10.06	0.9229	0.017618	0.005657
7.06	0.7061	0.012200	0.004328
5.07	0.5476	0.008667	0.003357
3.06	0.3746	0.005199	0.002296

Table E.35.: CNT and CO_2 with 2 h equilibration time per data point continued

p [bar]	X [mmolg^{-1}]	ρ_{meas} [gcm^{-3}]	Δm_{meas} [g]
1.07	0.1825	0.001798	0.001118
8. cycle			
1.07	0.1802	0.001804	0.001105
1.95	0.2682	0.003312	0.001644
2.95	0.3614	0.005033	0.002215
3.95	0.4483	0.006758	0.002748
5.95	0.6154	0.010231	0.003772
7.95	0.7695	0.013780	0.004717
9.95	0.9104	0.017400	0.005581
11.95	1.0398	0.021074	0.006373
13.95	1.1597	0.024837	0.007108
15.95	1.2708	0.028666	0.007789
17.95	1.3731	0.032578	0.008416
19.95	1.4700	0.036574	0.009011
24.87	1.6879	0.046787	0.010346
29.88	1.8895	0.057780	0.011582
34.88	2.0823	0.069472	0.012763
39.88	2.2751	0.082371	0.013945
44.73	2.4570	0.095438	0.015060
49.73	2.6478	0.110114	0.016229
54.74	2.8440	0.126254	0.017432
59.75	3.0491	0.144251	0.018689
69.84	3.5047	0.188801	0.021482
59.93	3.0610	0.145114	0.018762
39.95	2.2840	0.082554	0.014000
20.03	1.4809	0.036754	0.009077
10.06	0.9242	0.017601	0.005665
7.06	0.7090	0.012190	0.004346
5.07	0.5488	0.008667	0.003364
3.06	0.3775	0.005193	0.002314
1.07	0.1854	0.001782	0.001136

Table E.35.: CNT and CO_2 with 2 h equilibration time per data point continued

p [bar]	X [mmolg^{-1}]	ρ_{meas} [gcm^{-3}]	Δm_{meas} [g]
9. cycle			
1.07	0.1841	0.001780	0.001129
1.95	0.2720	0.003284	0.001667
2.95	0.3639	0.004985	0.002230
3.95	0.4520	0.006710	0.002770
5.95	0.6178	0.010203	0.003787
7.95	0.7700	0.013754	0.004720
9.95	0.9108	0.017373	0.005583
11.95	1.0407	0.021064	0.006379
13.95	1.1610	0.024827	0.007116
15.95	1.2716	0.028655	0.007794
17.95	1.3744	0.032564	0.008424
19.95	1.4708	0.036551	0.009015
24.87	1.6882	0.046742	0.010347
29.87	1.8905	0.057716	0.011588
34.88	2.0819	0.069398	0.012761
39.88	2.2743	0.082269	0.013940
44.72	2.4555	0.095328	0.015051
49.72	2.6464	0.110021	0.016221
54.72	2.8436	0.126203	0.017429
59.74	3.0502	0.144257	0.018696
69.83	3.5049	0.188875	0.021483
59.94	3.0619	0.145173	0.018768
39.95	2.2841	0.082575	0.014000
20.03	1.4827	0.036750	0.009088
10.06	0.9257	0.017591	0.005674
7.06	0.7098	0.012184	0.004351
5.06	0.5512	0.008654	0.003378
3.06	0.3783	0.005192	0.002319
1.07	0.1873	0.001790	0.001148

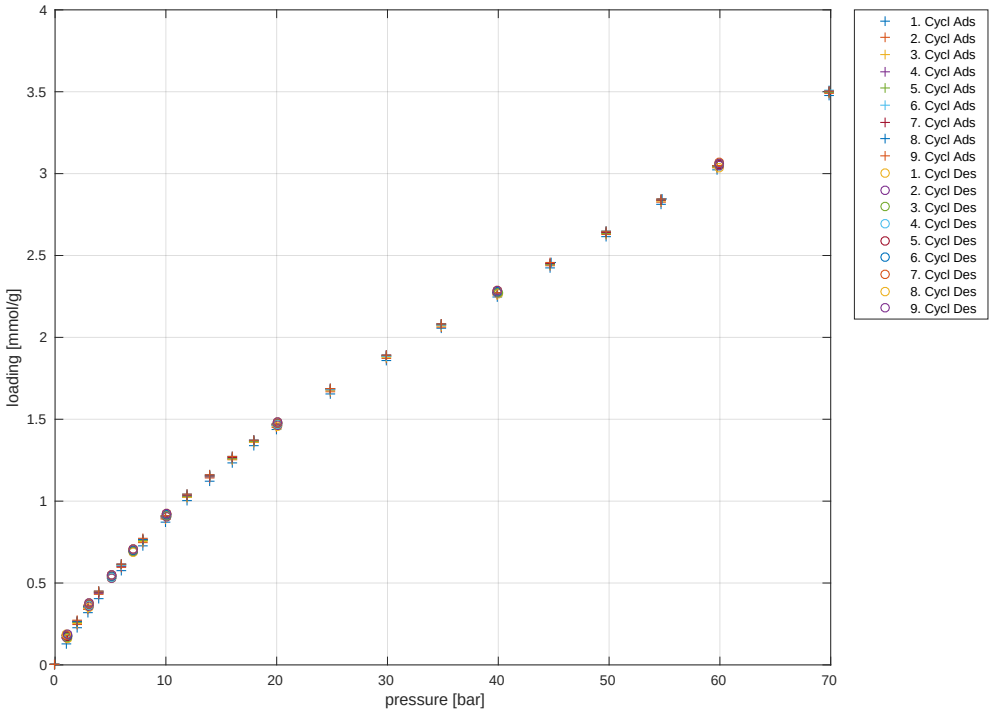

Figure E.41.: CNT and CO_2 at $40\,^{\circ}\mathrm{C}$ 9 cycles with $2\,\mathrm{h}$ equilibration time per data point

Table E.36.: Model fit parameter for CNT data and CO_2 - Langmuir and Freundlich model

Adsorption - Langmuir model						
T [°C]	k_L	k_L min	k_L max	q_max	q_max min	q_max max
0	0.0563	0.0089	0.0089	5.0238	0.4597	0.4597
25	0.0167	0.0062	0.0062	7.6278	1.9737	1.9737
50	0.0208	0.0019	0.0019	4.7248	0.2654	0.2654
50	0.0201	0.0019	0.0019	4.8830	0.2932	0.2932
75	0.0187	0.0008	0.0008	3.8191	0.1082	0.1082
Desorption - Langmuir model						
T [°C]	k_L	k_L min	k_L max	q_max	q_max min	q_max max
0	0.0422	0.0250	0.0594	5.8478	4.3391	7.3565
25	-0.0841	-0.1738	0.0057	0.1443	-1.0321	1.3207
50	0.0319	0.0197	0.0442	3.7883	2.9523	4.6242
50	0.0264	0.0199	0.0330	4.2135	3.5780	4.8490
75	0.0234	0.0175	0.0293	3.3686	2.8475	3.8897
Adsorption - Freundlich model						
T [°C]	K	K min	K max	n	n min	n max
0	0.3766	0.0313	0.0313	0.6641	0.0317	0.0317
25	0.1966	0.0456	0.0456	0.7510	0.0713	0.0713
50	0.1644	0.0124	0.0124	0.6964	0.0219	0.0219
50	0.1686	0.0127	0.0127	0.6937	0.0219	0.0219
75	0.1231	0.0114	0.0114	0.7006	0.0268	0.0268
Desorption - Freundlich model						
T [°C]	K	K min	K max	n	n min	n max
0	0.3230	0.0382	0.0382	0.7098	0.0443	0.0443
25						
50	0.2008	0.0159	0.0159	0.6451	0.0244	0.0244
50	0.1761	0.0198	0.0198	0.6853	0.0345	0.0345
75	0.1394	0.0162	0.0162	0.6696	0.0349	0.0349

Table E.37.: Model fit parameter for CNT data and CO_2 - BET and DR model

Adsorption - BET model						
T [°C]	K_BET	K_BET min	K_BET max	q_max_BET	q_max_BET max	q_max_BET min
0	7.2897	1.6490	1.6490	1.7292	0.1486	0.1486
25	6.6040	6.6040	-6.6040	1.7629	1.7629	-1.7629
50	6.0936	0.4317	0.4317	1.4531	0.0430	0.0430
50	6.1075	0.4820	0.4820	1.4723	0.0484	0.0484
75	5.4234	0.3062	0.3062	1.1373	0.0283	0.0283
Desorption - BET model						
T [°C]	K_BET	K_BET min	K_BET max	q_max_BET	q_max_BET max	q_max_BET min
0	6.8251	4.9461	4.9461	1.6355	0.4405	0.4405
25						
50	8.0941	0.4698	0.4698	1.3759	0.0309	0.0309
50	6.9731	0.8238	0.8238	1.4287	0.0697	0.0697
75	9.5372	2.3592	2.3592	0.9406	0.0569	0.0569
Adsorption - DR model						
T [°C]	k_DR	k_DR min	k_DR max	q_s	q_s min	q_s max
0	213.8202	54.9594	54.9594	3.1558	0.3935	0.3935
25	516.8250	110.9067	110.9067	3.8869	0.5398	0.5398
50	263.2308	56.4785	56.4785	1.8928	0.2528	0.2528
50	262.9459	55.2367	55.2367	1.9183	0.2508	0.2508
75	277.5311	61.9648	61.9648	1.4552	0.2103	0.2103
Desorption - DR model						
T [°C]	k_DR	k_DR min	k_DR max	q_s	q_s min	q_s max
0	252.5850	179.3072	179.3072	3.3874	1.4474	1.4474
25						
50	245.5740	137.8248	137.8248	1.9676	0.7574	0.7574
50	262.6356	137.1946	137.1946	2.0144	0.7550	0.7550
75	357.1483	81.1074	81.1074	1.8605	0.2584	0.2584

Table E.38.: Model fit parameter for CNT data and CO_2 - Temkin and Tóth model

Adsorption - Temkin model									
T [°C]	A_T	A_T min	A_T max	RTb_T	RTb_T max	RTb_T min			
0									
25									
50									
50									
75									
Desorption - Temkin model									
T [°C]	A_T	A_T min	A_T max	RTb_T	RTb_T max	RTb_T min			
0									
25									
50									
50									
75									
Adsorption - Tóth model									
T [°C]	K_T	K_T min	K_T max	a_T	a_T min	a_T max	t	t min	tmax
0									
25									
50	0.3259	0.1237	0.1237	9.9707	4.4062	4.4062	2.1802	0.4396	0.4396
50	0.4707	0.1913	0.1913	14.0172	4.5829	4.5829	1.8420	0.3223	0.3223
75	0.1729	0.0484	0.0484	8.2325	3.8663	3.8663	2.7711	0.5353	0.5353
Desorption - Tóth model									
T [°C]	K_T	K_T min	K_T max	a_T	a_T min	a_T max	t	t min	tmax
0									
25									
50	0.2266	0.2527	0.2527	1.8974	10.4756	10.4756	2.6546	2.1547	2.1547
50	0.3019	0.6213	0.6213	6.5943	21.6146	21.6146	2.2586	2.6502	2.6502
75	0.2208	0.0509	0.0509	7.1496	3.0581	3.0581	2.3014	0.2876	0.2876

E.2 MWCNT

E.2.1 MWCNT and SO_2 at 25 °C

Table E.39.: MWCNT and SO_2 at 25 °C

sample:	MWCNT		
gas:	SO_2		
temperature in [°C]:	25.1	+0.1	-0.3
$m_{S,meas}$ in [mg]:	95.82		
V_S in [cm^3]:	0.044638		

p [bar]	X [$mmolg^{-1}$]	ρ_{meas} [gcm^{-3}]	Δm_{meas} [g]
0.00	0.0000	0.000000	0.000000
0.15	0.2666	0.000393	0.001637
0.41	0.6958	0.001082	0.004272
0.62	1.0586	0.001616	0.006499
0.89	1.4950	0.002339	0.009179
1.42	2.1494	0.003764	0.013196
1.91	2.6332	0.005081	0.016166
2.32	3.1326	0.006231	0.019233
2.87	4.1114	0.007765	0.025242
3.34	5.9450	0.009157	0.036500
3.73	12.4895	0.010287	0.076680
3.21	5.5787	0.008777	0.034251
2.63	3.7487	0.007110	0.023016
2.12	2.9338	0.005669	0.018012
1.60	2.3681	0.004236	0.014539
1.12	1.8685	0.002910	0.011472
0.95	1.6668	0.002474	0.010234
0.62	1.1567	0.001602	0.007102
0.35	0.6866	0.000905	0.004215

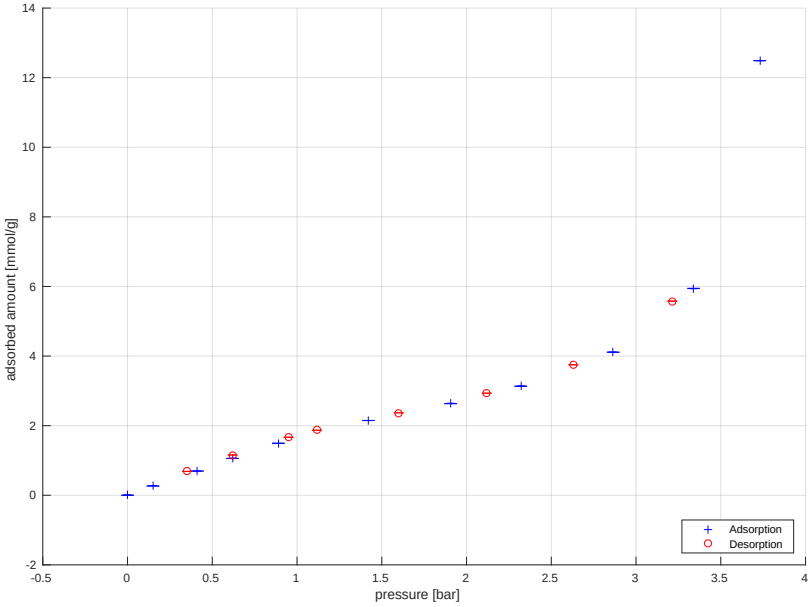

Figure E.42.: MWCNT and SO_2 at 25 °C

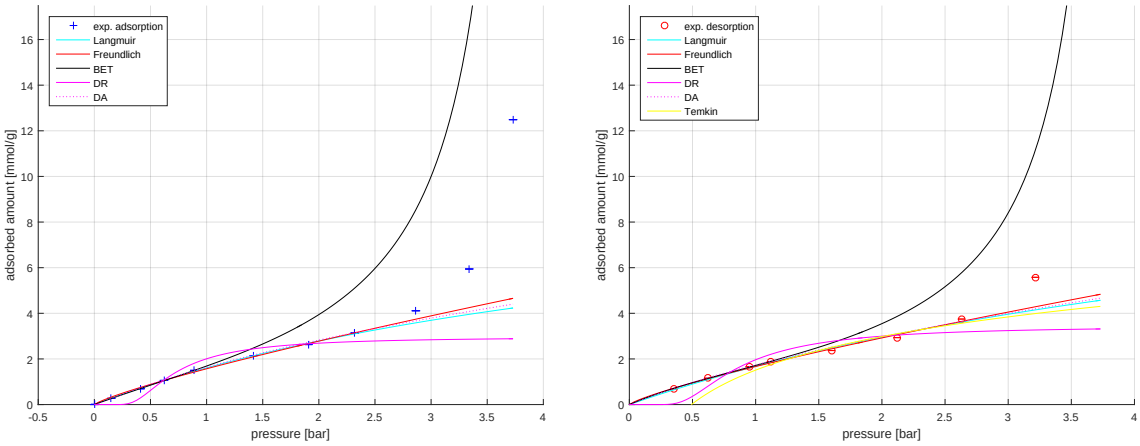

(a) adsorption **(b)** desorption

Figure E.43.: MWCNT and SO_2 at 25 °C data (marks) and fits (lines) adsorption branch (a) and desorption branch (b)

E.2.2 MWCNT and SO_2 at 50 °C

Table E.40.: MWCNT and SO_2 at 50 °C

sample:	MWCNT		
gas:	SO_2		
temperature in [°C]:	50.0	+0.1	-0.0
$m_{S,meas}$ in [mg]:	95.43		
V_S in [cm^3]:	0.044918		

p [bar]	X [mmolg^{-1}]	ρ_{meas} [gcm^{-3}]	Δm_{meas} [g]
0.00	0.0000	0.000000	0.000000
0.16	0.1627	0.000388	0.000995
0.37	0.3133	0.000904	0.001915
0.74	0.5820	0.001783	0.003558
0.97	0.7780	0.002318	0.004757
1.46	1.1394	0.003535	0.006966
2.06	1.5320	0.005036	0.009366
3.15	2.0804	0.007812	0.012719
4.84	2.9058	0.012295	0.017766
6.14	3.8415	0.015882	0.023486
6.87	4.7489	0.017974	0.029034
7.40	5.9137	0.019543	0.036155
7.91	8.5726	0.021079	0.052411
8.18	13.4891	0.021851	0.082470
7.68	7.3882	0.020344	0.045170
6.90	4.9404	0.018038	0.030205
5.94	3.7335	0.015301	0.022826
4.40	2.7297	0.011073	0.016689
2.83	1.9868	0.006953	0.012147
1.65	1.3320	0.003987	0.008144
1.13	0.9628	0.002726	0.005886
0.92	0.8029	0.002197	0.004909

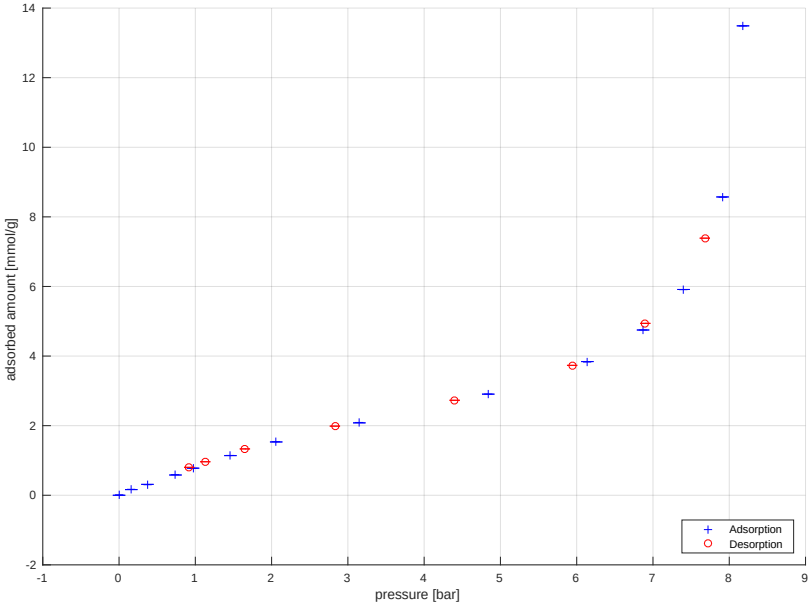

Figure E.44.: MWCNT and SO_2 at 50 °C

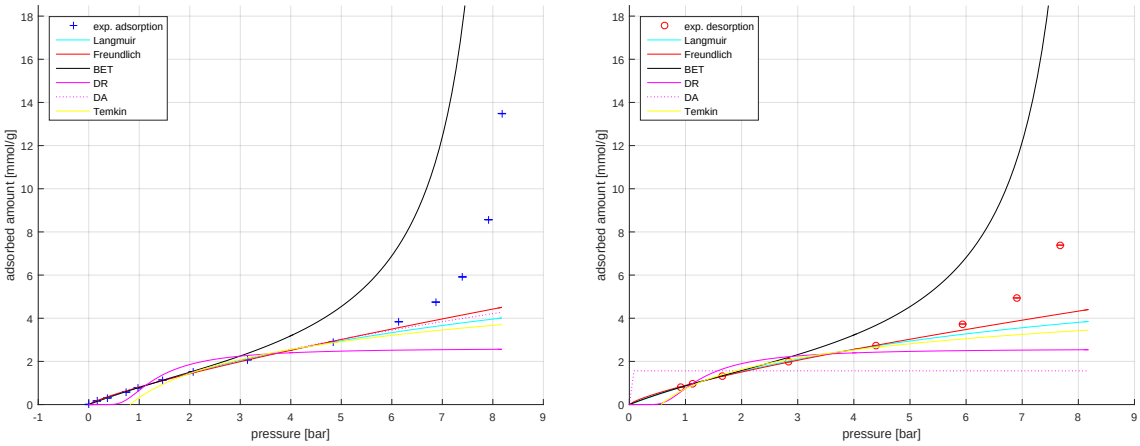

(a) adsorption **(b)** desorption

Figure E.45.: MWCNT and SO_2 at 50 °C data (marks) and fits (lines) adsorption branch (a) and desorption branch (b)

E.2.3 MWCNT and SO_2 at 75 °C

Table E.41.: MWCNT and SO_2 at 75 °C

sample:	MWCNT		
gas:	SO_2		
temperature in [°C]:	74.9	+0.9	-0.3
$m_{S,meas}$ in [mg]:	95.61		
V_S in [cm^3]:	0.041060		

p [bar]	X [$mmolg^{-1}$]	ρ_{meas} [gcm^{-3}]	Δm_{meas} [g]
0.00	0.0000	0.000000	0.000000
0.18	0.0770	0.000387	0.000471
0.52	0.2038	0.001135	0.001248
0.87	0.3258	0.001915	0.001995
1.24	0.4748	0.002724	0.002908
1.84	0.6841	0.004099	0.004191
3.93	1.3681	0.008980	0.008380
6.90	2.1093	0.016297	0.012921
9.81	2.8647	0.023984	0.017548
11.44	3.4450	0.028582	0.021102
12.89	4.1881	0.032850	0.025654
14.04	5.1686	0.036395	0.031660
14.87	6.5141	0.039015	0.039902
15.71	10.8745	0.041769	0.066612
12.40	3.9690	0.031385	0.024312
8.86	2.6636	0.021427	0.016316
7.37	2.2875	0.017514	0.014012
4.90	1.6990	0.011346	0.010407
2.91	1.1157	0.006597	0.006834
0.95	0.4257	0.002119	0.002608

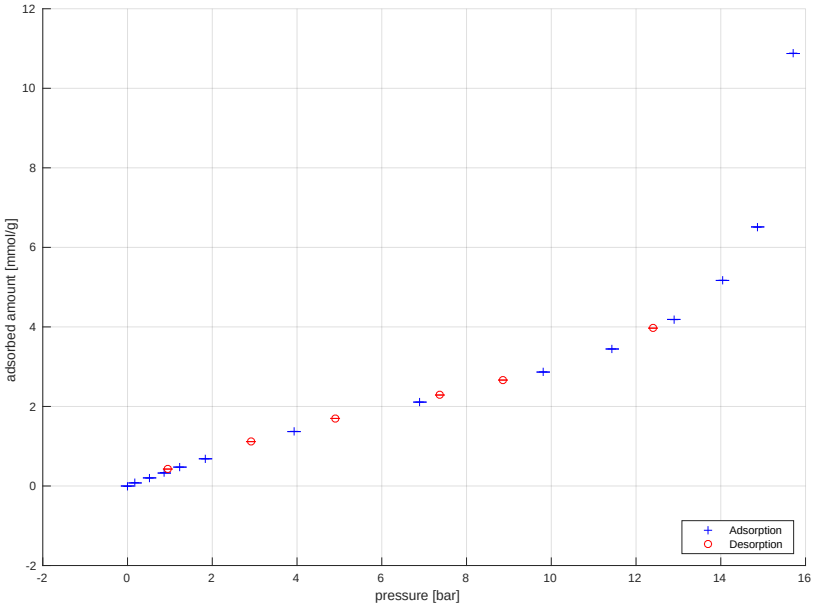

Figure E.46.: MWCNT and SO_2 at 75 °C

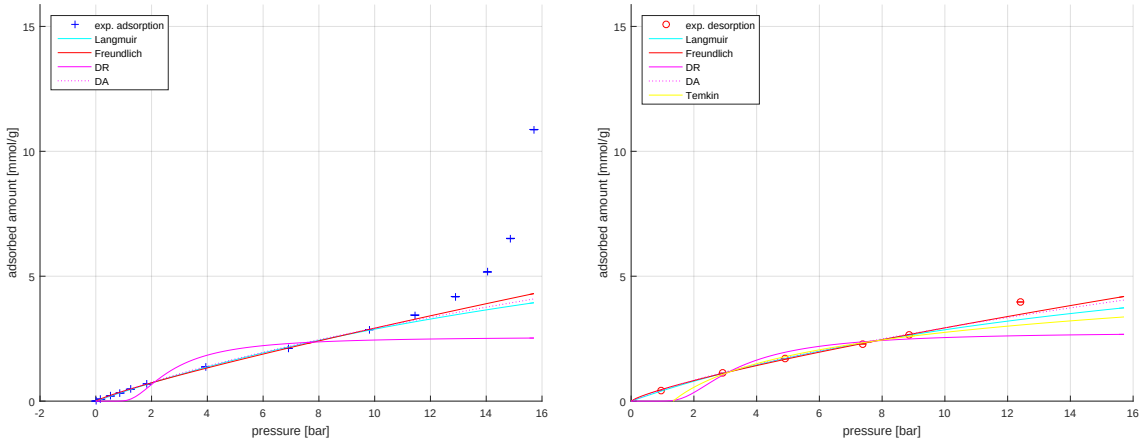

(a) adsorption **(b)** desorption

Figure E.47.: MWCNT and SO_2 at 75 °C data (marks) and fits (lines) adsorption branch (a) and desorption branch (b)

Table E.42.: MWCNT and SO_2 at 100 °C

sample:	MWCNT		
gas:	SO_2		
temperature in [°C]:	99.8	+0.4	-0.2
$m_{S,meas}$ in [mg]:	130.09		
V_S in [cm^3]:	0.059172		

p [bar]	X [$mmolg^{-1}$]	ρ_{meas} [gcm^{-3}]	Δm_{meas} [g]
0.00	0.0000	0.000000	0.000000
0.17	0.0767	0.000369	0.000639
0.61	0.1890	0.001264	0.001574
0.99	0.2818	0.002071	0.002348
2.04	0.5103	0.004280	0.004252
2.99	0.7093	0.006307	0.005910
4.94	1.0931	0.010576	0.009108
7.51	1.5587	0.016401	0.012987
10.00	1.9128	0.022298	0.015938
15.06	2.6146	0.035245	0.021786
20.04	3.5113	0.049553	0.029257
24.90	5.3109	0.065653	0.044252
27.44	10.7524	0.075368	0.089592
19.38	3.4084	0.047574	0.028399
17.21	3.0015	0.041236	0.025010
11.39	2.1471	0.025746	0.017890
7.36	1.5710	0.016053	0.013090
4.59	1.0934	0.009794	0.009111
3.95	0.9683	0.008392	0.008068
2.44	0.6593	0.005127	0.005494
1.08	0.3703	0.002245	0.003085
0.61	0.2612	0.001263	0.002177
0.26	0.1733	0.000550	0.001444

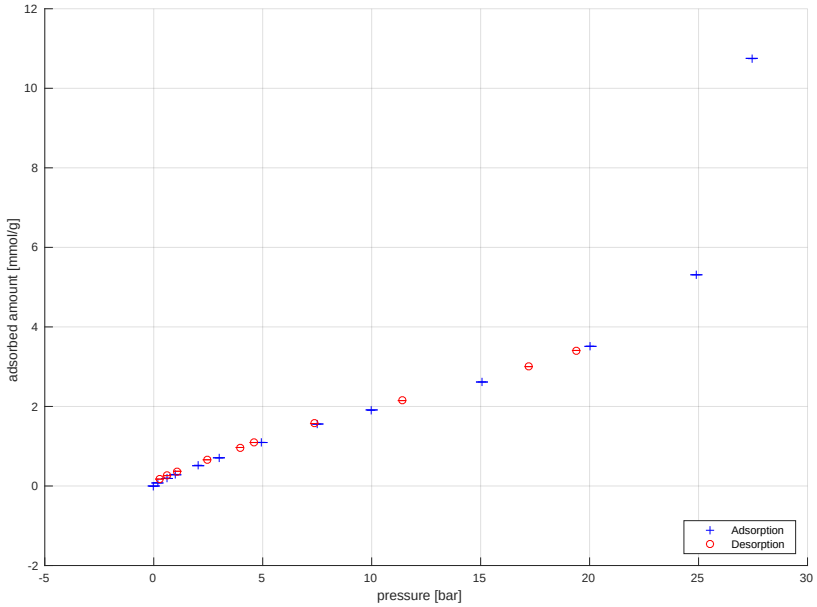

Figure E.48.: MWCNT and SO_2 at 100 °C

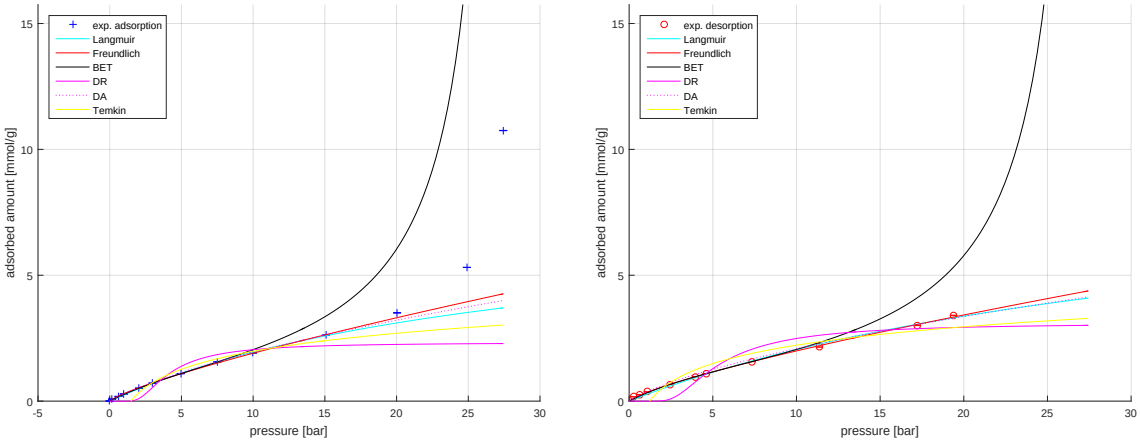

(a) adsorption **(b)** desorption

Figure E.49.: MWCNT and SO_2 at 100 °C data (marks) and fits (lines) adsorption branch (a) and desorption branch (b)

E.2.5 MWCNT and SO_2 at 125 °C

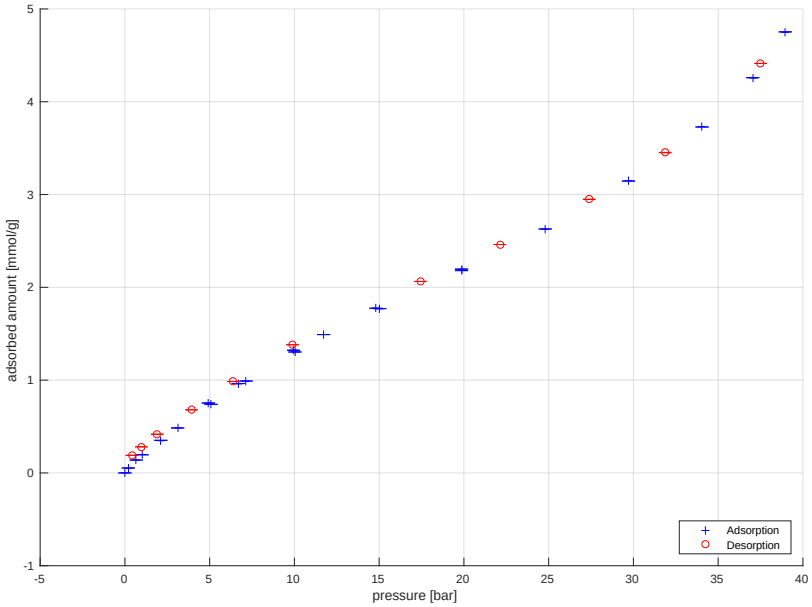

Figure E.50.: MWCNT and SO_2 at 125 °C

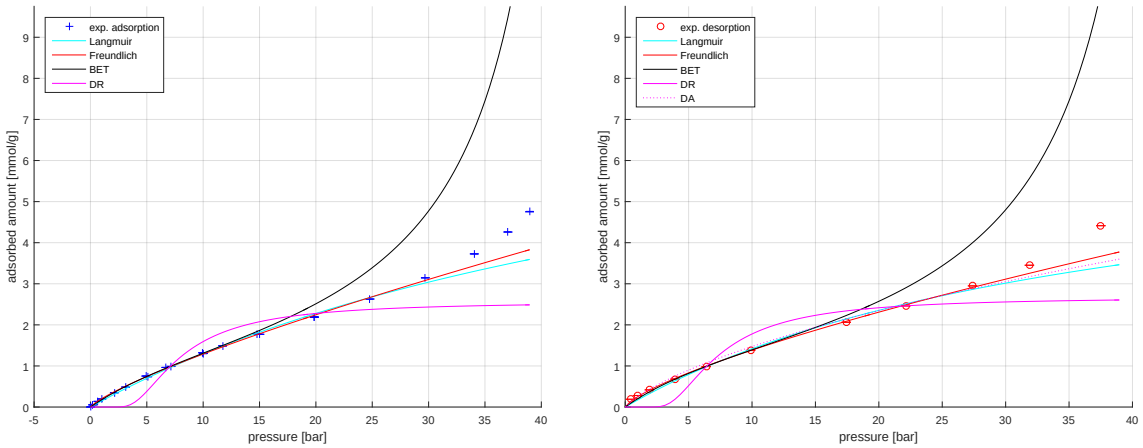

(a) adsorption **(b)** desorption

Figure E.51.: MWCNT and SO_2 at 125 °C data (marks) and fits (lines) adsorption branch (a) and desorption branch (b)

Table E.43.: MWCNT and SO_2 at 125 °C

sample:	MWCNT		
gas:	SO_2		
temperature in [°C]:	124.7	+0.1	-0.1
$m_{S,meas}$ in [mg]:	129.19		
V_S in [cm^3]:	0.061527		

p [bar]	X [$mmolg^{-1}$]	ρ_{meas} [gcm^{-3}]	Δm_{meas} [g]
0.00	0.0000	0.000000	0.000000
0.20	0.0533	0.000390	0.000441
0.67	0.1387	0.001299	0.001148
1.01	0.1953	0.001972	0.001617
2.12	0.3515	0.004156	0.002910
3.11	0.4847	0.006121	0.004012
5.08	0.7397	0.010117	0.006123
7.15	0.9905	0.014424	0.008199
10.03	1.3034	0.020623	0.010788
15.03	1.7705	0.032003	0.014655
19.86	2.1803	0.043896	0.018047
11.72	1.4906	0.024382	0.012338
6.69	0.9637	0.013453	0.007976
4.92	0.7537	0.009778	0.006239
9.95	1.3220	0.020430	0.010943
14.81	1.7744	0.031476	0.014687
19.86	2.1969	0.043898	0.018184
24.80	2.6290	0.057192	0.021761
29.71	3.1454	0.071940	0.026035
34.05	3.7280	0.086568	0.030857
37.04	4.2592	0.097816	0.035254
38.96	4.7528	0.105811	0.039340
37.51	4.4135	0.099811	0.036531
31.87	3.4518	0.078895	0.028571
27.39	2.9488	0.064779	0.024408
22.12	2.4616	0.049864	0.020375
17.43	2.0636	0.037820	0.017081
9.89	1.3809	0.020327	0.011430
6.39	0.9852	0.012816	0.008155
3.93	0.6799	0.007752	0.005628
1.91	0.4175	0.003716	0.003455
0.97	0.2812	0.001875	0.002328
0.41	0.1899	0.000794	0.001572

Table E.44.: Model fit parameter for MWCNT data and SO_2 - Langmuir and Freundlich model

Adsorption - Langmuir model						
T [°C]	k_L	k_L min	k_L max	q_max	q_max min	q_max max
25	0.1788	0.0474	0.0474	10.5792	2.1450	2.1450
50	0.0963	0.0157	0.0157	9.0991	1.1253	1.1253
75	0.0353	0.0089	0.0089	11.0433	2.2104	2.2104
100	0.0338	0.0063	0.0063	7.7017	1.0660	1.0660
125	0.0165	0.0040	0.0040	9.1936	1.6889	1.6889
Desorption - Langmuir model						
T [°C]	k_L	k_L min	k_L max	q_max	q_max min	q_max max
25	0.1550	0.1203	0.1203	12.4762	7.4921	7.4921
50	0.1303	0.0209	0.0209	7.4636	0.8556	0.8556
75	0.0545	0.0207	0.0207	8.0980	2.2370	2.2370
100	0.0274	0.0132	0.0132	9.5440	3.3097	3.3097
125	0.0259	0.0133	0.0133	6.8968	2.3434	2.3434
Adsorption - Freundlich model						
T [°C]	K	K min	K max	n	n min	n max
25	1.5690	0.0614	0.0614	0.8263	0.0576	0.0576
50	0.8121	0.0456	0.0456	0.8153	0.0438	0.0438
75	0.4041	0.0277	0.0277	0.8590	0.0337	0.0337
100	0.3022	0.0181	0.0181	0.7991	0.0253	0.0253
125	0.2043	0.0114	0.0114	0.8002	0.0191	0.0191
Desorption - Freundlich model						
T [°C]	K	K min	K max	n	n min	n max
25	1.6689	0.1083	0.1083	0.8079	0.0876	0.0876
50	0.8893	0.0559	0.0559	0.7611	0.0525	0.0525
75	0.4763	0.0508	0.0508	0.7893	0.0546	0.0546
100	0.3312	0.0302	0.0302	0.7795	0.0342	0.0342
125	0.2544	0.0238	0.0238	0.7363	0.0312	0.0312

Table E.45.: Model fit parameter for MWCNT data and SO_2 - BET and DR model

Adsorption - BET model						
T [°C]	K_BET	K_BET min	K_BET max	q_max_BET	q_max_BET max	q_max_BET min
25	2.6995	3.6120	3.6120	2.6222	2.1703	2.1703
50	3.4282	1.5554	1.5554	2.2123	0.5637	0.5637
75	3.3478	0.7100	0.7100	1.9815	0.2396	0.2396
100	4.3628	0.3023	0.3023	1.8429	0.0619	0.0619
125	4.8476	0.6761	0.6761	1.7569	0.1163	0.1163
Desorption - BET model						
T [°C]	K_BET	K_BET min	K_BET max	q_max_BET	q_max_BET max	q_max_BET min
25	4.4708	2.1530	2.1530	2.1133	0.4456	0.4456
50	4.0681	0.8731	0.8731	2.1513	0.2627	0.2627
75						
100	5.5646	0.4910	0.4910	1.7329	0.0675	0.0675
125	5.7498	2.2220	2.2220	1.7415	0.3136	0.3136
Adsorption - DR model						
T [°C]	k_DR	k_DR min	k_DR max	q_s	q_s min	q_s max
25						
50	61.5588	18.7477	18.7477	3.7844	0.7958	0.7958
75	109.4526	42.9509	42.9509	3.6039	0.8418	0.8418
100	160.5985	56.2524	56.2524	3.3327	0.7484	0.7484
125	289.1143	61.9000	61.9000	3.7218	0.5378	0.5378
Desorption - DR model						
T [°C]	k_DR	k_DR min	k_DR max	q_s	q_s min	q_s max
25	39.3035	17.4732	17.4732	4.8567	1.4260	1.4260
50	58.3144	20.9043	20.9043	3.7099	0.9240	0.9240
75	120.4123	90.1474	90.1474	3.7438	1.6722	1.6722
100	205.9092	73.7785	73.7785	4.3204	0.9604	0.9604
125	247.9671	110.8883	110.8883	3.6155	0.9026	0.9026

Table E.46.: Model fit parameter for MWCNT data and SO_2 - Temkin and Tóth model

Adsorption - Temkin model									
T [°C]	A_T	A_T min	A_T max	RTb_T	RTb_T min	RTb_T max			
25									
50	1.2232	2.4528	2.4528	1.6088	2.3129	2.3129			
75									
100	0.6827	0.2889	0.2889	1.0309	0.2867	0.2867			
125									
Desorption - Temkin model									
T [°C]	A_T	A_T min	A_T max	RTb_T	RTb_T min	RTb_T max			
25	2.0366	1.8953	1.8953	2.1226	1.4903	1.4903			
50	1.7684	0.8732	0.8732	1.2924	0.4396	0.4396			
75	0.7498	0.3765	0.3765	1.3661	0.4622	0.4622			
100	0.8213	0.4976	0.4976	1.0550	0.3509	0.3509			
125									
Adsorption									
T [°C]	K_T	K_T min	K_T max	a_T	a_T min	a_T max	t	t min	tmax
25									
50									
75									
100									
125									
Desorption									
T [°C]	K_T	K_T min	K_T max	a_T	a_T min	a_T max	t	t min	tmax
25									
50									
75									
100									
125									

E.2.7 MWCNT and N_2 at 25 °C

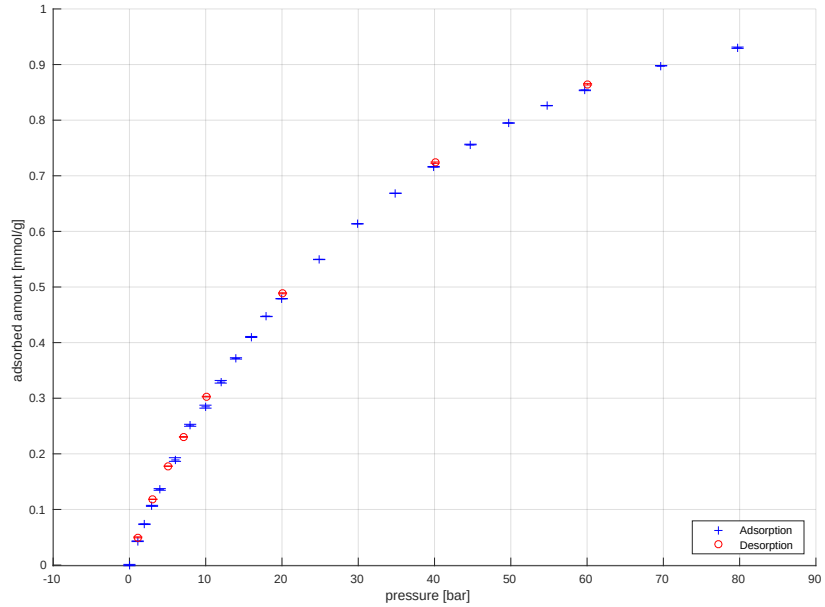

Figure E.52.: MWCNT and N_2 at 25 °C

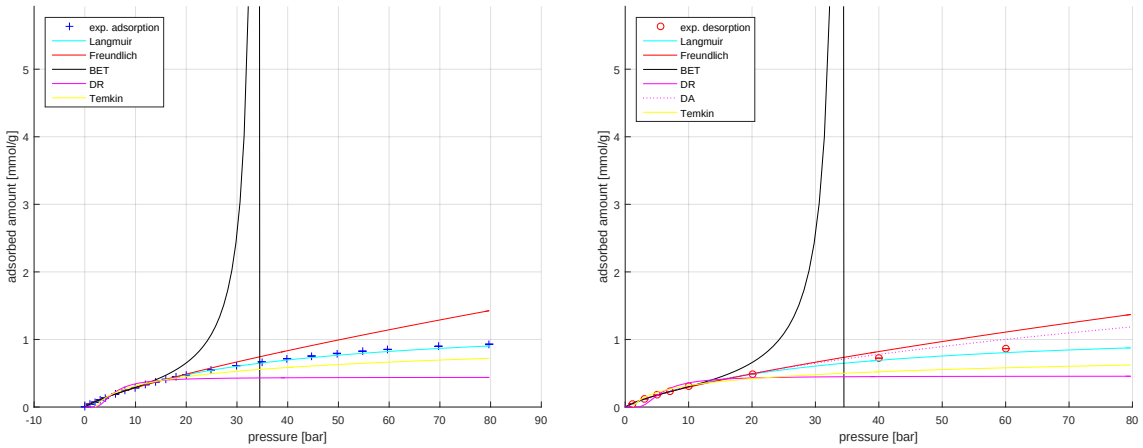

(a) adsorption **(b)** desorption

Figure E.53.: MWCNT and N_2 at 25 °C data (marks) and fits (lines) adsorption branch (a) and desorption branch (b)

Table E.47.: MWCNT and N_2 at 25 °C

sample:	MWCNT		
gas:	N_2		
temperature in [°C]:	25.1	+0.3	-0.0
$m_{S,meas}$ in [mg]:	119.91		
V_S in [cm^3]:	0.055991		

p [bar]	X [$mmolg^{-1}$]	ρ_{meas} [gcm^{-3}]	Δm_{meas} [g]
0.00	0.0000	0.000000	0.000000
1.08	0.0428	0.001212	0.000144
1.97	0.0735	0.002205	0.000247
2.96	0.1065	0.003321	0.000358
3.97	0.1360	0.004456	0.000457
5.97	0.1898	0.006718	0.000638
7.96	0.2513	0.008999	0.000845
9.97	0.2848	0.011255	0.000957
11.97	0.3296	0.013528	0.001107
13.97	0.3716	0.015795	0.001249
15.97	0.4102	0.018064	0.001378
17.96	0.4470	0.020336	0.001502
19.96	0.4790	0.022602	0.001609
24.87	0.5495	0.028193	0.001847
29.89	0.6136	0.033892	0.002062
34.88	0.6686	0.039564	0.002247
39.88	0.7161	0.045411	0.002406
44.71	0.7562	0.050897	0.002541
49.71	0.7949	0.056555	0.002671
54.71	0.8262	0.062222	0.002776
59.71	0.8536	0.067875	0.002869
69.70	0.8979	0.079125	0.003017
79.73	0.9303	0.090338	0.003126
60.07	0.8644	0.068235	0.002905
40.06	0.7236	0.045576	0.002432
20.08	0.4887	0.022729	0.001642
10.08	0.3029	0.011388	0.001018
7.08	0.2304	0.007987	0.000774
5.08	0.1778	0.005722	0.000598
3.08	0.1183	0.003458	0.000397
1.10	0.0498	0.001220	0.000167

E.2.8 MWCNT and N_2 at 25 °C after activation first N_2 measurement then He measurement

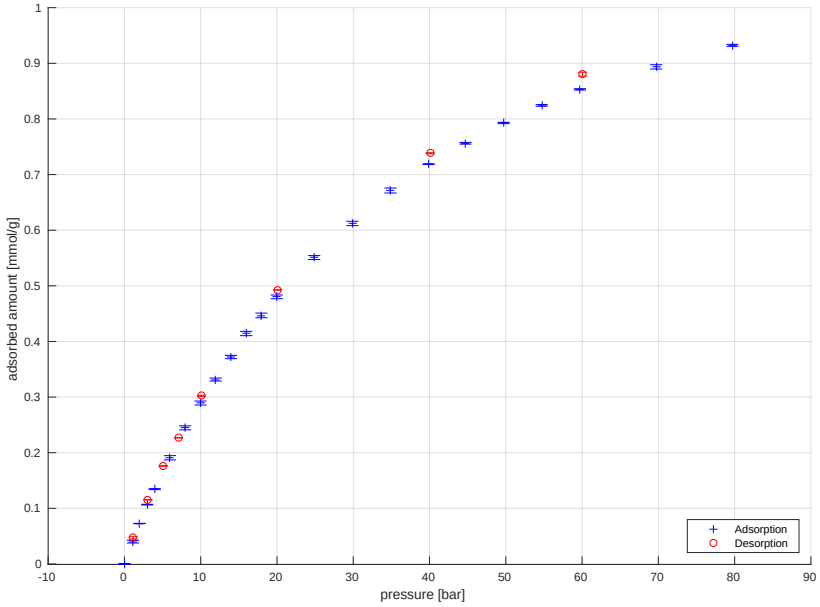

Figure E.54.: MWCNT and N_2 at 25 °C after activation first N_2 measurement then He measurement

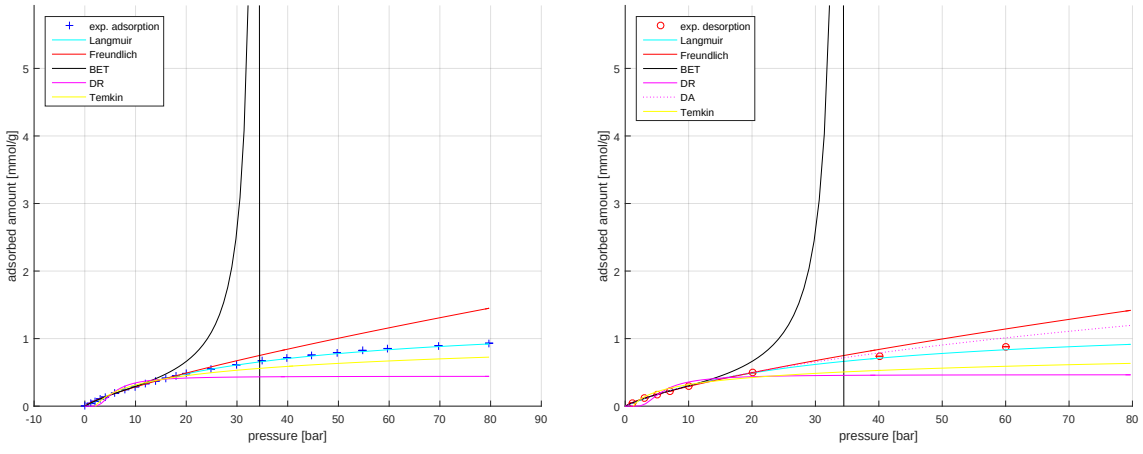

(a) adsorption **(b)** desorption

Figure E.55.: MWCNT and N_2 at 25 °C data (marks) and fits (lines) adsorption branch (a) and desorption branch (b) after activation first N_2 measurement then He measurement

Table E.48.: MWCNT and N_2 at 25 °C after activation first N_2 measurement then He measurement

sample:	MWCNT after activation first N_2 measurement then He measurement		
gas:	N_2		
temperature in [°C]:	25.1	+0.4	-0.0
$m_{S,meas}$ in [mg]:	119.91		
V_S in [cm^3]:	0.056398		

p [bar]	X [$mmolg^{-1}$]	ρ_{meas} [gcm^{-3}]	Δm_{meas} [g]
0.00	0.0000	0.000000	0.000000
1.13	0.0401	0.001251	0.000135
1.98	0.0727	0.002226	0.000244
2.99	0.1066	0.003370	0.000358
3.97	0.1345	0.004475	0.000452
5.97	0.1909	0.006741	0.000641
7.96	0.2447	0.009022	0.000822
9.96	0.2893	0.011293	0.000972
11.96	0.3315	0.013544	0.001114
13.97	0.3720	0.015812	0.001250
15.96	0.4143	0.018095	0.001392
17.96	0.4468	0.020362	0.001501
19.96	0.4802	0.022632	0.001614
24.88	0.5508	0.028213	0.001851
29.88	0.6121	0.033891	0.002057
34.88	0.6713	0.039586	0.002256
39.88	0.7186	0.045434	0.002415
44.72	0.7563	0.050918	0.002542
49.71	0.7928	0.056584	0.002664
54.71	0.8243	0.062240	0.002770
59.72	0.8532	0.067898	0.002867
69.72	0.8936	0.079156	0.003003
79.71	0.9322	0.090331	0.003133
60.07	0.8804	0.068327	0.002959
40.07	0.7384	0.045631	0.002482
20.08	0.4926	0.022732	0.001655
10.08	0.3020	0.011390	0.001015
7.08	0.2268	0.007995	0.000762
5.08	0.1761	0.005732	0.000592
3.08	0.1154	0.003465	0.000388
1.16	0.0469	0.001281	0.000158

E.2.9 MWCNT and N_2 at 50 °C

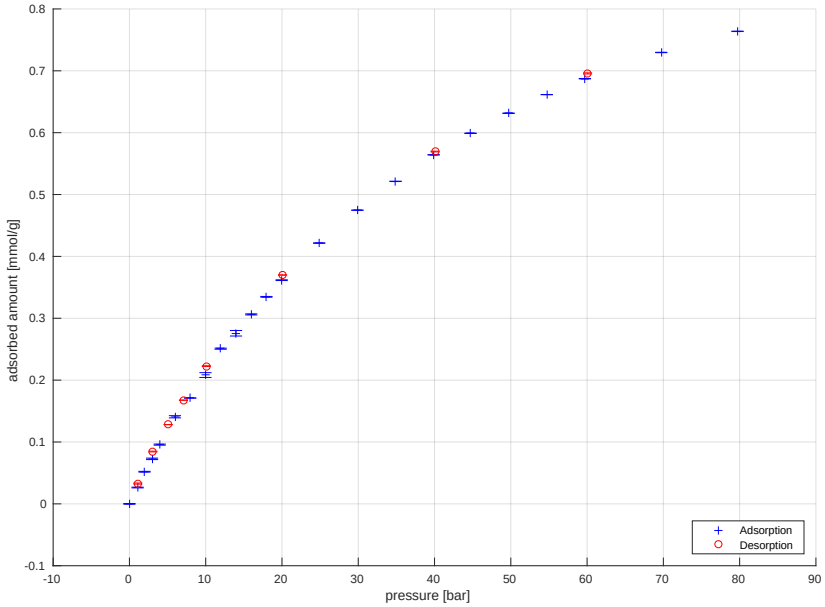

Figure E.56.: MWCNT and N_2 at 50 °C

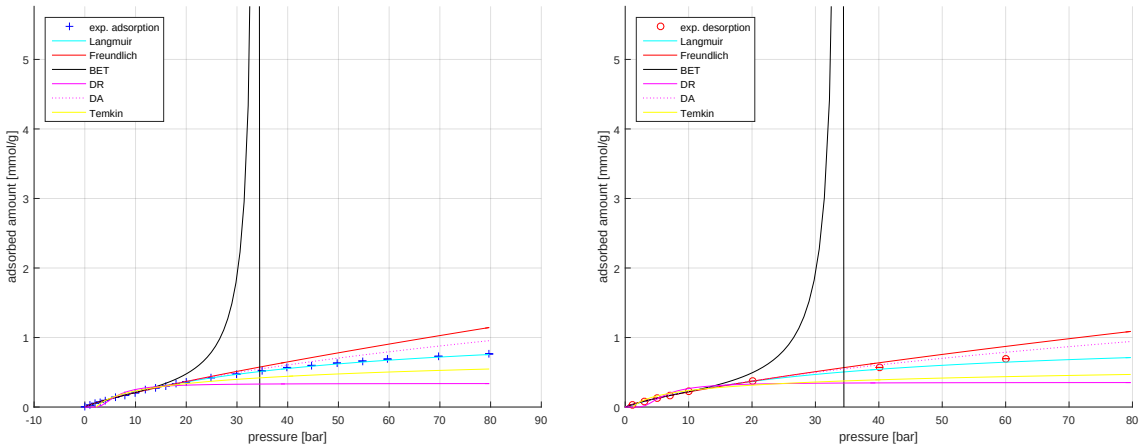

(a) adsorption **(b)** desorption

Figure E.57.: MWCNT and N_2 at 50 °C data (marks) and fits (lines) adsorption branch (a) and desorption branch (b)

Table E.49.: MWCNT and N_2 at 50 °C

sample:	MWCNT		
gas:	N_2		
temperature in [°C]:	50.0	+0.5	-0.1
$m_{S,meas}$ in [mg]:	119.48		
V_S in [cm^3]:	0.055395		

p [bar]	X [$mmol g^{-1}$]	ρ_{meas} [$g cm^{-3}$]	Δm_{meas} [g]
0.00	0.0000	0.000000	0.000000
1.07	0.0264	0.001110	0.000088
1.98	0.0519	0.002044	0.000174
2.97	0.0727	0.003077	0.000244
3.97	0.0958	0.004112	0.000321
5.97	0.1408	0.006203	0.000471
7.97	0.1710	0.008282	0.000573
9.97	0.2082	0.010374	0.000697
11.96	0.2508	0.012465	0.000840
13.97	0.2758	0.014540	0.000923
15.97	0.3062	0.016617	0.001025
17.96	0.3347	0.018690	0.001121
19.96	0.3616	0.020773	0.001211
24.88	0.4215	0.025900	0.001412
29.89	0.4747	0.031102	0.001590
34.89	0.5213	0.036287	0.001746
39.89	0.5642	0.041613	0.001889
44.72	0.5990	0.046602	0.002006
49.71	0.6314	0.051750	0.002114
54.72	0.6615	0.056896	0.002215
59.71	0.6873	0.062018	0.002301
69.72	0.7296	0.072228	0.002443
79.72	0.7638	0.082360	0.002558
60.07	0.6958	0.062347	0.002330
40.07	0.5695	0.041763	0.001907
20.08	0.3699	0.020889	0.001239
10.08	0.2227	0.010485	0.000746
7.08	0.1676	0.007361	0.000561
5.08	0.1281	0.005275	0.000429
3.08	0.0846	0.003191	0.000283
1.10	0.0328	0.001128	0.000110

E.2.10 MWCNT and N_2 at 75 °C

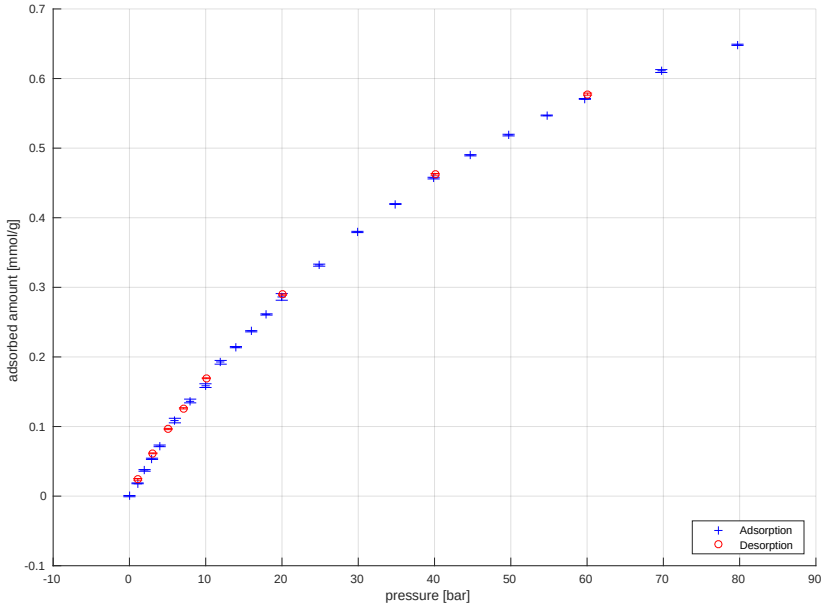

Figure E.58.: MWCNT and N_2 at 75 °C

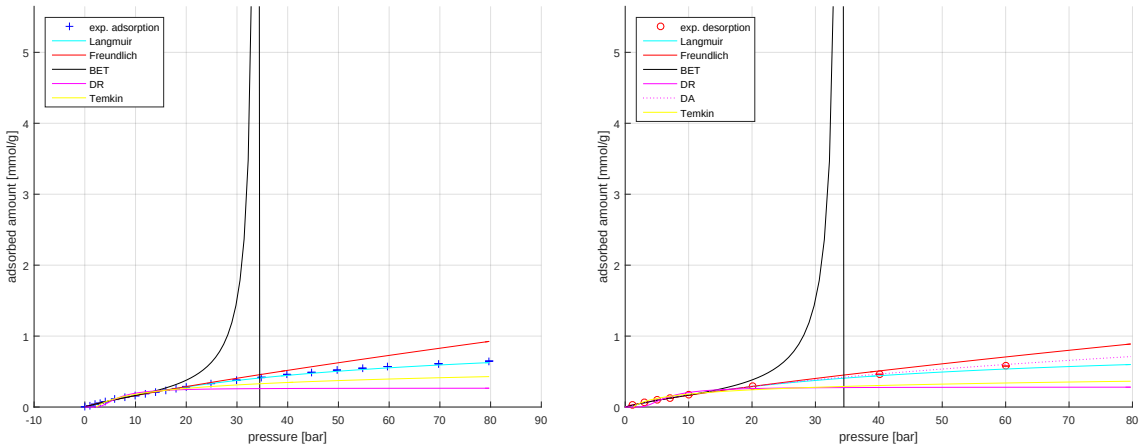

(a) adsorption **(b)** desorption

Figure E.59.: MWCNT and N_2 at 75 °C data (marks) and fits (lines) adsorption branch (a) and desorption branch (b)

Table E.50.: MWCNT and N_2 at 75 °C

sample:	MWCNT		
gas:	N_2		
temperature in [°C]:	74.9	+0.7	-0.3
$m_{S,meas}$ in [mg]:	119.87		
V_S in [cm^3]:	0.056408		

p [bar]	X [$mmolg^{-1}$]	ρ_{meas} [gcm^{-3}]	Δm_{meas} [g]
0.00	0.0000	0.000000	0.000000
1.07	0.0184	0.001026	0.000062
1.99	0.0370	0.001897	0.000124
2.96	0.0536	0.002836	0.000180
3.96	0.0722	0.003813	0.000243
5.96	0.1086	0.005747	0.000365
7.96	0.1367	0.007663	0.000459
9.97	0.1588	0.009590	0.000533
11.96	0.1923	0.011519	0.000646
13.96	0.2141	0.013436	0.000719
15.97	0.2369	0.015368	0.000796
17.97	0.2610	0.017292	0.000877
19.97	0.2862	0.019224	0.000961
24.88	0.3319	0.023934	0.001115
29.89	0.3795	0.028724	0.001275
34.87	0.4197	0.033485	0.001410
39.88	0.4569	0.038395	0.001535
44.70	0.4898	0.042979	0.001645
49.71	0.5188	0.047712	0.001743
54.71	0.5470	0.052427	0.001837
59.71	0.5707	0.057132	0.001917
69.73	0.6108	0.066496	0.002052
79.72	0.6485	0.075760	0.002178
60.07	0.5776	0.057437	0.001940
40.07	0.4624	0.038540	0.001553
20.08	0.2896	0.019306	0.000973
10.08	0.1694	0.009694	0.000569
7.08	0.1262	0.006805	0.000424
5.08	0.0964	0.004874	0.000324
3.08	0.0615	0.002944	0.000207
1.09	0.0242	0.001028	0.000081

E.2.11 MWCNT and N_2 at 100 °C

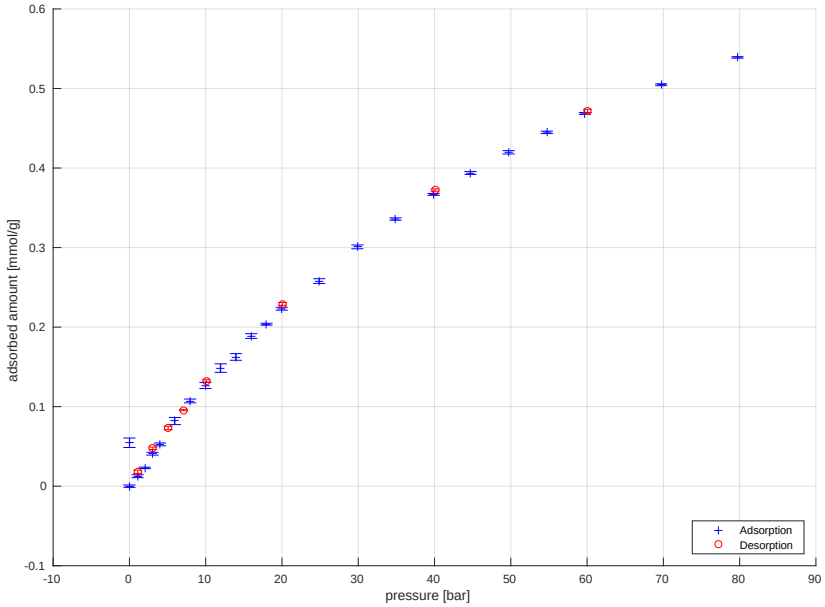

Figure E.60.: MWCNT and N_2 at 100 °C

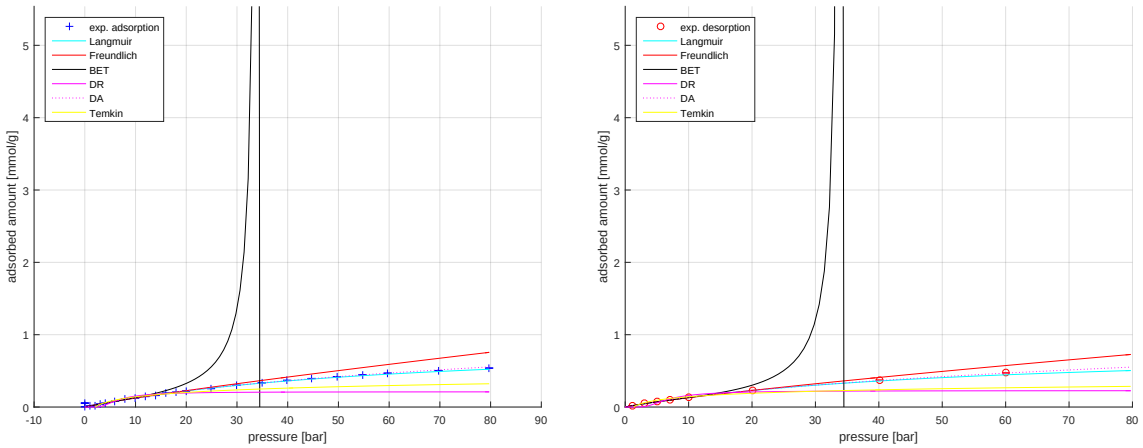

(a) adsorption **(b)** desorption

Figure E.61.: MWCNT and N_2 at 100 °C data (marks) and fits (lines) adsorption branch (a) and desorption branch (b)

Table E.51.: MWCNT and N_2 at 100 °C

sample:	MWCNT		
gas:	N_2		
temperature in [°C]:	99.8	+0.2	-0.1
$m_{S,meas}$ in [mg]:	120.05		
V_S in [cm^3]:	0.056474		

p [bar]	X [$mmolg^{-1}$]	ρ_{meas} [gcm^{-3}]	Δm_{meas} [g]
0.00	0.0546	0.000000	0.000183
0.00	0.0000	0.000071	0.000000
1.07	0.0125	0.001023	0.000042
2.01	0.0231	0.001858	0.000077
3.02	0.0408	0.002758	0.000137
3.99	0.0525	0.003633	0.000176
5.96	0.0819	0.005416	0.000275
7.96	0.1072	0.007215	0.000360
9.97	0.1267	0.009005	0.000425
11.97	0.1485	0.010796	0.000499
13.97	0.1625	0.012581	0.000546
15.96	0.1888	0.014375	0.000634
17.97	0.2037	0.016157	0.000684
19.97	0.2231	0.017951	0.000749
24.89	0.2579	0.022335	0.000866
29.88	0.3009	0.026783	0.001011
34.88	0.3359	0.031211	0.001128
39.88	0.3668	0.035760	0.001232
44.72	0.3938	0.040012	0.001323
49.71	0.4198	0.044384	0.001410
54.72	0.4448	0.048770	0.001494
59.71	0.4686	0.053107	0.001574
69.72	0.5047	0.061770	0.001695
79.72	0.5390	0.070340	0.001810
60.07	0.4717	0.053388	0.001584
40.07	0.3724	0.035894	0.001251
20.07	0.2291	0.018040	0.000769
10.08	0.1323	0.009095	0.000444
7.08	0.0957	0.006401	0.000321
5.08	0.0732	0.004607	0.000246
3.08	0.0477	0.002808	0.000160
1.09	0.0180	0.001018	0.000061

E.2.12 MWCNT and N_2 at 125 °C activation temperature 150 °C

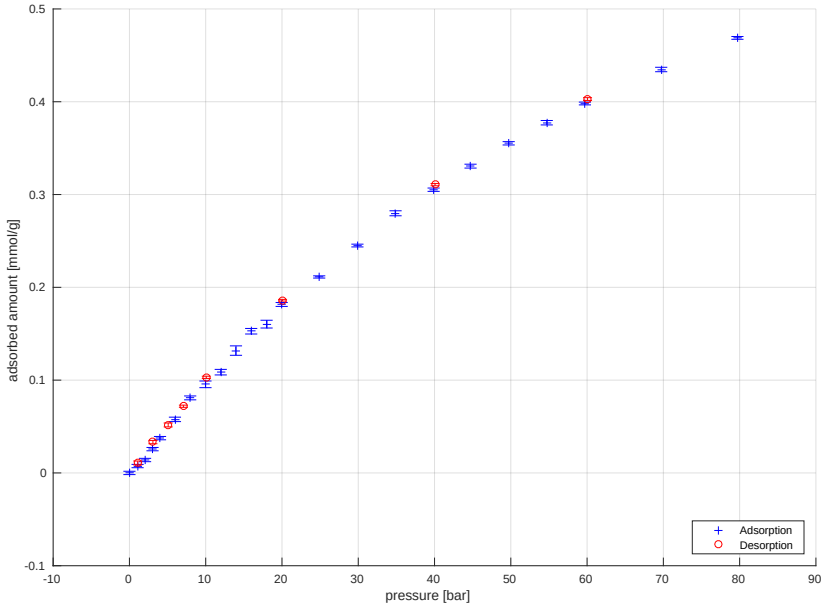

Figure E.62.: MWCNT and N_2 at 125 °C activation at 150 °C

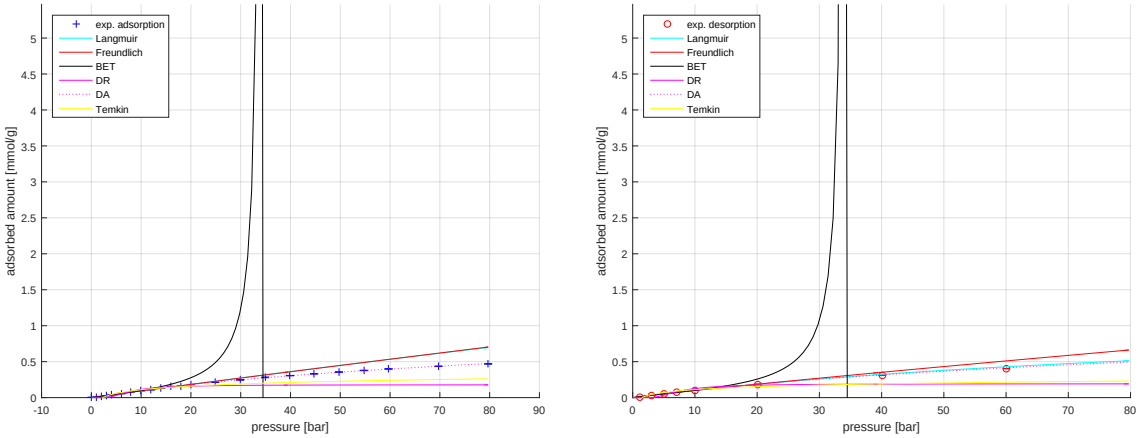

(a) adsorption **(b)** desorption

Figure E.63.: MWCNT and N_2 at 125 °C data (marks) and fits (lines) adsorption branch (a) and desorption branch (b) of activation at 150 °C

Table E.52.: MWCNT and N_2 at 125 °C activation at 150 °C

sample:	MWCNT activation at 150 °C		
gas:	N_2		
temperature in [°C]:	124.7	+0.2	-0.1
$m_{S,meas}$ in [mg]:	119.41		
V_S in [cm^3]:	0.058570		

p [bar]	X [$mmolg^{-1}$]	ρ_{meas} [gcm^{-3}]	Δm_{meas} [g]
0.00	0.0000	0.000000	0.000000
1.07	0.0074	0.000900	0.000025
2.05	0.0139	0.001717	0.000047
3.03	0.0257	0.002539	0.000086
4.01	0.0375	0.003363	0.000125
5.97	0.0577	0.005020	0.000193
7.97	0.0809	0.006704	0.000271
9.97	0.0955	0.008380	0.000319
11.97	0.1086	0.010056	0.000363
13.97	0.1318	0.011739	0.000441
15.96	0.1527	0.013422	0.000511
17.98	0.1603	0.015089	0.000536
19.96	0.1815	0.016765	0.000607
24.88	0.2112	0.020855	0.000707
29.89	0.2450	0.025025	0.000820
34.89	0.2798	0.029168	0.000936
39.88	0.3052	0.033402	0.001021
44.72	0.3306	0.037383	0.001106
49.72	0.3552	0.041476	0.001188
54.71	0.3774	0.045546	0.001263
59.71	0.3981	0.049606	0.001332
69.72	0.4347	0.057679	0.001455
79.71	0.4688	0.065661	0.001568
60.06	0.4029	0.049869	0.001348
40.07	0.3106	0.033538	0.001039
20.07	0.1861	0.016844	0.000623
10.08	0.1030	0.008469	0.000345
7.08	0.0719	0.005948	0.000240
5.08	0.0517	0.004264	0.000173
3.08	0.0332	0.002581	0.000111
1.09	0.0107	0.000903	0.000036

E.2.13 MWCNT and N_2 at 125 °C activation temperature 300 °C

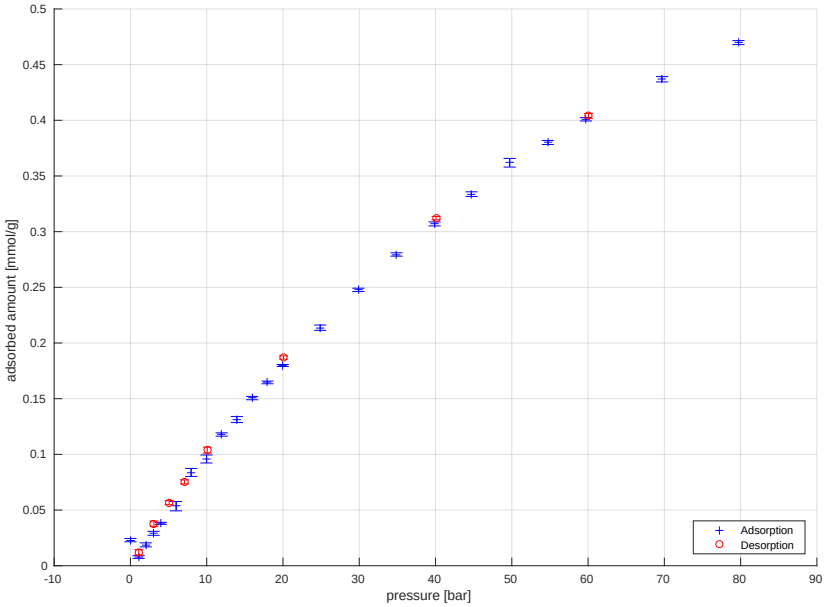

Figure E.64.: MWCNT and N_2 at 125 °C activation at 300 °C

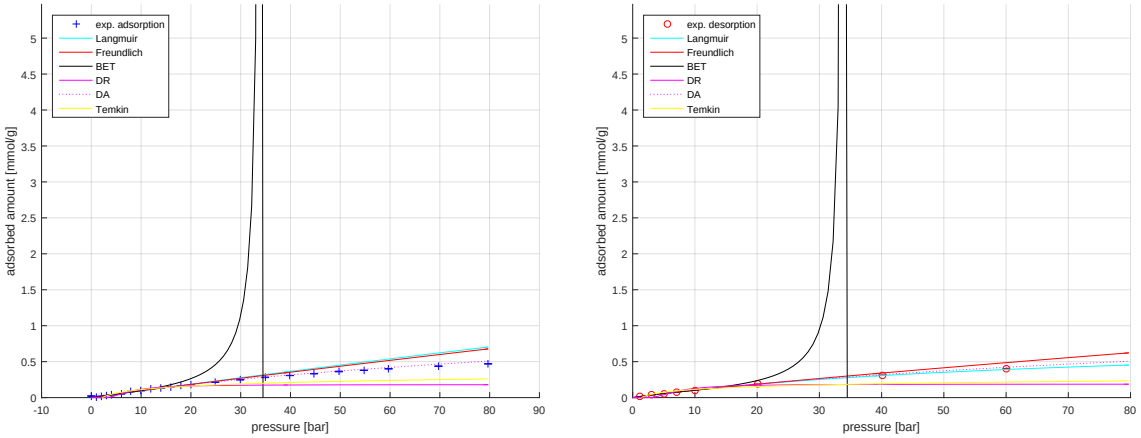

(a) adsorption **(b)** desorption

Figure E.65.: MWCNT and N_2 at 125 °C data (marks) and fits (lines) adsorption branch (a) and desorption branch (b) of activation at 300 °C

Table E.53.: MWCNT and N_2 at 125 °C activation at 300 °C

sample:	MWCNT activation at 300 °C		
gas:	N_2		
temperature in [°C]:	124.7	+0.2	-0.0
$m_{S,meas}$ in [mg]:	119.41		
V_S in [cm^3]:	0.058570		

p [bar]	X [$mmolg^{-1}$]	ρ_{meas} [gcm^{-3}]	Δm_{meas} [g]
0.00	0.0230	0.000000	0.000077
1.07	0.0078	0.000899	0.000026
2.01	0.0187	0.001680	0.000063
3.03	0.0291	0.002537	0.000097
3.98	0.0381	0.003340	0.000127
5.97	0.0535	0.005014	0.000179
7.96	0.0838	0.006708	0.000280
9.97	0.0959	0.008389	0.000321
11.96	0.1178	0.010073	0.000394
13.96	0.1312	0.011749	0.000439
15.96	0.1505	0.013426	0.000504
17.97	0.1646	0.015095	0.000551
19.96	0.1798	0.016761	0.000602
24.88	0.2138	0.020863	0.000715
29.89	0.2477	0.025025	0.000829
34.88	0.2795	0.029158	0.000935
39.88	0.3069	0.033416	0.001027
44.72	0.3337	0.037392	0.001116
49.72	0.3619	0.041495	0.001211
54.72	0.3801	0.045566	0.001272
59.72	0.4009	0.049628	0.001341
69.70	0.4369	0.057682	0.001462
79.71	0.4698	0.065680	0.001572
60.06	0.4041	0.049889	0.001352
40.07	0.3121	0.033558	0.001044
20.07	0.1870	0.016861	0.000626
10.08	0.1038	0.008487	0.000347
7.08	0.0753	0.005960	0.000252
5.08	0.0566	0.004276	0.000189
3.08	0.0378	0.002587	0.000126
1.09	0.0120	0.000909	0.000040

Table E.54.: Model fit parameter for MWCNT data and N_2 - Langmuir model

Adsorption						
T [°C]	k_L	k_L min	k_L max	q_max	q_max min	q_max max
25	0.0292	0.0037	0.0037	1.2918	0.1154	0.1154
25[a]	0.0280	0.0019	0.0019	1.3327	0.0651	0.0651
50	0.0217	0.0031	0.0031	1.1913	0.1294	0.1294
75	0.0184	0.0033	0.0033	1.0523	0.1476	0.1476
100	0.0153	0.0247	0.0247	0.9514	1.2566	1.2566
125[b]	0.0009	0.0118	0.0118	10.1563	126.7793	126.7793
125[c]	0.0009	0.0059	0.0059	10.1563	63.9892	63.9892
Desorption						
T [°C]	k_L	k_L min	k_L max	q_max	q_max min	q_max max
25	0.0341	0.0064	0.0064	1.1981	0.1541	0.1541
25[a]	0.0307	0.0045	0.0045	1.2880	0.1330	0.1330
50	0.0276	0.0044	0.0044	1.0353	0.1208	0.1208
75	0.0222	0.0036	0.0036	0.9387	0.1177	0.1177
100	0.0184	0.0041	0.0041	0.8487	0.1491	0.1491
125[b]	0.0135	0.0046	0.0046	0.8747	0.2477	0.2477
125[c]	0.0087	0.0035	0.0035	1.2481	0.4461	0.4461

[a] after activation first N_2 measurement then He measurement

[b] activation temperature 150 °C

[b] activation temperature 300 °C

Table E.55.: Model fit parameter for MWCNT data and N_2 - Freundlich model

Adsorption T [°C]	K	K min	K max	n	n min	n max
25	0.0475	0.0036	0.0036	0.7767	0.0286	0.0286
25[a]	0.0466	0.0037	0.0037	0.7849	0.0300	0.0300
50	0.0314	0.0026	0.0026	0.8207	0.0315	0.0315
75	0.0230	0.0021	0.0021	0.8434	0.0336	0.0336
100	0.0166	0.0085	0.0085	0.8720	0.1908	0.1908
125[b]	0.0109	0.0037	0.0037	0.9437	0.1241	0.1241
125[c]	0.0100	0.0018	0.0018	0.9720	0.0651	0.0651
Desorption						
T [°C]	K	K min	K max	n	n min	n max
25	0.0533	0.0062	0.0062	0.7415	0.0443	0.0443
25[a]	0.0507	0.0068	0.0068	0.7608	0.0511	0.0511
50	0.0362	0.0041	0.0041	0.7771	0.0427	0.0427
75	0.0257	0.0024	0.0024	0.8095	0.0352	0.0352
100	0.0189	0.0016	0.0016	0.8341	0.0325	0.0325
125[b]	0.0138	0.0013	0.0013	0.8706	0.0355	0.0355
125[c]	0.0120	0.0017	0.0017	0.9155	0.0519	0.0519

[a] after activation first N_2 measurement then He measurement

[b] activation temperature 150 °C

[b] activation temperature 300 °C

Table E.56.: Model fit parameter for MWCNT data and N_2 - BET model

Adsorption						
T [°C]	K_BET	K_BET min	K_BET max	q_max_BET	q_max_BET max	q_max_BET min
25	4.9331	1.5935	1.5935	0.3064	0.0440	0.0440
25[a]	4.6863	0.6636	0.6636	0.3127	0.0201	0.0201
50	4.5756	1.0607	1.0607	0.2257	0.0240	0.0240
75	4.1737	1.6887	1.6887	0.1815	0.0350	0.0350
100	3.0041	1.5741	1.5741	0.1655	0.0472	0.0472
125[b]	2.3616	1.8652	1.8652	0.1408	0.0660	0.0660
125[c]	2.0137	1.6682	1.6682	0.1531	0.0794	0.0794
Desorption						
T [°C]	K_BET	K_BET min	K_BET max	q_max_BET	q_max_BET max	q_max_BET min
25	5.5789	0.8790	0.8790	0.3044	0.0193	0.0193
25[a]	5.2838	0.8101	0.8101	0.3081	0.0195	0.0195
50	5.1191	0.6687	0.6687	0.2296	0.0126	0.0126
75	4.6468	1.0467	1.0467	0.1805	0.0178	0.0178
100	4.2899	0.7020	0.7020	0.1440	0.0107	0.0107
125[b]	4.2479	0.7832	0.7832	0.1134	0.0096	0.0096
125[c]	2.9263	0.6250	0.6250	0.1309	0.0150	0.0150

[a] after activation first N_2 measurement then He measurement

[b] activation temperature 150 °C

[b] activation temperature 300 °C

Table E.57.: Model fit parameter for MWCNT data and N_2 - DR model

Adsorption T [°C]	k_DR	k_DR min	k_DR max	q_s	q_s min	q_s max
25	259.3317	66.2984	66.2984	0.6078	0.0889	0.0889
25[a]	263.1017	65.0668	65.0668	0.6139	0.0877	0.0877
50	263.9264	66.4259	66.4259	0.4755	0.0728	0.0728
75	254.1138	62.3715	62.3715	0.3776	0.0577	0.0577
100	249.9321	86.3909	86.3909	0.3032	0.0676	0.0676
125[b]	274.1896	72.6645	72.6645	0.2652	0.0504	0.0504
125[c]	281.8016	59.7962	59.7962	0.2675	0.0415	0.0415
Desorption						
T [°C]	**k_DR**	**k_DR min**	**k_DR max**	**q_s**	**q_s min**	**q_s max**
25	266.4928	129.2878	129.2878	0.6426	0.2162	0.2162
25[a]	275.0180	129.9323	129.9323	0.6552	0.2184	0.2184
50	263.1284	123.3692	123.3692	0.4986	0.1682	0.1682
75	260.2474	119.6111	119.6111	0.4002	0.1370	0.1370
100	254.9250	117.4832	117.4832	0.3234	0.1139	0.1139
125[b]	253.3848	116.7355	116.7355	0.2702	0.0981	0.0981
125[c]	274.0642	110.1573	110.1573	0.2812	0.0928	0.0928

[a] after activation first N_2 measurement then He measurement

[b] activation temperature 150 °C

[b] activation temperature 300 °C

Table E.58.: Model fit parameter for MWCNT data and N_2 - Temkin model

Adsorption T [°C]	A_T	A_T min	A_T max	RTb_T	RTb_T max	RTb_T min
25	0.4919	0.1134	0.1134	0.1964	0.0275	0.0275
25[a]	0.4847	0.1086	0.1086	0.1986	0.0272	0.0272
50	0.4578	0.1089	0.1089	0.1520	0.0228	0.0228
75	0.4465	0.1071	0.1071	0.1201	0.0185	0.0185
100	0.5054	0.1268	0.1268	0.0870	0.0137	0.0137
125[b]	0.4721	0.1385	0.1385	0.0715	0.0136	0.0136
125[c]	0.4488	0.1212	0.1212	0.0730	0.0132	0.0132
Desorption						
T [°C]	A_T	A_T min	A_T max	RTb_T	RTb_T max	RTb_T min
25	0.8797	0.7295	0.7295	0.1464	0.1464	0.0672
25[a]	0.8210	0.6465	0.6465	0.1514	0.1514	0.0682
50	0.8294	0.6999	0.6999	0.1119	0.1119	0.0537
75	0.7994	0.7065	0.7065	0.0876	0.0876	0.0449
100	0.7799	0.7136	0.7136	0.0692	0.0692	0.0372
125[b]	0.7424	0.6842	0.6842	0.0568	0.0568	0.0315
125[c]	0.7011	0.6587	0.6587	0.0573	0.0573	0.0333

[a] after activation first N_2 measurement then He measurement

[b] activation temperature 150 °C

[b] activation temperature 300 °C

Table E.59.: Model fit parameter for MWCNT data and N_2 - Tóth model

Adsorption									
T [°C]	K_T	K_T min	K_T max	a_T	a_T min	a_T max	t	t min	tmax
25									
25[a]									
50									
75									
100									
125[b]									
125[c]									
Desorption									
T [°C]	K_T	K_T min	K_T max	a_T	a_T min	a_T max	t	t min	tmax
25									
25[a]									
50									
75									
100									
125[b]									
125[c]									

[a] after activation first N_2 measurement then He measurement

[b] activation temperature 150 °C

[b] activation temperature 300 °C

E.3 SWCNT

E.3.1 SWCNT and SO_2 at 25 °C

Table E.60.: SWCNT and SO_2 at 25 °C

sample:	SWCNT		
gas:	SO_2		
temperature in [°C]:	25.1	+0.0	-0.0
$m_{S,meas}$ in [mg]:	112.87		
V_S in [cm^3]:	0.045915		

p [bar]	X [mmolg^{-1}]	ρ_{meas} [gcm^{-3}]	Δm_{meas} [g]
0.00	0.0000	0.000000	0.000000
0.19	1.0344	0.000499	0.007480
0.59	2.2844	0.001551	0.016520
1.05	3.3922	0.002783	0.024531
1.56	4.3364	0.004144	0.031359
2.49	6.4012	0.006738	0.046292
3.00	8.4685	0.008182	0.061242
3.57	14.8088	0.009846	0.107093
3.85	22.6422	0.010662	0.163742
3.84	22.7087	0.010663	0.164223
3.84	22.5413	0.010613	0.163012
3.13	10.5206	0.008557	0.076082
2.97	9.0368	0.008091	0.065351
2.01	5.3473	0.005376	0.038670
1.28	3.9614	0.003368	0.028648
1.04	3.4979	0.002730	0.025296
0.98	3.3829	0.002585	0.024464
0.77	2.8896	0.002006	0.020897
0.57	2.3775	0.001498	0.017193
0.38	1.8049	0.000984	0.013053

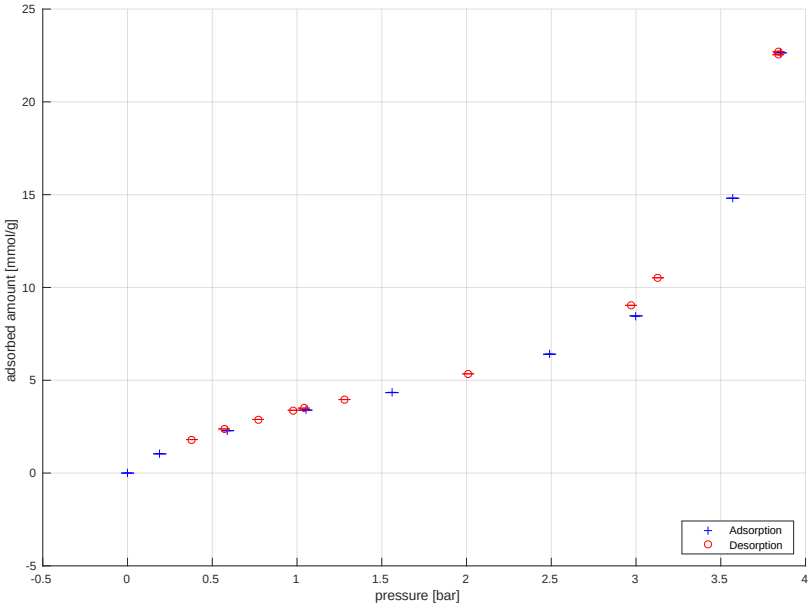

Figure E.66.: SWCNT and SO_2 at 25 °C

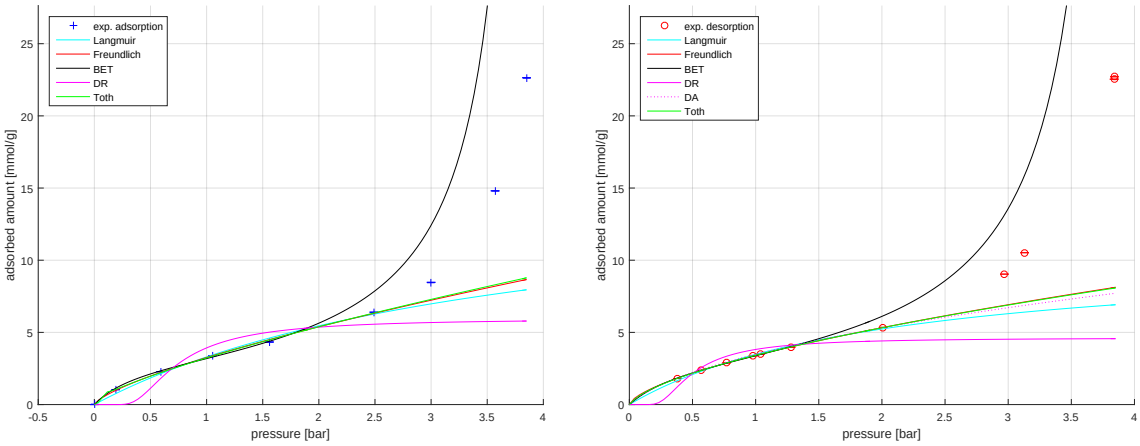

(a) adsorption **(b)** desorption

Figure E.67.: SWCNT and SO_2 at 25 °C data (marks) and fits (lines) adsorption branch (a) and desorption branch (b)

Table E.61.: SWCNT and SO_2 at 50 °C

sample:	SWCNT		
gas:	SO_2		
temperature in [°C]:	50.0	+0.1	-0.0
$m_{S,meas}$ in [mg]:	60.46		
V_S in [cm^3]:	0.021514		

p [bar]	X [mmolg^{-1}]	ρ_{meas} [gcm^{-3}]	Δm_{meas} [g]
0.00	0.0000	0.000000	0.000000
0.17	0.5656	0.000394	0.002191
0.39	0.9836	0.000921	0.003809
0.60	1.3230	0.001440	0.005124
0.92	1.7656	0.002212	0.006838
3.06	3.8815	0.007572	0.015033
4.91	5.4650	0.012491	0.021166
6.04	6.8880	0.015639	0.026677
6.90	8.7647	0.018103	0.033946
7.38	10.7465	0.019529	0.041621
7.92	15.0698	0.021156	0.058365
8.27	20.1310	0.022223	0.077967
7.49	13.2445	0.019854	0.051296
5.02	5.6860	0.012803	0.022022
2.33	3.3748	0.005714	0.013071
1.07	2.0404	0.002571	0.007902
0.56	1.3445	0.001349	0.005207

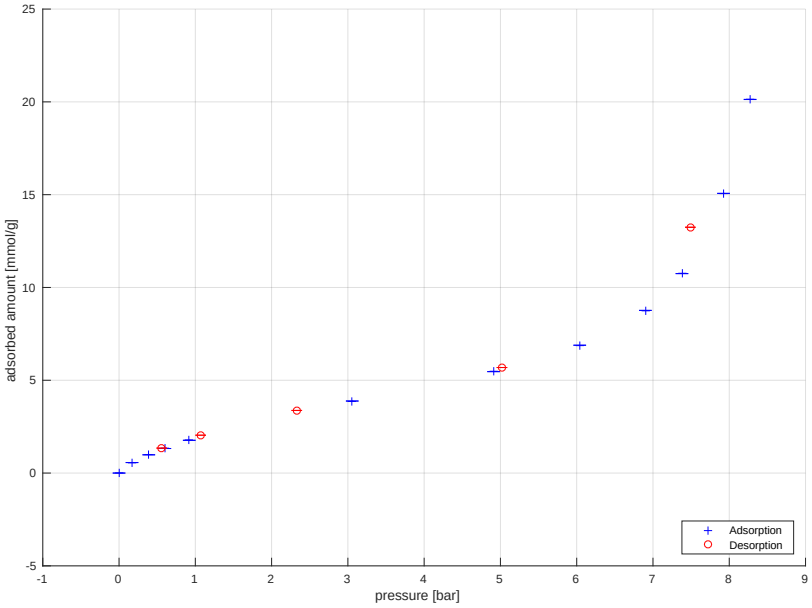

Figure E.68.: SWCNT and SO_2 at 50 °C

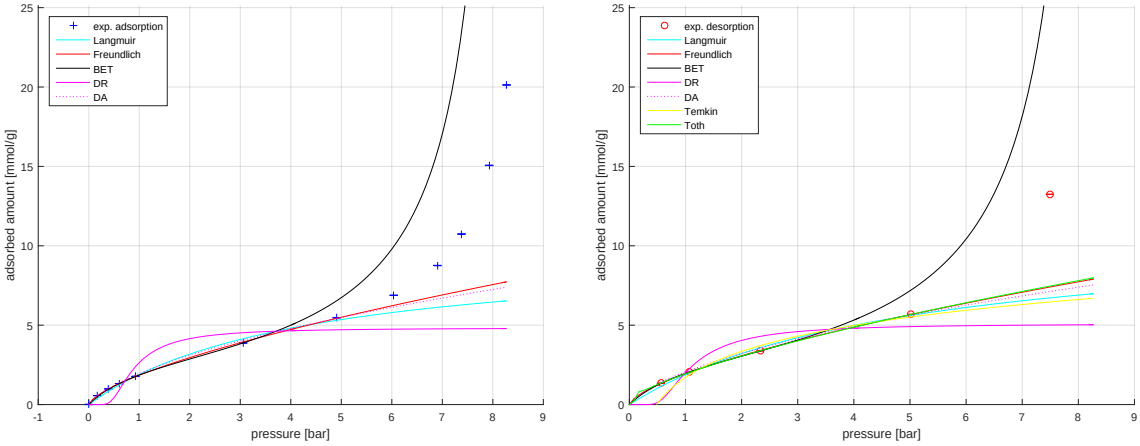

(a) adsorption **(b)** desorption

Figure E.69.: SWCNT and SO_2 at 50 °C data (marks) and fits (lines) adsorption branch (a) and desorption branch (b)

E.3.3 SWCNT and SO_2 at 75 °C

Table E.62.: SWCNT and SO_2 at 75 °C

sample:	SWCNT		
gas:	SO_2		
temperature in [°C]:	74.9	+0.1	-0.0
$m_{S,meas}$ in [mg]:	112.33		
V_S in [cm^3]:	0.045726		

p [bar]	X [mmolg^{-1}]	ρ_{meas} [gcm^{-3}]	Δm_{meas} [g]
0.00	0.0000	0.000000	0.000000
0.51	0.6739	0.001134	0.004849
1.07	1.1240	0.002383	0.008087
2.05	1.7815	0.004611	0.012818
3.11	2.3880	0.007085	0.017182
4.70	3.1307	0.010863	0.022526
6.93	4.0204	0.016407	0.028927
9.81	5.2626	0.024029	0.037866
12.55	7.0732	0.031865	0.050893
14.68	10.6838	0.038438	0.076871
15.58	14.9376	0.041359	0.107479
12.53	7.1420	0.031772	0.051388
10.05	5.4567	0.024676	0.039262
7.40	4.2918	0.017608	0.030881
5.13	3.3976	0.011905	0.024446
2.53	2.1599	0.005740	0.015541
1.07	1.2063	0.002378	0.008680
1.08	1.2066	0.002397	0.008682
0.45	0.7066	0.000999	0.005084
0.25	0.5135	0.000552	0.003695

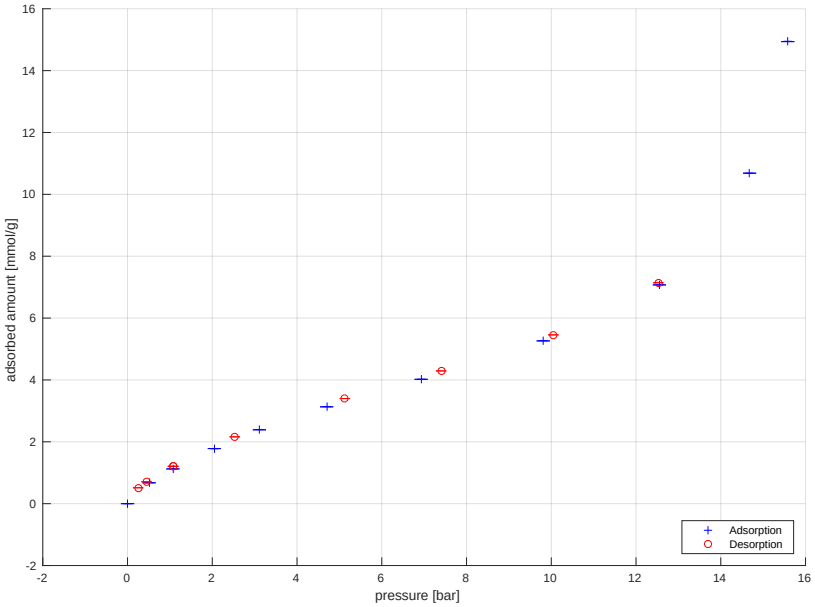

Figure E.70.: SWCNT and SO_2 at 75 °C

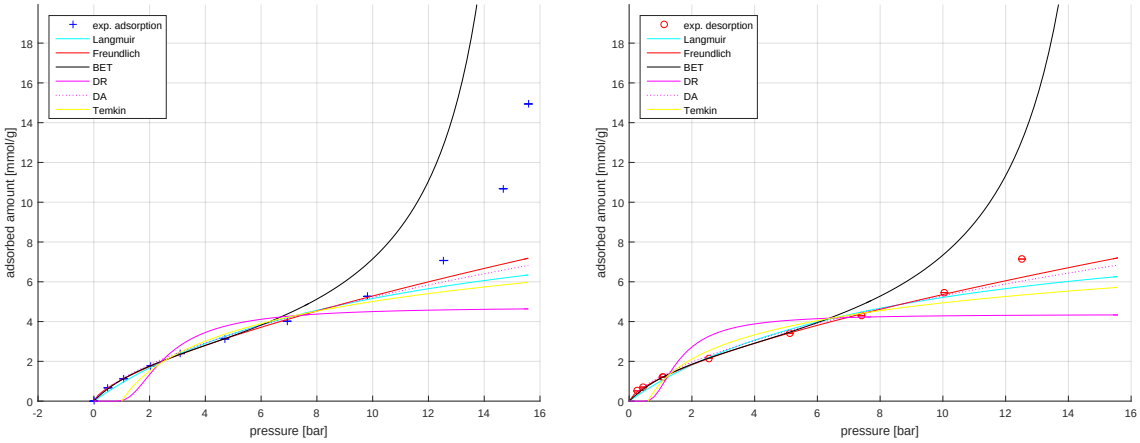

(a) adsorption **(b)** desorption

Figure E.71.: SWCNT and SO_2 at 75 °C data (marks) and fits (lines) adsorption branch (a) and desorption branch (b)

E.3.4 SWCNT and SO_2 at 75 °C second cycle

Table E.63.: SWCNT and SO_2 at 75 °C second cycle

sample:	SWCNT 2. cycle		
gas:	SO_2		
temperature in [°C]:	74.9	+0.1	-0.0
$m_{S,meas}$ in [mg]:	112.54		
V_S in [cm^3]:	0.046780		

p [bar]	X [mmolg^{-1}]	ρ_{meas} [gcm^{-3}]	Δm_{meas} [g]
0.00	0.0000	0.000000	0.000000
0.51	0.6487	0.001134	0.004676
1.02	1.0640	0.002280	0.007670
2.16	1.8221	0.004868	0.013135
3.30	2.4574	0.007534	0.017715
4.65	3.0829	0.010752	0.022224
6.82	3.9505	0.016157	0.028477
9.54	5.0909	0.023288	0.036698
12.42	6.9177	0.031480	0.049867
14.39	9.7858	0.037510	0.070542
15.65	15.3134	0.041569	0.110388
13.95	9.4265	0.036099	0.067951
11.19	6.0590	0.027900	0.043677
9.09	4.9526	0.022077	0.035701
6.51	3.9038	0.015362	0.028141
4.07	2.9004	0.009360	0.020908
1.47	1.4526	0.003279	0.010471
0.97	1.0951	0.002151	0.007894
0.65	0.8454	0.001440	0.006094
0.29	0.5207	0.000639	0.003753

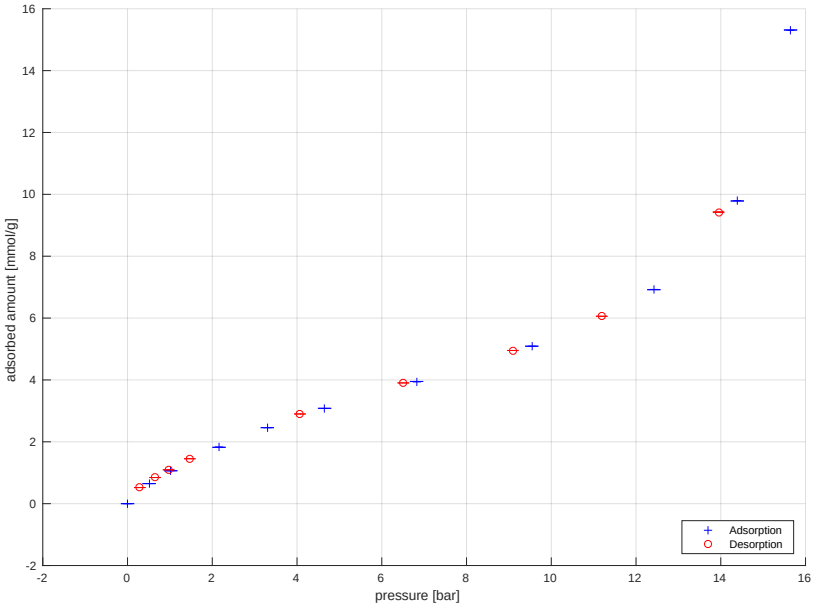

Figure E.72.: SWCNT and SO_2 at 75 °C second cycle

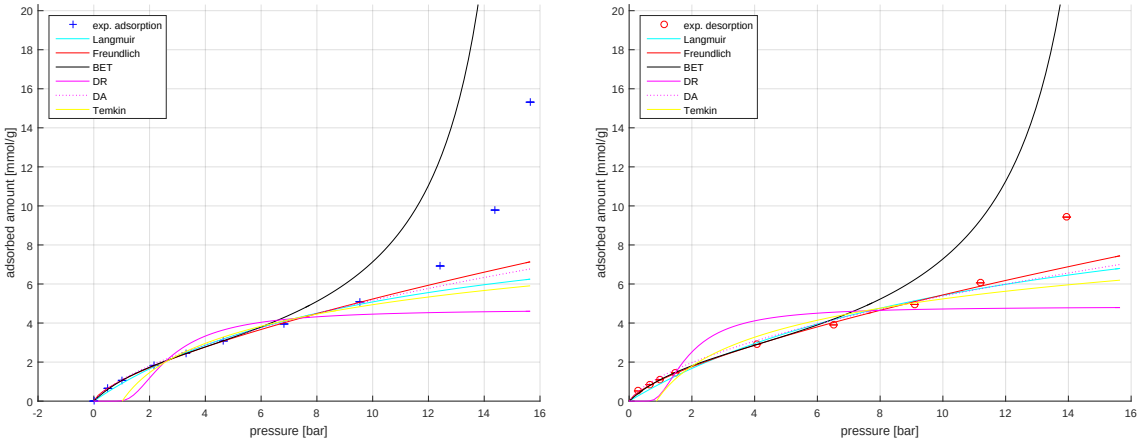

(a) adsorption **(b)** desorption

Figure E.73.: SWCNT and SO_2 at 75 °C data (marks) and fits (lines) adsorption branch (a) and desorption branch (b)

Table E.64.: SWCNT and SO_2 at 100 °C

sample:	SWCNT		
gas:	SO_2		
temperature in [°C]:	99.8	+0.3	-0.1
$m_{S,meas}$ in [mg]:	60.10		
V_S in [cm^3]:	0.026487		

p [bar]	X [mmolg^{-1}]	ρ_{meas} [gcm^{-3}]	Δm_{meas} [g]
0.00	0.0000	0.000000	0.000000
0.41	0.3706	0.000827	0.001427
1.08	0.7340	0.002197	0.002826
1.98	1.1363	0.004104	0.004375
3.13	1.5745	0.006561	0.006062
5.15	2.2290	0.011006	0.008582
7.51	2.8682	0.016381	0.011043
10.18	3.4796	0.022719	0.013397
14.92	4.5171	0.034831	0.017391
19.93	5.8985	0.049194	0.022710
24.25	8.0807	0.063275	0.031112
27.38	14.2675	0.075036	0.054932
22.38	7.0363	0.057005	0.027090
17.56	5.2597	0.042160	0.020251
12.47	4.0502	0.028416	0.015594
7.16	2.8818	0.015577	0.011095
3.93	1.9641	0.008323	0.007562
2.54	1.4797	0.005342	0.005697
1.47	1.0455	0.003050	0.004025
1.05	0.8571	0.002194	0.003300
0.66	0.6603	0.001369	0.002542
0.27	0.4311	0.000571	0.001660

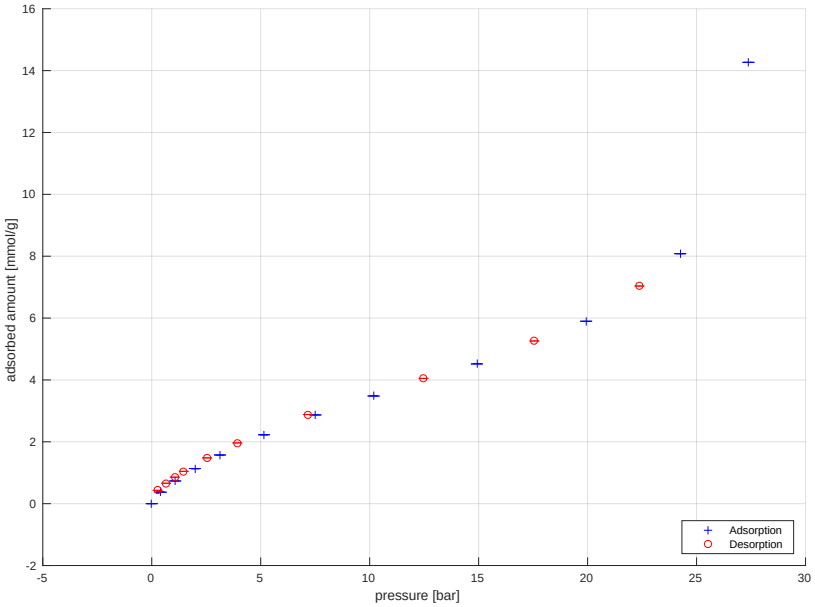

Figure E.74.: SWCNT and SO_2 at 100 °C

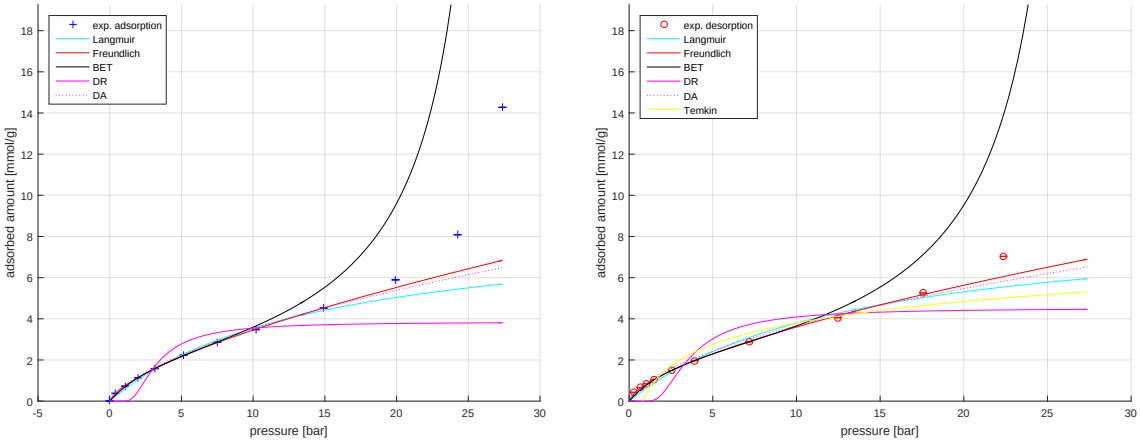

(a) adsorption **(b)** desorption

Figure E.75.: SWCNT and SO_2 at 100 °C data (marks) and fits (lines) adsorption branch (a) and desorption branch (b)

E.3.6 SWCNT and SO_2 at 125 °C

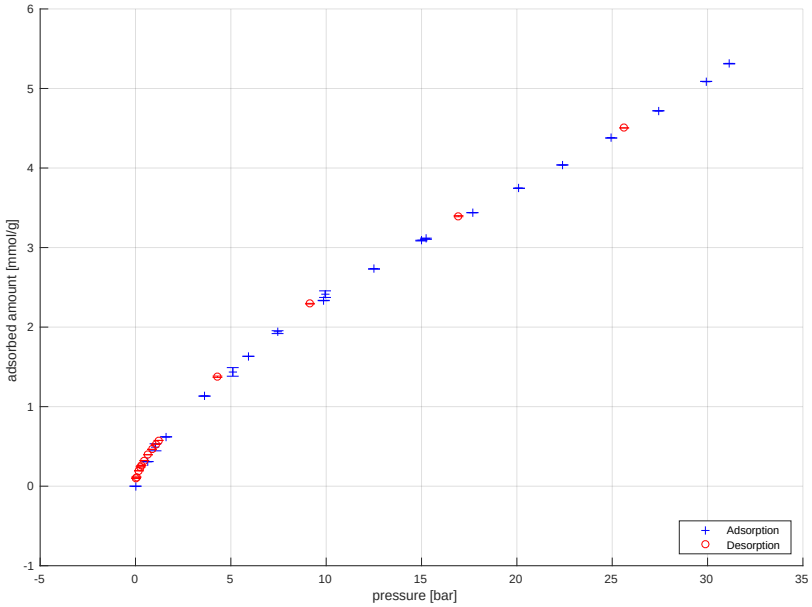

Figure E.76.: SWCNT and SO_2 at 125 °C

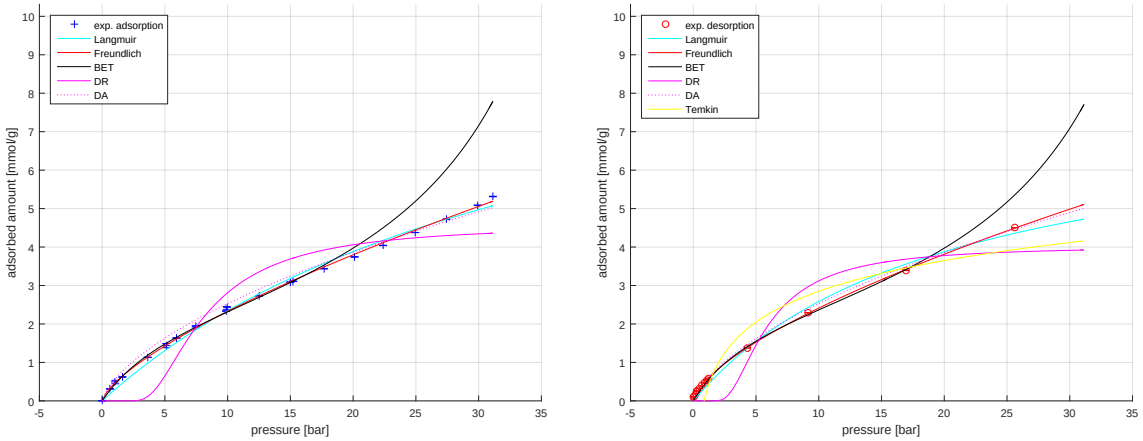

(a) adsorption **(b)** desorption

Figure E.77.: SWCNT and SO_2 at 125 °C data (marks) and fits (lines) adsorption branch (a) and desorption branch (b)

Table E.65.: SWCNT and SO_2 at 125 °C

sample:	SWCNT		
gas:	SO_2		
temperature in [°C]:	124.7	+0.1	-0.2
$m_{S,meas}$ in [mg]:	112.27		
V_S in [cm^3]:	0.054186		

p [bar]	X [$mmolg^{-1}$]	ρ_{meas} [gcm^{-3}]	Δm_{meas} [g]
0.00	0.0000	0.000000	0.000000
0.63	0.3092	0.001213	0.002223
1.05	0.4890	0.002006	0.003515
1.61	0.6206	0.003132	0.004461
3.62	1.1327	0.007139	0.008143
5.10	1.4367	0.010044	0.010328
5.92	1.6330	0.011845	0.011739
7.45	1.9365	0.015031	0.013921
9.87	2.3344	0.020265	0.016782
9.94	2.4143	0.020464	0.017356
12.51	2.7309	0.026144	0.019632
14.99	3.0877	0.031870	0.022197
15.23	3.1104	0.032472	0.022360
17.67	3.4389	0.038330	0.024722
20.11	3.7453	0.044469	0.026924
22.39	4.0386	0.050471	0.029033
24.95	4.3776	0.057547	0.031470
27.42	4.7196	0.064743	0.033928
29.93	5.0888	0.072458	0.036582
31.14	5.3117	0.076393	0.038185
25.63	4.5042	0.059504	0.032380
16.94	3.3946	0.036535	0.024404
9.15	2.2942	0.018671	0.016492
4.30	1.3760	0.008537	0.009892
1.21	0.5754	0.002336	0.004137
1.06	0.5278	0.002035	0.003794
0.86	0.4632	0.001643	0.003330
0.66	0.3955	0.001260	0.002843
0.46	0.3226	0.000882	0.002319
0.31	0.2604	0.000594	0.001872
0.27	0.2426	0.000518	0.001744
0.18	0.1938	0.000330	0.001393
0.05	0.1144	0.000077	0.000823
0.03	0.0991	0.000038	0.000712

Table E.66.: Model fit parameter for SWCNT data and SO_2 - Langmuir model

Adsorption						
T [°C]	k_L	k_L min	k_L max	q_max	q_max min	q_max max
25	0.2658	0.2161	0.2161	15.7222	8.7084	8.7084
50	0.2390	0.1270	0.1270	9.8322	2.9029	2.9029
75	0.0922	0.0407	0.0407	10.7565	2.9895	2.9895
75[a]	0.0934	0.0378	0.0378	10.5208	2.6947	2.6947
100	0.0686	0.0223	0.0223	8.7152	1.7314	1.7314
125	0.0261	0.0060	0.0060	11.3080	1.6857	1.6857
Desorption						
T [°C]	k_L	k_L min	k_L max	q_max	q_max min	q_max max
25	0.4891	0.1492	0.1492	10.5890	2.0387	2.0387
50	0.2025	0.2201	0.2201	11.1503	7.1713	7.1713
75	0.1139	0.0664	0.0664	9.7934	3.2553	3.2553
75[a]	0.0786	0.0583	0.0583	12.3278	5.6201	5.6201
100	0.0746	0.0391	0.0391	8.8668	2.5844	2.5844
125	0.0496	0.0203	0.0203	7.7875	1.7489	1.7489

[a] 2. cycle

Table E.67.: Model fit parameter for SWCNT data and SO_2 - Freundlich model

Adsorption T [°C]	K	K min	K max	n	n min	n max
25	3.2622	0.1545	0.1545	0.7243	0.0649	0.0649
50	1.8505	0.0454	0.0454	0.6767	0.0179	0.0179
75	1.0743	0.0460	0.0460	0.6920	0.0223	0.0223
75[a]	1.0597	0.0372	0.0372	0.6934	0.0185	0.0185
100	0.7229	0.0208	0.0208	0.6790	0.0125	0.0125
125	0.4583	0.0231	0.0231	0.7059	0.0165	0.0165
Desorption						
T [°C]	K	K min	K max	n	n min	n max
25	3.4058	0.0211	0.0211	0.6450	0.0127	0.0127
50	1.9436	0.0815	0.0815	0.6640	0.0307	0.0307
75	1.1523	0.0646	0.0646	0.6675	0.0283	0.0283
75[a]	1.0830	0.1213	0.1213	0.7009	0.0527	0.0527
100	0.8146	0.0530	0.0530	0.6453	0.0263	0.0263
125	0.5270	0.0179	0.0179	0.6606	0.0118	0.0118

[a] 2. cycle

Table E.68.: Model fit parameter for SWCNT data and SO_2 - BET model

Adsorption						
T [°C]	K_BET	K_BET min	K_BET max	q_max_BET	q_max_BET max	q_max_BET min
25						
50						
75	8.0425	1.4154	1.4154	2.8838	0.1745	0.1745
75[a]	7.8140	1.4074	1.4074	2.8827	0.1782	0.1782
100	7.7750	0.8022	0.8022	2.8255	0.1080	0.1080
125	7.0707	1.3996	1.3996	2.7432	0.2068	0.2068
Desorption						
T [°C]	K_BET	K_BET min	K_BET max	q_max_BET	q_max_BET max	q_max_BET min
25	8.6057	0.7151	0.7151	3.4147	0.0906	0.0906
50	9.2678	4.5010	4.5010	3.1247	0.5097	0.5097
75	8.5804	1.9487	1.9487	2.9473	0.3260	0.3260
75[a]	8.2225	3.9091	3.9091	2.9324	0.5342	0.5342
100	9.5437	1.9377	1.9377	2.7766	0.2059	0.2059
125						

[a] 2. cycle

Table E.69.: Model fit parameter for SWCNT data and SO_2 - DR model

Adsorption T [°C]	k_DR	k_DR min	k_DR max	q_s	q_s min	q_s max
25	34.1969	24.9280	24.9280	8.3142	3.6876	3.6876
50	36.4583	18.2890	18.2890	6.0541	1.5600	1.5600
75	90.7874	45.7705	45.7705	6.1764	1.7401	1.7401
75[a]	91.4223	47.0642	47.0642	6.0703	1.7460	1.7460
100	116.7846	51.1618	51.1618	5.1445	1.2154	1.2154
125	277.4937	61.1019	61.1019	6.3319	0.7854	0.7854
Desorption						
T [°C]	k_DR	k_DR min	k_DR max	q_s	q_s min	q_s max
25	23.9660	8.6068	8.6068	6.5946	1.4365	1.4365
50	45.6921	57.5451	57.5451	6.7372	4.6728	4.6728
75	70.4290	40.0338	40.0338	5.8429	1.5757	1.5757
75[a]	80.3139	53.5601	53.5601	6.3923	1.8463	1.8463
100	111.6300	61.2959	61.2959	5.5933	1.5539	1.5539
125	207.1178	96.8093	96.8093	5.4643	1.3190	1.3190

[a] 2. cycle

Table E.70.: Model fit parameter for SWCNT data and SO_2 - Temkin model

Adsorption T [°C]	A_T	A_T min	A_T max	RTb_T	RTb_T min	RTb_T max
25						
50						
75	1.0030	0.5361	0.5361	2.1720	0.7144	0.7144
75[a]	0.9829	0.4816	0.4816	2.1613	0.6595	0.6595
100						
125						
Desorption T [°C]	**A_T**	**A_T min**	**A_T max**	**RTb_T**	**RTb_T min**	**RTb_T max**
25						
50						
75	1.6713	0.9087	0.9087	1.7546	0.5020	0.5020
75[a]	1.1525	1.0538	1.0538	2.1423	1.0107	1.0107
100	1.2547	0.7218	0.7218	1.5010	0.4456	0.4456
125	1.1772	0.9759	0.9759	1.1548	0.4353	0.4353

[a] 2. cycle

Table E.71.: Model fit parameter for SWCNT data and SO_2 - Tóth model

Adsorption T [°C]	K_T	K_T min	K_T max	a_T	a_T min	a_T max	t	t min	tmax
25	3.1604	0.3307	0.3307	-0.0874	0.2342	0.2342	4.0615	1.9411	1.9411
50									
75									
75[a]									
100									
125									
Desorption									
T [°C]	K_T	K_T min	K_T max	a_T	a_T min	a_T max	t	t min	tmax
25	3.4477	0.2048	0.2048	0.0305	0.1456	0.1456	2.7311	0.4079	0.4079
50	1.8631	0.4751	0.4751	-0.1205	0.6795	0.6795	3.1902	1.4646	1.4646
75									
75[a]									
100									
125									

[a] 2. cycle

E.3.8 SWCNT and N_2 at 25 °C

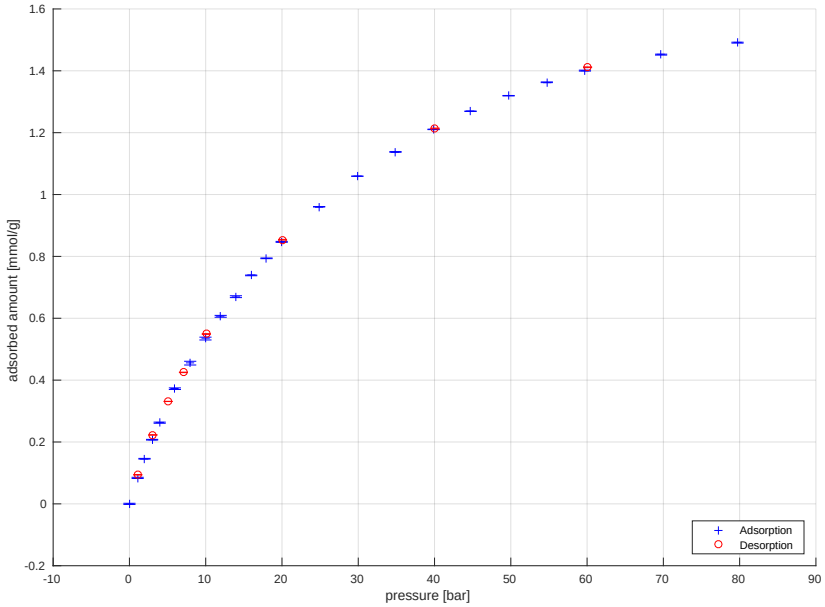

Figure E.78.: SWCNT and N_2 at 25 °C

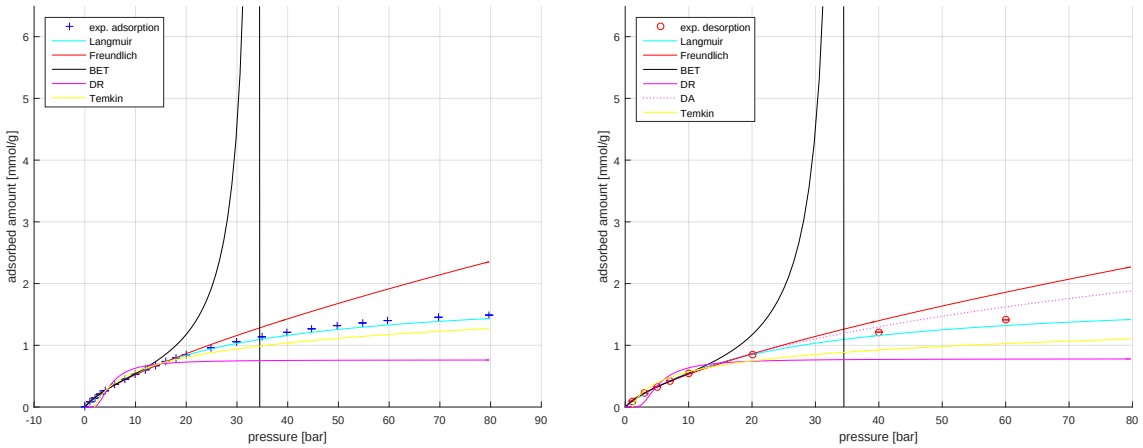

(a) adsorption **(b)** desorption

Figure E.79.: SWCNT and N_2 at 25 °C data (marks) and fits (lines) adsorption branch (a) and desorption branch (b)

Table E.72.: SWCNT and N_2 at 25 °C

sample:	SWCNT		
gas:	N_2		
temperature in [°C]:	22.4	+0.2	-0.4
$m_{S,meas}$ in [mg]:	94.76		
V_S in [cm^3]:	0.038992		

p [bar]	X [$mmolg^{-1}$]	ρ_{meas} [gcm^{-3}]	Δm_{meas} [g]
0.00	0.0000	0.000000	0.000000
1.08	0.0840	0.001228	0.000223
1.98	0.1458	0.002258	0.000388
2.97	0.2074	0.003391	0.000551
3.96	0.2624	0.004528	0.000697
5.96	0.3723	0.006825	0.000989
7.97	0.4549	0.009105	0.001209
9.97	0.5344	0.011399	0.001420
11.96	0.6063	0.013677	0.001611
13.96	0.6698	0.015969	0.001780
15.96	0.7386	0.018267	0.001962
17.97	0.7938	0.020565	0.002109
19.96	0.8470	0.022855	0.002251
24.87	0.9605	0.028498	0.002552
29.88	1.0593	0.034241	0.002815
34.88	1.1378	0.039984	0.003023
39.88	1.2106	0.045896	0.003217
44.72	1.2692	0.051460	0.003372
49.71	1.3195	0.057178	0.003506
54.72	1.3630	0.062921	0.003621
59.72	1.4007	0.068640	0.003722
69.70	1.4523	0.080016	0.003859
79.72	1.4910	0.091368	0.003962
60.07	1.4115	0.069017	0.003750
40.06	1.2138	0.046105	0.003225
20.07	0.8539	0.023017	0.002269
10.08	0.5491	0.011562	0.001459
7.08	0.4250	0.008129	0.001129
5.08	0.3312	0.005842	0.000880
3.08	0.2228	0.003557	0.000592
1.10	0.0940	0.001295	0.000250

E.3.9 SWCNT and N_2 at 75 °C

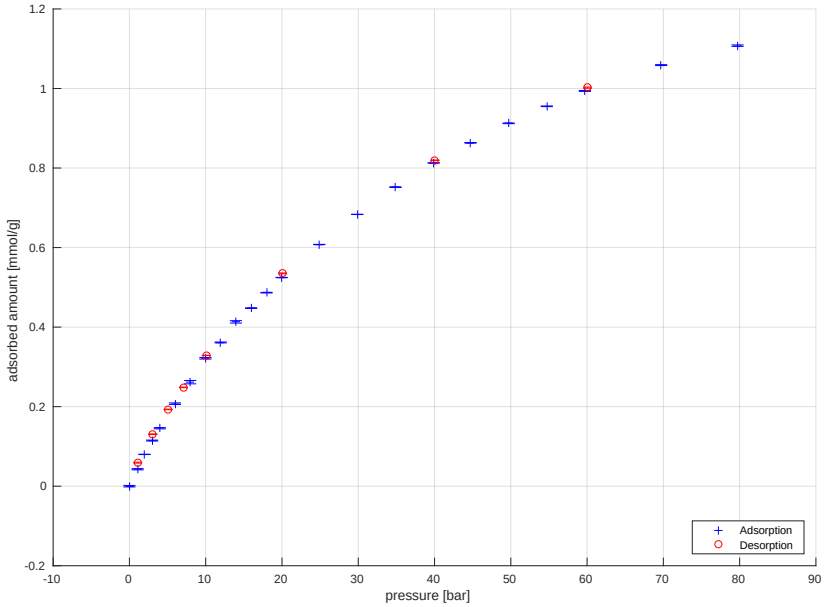

Figure E.80.: SWCNT and N_2 at 75 °C

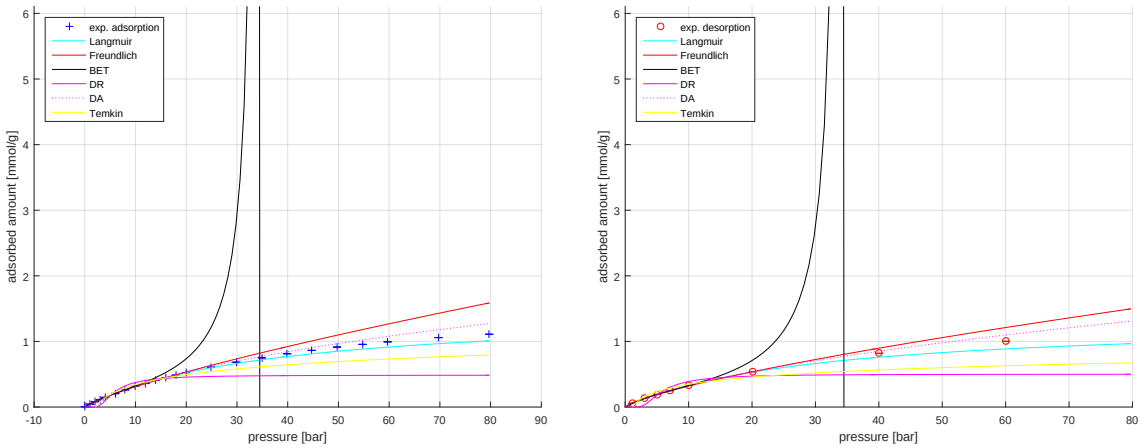

(a) adsorption **(b)** desorption

Figure E.81.: SWCNT and N_2 at 75 °C data (marks) and fits (lines) adsorption branch (a) and desorption branch (b)

Table E.73.: SWCNT and N_2 at 75 °C

sample:	SWCNT		
gas:	N_2		
temperature in [°C]:	71.7	+0.4	-0.1
$m_{S,meas}$ in [mg]:	94.71		
V_S in [cm^3]:	0.041350		

p [bar]	X [$mmolg^{-1}$]	ρ_{meas} [gcm^{-3}]	Δm_{meas} [g]
0.00	0.0000	0.000000	0.000000
1.07	0.0426	0.001046	0.000113
1.98	0.0799	0.001924	0.000212
2.98	0.1148	0.002902	0.000305
3.98	0.1457	0.003872	0.000387
5.97	0.2075	0.005818	0.000551
7.97	0.2615	0.007773	0.000694
9.96	0.3215	0.009725	0.000853
11.97	0.3614	0.011656	0.000959
13.96	0.4132	0.013611	0.001096
15.96	0.4477	0.015543	0.001188
17.97	0.4866	0.017498	0.001291
19.96	0.5247	0.019422	0.001392
24.88	0.6077	0.024189	0.001613
29.87	0.6835	0.029014	0.001814
34.88	0.7519	0.033843	0.001995
39.89	0.8128	0.038802	0.002157
44.72	0.8634	0.043427	0.002291
49.72	0.9123	0.048215	0.002421
54.72	0.9552	0.052977	0.002535
59.71	0.9939	0.057718	0.002638
69.71	1.0588	0.067162	0.002810
79.73	1.1077	0.076544	0.002940
60.07	1.0022	0.058012	0.002659
40.06	0.8194	0.038911	0.002175
20.08	0.5351	0.019483	0.001420
10.08	0.3288	0.009775	0.000872
7.08	0.2484	0.006853	0.000659
5.08	0.1930	0.004907	0.000512
3.08	0.1307	0.002964	0.000347
1.09	0.0592	0.001033	0.000157

E.3.10 SWCNT and N_2 at 125 °C

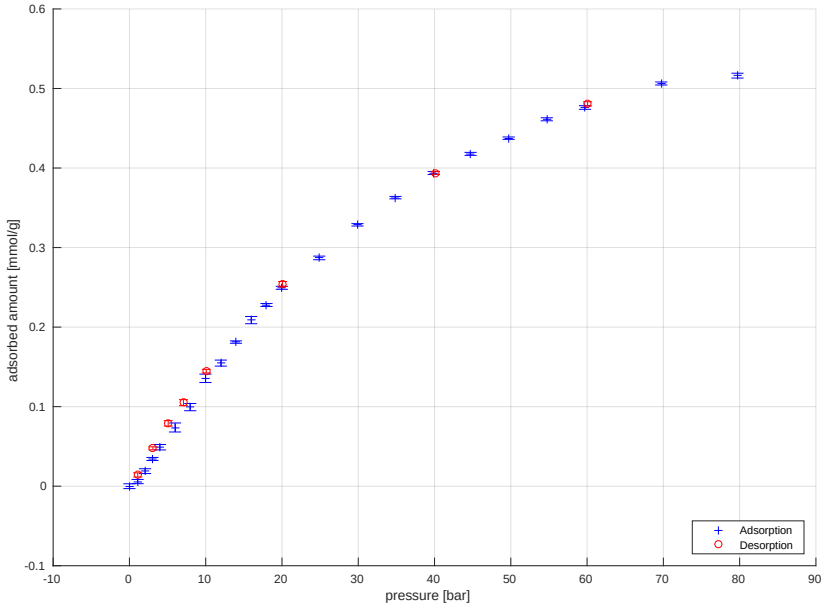

Figure E.82.: SWCNT and N_2 at 125 °C

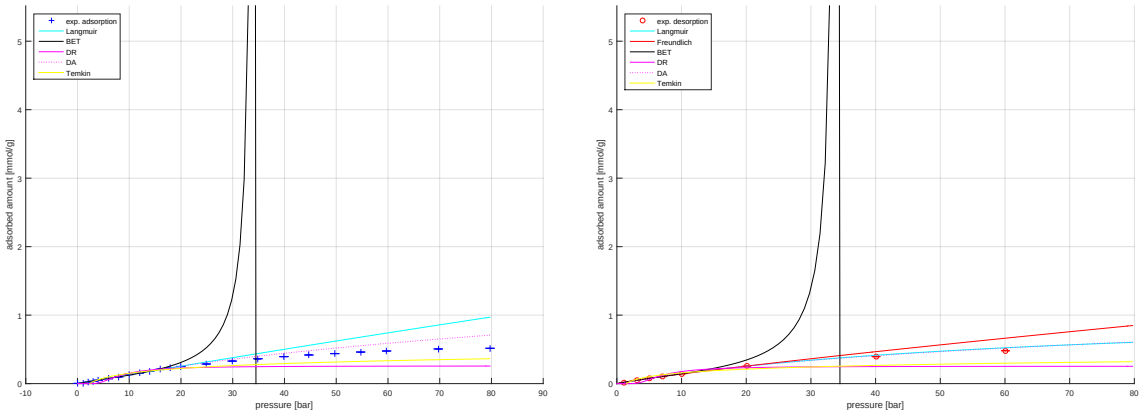

(a) adsorption **(b)** desorption

Figure E.83.: SWCNT and N_2 at 125 °C data (marks) and fits (lines) adsorption branch (a) and desorption branch (b)

Table E.74.: SWCNT and N_2 at 125 °C

sample:	SWCNT		
gas:	N_2		
temperature in [°C]:	124.4	+0.5	-0.2
$m_{S,meas}$ in [mg]:	171.84		
V_S in [cm^3]:	0.086896		

p [bar]	X [$mmol g^{-1}$]	ρ_{meas} [$g cm^{-3}$]	Δm_{meas} [g]
0.00	0.0000	0.000000	0.000000
1.07	0.0054	0.000884	0.000026
2.02	0.0178	0.001676	0.000085
2.97	0.0264	0.002471	0.000126
3.98	0.0365	0.003315	0.000175
5.98	0.0568	0.004992	0.000272
7.98	0.0740	0.006678	0.000355
9.96	0.0946	0.008338	0.000453
11.96	0.1123	0.010005	0.000538
13.96	0.1268	0.011674	0.000607
15.97	0.1452	0.013351	0.000695
17.98	0.1639	0.015034	0.000785
19.99	0.1780	0.016706	0.000852
24.89	0.2135	0.020788	0.001023
29.88	0.2484	0.024934	0.001189
34.90	0.2832	0.029084	0.001356
39.90	0.3115	0.033316	0.001492
44.71	0.3401	0.037266	0.001629
49.72	0.3693	0.041353	0.001769
54.73	0.3935	0.045425	0.001885
59.73	0.4161	0.049468	0.001993
69.72	0.4599	0.057509	0.002203
79.72	0.5023	0.065487	0.002406
60.06	0.4206	0.049727	0.002014
40.07	0.3162	0.033435	0.001514
20.07	0.1829	0.016781	0.000876
10.08	0.0987	0.008428	0.000473
7.08	0.0696	0.005914	0.000333
5.08	0.0514	0.004236	0.000246
3.08	0.0310	0.002554	0.000149
1.09	0.0093	0.000873	0.000045

Table E.75.: Model fit parameter for SWCNT data and N_2 - Langmuir and Freundlich model

Adsorption - Langmuir model						
T [°C]	k_L	k_L min	k_L max	q_max	q_max min	q_max max
25	0.0406	0.0034	0.0034	1.8765	0.1001	0.1001
75	0.0278	0.0023	0.0023	1.4637	0.0873	0.0873
125	0.0008	0.0055	0.0055	16.6081	115.7041	115.7041
Desorption - Langmuir model						
T [°C]	k_L	k_L min	k_L max	q_max	q_max min	q_max max
25	0.0434	0.0070	0.0070	1.8270	0.1905	0.1905
75	0.0332	0.0102	0.0102	1.3303	0.2846	0.2846
125	0.0147	0.0039	0.0039	1.1157	0.2409	0.2409
Adsorption - Freundlich model						
T [°C]	K	K min	K max	n	n min	n max
25	0.0988	0.0083	0.0083	0.7242	0.0316	0.0316
75	0.0507	0.0045	0.0045	0.7864	0.0333	0.0333
125						
Desorption - Freundlich model						
T [°C]	K	K min	K max	n	n min	n max
25	0.1057	0.0158	0.0158	0.7003	0.0578	0.0578
75	0.0581	0.0040	0.0040	0.7421	0.0264	0.0264
125	0.0190	0.0033	0.0033	0.8678	0.0655	0.0655

Table E.76.: Model fit parameter for SWCNT data and N_2 - BET and DR model

Adsorption - BET model						
T [°C]	K_BET	K_BET min	K_BET max	q_max_BET	q_max_BET max	q_max_BET min
25	5.7197	1.0849	1.0849	0.5428	0.0429	0.0429
75	4.4037	0.2664	0.2664	0.3507	0.0099	0.0099
125	1.4007	0.7340	0.7340	0.2591	0.0947	0.0947
Desorption - BET model						
T [°C]	K_BET	K_BET min	K_BET max	q_max_BET	q_max_BET max	q_max_BET min
25	6.2891	1.4208	1.4208	0.5341	0.0456	0.0456
75	5.7382	0.0245	0.0245	0.3267	0.0006	0.0006
125	3.6702	1.4016	1.4016	0.1681	0.0313	0.0313
Adsorption - DR model						
T [°C]	k_DR	k_DR min	k_DR max	q_s	q_s min	q_s max
25	228.5147	56.5292	56.5292	1.0354	0.1359	0.1359
75	227.9201	55.6505	55.6505	0.6743	0.0958	0.0958
125	306.1199	59.1874	59.1874	0.3912	0.0585	0.0585
Desorption - DR model						
T [°C]	k_DR	k_DR min	k_DR max	q_s	q_s min	q_s max
25	242.9448	119.2149	119.2149	1.0889	0.3519	0.3519
75	230.4186	119.1711	119.1711	0.7045	0.2540	0.2540
125	249.9377	99.8835	99.8835	0.3672	0.1148	0.1148

Table E.77.: Model fit parameter for SWCNT data and N_2 - Temkin and Tóth model

Adsorption - Temkin model						
T [°C]	A_T	A_T min	A_T max	RTb_T	RTb_T max	RTb_T min
25	0.5406	0.1098	0.1098	0.3378	0.0395	0.0395
75	0.4803	0.1052	0.1052	0.2179	0.0293	0.0293
125	0.4349	0.1229	0.1229	0.1025	0.0197	0.0197
Desorption - Temkin model						
T [°C]	A_T	A_T min	A_T max	RTb_T	RTb_T max	RTb_T min
25	0.9336	0.7180	0.7180	0.2553	0.2553	0.1056
75	0.9017	0.8004	0.8004	0.1577	0.1577	0.0766
125	0.7245	0.6221	0.6221	0.0789	0.0789	0.0413
Adsorption - Tóth model									
T [°C]	K_T	K_T min	K_T max	a_T	a_T min	a_T max	t	t min	tmax
25									
75									
125									
Desorption - Tóth model									
T [°C]	K_T	K_T min	K_T max	a_T	a_T min	a_T max	t	t min	tmax
25									
75									
125									

E.3.12 SWCNT and CO_2 at 0 °C

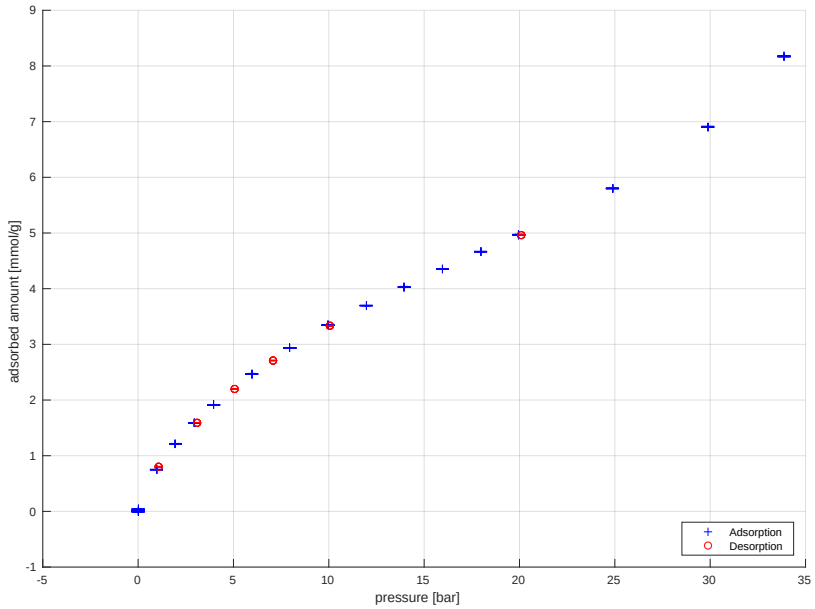

Figure E.84.: SWCNT and CO_2 at 0 °C

Table E.78.: SWCNT and CO_2 at 0 °C

sample:	SWCNT		
gas:	CO_2		
temperature in [°C]:	4.5	+2.1	-2.1
$m_{S,meas}$ in [mg]:	94.27		
V_S in [cm^3]:	0.034019		

p [bar]	X [$mmolg^{-1}$]	ρ_{meas} [gcm^{-3}]	Δm_{meas} [g]
0.00	0.0000	0.000000	0.000000
0.00	0.0045	-0.000002	0.000019
0.00	0.0158	-0.000005	0.000066
0.00	0.0439	0.000020	0.000182
0.96	0.7549	0.001860	0.003137
1.96	1.2201	0.003805	0.005071
2.96	1.5944	0.005753	0.006626
3.96	1.9182	0.007725	0.007972
5.95	2.4710	0.011761	0.010270
7.96	2.9389	0.015918	0.012214
9.96	3.3498	0.020230	0.013922
11.96	3.7017	0.024647	0.015385
13.96	4.0336	0.029219	0.016764
15.96	4.3552	0.033956	0.018101
17.96	4.6698	0.038829	0.019408
19.96	4.9734	0.043871	0.020669
24.87	5.8056	0.057314	0.024128
29.87	6.9103	0.072782	0.028719
33.87	8.1793	0.086919	0.033993
20.07	4.9656	0.044062	0.020637
10.08	3.3346	0.020387	0.013859
7.08	2.7148	0.013999	0.011283
5.08	2.2061	0.009888	0.009169
3.08	1.5969	0.005905	0.006637
1.08	0.8074	0.002037	0.003356

E.4 VACNT

E.4.1 VACNT and SO_2 at 15 °C

Table E.79.: VACNT and SO_2 at 15 °C

sample:	VACNT		
gas:	SO_2		
temperature in [°C]:	15.3	+0.0	-0.0
$m_{S,meas}$ in [mg]:	16.25		
V_S in [cm^3]:	0.007440		

p [bar]	X [mmolg^{-1}]	ρ_{meas} [gcm^{-3}]	Δm_{meas} [g]
0.00	0.0000	0.000000	0.000000
0.23	0.9936	0.000630	0.001034
0.55	2.4996	0.001473	0.002602
0.96	3.7817	0.002621	0.003936
1.32	4.9333	0.003629	0.005135
1.79	7.0754	0.004968	0.007364
2.29	10.1567	0.006414	0.010571
2.68	17.3376	0.007561	0.018045
2.24	10.1190	0.006255	0.010532
1.90	8.5746	0.005275	0.008924
1.64	7.6529	0.004526	0.007965
1.36	5.5859	0.003734	0.005814
0.95	4.3455	0.002579	0.004523
0.48	2.7761	0.001291	0.002889

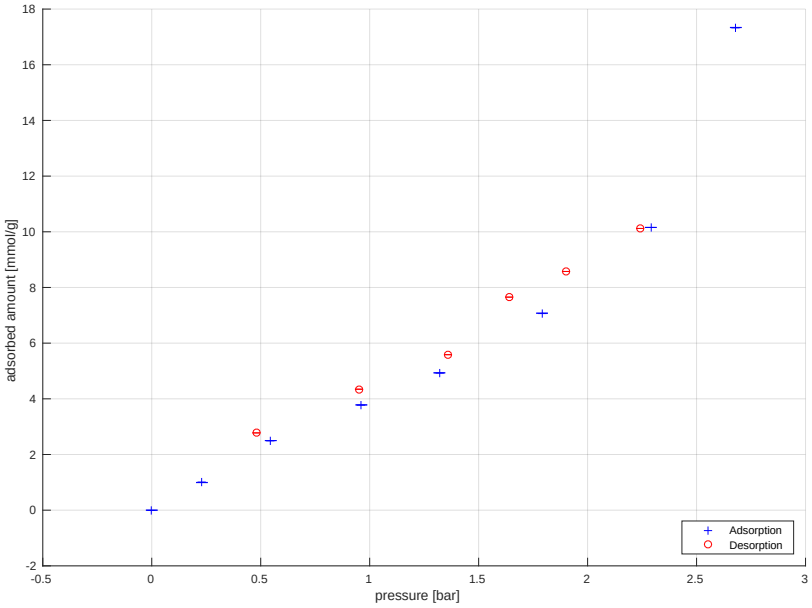

Figure E.85.: VACNT and SO_2 at 15 °C

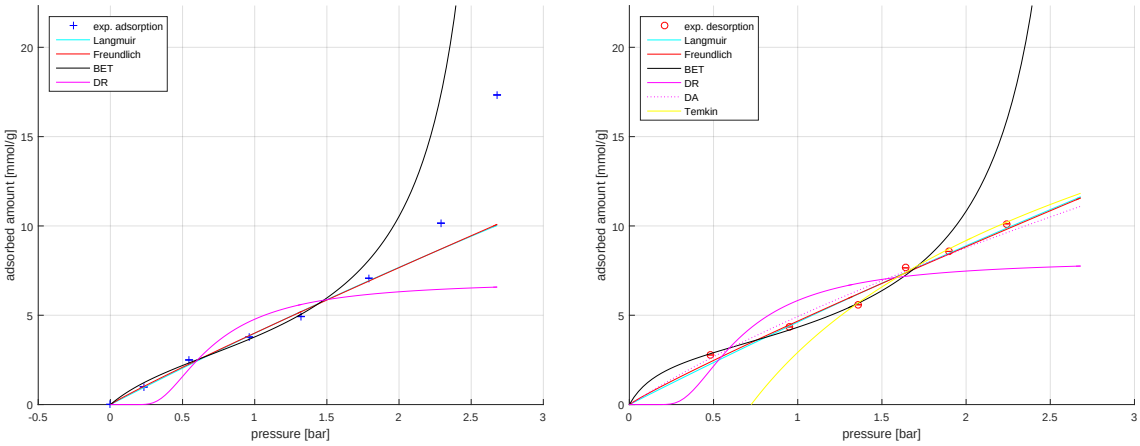

(a) adsorption **(b)** desorption

Figure E.86.: VACNT and SO_2 at 15 °C data (marks) and fits (lines) adsorption branch (a) and desorption branch (b)

E.4.2 VACNT and SO_2 at 25 °C

Table E.80.: VACNT and SO_2 at 25 °C

sample:	VACNT		
gas:	SO_2		
temperature in [°C]:	25.2	+0.0	-0.0
$m_{S,meas}$ in [mg]:	16.08		
V_S in [cm^3]:	0.009116		

p [bar]	X [$mmolg^{-1}$]	ρ_{meas} [gcm^{-3}]	Δm_{meas} [g]
0.00	0.0000	0.000000	0.000000
0.21	0.5612	0.000538	0.000578
0.54	1.7415	0.001420	0.001794
0.96	2.9650	0.002527	0.003055
1.28	3.6440	0.003385	0.003755
1.65	4.3785	0.004400	0.004512
2.01	5.3273	0.005378	0.005489
2.41	6.4731	0.006491	0.006670
2.74	7.8413	0.007423	0.008080
3.25	10.1475	0.008872	0.010456
3.71	14.2241	0.010223	0.014657
3.29	10.7666	0.009004	0.011094
2.61	8.5055	0.007075	0.008764
1.99	5.6566	0.005320	0.005829
1.48	4.5875	0.003929	0.004727
0.95	3.4561	0.002484	0.003561
0.48	1.9752	0.001240	0.002035

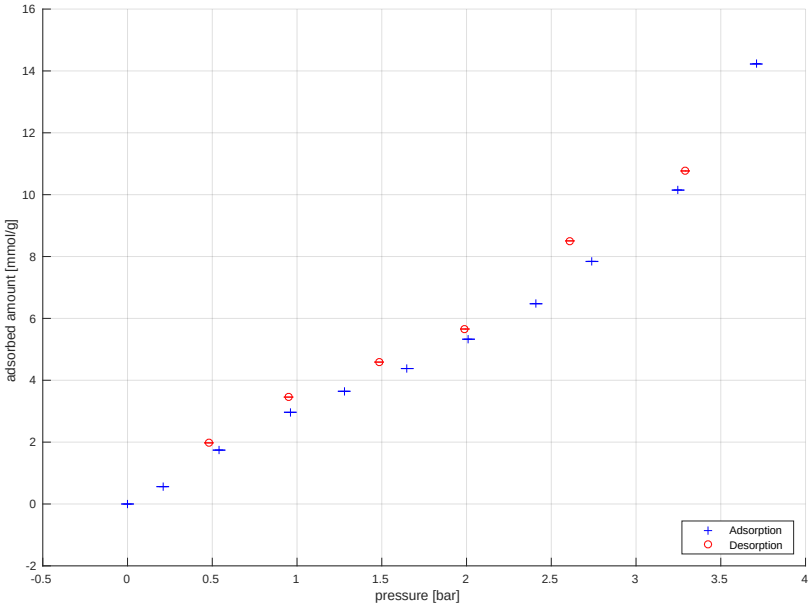

Figure E.87.: VACNT and SO_2 at 25 °C

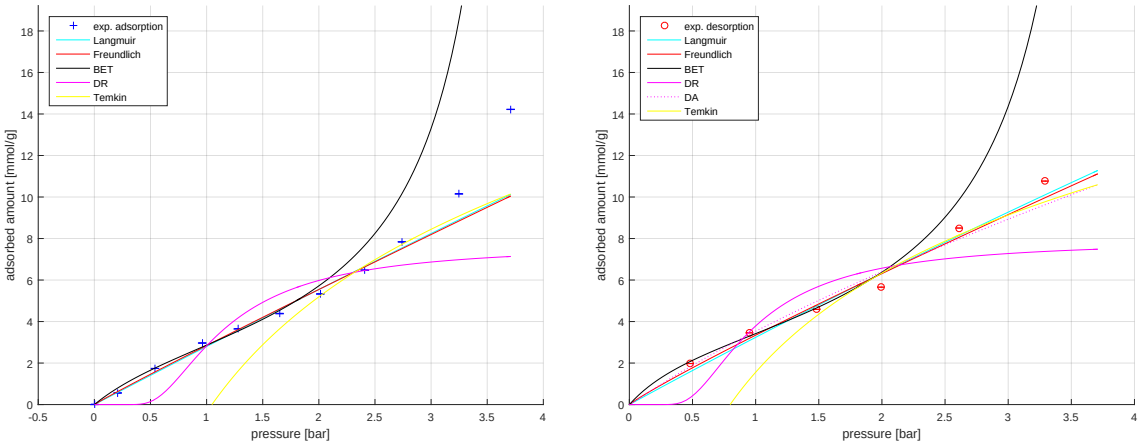

(a) adsorption **(b)** desorption

Figure E.88.: VACNT and SO_2 at 25 °C data (marks) and fits (lines) adsorption branch (a) and desorption branch (b)

E.4.3 VACNT and SO_2 at 35 °C

Table E.81.: VACNT and SO_2 at 35 °C

sample:	VACNT		
gas:	SO_2		
temperature in [°C]:	35.3	+0.2	-0.3
$m_{S,meas}$ in [mg]:	16.25		
V_S in [cm^3]:	0.008222		

p [bar]	X [$mmolg^{-1}$]	ρ_{meas} [gcm^{-3}]	Δm_{meas} [g]
0.00	0.0000	0.000000	0.000000
0.29	0.5755	0.000742	0.000599
0.67	1.4734	0.001702	0.001535
0.96	2.1483	0.002448	0.002238
1.39	2.9250	0.003560	0.003047
1.97	3.7985	0.005110	0.003956
2.40	4.4460	0.006212	0.004631
2.99	5.3547	0.007820	0.005577
3.44	6.3521	0.009067	0.006616
3.89	7.7203	0.010356	0.008041
4.34	9.1885	0.011633	0.009570
4.91	11.6080	0.013305	0.012090
5.36	27.4343	0.014632	0.028574
4.95	12.6531	0.013398	0.013179
4.07	9.2437	0.010857	0.009628
3.42	7.3511	0.009034	0.007656
2.96	5.9268	0.007749	0.006173
2.45	5.0758	0.006378	0.005287
1.91	4.2085	0.004904	0.004383
1.45	3.5557	0.003712	0.003703
0.92	2.5675	0.002352	0.002674
0.46	1.3983	0.001168	0.001456
0.20	0.7835	0.000520	0.000816

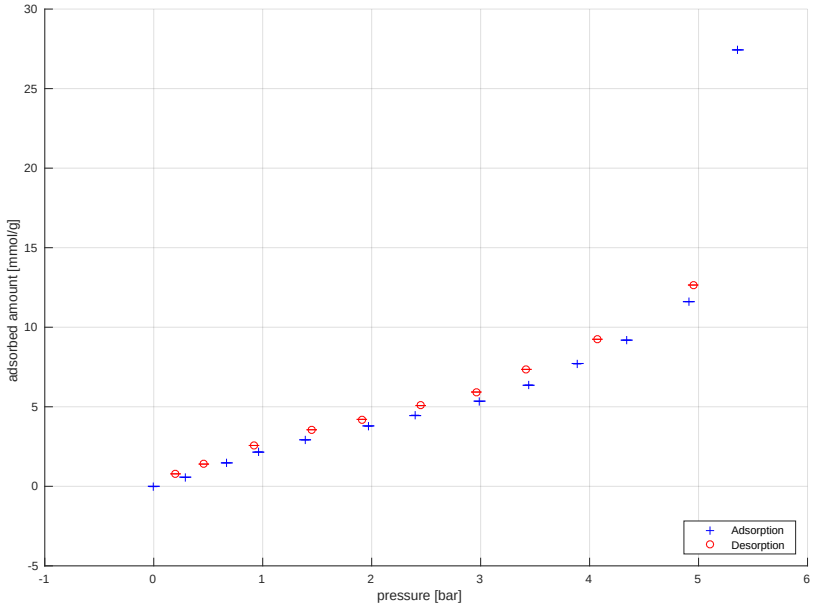

Figure E.89.: VACNT and SO_2 at 35 °C

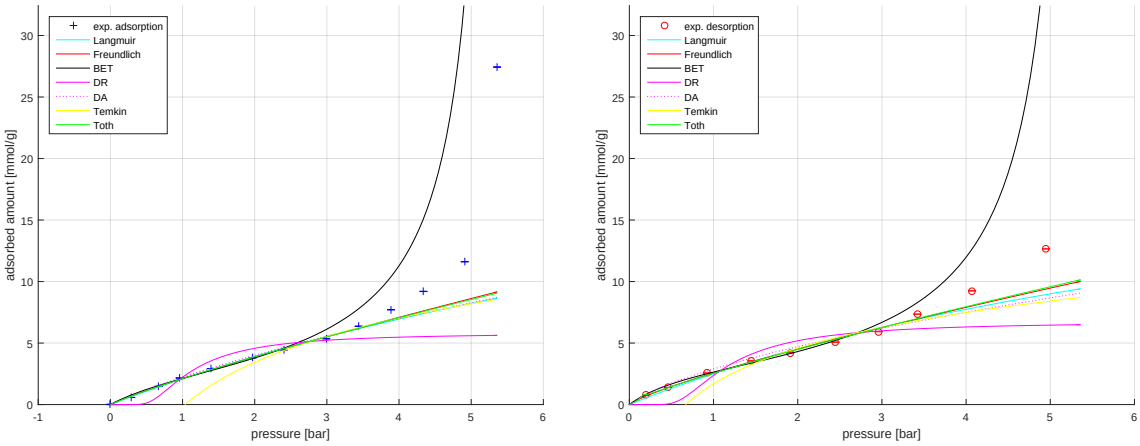

(a) adsorption **(b)** desorption

Figure E.90.: VACNT and SO_2 at 35 °C data (marks) and fits (lines) adsorption branch (a) and desorption branch (b)

E.4.4 VACNT and SO_2 at 50 °C

Table E.82.: VACNT and SO_2 at 50 °C

sample:	VACNT		
gas:	SO_2		
temperature in [°C]:	50.3	+0.1	-0.0
$m_{S,meas}$ in [mg]:	15.88		
V_S in [cm^3]:	0.007733		

p [bar]	X [mmolg^{-1}]	ρ_{meas} [gcm^{-3}]	Δm_{meas} [g]
0.00	0.0000	0.000000	0.000000
0.33	0.4302	0.000778	0.000438
0.67	0.9161	0.001600	0.000932
0.99	1.3937	0.002386	0.001418
2.94	3.6408	0.007260	0.003704
5.10	5.8332	0.013007	0.005934
5.95	7.4657	0.015336	0.007595
6.91	9.5460	0.018115	0.009711
7.43	10.7952	0.019621	0.010982
7.93	12.7708	0.021110	0.012992
8.08	13.8394	0.021561	0.014079
7.37	10.8163	0.019454	0.011003
5.91	7.9877	0.015253	0.008126
3.92	4.9469	0.009812	0.005032
2.45	3.5347	0.006017	0.003596
1.45	2.3970	0.003504	0.002438
0.97	1.6971	0.002327	0.001726
0.49	0.9062	0.001166	0.000922
0.29	0.5853	0.000676	0.000595

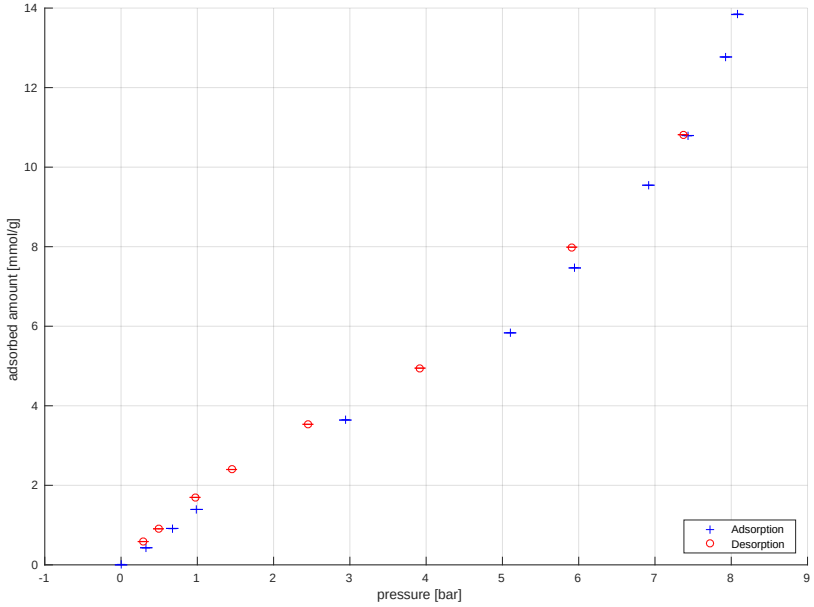

Figure E.91.: VACNT and SO_2 at 50 °C

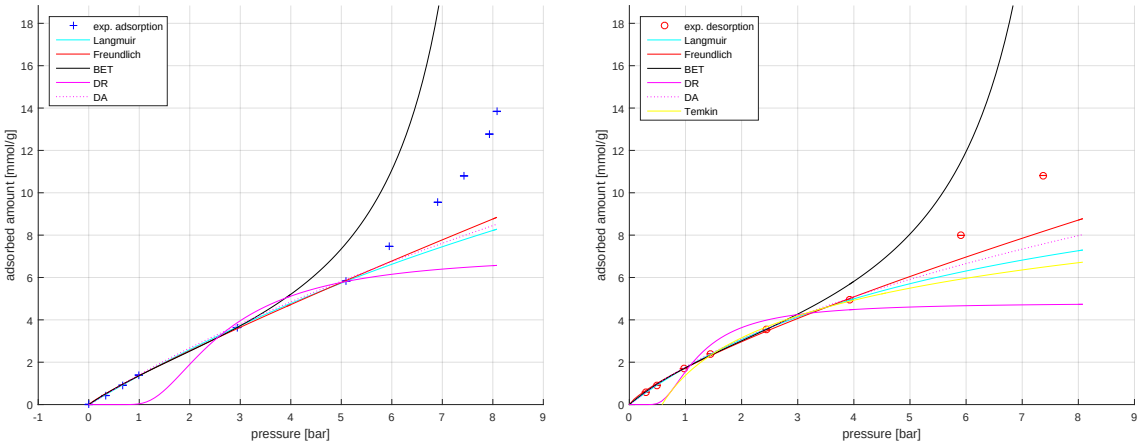

(a) adsorption **(b)** desorption

Figure E.92.: VACNT and SO_2 at 50 °C data (marks) and fits (lines) adsorption branch (a) and desorption branch (b)

Table E.83.: VACNT and SO_2 at 75 °C

sample:	VACNT		
gas:	SO_2		
temperature in [°C]:	75.2	+0.2	-0.2
$m_{S,meas}$ in [mg]:	16.32		
V_S in [cm^3]:	0.008049		

p [bar]	X [$mmolg^{-1}$]	ρ_{meas} [gcm^{-3}]	Δm_{meas} [g]
0.00	0.0000	0.000000	0.000000
0.42	0.2753	0.000928	0.000287
0.99	0.6495	0.002181	0.000678
1.55	1.0607	0.003458	0.001107
2.14	1.4877	0.004822	0.001553
3.88	2.7301	0.008947	0.002851
5.58	3.4798	0.012996	0.003633
7.24	4.2042	0.017166	0.004390
10.02	5.6700	0.024578	0.005920
10.86	6.2853	0.026904	0.006563
12.03	7.4159	0.030279	0.007743
13.26	8.8753	0.033942	0.009267
13.95	10.0063	0.036058	0.010448
15.59	13.6990	0.041354	0.014303
14.08	10.3557	0.036513	0.010813
12.56	8.4868	0.031831	0.008861
9.89	6.0222	0.024230	0.006288
7.01	4.4145	0.016607	0.004609
4.94	3.4628	0.011440	0.003616
2.51	2.1082	0.005666	0.002201
1.41	1.3008	0.003133	0.001358
0.98	0.9730	0.002156	0.001016

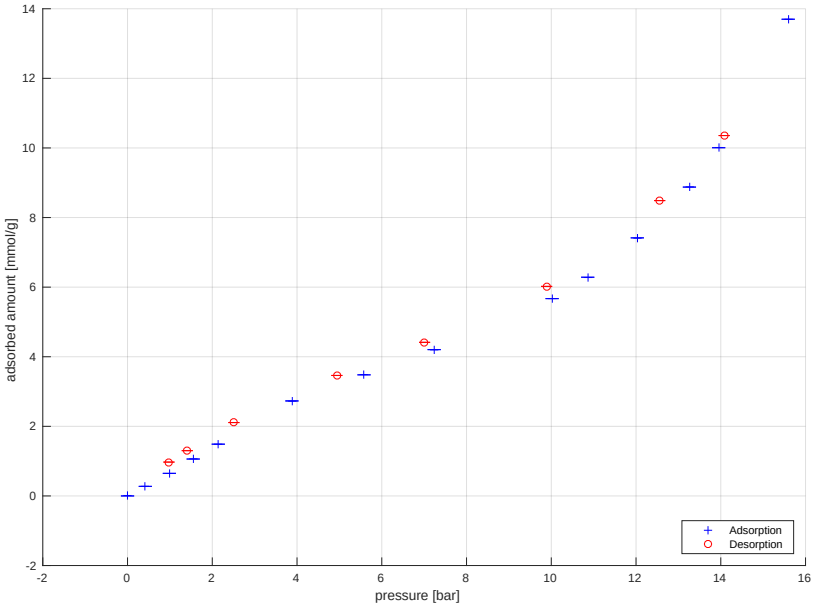

Figure E.93.: VACNT and SO_2 at 75 °C

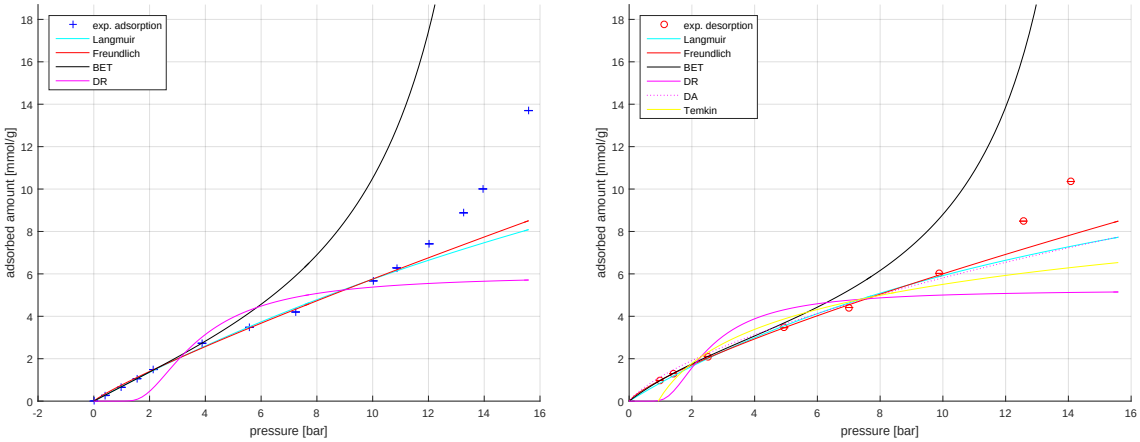

(a) adsorption **(b)** desorption

Figure E.94.: VACNT and SO_2 at 75 °C data (marks) and fits (lines) adsorption branch (a) and desorption branch (b)

Table E.84.: Model fit parameter for VACNT data and SO_2 - Langmuir and Freundlich model

Adsorption - Langmuir model						
T [°C]	k_L	k_L min	k_L max	q_max	q_max min	q_max max
15	0.0411	-0.1268	0.2090	101.0899	-288.5843	490.7641
25	0.0093	-0.0655	0.0840	304.2872	-2097.6556	2706.2301
35	0.0727	0.0241	0.1213	30.8192	13.5213	48.1171
50	0.0480	0.0348	0.0611	29.6344	22.8730	36.3957
75	0.0239	0.0102	0.0376	29.7669	15.5951	43.9387
Desorption - Langmuir model						
T [°C]	k_L	k_L min	k_L max	q_max	q_max min	q_max max
15	0.0394	-0.3183	0.3971	121.7262	-918.9820	1162.4344
25	0.0245	-0.2540	0.3029	135.5148	-1330.9066	1601.9362
35	0.1079	-0.0152	0.2310	25.6877	2.7626	48.6127
50	0.1498	0.1295	0.1701	13.3235	12.0432	14.6038
75	0.0532	0.0146	0.0919	17.0354	8.0970	25.9738
Adsorption - Freundlich model						
T [°C]	K	K min	K max	n	n min	n max
15	4.0013	3.7089	4.2937	0.9381	0.7870	1.0891
25	2.8447	2.5809	3.1085	0.9627	0.8478	1.0777
35	2.1097	1.9759	2.2435	0.8746	0.8114	0.9377
50	1.3689	1.2749	1.4629	0.8927	0.8456	0.9399
75	0.7598	0.6651	0.8545	0.8795	0.8212	0.9377
Desorption - Freundlich model						
T [°C]	K	K min	K max	n	n min	n max
15	4.6720	3.7951	5.5489	0.9196	0.5518	1.2874
25	3.3425	2.3596	4.3254	0.9168	0.5356	1.2980
35	2.5720	2.2745	2.8695	0.8096	0.6936	0.9257
50	1.7312	1.6093	1.8530	0.7770	0.7140	0.8400
75	0.9930	0.8851	1.1008	0.7812	0.7268	0.8356

Table E.85.: Model fit parameter for VACNT data and SO_2 - BET and DR model

Adsorption - BET model						
T [°C]	K_BET	K_BET min	K_BET max	q_max_BET	q_max_BET max	q_max_BET min
15	6.1631	-1.9921	14.3183	3.1145	2.0975	4.1316
25	5.2838	0.4555	10.1120	3.3146	2.3833	4.2459
35	5.4261	2.4933	8.3589	3.1405	2.6290	3.6520
50	3.8761	-1.0746	8.8269	3.5108	1.6663	5.3554
75	5.2698	1.6841	8.8556	2.9544	2.3319	3.5768
Desorption - BET model						
T [°C]	K_BET	K_BET min	K_BET max	q_max_BET	q_max_BET max	q_max_BET min
15	15.2738	-74.4029	104.9506	3.0874	0.9460	5.2288
25	7.6537	-24.3493	39.6568	3.5193	-0.3869	7.4254
35	8.5851	2.7129	14.4573	3.2590	2.7620	3.7561
50	7.6307	3.0113	12.2500	3.1154	2.6213	3.6094
75	7.4680	4.0462	10.8897	2.9752	2.6026	3.3477
Adsorption - DR model						
T [°C]	k_DR	k_DR min	k_DR max	q_s	q_s min	q_s max
15	675.5941	-64.5119	1415.7001	6.9265	4.2269	9.6262
25	1696.0990	484.5536	2907.6444	7.6720	5.6333	9.7108
35	1529.2503	582.6766	2475.8240	5.8161	4.6416	6.9907
50	7651.9761	-5779.1300	21083.0822	7.1243	2.2163	12.0323
75	12769.3042	3081.8171	22456.7912	5.9562	4.5919	7.3205
Desorption - DR model						
T [°C]	k_DR	k_DR min	k_DR max	q_s	q_s min	q_s max
15	604.3537	-339.4330	1548.1404	8.1208	4.5267	11.7149
25	1248.8646	-1126.1075	3623.8366	7.8948	2.8653	12.9243
35	1662.0662	129.1305	3195.0018	6.7325	4.8131	8.6518
50	1633.3351	-13.6098	3280.2800	4.8164	3.0286	6.6043
75	6021.9916	-2224.1526	14268.1357	5.2498	3.2036	7.2961

Table E.86.: Model fit parameter for VACNT data and SO_2 - Temkin and Tóth model

Adsorption - Temkin model									
T [°C]	A_T	A_T min	A_T max	RTb_T	RTb_T min	RTb_T max			
15									
25	0.9548	-0.5414	2.4511	8.0234	-7.2017	23.2486			
35	0.9689	-1.0307	2.9684	5.1917	-5.0358	15.4191			
50									
75									
Desorption - Temkin model									
T [°C]	A_T	A_T min	A_T max	RTb_T	RTb_T min	RTb_T max			
15	1.3822	-0.7657	3.5302	9.0320	-8.1562	26.2203			
25	1.2533	-3.0164	5.5229	6.8946	-18.2177	32.0069			
35	1.4982	0.5232	2.4732	4.1782	2.0661	6.2902			
50	1.7171	-1.3087	4.7429	2.5563	-0.4966	5.6092			
75	1.0779	0.3361	1.8197	2.3155	1.3511	3.2799			
Adsorption - Tóth model									
T [°C]	K_T	K_T min	K_T max	a_T	a_T min	a_T max	t	t min	tmax
15									
25									
35	2.2241	0.8773	3.5709	0.3797	-3.9868	4.7462	6.3723	-7.2837	20.0283
50									
75									
Desorption - Tóth model									
T [°C]	K_T	K_T min	K_T max	a_T	a_T min	a_T max	t	t min	tmax
15									
25									
35	2.4814	2.0774	2.8854	-0.1475	-0.5095	0.2145	6.0996	0.3864	11.8128
50									
75									

E.5 13X

E.5.1 13X and N_2 at 25 °C

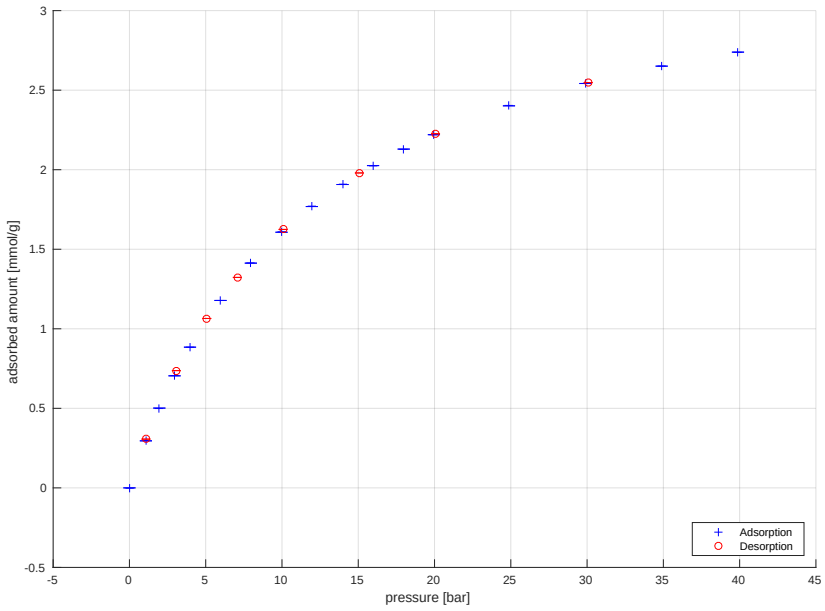

Figure E.95.: 13X and N_2 at 25 °C

Table E.87.: 13X and N_2 at 25 °C

sample:	13X		
gas:	N_2		
temperature in [°C]:	25.3	+0.2	-0.0
$m_{S,meas}$ in [mg]:	1971.50		
V_S in [cm^3]:	0.825486		

p [bar]	X [$mmolg^{-1}$]	ρ_{meas} [gcm^{-3}]	Δm_{meas} [g]
0.00	0.0000	0.000000	0.000000
1.08	0.2957	0.001197	0.016334
1.96	0.5016	0.002183	0.027711
2.96	0.7043	0.003304	0.038913
3.97	0.8845	0.004448	0.048867
5.97	1.1782	0.006689	0.065096
7.96	1.4127	0.008921	0.078053
9.97	1.6070	0.011178	0.088788
11.96	1.7684	0.013415	0.097705
13.97	1.9069	0.015676	0.105356
15.97	2.0258	0.017931	0.111926
17.98	2.1296	0.020194	0.117658
19.96	2.2202	0.022428	0.122663
24.88	2.4016	0.027980	0.132685
29.89	2.5420	0.033622	0.140442
34.89	2.6510	0.039268	0.146467
39.89	2.7391	0.045093	0.151334
30.07	2.5480	0.033840	0.140773
20.07	2.2264	0.022570	0.123007
15.07	1.9797	0.016942	0.109377
10.07	1.6246	0.011321	0.089760
7.07	1.3231	0.007945	0.073098
5.07	1.0650	0.005695	0.058838
3.07	0.7372	0.003448	0.040728
1.08	0.3064	0.001204	0.016931

E.5.2 13X and N_2 at 25 °C second measurement

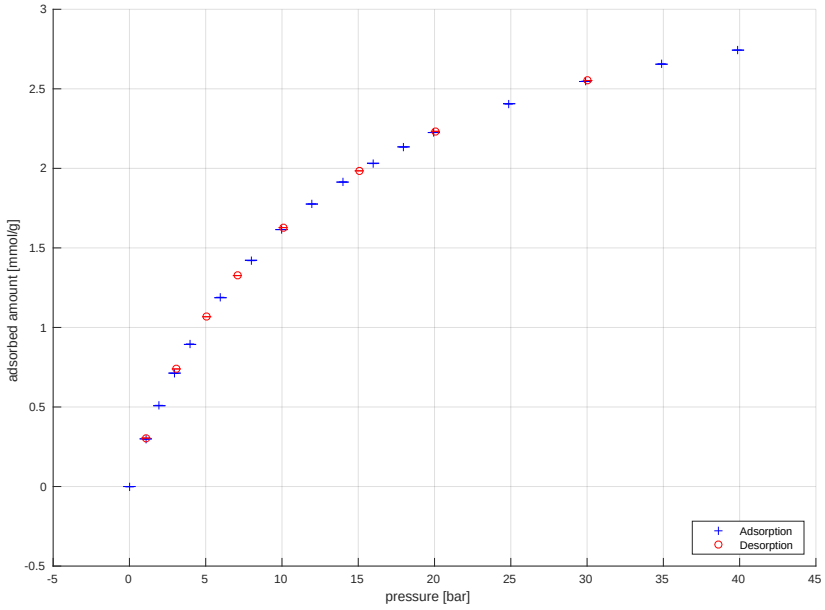

Figure E.96.: 13X and N_2 at 25 °C second measurement

Table E.88.: 13X and N_2 at 25 °C second measurement

sample:	13X		
gas:	N_2		
temperature in [°C]:	25.3	+0.1	-0.0
$m_{S,meas}$ in [mg]:	1971.50		
V_S in [cm^3]:	0.825486		

p [bar]	X [mmolg^{-1}]	ρ_{meas} [gcm^{-3}]	Δm_{meas} [g]
0.00	0.0000	0.000000	0.000000
1.07	0.2997	0.001213	0.016556
1.96	0.5081	0.002210	0.028072
2.96	0.7129	0.003342	0.039389
3.97	0.8933	0.004484	0.049355
5.97	1.1870	0.006731	0.065583
7.97	1.4221	0.008983	0.078571
9.97	1.6152	0.011238	0.089236
11.96	1.7757	0.013478	0.098108
13.97	1.9137	0.015748	0.105730
15.97	2.0320	0.018011	0.112268
17.97	2.1352	0.020291	0.117966
19.96	2.2252	0.022545	0.122940
24.89	2.4065	0.028134	0.132958
29.88	2.5461	0.033795	0.140669
34.88	2.6548	0.039465	0.146674
39.89	2.7431	0.045320	0.151555
30.05	2.5524	0.033988	0.141018
20.05	2.2329	0.022654	0.123365
15.06	1.9844	0.016994	0.109635
10.07	1.6277	0.011340	0.089928
7.07	1.3260	0.007950	0.073259
5.07	1.0673	0.005696	0.058967
3.07	0.7390	0.003443	0.040830
1.08	0.3049	0.001198	0.016848

E.6 BET measurements

E.6.1 CNT and N_2 at $77\,\mathrm{K}$

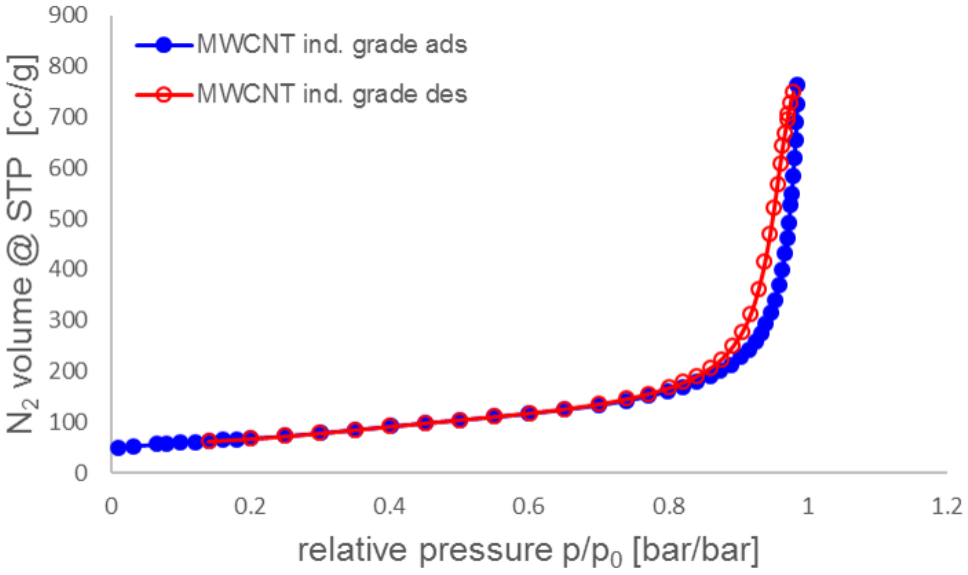

Figure E.97.: CNT and N_2 at $77\,\mathrm{K}$

Table E.89.: CNT and N_2 at 77 K

sample:		CNT			
rel. pressure $\frac{p}{p_0}$ [-]	volume @ STP [cm^3g^{-1}]	rel. pres. $\frac{p}{p_0}$ [-]	vol. @ STP [cm^3g^{-1}]	rel. pres. $\frac{p}{p_0}$ [-]	vol. @ STP [cm^3g^{-1}]
0.0108222	48.470	0.9587170	369.741	0.7010230	136.103
0.0310512	52.669	0.9636951	400.828	0.6508189	126.182
0.0658229	56.397	0.9674432	431.901	0.6012799	118.182
0.0797398	57.638	0.9709207	462.936	0.5508378	111.158
0.0999246	59.363	0.9726962	493.262	0.5007861	104.747
0.1203620	61.029	0.9758943	527.869	0.4505793	98.461
0.1398037	62.639	0.9771407	550.375	0.4001123	91.768
0.1600213	64.338	0.9788552	584.848	0.3494551	84.907
0.1805638	66.112	0.9809450	619.415	0.2994607	78.355
0.1998430	67.857	0.9823803	654.578	0.2499189	72.564
0.2489354	72.702	0.9840844	691.006	0.2002161	67.603
0.3002258	78.602	0.9847979	726.839	0.1402781	62.392
0.3502696	85.116	0.9856813	762.975		
0.4012637	91.912	0.9796660	749.984		
0.4512896	98.316	0.9752399	727.666		
0.5010410	104.444	0.9717262	705.632		
0.5509545	110.551	0.9705675	695.928		
0.5999946	117.096	0.9671882	668.750		
0.6500124	124.731	0.9642876	644.582		
0.6998497	133.837	0.9605566	610.201		
0.7398920	142.973	0.9565786	569.101		
0.7706353	151.388	0.9517900	522.407		
0.7996123	161.102	0.9459807	470.509		
0.8206513	169.456	0.9387061	416.303		
0.8400761	178.629	0.9295509	362.005		
0.8598752	190.137	0.9178653	312.223		
0.8753667	200.878	0.9059862	277.558		
0.8900406	213.224	0.8925443	249.126		
0.9046168	228.969	0.8763579	224.554		
0.9154222	243.440	0.8615764	208.077		
0.9249641	259.288	0.8413806	191.401		
0.9330865	276.030	0.8215661	178.664		
0.9399198	293.812	0.8009749	168.070		
0.9469831	316.139	0.7706538	155.838		
0.9528193	339.506	0.7408899	146.336		

E.6.2 MWCNT and N_2 at 77 K

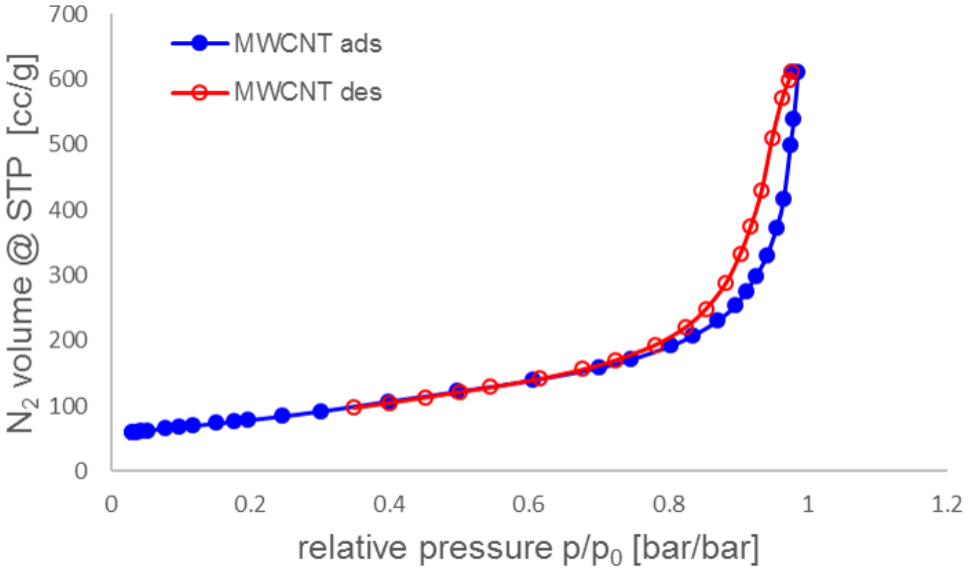

Figure E.98.: MWCNT and N_2 at 77 K

Table E.90.: MWCNT and N_2 at 77 K

sample:		MWCNT	
rel. pressure $\frac{p}{p_0}$ [-]	volume @ STP [cm^3g^{-1}]	rel. pres. $\frac{p}{p_0}$ [-]	vol. @ STP [cm^3g^{-1}]
0.0299340	59.901	0.9769150	610.875
0.0295230	59.847	0.9735140	598.159
0.0348370	60.733	0.9643060	571.152
0.0423490	61.794	0.9500270	511.053
0.0512530	62.903	0.9345140	429.349
0.0764300	65.869	0.9186640	374.165
0.0964240	67.991	0.9036960	332.739
0.1164550	70.104	0.8828900	287.680
0.1513330	73.792	0.8537580	248.072
0.1770960	76.641	0.8241240	220.021
0.1967290	78.855	0.7809620	193.518
0.2462920	84.831	0.7245150	170.621
0.3010240	92.340	0.6770730	156.218
0.3976090	107.250	0.6159570	141.989
0.4966260	122.406	0.5437800	128.830
0.6062460	139.982	0.5004250	121.823
0.7003690	158.998	0.4510520	113.529
0.7455260	171.162	0.3998770	105.448
0.8040920	192.877	0.3490460	97.555
0.8356180	208.148		
0.8699720	230.171		
0.8959510	253.728		
0.9113500	275.867		
0.9256650	298.470		
0.9410320	329.568		
0.9558210	373.782		
0.9655790	416.919		
0.9755480	500.361		
0.9799980	539.057		
0.9855090	611.112		
0.9771730	611.330		

E.6.3 SWCNT and N_2 at $77\,\mathrm{K}$

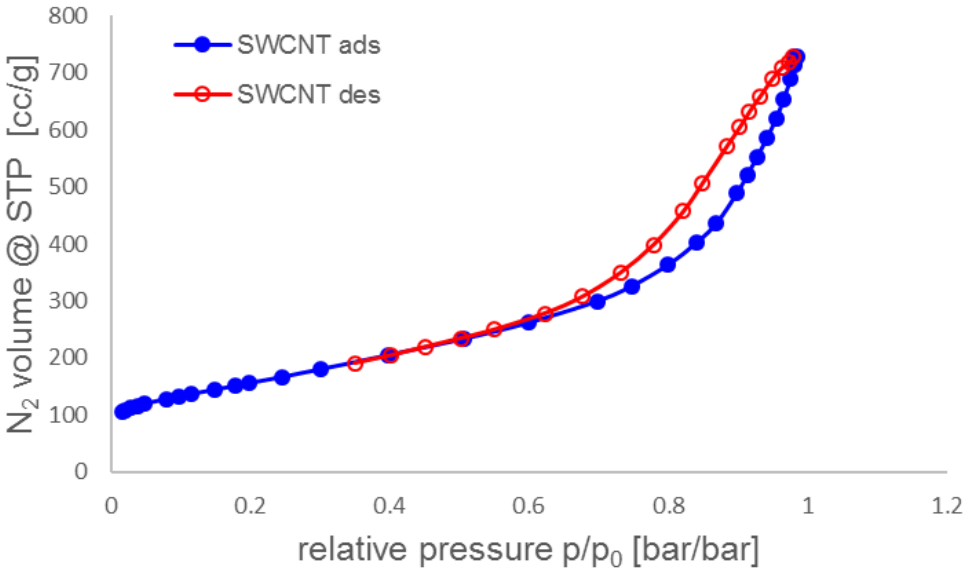

Figure E.99.: SWCNT and N_2 at $77\,\mathrm{K}$

Table E.91.: SWCNT and N_2 at 77 K

sample:		MWCNT	
rel. pressure $\frac{p}{p_0}$ [-]	volume @ STP [cm^3g^{-1}]	rel. pres. $\frac{p}{p_0}$ [-]	vol. @ STP [cm^3g^{-1}]
0.0154290	106.099	0.9801070	727.550
0.0195250	108.538	0.9742760	719.958
0.0273870	112.234	0.9625330	708.419
0.0367810	115.813	0.9494240	689.615
0.0471190	118.910	0.9315990	658.118
0.0782450	127.415	0.9164500	631.762
0.0962050	131.774	0.9029940	605.127
0.1152050	136.241	0.8841580	571.144
0.1488550	143.934	0.8495180	506.841
0.1789210	150.812	0.8216390	456.902
0.1969990	154.974	0.7789570	398.472
0.2452410	166.203	0.7315310	349.379
0.3001870	179.562	0.6767300	307.175
0.3970180	204.235	0.6223650	277.660
0.5073230	233.385	0.5507640	249.642
0.6004680	261.710	0.5022270	234.124
0.6976730	298.964	0.4519100	219.163
0.7474520	325.593	0.4013700	204.044
0.8001100	363.181	0.3494960	190.218
0.8401870	401.435		
0.8689500	435.724		
0.8990180	489.705		
0.9135780	521.213		
0.9277770	552.485		
0.9415010	585.688		
0.9550470	620.565		
0.9654560	653.383		
0.9754330	689.426		
0.9817800	713.891		
0.9854150	728.597		
0.9805160	729.262		

E.6.4 VACNT and N_2 at 77 K

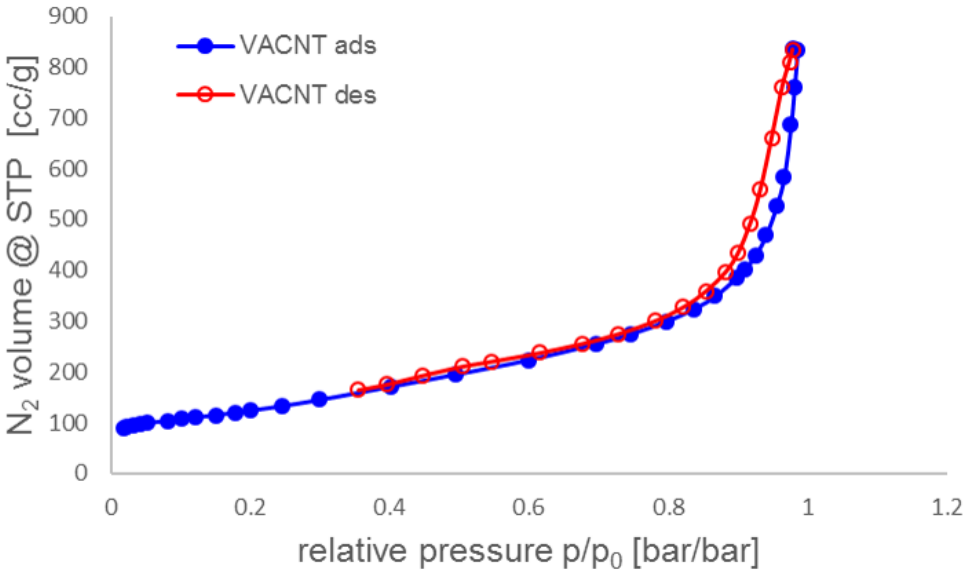

Figure E.100.: VACNT and N_2 at 77 K

Table E.92.: VACNT and N_2 at 77 K

sample:		MWCNT	
rel. pressure $\frac{p}{p_0}$ [-]	volume @ STP [cm^3g^{-1}]	rel. pres. $\frac{p}{p_0}$ [-]	vol. @ STP [cm^3g^{-1}]
0.0179160	90.709	0.9790680	835.056
0.0224280	92.799	0.9743930	810.080
0.0317420	95.515	0.9642120	760.932
0.0416080	97.720	0.9487900	659.041
0.0517780	99.587	0.9327180	558.187
0.0804920	104.029	0.9183280	492.764
0.1004860	107.123	0.9008240	434.609
0.1203690	110.508	0.8831710	397.482
0.1495520	115.199	0.8544910	359.030
0.1789160	120.187	0.8220000	327.648
0.1991230	123.984	0.7811430	300.297
0.2463550	133.376	0.7286210	275.095
0.2984810	145.186	0.6763630	255.739
0.4010520	171.060	0.6151410	237.625
0.4951920	195.306	0.5457130	220.693
0.5990410	223.489	0.5043590	211.031
0.6969210	255.750	0.4467490	192.999
0.7457310	274.601	0.3957660	175.650
0.7968350	299.443	0.3547940	164.741
0.8367380	324.388		
0.8670360	348.923		
0.8978360	385.595		
0.9101570	402.776		
0.9250170	429.443		
0.9400140	468.567		
0.9555020	527.404		
0.9663670	585.238		
0.9761230	688.315		
0.9808110	760.858		
0.9850910	834.407		
0.9793400	836.397		

E.7 Heat of adsorption

Here the parameters for the fits of the Virial-type thermal equation are given for the different CNT types measured in experiments. In the tables also the fitting values for the 95 % confidence interval are given.

Table E.93.: Fit parameters for Virial-type thermal equation for different CNT types and SO_2

Adsorption type	fit				min. 95% confidence intervall				max. 95% confidence intervall			
	a_0	a_1	a_2	b_0	a_0	a_1	a_2	b_0	a_0	a_1	a_2	b_0
VACNT	-3105.308	4.157	-0.569	9.339	-3211.600	0.915	-0.712	9.005	-2999.017	7.399	-0.427	9.672
SWCNT	-3446.288	51.950	-2.628	9.753	-3654.134	40.852	-3.184	9.186	-3238.442	63.047	-2.073	10.320
MWCNT	-2981.757	47.387	-5.092	9.336	-3119.659	34.339	-6.175	8.954	-2843.856	60.434	-4.009	9.717
CNT	-3093.150	25.125	-3.562	9.929	-3220.242	12.665	-4.557	9.573	-2966.057	37.585	-2.567	10.286

Desorption type	fit				min. 95% confidence intervall				max. 95% confidence intervall			
	a_0	a_1	a_2	b_0	a_0	a_1	a_2	b_0	a_0	a_1	a_2	b_0
VACNT	-3422.903	52.113	-3.562	9.758	-3534.733	44.357	-4.182	9.422	-3311.073	59.869	-2.942	10.094
SWCNT	-3019.461	87.227	-3.815	8.052	-3511.862	61.723	-4.921	6.732	-2527.061	112.731	-2.709	9.372
MWCNT	-3120.366	165.331	-21.387	9.252	-3349.341	125.507	-27.358	8.639	-2891.392	205.154	-15.415	9.866
CNT	-3300.498	139.484	-19.100	10.107	-3472.075	111.321	-23.812	9.628	-3128.920	167.647	-14.389	10.585

Table E.94.: Fit parameters for Virial-type thermal equation for different CNT types and N_2

Adsorption type	fit				min. 95% confidence intervall				max. 95% confidence intervall			
	a_0	a_1	a_2	b_0	a_0	a_1	a_2	b_0	a_0	a_1	a_2	b_0
SWCNT	-2247.346	132.992	107.929	10.024	-2424.547	-10.234	12.512	9.555	-2070.145	276.218	203.345	10.493
MWCNT	-1721.001	290.667	108.765	8.964	-1762.029	236.361	47.419	8.852	-1679.973	344.973	170.111	9.075
CNT	-1557.637	334.951	103.274	8.628	-1607.446	264.603	19.798	8.486	-1507.828	405.298	186.749	8.770

Desorption type	fit				min. 95% confidence intervall				max. 95% confidence intervall			
	a_0	a_1	a_2	b_0	a_0	a_1	a_2	b_0	a_0	a_1	a_2	b_0
SWCNT	-2187.721	378.571	-46.174	9.587	-2454.350	135.199	-217.875	8.871	-1921.092	621.943	125.527	10.302
MWCNT	-1728.257	596.828	-212.569	8.795	-1803.280	488.160	-342.146	8.589	-1653.234	705.496	-82.992	9.001
CNT	-1596.407	582.840	-232.315	8.604	-1669.420	468.372	-378.973	8.395	-1523.395	697.307	-85.656	8.812